

Development of Flow Platform Designs and their Application for the Synthesis of Natural Products, Ferrocenyl Azides, and Benzotriazoles

Inaugural-Dissertation
to obtain the academic degree
Doctor rerum naturalium (Dr. rer. nat.)

submitted to the Department of Biology, Chemistry, Pharmacy
Freie Universität Berlin

by
Merlin Kleoff
from Berlin

September 2021

Hereby, I declare that the submitted thesis is my own work and was prepared autonomously without the help of other sources than the ones cited and acknowledged. The work was not submitted to any prior doctoral procedure.

Merlin Kleoff, September 2021

The following work was carried out within the research groups of Prof. Dr. PHILIPP HERETSCH and Prof. Dr. MATHIAS CHRISTMANN from July 2018 until March 2021 at the Institute of Chemistry and Biochemistry of the Freie Universität Berlin.

Date of Disputation: 07.10.2021

1st reviewer: Prof. Dr. PHILIPP HERETSCH

(Institute of Organic Chemistry, Leibniz Universität Hannover)

2nd reviewer: Prof. Dr. MATHIAS CHRISTMANN

(Institute of Chemistry and Biochemistry, Freie Universität Berlin)

Parts of this dissertation have already been published in:

M. Kleoff, J. Schwan, L. Boeser, B. Hartmayer, M. Christmann, B. Sarkar, P. Heretsch, Scalable Synthesis of Functionalized Ferrocenyl Azides and Amines Enabled by Flow Chemistry. *Org. Lett.* **2020**, *22*, 902–907.

M. Kleoff, L. Boeser, L. Baranyi, P. Heretsch, Scalable Synthesis of Benzotriazoles via [3+2] Cycloaddition of Azides and Arynes in Flow. *Eur. J. Org. Chem.* **2021**, 979–982.

M. Kleoff, J. Schwan, M. Christmann, P. Heretsch, A Modular, Argon-Driven Flow Platform for Natural Product Synthesis and Late-Stage Transformations. *Org. Lett.* **2021**, *23*, 2370–2374.

Not included in this dissertation are the following publications:

L. Suntrup, **M. Kleoff**, B. Sarkar, Serendipitous discoveries of new coordination modes of the 1,5-regioisomer of 1,2,3-triazoles enroute to the attempted synthesis of a carbon-anchored tri-mesoionic carbene. *Dalton Trans.* **2018**, *47*, 7992–8002.

L. Suntrup, F. Stein, G. Hermann, **M. Kleoff**, M. Kuss-Petermann, J. Klein, O. S. Wenger, J. C. Tremblay, B. Sarkar, Influence of Mesoionic Carbenes on Electro- and Photoactive Ru and Os Complexes: A Combined (Spectro-)Electrochemical, Photochemical, and Computational Study. *Inorg. Chem.* **2018**, *57*, 13973–13984.

M. Kleoff, K. Omoregbee, R. Zimmer, Science of Synthesis Knowledge Updates: Tetraheterosubstituted Methanes bearing a Carbon–Halogen Bond, Thieme, Stuttgart, **2018**, *4*, 209–240.

J. Schwan, **M. Kleoff**, B. Hartmayer, P. Heretsch, M. Christmann, Synthesis of Quinolinone Alkaloids via Aryne Insertions into Unsymmetric Imides in Flow. *Org. Lett.* **2018**, *20*, 7661–7664.

M. Kleoff, S. Suhr, B. Sarkar, R. Zimmer, H.-U. Reissig, M. Marin-Luna, H. Zipse, Efficient Syntheses of New Super Lewis Basic Tris(dialkylamino)-Substituted Terpyridines and Comparison of Their Methyl Cation Affinities. *Chem. Eur. J.* **2019**, *25*, 7526–7533.

J. Schwan, **M. Kleoff**, P. Heretsch, M. Christmann, Five-Step Synthesis of Yaequinolones J1 and J2. *Org. Lett.* **2020**, *22*, 675–678.

„Pressure is like medicine. Take it to get better.“

-Zlatan Ibrahimović

Content

Danksagung	1
Abbreviations	3
Zusammenfassung.....	5
Abstract.....	7
1 Introduction.....	9
1.1 Flow Chemistry.....	9
1.2 Natural Product Synthesis and Late-Stage Transformations	16
1.3 Ferrocenyl Derivatives as Versatile Building Blocks	19
1.4 Benzotriazoles.....	25
1.5 Synthetic Applications of Arynes	29
1.6 Scientific Goal	33
2 List of References and Illustration Credits	35
2.1 References	35
2.2 Illustration Credits	51
Appendices	52

Danksagung

An erster Stelle möchte ich mich bei meinem Doktorvater Prof. Dr. Philipp Heretsch für die Übernahme des Erstgutachtens und für die große wissenschaftliche Freiheit während der Promotion bedanken. Vor allem aber danke ich ihm dafür, dass er es mir ermöglichte, an der Flowchemie zu forschen.

Ich danke Prof. Dr. Mathias Christmann für die Übernahme des Zweitgutachtens, für interessante Gespräche und für die lehrreichen, gemeinsamen Korrekturarbeiten an den „Papieren“.

Mein großer Dank gilt Prof. Dr. Hans-Ulrich Reißig für die fortwährende Unterstützung seit meinem Masterstudium.

Auch danke ich Prof. Dr. Biprajit Sarkar für wertvolle wissenschaftliche Ratschläge und für die kreative Zusammenarbeit seit meiner Masterarbeit.

Ganz besonders danke ich Dr. Reinhold Zimmer, von dem ich über die Jahre unendlich viel gelernt habe. Ich danke ihm dafür, dass er immer ein offenes Ohr für Probleme hatte, für zahlreiche wissenschaftliche und nicht-wissenschaftliche Diskussionen und für das Korrekturlesen fast all meiner Publikationen.

Dr. Simon Steinhauer, Dr. Carlo Fasting und Prof. Dr. Kerry Gilmore danke ich für ihren Rat und ihre Hilfe bei vielen technischen Fragestellungen.

Danke auch an alle, die diese Arbeit korrekturgelesen haben: Lorenz Wiese, Lisa Böser, Bence Hartmayer, Dr. Sebastian Ponath, Dr. Johannes Schwan, Dr. Reinhold Zimmer.

Der Deutschen Forschungsgemeinschaft danke ich für die finanzielle Unterstützung.

Der Arbeitsgruppe Heretsch und der Arbeitsgruppe Christmann danke ich für die freundliche und hilfsbereite Atmosphäre. Ganz besonders danke ich Dr. Johannes Schwan für zwei sehr schöne, gemeinsame Jahre im Labor 22.14, für die wunderbare Zusammenarbeit an insgesamt fünf (!) Projekten und für zahlreiche interessante Gespräche. Auch Lorenz Wiese danke ich für die sehr angenehme und humorvolle Zeit im Labor 23.06.

Weiterhin danke ich Dr. Florian Howaldt, Dr. Sebastian Ponath und Bence Hartmayer für ihre Unterstützung bei meiner Arbeit und für aufbauende Gespräche. Stefan Leisering danke ich dafür, dass er mir sein enzyklopädisches Wissen in vielen Diskussionen weitergab.

Patrick Voßnacker danke ich für die sehr gute Zusammenarbeit seit nunmehr fast zehn Jahren.

Meinen Studentinnen Lisa Böser und Linda Baranyi danke ich für ihre tatkräftige Mitarbeit und die sehr schöne gemeinsame Zeit.

Abschließend gilt mein größter Dank meinen Freunden und meiner Familie für ihre bedingungslose Unterstützung über all die Jahre.

Abbreviations

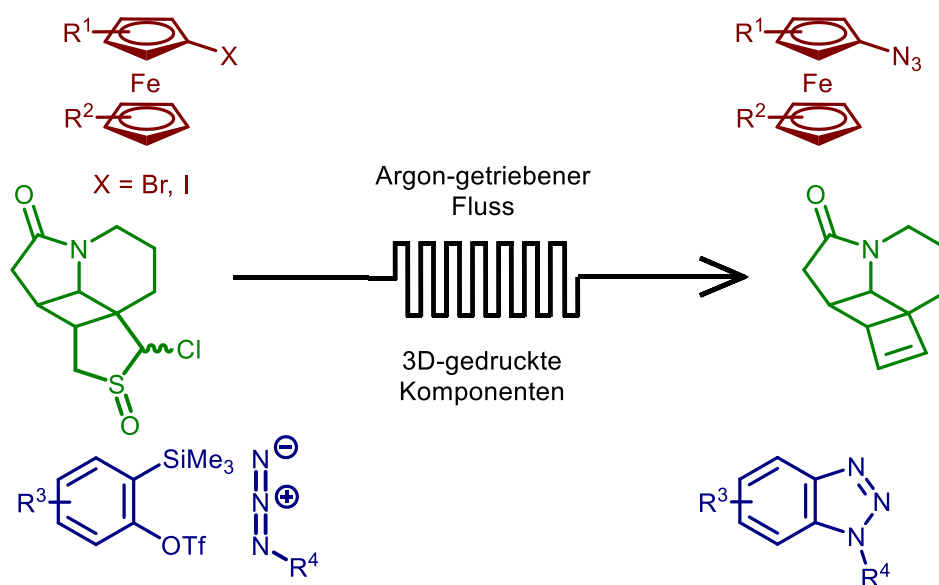
Ac	acetyl
Ar	arene
Bn	benzyl
bpy	2,2'-bipyridine
Bu	butyl
c	concentration/ cyclo-/ centi-
Cbz	benzyloxycarbonyl
COX	cyclooxygenase
Δ	elevated temperature
d	day
DME	dimethoxyethane
DMF	<i>N,N</i> -dimethylformamide
DNA	deoxyribonucleic acid
E	electrophile
equiv	equivalents
Et	ethyl
FEP	fluorinated ethylene propylene
g	gram
HIV	human immunodeficiency viruses
<i>i</i>	<i>iso</i>
λ	wavelength
LG	leaving group
m	<i>meta</i> -/ milli-/ meter
M	molar (mol/L)/ mega-/metal
μ	micro-
Me	methyl
Mes	mesityl
MFC	mass flow controller
min	minute
NMR	nuclear magnetic resonance
Nu	nucleophile
[O]	oxidation
p	piko
Ph	phenyl

Pr	propyl
R	rest
rt	room temperature
t	time/ <i>tert</i>
T	temperature
TBAF	tetrabutylammonium fluoride
TBAT	tetrabutylammonium triphenyldifluorosilicate
TBS	<i>tert</i> -butyldimethyl silyl
Tf	trifluoromethanesulfonyl
THF	tetrahydrofuran
Ts	<i>para</i> -toluenesulfonyl
X	halogenide

Zusammenfassung

In dieser Arbeit wurde eine modulare Fluss-Plattform entworfen und für die Synthese von Naturstoffen und für zwei methodische Arbeiten verwendet. Der etablierte, flüssigkeitsgetriebene Fluss weist diverse Nachteile auf und geht vor allem mit dem Auftreten von Dispersions-Phänomenen zwischen Lösungsmitteln und Reagenzlösungen einher, die zu großen Reagenzverlusten führen. Deshalb wurde das neue Konzept des Argon-getriebenen Flusses verfolgt. Dadurch können Dispersions-Phänomene unterdrückt werden, was neue Wege bei der Handhabung von wertvollen Intermediaten im Fluss, vor allem im kleinen Maßstab, eröffnet. Um standardmäßige, nicht nachhaltige Trocknungsprotokolle von Flussreaktoren zu vermeiden, wurden „Schlenk-im-Fluss“-Prozeduren entwickelt, die die verbreiteten Schlenk-Techniken für die Chemie im Fluss adaptieren. Um diese Konzepte zu realisieren, stellte sich der starke Einsatz vom 3D-Druck als Schlüsseltechnik heraus, der die Fertigung von maßgeschneiderten Komponenten ermöglichte.

Als Beweis des Konzeptes wurden unter Verwendung der Fluss-Plattform zwei Intermediate von Naturstoffsynthesen in reproduzierbaren Ausbeuten dargestellt. Weiterhin wurde eine neue Methode zur Dekawolfram-katalysierten, seitenselektiven C-H-Chlorierung von (+)-Sklareolid entwickelt, die im Fluss mit einer besseren Skalierbarkeit und einer höheren Reaktionsgeschwindigkeit realisiert wurde.



Scheme 1: Eine modulare Fluss-Plattform, die auf einem Argon-getriebenem Fluss und 3D-gedruckten Komponenten basiert, wurde verwendet, um Ferrocenylazide (rot), Intermediate in Naturstoffsynthesen (grün) und Benzotriazole (blau) zu synthetisieren.

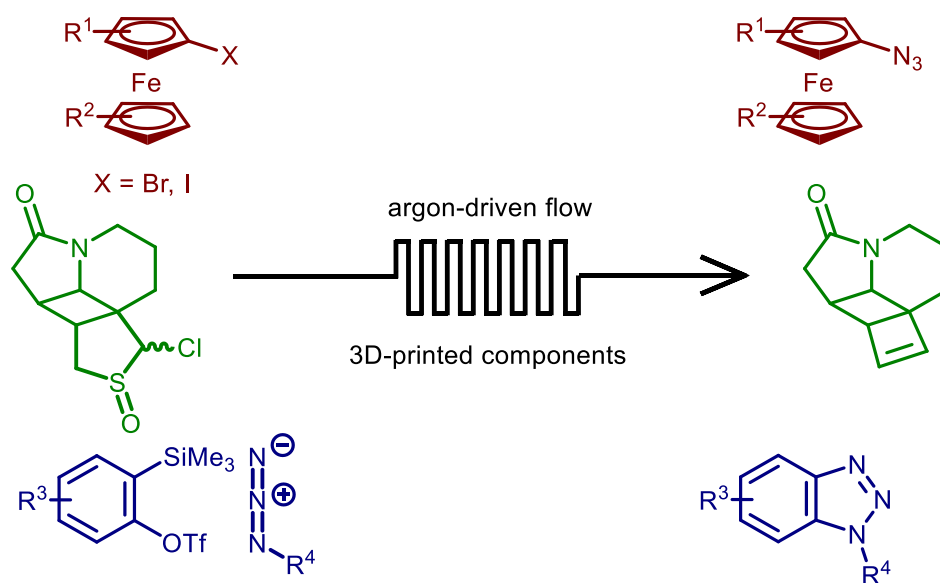
Außerdem wurde eine generelle Methode zur Synthese von funktionalisierten Ferrocenylaziden und -aminen im Kolben und im Fluss entwickelt. Durch Halogen-Lithium-Austausch von Ferrocenylhalogeniden und anschließendem Abfangen mit Tosylazid wurde eine Reihe von

Ferrocenylaziden erhalten. Im Fluss konnten aufgrund besserer Durchmischung der Halogen-Lithium-Austausch und die Reaktion mit Tosylazid signifikant schneller durchgeführt werden. Auch die folgende Thermolyse von Ferrocenyltriazenen konnte bei erhöhten Temperaturen im Fluss beschleunigt werden, da Schlauchreaktoren einen gesteigerten Wärmetransfer aufweisen, während die thermische Belastung von gefährlichen Ferrocenylaziden reduziert werden konnte. Ausfallende *para*-Toluylsulfinate wurden in einem dreiphasigen Flussregime effizient im Fluss gehalten. Das überlegene Sicherheits- und Skalierbarkeitsprofil des Flussprozesses wurde im Grammmaßstab demonstriert. In einem Staudingerprotokoll wurden die Ferrocenylazide in durchgängig guten Ausbeuten zu den entsprechenden Ferrocenylaminen reduziert.

Unter Verwendung der Fluss-Plattform und einiger der zuvor dargestellten Ferrocenylazide wurde ein Protokoll zur schnellen und skalierbaren Synthese von Benzotriazolen durch [3+2]-Zykloaddition von Aziden und Arinen entwickelt. Im Fluss konnte der Prozess bei erhöhten Temperaturen durchgeführt werden, wobei die sichere Handhabung von potentiell explosiven Aziden und die vorteilhafte Reaktionskontrolle von hochreaktiven Arinen im Fluss ausgenutzt wurde. Dadurch konnten höhere Reaktionsgeschwindigkeiten und eine gesteigerte Produktivität erreicht werden. Die Skalierbarkeit des Flussprotokolls wurde für die Synthese eines antibakteriellen und antiviralen Benzotriazols im Grammmaßstab demonstriert.

Abstract

In this work, a modular flow platform was designed and employed in the synthesis of natural products and for two methodology projects. As the established liquid-driven flow shows several disadvantages, in particular the occurrence of dispersion phenomena between solvent and reagent solutions resulting in high reagent losses, the new concept of an argon-driven flow was pursued. In this way, dispersion phenomena were suppressed, opening up new ways for the handling of valuable intermediates in flow on small scale. To avoid common, unsustainable drying protocols of flow reactors, “Schlenk-in-flow” procedures were developed adopting well-established Schlenk techniques to flow chemistry. To realize these concepts, the extensive use of 3D-printing to enable the manufacturing of tailor-made equipment turned out as a key technique. As a proof of concept, two intermediates in natural product synthesis were prepared in reproducible yields slightly higher than in batch. In addition, a new method for the site-selective C–H chlorination of (+)-sclareolide by decatungstate catalysis was developed, allowing improved scalability and higher reaction rates in flow.



Scheme 2: Using the modular flow platform based on argon-driven flow and 3D-printed parts, ferrocenyl azides (red), intermediates in natural product synthesis (green) and benzotriazoles (blue) were synthesized.

Furthermore, a general method for the synthesis of functionalized ferrocenyl azides and amines was developed in batch and flow. By halogen-lithium exchange of ferrocenyl halides and subsequent trapping with tosyl azide, a variety of ferrocenyl azides was obtained. In flow, the halogen-lithium exchange and the reaction with tosyl azide proceeded significantly faster due to improved mixing. Also, the subsequent thermolysis of ferrocenyl triazene intermediates could be accelerated at elevated temperature in flow as a result of the enhanced heat-transfer in tube reactors, while thermal strain of hazardous ferrocenyl azides could be minimized. Precipitating *para*-tolyl sulfinates were efficiently kept in turbid flow by utilizing a triphasic flow regime. The

advantageous safety and scalability profile of the flow process was demonstrated on gram scale. Using a Staudinger protocol, ferrocenyl azides were reduced in consistently good yields to the corresponding ferrocenyl amines.

Employing the flow platform and a selection of the prepared ferrocenyl azides, a protocol for the rapid and scalable synthesis of benzotriazoles via [3+2] cycloaddition of azides and arynes was developed. By making use of the advantages of flow chemistry in the safe handling of potentially explosive azides and the improved reaction control of highly reactive arynes, the process could be performed at elevated temperature providing faster reactions and an increased productivity. The scalability of the flow protocol was demonstrated for the synthesis of an antibacterial and antifungal benzotriazole on gram scale.

1 Introduction

1.1 Flow Chemistry

Since the dawn of organic chemistry, the synthesis of organic molecules has evolved as a central science for modern society. May it be for the development of agrochemicals, of pharmaceuticals in the fight against diseases, or for more aesthetic interests as cosmetics and fragrances, synthetic organic chemistry plays a central role. Over time, organic synthesis was consistently enriched by innovative technologies such as spectroscopy or chromatography opening up new research areas and pushing the frontiers of synthetic chemistry.^[1-4]

In the last decades, flow technology has entered the field of organic chemistry.^[5-82] Originally, continuously operating reactors were developed in petrochemical industry to achieve higher productivity and scalability. Today, literally all petrochemical processes, beginning with the heating of crude oil, then cracking, refining, and production of bulk chemicals are performed in continuous flow.^[83] Even in the production of pharmaceuticals and other fine chemicals, more and more reactions are conducted in flow offering improved scalability, higher purity of products, and decreased manufacturing costs.^[84-92]

For many years, flow chemistry seemed to be a prerogative of process chemists and engineers. This changed in particular when Steven Ley started a research program for the systematic application of flow chemistry in methodology and natural product synthesis.^[93-99] Confronted with underdeveloped equipment, impractical flow procedures, and other limitations, many pioneering – and sometimes highly artificial – technologies were developed in the Ley laboratories.^[100-115]

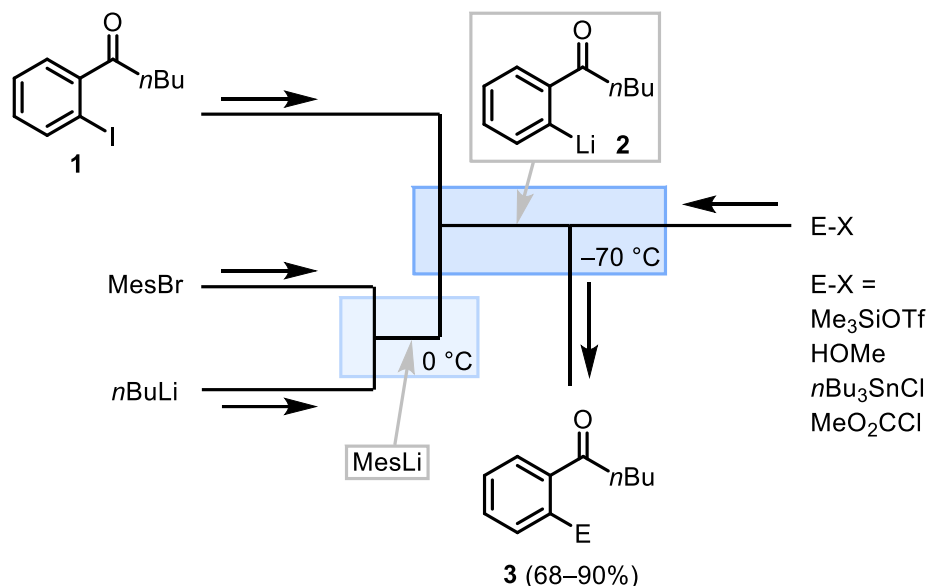
In the last decade, flow chemistry has been increasingly applied as a technology to expand synthetic options, while continuous process technology has been emphasized as a key technology for sustainable manufacturing.^[116-118] In general, flow reactors show many advantages including:

- enhanced heat-, mass-, and photon transfer
- improved safety profile
- broad scalability
- higher sustainability

The advances of fast heat- and mass transfer were exploited especially by Yoshida and coworkers, coining the term “flash chemistry” for reactions that are essentially diffusion limited and completed within milliseconds when proper mixing is ensured.^[119-121] Applying flash chemistry, chemical transformations previously considered impossible were realized in flow.^[119,122-135]

One impressive example for the application of flash chemistry is the generation of organolithiums in the presence of ketones by Yoshida and coworkers (Scheme 3).^[135] After reaction of mesityl bromide and *n*-butyl lithium, the formed mesityl lithium is mixed with acylidobenzene **1**

generating organolithium species **2** by iodine-lithium exchange at $-70\text{ }^{\circ}\text{C}$. After a residence time of only 3 ms the highly instable intermediate **2** is trapped with an electrophile (E-X) forming substituted ketones **3** in good to excellent yields. Those transformations are only possible due to the ultrafast mixing of reagents and the almost perfect cooling provided by microreactors.^[135]



Scheme 3: Flash chemistry approach for the generation of organolithium **2** in presence of a ketone followed by trapping with various electrophiles leading to substituted ketones **3**. The iodine-lithium exchange is performed with mesityl lithium prepared from mesityl bromide and *n*-butyl lithium in flow.

In analogy to the increased heat- and mass transfer, also the significantly higher photon transfer is a key advantage of flow reactors.^[6,136] This is a consequence of the Lambert–Beer law, describing that the attenuation of light A (also expressed as the logarithm of the ratio of the initial power of light I_0 and the power of transmitted light I) is dependent on the molar attenuation coefficient of a molecule ϵ , the concentration of a attenuating species c and the optical path length l (Eq. 1).

$$A = \log_{10} \frac{I_0}{I} = \epsilon cl \quad (\text{Eq. 1})$$

In the case of a species with a high molar attenuation coefficient such as the important photocatalyst tris(bipyridine)ruthenium(II) chloride [Ru(bpy)₃]Cl₂ in a concentration of 0.5 mM, a significant amount of the incident light is already absorbed after passing a path length of only 0.2 cm (Figure 1). Hence, even in a small reaction vial with a diameter of 1 cm, the major part of the reaction mixture is not irradiated.^[6,136]

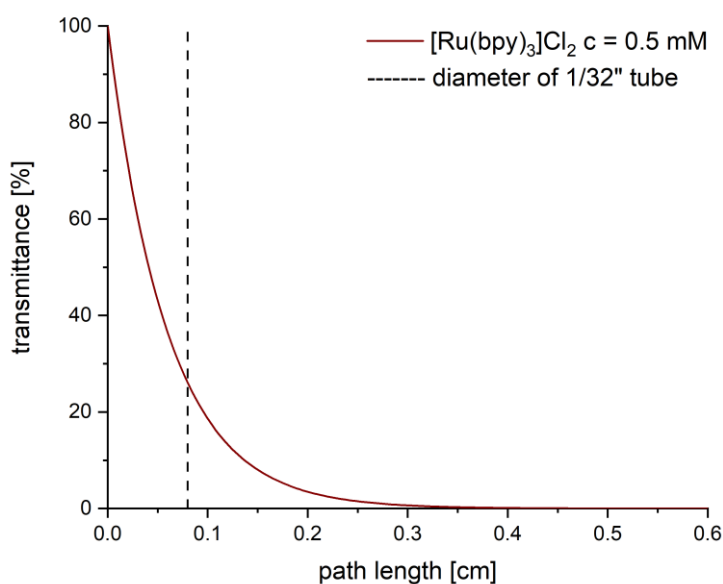
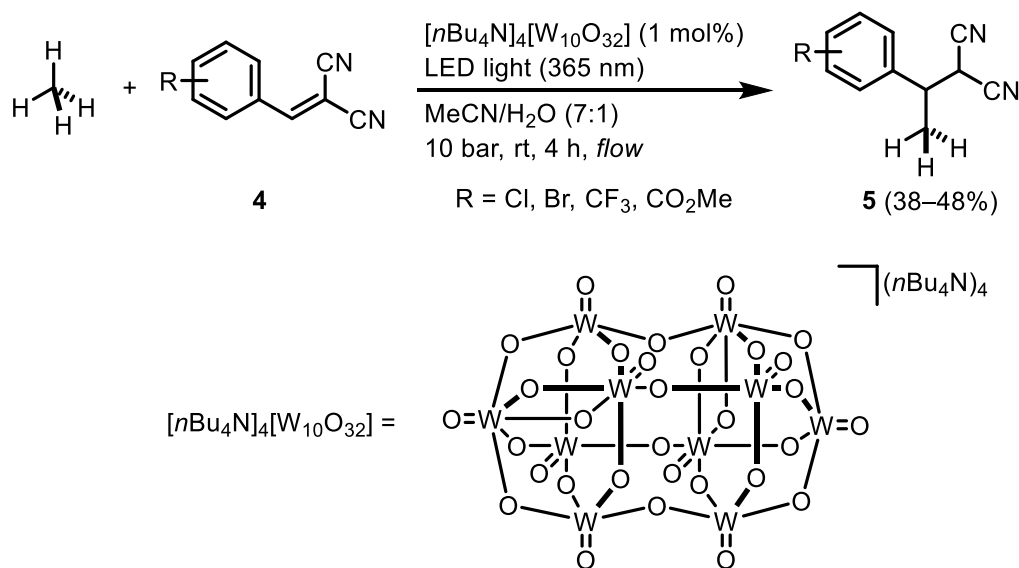


Figure 1: Transmittance of light plotted against the path length for $[\text{Ru}(\text{bpy})_3]\text{Cl}_2$ with a concentration of $c = 0.5 \text{ mM}$ in methanol ($\epsilon = 14600 \text{ M}^{-1} \text{ cm}^{-1}$). The dashed vertical line represents the inner diameter ($1/32'' \approx 0.08 \text{ cm}$) of a common FEP tube employed in flow chemistry. Transmittance = $10^{-(\epsilon c l)}$.^[6]

As a result, scaling up photoreactions in large reaction vessels results in very long reaction times potentially leading to increased side reactions due to over-irradiation – a limitation which can easily be overcome in flow.^[137,138] As in many academic flow reactors tubes with an inner diameter of 0.08 cm are used, the light intensity in the tubes is significantly higher. Consequently, many photochemical reactions can be enormously accelerated in flow, while the continuous removal of the reaction mixture from the light source can reduce degradation of the product.^[139-142]

Very recently, Noël and coworkers made use of the efficient irradiation in flow for the $\text{C}(\text{sp}^3)\text{-H}$ functionalization of gaseous hydrocarbons.^[139] The reaction is catalyzed by decatungstate ($[\text{W}_{10}\text{O}_{32}]^{4-}$), which forms upon irradiation with light (UV-A, $\sim 365 \text{ nm}$) the excited state $[\text{W}_{10}\text{O}_{32}]^{4-*}$ which decays within 30 ps to an extremely reactive transient species.^[143,144] This species reacts by capturing an electron or a hydrogen atom from virtually any organic substrate, making decatungstate a versatile hydrogen atom transfer (HAT) photocatalyst with growing applications in organic synthesis.^[140,145-157] Noël and coworkers extended the scope of organic substrates activated by decatungstate to light hydrocarbons such as ethane and methane (Scheme 4). By premixing gaseous methane and a solution of decatungstate and electron-poor olefins **4**, a pressurized reaction mixture is formed that can be safely handled in flow. This mixture is then irradiated with LED light with a wavelength of 365 nm to initiate C–H functionalization of methane providing the C–C coupled products **5**.^[139]

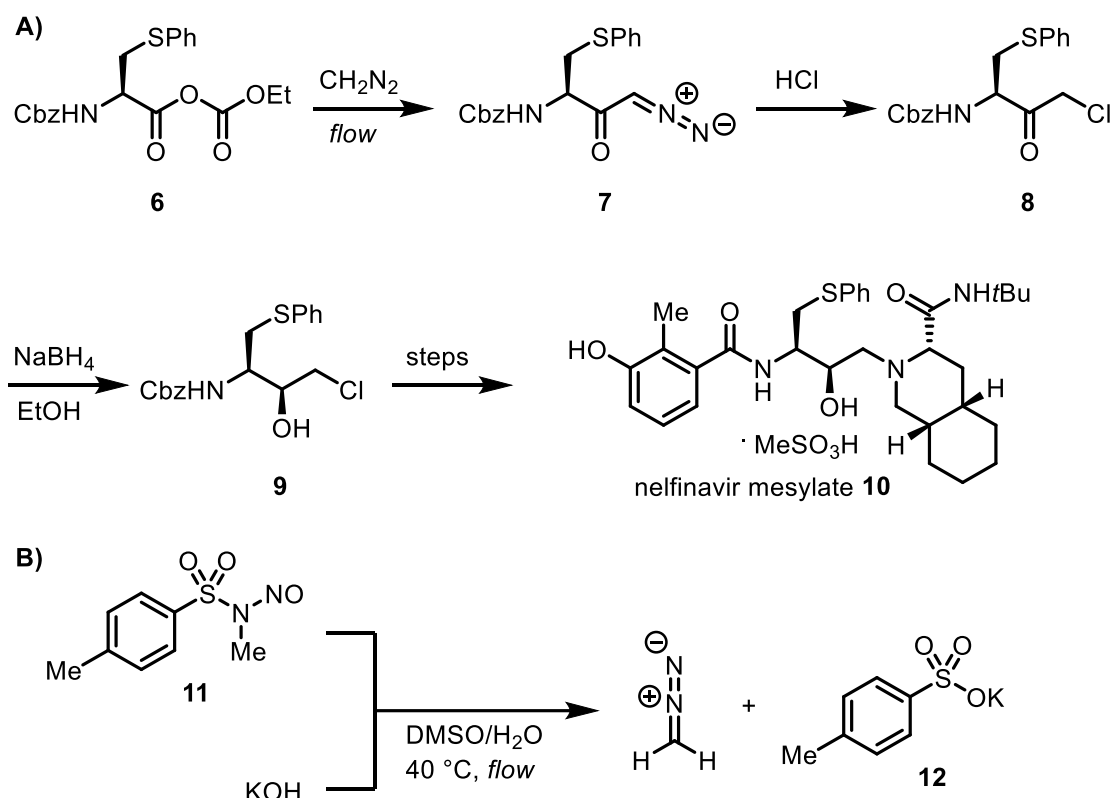


Scheme 4: C-C coupling of methane with electron-poor olefins **4** via decatungstate catalyzed C(sp³)-H functionalization in flow.

This work showcases the benefits of flow chemistry for photoreactions offering not only short reaction times and better scalability, but also improved safety when pressurized reaction mixtures are handled.^[139]

Although dangers of hazardous reactions are sometimes belittled in academia, there is pervasive emphasis and awareness of safety in industrial laboratories.^[158] Therefore, a significant number of industrial reactions and processes have been translated into continuous flow. The precise reaction control and the comparable small dimensions of flow reactors make flow processes attractive for taming poisonous chemicals, e.g., phosgene or fluorine, or explosive compounds, such as diazonium salts or azides, especially when upscaling is the purpose.^[159–163]

Probably, one of the most dangerous reagents in organic synthesis is diazomethane.^[47] This yellow gas is a valuable methylating agent primarily used for Arndt–Eistert reactions, but also shows high toxicity and explosiveness limiting its use on larger scale.^[164] Already the discoverer of diazomethane, Hans von Pechmann, noted in 1895, while suffering from the complications of a diazomethane intoxication that this reagent would only find applications “where operations are carried out in smallest quantities” (“... wo es sich um Operationen im kleinsten Maassstab [sic] handelt”).^[165] More than 100 years later, Proctor and Warr from Phoenix Chemicals noted that diazomethane was indispensable for the ton scale production of the HIV protease inhibitor nelfinavir mesylate **10** (Scheme 5A). In the course of the synthesis, the mixed anhydride **6** was reacted with diazomethane in a modified Arndt–Eistert reaction to afford diazo compound **7** which is treated with hydrogen chloride leading to chloromethyl ketone **8** and subsequently reduced to alcohol **9**.^[166]



Scheme 5: A) Industrial synthesis of nelfinavir mesylate **10** involving reaction of mixed anhydride **6** with diazomethane in continuous flow. B) Preparation of diazomethane from diazald® (**11**) and potassium hydroxide under formation of potassium *para*-toluenesulfonate (**12**) in flow.

To realize this reaction on ton scale fulfilling all safety requirements, the process is conducted in continuous flow. Thus, diazomethane is generated in a mixture of dimethyl sulfoxide and water by reaction of diazald® (**11**) with potassium hydroxide at 40 °C producing 90–93 g diazomethane per hour (Scheme 5B). A stream of nitrogen is employed for continuously stripping diazomethane from the reaction mixture which is then carried into a solution of mixed anhydride **6** where the introduced diazomethane is continuously consumed (Scheme 5A). In this way, an overall inventory of diazomethane of less than 80 g at any time is ensured, demonstrating the virtue of flow chemistry for controlling hazardous chemicals in large scale processes.^[166] Following this blueprint, numerous other methods for the safe generation of diazo compounds in flow were developed in the following years.^[167–180]

Although flow chemistry is a valuable tool to extend the borders of organic synthesis, translating reactions in flow frequently requires dealing with technological limitations.^[6] Furthermore, flow reactors show some disadvantages that do not (or only to a small degree) exist in batch. One of the most important problems of flow reactors is the occurrence of dispersion phenomena when e.g., a reagent solution is introduced in a stream of pure solvent.^[6] Due to the concentration difference between the reagent solution and the solvent, a gradient is formed resulting in leaching of the reagent into the solvent slug (Figure 2). The axial dispersion is primarily depending on the flow speed (the higher the flow speed, the higher the dispersion) and on the time (the dispersion

increases with time).^[181] Only within a part of the introduced reagent solution the initial concentration is retained reflecting the so-called “steady-state conditions”. Therefore, typically, only the part of the reaction under steady state conditions is collected while the pre- and postrun are discarded.^[6] The resulting material loss is relatively high, when small reagent slugs are introduced, in particular in combination with reactions that are performed in large tube reactors and with high flow rates leading to a high dispersion. It has been outlined that dispersion phenomena are a significant issue in flow chemistry, especially for small scale operations of valuable substrates and for multi-step sequences resulting in dispersion losses with each step.^[107]

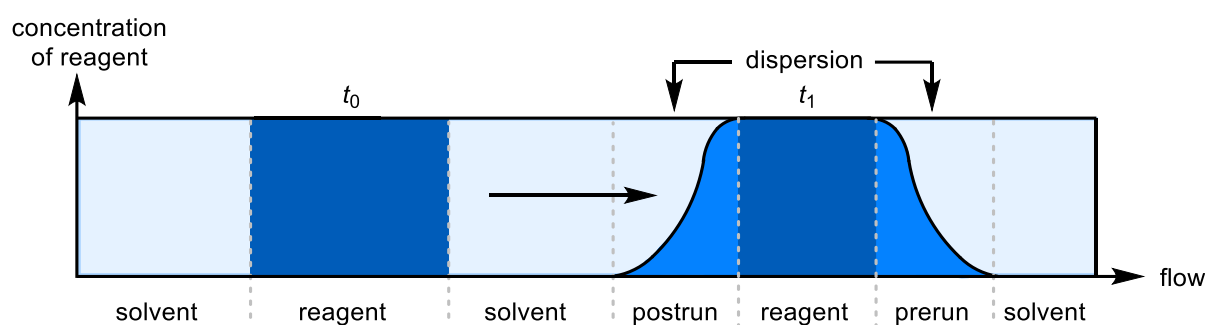


Figure 2: Simplified representation of dispersion between solvent and reagent directly after introduction of a reagent slug (t_0) and after a given time (t_1).

To address these shortcomings, the concept of the segmented gas-liquid flow has been developed by Jansen and coworkers. Reagent solutions are mixed with a stream of a carrier gas resulting in the formation of alternating liquid and gas slugs, while the gas slugs act as barriers between the liquid volumes. In this way, a direct contact between a reagent solution and pure solvent is avoided and dispersion phenomena are minimized.^[182-188] Very recently, this concept has been adopted by Gilmore and coworkers to design an automated synthesizer for multistep sequences in flow.^[189]

Another common problem in flow chemistry are suspensions caused either by insoluble reagents or precipitation formed during a reaction. As they tend to block tubes or movable parts (valves, pumps, etc.), performing reactions with suspensions in flow is still challenging. To suppress sedimentation of solids, concepts including continuous mechanical agitation or sonication using ultrasound were developed.^[111,190-193] Recently, Gilmore and coworkers presented a simple and elegant solution by pumping suspensions in a segmented flow (Figure 3).^[194]

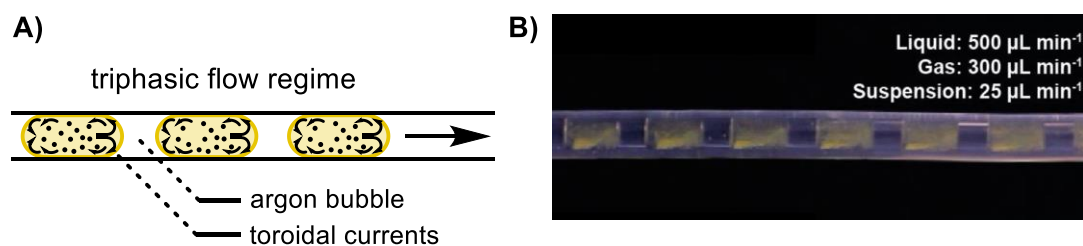


Figure 3: A) Formation of toroidal currents between liquid and argon bubbles in a triphasic flow regime. B) Picture of a pumped suspension in segmented flow.

The suspension is mixed with argon to form a triphasic flow regime in which strong toroidal currents continuously resuspend the solids within the liquid segments preventing clogging of the tubes. Using this technique, decarboxylative fluorinations mediated by an insoluble photocatalyst were realized in flow.^[194]

To deal with such engineering challenges frequently customized solutions must be found, resulting in the development of specially designed flow equipment.^[189,195-198] Recently, engineering tasks were enormously simplified by the evolution of 3D-printing. By using software for computer aided design (CAD) and an inexpensive 3D-printer to manufacture prototypes, the development of simple solutions for complex engineering problems is significantly accelerated.^[199-208]

However, printing of materials that are resistant against different organic solvents is challenging and requires much more expensive industrial printers.^[206,209,210] 3D printing of reactors and other so called “labware” with only moderately resistant polymers such as polypropylene as invented by Cronin and coworkers is rarely practical, restricting their applicability on relatively few organic reactions.^[211-213] Therefore, 3D-printing is not a one-fits-all solution to replace established technologies or inexpensive lab equipment but rather a supporting tool and an enabling technique for prototyping.^[206,208,214] For instance, 3D printing of highly chemical resistant materials such as stainless steel 316L or titanium enabled the construction of tailor-made reactors with superior mixing properties.^[215]

As 3D printing lowers the barrier for inventing technological solutions, more recently, it also facilitated the adaption of flow processes for automation and high-throughput optimization processes.^[216-218] This is of great importance, since reactions in flow require usually stricter supervision and consequently more time at the lab bench than batch processes.^[219] Additionally, in most cases it is necessary to reconfigure the flow system when different types of reactions are performed. To overcome these limitations, many flow chemists and engineers focused on the development of partially automated and autonomous flow systems or modular approaches that simplify switching between different reaction types.^[220]

Among the different areas of organic chemistry, the total synthesis of natural products has the highest demand on the flexibility and modularity of a flow system. To approach structurally complex natural products, various reaction types are regularly conducted, including fast reactions at low temperatures, slow reactions at elevated temperatures, reactions involving gases under pressure and photochemical reactions. Besides these requisites on flexibility, natural product synthesis calls for broad scalability, reaching from decagrams in the early steps of a synthesis to milligrams in the “end game”. Therefore, designing such a flow system is both a chemical and an engineering challenge.^[8,40,93,221]

1.2 Natural Product Synthesis and Late-Stage Transformations

Nature is an almost infinite source of molecules with an enormous structural diversity. Most of them are secondary metabolites meaning that these compounds are not necessarily required for survival but may help the organism for instance to defend itself against predators or to attract insects for pollination.^[222–224] However, these natural products are of great importance for human civilization as they are frequently used to treat diseases (65% of the newly approved small molecule drugs have been natural products or derivatives thereof) or to serve as flavors and fragrances.^[225–227]

The use (and misuse) of opium as an analgesic and anesthetic was already described by “the father of medicine”, Hippocrates of Kos (460–377 BC).^[228] In 1803, one of the most important opiates, (–)-morphine (**13**), was isolated by Sertürner, which was, in fact, the first isolation of an alkaloid from a plant.^[229] Today, (–)-morphine (**13**) is on the World Health Organization’s list of essential medicines – and is still isolated from the opium poppy in quantities of ~500 t/a.^[230,231]

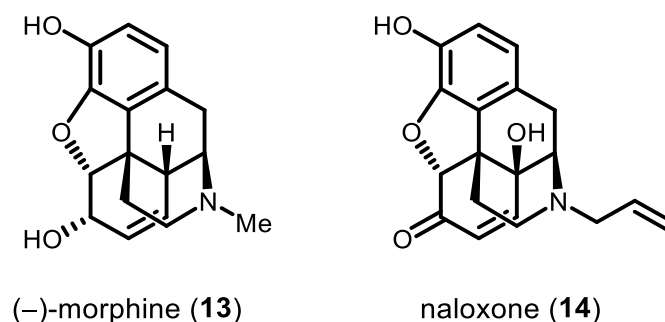


Figure 4: The essential opioids (–)-morphine (**13**) and its antagonist naloxone (**14**).

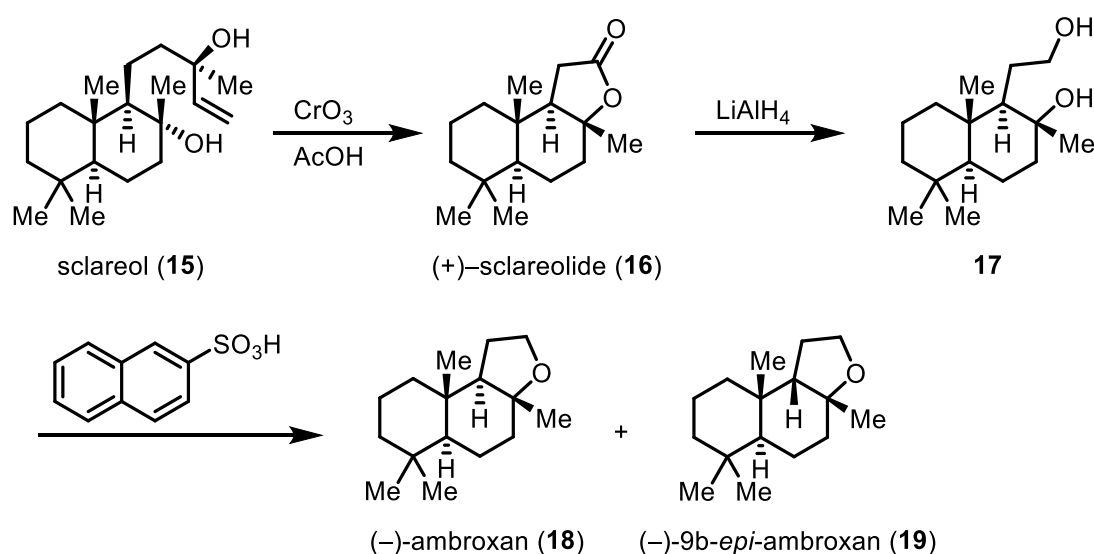
However, the structure of (–)-morphine (**13**) was unknown at that time and could only be elucidated by the first total synthesis of (–)-morphine (**13**) in 1952 by Gates and Tschudi.^[232,233] For many decades, one of the primary motivations for the natural product synthesis was to determine their structure. This has been changed in the last fifty years, in particular due to the achievements in NMR spectroscopy and X-ray crystallography,^[221] but even today, the total synthesis of a natural product occasionally leads to a revision of its proposed structure.^[234–236] Nevertheless, after solving the structure of (–)-morphine (**13**) by total synthesis, many other syntheses followed.^[237–254] This may be rationalized by achieving independency of natural sources,^[255] but also to demonstrate the virtue of new synthetic methods for the preparation of an attractive target such as morphine (**13**).^[256]

To understand the structure-activity relationship and to identify molecules that show enhanced pharmacological profiles, derivatization of natural products is of great interest.^[257] Thus, total synthesis of natural products can serve as an access hub to a plethora of derivatives. In particular, as a result of the tremendous achievements in C–H functionalization in recent years, which allow

activation even of the strongest C(sp³)-H bonds in a molecule, late stage-functionalization of natural products receives more and more attention.^[258,259]

Already the first derivatives of morphine (**13**) have been prepared by functionalization of morphine (**13**) in a semisynthetic fashion before its first total synthesis was completed.^[230] A breakthrough in the synthesis of opioid drugs was the synthesis of naloxone (**14**), which is obtained from morphine (**13**) in few steps.^[260] It is a competitive opioid receptor antagonist able to block the effect of other opioids and saves lives in case of an opioid overdose. Consequently, naloxone (**14**) was also included in the World Health Organization's list of essential medicines.^[261] Beside the importance of natural products for medicine, they have found numerous applications as odorants. In modern perfumery, animal notes such as amber, musk, and civet are employed as base notes in almost any fragrance. The primary odorous constituent of natural ambergris is (-)-ambroxan (**18**), adding a slightly sweet, woody, and fresh note to a perfume (a high concentration is used in e.g., *Dior Sauvage*). Due to its full and pleasant smell, it is even sold as a single-ingredient fragrance (e.g., *Escentric Molecules: Molecule 02*).^[226,262,263]

As natural ambergris is only produced in very small amounts by sperm whales, the need for (-)-ambroxan (**18**) cannot be covered by natural sources. Therefore, it is produced in a combined scale of ~100 t/a, typically by semi-synthesis starting from sclareol (**15**), a diterpene that is isolated from clary sage (Scheme 6).^[226,263] Sclareol (**15**) is oxidized by chromium(VI) oxide in acetic acid to provide (+)-sclareolide (**16**), which is then reduced to the corresponding diol **17** and cyclized to (-)-ambroxan (**18**) using naphthalene-2-sulfonic acid.^[263] In the last step, careful reaction control is necessary to suppress formation of the thermodynamically more stable 9b-*epi*-ambroxan (**19**). Alternative synthetic routes towards (-)-ambroxan (**18**) including biocatalytic processes were developed, but most of them are still semi-synthetic approaches.^[226,264–266]



Scheme 6: Industrial synthesis of (-)-ambroxan (**18**) by oxidation of sclareol (**15**) to (+)-sclareolide (**16**) followed by reduction and cyclization of diol **17** under acidic conditions.

1.3 Ferrocenyl Derivatives as Versatile Building Blocks

The discovery of ferrocene in 1951 is one of the most popular events in organometallic chemistry. Already the structural elucidation of ferrocene led to a scientific debate recognized beyond the borders of chemistry, prompting Laszlo and Hoffmann to re-narrate the years of discovery and its structural elucidation fifty years later.^[270,271]

Initially, the structure of ferrocene was described as an iron(II) center coordinated by two η^1 -cyclopentadienyl ligands ($[\text{Fe}(\eta^1\text{-C}_5\text{H}_5)_2]$), but was revised shortly afterwards. Wilkinson and Woodward and, independently, Fischer and Pfab suggested a “sandwich-type” or “double-cone” structure, respectively. One year later, their structural proposal was proven unambiguously by X-ray crystallography. While Woodward coined the name “ferrocene” underlining its aromaticity in analogy to benzene, Wilkinson and Fischer as key protagonists in the early history of metallocenes were honored with the Nobel prize in chemistry in 1973.^[271]

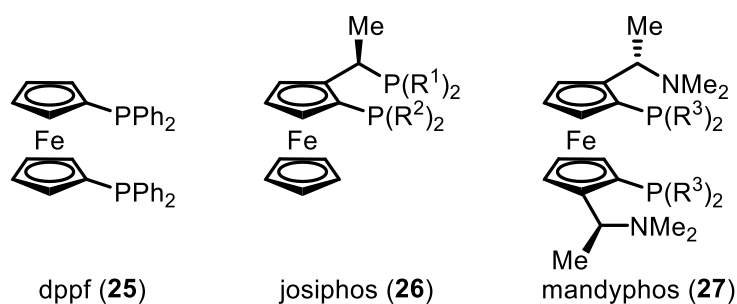
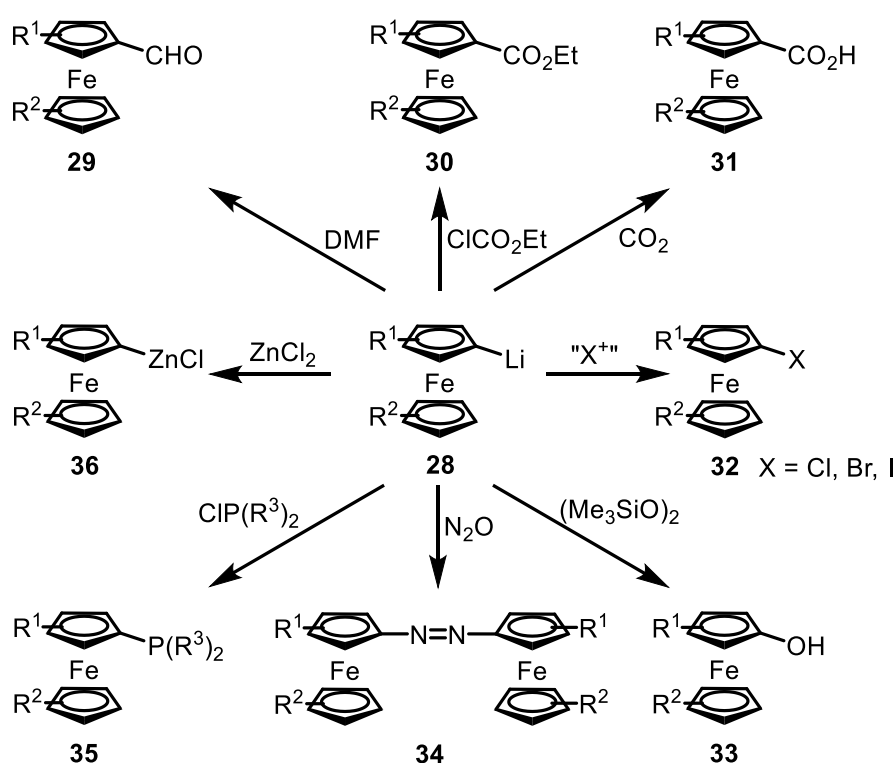


Figure 5: The structures of 1,1'-bis(diphenylphosphino)ferrocene (**25**, dppf), and the chiral catalysts josiphos (**26**) and mandyphos (**27**).

Over the last decades, ferrocene derivatives have found numerous applications in almost all areas of chemistry due to the striking combination of unique redox properties, high chemical and physical stability, and simple methods for their preparation.^[270] In homogeneous catalysis, ferrocene serves as a stable backbone for ligands such as 1,1'-bis(diphenylphosphino)ferrocene (**25**, dppf). Since ferrocenes bearing at least two different substituents on one cyclopentadienyl rings are planar chiral, ferrocene derivatives have been utilized as platform for an array of chiral ligands, e.g., josiphos (**26**) or mandyphos (**27**) which are employed for asymmetric catalysis, even on industrial scale.^[272-277]

One of the most intriguing properties of ferrocene is its reversible oxidation from ferrocene (iron(II)) to the ferrocenium cation (iron(III)).^[270] Due to the high stability of the ferrocenium cation in many organic solvents, the ferrocene/ferrocenium couple is frequently used as internal standard for electrochemical measurements but also as redox mediator in preparative electrochemistry.^[278-281] In addition, ferrocene derivatives are further utilized as redox switches for inorganic materials and molecular electronics.^[282-285] If more than one ferrocene unit is present in the molecule, the redox state of each ferrocenyl unit can be switched separately or cooperatively, allowing the controlled switch of polarity, charge, or color.^[277,286-299]

For the synthesis of these compounds, easily accessible and versatile ferrocenyl building blocks are required. Therefore, new methods for the functionalization of ferrocene are developed until today. Despite the aromaticity of ferrocene, many substitution reactions which are commonly used for aromatic compounds cannot be applied to ferrocene derivatives, as under oxidizing reaction conditions the ferrocene moiety is readily oxidized changing its reactivity.^[277] More recently, methods for the directed C–H functionalization of ferrocene derivatives using transition metal catalysis have been reported.^[300–305] Nevertheless, most functional groups are typically introduced to ferrocene derivatives using stoichiometric organometallics. Especially ferrocenyl lithiums **28** have been established as versatile precursors (Scheme 8). They are commonly prepared by lithiation or by halogen-lithium exchange of ferrocenyl halides.^[277]



Scheme 8: Overview of reactions of ferrocenyl lithiums **28** with selected electrophiles to the corresponding functionalized ferrocene derivatives.

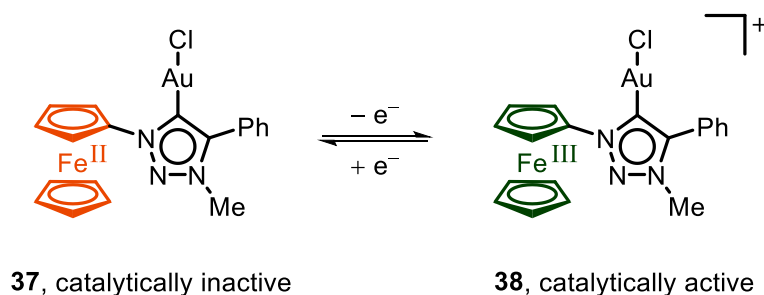
In general, ferrocenyl lithiums **28** can be reacted with a variety of electrophiles for the construction of C–C bonds and the introduction of heteroatoms. Trapping of **28** with *N,N*-dimethylformamide (DMF) provides the corresponding aldehyde **29**,^[306] while reaction with ethyl chloroformate leads to ester **30**.^[307] By introduction of gaseous carbon dioxide to a solution of ferrocenyl lithiums **28** at low temperatures, ferrocenyl carboxylic acids **31** can easily be prepared.^[308] The preparatively useful ferrocenyl halides **32** are accessed by reaction with electrophilic halogen sources such as *para*-toluenesulfonyl chloride, 1,2-dibromoethane, or iodine.^[309–311]

By formal oxidation of the C–Li bond with bis(trimethylsilyl)peroxide, the oxygen-labile ferrocenols **33** can be synthesized,^[312] while reaction of ferrocenyl lithiums **28** with gaseous dinitrogen oxide gives access to the deep violet azoferrocenes **34**.^[313] One of the most important reactions of ferrocenyl lithiums **28** is the reactions with chlorophosphines to phosphines **35**, introducing a donor-functionality present in many ferrocene based ligands.^[310,314–316] In addition, ferrocenyl lithiums **28** can undergo salt metathesis with e.g., zinc chloride, affording the corresponding ferrocenyl zinc species **36** which are primarily employed in Negishi cross coupling reactions.^[317,318]

Based on these methods, countless ferrocene building blocks were prepared resulting in a broad spectrum of applications. However, for the installation of some versatile functionalities such as azides and amines, reliable synthetic methods are underexplored.^[314,319]

The synthetic value of azides was already demonstrated by Staudinger and Curtius, however, only recently, organic azides have emerged as one of the most important compound classes in chemistry and biochemistry.^[320–322] This elevation was initiated by the simultaneous and independent discovery of Sharpless and Fokin that the copper-catalyzed azide alkyne cycloaddition (CuAAC) forms exclusively the 1,4-regioisomers of 1,2,3-triazoles in contrast to the uncatalyzed, thermal Huisgen cycloaddition of azides and alkynes resulting in mixtures of the 1,4- and the 1,5-triazoles.^[323] As the CuAAC reliably offers also high yields and a broad tolerance of functional groups and solvents, it has been outlined as a premier example of a “click” reaction, a term coined by Sharpless to characterize “nearly perfect” bond-forming reactions to create covalent links between diverse building blocks.^[324] Already in the years after its discovery, the CuAAC crossed traditional disciplinary borders and found broad applications in biochemistry, medicinal chemistry, polymer and material sciences as well as inorganic chemistry.^[325–330]

Shortly after, the first examples of ferrocenyl-substituted 1,2,3-triazoles were presented, merging the unique redox properties of ferrocene with the synthetic possibilities opened up by click chemistry to access unprecedented ligands, complexes, and molecular electronics.^[294–296,328]

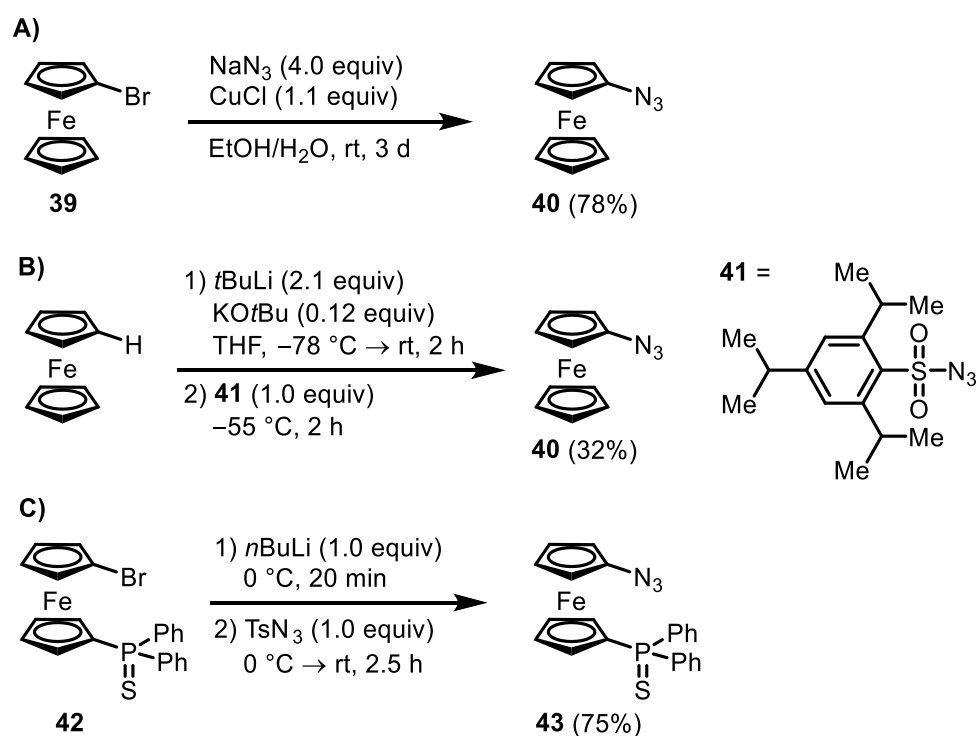


Scheme 9: The redox switchable gold(I) catalyst **37**. By oxidation of the ferrocene moiety, the catalytically active cationic complex **38** is formed. Reduction of **38** leads back to the catalytically inactive neutral complex **37**.

For instance, in the gold(I)-complex **37**, the ferrocenyl substituent serves as a stable redox-switch while the 1,2,3-triazole-5-ylidene (a mesoionic carbene) derived from the corresponding 1,2,3-triazole coordinates to the gold(I) center (Scheme 9).^[285,331]

Typically, the gold(I) catalyst is activated by removing the anionic counter ion (e.g., using silver(I) salts), to obtain a cationic gold(I) catalyst. In contrast, complex **37** can be activated for the gold(I) catalyzed synthesis of heterocycles by oxidizing the ferrocenyl moiety. As the oxidation of ferrocene is completely reversible, the oxidized species **38** can be reduced leading back to the native form **37** which also shuts down the catalytic activity, rendering complex **37** the first redox-switchable gold(I) catalyst.^[285]

To construct ferrocenes such as catalyst **37**, ferrocenyl azides are required as precursors to forge the 1,2,3-triazole heterocycle via CuAAC. Although ferrocenyl azides have found numerous applications as building blocks, no general methods for the synthesis of ferrocenyl azides have been developed. Among the published procedures for the synthesis of ferrocenyl azides, in particular three approaches have been employed.^[314]



Scheme 10: Selected examples for the synthesis of ferrocenyl azides. A) Copper mediated nucleophilic substitution of bromoferrocene. B) Lithiation of ferrocene with subsequent electrophilic trapping using 2,4,6-triisopropylbenzenesulfonyl azide (**41**). C) Bromine-lithium exchange of ferrocenyl bromide **42** followed by reaction with tosyl azide.

In the first approach, azidoferrocene (**40**) is prepared by the copper-mediated nucleophilic substitution of bromoferrocene (**39**) with sodium azide (Scheme 10A). Typically, stoichiometric amounts of copper(I) or copper(II) mediators are employed, resulting in the formation of highly explosive copper azides as intermediates. As the functional group tolerance under these

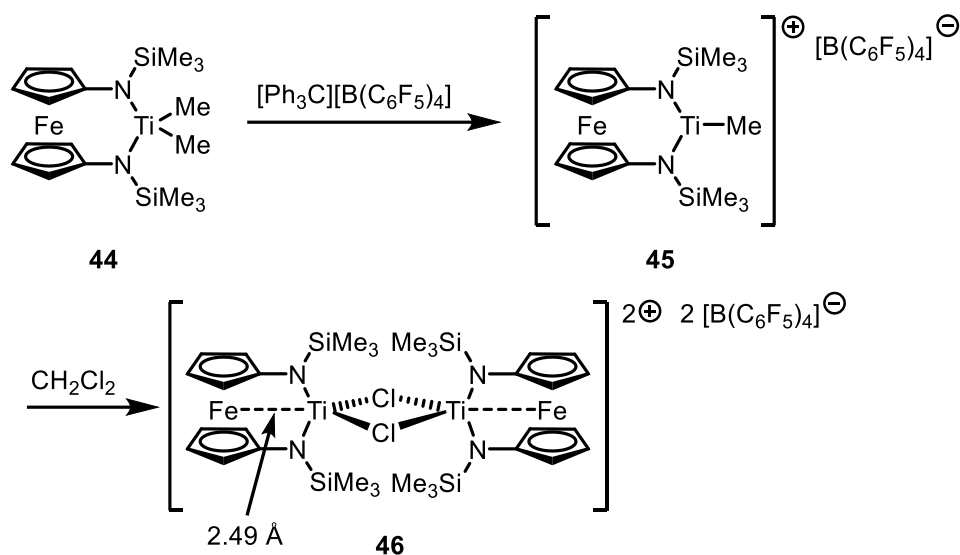
conditions is limited, this approach is primarily used for the synthesis of unfunctionalized ferrocenyl azides such as azidoferrocene (**40**) or 1,1'-diazidoferrocene.^[319,332]

In the second approach stoichiometric amounts of organolithium bases are used for the C-H lithiation of ferrocene, followed by trapping with 2,4,6-triisopropylbenzenesulfonyl azide (**41**, Scheme 10B).^[333] The monolithiation of ferrocene requires the use of the extremely strong Lochmann-Schlosser base while dilithiation of ferrocene is achieved using *n*-butyl lithium in combination with *N,N,N',N'*-tetramethylethylenediamine.^[310] However, metalation of ferrocenes bearing directing groups can be performed under milder conditions.^[275,309]

In the third approach, the functionalized ferrocenyl azide **43** is generated by bromine-lithium exchange of **42** and subsequently reacted with tosyl azide (Scheme 10C). This approach has recently been used for the preparation of silver(I)- and gold(I) complexes with ferrocenyl isocyanide ligands.^[314]

All three approaches have in common that they prepare ferrocenyl azides via hazardous intermediates, leading to safety concerns in particular on larger scale. Notably, ferrocenyl azides are – in contrast to other aryl azides – relatively unstable compounds that are light sensitive, decompose at ambient temperature, and can be even prone to explosion.^[319,334] Although the reason for the unusual instability of ferrocenyl azides is still under debate, it has been suggested that the iron(II) center facilitates decomposition processes. Either via non-bonding electrons of the iron atom, or by σ - π carbon-iron hyperconjugation, nitrene intermediates could be stabilized, thus lowering the kinetic barrier for fragmentation of the azide.^[335]

Frequently, ferrocenyl azides are reduced to the corresponding ferrocenyl amines, which have found numerous applications for the preparation of biologically active compounds, chromophores, peptides and especially as platform for ligands.^[336] For instance, after hydrogenation of 1,1'-diazidoferrocene under palladium catalysis, the thus-obtained 1,1'-diaminoferrocene was used to prepare titanium (IV) complex **44** (Scheme 11). Upon treatment with the strong Lewis acid triphenylmethylium tetrakis(pentafluorophenyl)borate ($[\text{Ph}_3\text{C}][\text{B}(\text{C}_6\text{F}_5)_4]$) the cationic titanium (IV) complex **45** was obtained. Further reaction with dichloromethane led to the dimer **46** which could be crystallized and analyzed by X-ray diffraction revealing a short Fe–Ti distance of 2.49 Å which is similar to the sum of the covalent radii of iron and titanium for Fe–Ti single bonds. Thus, the iron(II) center of the ferrocene moiety can be considered as a Lewis base that coordinates within the complex to the Lewis acidic titanium (IV) moiety.^[337,338]

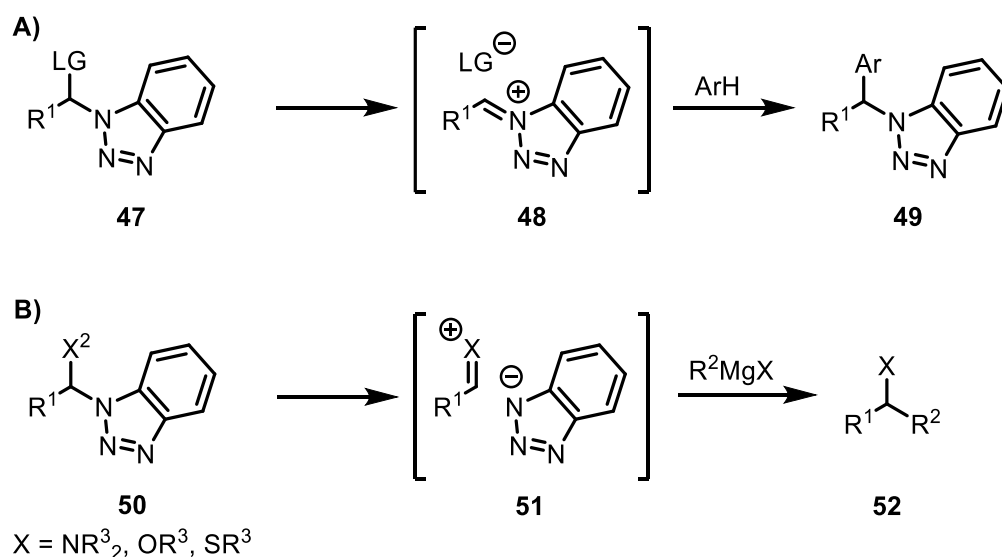


Scheme 11: Synthesis of the dimeric complex **46** with a dative Fe–Ti bond.

Relatively often, complexes with ferrocene-based ligands show unique features and superior catalytic properties.^[282] In many cases, they are functionalized with additional donating groups, especially nitrogen heterocycles, such as pyridines,^[333,339–342] triazoles,^[285,328,333,343] or benzotriazoles.^[344–347]

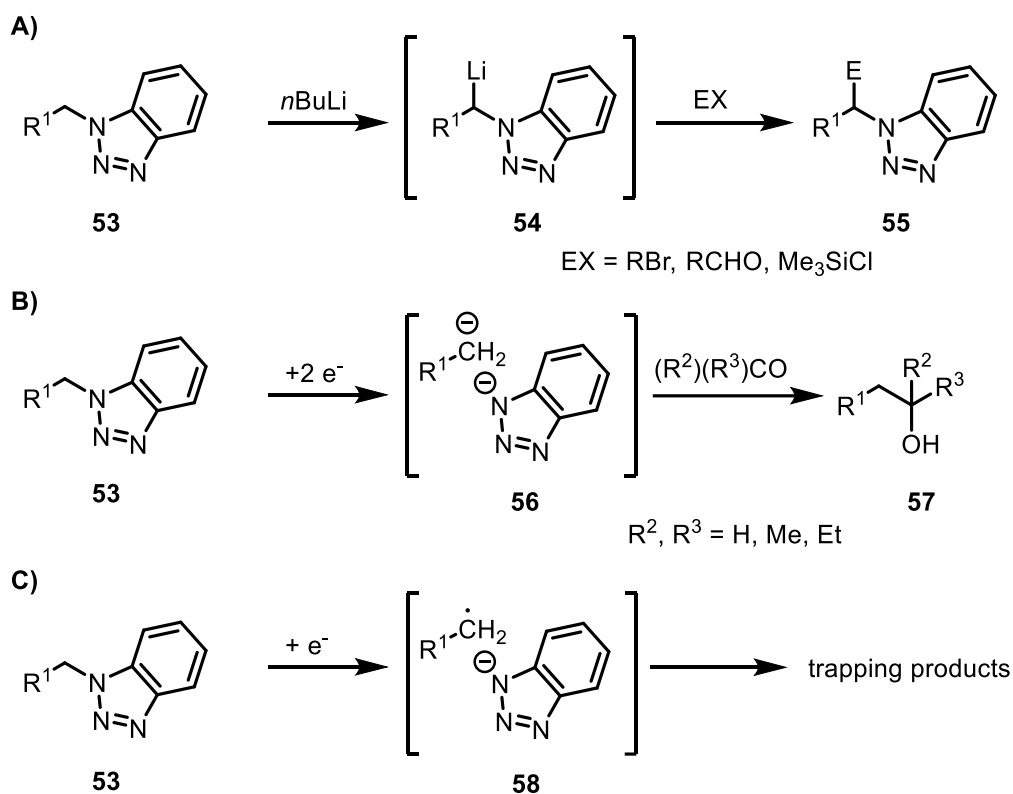
1.4 Benzotriazoles

Benzotriazoles constitute a versatile class of aromatic heterocycles with applications in synthetic organic chemistry and medicine.^[348] Katritzky and coworkers established benzotriazole as a synthetic auxiliary, which is easily introduced, activates the molecule towards various transformations and can then be removed under mild conditions.^[349–351] Interestingly, a benzotriazole substituent is able to guide functionalizations both via ionic and radical pathways allowing a plethora of transformations (Scheme 12).^[349] Alkyl benzotriazoles **47** bearing a good leaving group can form the cationic intermediate **48** which is stabilized by conjugation with the benzotriazole moiety (Scheme 12A). For instance, **48** can be attacked by electron-rich arenes in a Friedel–Crafts type reaction leading to the α -arylated species **49**. If the functionality in α -position to the benzotriazole is an electron donating group such as an amine, ether, or sulfide, the benzotriazole **50** acts as a leaving group leading to **51** which can be attacked by e.g., organomagnesiums providing the C–C coupling product **52** (Scheme 12B).^[349]



Scheme 12: The benzotriazole auxiliary activates the adjacent carbon atom. A) By stabilization of α -cations enabling reactions with arenes. B) By behaving as a leaving group in the reaction with organomagnesiums.

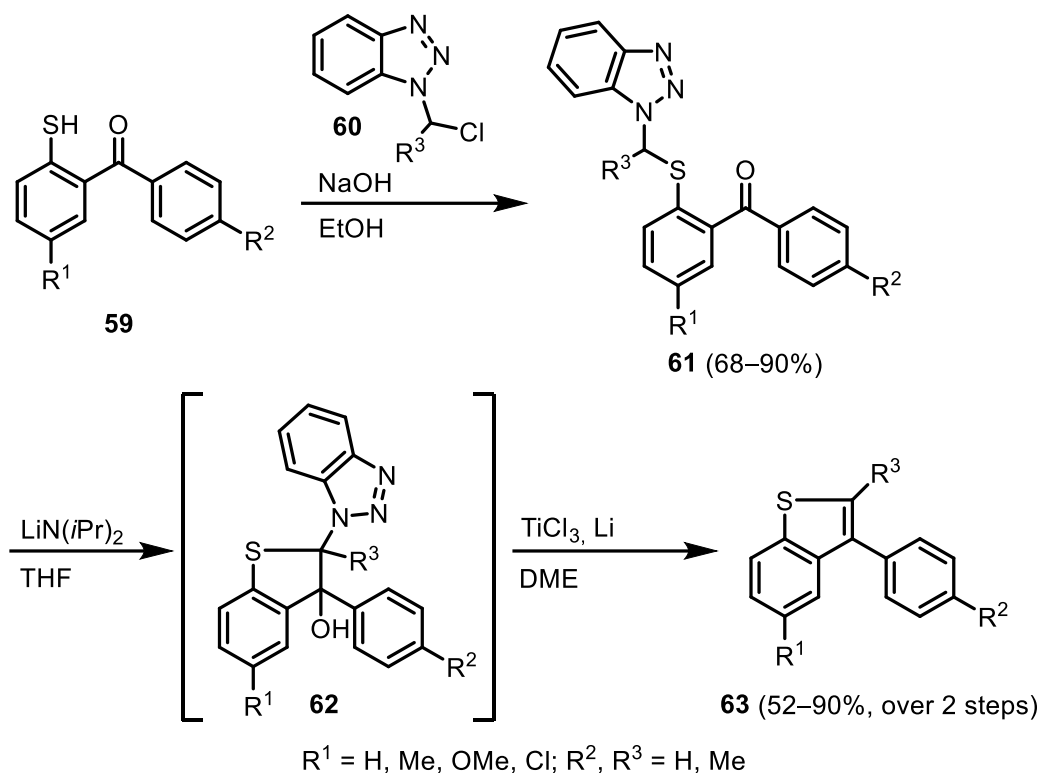
Alternatively, alkylated benzotriazoles **53** can be lithiated in α -position due to the electron-withdrawing effect of the adjacent heterocycle providing organolithium **54** and subsequently be trapped with various electrophiles to give benzotriazoles **55** (Scheme 13A). Precursor **53** can also be reduced by strong reducing agents e.g., samarium diiodide, to generate either anionic intermediates **56** which can attack carbonyls to afford alcohols **57** (Scheme 13B) or radical species **58** that can be trapped for example with alkenes (Scheme 13C).^[349,352]



Scheme 13: Further modes of activation by a benzotriazole substituent. A) By facilitating lithiation and subsequent reaction with electrophiles. B) By reduction to generate anions which are reacted with electrophiles. C) By forming radicals allowing radical trapping reactions.

When the benzotriazole moiety serves as an auxiliary and is not replaced in the course of the transformation (Scheme 12A and Scheme 13A), the benzotriazole can easily be removed under acidic or reductive conditions, afterwards. Utilizing benzotriazole as a directing group, Katritzky and coworkers disclosed an access for the preparation of pharmaceutically valuable 2,3-disubstituted benzothiophenes **63** from *o*-sulfanylphenyl ketones **59** (Scheme 14). By deprotonation of **59** and reaction with benzotriazole-substituted alkyl chlorides **60** the sulfides **61** were obtained. Upon treatment with lithium diisopropylamide the sulfides **61** undergo a benzotriazole-directed α -lithiation leading to the cyclization products **62**. Without further purification, these intermediates were treated with a low-valent titanium species prepared from lithium and titanium(III) chloride in dimethoxyethane (DME) providing the 2,3-disubstituted benzothiophenes **63** under removal of the benzotriazole moiety.^[353]

Given the ability of benzotriazole to enable various chemical transformations, a broad spectrum of functionalized benzotriazoles and related heterocycles were synthesized, which are particularly important for the development of new pharmaceuticals.



Scheme 14: Synthesis of 2,3-disubstituted benzothiophenes **63** utilizing a benzotriazole moiety as directing group.

In recent years, more and more microbes were identified that are resistant against commonazole-based pharmaceuticals. Thus, there is a growing demand for analogs of established drugs utilizing related heterocycles such as benzotriazoles for antibacterial and antiviral agents. As a result, benzotriazoles have evolved as valuable substitutes for antibacterial and antiviral agents.^[354-358] One of the most prominent benzotriazole derivatives is vorozole (**64**), a third generation aromatase inhibitor able to cause a selective, reversible inhibition of intratumoral cytochrome P₄₅₀ aromatase in postmenopausal breast cancer. Compared to previously developed drugs for the treatment of breast cancer such as aminoglutethimide, a significantly better quality of life of the patients was associated with vorozole (**64**).^[359-361] As aromatase is a catalyst in estrogen biosynthesis, mediating the aromatization of the A ring of e.g., testosterone to estradiol, the activity of aromatase has been associated with neurophysiological and behavioral functions including aggression and sexual behavior. Therefore, ¹¹C radiolabeled vorozole (**64**) was also used to investigate the distribution of aromatase in the human brain by positron emission tomography.^[362] More recently, in a systematic screening of thiazole-based drugs, the benzotriazole substituted compound **65** was found to be an anticonvulsant and a COX-2 inhibitor showing an anti-inflammatory activity almost as potent as ibuprofen.^[363]

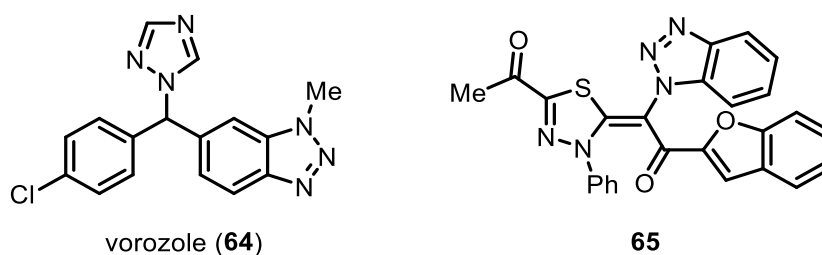
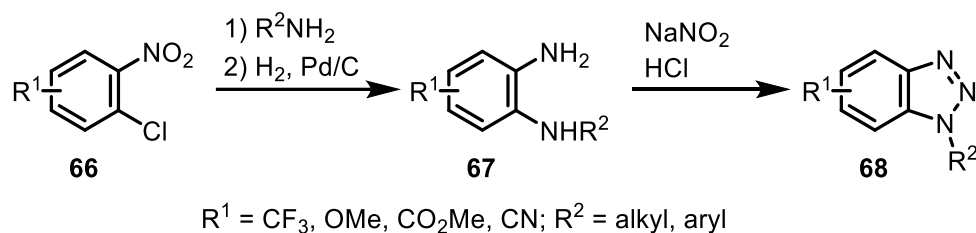


Figure 6: The structures of the antineoplastic agent vorozole (**64**) and of the thiazolidine **65** with anti-inflammatory activity.

Hence, methods for the preparation of functionalized benzotriazoles are of great interest and are continuously investigated.^[364–369] More recently, Buchwald and coworkers developed a multistep synthesis of 1-substituted benzotriazoles in flow (Scheme 15).^[367] Starting from *ortho*-chloronitroarenes **66**, the corresponding diamines **67** are formed via nucleophilic aromatic substitution or palladium catalyzed amination depending on the electronic properties of the *ortho*-chloronitroarene **66** and subsequent palladium-catalyzed hydrogenation. In a diazotization and cyclization sequence, a spectrum of functionalized benzotriazoles **68** with various *N*-substituents were regioselectively accessed in good to excellent yields.^[367]



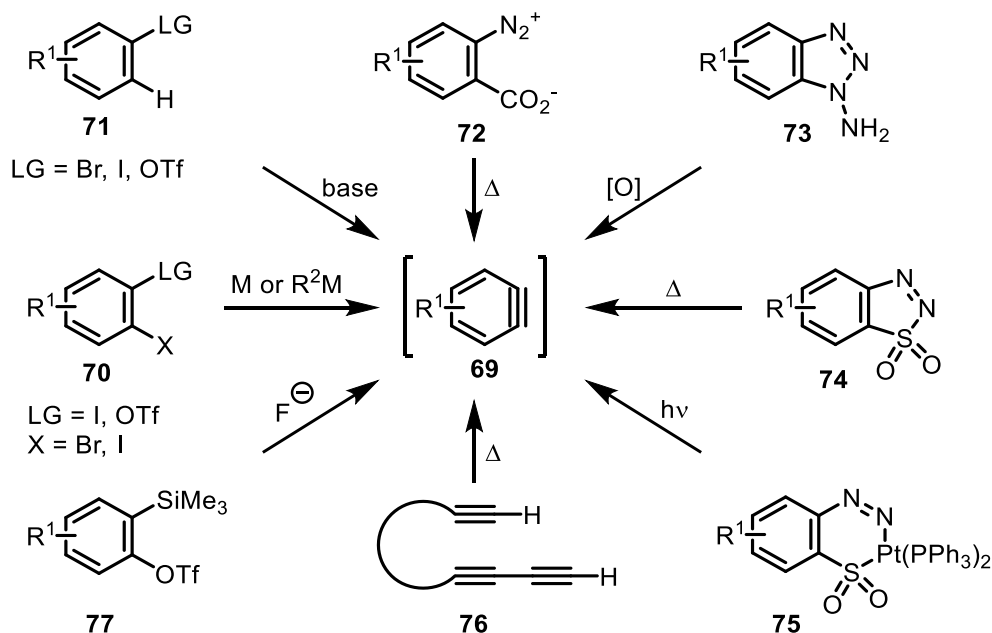
Scheme 15: Synthesis of benzotriazoles **68** from *ortho*-chloronitroarenes **66** by amination, hydrogenation and diazotization with subsequent cyclization.

This flow procedure represents an interesting and readily scalable alternative to the established methods for the preparation of 1-substituted benzotriazoles via *N*-functionalization of benzotriazoles or via [3+2] cycloaddition of azides and in situ generated arynes.^[370–376]

1.5 Synthetic Applications of Arynes

Among all intermediates in organic synthesis, arynes are energetically near the top. Formally, they are obtained by removal of two adjacent substituents from an aromatic system leading to a highly strained cyclic alkyne.^[377,378] As the alkyne moiety cannot adopt a linear geometry, it can be imagined that one π -bond is formed by overlap of two sp^2 -orbitals resulting in an extremely weak triple bond with a small HOMO-LUMO gap.^[379] Once regarded as laboratory curiosities, arynes have been evolved as versatile intermediates for countless reactions with applications in the synthesis of natural products and pharmaceuticals.^[377,380-395]

Due to their enormous reactivity, arynes allow transformations that are impossible with almost all other alkynes. Therefore, unless trapped at low temperatures in a matrix, arynes are transient species and have to be generated in situ.^[396] In the last century, more than 30 different types of aryne precursors have been developed and the search for the “ideal” aryne precursor continues until today (Scheme 16).^[377] One of the oldest preparation methods is the reaction of 1,2-dihalides with alkali or earth alkali metals, forming arynes **69** by elimination of metal salts.^[397] Later, this access was extended to precursors of type **70** bearing a good leaving group and either a bromide or an iodide in *ortho*-position capable of undergoing a halogen-metal exchange with organolithiums or organomagnesiums.^[398] More recently, this approach has found rejuvenated interest for the generation of arynes in flow.^[130]



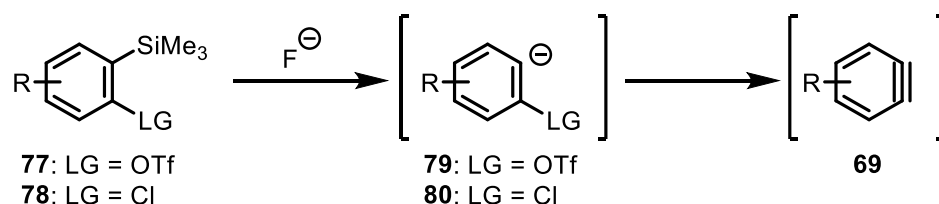
Scheme 16: Selected methods for the generation of arynes.

A related method is the directed *ortho*-deprotonation of arenes **71** bearing good leaving groups such as halides or triflates.^[399] As this method requires strong bases limiting the functional group tolerance, diazonium carboxylates **72** were developed which can be obtained by diazotization of anthranilic acid derivatives. Upon thermolysis, **72** release nitrogen and carbon dioxide forming

arynes **69**.^[400] Alternatively, upon oxidation of aminobenzotriazoles **73** with strong oxidants such as lead tetraacetate, presumably a nitrene intermediate is formed which rapidly disintegrates with the loss of two equivalents of nitrogen to give arynes **69**.^[401–403] Similarly, the benzothiadiazole dioxide **74** generates arynes **69** under formation of nitrogen and sulfur dioxide even at temperatures around 0 °C.^[404–407] Interestingly, it was found that also the structurally related platinum complex **75**, formed by reaction of **74** with tetrakis(triphenylphosphine)platinum(0), is capable to form arynes **69** by photolysis.^[408] However, as aryne precursors **72–75** release gases in exothermic reactions, they are potentially explosive compounds. In particular, diazonium carboxylates **72** are reportedly extremely dangerous and display “shock sensitivity when isolated”.^[160,409]

More recently, the generation of arynes from non-aromatic triynes **76** has received great interest. Upon thermal activation, these precursors undergo cycloaromatization in a hexadehydro-Diels–Alder (HDDA) reaction forging an aryne.^[410–412] This approach has the great advantage to form structurally complex arynes by thermal activation (typically at temperatures around ~100 °C) without any reagents and is not accompanied by the formation of gases.^[413,414]

The most important aryne precursors are *ortho*-trimethylsilylaryl triflates **77** that are also frequently called “Kobayashi aryne precursors”, named after their discoverer.^[377,415] In comparison, it was found that when related precursors **78** with a chloride as leaving group are employed, the elimination step proceeds comparably slow (Scheme 17).^[415,416] Thus, the anionic species **80** is persistent enough to react as a base with either traces of water or with acidic protons of the solvents, reagents, or intermediates.



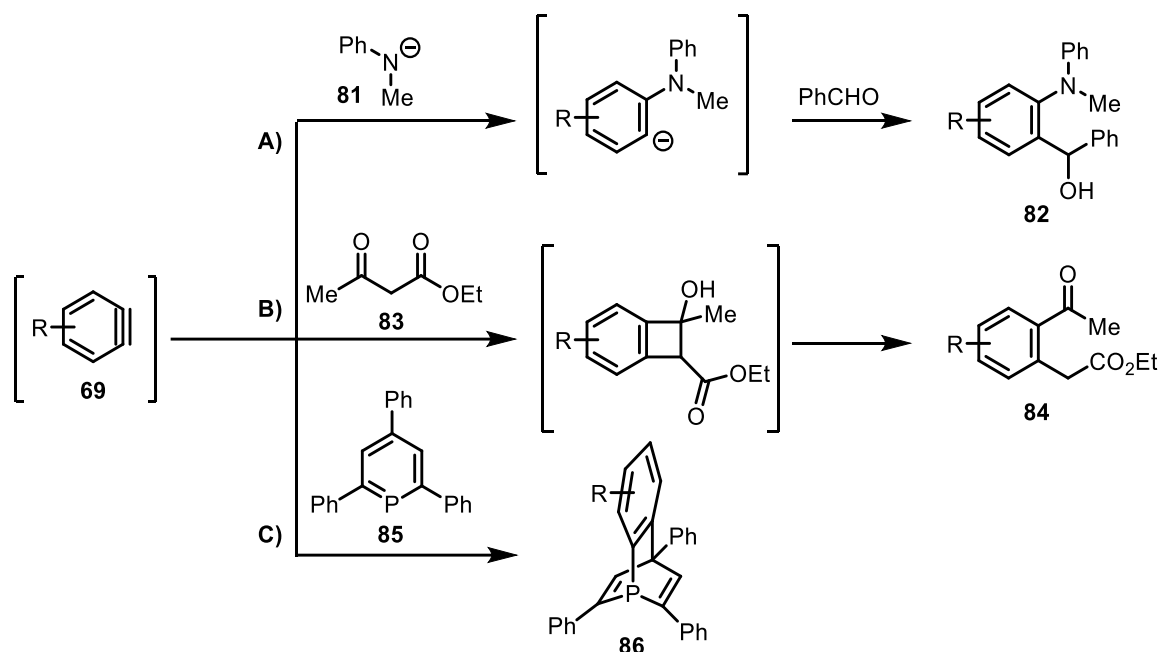
Scheme 17: Reaction of aryne precursors **77** and **78** leads to carbanions **79** and **80**, respectively, which undergo elimination to arynes **69**. In the case of intermediate **79** the elimination is very fast and undesired side reactions of the carbanion are minimized.

In 1983, it was realized by Kobayashi and coworkers that by changing the leaving group from chlorides to the superior triflates, the elimination is significantly accelerated and undesired side reactions of the corresponding carbanion **79** are substantially reduced.^[415] In fact, *ortho*-trimethylsilylaryl triflates **77** successfully generate arynes even in the presence of stoichiometric amounts of water.^[267,417–419] After the seminal work of Kobayashi, related aryne precursors with other leaving groups, other silyl groups and alternative protocols for cleaving the silyl group have been developed.^[420–425] As *ortho*-trimethylsilylaryl triflates can be readily prepared from phenols, are mostly bench-stable, and generate arynes under mild reaction conditions with fluoride ions, they are by far the most frequently used aryne precursors. However, very recently, it has been

outlined that the most distinct advantage of Kobayashi aryne precursors is actually their ability to generate arynes continuously at relatively low concentration. Thus, typical side reactions of arynes such as the trimerization of arynes in a [2+2+2] cycloaddition, are reduced. In fact, the tremendous progress of aryne chemistry in the last two decades can be mainly attributed to the application of Kobayashi aryne precursors.^[377]

Given the broad range of aryne precursors and the various transformations that arynes can undergo, the scope of products accessible by aryne chemistry is consistently expanding. As arynes contain an electron poor triple bond, they are attacked by various nucleophiles, while the formed carbanionic intermediates can be trapped with a broad array of electrophiles. As demonstrated by Knochel and coworkers, nucleophilic attack of phenylmethyl amide (**81**) followed by trapping with benzaldehyde gives the *ortho*-functionalized arene **82** (Scheme 18).^[398]

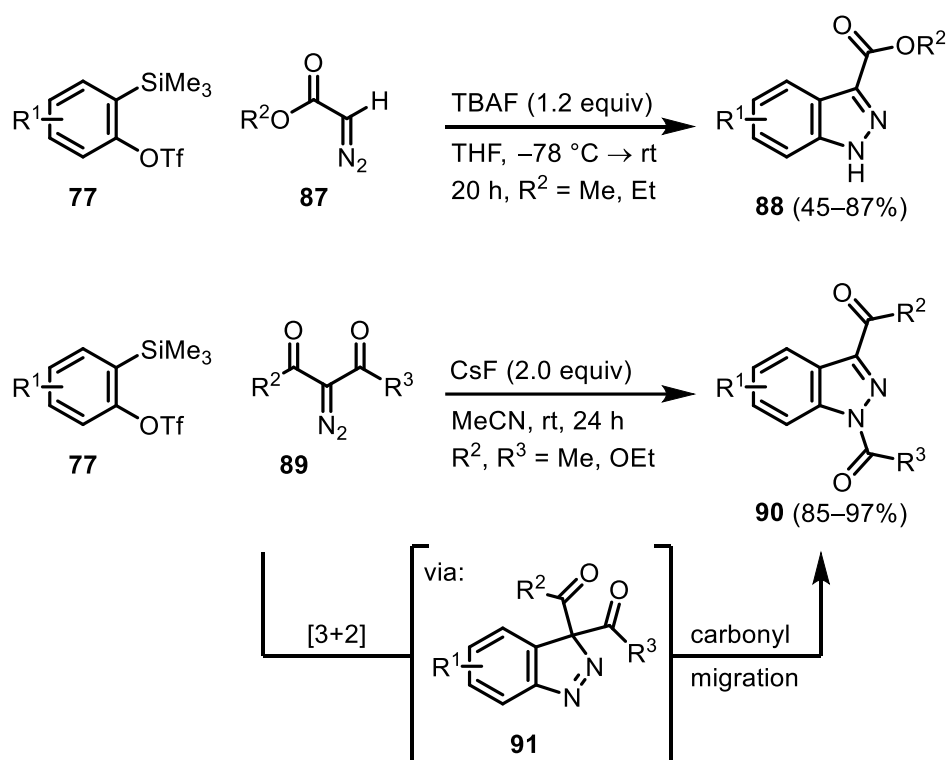
In the case that a single substrate consists both of a nucleophilic and an electrophilic moiety, the aryne can react in a formal σ -bond insertion. For instance, Stoltz and coworkers described the insertion of arynes into β -ketoesters **83** leading to acyl-alkylated arenes **84**. In analogy, cyclic β -ketoesters could be expanded to carbocycles that would otherwise be laborious to prepare.^[426]



Scheme 18: Selected examples for the reaction of arynes. A) Nucleophilic attack of amide **81** with arynes followed by electrophilic trapping with benzaldehyde. B) σ -Insertion of arynes into β -ketoester **83**. C) Diels-Alder reaction of arynes and phosphinine **85**.

However, the earliest, and, until today most well-investigated applications of arynes are pericyclic reactions. Due to the small HOMO-LUMO gap of an aryne, it is an extremely reactive dienophile in [4+2] cycloadditions that can even react with benzene in a Diels-Alder reaction.^[389] For example, the same reactivity can be adopted to 2,4,6-triphenylphosphinine (**85**) leading to the corresponding phosphabarrelene **86**.^[427] These phosphor(III) compounds were later employed as unique ligands for coordination chemistry and catalysis.^[428-434]

In addition, numerous 1,3-dipolar cycloadditions were studied with formal [3+2] cycloadditions of arynes and 1,3-dipoles including, e.g., diazo compounds,^[435–439] azides,^[370–375] nitrones^[440–443] and hydrazones.^[444,445] For these reactions, Kobayashi aryne precursors **77** are employed very frequently, since they generate arynes under mild conditions and thus allow a variety of 1,3-dipoles to be used.^[377] As described by Larock and coworkers, arynes can be reacted with diazo compounds to indazoles in high yields under mild conditions (cesium fluoride in acetonitrile at room temperature, Scheme 19). In the reaction of monosubstituted diazomethane derivatives **87**, the corresponding 1*H*-indazoles **88** are formed via [3+2] cycloaddition in moderate to very good yields.^[435]



Scheme 19: 1,3-Dipolar cycloaddition of arynes with mono- and disubstituted diazo compounds.

In contrast, when disubstituted diazo compounds **89** are employed under slightly different reaction conditions, the intermediate **91** is formed which reacts in a carbonyl migration to 1-acyl and 1-alkoxycarbonyl indazoles in very good to excellent yields.^[435] This example demonstrates not only the value of arynes to construct heterocycles but is also a testament for the countless unexpected reactions and mechanistic pathways serendipitously discovered in aryne chemistry.^[377]

1.6 Scientific Goal

Motivated by the advantages of flow chemistry, a new platform should be designed and applied for the synthesis of natural products, ferrocenyl azides, and benzotriazoles (Figure 7). As most commercially available flow systems are based on a liquid-driven flow resulting in dispersion phenomena between solvent and reagent solution, a gas-driven flow platform should be developed. In this way, dispersion effects would be minimized, and valuable substrates could be preserved.

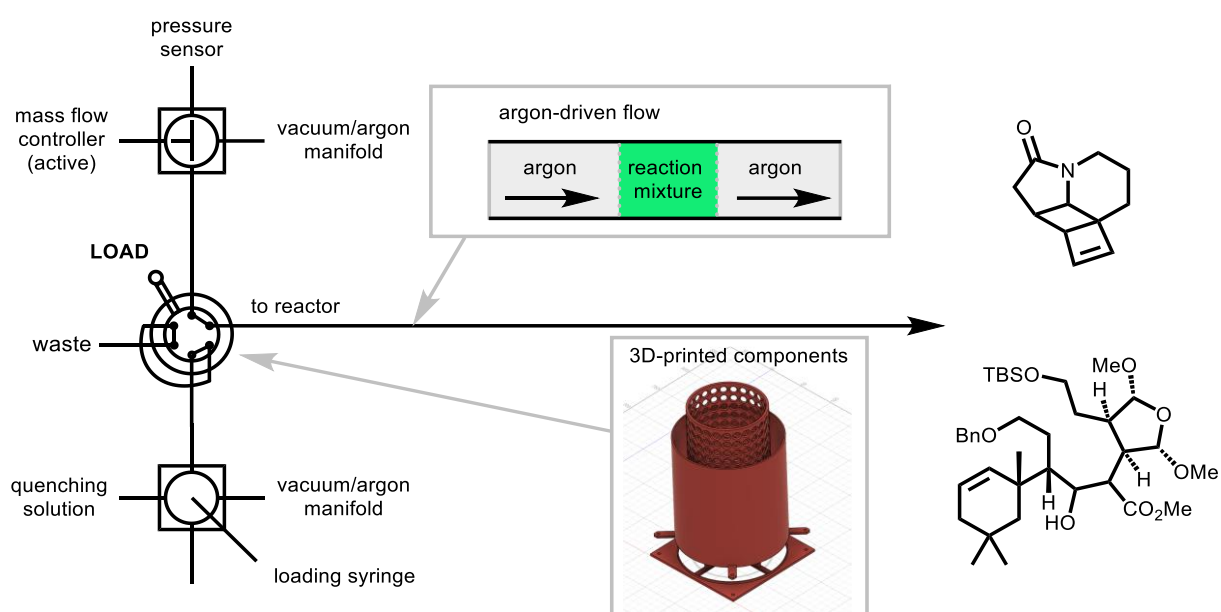
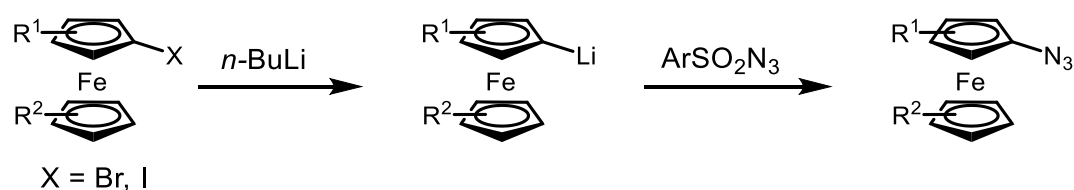


Figure 7: Concept sketch of the flow platform for the synthesis of natural product intermediates in an argon-driven flow utilizing 3D-printed components.

Adhering to the idea of sustainable manufacturing, solvent- and reagent demanding drying procedures should be overcome by the adaptation of common Schlenk techniques to efficient drying procedures in flow. Confronted with the broad spectrum of reaction conditions that are typically used in organic synthesis, the flow platform should be constructed of interchangeable and independent modules offering more flexibility. In addition, the platform should be suitable for screening reactions on small scale as well as for large scale processes without circumstantial modifications. As it was expected that these technical ambitions would be hard to realize employing only commercially available components, it was envisaged to use 3D-printing for the manufacturing of tailor-made prototypes.

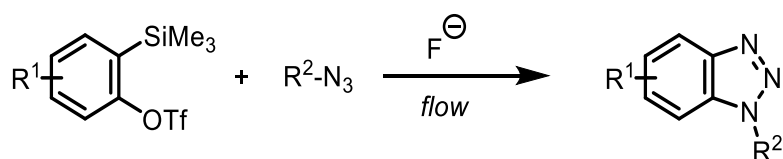
Finally, it should be demonstrated that the developed flow platform can be applied for the substrate economical handling of valuable intermediates in natural product syntheses while offering reproducible yields on small and large scale. Thus, key steps in the total synthesis of (+)-darwinolide and aspidodispermine should be performed in flow. Additionally, a flow protocol for the scalable decatungstate catalyzed C–H chlorination of (+)-sclareolide was envisaged.

After this proof of concept, it was planned to utilize selected modules of the flow platform for the synthesis of ferrocenyl azides via halogen-lithium exchange of functionalized ferrocenyl halides followed by trapping with aryl sulfonyl azides (Scheme 20). The influence of the superior mixing and cooling in flow reactors on yields and selectivities should be investigated by preparing a variety of functionalized ferrocenyl azides in batch and in flow allowing a direct comparison. To avoid accumulation of hazardous intermediates and to overcome resulting scalability limitations, a flow protocol should be developed that allows the safe synthesis of ferrocenyl azides on gram scale. Intrigued by the numerous applications of ferrocenyl amines, in addition, a reliable and functional group tolerant protocol for the reduction of ferrocenyl azides to the corresponding amines should be developed.



Scheme 20: Intended transformation of ferrocenyl bromides and iodides to ferrocenyl lithiums and subsequent reaction ferrocenyl azides in batch and flow.

To further emphasize the benefits of flow chemistry for reactions of organic azides, a flow protocol for the synthesis of benzotriazoles by [3+2] cycloaddition of azides and arynes should be developed (Scheme 21). In order to provide a rapid and scalable access to benzotriazoles, the reaction should be performed at elevated temperature exploiting the safe handling of potentially explosive azides in flow. It was planned to investigate the scope of the reaction with respect to a broad variety of functional groups. Due to the importance of benzotriazoles in medicinal chemistry, the scalability of the process should be demonstrated on gram scale for a biologically active benzotriazole.



Scheme 21: Planned reaction of in situ generated arynes with azides leading to functionalized benzotriazoles in flow.

2 List of References and Illustration Credits

2.1 References

- [1] J. Weyer, *Geschichte der Chemie Band 2 – 19. und 20. Jahrhundert*, Springer, Berlin, Heidelberg, **2018**.
- [2] S. V. Ley, D. E. Fitzpatrick, R. J. Ingham, R. M. Myers, *Angew. Chem. Int. Ed.* **2015**, *54*, 3449–3464.
- [3] C. K. Winkler, J. H. Schrittwieser, W. Kroutil, *ACS Cent. Sci.* **2021**, *7*, 55–71.
- [4] K. C. Nicolaou, S. Rigol, *J. Antibiot.* **2018**, *71*, 153–184.
- [5] M. Guidi, P. H. Seeberger, K. Gilmore, *Chem. Soc. Rev.* **2020**, *49*, 8910–8932.
- [6] M. B. Plutschack, B. Pieber, K. Gilmore, P. H. Seeberger, *Chem. Rev.* **2017**, *117*, 11796–11893.
- [7] M. Power, E. Alcock, G. P. McGlacken, *Org. Process Res. Dev.* **2020**, *24*, 1814–1838.
- [8] J. C. Pastre, D. L. Browne, S. V. Ley, *Chem. Soc. Rev.* **2013**, *42*, 8849–8869.
- [9] S. V. Ley, *Tetrahedron* **2010**, *66*, 6270–6292.
- [10] I. Atodiresei, C. Vila, M. Rueping, *ACS Catal.* **2015**, *5*, 1972–1985.
- [11] J. H. Bannock, S. H. Krishnadasan, M. Heeney, J. C. de Mello, *Mater. Horiz.* **2014**, *1*, 373–378.
- [12] J. Bao, G. K. Tranmer, *Chem. Commun.* **2015**, *51*, 3037–3044.
- [13] M. Baumann, I. R. Baxendale, *Beilstein J. Org. Chem.* **2015**, *11*, 1194–1219.
- [14] T. Noël, S. L. Buchwald, *Chem. Soc. Rev.* **2011**, *40*, 5010–5029.
- [15] J. Britton, C. L. Raston, *Chem. Soc. Rev.* **2017**, *46*, 1250–1271.
- [16] M. Brzozowski, M. O'Brien, S. V. Ley, A. Polyzos, *Acc. Chem. Res.* **2015**, *48*, 349–362.
- [17] D. Cambié, C. Bottecchia, N. J. W. Straathof, V. Hessel, T. Noël, *Chem. Rev.* **2016**, *116*, 10276–10341.
- [18] D. Cantillo, C. O. Kappe, *ChemCatChem* **2014**, *6*, 3286–3305.
- [19] D. Cantillo, C. O. Kappe, *React. Chem. Eng.* **2017**, *2*, 7–19.
- [20] P. J. Cossar, L. Hizartzidis, M. I. Simone, A. McCluskey, C. P. Gordon, *Org. Biomol. Chem.* **2015**, *13*, 7119–7130.
- [21] K. S. Elvira, X. Casadevall i Solvas, R. C. R. Wootton, A. J. de Mello, *Nat. Chem.* **2013**, *5*, 905–915.
- [22] F. G. Finelli, L. S. M. Miranda, R. O. M. A. D. Souza, *Chem. Commun.* **2015**, *51*, 3708–3722.
- [23] C. K. Fredrickson, Z. H. Fan, *Lab Chip* **2004**, *4*, 526–533.
- [24] C. G. Frost, L. Mutton, *Green Chem.* **2010**, *12*, 1687–1703.
- [25] T. Fukuyama, T. Totoki, I. Ryu, *Green Chem.* **2014**, *16*, 2042–2050.
- [26] H. P. L. Gemoets, Y. Su, M. Shang, V. Hessel, R. Luque, T. Noël, *Chem. Soc. Rev.* **2016**, *45*, 83–117.
- [27] T. N. Glasnov, C. O. Kappe, *Macromol. Rapid Commun.* **2007**, *28*, 395–410.
- [28] A. Günther, K. F. Jensen, *Lab Chip* **2006**, *6*, 1487–1503.
- [29] B. Gutmann, D. Cantillo, C. O. Kappe, *Angew. Chem. Int. Ed.* **2015**, *54*, 6688–6728.

- [30] R. L. Hartman, K. F. Jensen, *Lab Chip* **2009**, *9*, 2495–2507.
- [31] R. L. Hartman, J. P. McMullen, K. F. Jensen, *Angew. Chem. Int. Ed.* **2011**, *50*, 7502–7519.
- [32] V. Hessel, *Chem. Eng. Technol.* **2009**, *32*, 1655–1681.
- [33] V. Hessel, D. Kralisch, N. Kockmann, T. Noël, Q. Wang, *ChemSusChem* **2013**, *6*, 746–789.
- [34] V. Hessel, H. Löwe, F. Schönfeld, *Chem. Eng. Sci.* **2005**, *60*, 2479–2501.
- [35] M. Irfan, T. N. Glasnov, C. O. Kappe, *ChemSusChem* **2011**, *4*, 300–316.
- [36] K. Jähnisch, V. Hessel, H. Löwe, M. Baerns, *Angew. Chem. Int. Ed.* **2004**, *43*, 406–446.
- [37] G. Jas, A. Kirschning, *Chem. Eur. J.* **2003**, *9*, 5708–5723.
- [38] K. F. Jensen, B. J. Reizman, S. G. Newman, *Lab Chip* **2014**, *14*, 3206–3212.
- [39] M. N. Kashid, L. Kiwi-Minsker, *Ind. Eng. Chem. Res.* **2009**, *48*, 6465–6485.
- [40] S. Kobayashi, *Chem. Asian J.* **2016**, *11*, 425–436.
- [41] N. Kockmann, D. M. Roberge, *Chem. Eng. Technol.* **2009**, *32*, 1682–1694.
- [42] S. V. Ley, D. E. Fitzpatrick, R. M. Myers, C. Battilocchio, R. J. Ingham, *Angew. Chem. Int. Ed.* **2015**, *54*, 10122–10136.
- [43] L. Malet-Sanz, F. Susanne, *J. Med. Chem.* **2012**, *55*, 4062–4098.
- [44] C. J. Mallia, I. R. Baxendale, *Org. Process Res. Dev.* **2016**, *20*, 327–360.
- [45] B. P. Mason, K. E. Price, J. L. Steinbacher, A. R. Bogdan, D. T. McQuade, *Chem. Rev.* **2007**, *107*, 2300–2318.
- [46] D. T. McQuade, P. H. Seeberger, *J. Org. Chem.* **2013**, *78*, 6384–6389.
- [47] S. T. R. Müller, T. Wirth, *ChemSusChem* **2015**, *8*, 245–250.
- [48] R. Munirathinam, J. Huskens, W. Verboom, *Adv. Synth. Catal.* **2015**, *357*, 1093–1123.
- [49] S. G. Newman, K. F. Jensen, *Green Chem* **2013**, *15*, 1456–1472.
- [50] M. Oelgemöller, *Chem. Rev.* **2016**, *116*, 9664–9682.
- [51] T. Noël, V. Hessel, *ChemSusChem* **2013**, *6*, 405–407.
- [52] R. Porta, M. Benaglia, A. Puglisi, *Org. Process Res. Dev.* **2016**, *20*, 2–25.
- [53] T. Razzaq, C. O. Kappe, *Chem. Asian J.* **2010**, *5*, 1274–1289.
- [54] T. H. Rehm, *Chem. Eng. Technol.* **2016**, *39*, 66–80.
- [55] R. Ricciardi, J. Huskens, W. Verboom, *ChemSusChem* **2015**, *8*, 2586–2605.
- [56] T. Rodrigues, P. Schneider, G. Schneider, *Angew. Chem. Int. Ed.* **2014**, *53*, 5750–5758.
- [57] C. Rodríguez-Esrich, M. A. Pericàs, *Eur. J. Org. Chem.* **2015**, 1173–1188.
- [58] H. Song, D. L. Chen, R. F. Ismagilov, *Angew. Chem. Int. Ed.* **2006**, *45*, 7336–7356.
- [59] D. Webb, T. F. Jamison, *Chem. Sci.* **2010**, *1*, 675.
- [60] J. Wegner, S. Ceylan, A. Kirschning, *Chem. Commun.* **2011**, *47*, 4583–4592.
- [61] J. Wegner, S. Ceylan, A. Kirschning, *Adv. Synth. Catal.* **2012**, *354*, 17–57.
- [62] J.-I. Yoshida, H. Kim, A. Nagaki, *ChemSusChem* **2011**, *4*, 331–340.
- [63] P. Bana, R. Örkényi, K. Lövei, Á. Lakó, G. I. Túrós, J. Éles, F. Faigl, I. Greiner, *Bioorg. Med. Chem.* **2017**, *25*, 6180–6189.

- [64] P. Bianchi, J. D. Williams, C. O. Kappe, *J. Flow Chem.* **2020**, *10*, 475–490.
- [65] J. Britton, S. Majumdar, G. A. Weiss, *Chem. Soc. Rev.* **2018**, *47*, 5891–5918.
- [66] M. Colella, A. Nagaki, R. Luisi, *Chem. Eur. J.* **2020**, *26*, 19–32.
- [67] F. Fanelli, G. Parisi, L. Degennaro, R. Luisi, *Beilstein J. Org. Chem.* **2017**, *13*, 520–542.
- [68] A. Gavriilidis, A. Constantinou, K. Hellgardt, K. K. Hii, G. J. Hutchings, G. L. Brett, S. Kuhn, S. P. Marsden, *React. Chem. Eng.* **2016**, *1*, 595–612.
- [69] A. Gioiello, V. Mancino, P. Filipponi, S. Mostarda, B. Cerra, *J. Flow Chem.* **2016**, *6*, 167–180.
- [70] M. V. Gomez, A. de La Hoz, *Beilstein J. Org. Chem.* **2017**, *13*, 285–300.
- [71] C. A. Hone, D. M. Roberge, C. O. Kappe, *ChemSusChem* **2017**, *10*, 32–41.
- [72] X. Hu, N. Zhu, Z. Fang, K. Guo, *React. Chem. Eng.* **2017**, *2*, 20–26.
- [73] P. D. Morse, R. L. Beingessner, T. F. Jamison, *Isr. J. Chem.* **2017**, *57*, 218–227.
- [74] A. Nagaki, *Tetrahedron Lett.* **2019**, *60*, 150923.
- [75] T. Noël, Y. Cao, G. Laudadio, *Acc. Chem. Res.* **2019**, *52*, 2858–2869.
- [76] B. R. Pinkard, D. J. Gorman, K. Tiwari, J. C. Kramlich, P. G. Reinhall, I. V. Novosselov, *Ind. Eng. Chem. Res.* **2018**, *57*, 3471–3481.
- [77] F. Politano, G. Oksdath-Mansilla, *Org. Process Res. Dev.* **2018**, *22*, 1045–1062.
- [78] B. J. Reizman, K. F. Jensen, *Acc. Chem. Res.* **2016**, *49*, 1786–1796.
- [79] C. Sambaglio, T. Noël, *Trends Chem.* **2020**, *2*, 92–106.
- [80] S. Santoro, F. Ferlin, L. Ackermann, L. Vaccaro, *Chem. Soc. Rev.* **2019**, *48*, 2767–2782.
- [81] V. Sebastian, S. A. Khan, A. A. Kulkarni, *J. Flow Chem.* **2017**, *7*, 96–105.
- [82] J. Zhang, J. Chen, S. Peng, S. Peng, Z. Zhang, Y. Tong, P. W. Miller, X.-P. Yan, *Chem. Soc. Rev.* **2019**, *48*, 2566–2595.
- [83] S. V. Luis, E. Garcia-Verdugo (Eds.) *Chemical Reactions and Processes under Flow Conditions*, RSC Publishing, Cambridge, **2009**.
- [84] K. P. Cole, J. McClary Groh, M. D. Johnson, C. L. Burcham, B. M. Campbell, W. D. Diserod, M. R. Heller, J. R. Howell, N. J. Kallman, T. M. Koenig et al., *Science* **2017**, *356*, 1144–1150.
- [85] K. P. Cole, M. D. Argentine, E. W. Conder, R. K. Vaid, P. Feng, M. Jia, P. Huang, P. Liu, B. Sun, S. Tadayon et al., *Org. Process Res. Dev.* **2020**, *24*, 2043–2054.
- [86] J. D. Williams, W. J. Kerr, S. G. Leach, D. M. Lindsay, *Angew. Chem. Int. Ed.* **2018**, *57*, 12126–12130.
- [87] Y. Ma, S. Wu, E. G. J. Macaringue, T. Zhang, J. Gong, J. Wang, *Org. Process Res. Dev.* **2020**, *24*, 1785–1801.
- [88] E. İçten, A. J. Maloney, M. G. Beaver, D. E. Shen, X. Zhu, L. R. Graham, J. A. Robinson, S. Huggins, A. Allian, R. Hart et al., *Org. Process Res. Dev.* **2020**, *24*, 1861–1875.
- [89] E. İçten, A. J. Maloney, M. G. Beaver, X. Zhu, D. E. Shen, J. A. Robinson, A. T. Parsons, A. Allian, S. Huggins, R. Hart et al., *Org. Process Res. Dev.* **2020**, *24*, 1876–1890.

- [90] A. J. Maloney, E. İçten, G. Capellades, M. G. Beaver, X. Zhu, L. R. Graham, D. B. Brown, D. J. Griffin, R. Sangodkar, A. Allian et al., *Org. Process Res. Dev.* **2020**, *24*, 1891–1908.
- [91] N. Uhlig, A. Martins, D. Gao, *Org. Process Res. Dev.* **2020**, *24*, 2326–2335.
- [92] S. V. Ley, Y. Chen, A. Robinson, B. Otter, E. Godineau, C. Battilocchio, *Org. Process Res. Dev.* **2021**, *25*, 713–720.
- [93] S. Newton, C. F. Carter, C. M. Pearson, L. de C. Alves, H. Lange, P. Thansandote, S. V. Ley, *Angew. Chem. Int. Ed.* **2014**, *53*, 4915–4920.
- [94] T. Ouchi, R. J. Mutton, V. Rojas, D. E. Fitzpatrick, D. G. Cork, C. Battilocchio, S. V. Ley, *ACS Sustainable Chem. Eng.* **2016**, *4*, 1912–1916.
- [95] S. V. Ley, I. R. Baxendale, *Chem. Rec.* **2002**, *2*, 377–388.
- [96] C. D. Smith, I. R. Baxendale, S. Lanners, J. J. Hayward, S. C. Smith, S. V. Ley, *Org. Biomol. Chem.* **2007**, *5*, 1559–1561.
- [97] S. V. Ley, I. R. Baxendale, *Nature Rev.* **2002**, *1*, 573–586.
- [98] C. K. Y. Lee, A. B. Holmes, S. V. Ley, I. F. McConvey, B. Al-Duri, G. A. Leeke, R. C. D. Santos, J. P. K. Seville, *Chem. Commun.* **2005**, 2175–2177.
- [99] S. Saaby, K. R. Knudsen, M. Ladlow, S. V. Ley, *Chem. Commun.* **2005**, 2909–2911.
- [100] D. E. Fitzpatrick, C. Battilocchio, S. V. Ley, *Org. Process Res. Dev.* **2016**, *20*, 386–394.
- [101] D. L. Browne, M. Baumann, B. H. Harji, I. R. Baxendale, S. V. Ley, *Org. Lett.* **2011**, *13*, 3312–3315.
- [102] B. J. Deadman, C. Battilocchio, E. Sliwinski, S. V. Ley, *Green Chem.* **2013**, *15*, 2050–2055.
- [103] P. Koos, D. L. Browne, S. V. Ley, *Green Process Synth.* **2012**, *1*, 11–18.
- [104] C. F. Carter, H. Lange, S. V. Ley, I. R. Baxendale, B. Wittkamp, J. G. Goode, N. L. Gaunt, *Org. Process Res. Dev.* **2010**, *14*, 393–404.
- [105] M. O'Brien, I. R. Baxendale, S. V. Ley, *Org. Lett.* **2010**, *12*, 1596–1598.
- [106] C. H. Hornung, M. R. Mackley, I. R. Baxendale, S. V. Ley, *Org. Process Res. Dev.* **2007**, *11*, 399–405.
- [107] H. Lange, C. F. Carter, M. D. Hopkin, A. Burke, J. G. Goode, I. R. Baxendale, S. V. Ley, *Chem. Sci.* **2011**, *2*, 765.
- [108] D. L. Browne, S. Wright, B. J. Deadman, S. Dunnage, I. R. Baxendale, R. M. Turner, S. V. Ley, *Rapid Commun. Mass. Spectrom.* **2012**, *26*, 1999–2010.
- [109] M. O'Brien, P. Koos, D. L. Browne, S. V. Ley, *Org. Biomol. Chem.* **2012**, *10*, 7031–7036.
- [110] C. H. Hornung, B. Hallmark, M. Baumann, I. R. Baxendale, S. V. Ley, P. Hester, P. Clayton, M. R. Mackley, *Ind. Eng. Chem. Res.* **2010**, *49*, 4576–4582.
- [111] D. L. Browne, B. J. Deadman, R. Ashe, I. R. Baxendale, S. V. Ley, *Org. Process Res. Dev.* **2011**, *15*, 693–697.
- [112] S. V. F. Hansen, Z. E. Wilson, T. Ulven, S. V. Ley, *React. Chem. Eng.* **2016**, *1*, 280–287.

- [113] D. E. Fitzpatrick, T. Maujean, A. C. Evans, S. V. Ley, *Angew. Chem. Int. Ed.* **2018**, *57*, 15128–15132.
- [114] D. E. Fitzpatrick, S. V. Ley, *React. Chem. Eng.* **2016**, *1*, 629–635.
- [115] J. A. Newby, D. W. Blaylock, P. M. Witt, J. C. Pastre, M. K. Zacharova, S. V. Ley, D. L. Browne, *Org. Process Res. Dev.* **2014**, *18*, 1211–1220.
- [116] C. Wiles, P. Watts, *Green Chem.* **2012**, *14*, 38–54.
- [117] C. Wiles, P. Watts, *Green Chem.* **2014**, *16*, 55–62.
- [118] F. M. Akwi, P. Watts, *Chem. Commun.* **2018**, *54*, 13894–13928.
- [119] J.-I. Yoshida, A. Nagaki, T. Yamada, *Chem. Eur. J.* **2008**, *14*, 7450–7459.
- [120] J.-I. Yoshida, *Chem. Commun.* **2005**, 4509–4516.
- [121] J.-I. Yoshida, *Chem. Rec.* **2010**, *10*, 332–341.
- [122] C. A. Correia, K. Gilmore, D. T. McQuade, P. H. Seeberger, *Angew. Chem. Int. Ed.* **2015**, *54*, 4945–4948.
- [123] J.-I. Yoshida, H. Kim, A. Nagaki, *J. Flow Chem.* **2017**, *7*, 60–64.
- [124] J.-I. Yoshida, Y. Takahashi, A. Nagaki, *Chem. Commun.* **2013**, *49*, 9896–9904.
- [125] A. Nagaki, H. Yamashita, K. Hirose, Y. Tsuchihashi, J.-I. Yoshida, *Angew. Chem. Int. Ed.* **2019**, *58*, 4027–4030.
- [126] A. Nagaki, K. Imai, S. Ishiuchi, J.-I. Yoshida, *Angew. Chem. Int. Ed.* **2015**, *54*, 1914–1918.
- [127] A. Nagaki, Y. Takahashi, J.-I. Yoshida, *Angew. Chem. Int. Ed.* **2016**, *55*, 5327–5331.
- [128] H. Kim, Y. Yonekura, J.-I. Yoshida, *Angew. Chem. Int. Ed.* **2018**, *57*, 4063–4066.
- [129] J. Wu, X. Yang, Z. He, X. Mao, T. A. Hatton, T. F. Jamison, *Angew. Chem. Int. Ed.* **2014**, *53*, 8416–8420.
- [130] A. Nagaki, D. Ichinari, J.-I. Yoshida, *J. Am. Chem. Soc.* **2014**, *136*, 12245–12248.
- [131] N. Bhuma, L. Lebedel, H. Yamashita, Y. Shimizu, Z. Abada, A. Ardá, J. Désiré, B. Michelet, A. Martin-Mingot, A. Abou-Hassan et al., *Angew. Chem. Int. Ed.* **2021**, *60*, 2036–2041.
- [132] T. von Keutz, D. Cantillo, C. O. Kappe, *Org. Lett.* **2020**, *22*, 7537–7541.
- [133] A. Nagaki, Y. Ashikari, M. Takumi, T. Tamaki, *Chem. Lett.* **2021**, *50*, 485–492.
- [134] M. Seto, S. Masada, H. Usutani, D. G. Cork, K. Fukuda, T. Kawamoto, *Org. Process Res. Dev.* **2019**, *23*, 1420–1428.
- [135] H. Kim, A. Nagaki, J.-I. Yoshida, *Nat. Commun.* **2011**, *2*, 264.
- [136] Y. Su, N. J. W. Straathof, V. Hessel, T. Noël, *Chem. Eur. J.* **2014**, *20*, 10562–10589.
- [137] M. G. Beaver, E.-x. Zhang, Z.-q. Liu, S.-y. Zheng, B. Wang, J.-p. Lu, J. Tao, M. Gonzalez, S. Jones, J. S. Tedrow, *Org. Process Res. Dev.* **2020**, *24*, 2139–2146.
- [138] E. Herrero-Gomez, C. H. M. van der Loo, L. Huck, A. Rioz-Martínez, N. F. Keene, B. Li, K. Pouwer, C. Allais, *Org. Process Res. Dev.* **2020**, *24*, 2304–2310.
- [139] G. Laudadio, Y. Deng, K. van der Wal, D. Ravelli, M. Nuño, M. Fagnoni, D. Guthrie, Y. Sun, T. Noël, *Science* **2020**, *369*, 92–96.

- [140] Z. Wen, A. Maheshwari, C. Sambigiato, Y. Deng, G. Laudadio, K. van Aken, Y. Sun, H. P. L. Gemoets, T. Noël, *Org. Process Res. Dev.* **2020**, *24*, 2356–2361.
- [141] K. Gilmore, P. H. Seeberger, *Chem. Rec.* **2014**, *14*, 410–418.
- [142] C. S. Teschers, R. Gilmour, *Org. Process Res. Dev.* **2020**, *24*, 2234–2239.
- [143] I. Texier, J.-F. Delouis, J. A. Delaire, C. Giannotti, P. Plaza, M. M. Martin, *Chem. Phys. Lett.* **1999**, *311*, 139–145.
- [144] C. Tanielian, F. Cougnon, R. Seghrouchni, *J. Mol. Catal. A Chem.* **2007**, *262*, 164–169.
- [145] G. Laudadio, S. Govaerts, Y. Wang, D. Ravelli, H. F. Koolman, M. Fagnoni, S. W. Djuric, T. Noël, *Angew. Chem. Int. Ed.* **2018**, *57*, 4078–4082.
- [146] S. D. Halperin, H. Fan, S. Chang, R. E. Martin, R. Britton, *Angew. Chem. Int. Ed.* **2014**, *53*, 4690–4693.
- [147] S. Montanaro, D. Ravelli, D. Merli, M. Fagnoni, A. Albini, *Org. Lett.* **2012**, *14*, 4218–4221.
- [148] I. B. Perry, T. F. Brewer, P. J. Sarver, D. M. Schultz, D. A. DiRocco, D. W. C. MacMillan, *Nature* **2018**, *560*, 70–75.
- [149] M. C. Quattrini, S. Fujii, K. Yamada, T. Fukuyama, D. Ravelli, M. Fagnoni, I. Ryu, *Chem. Commun.* **2017**, *53*, 2335–2338.
- [150] D. Ravelli, M. Fagnoni, T. Fukuyama, T. Nishikawa, I. Ryu, *ACS Catal.* **2018**, *8*, 701–713.
- [151] P. J. Sarver, V. Bacauanu, D. M. Schultz, D. A. DiRocco, Y.-H. Lam, E. C. Sherer, D. W. C. MacMillan, *Nature Chem.* **2020**, *12*, 459–467.
- [152] D. M. Schultz, F. Lévesque, D. A. DiRocco, M. Reibarkh, Y. Ji, L. A. Joyce, J. F. Dropinski, H. Sheng, B. D. Sherry, I. W. Davies, *Angew. Chem. Int. Ed.* **2017**, *56*, 15274–15278.
- [153] C. Tanielian, *Coord. Chem. Rev.* **1998**, *178-180*, 1165–1181.
- [154] M. D. Tzirakis, I. N. Lykakis, M. Orfanopoulos, *Chem. Soc. Rev.* **2009**, *38*, 2609–2621.
- [155] Z. Yuan, H. Yang, N. Malik, M. Čolović, D. S. Weber, D. Wilson, F. Bénard, R. E. Martin, J. J. Warren, P. Schaffer et al., *ACS Catal.* **2019**, *9*, 8276–8284.
- [156] S. Esposti, D. Dondi, M. Fagnoni, A. Albini, *Angew. Chem. Int. Ed.* **2007**, *46*, 2531–2534.
- [157] D. Ravelli, S. Protti, M. Fagnoni, *Acc. Chem. Res.* **2016**, *49*, 2232–2242.
- [158] K. A. McGarry, K. R. Hurley, K. A. Volp, I. M. Hill, B. A. Merritt, K. L. Peterson, P. A. Rudd, N. C. Erickson, L. A. Seiler, P. Gupta et al., *J. Chem. Educ.* **2013**, *90*, 1414–1417.
- [159] C. Schotten, S. K. Leprevost, L. M. Yong, C. E. Hughes, K. D. M. Harris, D. L. Browne, *Org. Process Res. Dev.* **2020**, *24*, 2336–2341.
- [160] A. V. Kelleghan, C. A. Busacca, M. Sarvestani, I. Volchkov, J. M. Medina, N. K. Garg, *Org. Lett.* **2020**, *22*, 1665–1669.
- [161] M. Teci, M. Tilley, M. A. McGuire, M. G. Organ, *Org. Process Res. Dev.* **2016**, *20*, 1967–1973.
- [162] M. Movsisyan, E. I. P. Delbeke, J. K. E. T. Berton, C. Battilocchio, S. V. Ley, C. V. Stevens, *Chem. Soc. Rev.* **2016**, *45*, 4892–4928.
- [163] C. B. McPake, G. Sandford, *Org. Process Res. Dev.* **2012**, *16*, 844–851.

- [164] D. Dallinger, C. O. Kappe, *Aldrichimica Acta* **2016**, *49*, 57–66.
- [165] H. von Pechmann, *Ber. Dtsch. Chem. Ges.* **1895**, *28*, 855–861.
- [166] L. D. Proctor, A. J. Warr, *Org. Process Res. Dev.* **2002**, *6*, 884–892.
- [167] M. Struempel, B. Ondruschka, R. Daute, A. Stark, *Green Chem.* **2008**, *10*, 41–43.
- [168] R. A. Maurya, C. P. Park, J. H. Lee, D.-P. Kim, *Angew. Chem. Int. Ed.* **2011**, *50*, 5952–5955.
- [169] E. Rossi, P. Woehl, M. Maggini, *Org. Process Res. Dev.* **2012**, *16*, 1146–1149.
- [170] B. Pieber, C. O. Kappe, *Org. Lett.* **2016**, *18*, 1076–1079.
- [171] F. Mastronardi, B. Gutmann, C. O. Kappe, *Org. Lett.* **2013**, *15*, 5590–5593.
- [172] H. Lehmann, *Green Chem.* **2017**, *19*, 1449–1453.
- [173] H. Yang, B. Martin, B. Schenkel, *Org. Process Res. Dev.* **2018**, *22*, 446–456.
- [174] J. W. Sheeran, K. Campbell, C. P. Breen, G. Hummel, C. Huang, A. Datta, S. H. Boyer, S. J. Hecker, M. M. Bio, Y.-Q. Fang et al., *Org. Process Res. Dev.* **2021**, *25*, 522–528.
- [175] P. Rullière, G. Benoit, E. M. D. Allouche, A. B. Charette, *Angew. Chem. Int. Ed.* **2018**, *57*, 5777–5782.
- [176] A. Greb, J.-S. Poh, S. Greed, C. Battilocchio, P. Pasau, D. C. Blakemore, S. V. Ley, *Angew. Chem. Int. Ed.* **2017**, *56*, 16602–16605.
- [177] K. J. Hock, R. M. Koenigs, *Chem. Eur. J.* **2018**, *24*, 10571–10583.
- [178] S. T. R. Müller, A. Murat, P. Hellier, T. Wirth, *Org. Process Res. Dev.* **2016**, *20*, 495–502.
- [179] S. T. R. Müller, A. Murat, D. Maillos, P. Lesimple, P. Hellier, T. Wirth, *Chem. Eur. J.* **2015**, *21*, 7016–7020.
- [180] B. J. Deadman, S. G. Collins, A. R. Maguire, *Chem. Eur. J.* **2015**, *21*, 2298–2308.
- [181] R. E. Thiers, A. H. Reed, K. Delander, *Clin. Chem.* **1971**, *17*, 42–48.
- [182] M. T. Kreutzer, A. Günther, K. F. Jensen, *Anal. Chem.* **2008**, *80*, 1558–1567.
- [183] A. Günther, S. A. Khan, M. Thalmann, F. Trachsel, K. F. Jensen, *Lab Chip* **2004**, *4*, 278–286.
- [184] B. K. H. Yen, A. Günther, M. A. Schmidt, K. F. Jensen, M. G. Bawendi, *Angew. Chem. Int. Ed.* **2005**, *44*, 5447–5451.
- [185] V. S. Cabeza, S. Kuhn, A. A. Kulkarni, K. F. Jensen, *Langmuir* **2012**, *28*, 7007–7013.
- [186] A. Günther, M. Jhunhunwala, M. Thalmann, M. A. Schmidt, K. F. Jensen, *Langmuir* **2005**, *21*, 1547–1555.
- [187] R. L. Hartman, H. R. Sahoo, B. C. Yen, K. F. Jensen, *Lab Chip* **2009**, *9*, 1843–1849.
- [188] H.-W. Hsieh, C. W. Coley, L. M. Baumgartner, K. F. Jensen, R. I. Robinson, *Org. Process Res. Dev.* **2018**, *22*, 542–550.
- [189] S. Chatterjee, M. Guidi, P. H. Seeberger, K. Gilmore, *Nature* **2020**, *579*, 379–385.
- [190] W. Debrouwer, W. Kimpe, R. Dangreau, K. Huvaere, H. P. L. Gemoets, M. Mottaghi, S. Kuhn, K. van Aken, *Org. Process Res. Dev.* **2020**, *24*, 2319–2325.

- [191] M. R. Chapman, M. H. T. Kwan, G. King, K. E. Jolley, M. Hussain, S. Hussain, I. E. Salama, C. González Niño, L. A. Thompson, M. E. Bayana et al., *Org. Process Res. Dev.* **2017**, *21*, 1294–1301.
- [192] T. Noël, J. R. Naber, R. L. Hartman, J. P. McMullen, K. F. Jensen, S. L. Buchwald, *Chem. Sci.* **2011**, *2*, 287–290.
- [193] J. Sedelmeier, S. V. Ley, I. R. Baxendale, M. Baumann, *Org. Lett.* **2010**, *12*, 3618–3621.
- [194] B. Pieber, M. Shalom, M. Antonietti, P. H. Seeberger, K. Gilmore, *Angew. Chem. Int. Ed.* **2018**, *57*, 9976–9979.
- [195] L. Rogers, N. Briggs, R. Achermann, A. Adamo, M. Azad, D. Brancazio, G. Capellades, G. Hammersmith, T. Hart, J. Imbrogno et al., *Org. Process Res. Dev.* **2020**, *24*, 2183–2196.
- [196] C. P. Breen, C. Parrish, N. Shanguan, S. Majumdar, H. Murnen, T. F. Jamison, M. M. Bio, *Org. Process Res. Dev.* **2020**, *24*, 2298–2303.
- [197] J. Bobers, J. Grün, S. Höving, T. Pyka, N. Kockmann, *Org. Process Res. Dev.* **2020**, *24*, 2094–2104.
- [198] T. Hart, V. L. Schultz, D. Thomas, T. Kulesza, K. F. Jensen, *Org. Process Res. Dev.* **2020**, *24*, 2105–2112.
- [199] M. Coakley, D. E. Hurt, *J. Lab. Autom.* **2016**, *21*, 489–495.
- [200] T. Chen, Y.-C. Lin, *Int. J. Intell. Syst.* **2017**, *32*, 394–413.
- [201] M. R. Hartings, Z. Ahmed, *Nat. Rev. Chem.* **2019**, *3*, 305–314.
- [202] Y. He, Y. Wu, J.-z. Fu, Q. Gao, J.-j. Qiu, *Electroanalysis* **2016**, *28*, 1658–1678.
- [203] C. Hurt, M. Brandt, S. S. Priya, T. Bhatelia, J. Patel, P. Selvakannan, S. Bhargava, *Catal. Sci. Technol.* **2017**, *7*, 3421–3439.
- [204] P. N. Nesterenko, *Pure Appl. Chem.* **2020**, *92*, 1341–1355.
- [205] C. W. Pinger, M. K. Geiger, D. M. Spence, *J. Chem. Educ.* **2020**, *97*, 112–117.
- [206] C. R. Sagandira, M. Siyawamwaya, P. Watts, *Arab. J. Chem.* **2020**, *13*, 7886–7908.
- [207] Q. Yan, H. Dong, J. Su, J. Han, B. Song, Q. Wei, Y. Shi, *Engineering* **2018**, *4*, 729–742.
- [208] S. Rossi, A. Puglisi, M. Benaglia, *ChemCatChem* **2018**, *10*, 1512–1525.
- [209] M. J. Harding, S. Brady, H. O'Connor, R. Lopez-Rodriguez, M. D. Edwards, S. Tracy, D. Dowling, G. Gibson, K. P. Girard, S. Ferguson, *React. Chem. Eng.* **2020**, *5*, 728–735.
- [210] F. Kotz, P. Risch, D. Helmer, B. E. Rapp, *Adv. Mater.* **2019**, *31*, 1805982.
- [211] P. J. Kitson, M. H. Rosnes, V. Sans, V. Dragone, L. Cronin, *Lab Chip* **2012**, *12*, 3267–3271.
- [212] P. J. Kitson, G. Marie, J.-P. Francoia, S. S. Zaleskiy, R. C. Sigerson, J. S. Mathieson, L. Cronin, *Science* **2018**, *359*, 314–318.
- [213] P. J. Kitson, S. Glatzel, W. Chen, C.-G. Lin, Y.-F. Song, L. Cronin, *Nat. Protoc.* **2016**, *11*, 920–936.
- [214] M. B. Spano, B. H. Tran, S. Majumdar, G. A. Weiss, *J. Org. Chem.* **2020**, *85*, 8480–8488.

- [215] M. C. Maier, A. Valotta, K. Hiebler, S. Soritz, K. Gavric, B. Grabner, H. Gruber-Woelfler, *Org. Process Res. Dev.* **2020**, *24*, 2197–2207.
- [216] D. E. Fitzpatrick, C. Battilocchio, S. V. Ley, *ACS Cent. Sci.* **2016**, *2*, 131–138.
- [217] M. Baumann, T. S. Moody, M. Smyth, S. Wharry, *Org. Process Res. Dev.* **2020**, *24*, 1802–1813.
- [218] Z. Chen, J. Y. Han, L. Shumate, R. Fedak, D. L. DeVoe, *Adv. Mater. Technol.* **2019**, *4*, 1800511.
- [219] R. J. Ingham, C. Battilocchio, D. E. Fitzpatrick, E. Sliwinski, J. M. Hawkins, S. V. Ley, *Angew. Chem. Int. Ed.* **2015**, *54*, 144–148.
- [220] N. Cherkasov, Y. Bai, A. J. Expósito, E. V. Rebrov, *React. Chem. Eng.* **2018**, *3*, 769–780.
- [221] K. C. Nicolaou, D. Vourloumis, N. Winssinger, P. S. Baran, *Angew. Chem. Int. Ed.* **2000**, *39*, 44–122.
- [222] R. A. Maplestone, M. J. Stone, D. H. Williams, *Gene* **1992**, *115*, 151–157.
- [223] R. Nishida, *Biosci. Biotechnol. Biochem.* **2014**, *78*, 1–13.
- [224] W. O. Foye, T. L. Lemke, D. A. Williams, *Foye's principles of medicinal chemistry*, Lippincott Williams & Wilkins, Philadelphia, **2008**.
- [225] D. J. Newman, G. M. Cragg, *J. Nat. Prod.* **2016**, *79*, 629–661.
- [226] N. Armanino, J. Charpentier, F. Flachsmann, A. Goeke, M. Liniger, P. Kraft, *Angew. Chem. Int. Ed.* **2020**, *59*, 16310–16344.
- [227] P. Kraft, J. A. Bajgrowicz, C. Denis, G. Frater, *Angew. Chem. Int. Ed.* **2000**, *39*, 2980–3010.
- [228] P. L. Schiff jr., *Am. J. Pharm. Educ.* **2002**, *66*, 186–194.
- [229] F. Sertürner, *J. Pharm. Ärzte Apotheker* **1805**, *13*, 229–243.
- [230] J. Frackenpohl, *Chem. Unserer Zeit* **2000**, *34*, 99–112.
- [231] B. Schäfer, *Naturstoffe der chemischen Industrie*, Spektrum Akademischer Verlage, München, **2007**.
- [232] M. Gates, G. Tschudi, *J. Am. Chem. Soc.* **1952**, *74*, 1109–1110.
- [233] M. Gates, G. Tschudi, *J. Am. Chem. Soc.* **1955**, *78*, 1380–1393.
- [234] V. M. Schmiedel, Y. J. Hong, D. Lentz, D. J. Tantillo, M. Christmann, *Angew. Chem. Int. Ed.* **2018**, *57*, 2419–2422.
- [235] T. Seitz, P. Fu, F.-L. Haut, L. Adam, M. Habicht, D. Lentz, J. B. MacMillan, M. Christmann, *Org. Lett.* **2016**, *18*, 3070–3073.
- [236] S. Gao, Q. Wang, C. Chen, *J. Am. Chem. Soc.* **2009**, *131*, 1410–1412.
- [237] T. H. J. Zezula, *Synlett* **2005**, 388–405.
- [238] B. M. Trost, W. Tang, F. D. Toste, *J. Am. Chem. Soc.* **2005**, *127*, 14785–14803.
- [239] J. Brousseau, A. Xolin, L. Barriault, *Org. Lett.* **2019**, *21*, 1347–1349.
- [240] C. Y. Hong, N. Kado, L. E. Overman, *J. Am. Chem. Soc.* **1993**, *115*, 11028–11029.
- [241] S. Chu, N. Münster, T. Balan, M. D. Smith, *Angew. Chem. Int. Ed.* **2016**, *55*, 14306–14309.
- [242] D. A. Evans, C. H. Mitch, *Tetrahedron Lett.* **1982**, *23*, 285–288.
- [243] M. Geffe, T. Opatz, *Org. Lett.* **2014**, *16*, 5282–5285.

- [244] M. Ichiki, H. Tanimoto, S. Miwa, R. Saito, T. Sato, N. Chida, *Chem. Eur. J.* **2013**, *19*, 264–269.
- [245] J. E. Toth, P. R. Hamann, P. L. Fuchs, *J. Org. Chem.* **1988**, *53*, 4694–4708.
- [246] J. Mulzer, G. Dürner, D. Trauner, *Angew. Chem. Int. Ed. Engl.* **1996**, *35*, 2830–2832.
- [247] K. A. Parker, D. Fokas, *J. Am. Chem. Soc.* **1992**, *114*, 9688–9689.
- [248] K. A. Parker, D. Fokas, *J. Org. Chem.* **2006**, *71*, 449–455.
- [249] D. F. Taber, T. D. Neubert, A. L. Rheingold, *J. Am. Chem. Soc.* **2002**, *124*, 12416–12417.
- [250] H. Tanimoto, R. Saito, N. Chida, *Tetrahedron Lett.* **2008**, *49*, 358–362.
- [251] M. Tissot, R. J. Phipps, C. Lucas, R. M. Leon, R. D. M. Pace, T. Ngouansavanh, M. J. Gaunt, *Angew. Chem. Int. Ed.* **2014**, *53*, 13498–13501.
- [252] B. M. Trost, W. Tang, *J. Am. Chem. Soc.* **2002**, *124*, 14542–14543.
- [253] K. Uchida, S. Yokoshima, T. Kan, T. Fukuyama, *Org. Lett.* **2006**, *8*, 5311–5313.
- [254] H. Umihara, S. Yokoshima, M. Inoue, T. Fukuyama, *Chem. Eur. J.* **2017**, *23*, 6993–6995.
- [255] J. W. Reed, T. Hudlicky, *Acc. Chem. Res.* **2015**, *48*, 674–687.
- [256] J. Schwan, M. Christmann, *Chem. Soc. Rev.* **2018**, *47*, 7985–7995.
- [257] J. Heilmann, *Chem. Unserer Zeit* **2007**, *41*, 376–389.
- [258] R. R. Karimov, J. F. Hartwig, *Angew. Chem. Int. Ed.* **2018**, *57*, 4234–4241.
- [259] W. R. Gutekunst, P. S. Baran, *Chem. Soc. Rev.* **2011**, *40*, 1976–1991.
- [260] M. A. A. Endoma-Arias, D. P. Cox, T. Hudlicky, *Adv. Synth. Catal.* **2013**, *355*, 1869–1873.
- [261] H.-D. Arndt, C. P. R. Hackenberger, D. Schwarzer, *Chem. Unserer Zeit* **2010**, *44*, 130–137.
- [262] G. Schön, *Chem. Biodiversity* **2008**, *5*, 1154–1158.
- [263] B. Schäfer, *Chem. Unserer Zeit* **2011**, *45*, 374–388.
- [264] S. Yang, H. Tian, B. Sun, Y. Liu, Y. Hao, Y. Lv, *Sci. Rep.* **2016**, *6*, 32650.
- [265] M. Schalk, L. Pastore, M. A. Mirata, S. Khim, M. Schouwey, F. Deguerry, V. Pineda, L. Rocci, L. Daviet, *J. Am. Chem. Soc.* **2012**, *134*, 18900–18903.
- [266] R. L. Snowden, *Chem Biodiversity* **2008**, *5*, 958–969.
- [267] J. Schwan, M. Kleoff, B. Hartmayer, P. Heretsch, M. Christmann, *Org. Lett.* **2018**, *20*, 7661–7664.
- [268] S. O. Simonetti, E. L. Larghi, T. S. Kaufman, *Nat. Prod. Rep.* **2016**, *33*, 1425–1446.
- [269] J. Schwan, M. Kleoff, P. Heretsch, M. Christmann, *Org. Lett.* **2020**, *22*, 675–678.
- [270] D. Astruc, *Eur. J. Inorg. Chem.* **2017**, 6–29.
- [271] P. Laszlo, R. Hoffmann, *Angew. Chem. Int. Ed.* **2000**, *39*, 123–124.
- [272] H.-U. Blaser, F. Spindler, *Chimia* **1997**, *51*, 297–299.
- [273] L.-X. Dai, T. Tu, S.-L. You, W.-P. Deng, X.-L. Hou, *Acc. Chem. Res.* **2003**, *36*, 659–667.
- [274] M. Mato, C. Pérez-Caaveiro, L. A. Sarandeses, J. Pérez Sestelo, *Adv. Synth. Catal.* **2017**, *359*, 1388–1393.
- [275] R. Haraguchi, S. Hoshino, T. Yamazaki, S.-I. Fukuzawa, *Chem. Commun.* **2018**, *54*, 2110–2113.
- [276] R. Gómez Arrayás, J. Adrio, J. C. Carretero, *Angew. Chem. Int. Ed.* **2006**, *45*, 7674–7715.

- [277] A. Togni, T. Hayashi (Eds.) *Ferrocenes: Homogeneous Catalysis, Organic Synthesis, Material Science*, Wiley-VCH, Weinheim, **1995**.
- [278] A. Wiebe, T. Gieshoff, S. Möhle, E. Rodrigo, M. Zirbes, S. R. Waldvogel, *Angew. Chem. Int. Ed.* **2018**, *57*, 5594–5619.
- [279] S. D. Waniek, J. Klett, C. Förster, K. Heinze, *Beilstein J. Org. Chem.* **2018**, *14*, 1004–1015.
- [280] N. G. Connelly, W. E. Geiger, *Chem. Rev.* **1996**, *96*, 877–910.
- [281] R. R. Gagné, C. A. Koval, G. C. Lisensky, *Inorg. Chem.* **1980**, *19*, 2854–2855.
- [282] J. Wei, P. L. Diaconescu, *Acc. Chem. Res.* **2019**, *52*, 415–424.
- [283] V. Blanco, D. A. Leigh, V. Marcos, *Chem. Soc. Rev.* **2015**, *44*, 5341–5370.
- [284] A. J. Teator, D. N. Lastovickova, C. W. Bielawski, *Chem. Rev.* **2016**, *116*, 1969–1992.
- [285] S. Klenk, S. Rupf, L. Suntrup, M. van der Meer, B. Sarkar, *Organometallics* **2017**, *36*, 2026–2035.
- [286] M. S. Inkpen, S. Scheerer, M. Linseis, A. J. P. White, R. F. Winter, T. Albrecht, N. J. Long, *Nat. Chem.* **2016**, *8*, 825–830.
- [287] N. J. Long, A. J. Martin, R. Vilar, A. J. P. White, D. J. Williams, M. Younus, *Organometallics* **1999**, *19*, 4261–4269.
- [288] L. E. Wilson, C. Hassenrück, R. F. Winter, A. J. P. White, T. Albrecht, N. J. Long, *Eur. J. Inorg. Chem.* **2017**, 496–504.
- [289] L. E. Wilson, C. Hassenrück, R. F. Winter, A. J. P. White, T. Albrecht, N. J. Long, *Angew. Chem. Int. Ed.* **2017**, *56*, 6838–6842.
- [290] Y. Wang, A. Rapakousiou, G. Chastanet, L. Salmon, J. Ruiz, D. Astruc, *Organometallics* **2013**, *32*, 6136–6146.
- [291] M. Lohan, F. Justaud, T. Roisnel, P. Ecorchard, H. Lang, C. Lapinte, *Organometallics* **2010**, *29*, 4804–4817.
- [292] M. Lohan, P. Ecorchard, T. Rüffer, F. Justaud, C. Lapinte, H. Lang, *Organometallics* **2009**, *28*, 1878–1890.
- [293] R. Warratz, H. Aboufadel, T. Bally, F. Tucek, *Chem. Eur. J.* **2009**, *15*, 1604–1617.
- [294] A. Rapakousiou, R. Djeda, M. Grillaud, N. Li, J. Ruiz, D. Astruc, *Organometallics* **2014**, *33*, 6953–6962.
- [295] A. Rapakousiou, C. Deraedt, H. Gu, L. Salmon, C. Belin, J. Ruiz, D. Astruc, *J. Am. Chem. Soc.* **2014**, *136*, 13995–13998.
- [296] R. Djeda, A. Rapakousiou, L. Liang, N. Guidolin, J. Ruiz, D. Astruc, *Angew. Chem. Int. Ed.* **2010**, *49*, 8152–8156.
- [297] T.-Y. Dong, S.-W. Chang, S.-F. Lin, M.-c. Lin, Y.-S. Wen, L. Lee, *Organometallics* **2006**, *25*, 2018–2024.
- [298] R. Breuer, M. Schmittel, *Organometallics* **2012**, *31*, 6642–6651.

- [299] L.-A. Hore, C. J. McAdam, J. L. Kerr, N. W. Duffy, B. H. Robinson, J. Simpson, *Organometallics* **2000**, *19*, 5039–5048.
- [300] D. Schmiel, R. Gathy, H. Butenschön, *Organometallics* **2018**, *37*, 2095–2110.
- [301] C. Pi, X. Cui, X. Liu, M. Guo, H. Zhang, Y. Wu, *Org. Lett.* **2014**, *16*, 5164–5167.
- [302] M. Deb, S. Hazra, A. Gupta, A. J. Elias, *Dalton Trans.* **2018**, *47*, 7229–7236.
- [303] M. Sattar, K. Patidar, R. A. Thorat, S. Kumar, *J. Org. Chem.* **2019**, *84*, 6669–6678.
- [304] J. Xu, Y. Liu, J. Zhang, X. Xu, Z. Jin, *Chem. Commun.* **2018**, *54*, 689–692.
- [305] Z.-J. Cai, C.-X. Liu, Q. Gu, S.-L. You, *Angew. Chem. Int. Ed.* **2018**, *57*, 1296–1299.
- [306] R. Sanders, U. T. Mueller-Westerhoff, *J. Organomet. Chem.* **1996**, *512*, 219–224.
- [307] S. Dey, J. W. Quail, J. Müller, *Organometallics* **2015**, *34*, 3039–3046.
- [308] S. A. Herbert, D. C. Castell, J. Clayden, G. E. Arnott, *Org. Lett.* **2013**, *15*, 3334–3337.
- [309] G. Werner, H. Butenschön, *Eur. J. Inorg. Chem.* **2017**, 378–387.
- [310] D. A. Khobragade, S. G. Mahamulkar, L. Pospišil, I. Císařová, L. Rulíšek, U. Jahn, *Chem. Eur. J.* **2012**, *18*, 12267–12277.
- [311] H. Butenschön, *Synthesis* **2018**, *50*, 3787–3808.
- [312] R. C. J. Atkinson, V. C. Gibson, N. J. Long, A. J. P. White, D. J. Williams, *Organometallics* **2004**, *23*, 2744–2751.
- [313] A. N. Nesmeyanov, E. G. Perevalova, T. V. Nikitina, *Tetrahedron Lett.* **1960**, *1*, 1–2.
- [314] K. Škoch, I. Císařová, J. Schulz, U. Siemeling, P. Štěpnička, *Dalton Trans.* **2017**, *46*, 10339–10354.
- [315] Z. Jian, S. Krupski, K. Škoch, G. Kehr, C. G. Daniliuc, I. Císařová, P. Štěpnička, G. Erker, *Organometallics* **2017**, *36*, 2940–2946.
- [316] T. J. Colacot, *Chem. Rev.* **2003**, *103*, 3101–3118.
- [317] M. Malessa, J. Heck, J. Kopf, M. H. Garcia, *Eur. J. Inorg. Chem.* **2006**, 857–867.
- [318] M.-T. Lee, B. M. Foxman, M. Rosenblum, *Organometallics* **1985**, *4*, 539–547.
- [319] A. Shafir, M. P. Power, G. D. Whitener, J. Arnold, *Organometallics* **2000**, *19*, 3978–3982.
- [320] S. Bräse, C. Gil, K. Knepper, V. Zimmermann, *Angew. Chem. Int. Ed.* **2005**, *44*, 5188–5240.
- [321] K. Banert, *Synthesis* **2016**, *48*, 2361–2375.
- [322] D. Huang, G. Yan, *Adv. Synth. Catal.* **2017**, *359*, 1600–1619.
- [323] V. V. Rostovtsev, L. G. Green, V. V. Fokin, K. B. Sharpless, *Angew. Chem. Int. Ed.* **2002**, *41*, 2596–2599.
- [324] H. C. Kolb, M. G. Finn, K. B. Sharpless, *Angew. Chem. Int. Ed.* **2001**, *40*, 2004–2021.
- [325] J. E. Hein, V. V. Fokin, *Chem. Soc. Rev.* **2010**, *39*, 1302–1315.
- [326] E. M. Sletten, C. R. Bertozzi, *Angew. Chem. Int. Ed.* **2009**, *48*, 6974–6998.
- [327] A. H. El-Sagheer, T. Brown, *Chem. Soc. Rev.* **2010**, *39*, 1388–1405.
- [328] D. Schweinfurth, L. Hettmanczyk, L. Suntrup, B. Sarkar, *Z. Anorg. Allg. Chem.* **2017**, *643*, 554–584.

- [329] P. L. Golas, K. Matyjaszewski, *Chem. Soc. Rev.* **2010**, *39*, 1338–1354.
- [330] P. Thirumurugan, D. Matosiuk, K. Jozwiak, *Chem. Rev.* **2013**, *113*, 4905–4979.
- [331] M. N. Hopkinson, C. Richter, M. Schedler, F. Glorius, *Nature* **2014**, *510*, 485–496.
- [332] D. Plažuk, B. Rychlik, A. Błaż, S. Domagała, *J. Organomet. Chem.* **2012**, *715*, 102–112.
- [333] T. Romero, R. A. Orenes, A. Espinosa, A. Tárraga, P. Molina, *Inorg. Chem.* **2011**, *50*, 8214–8224.
- [334] C. Steel, M. Rosenblum, *Int. J. Chem. Kinet.* **1994**, *26*, 631–641.
- [335] R. G. Sutherland, *Chem. Commun.* **1971**, 134–135.
- [336] A. Shafir, M. P. Power, G. D. Whitener, J. Arnold, *Organometallics* **2001**, *20*, 1365–1369.
- [337] A. Shafir, J. Arnold, *J. Am. Chem. Soc.* **2001**, *123*, 9212–9213.
- [338] U. Siemeling, T.-C. Auch, *Chem. Soc. Rev.* **2005**, *34*, 584–594.
- [339] U. Siemeling, B. Neumann, H.-G. Stammer, A. Salmon, *Z. Anorg. Allg. Chem.* **2002**, *628*, 2315–2320.
- [340] K. Tani, T. Mihana, T. Yamagata, T. Saito, *Chem. Lett.* **1991**, *20*, 2047–2050.
- [341] S.-H. Wu, J.-J. Shen, J. Yao, Y.-W. Zhong, *Chem. Asian. J.* **2013**, *8*, 138–147.
- [342] M. Auzias, B. Therrien, G. Süß-Fink, P. Štěpnička, W. H. Ang, P. J. Dyson, *Inorg. Chem.* **2008**, *47*, 578–583.
- [343] L. Hettmanczyk, L. Suntrup, S. Klenk, C. Hoyer, B. Sarkar, *Chem. Eur. J.* **2017**, *23*, 576–585.
- [344] P. Štěpnička, H. Solařová, I. Čísařová, *J. Organomet. Chem.* **2011**, *696*, 3727–3740.
- [345] T. Sakano, M. Okano, K. Osakada, *J. Inorg. Organomet. Polym.* **2009**, *19*, 35–45.
- [346] L. V. Snegur, Y. S. Nekrasov, N. S. Sergeeva, Z. V. Zhilina, V. V. Gumenyuk, Z. A. Starikova, A. A. Simenel, N. B. Morozova, I. K. Sviridova, V. N. Babin, *Appl. Organometal. Chem.* **2008**, *22*, 139–147.
- [347] E. Loukopoulos, G. E. Kostakis, *Coord. Chem. Rev.* **2019**, *395*, 193–229.
- [348] Y. Wang, Z. Wang, Y. Tang, *Chem. Rec.* **2020**, *20*, 693–709.
- [349] A. R. Katritzky, S. Rachwal, *Chem. Rev.* **2010**, *110*, 1564–1610.
- [350] A. R. Katritzky, S. Rachwal, *Chem. Rev.* **2011**, *111*, 7063–7120.
- [351] A. R. Katritzky, B. V. Rogovoy, *Chem. Eur. J.* **2003**, *9*, 4586–4593.
- [352] A. R. Katritzky, Y. Fang, M. Qi, D. Feng, *Heterocycles* **1998**, *12*, 2535–2541.
- [353] A. R. Katritzky, K. Kirichenko, Y. Ji, I. Prakash, *Chem. Heterocycl. Compd.* **2002**, *38*, 156–164.
- [354] I. Briguglio, S. Piras, P. Corona, E. Gavini, M. Nieddu, G. Boatto, A. Carta, *Eur. J. Med. Chem.* **2015**, *97*, 612–648.
- [355] Y. Ren, L. Zhang, C.-H. Zhou, R.-X. Geng, *Med. Chem.* **2014**, *4*, 640–662.
- [356] X.-M. Peng, G.-X. Cai, C.-H. Zhou, *Curr. Top. Med. Chem.* **2013**, *13*, 1963–2010.
- [357] R. R. Kale, V. Prasad, P. P. Mohapatra, V. K. Tiwari, *Monatsh. Chem.* **2010**, *141*, 1159–1182.
- [358] R. Ramachandran, M. Rani, S. Senthana, Y. T. Jeong, S. Kabilan, *Eur. J. Med. Chem.* **2011**, *46*, 1926–1934.

- [359] P. E. Goss, *Breast Cancer Res. Treat.* **1998**, *49*, 59–65.
- [360] L. R. Wiseman, C. M. Spencer, *Drugs Aging* **1997**, *3*, 245–250.
- [361] Y. Hu, C.-Y. Li, X.-M. Wang, Y.-H. Yang, H.-L. Zhu, *Chem. Rev.* **2014**, *114*, 5572–5610.
- [362] A. Biegón, S. W. Kim, D. L. Alexoff, M. Jayne, P. Carter, B. Hubbard, P. King, J. Logan, L. Muench, D. Pareto et al., *Synapse* **2010**, *64*, 801–807.
- [363] K. M. Dawood, H. Abdel-Gawad, E. A. Rageb, M. Ellithey, H. A. Mohamed, *Bioorg. Med. Chem.* **2006**, *14*, 3672–3680.
- [364] R. K. Kumar, M. A. Ali, T. Punniyamurthy, *Org. Lett.* **2011**, *13*, 2102–2105.
- [365] C. Mukhopadhyay, P. K. Tapaswi, R. J. Butcher, *Org. Biomol. Chem.* **2010**, *8*, 4720–4729.
- [366] V. Zimmermann, S. Bräse, *J. Comb. Chem.* **2007**, *9*, 1114–1137.
- [367] M. Chen, S. L. Buchwald, *Angew. Chem. Int. Ed.* **2013**, *52*, 4247–4250.
- [368] R. J. Faggyas, N. L. Sloan, N. Buijs, A. Sutherland, *Eur. J. Org. Chem.* **2019**, 5344–5353.
- [369] V. Gurram, H. K. Akula, R. Garlapati, N. Pottabathini, M. K. Lakshman, *Adv. Synth. Catal.* **2015**, *357*, 451–462.
- [370] F. Shi, J. P. Waldo, Y. Chen, R. C. Larock, *Org. Lett.* **2008**, *10*, 2409–2412.
- [371] S. Chandrasekhar, M. Seenaiiah, C. L. Rao, C. R. Reddy, *Tetrahedron* **2008**, *64*, 11325–11327.
- [372] G. Singh, R. Kumar, J. Swett, B. Zajc, *Org. Lett.* **2013**, *15*, 4086–4089.
- [373] L. Campbell-Verduyn, P. H. Elsinga, L. Mirfeizi, R. A. Dierckx, B. L. Feringa, *Org. Biomol. Chem.* **2008**, *6*, 3461–3463.
- [374] A. Guin, R. N. Gaykar, S. Bhattacharjee, A. T. Biju, *J. Org. Chem.* **2019**, *84*, 12692–12699.
- [375] H. Ankati, E. Biehl, *Tetrahedron Lett.* **2009**, *50*, 4677–4682.
- [376] H.-G. Lee, J.-E. Won, M.-J. Kim, S.-E. Park, K.-J. Jung, B. R. Kim, S.-G. Lee, Y.-J. Yoon, *J. Org. Chem.* **2009**, *74*, 5675–5678.
- [377] J. Shi, L. Li, Y. Li, *Chem. Rev.* **2021**, *121*, 3892–4044.
- [378] H. H. Wenk, M. Winkler, W. Sander, *Angew. Chem. Int. Ed.* **2003**, *42*, 502–528.
- [379] N. G. Rondan, L. N. Domelsmith, K. N. Houk, *Tetrahedron Lett.* **1979**, *20*, 3237–3240.
- [380] R. Sanz, *Org. Prep. Proced. Int.* **2008**, *40*, 215–291.
- [381] D. B. Werz, A. T. Biju, *Angew. Chem. Int. Ed.* **2020**, *59*, 3385–3398.
- [382] C. Wentrup, *Aust. J. Chem.* **2010**, *63*, 979–986.
- [383] S. Yoshida, T. Hosoya, *Chem. Lett.* **2015**, *44*, 1450–1460.
- [384] C. M. Gampe, E. M. Carreira, *Angew. Chem. Int. Ed.* **2012**, *51*, 3766–3778.
- [385] A. E. Goetz, T. K. Shah, N. K. Garg, *Chem. Commun.* **2015**, *51*, 34–45.
- [386] J. He, D. Qiu, Y. Li, *Acc. Chem. Res.* **2020**, *53*, 508–519.
- [387] P. M. Tadross, B. M. Stoltz, *Chem. Rev.* **2012**, *112*, 3550–3577.
- [388] H. Takikawa, A. Nishii, T. Sakai, K. Suzuki, *Chem. Soc. Rev.* **2018**, *47*, 8030–8056.
- [389] R. Karmakar, D. Lee, *Chem. Soc. Rev.* **2016**, *45*, 4459–4470.
- [390] M. Asamdi, K. H. Chikhaliya, *Asian J. Org. Chem.* **2017**, *6*, 1331–1348.

- [391] J. Shi, Y. Li, Y. Li, *Chem. Soc. Rev.* **2017**, *46*, 1707–1719.
- [392] C. Wu, F. Shi, *Asian J. Org. Chem.* **2013**, *2*, 116–125.
- [393] D. Pérez, D. Peña, E. Guitián, *Eur. J. Org. Chem.* **2013**, 5981–6013.
- [394] R. A. Dhokale, S. B. Mhaske, *Synthesis* **2018**, *50*, 1–16.
- [395] T. Roy, A. T. Biju, *Chem. Commun.* **2018**, *54*, 2580–2594.
- [396] F. I. M. Idiris, C. R. Jones, *Org. Biomol. Chem.* **2017**, *15*, 9044–9056.
- [397] G. Wittig, L. Pohmer, *Angew. Chem.* **1955**, *67*, 348.
- [398] W. Lin, I. Sapountzis, P. Knochel, *Angew. Chem. Int. Ed.* **2005**, *44*, 4258–4261.
- [399] H. Gilman, T. S. Soddy, *J. Org. Chem.* **1957**, *22*, 1715–1716.
- [400] L. Friedman, F. M. Logullo, *J. Am. Chem. Soc.* **1963**, *85*, 1549.
- [401] C. D. Campbell, C. W. Rees, *J. Chem. Soc. C.* **1969**, 742–747.
- [402] M. A. Birkett, D. W. Knight, R. G. Giles, M. B. Mitchell, *J. Chem. Soc., Perkin Trans. 1* **1998**, 2301–2305.
- [403] M. A. Birkett, D. W. Knight, P. B. Little, M. B. Mitchell, *Tetrahedron* **2000**, *56*, 1013–1023.
- [404] G. Wittig, R. W. Hoffmann, *Chem. Ber.* **1962**, *95*, 2718–2728.
- [405] G. Wittig, R. W. Hoffmann, *Org. Synth.* **1967**, *47*, 4–9.
- [406] R. W. Hoffmann, W. Sieber, G. Guhn, *Chem. Ber.* **1965**, *98*, 3470–3478.
- [407] G. Wittig, R. W. Hoffmann, *Angew. Chem.* **1961**, *73*, 435–436.
- [408] T. L. Gilchrist, F. J. Graveling, C. W. Rees, *J. Chem. Soc. C.* **1971**, 977–980.
- [409] E. M. Serum, S. Selvakumar, N. Zimmermann, M. P. Sibi, *Green Chem.* **2018**, *20*, 1448–1454.
- [410] T. R. Hoye, B. Baire, D. Niu, P. H. Willoughby, B. P. Woods, *Nature* **2012**, *490*, 208–212.
- [411] S. Ghorai, D. Lee, *Tetrahedron* **2017**, *73*, 4062–4069.
- [412] A. Z. Bradley, R. P. Johnson, *J. Am. Chem. Soc.* **1997**, *119*, 9917–9918.
- [413] O. J. Diamond, T. B. Marder, *Org. Chem. Front.* **2017**, *4*, 891–910.
- [414] J. Chen, V. Palani, T. R. Hoye, *J. Am. Chem. Soc.* **2016**, *138*, 4318–4321.
- [415] Y. Himeshima, T. Sonoda, H. Kobayashi, *Chem. Lett.* **1983**, *12*, 1211–1214.
- [416] R. F. Cunico, E. M. Dexheimer, *J. Organomet. Chem.* **1973**, *59*, 153–160.
- [417] T. Roy, D. R. Baviskar, A. T. Biju, *J. Org. Chem.* **2015**, *80*, 11131–11137.
- [418] M. Serafini, A. Griglio, S. Viarengo, S. Aprile, T. Pirali, *Org. Biomol. Chem.* **2017**, *15*, 6604–6612.
- [419] T. Kaicharla, M. Thangaraj, A. T. Biju, *Org. Lett.* **2014**, *16*, 1728–1731.
- [420] T. Ikawa, T. Nishiyama, T. Nosaki, A. Takagi, S. Akai, *Org. Lett.* **2011**, *13*, 1730–1733.
- [421] T. Kitamura, Y. Aoki, S. Isshiki, K. Wasai, Y. Fujiwara, *Tetrahedron Lett.* **2006**, *47*, 1709–1712.
- [422] S. Kovács, Á. I. Csincsi, T. Z. Nagy, S. Boros, G. Timári, Z. Novák, *Org. Lett.* **2012**, *14*, 2022–2025.
- [423] M. Mesgar, O. Daugulis, *Org. Lett.* **2016**, *18*, 3910–3913.
- [424] Q. Chen, H. Yu, Z. Xu, L. Lin, X. Jiang, R. Wang, *J. Org. Chem.* **2015**, *80*, 6890–6896.

- [425] A. C. A. Muraca, C. Raminelli, *ACS Omega* **2020**, *5*, 2440–2457.
- [426] U. K. Tambar, B. M. Stoltz, *J. Am. Chem. Soc.* **2005**, *127*, 5340–5341.
- [427] G. Märkl, F. Lieb, C. Martin, *Tetrahedron Lett.* **1971**, *13*, 1249–1252.
- [428] P. S. Bäuerlein, I. A. Gonzalez, J. J. M. Weemers, M. Lutz, A. L. Spek, D. Vogt, C. Müller, *Chem. Commun.* **2009**, 4944–4946.
- [429] M. Blug, C. Guibert, X.-F. Le Goff, N. Mézailles, P. Le Floch, *Chem. Commun.* **2009**, 201–203.
- [430] B. Breit, E. Fuchs, *Chem. Commun.* **2004**, 694–695.
- [431] B. Breit, E. Fuchs, *Synthesis* **2006**, 2121–2128.
- [432] M. Bruce, M. Papke, A. W. Ehlers, M. Weber, D. Lentz, N. Mézailles, J. C. Slootweg, C. Müller, *Chem. Eur. J.* **2019**, *25*, 14332–14340.
- [433] M. Rigo, J. A. W. Sklorz, N. Hatje, F. Noack, M. Weber, J. Wiecko, C. Müller, *Dalton Trans.* **2016**, *45*, 2218–2226.
- [434] C. Wallis, P. G. Edwards, M. Hanton, P. D. Newman, A. Stasch, C. Jones, R. P. Tooze, *Dalton Trans.* **2009**, *38*, 2170–2177.
- [435] Z. Liu, F. Shi, P. D. G. Martinez, C. Raminelli, R. C. Larock, *J. Org. Chem.* **2008**, *73*, 219–226.
- [436] T. Jin, Y. Yamamoto, *Angew. Chem. Int. Ed.* **2007**, *46*, 3323–3325.
- [437] Y. Hari, R. Sone, T. Aoyama, *Org. Biomol. Chem.* **2009**, *7*, 2804–2808.
- [438] B. Cheng, B. Zu, B. Bao, Y. Li, R. Wang, H. Zhai, *J. Org. Chem.* **2017**, *82*, 8228–8233.
- [439] L. Sun, J. Nie, Y. Zheng, J.-A. Ma, *J. Fluorine Chem.* **2015**, *174*, 88–94.
- [440] C. Lu, A. V. Dubrovskiy, R. C. Larock, *J. Org. Chem.* **2012**, *77*, 2279–2284.
- [441] R. K. Khangarot, K. P. Kaliappan, *Eur. J. Org. Chem.* **2012**, 5844–5854.
- [442] T. Yao, B. Ren, B. Wang, Y. Zhao, *Org. Lett.* **2017**, *19*, 3135–3138.
- [443] J. Son, K. H. Kim, D.-L. Mo, D. J. Wink, L. L. Anderson, *Angew. Chem. Int. Ed.* **2017**, *56*, 3059–3063.
- [444] P. Li, J. Zhao, C. Wu, R. C. Larock, F. Shi, *Org. Lett.* **2011**, *13*, 3340–3343.
- [445] P. Li, C. Wu, J. Zhao, D. C. Rogness, F. Shi, *J. Org. Chem.* **2012**, *77*, 3149–3158.

2.2 Illustration Credits

Figure 1, p. 11

Drawn with OriginPro 2020.

Figure 2, p. 14

Drawn with ChemDraw Professional 16.0.

Figure 3, p. 14

A: Drawn with ChemDraw Professional 16.0. B: A part of Figure 2B in the cited publication was used. Reprinted with permission from (B. Pieber, M. Shalom, P. H. Seeberger, K. Gilmore, *Angew. Chem. Int. Ed.* **2018**, *57*, 9976–9979, © 2018 Wiley-VCH Verlag GmbH & Co. KGaA, Weinheim (License No.: 5092971461238)

Figure 4, p. 16; Figure 5, p. 19; Figure 6, p. 28

Drawn with ChemDraw Professional 16.0.

Figure 7, p. 33

Drawn with ChemDraw Professional 16.0, showing also a picture (grey box, “3D printed components”) taken from Autodesk Fusion 360.

Appendices

Appendix A: A Modular, Argon-Driven Flow Platform for Natural Product Synthesis and Late-Stage Transformations

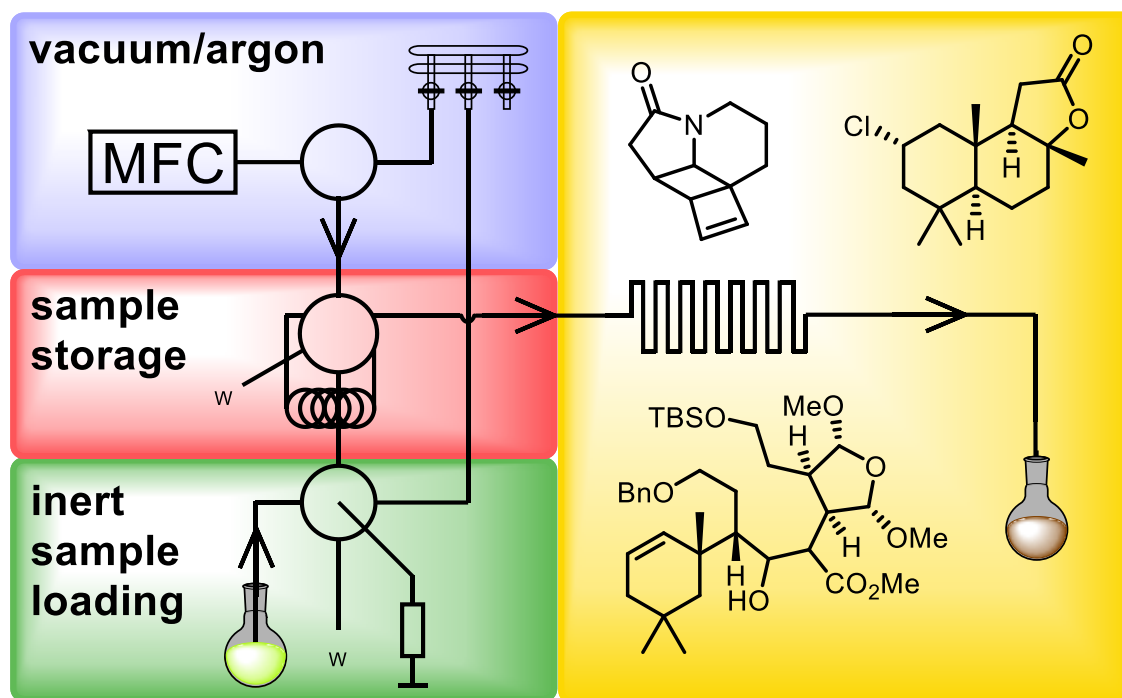
Appendix B: Scalable Synthesis of Functionalized Ferrocenyl Azides and Amines Enabled by Flow Chemistry

Appendix C: Scalable Synthesis of Benzotriazoles via [3+2] Cycloaddition of Azides and Arynes in Flow

Appendix A

A Modular, Argon-Driven Flow Platform for Natural Product Synthesis and Late-Stage Transformations

M. Kleoff, J. Schwan, M. Christmann, P. Heretsch



Institut für Chemie und Biochemie, Organische Chemie, Freie Universität Berlin, Takustraße 3,
14195 Berlin, Germany

This article is reproduced with permission from:

M. Kleoff, J. Schwan, M. Christmann, P. Heretsch, *Org. Lett.* **2021**, *23*, 2370–2374.

<https://doi.org/10.1021/acs.orglett.1c00661>

© American Chemical Society

Author contributions: M. Kleoff and J. Schwan designed and constructed the flow platform. M. Kleoff carried out the experimental work. The analytical data were collected and analyzed by M. Kleoff. The manuscript was prepared by M. Kleoff and revised by J. Schwan, M. Christmann, and P. Heretsch.

A Modular, Argon-Driven Flow Platform for Natural Product Synthesis and Late-Stage Transformations

Merlin Kleoff, Johannes Schwan, Mathias Christmann,* and Philipp Heretsch*

Freie Universität Berlin, Institut für Chemie und Biochemie, Takustraße 3, 14195 Berlin, Germany

Supporting Information

1. General Information	60
2. Construction of the Flow Platform.....	69
3. Handling of the Flow Platform.....	105
4. Experimental Procedures.....	120
5. NMR Spectra of Synthesized Compounds.....	143
6. References	147

General Information

1.1 Materials and Methods

Unless otherwise noted, all reactions and workups were performed open to air. All compounds sensitive to water and oxygen were handled under an argon atmosphere using standard Schlenk techniques and oil pump vacuum. Room temperature (rt) refers to 23 °C.

Anhydrous THF was distilled under an atmosphere of argon over sodium/benzophenone and stored over activated 3 Å mol sieves. Anhydrous MeCN was obtained from ACROS and stored over 3 Å mol sieves. Anhydrous HNiPr₂ was distilled from KOH and stored over activated 3 Å mol sieves.

EtOAc, Et₂O, *n*-pentane, and *n*-hexane were purified by distillation on a rotary evaporator. All other solvents and commercially available reagents were used without further purification unless otherwise stated.

3 Å mol sieves were activated by drying in an oven at 250 °C and 10⁻³ mbar for 2–3 h.

Medium pressure liquid chromatography (MPLC) was performed with a TELEDYNE ISCO Combi-Flash Rf or a TELEDYNE ISCO Combi-Flash Rf200 using prepacked SiO₂ columns and cartridges from TELEDYNE. UV response was monitored at 254 nm and 280 nm. As eluents, cyclohexane (99.5%+ quality) and EtOAc (HPLC grade) were used.

For column chromatography, silica 60 M (0.040-0.063 mm) from MACHERY-NAGEL was used. Concentration under reduced pressure was performed by rotary evaporation at 40 °C and the appropriate pressure.

The following compounds were prepared according to the literature: **4**,^[1] **5**,^[1] **7**,^[2] [nBu₄N]₄[W₁₀O₃₂],^[3] **S5**,^[4] **11**.^[4]

A zip file including 3D-printing files (.stl files, necessary to print the 3D-printed parts), LabVIEW software (.vi file) and Arduino code (.ino file, both necessary to control the flow platform) can be obtained from the corresponding author (philipp.heretsch@fu-berlin.de) upon request.

1.2 Analysis

Reaction monitoring: Reactions were monitored by TLC carried out on Merck Silica Gel 50 F₂₅₄ plates and visualized by fluorescence quenching under UV light ($\lambda = 254$ nm) or by using a stain of vanillin (6 g vanillin, 1.5 mL 96% aq. H₂SO₄, 100 mL EtOH) and heat as developing agent.

NMR spectroscopy: All NMR spectra were acquired on a JEOL ECP 500 (500 MHz), a Bruker Avance 500 (500 MHz), a Varian INOVA 600 (600 MHz), or a Bruker Avance 700 (700 MHz) in the reported deuterated solvents. Chemical shifts are reported in parts per million (ppm) with reference to the residual solvent peaks. The given multiplicities are phenomenological, thus, the actual appearance of the signals is stated and not the theoretically expected one. The following abbreviations were used to designate multiplicities: s = singlet, d = doublet, t = triplet, q = quartet, quint = quintet. In case no multiplicity could be identified, the chemical shift range of the signal is given (m = multiplet).

Karl-Fischer titration: Karl-Fischer titrations were performed using a METTLER TOLEDO DL312 Karl-Fischer Coulometer.

1.3 Flow Equipment and Hardware

All flow experiments were carried out using the following equipment:

Flow equipment

Material	Provider
FEP tube (outer diameter 1/16", inner diameter 1/32")	BOLA
PTFE tube (outer diameter 1/16", inner diameter 1.0 mm)	BOLA
PTFE tube (outer diameter 1/8", inner diameter 1/16")	BOLA
T-mixers (stainless steel 316L)	VICI
Coned 10-32 UNF fittings (stainless steel 316L)	UPCHURCH SCIENTIFIC
Flat bottom 1/4-28 UNF gripper fittings (PP)	DIBAFIT
Adapters for 1/4-28 UNF (PP or PTFE)	UPCHURCH SCIENTIFIC
Manual 6-way-valves (stainless steel 316L)	KNAUER
Low pressure valves (4-port T-configuration, PTFE/PCTFE)	OMNIFIT (DIBA)
Low pressure valves (5-port 5 positions, PTFE/PCTFE)	OMNIFIT (DIBA)
Gastight glass syringe	VWR
Adjustable back pressure regulator	ZAIPUT

Electronics

All kind of tools (pliers, screwdrivers, soldering bolts, saw, etc.) were obtained from BAUHAUS.

Material	Provider
Pressure sensor Walfront3crb1gv75x, 0-12 bar, 0.5-4.5 V VDC, G1	WALFRONT
Shrinking tube in different sizes	CHILITEC
Threading tap for 1/4-28 UNF	GSR PROFI
M2-M5 Screws, flat washers, and nuts (stainless steel)	BAUHAUS
60 mm PC fan	NOISEBLOCKER
140 mm PC fan Arctic F14	ARCTIC
Linear guide 8 mm x 500 mm	ROBOMALL
Linear bearing LM8UU	UEETEK
M8 threaded bolt	BAUHAUS
Perforated plate 500x250x1.5 mm (anodized aluminum)	BAUHAUS
Aluminum rod (outer diameter = 6 mm, inner diameter = 4 mm)	BAUHAUS
Flexible shaft coupling (5 mm to 8 mm)	UEETEK

Luster terminal	KOPP
Circuit board 40x60 mm	VKTECH
4-Pin wire	FOXNOVO
1-Pin wires	CONRAD ELECTRONICS
Resistors	CONRAD ELECTRONICS
4 channel fan controller 12 V	RICHER-R
Coaxial power supply	WENTRONIC
Power adapter 1000 mA Goobay 59031	GOOBAY
Nema stepper motors (12 V, 1.7 A, 40 Ncm)	TOPDIRECT
Arduino Uno R3 + CNC engraver shield + 4 A4988 stepper drivers	KUMAN
Cable Conduit 5 m	CALLSTEL
140 mm Fan Grill	AAB Cooling
LED stripe (12 V, LED 2835, 385–400 nm)	DEEPDREAM
LED stripe (24 V, LED 2835, 365 nm)	LUXALIGHT

3D-Printing

In general, 3D-printing was performed with a Creality CR-10 Prusa using PLA as filament at 200 °C/65 °C (extruder/heat bed) on a glass bed sprayed with a fine layer of hair spray. PLA filament was stored in a “dry box” containing silica gel orange as desiccant. A zip file including 3D-printing files (.stl files) can be obtained from the corresponding author (philipp.heretsch@fu-berlin.de) upon request.

Material	Provider
3D-printer Creality CR10-S	CREALITY
Hair spray today Glanz&Halt	PENNY MARKT
PLA filament	AMZ3D

3D-printed files

A list of the 3D printed files and the respective infill used.

3D-file (.stl)	Infill
ArduinoCase_Backplate	25%
ArduinoCase_Case	25%
ArduinoCase_CoverTop	25%
Connector_tube_to_UNF14-28	100%

FlexValves_Mounts	50%
FlexValves_Clips	100%
FlexValves_Sledge_HPLC_valves	25%
FlexValves_Sledge_LP_valves	25%
MFC_Mount	40%
Photoreactor_Body	50%
Photoreactor_Body2	50%
Photoreactor_Ground	50%
Photoreactor_TubeReactor	50%
Photoreactor_Curve	50%
SyringePump_Body	50%
SyringePump_Sledge	50%

(Selected) Specifications of the used mass flow controllers (MFCs)

Bronkhorst EL-FLOW Prestige

$v_{\text{flow}} = 0.076 \dots 10 \text{ mL}_n/\text{min}$ ($\pm 0.5\%$ onset scale, $\pm 0.1\%$ full scale)

Medium: Argon

Operating temperature: 20 °C

Operating pressure (in): 30 bar

Operating pressure (out): 0 bar

Sealing: Viton 51415

Plunger: FFKM

Process fittings: G1/8 female

1.4 General Remarks and Advices for Performing Experiments

Tubes

Tubes for flow chemistry are typically made from PTFE, PFA, or FEP. All polymers show excellent chemical resistance. In fact, there are slight differences (PTFE is chemically more resistant than FEP or PFA), however, these differences are not significant for most reactions in flow. Typically, 1/16" tubes of PTFE have an inner diameter of 1.0 mm; tubes of FEP have an inner diameter of 0.8 mm, PFA have an inner diameter of 0.75 mm. In order to reduce dead volume between wetted parts, tubes with smaller inner diameter are preferable.

PTFE is a relatively stiff polymer that is easy to cut. FEP and PFA are more flexible making it more difficult to equip them with ferrules. On the other hand, they have the large advantage to be more permeable to light. Therefore, impurities (primarily solids!) are easier to detect. Because of their superior translucence and their smaller inner diameter, we use typically FEP tubes.

For additional tips about assembling a flow system, see the literature.^[5]

Blockages

Blockages are a big problem when performing flow chemistry. In general, the undesired formation of solids in tubes, valves, and connectors should be avoided. Especially, when moisture-sensitive organometallics are used, problems can arise. After passing a solution of organolithiums or organomagnesiums through a flow system, it is problematic to wash the system with water afterwards. In our experience, it is better to wash the system first one time (= volume of the sample loop; otherwise 1–2 mL) with *iso*-propanol, then with deionized water and finally two more times with *iso*-propanol to remove the water.

A good way to remove blockages is to wash the system with a solution of AcOH/MeOH/H₂O (0.1:1:1) as recommended by Williams *et al.*^[6] If this does not work, tubes and connectors can be sonicated in a bath of deionized water, *iso*-propanol for some minutes removing most of the solids.

To prevent blockages, only clear solutions of the reagents should be pumped in flow. Even small particles can lead to blockages. When possible, reagent solutions should be filtered through a plug of glass wool or using syringe filters.

Treatment of parts made from stainless steel 316L

Many parts that are used in HPLC and flow chemistry are made from stainless steel 316L. Although this steel shows broad chemical resistance, it is relatively sensitive against acids and, especially, chlorides. In general, components made from stainless steel 316L should never be treated with hydrochloric acid. If diluted solutions of chloride in organic solvents (such as magnesium chloride, when Grignard reactions are performed), or of compounds that can generate hydrochloric acid (such as titanium

tetrachloride) come in contact with components made from stainless steel 316L, it is recommended to wash these components as soon as possible with *iso*-propanol, deionized water and one more time with *iso*-propanol in order to prevent salt formation and corrosion.

Keeping the flow system in “stand-by” for longer times

After each flow experiment, all wetted parts should be washed thoroughly with an appropriate solvent. In most cases, *iso*-propanol can be used, as it dissolves both organic and inorganic residues and most polymers (even PLA) are chemically resistant against *iso*-propanol.

In the case, the flow platform is not used for several weeks, all wetted parts should be flushed with *iso*-propanol and stored with *iso*-propanol for the “stand-by” time. Equally recommendable are ethanol or acetonitrile instead of *iso*-propanol. However, prolonged contact of wetted parts with solvents such as tetrahydrofuran or dichloromethane should be avoided.

When tubes, mixers, or other wetted components are not used for a foreseeable time, they should be thoroughly flushed with *iso*-propanol. In order to dry these components, they can be stored in a drying cabinet at 50–90 °C also for longer time.

3D-Printing of wetted parts from polypropylene

3D-Printed components for chemical reactions are typically printed from polypropylene. Polypropylene shows a higher chemical resistance than PLA (polylactic acid) or PETG (polyethylene terephthalate, glycol-modified), but cannot compete with fluorinated polymers such as PTFE, FEP, or PFA. Hence, it has to be noted that these printed components are not suitable for a broad range of chemical reactions. Due to good, but still limited chemical resistance of polypropylene, typical solvents such as diethyl ether, tetrahydrofuran, dichloromethane, or 1,2-dichloroethane are not recommended.^[7]

We performed a test concerning the chemical resistance of a polypropylene filament (3dkTop kindly provided by 3dk.berlin):

The filament (10.0 g) was cut in 2–5 mm parts. The parts were transferred in a flask equipped with a reflux condenser and treated with THF (50 mL) at 65 °C for 3 h. After some minutes, the polymer started to swell. After 1 h, most of the THF was absorbed by the filament. On the walls of the flask, colorless gel deposited.



Left: The cut filament before treatment with THF. **Right:** Boiling the filament in THF.



Left: After 1 h, swelling of the filament was observed. **Right:** Colorless gel deposited on the walls of the flask after cooling to room temperature.

After these experiments, we stopped our efforts to employ 3D-printed components as reactors.

Unfortunately, printing of chemically more resistant polymers (PEEK, FEP, PFA) is challenging (for PTFE, it is not possible).^[8] In the case that specially designed components offering a high chemical resistance are required, we recommend to order these components from professional 3D-printers, either made from stainless steel 316L, or titanium (both metals can be printed).

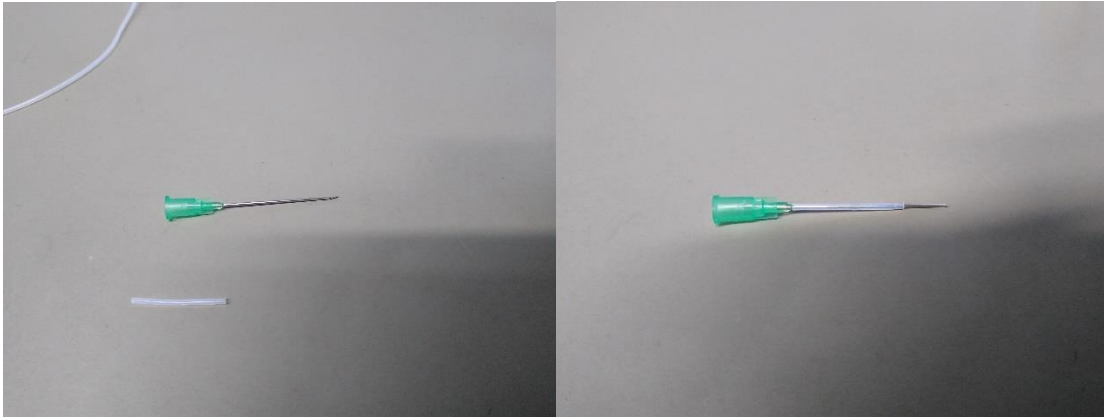
2. Construction of the Flow Platform

2.1 Hardware

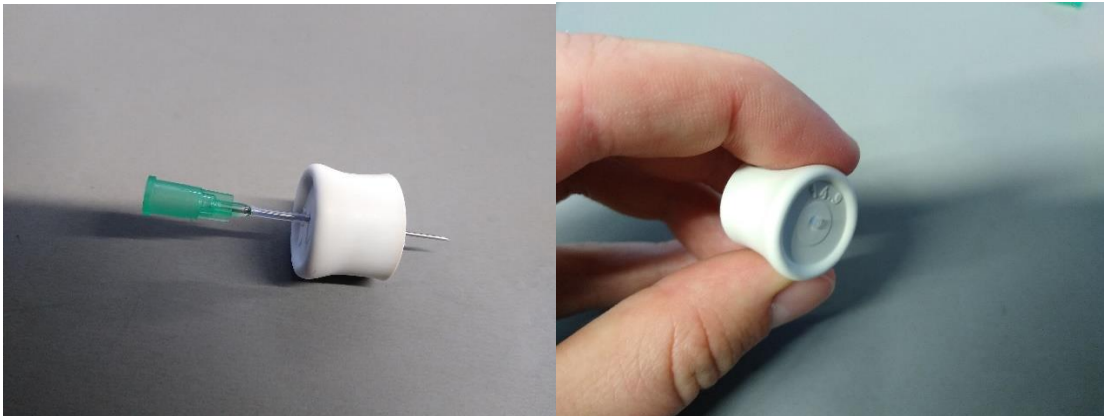
For a list of used materials, see 1.3.

Cutting of tubes and equipping tubes with ferrules and connectors

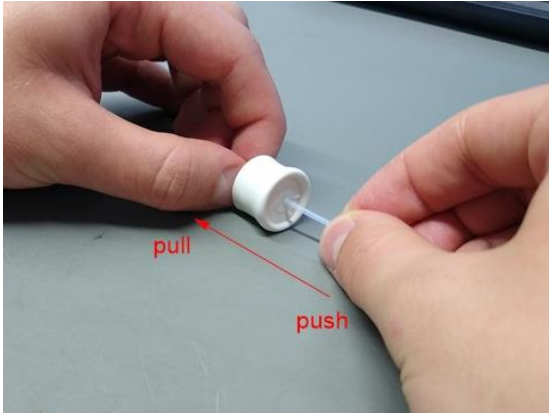
Introduction of tubes (1/16" outer diameter) through a septum.



Left: A small piece of a tube with an outer diameter of 1/16" is pulled over a short canula. **Right:** The canula equipped with the tube.

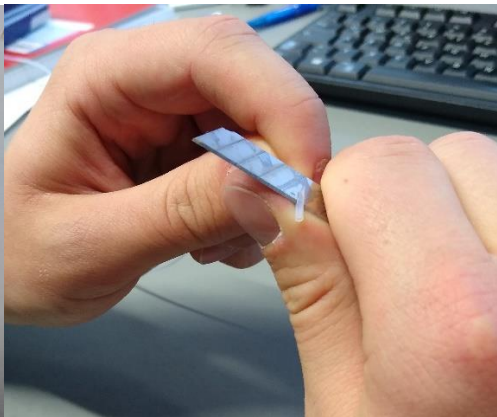
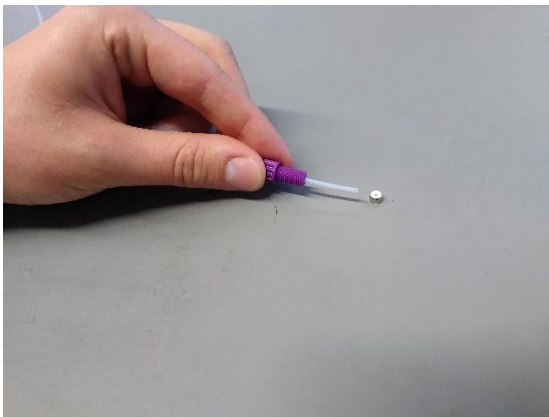


Left: The equipped canula is pierced through the septum. **Right:** The canula is removed, while the tube remains in the septum.



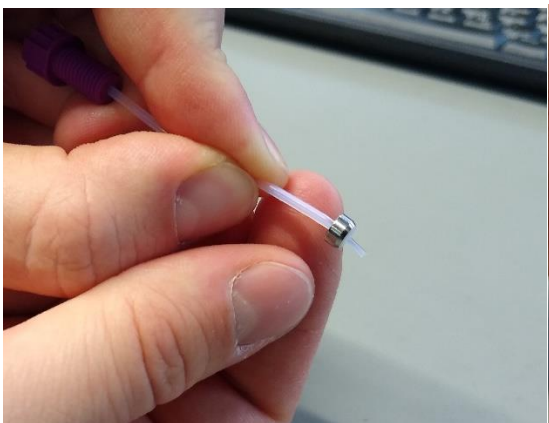
The tube to be introduced to the septum is pushed directly on the end of the pulled tube piece.

Fittings and ferrules:

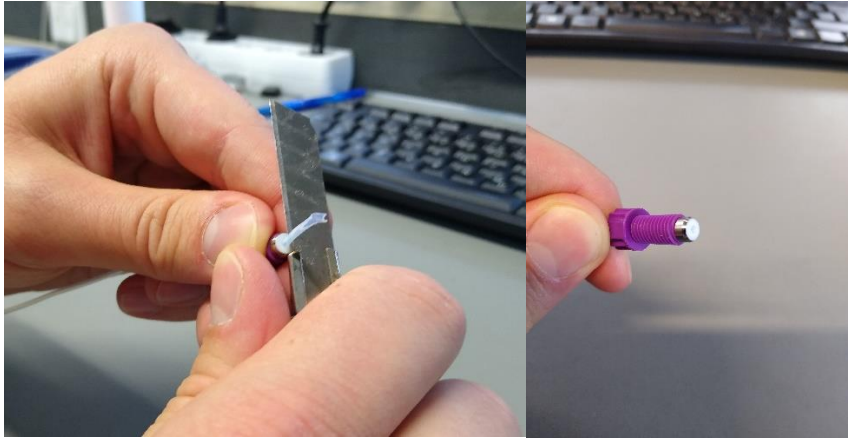


Left: The tube (outer diameter 1/16") is equipped with a fitting (flat bottom 1/4-28 UNF gripper fitting).

Right: The end of the tube is carefully cut in a slight angle.



Left: The ferrule is pulled on the tube. **Right:** The ferrule is further pulled on the tube by using a long-nose pliers.



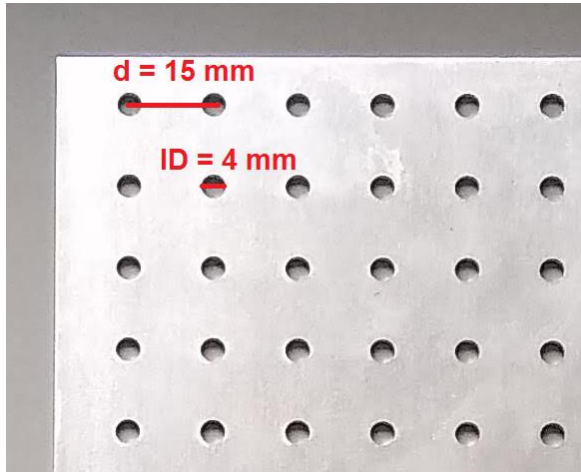
Left: The overhanging tube is cut to provide a plane surface on the end of the ferrule. **Right:** The tube equipped with fitting and ferrule.



Left: In the same way, tubes (outer diameter 1/16") are equipped with HPLC fittings (10-32 UNF fitting) and conical ferrules **Right:** A tube equipped with fitting and ferrule.

Assembly of the controller board

The controller board consists of valves arranged on a commercially available perforated plate made from anodized aluminum. The plate has a size of 500x250x1.5 mm and screwing holes with an inner diameter of 4 mm suitable for M4 screws and are assembled in a distance of 15 mm from center to center.



The perforated plate with an internal distance between each screwing hole of 15 mm and holes with an internal diameter of 4 mm for M4 screws.

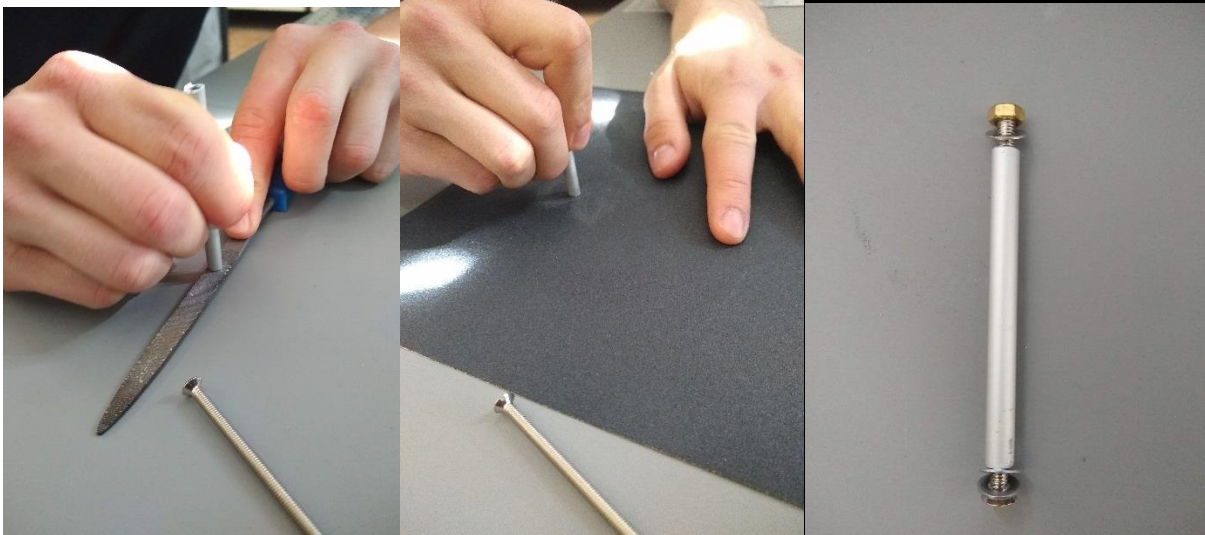
Mounting of the controller board in a fume hood

The controller board can be mounted in a fume hood using stands and cross sleeves. To do so, four holders were installed on the edges of each perforated plate. A holder consists of a M4x80 countersunk screw made from nickel plated brass, three M4 flat washers made from stainless steel, one M4 nut and a rod (outer diameter = 6 mm, inner diameter = 4 mm) made from anodized aluminum to armor the screw of the countersunk screw.



Left: Assembly of all material and tools used for the holders of the controller board. **Right:** Shortening of the aluminum rod with a jab saw.

The aluminum rod was shortened to four small rods with a length of approximately 65 mm using a jab saw. Afterwards, the ends of each rod were filed with a metal file and polished using sand paper. The ends of the rod should have a plane and smooth surface. This is important to allow direct contact between the rod and the flat washers.



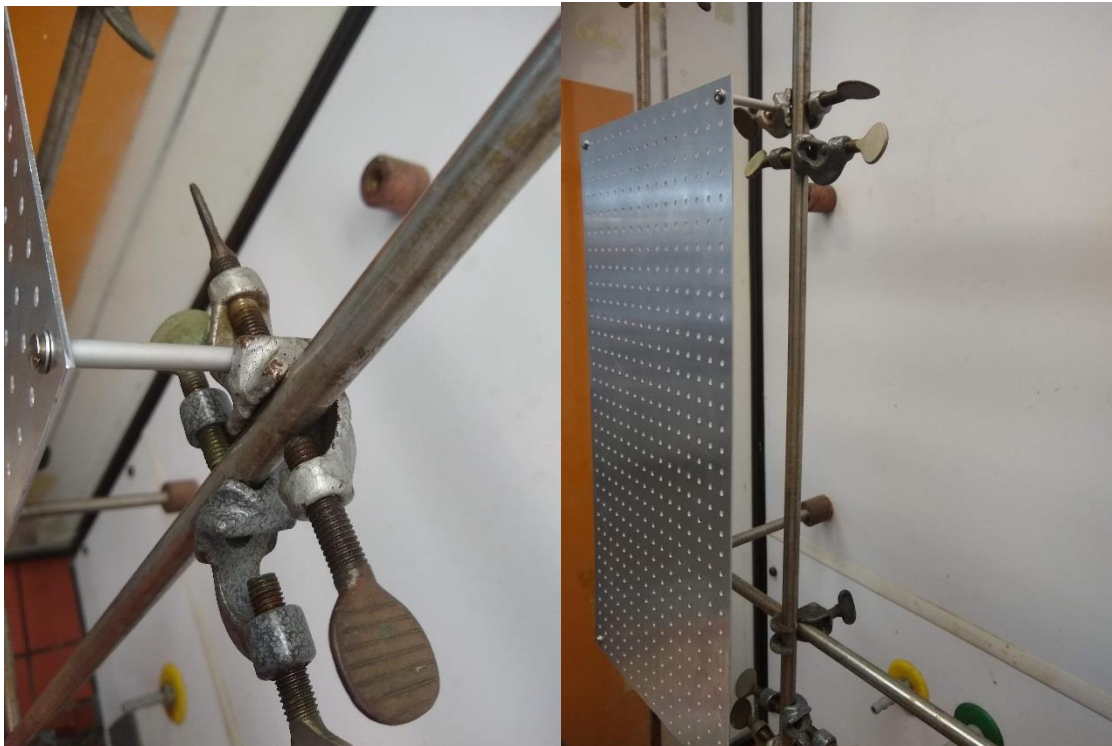
Left: Each aluminum rod was filed... **Center:** ...and subsequently polished. **Right:** Assembly of the countersunk screw, the rod, the flat washers, and the nut. The perforated plate will be mounted between the two flat washers (bottom).

Then, the holder is mounted on the perforated plate. First, the countersunk screw is equipped with one flat washer. Then, the countersunk screw is introduced through the perforated plate and the second flat washer is put on the other side to hold the perforated plate between the flat washers. The screw of the countersunk screw is covered with the aluminum rod. On the end of the screw, the third flat washer is placed, followed by the M4 brass nut to tighten the holder on the board.



Tightening of the holders on the perforated plate.

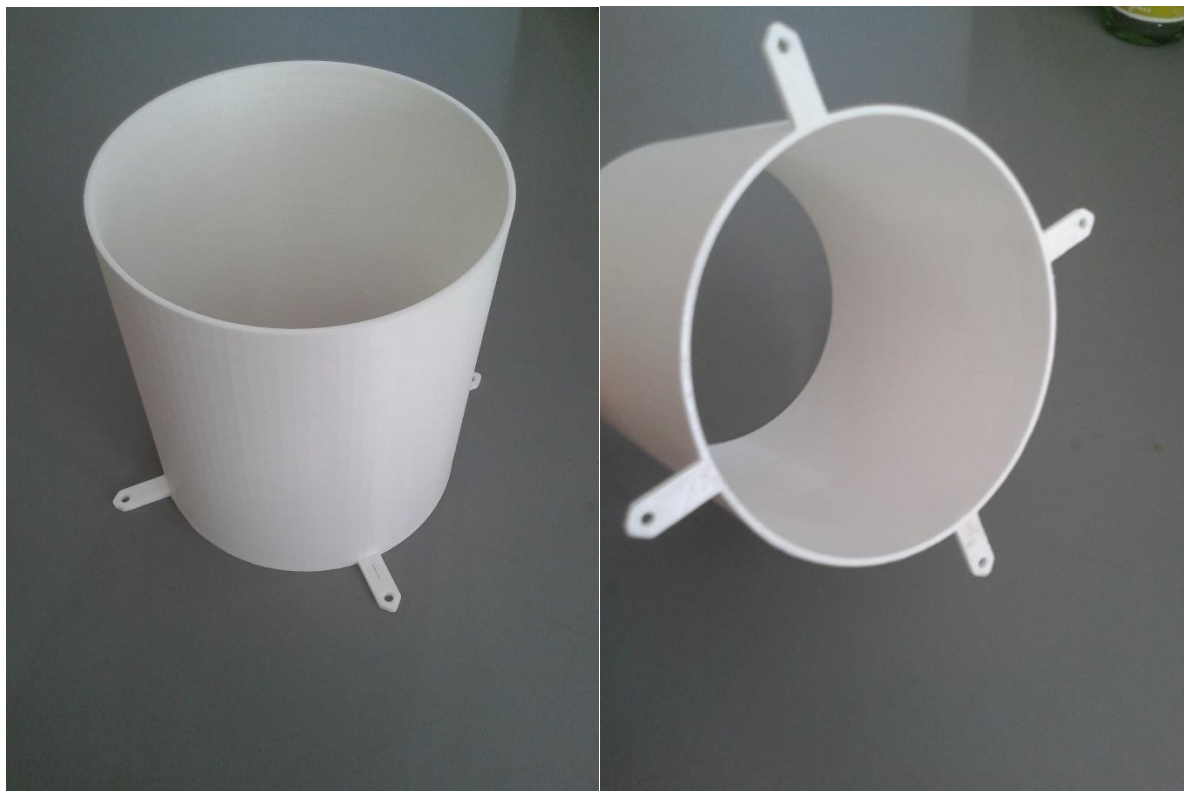
The board equipped with the four holders is then placed in a fume hood using cross sleeves. It is important to apply mechanical pressure only on the part of the holders that are covered by the aluminum rod.



Left: Mounting of the controller board in a fume hood using cross sleeves to secure the holders. **Right:** The controller board connected on four points to the stand of a fume hood.

Assembly of the photoreactor

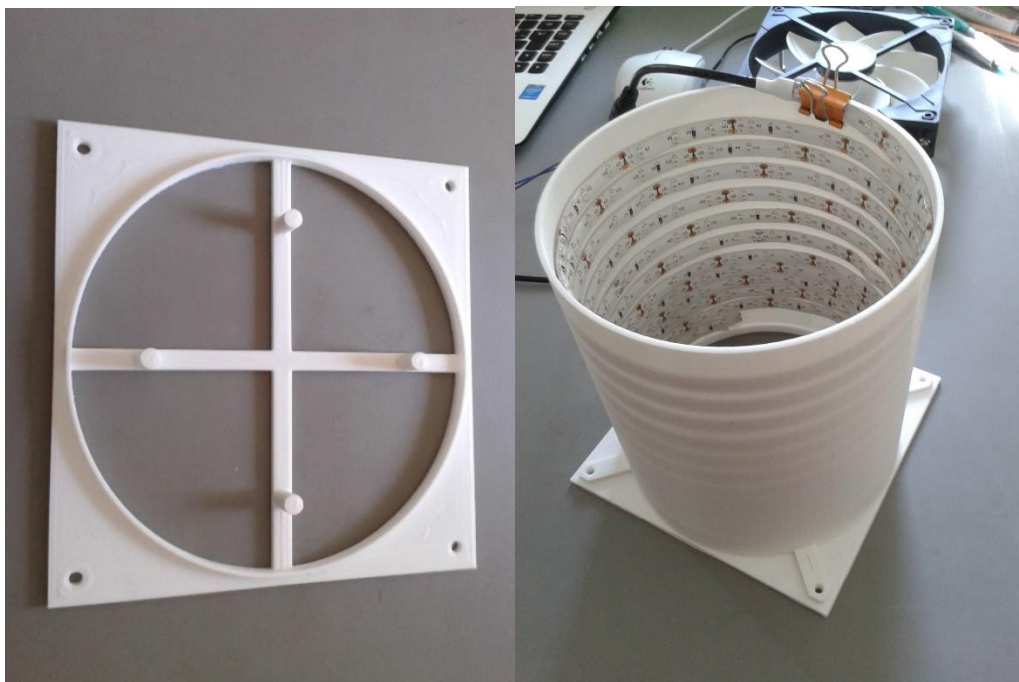
A self-made photoreactor was constructed from 3D-printed parts (white PLA, 25% infill), a 140 mm computer fan, a LED stripe (12 V, LED 2835, 385–400 nm) and FEP tube (outer diameter 1/16", inner diameter 1/32"). The 140 mm fan is used to cool both the LEDs and the reaction mixture in the FEP tube and is powered by a universal power supply.



Left: The body of the photoreactor printed from white PLA. **Right:** The bottom of the body.



Left: The LED stripe is secured with a clip on the top of the body of the photoreactor. **Right:** The LED stripe is coiled inside of the body.



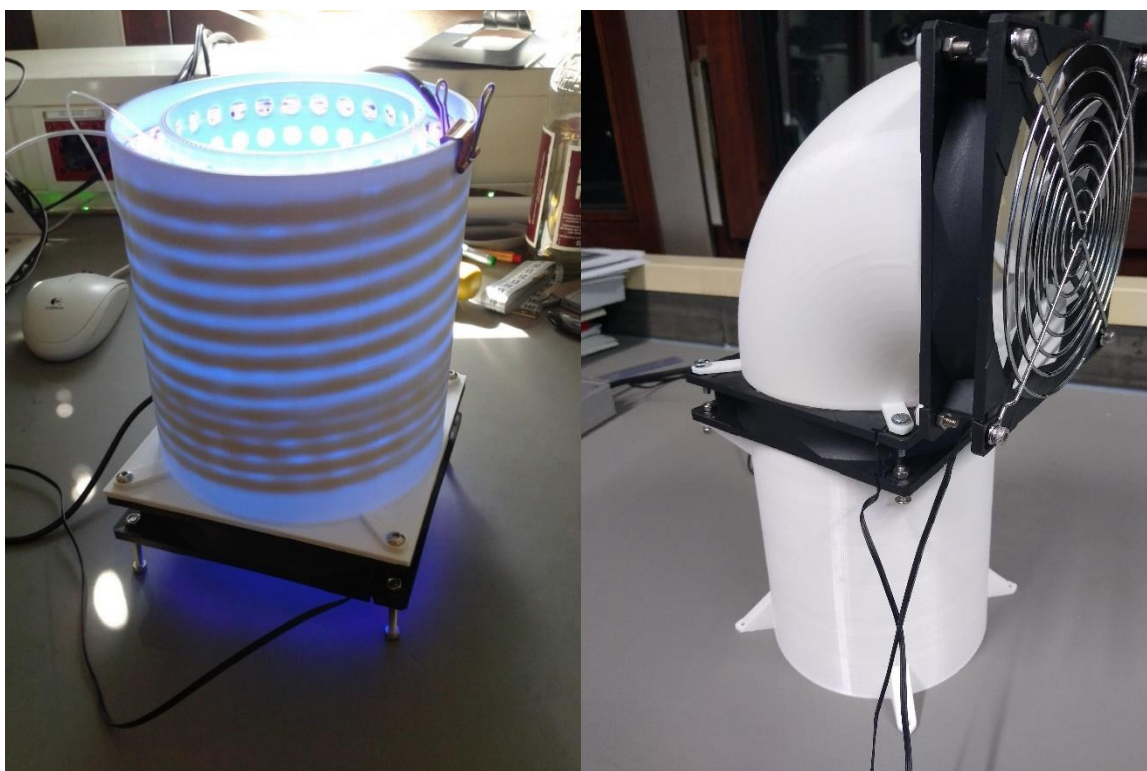
Left: The bottom plate of the photoreactor printed from white PLA. **Right:** The body of the photoreactor is placed on the bottom plate.



Left: The bottom plate and the fan are connected with a M4x16 screw. **Right:** The fan is equipped with a M4x30 screw. These screws serve as “foots” for the photoreactor to allow a proper air stream for the fan.



Left: The tube cage is equipped with FEP tube of the appropriate length. To secure the tube, it is threaded through some holes of the tube cage. When the tube is secured, the remaining tube is winded up on the tube cage. **Right:** The tube-cage equipped with 24 m ($V = 12$ mL) FEP tube.



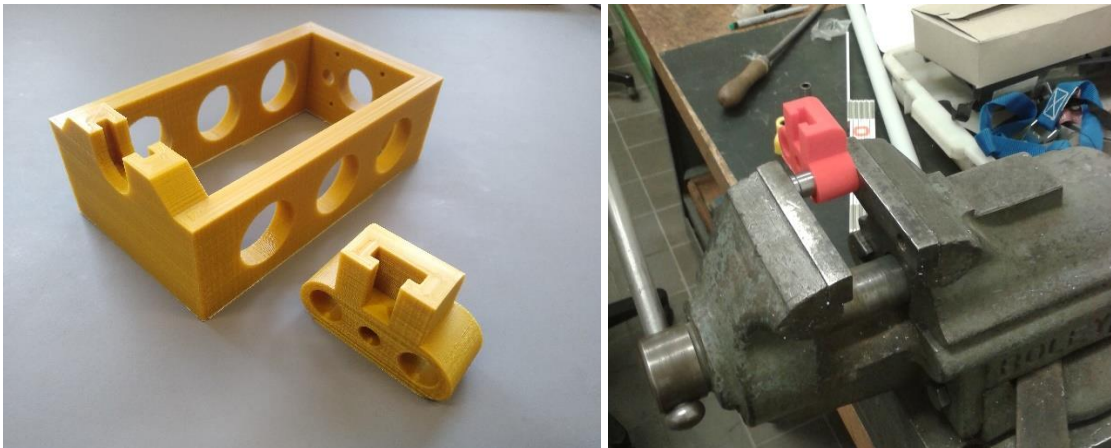
Left: The complete photoreactor. **Right:** Alternatively, the air is sucked from the ground through the photoreactor using a curved tube equipped with two 140 mm computer fans (analogously constructed as described above).

Assembly of the syringe pumps

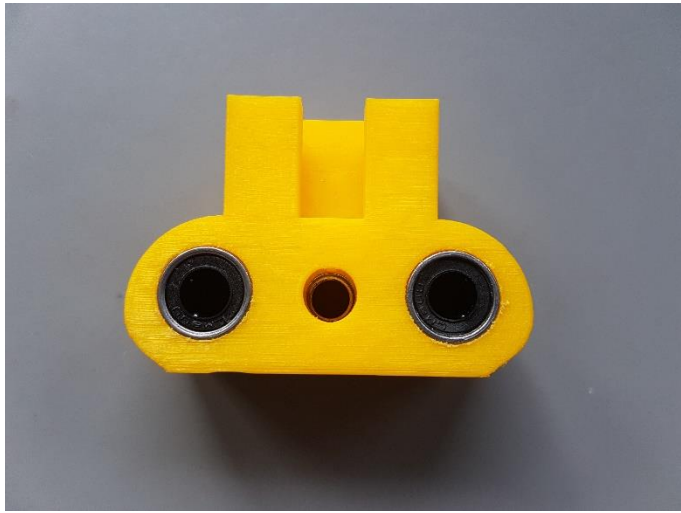
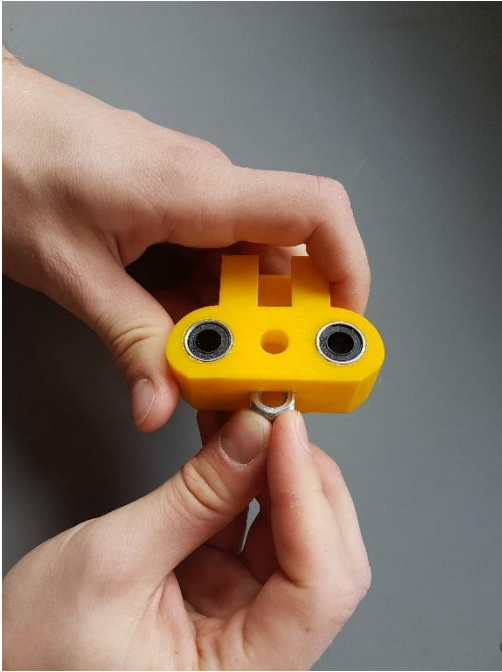
The syringe pumps consist of 3D-printed parts (PLA, 50% infill), threaded bolt, rods, linear bearings, and Nema 17 stepper motors (1.7 A, 40 Ncm) that are typically used for 3D-printers. The syringe pumps are specifically designed for 10 mL gastight glass syringes from VWR.



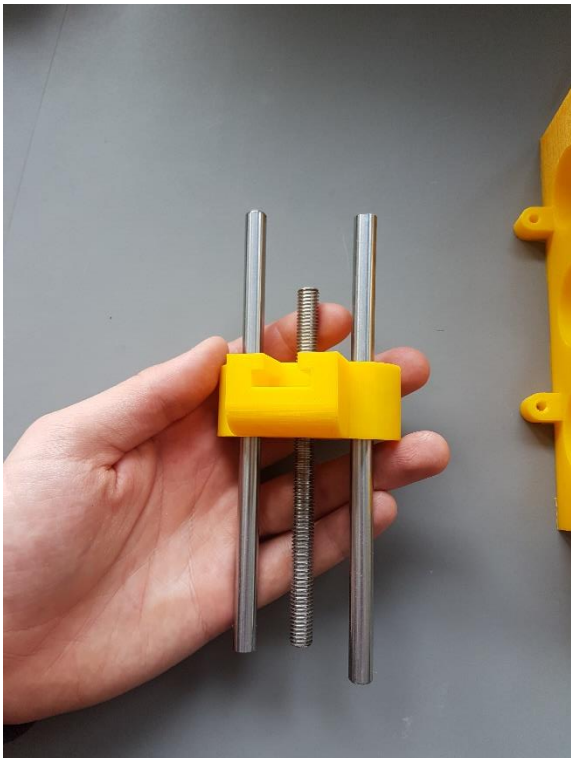
Left: Shortening of the linear rods and the threaded bolt using an angle grinder. **Right:** The ends of the linear rods and the threaded bolt are grinded using an electronic grindstone.



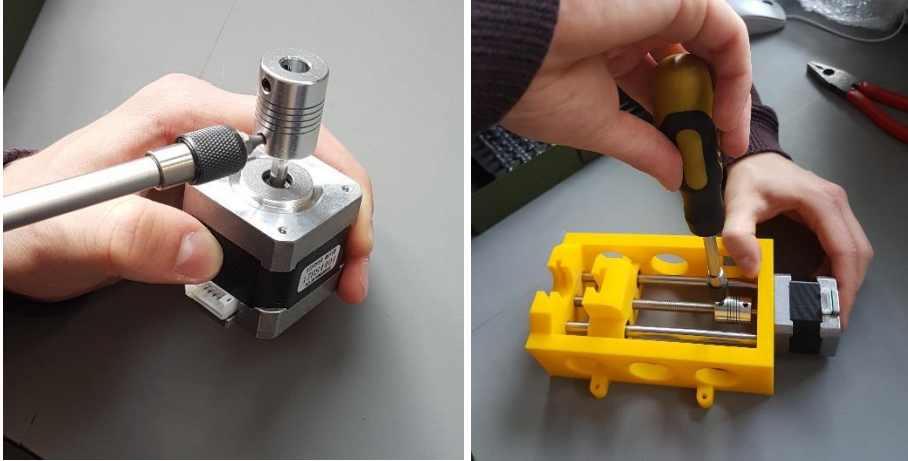
Left: The body (left) and the sledge (right) of a syringe pump. **Right:** The linear bearings are pressed in the sledge using a parallel vise. It is important, that the linear bearings are fixed precisely in the sledge. However, if the holes of the sledge are too tight and the linear bearings are pressed with too much pressure, the sledge can break. In this case, the holes of the sledge should be polished with a file or sandpaper before introducing the linear bearings.



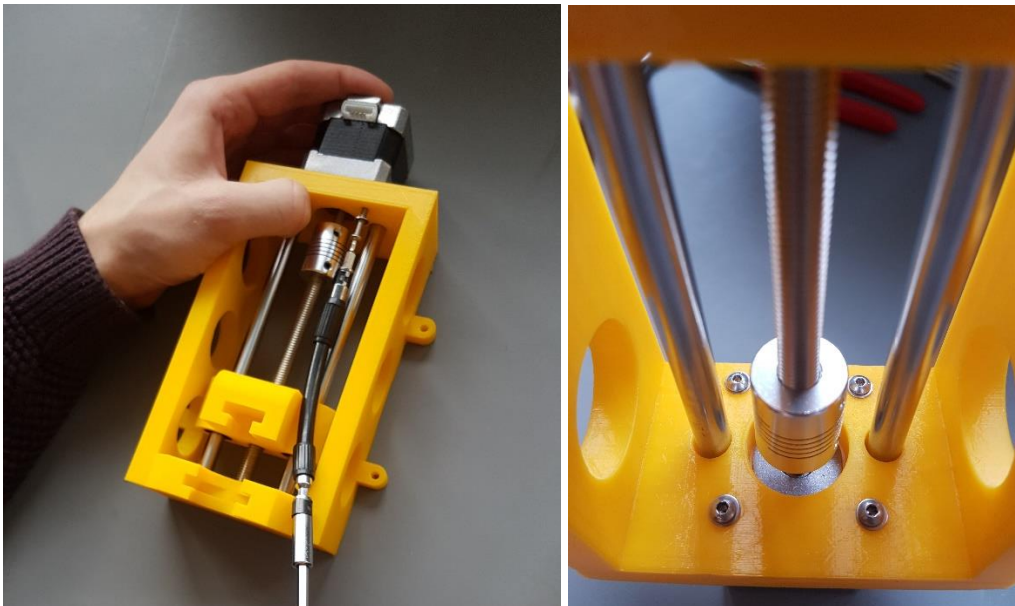
Left: The sledge is equipped with a M8 hexagonal nut. **Right:** The sledge with the linear guides and the hexagonal nut in the middle.



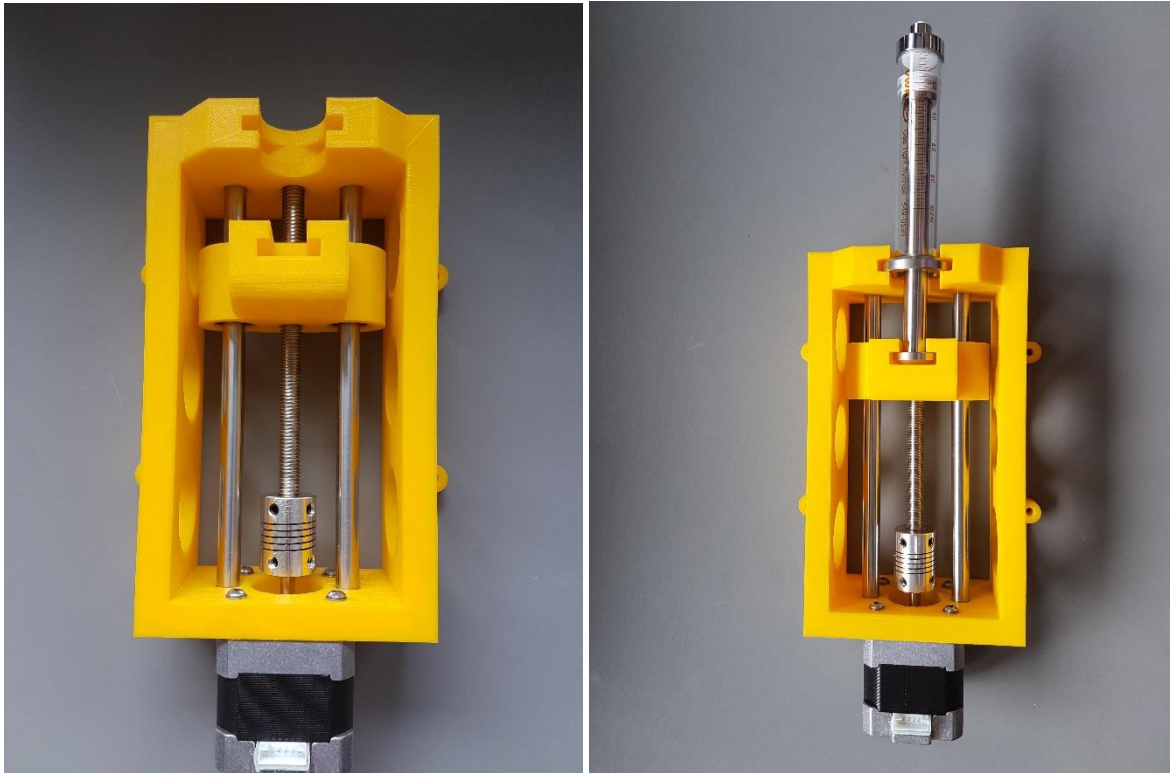
Left: The sledge with the linear rods and a M8 threaded bolt in the middle. Both the threaded bolt and the linear rods were shortened by a jab saw. **Right:** The sledge placed in the body of the syringe pump.



Left: The stepper motor is equipped with a flexible shaft coupling. **Right:** The threaded bolt and the stepper motor are connected using the flexible shaft coupling.



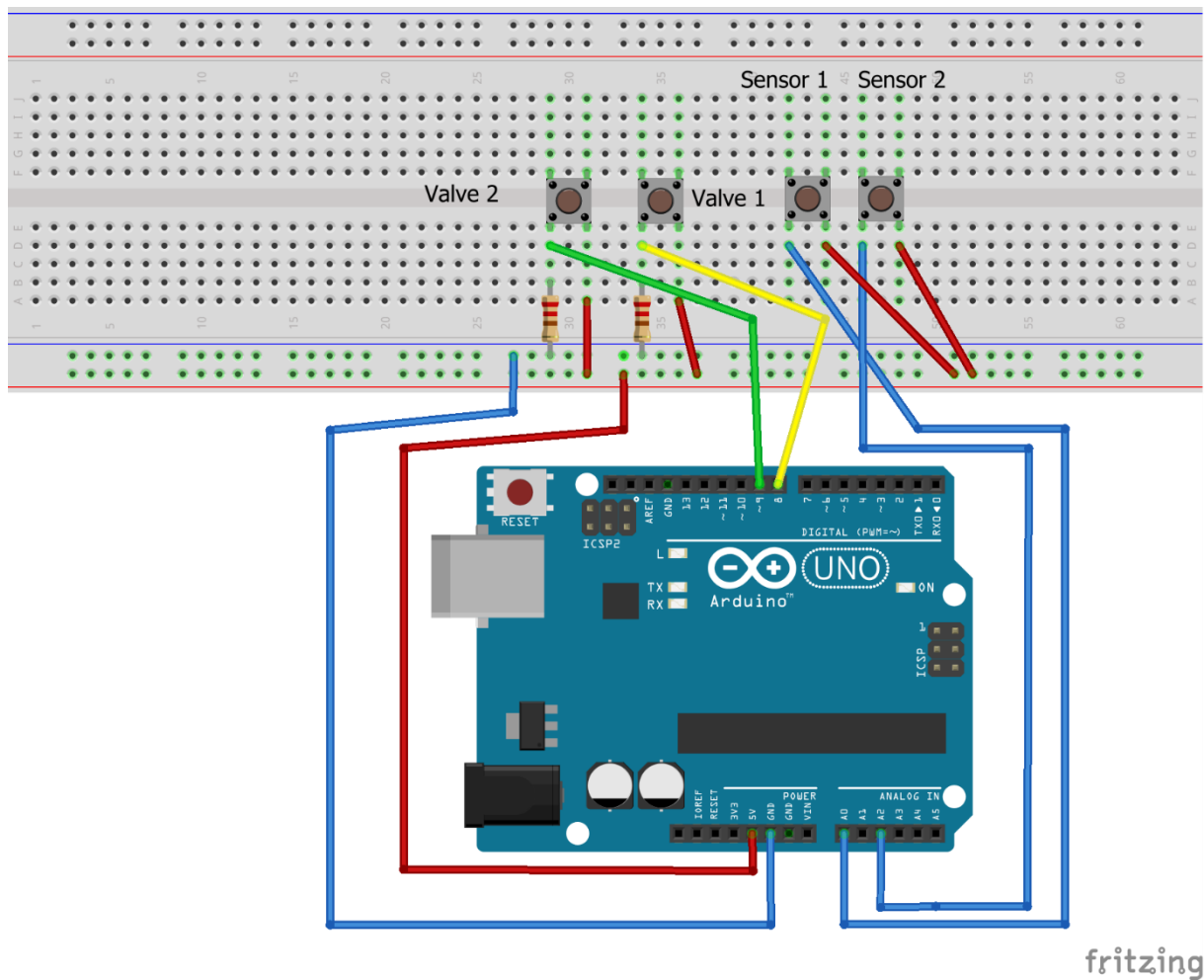
Left: The stepper motor is mounted with a M3x12 screw and a M3 washer. **Right:** The stepper motor mounted with four screws.



Left: The complete syringe pump. **Right:** The syringe pump equipped with a gastight glass syringe.

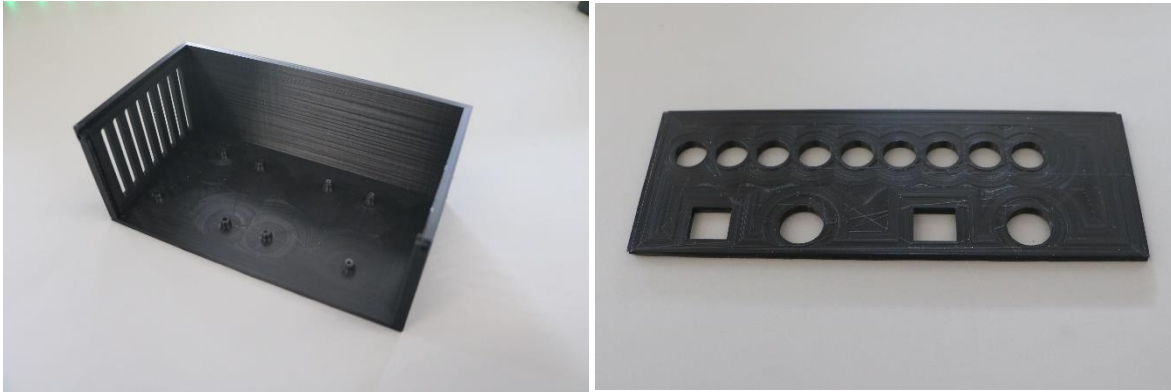
Electronic configuration of the Arduino

The MFC's and the Arduino Uno are connected to a computer via serial ports. For time reading, a circuit board was manufactured. Resistors with 10 k Ω or more are used.

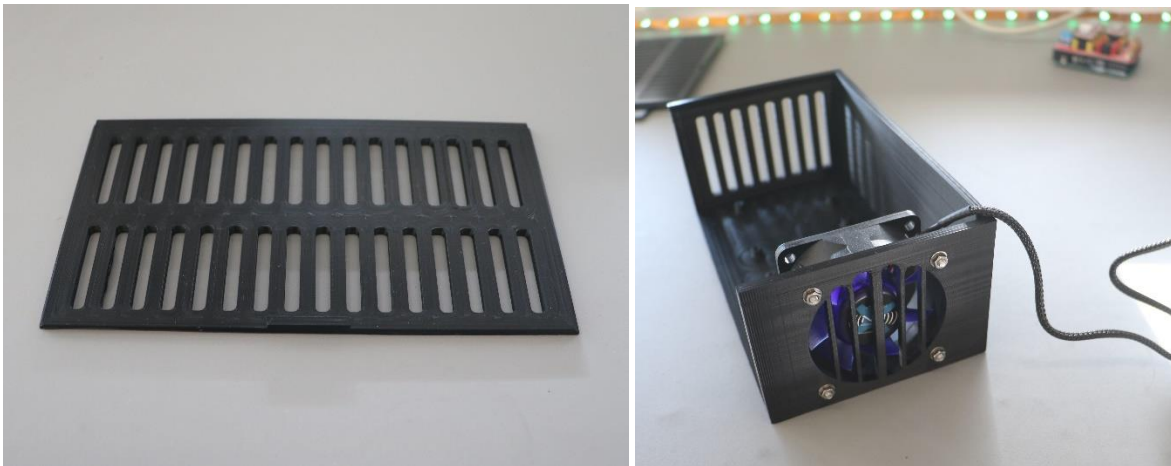


Assembly of the controller box

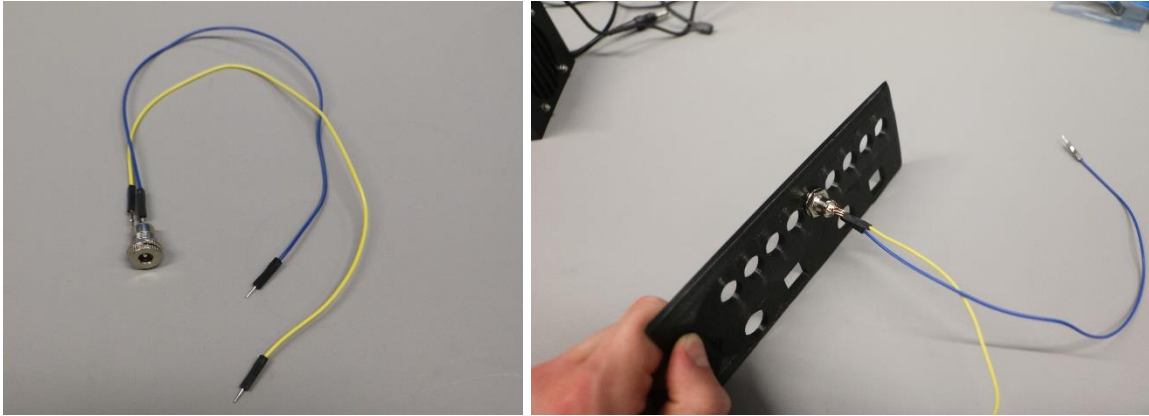
The microcontrollers are assembled in a 3D-printed controller box (PLA, 50% infill) to protect the electronics. One microcontroller is connected to a CNC shield with three stepper drivers that controls up to three syringe pumps. Since the stepper drivers heat up, they are cooled with a 60 mm computer fan from the side.



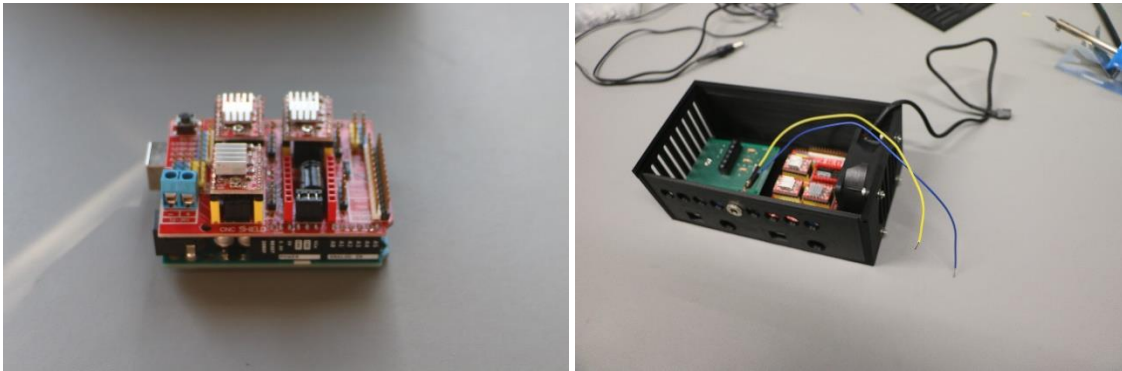
Left: The 3D-printed case of the controller box. **Right:** The 3D-printed side cover.



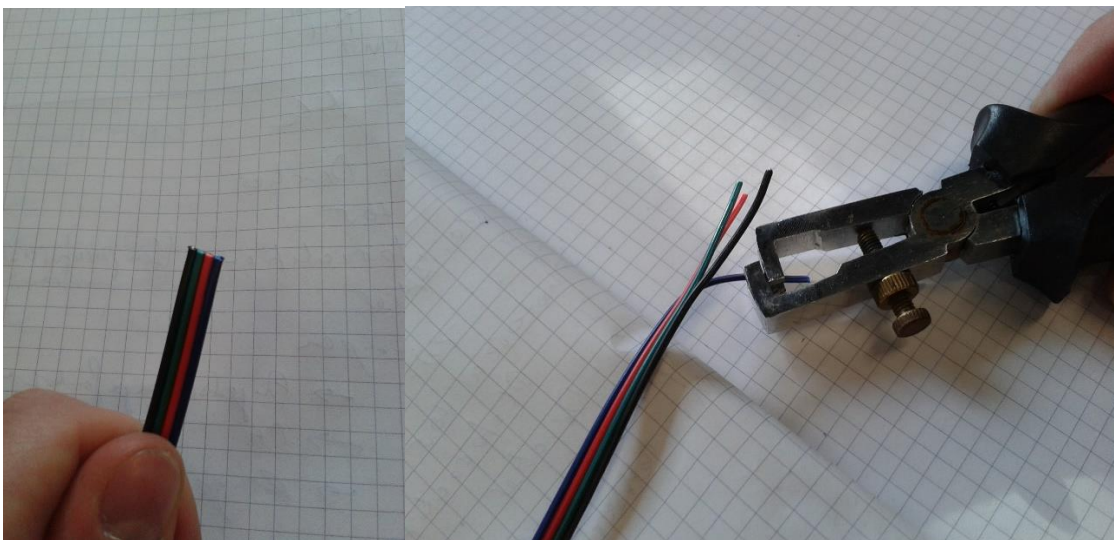
Left: The 3D-printed top cover. **Right:** The case is equipped with the 60 mm fan using M3x12 screws with washers.



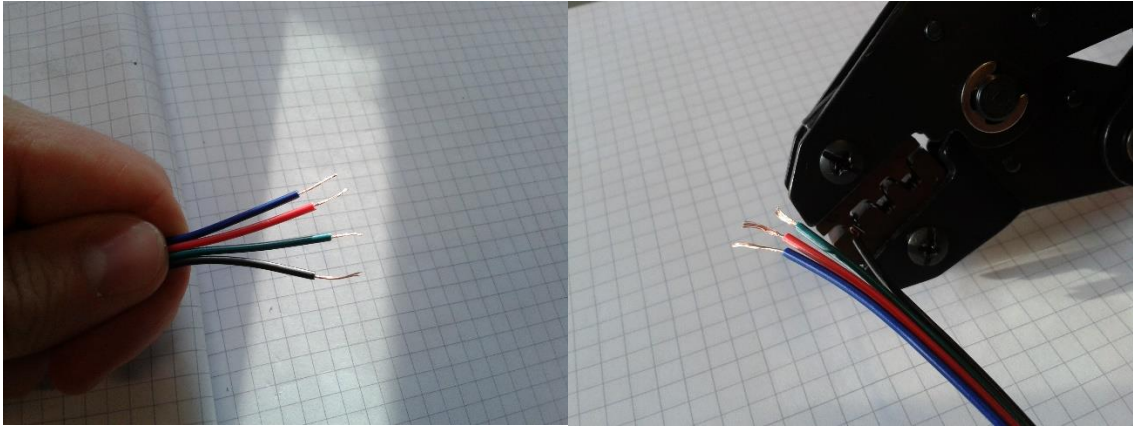
Left: A coaxial power supply is equipped with two wires. **Right:** The coaxial power supply is mounted on the side cover.



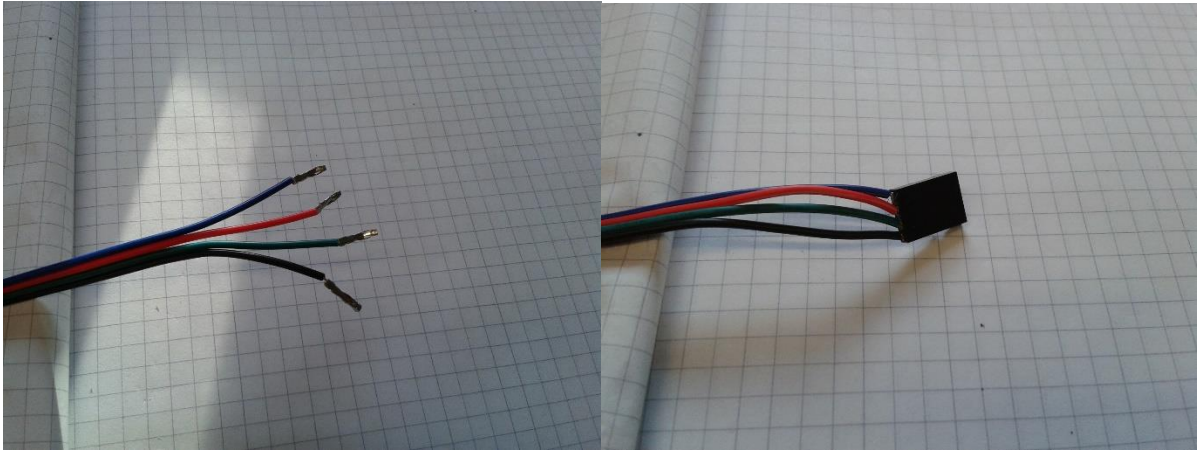
Left: An Arduino Uno equipped with CNC shield and three stepper drivers (positioned at X,Y,Z; A is free). **Right:** Both Arduinos are mounted in the case using M3x6 screws. The side cover is attached. Typically, Arduinos are connected with wires using crimp connections. Therefore, wires need to be terminated with crimp connectors. Detailed instructions can be found online.



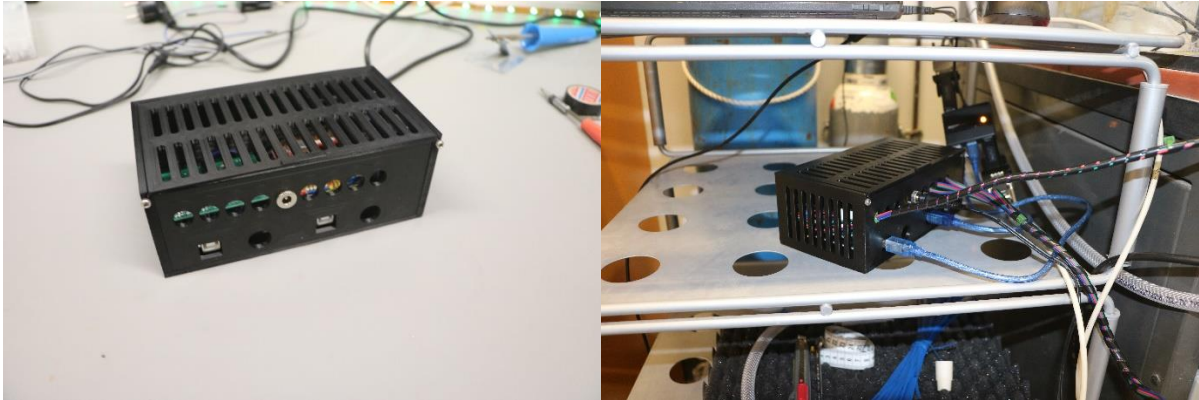
Left: A 4-conductor cable. **Right:** The wires are skinned using a wire stripper.



Left: The stripped 4-conductor cable. **Right:** The ends of the stranded wires are terminated with crimp connections using a crimp clamp.



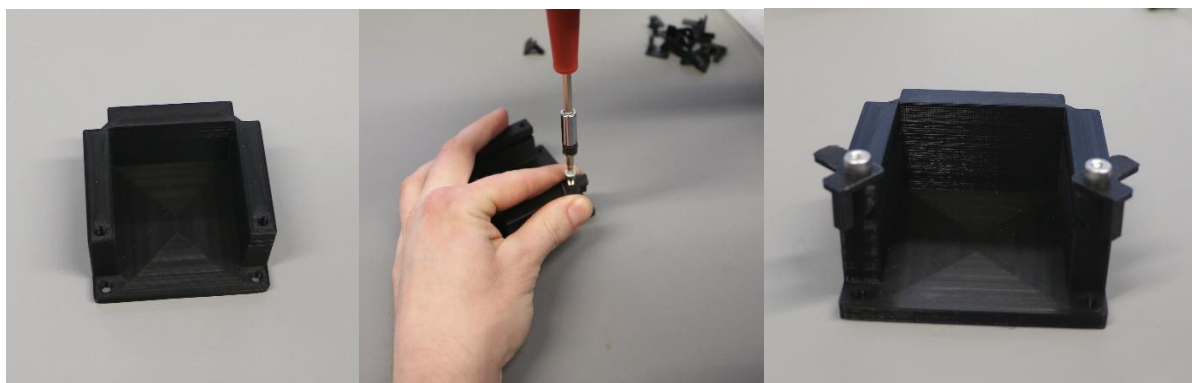
Left: The wires terminated with crimp connectors. **Right:** The crimp connectors are introduced in a Dupont connector.



Left: The complete controller box. **Right:** The controller box equipped with cables.

Assembly of the modular valve system

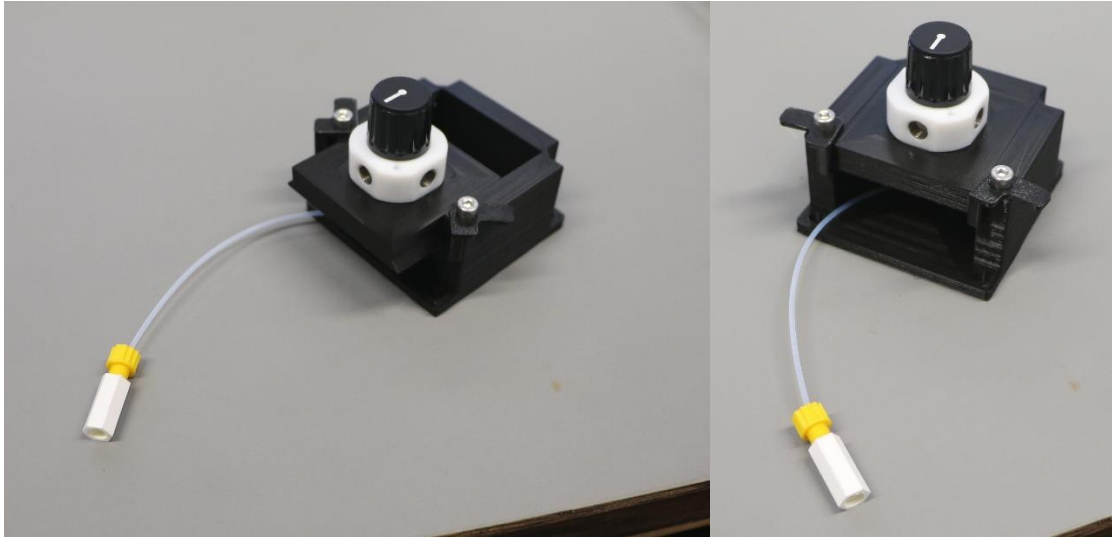
It is practical, when all valves can be easily disconnected from the controller board. In this way, cleaning of the valves or changing tubes becomes much easier. To allow as much flexibility as possible, we designed a modular valve system. Thus, the low pressure valves and the HPLC injection valves are mounted on 3D-printed mounts having a unified size. On the controller board, 3D-printed sockets are secured. The mounts of the valves can be placed in the sockets and further secured by using two 3D-printed clamps on the top of each socket.



Left: The 3D-printed socket. **Center:** The 3D-printed hooks are secured using M4 screws. **Right:** The socket equipped with two hooks.



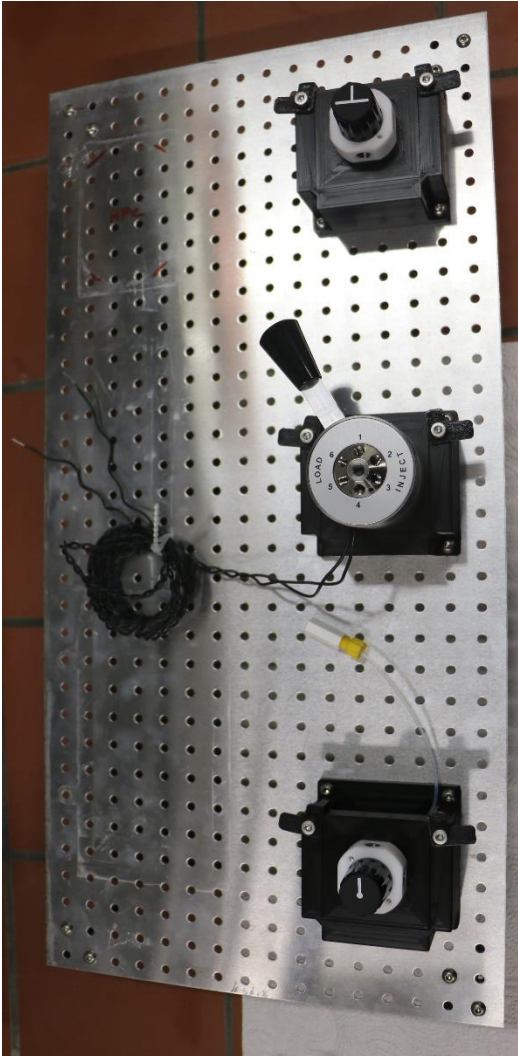
Left: The low-pressure valves are secured on the low-pressure valve mounts using M3 screws. **Right:** The HPLC injection valves are secured on the corresponding mounts using M4 screws.



Left: A mount equipped with a low pressure valve is introduced to the socket. **Right:** The mount is secured using the hooks.



Left: A small collection of the three different valves placed in the valve sockets. **Right:** The sockets are mounted on the controller board using M4 screws.



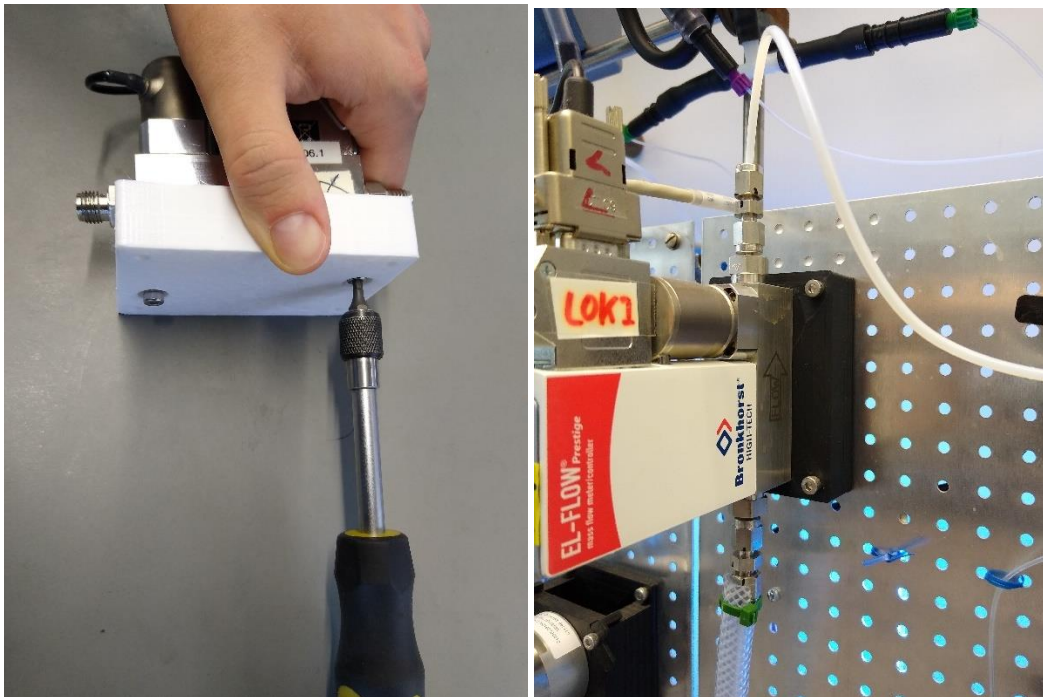
The controller board equipped with three sockets and valves.

Mounting of the MFCs

3D-printed mounts for the MFCs were designed to attach the MFCs to the controller board.



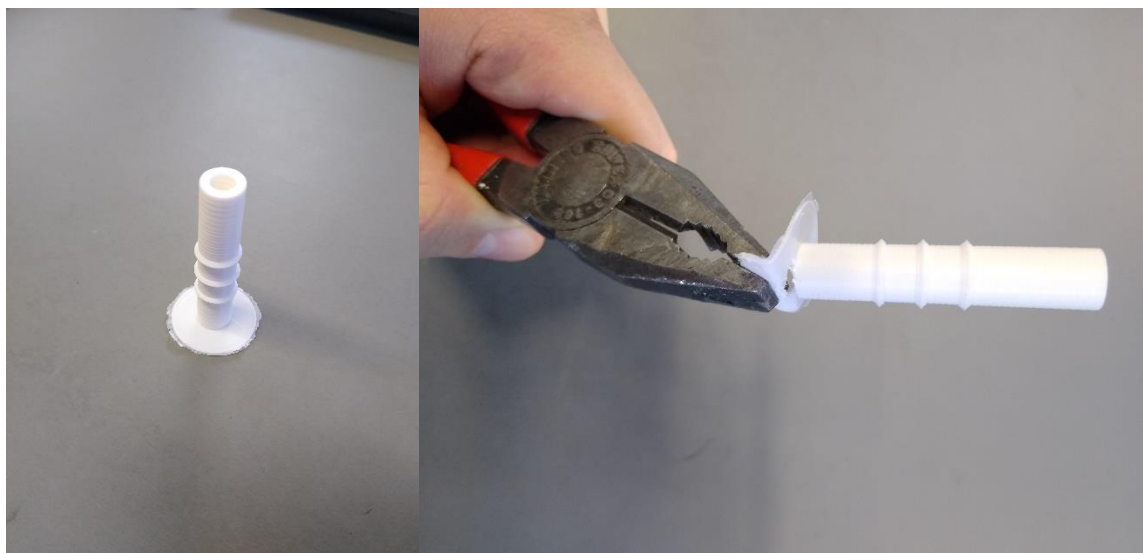
Left: The mount is designed to be connected with the MFC from the one and with the controller board from the other side. **Right:** M4x14 screws are screwed in the mount.



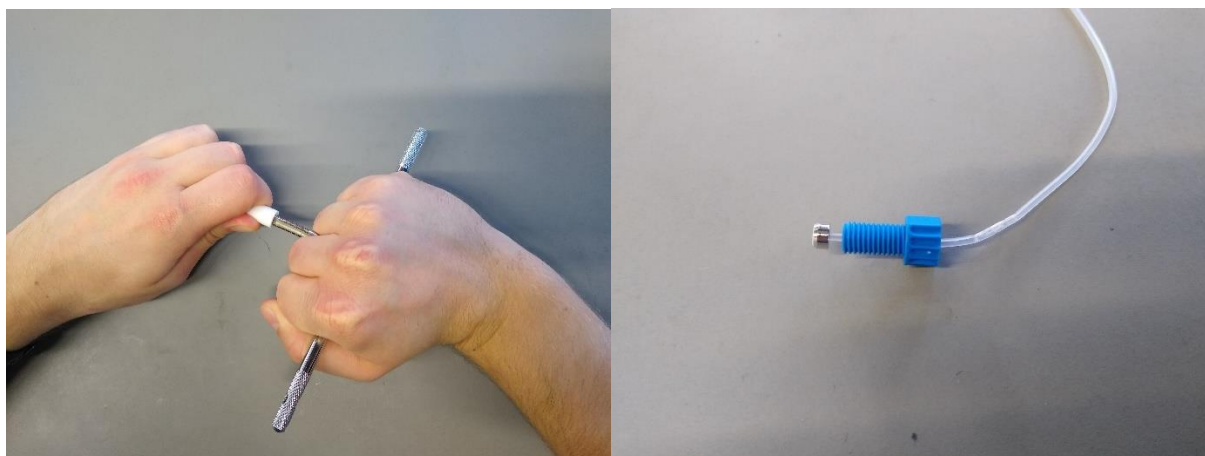
Left: A MFC is secured to the mount. **Right:** A fully equipped MFC secured via the mount to the controller board.

3D-printed connectors between the flow platform and a Schlenk line

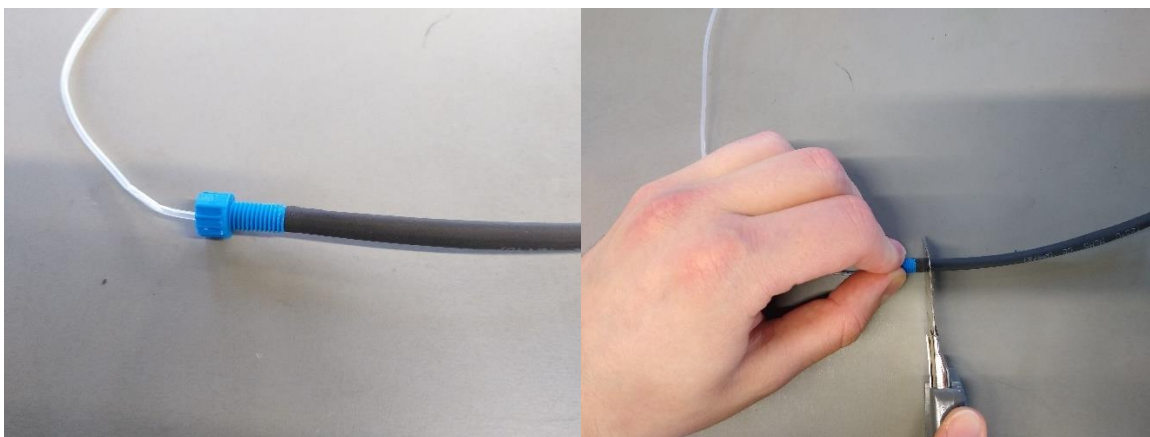
To connect the flow platform with a standard laboratory Schlenk line, 3D-printed connectors (PLA, 100% infill) were designed connecting a pipe nozzle (10 mm diameter) on one side and a 1/4-28 UNF thread on the other side. To enable tight contact between the connector and a 1/4-28 UNF fitting, a small piece of shrink tube is employed as seal.



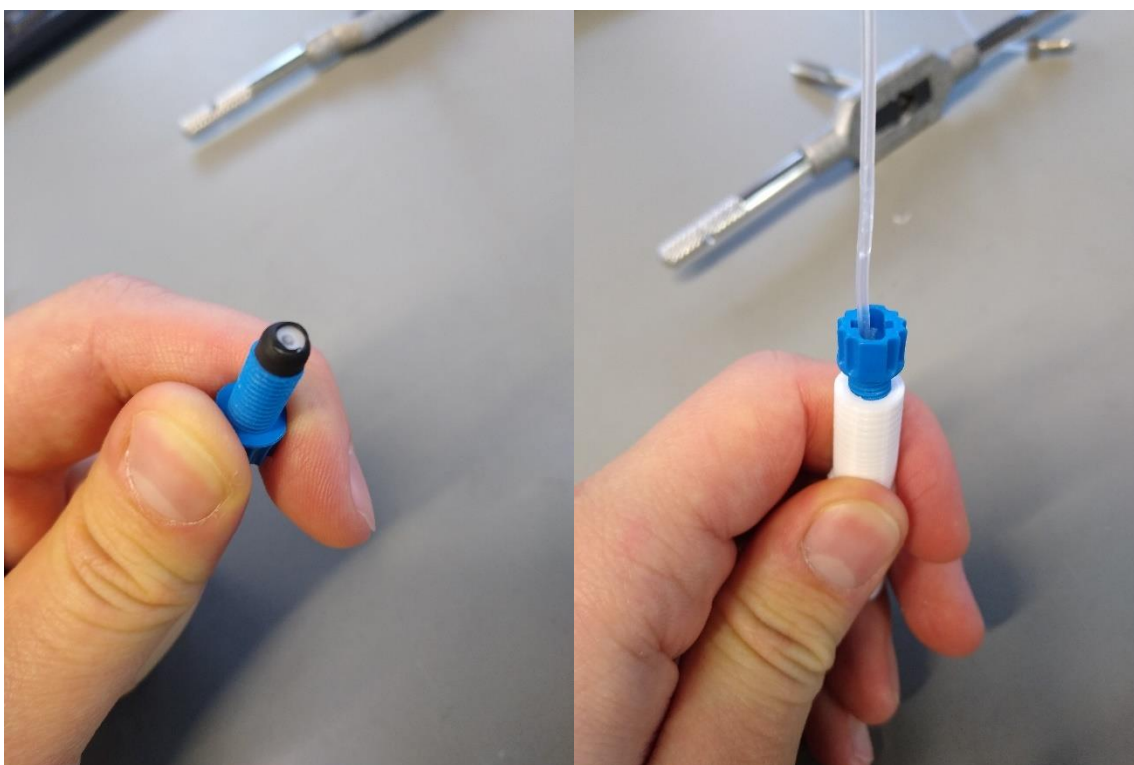
Left: A connector printed on a small raft. **Right:** The raft is removed using pliers.



Left: Using a 1/4-28 UNF screw tap, a thread is drilled. **Right:** A tube equipped with a 1/4-28 UNF fitting.

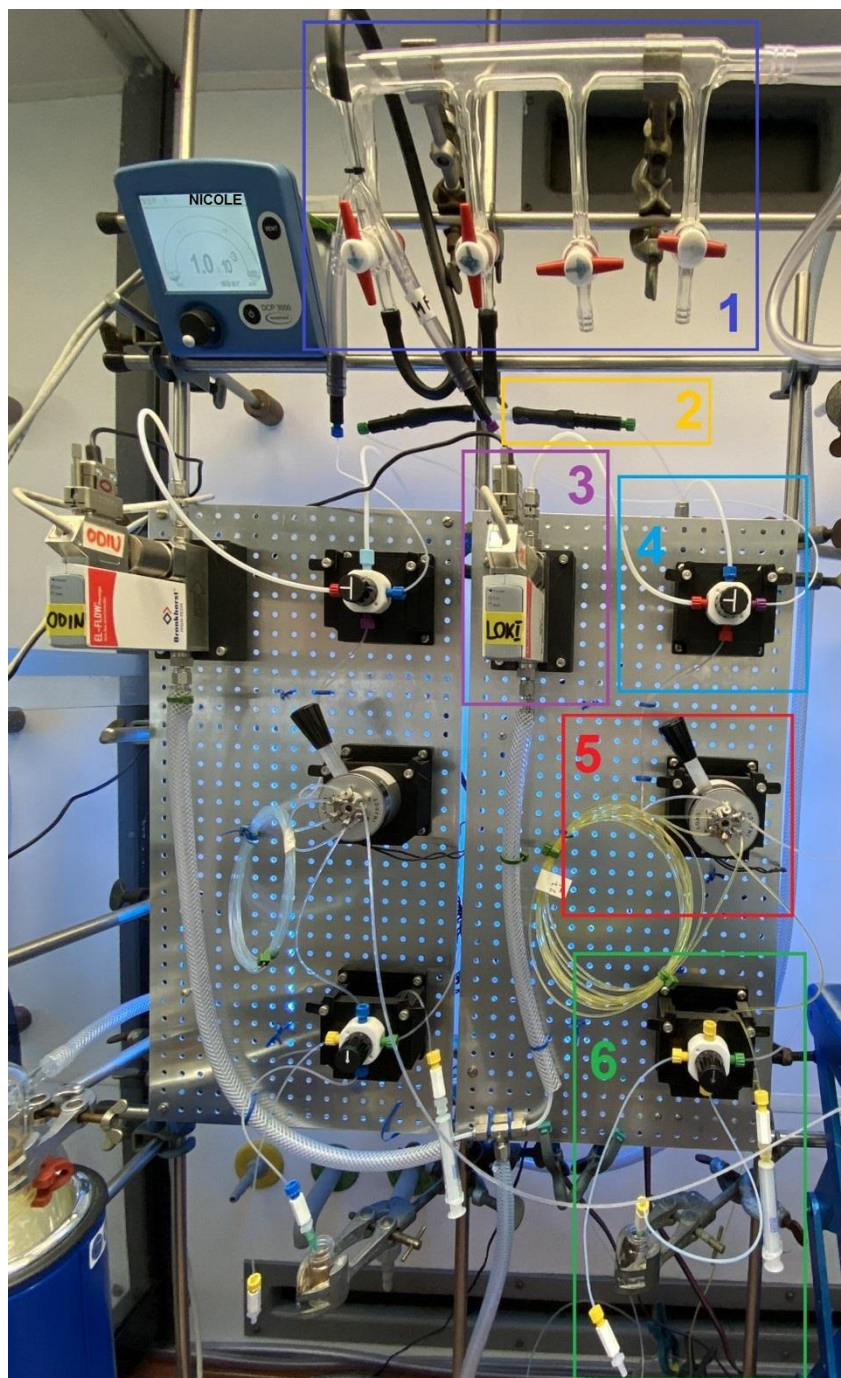


Left: The ferrule is covered with a shrink tube of appropriate size. **Right:** The shrink tube is shortened using a cutter and shrunk employing a heat gun.



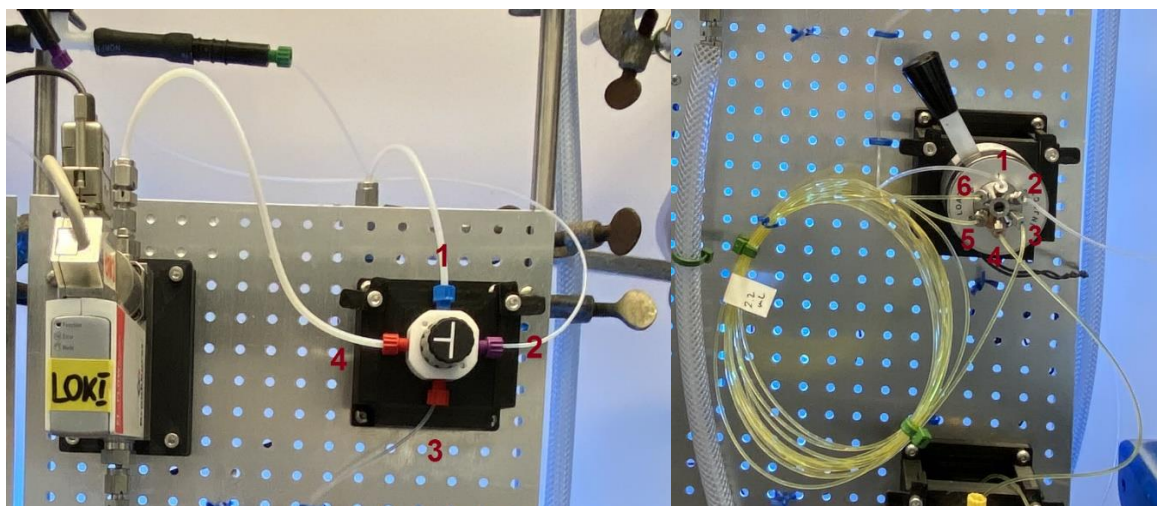
Left: The ferrule equipped with a small piece of shrink tube that serves a seal between the connector and the fitting. **Right:** The connector equipped with the fitting providing a vacuum tight connection between a Schlenk line and typical flow tubes.

The complete flow platform:

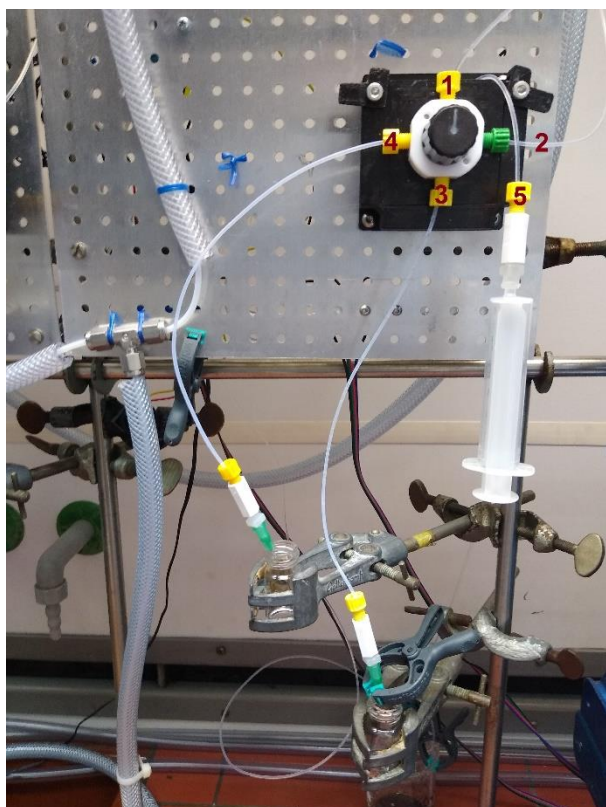


The complete flow platform consisting of two setups. **1:** Schlenk line. **2:** Connector between Schlenk line and flow platform. **3:** MFC. **4:** Vacuum/argon module. **5:** Reagent module. **6:** Inert sample loading module.

Detailed pictures



Left: The vacuum/argon module. 1: To pressure sensor. 2: To Schlenk line. 3: To HPLC injection valve. 4: To MFC. **Right:** The reagent module. 1: To the vacuum/argon module. 2: To reactor. 3: To sample loop I. 4: To the inert sample loading module. 5: To waste. 6: To sample loop II.



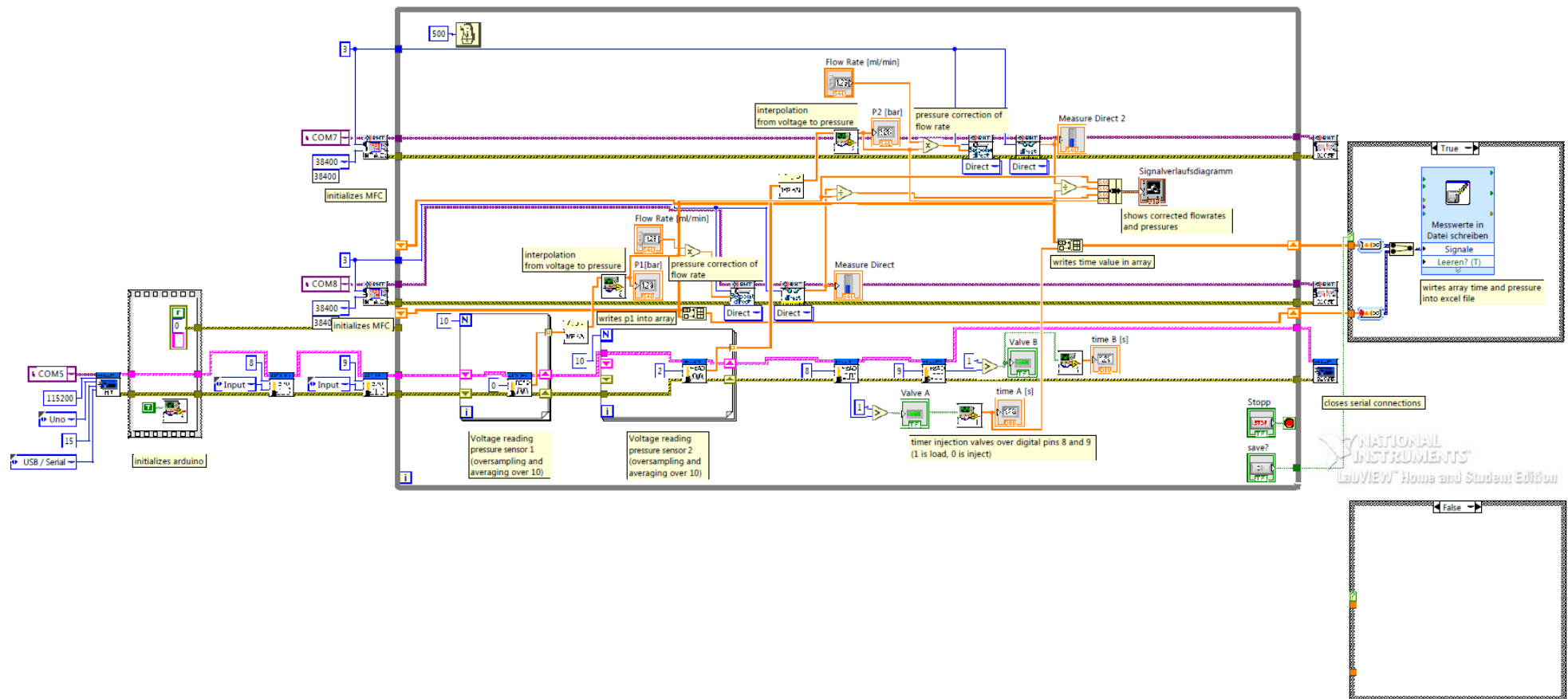
The inert sample load module. 1: To HPLC injection valve. 2: To Schlenk line. 3: To solution I. 4: To solution II. 5: To syringe (the tube is connected on the backside of the 5-port 5 positions valve).

2.2 Software

2.2.1 LabVIEW Software

In order to establish a defined flow rate, the MFCs are adjusted by a LabVIEW-based software. The mass flow rate of the MFC must also be correlated with the measured pressure in order to yield the desired volumetric flow rate. Thus, the software also reads the pressure at each individual MFC via analog pressure sensors that are connected to an Arduino Uno unit. Furthermore, the HPLC injection valves are also connected to the Arduino and act as a trigger to start a stopwatch. The Arduino® is implemented into the LabVIEW software by using the graphical LabVIEW interface for Arduinos.

The Bronkhorst MFC's are implemented into the software by using the Flow-BUS VI's developed by Bronkhorst. The program is depicted below and is available for download at <https://www.ni.com>.



2.2.2 Arduino Script for Controlling the Syringe Pumps

The following script is a modified version of a script provided by Michael B. Spano and can be copied in Arduino IDE (free of charge available at <https://www.arduino.cc/>). It uses Mike McCauley's AccelStepper library which can be downloaded for free via Arduino IDE.

```
////////////////////////////////////
//      Freie Universität Berlin      //
//      Merlin Kleoff, Johannes Schwan  //
//      October/2020                   //
//                                     //
//                                     //
//      Based on a script by:          //
//      University of North Carolina Greensboro //
//      Croatt Research Group          //
//      Division of Flow Chemistry     //
//      Michael B. Spano               //
//      brzusa@gmail.com               //
//      March/2016                     //
////////////////////////////////////
// Go to our homepage for info on how to build your own system //
//      https://chem.uncg.edu/croatt/flow-chemistry/ //
//                                     //
////////////////////////////////////DESCRIPTION OF THIS CODE////////////////////////////////////
//                                     //
// This program controls 3 syringe pumps simultaneously with the //
// aid of Mike McCauley's AccelStepper library. //
//                                     //
// The pumps can be controlled via a USB connection to the arduino //
// and sending commands via the Serial Monitor ( ctr + shft + m ). //
//                                     //
////////////////////////////////////COMMANDS (USE SERIAL MONITOR)////////////////////////////////////
// * The pound symbol (#) represents an arbitrary number //
// * The percent sign (%) represents a number from 1 to 6 //
//                                     //
// #,#,#,#,#,# - Sets the flowrate for all 6 pumps. //
// set%]###] - Sets the current volume that is in stepper[%] //
```



```

// reset] - Makes the current position correspond to 0mL      //
// volumes] - Returns how many mL are in the syringe          //
// diameter%]##] - Changes the internal diameter of syringe % //
// help] - Displays SPM, Diameters and Volumes               //
//                                                             //
////////////////////////////////////////////////////////////////

```

#include <AccelStepper.h> //Includes the functions found in the AccelStepper library used to control the stepper motors.

AccelStepper stepper[6]; // Six instances of the AccelStepper are instantiated with their default constructors.

String inputString = "", command;

boolean stringComplete = false, protect = false, bounce = false;

boolean rebound = false, sufficientSolvent, sufficientReagents;

//

int i;

float ThreadDensity = 0.8; // Thread density of lead screw, Unit: [Revolutions per millimeter]. This can be changed if a different lead screw was used to build the pumps.

float stepAngle = 0.1125; // This is the stepper motor step angle.

float Position[7];

float position1, position2, position3, rate1, rate2, stoich1 = 1.0, stoich2 = 1.0;

float Diameter[7] = { 14.5,14.5,14.5,14.5,14.5,14.5}; // The default value for syringe diameter is 20.0mm

float commandval;

float Rate[7];

float Limit[7];

int commaIndex[6];

int bracketIndex[3];

unsigned int startT, nowT;

float spm[7]; // spm is a acronym for 'Steps Per Milliliter'

// spm is calculated during void setup() and will differ based on

// Diameter, ThreadDensity and StepAngle

//

```

void setup() {
  startT = millis();
  Serial.begin(9600);
  inputString.reserve(50);
  for(i=0; i<3; i++){ // The instances of AccelStepper are constructed as DRIVER on pins 2,3; 4,5; 6,7;
8,9; 10,11; 12,13.
  stepper[i] = AccelStepper(1,2+i,5+i);
  stepper[i].setMaxSpeed(4000);
  stepper[i].setMinPulseWidth(20);
  stepper[i].setEnablePin(8);
  stepper[i].disableOutputs();
  spm[i] = (ThreadDensity*(360/stepAngle))/(3.1415*square(Diameter[i]/2.0)/1000.0);
  // ThreadDensity[revolutions/mm]*200[steps/revolution]/{Pi*r^2/1000}[mL/mm}
  }
}
/////////////////////////////////////////////////////////////////
void refreshPositions(){
  for(i=0; i<3; i++){
    Position[i] = stepper[i].currentPosition();
  }
}

/////////////////////////////////////////////////////////////////
void printVolumes(){
  refreshPositions();
  Serial.print(F("V"));
  for( i=0; i<3; i++){
    Serial.print(-milliliters(Position[i], i));
    Serial.print(',');
  }
  Serial.println();
}

/////////////////////////////////////////////////////////////////
float flowToStepRate(float flowRate, int x){
  return flowRate*spm[x]/60; // Accepts a flowrate ##.## mL and converts it to an int steps/s
}

/////////////////////////////////////////////////////////////////

```

```

float volumetosteps(float mL, int x){
//Accepts a volume ###.### and returns the corresponding integer of steps
//the motor must take make.
float s = mL * spm[x];
return s;
}
////////////////////////////////////
float milliliters(float motorposition, int x ){ //spm is steps per milliliter
return motorposition / spm[x];
}
////////////////////////////////////
// This function creates a string 'inputString' by compound addition
// of the characters stored in the serial buffer. The global boolean
// 'stringComplete' is then set to true to tell the main loop that
// a new user input is available.

void serialEvent() {
while (Serial.available()) {
// get the new byte:
char inChar = (char)Serial.read();
// add it to the inputString:
inputString += inChar;
// if the incoming character is a newline, set a flag
// so the main loop can do something about it:
if (inChar == '\n') {
stringComplete = true;
}
}
}
////////////////////////////////////
void loop() {
// First check the global boolean 'stringComplete'
if (stringComplete) {

// If there is a new user input, find where the five commas are.
// Store their position in commaIndex[].

```

```

for(int n = 0; n<6; n++){
    if(n == 0){
        commaIndex[n] = inputString.indexOf(',');
    }
    else {
        commaIndex[n] = inputString.indexOf(',',commaIndex[n-1]+1);
    }
}

// Now store the position of the brackets in the bracketIndex[].

bracketIndex[0] = inputString.indexOf('(');
bracketIndex[1] = inputString.indexOf(')', bracketIndex[0]+1);

// Now split the inputString at each commaIndex
// Convert the strings to a floats and store them in Rate[]

for(int j=0; j<6; j++){
    if(j == 0){
        String tempString = inputString.substring(j,commaIndex[j]);
        Rate[j] = tempString.toFloat();
    }
    else{
        String tempString = inputString.substring(commaIndex[j-1]+1,commaIndex[j]);
        Rate[j] = tempString.toFloat();
    }
}

// Do the same for the bracket indexes
// Store the first as a String type variable and the second as a Float type

String command = inputString.substring(0,bracketIndex[0]);
commandval = inputString.substring(bracketIndex[0]+1, bracketIndex[1]).toFloat();

// Now the original 'inputString' is cleared
// The global boolean 'stringComplete; is set to false.

```

```

inputString = "";
stringComplete = false;

// Now that the user input has been processed the code
// proceeds to manage the stepper motors. First thing
// is to refresh where each stepper is with respect to
// it's initial position.

refreshPositions();

// Now begins a multitude of 'if' statements to check what
// the program should do with the users input. Most procedures
// are evident in their functionality.

if (command == "volumes" )printVolumes();
if (command == "reset" ){
  for(int g = 0; g<6; g++){
    stepper[g].setCurrentPosition(0);
    Diameter[g] = 20.0;
  }
  refreshPositions();
  Serial.println(F("reset"));
}

// Ceck if the command string contains "set" and change the appropriate volume if so.
// Remember the steppers are zero indexed but the pumps are one indexed.

if(command.substring(0,3) == "set"){
  command.replace("set","");
  int r = command.toInt()-1;
  stepper[r].setCurrentPosition(-volumetosteps(commandval,r));
  printVolumes();
}

// Ceck if the command string contains "diameter" and change both the appropriate diameter
// and the spm[] calculation for that pump.

```

```

// Remember the steppers are zero indexed but the pumps are one indexed.

if (command.substring(0,8) == "diameter"){
  command.replace("diameter","");
  int r = command.toInt()-1;
  Diameter[r] = commandval;
  spm[r] = ThreadDensity*200.0/(3.1415*square(Diameter[r]/2.0)/1000.0);
}

if (command == "help"){
  Serial.println(F("spm"));
  for(int y=0; y<6; y++){
    Serial.println(spm[y]);
  }
  Serial.println(F("diameters"));
  for(int y=0; y<6; y++){
    Serial.println(Diameter[y]);
  }
  printVolumes();
}

////////////////////////////////////
//      Done handling the Serial Event      //
////////////////////////////////////

nowT = millis();
if(nowT-startT >= 1000){
  printVolumes();
  startT=nowT;
}

// Now that the serial event has been handled the motors must be polled
// This is done using the functions from the AccelStepper Class

for(int z = 0; z<6; z++){
  if(stepper[z].currentPosition() > 0)Rate[z]=0;
  //if(stepper[z].currentPosition() < Limit)Rate[z]=0;
  stepper[z].setSpeed(flowToStepRate(Rate[z],z));
  stepper[z].runSpeed();
}

```

}

}

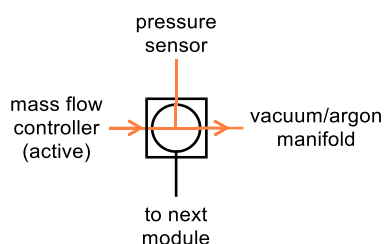
3. Handling of the Flow Platform

3.1 Functions of the Modules

3.1.1 Vacuum/Argon Module

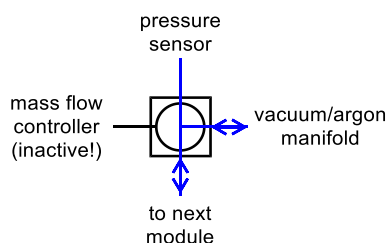
The vacuum/argon module allows switchable connection to either a MFC or a vacuum/argon manifold. The heart of the module is a 4-port-T-valve.

Mode 1: idle



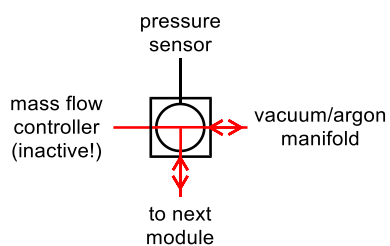
In this mode, the MFC feeds an argon flow to the vacuum/argon manifold, while the next module is disconnected. The pressure is measured by the pressure sensor. This mode is good for the warm-up period of the MFC (~30 min).

Mode 2: drying/flushing mode (“Schlenk-in-flow” (SiF) mode)



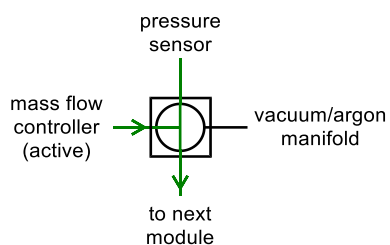
In this mode, the MFC is disconnected and has to be switched to a mass flow of 0 mL/min to avoid the build-up of pressure. The pressure sensor, the vacuum/argon manifold, and the next module are connected. By using the vacuum/argon manifold, the next module can be evacuated, solvents can be evaporated or the next module can be flushed with argon. This mode allows the “Schlenk-in-flow” (SiF) techniques. The pressure sensors are quite resistant against most solvents and can be easily replaced as they are relatively inexpensive.

Mode 3: not recommended!



This mode works in the same way as mode 2. In this mode, the MFC has to be switched to a mass flow of 0 mL/min, to allow a proper vacuum. The build-up of pressure is avoided in this mode, but the MFC is connected to the next module and can be damaged by solvent or reagent vapors.

Mode 4: Reaction mode

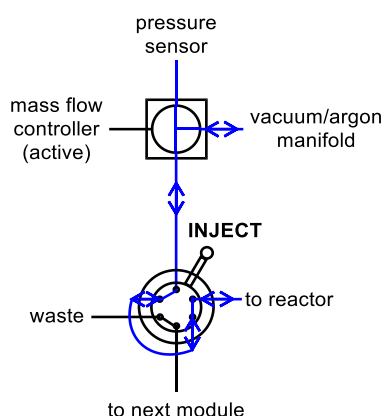


This mode enables the argon-driven flow of reagents. The MFC, the pressure sensor and the next module are connected. The argon stream provided by the MFC is corrected by continuous measurement of the system pressure. The argon stream is directed to the next module, while the vacuum/argon manifold is disconnected.

3.1.2 Vacuum/Argon Module Connected to the Reagent Module

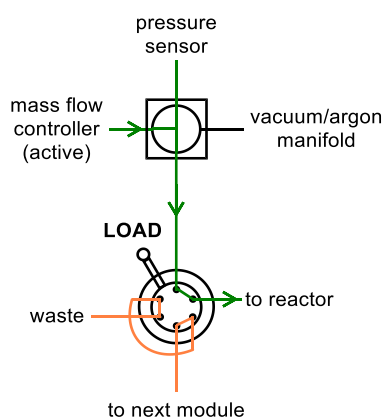
Typically, the vacuum/argon module is connected to the reagent module. The reagent module consists of a HPLC injection valve (6-port-2-ways) and is equipped with a sample loop for storage of reagent solutions.

Mode 1: drying/flushing mode (SiF mode)



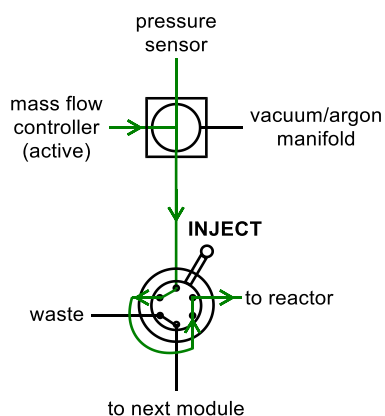
In this mode, the vacuum/argon manifold is connected to the sample loop and the reactor. Thus, the sample loop and the reactor can be dried in vacuum and flushed with argon. To allow evacuation of the reactor, the end of the reactor is either a) sealed with plunger; b) is equipped with a canula and the canula is introduced through a septum of a closed (Schlenk-)flask; or c) is connected with a valve that switches between a plunger and an outlet in a collection flask.

Mode 2: sample loading mode



In this mode, the MFC flushes the reactor consistently with argon, while the sample loop can be loaded with a reagent solution.

Mode 3: reaction mode

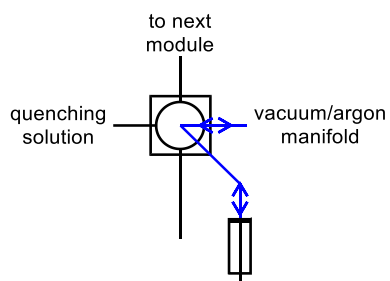


The HPLC injection valve is switched to the injection-position and a liquid slug of the reagent solution is inserted in the argon flow provided by the MFC.

3.1.3 Inert Sample Loading Module

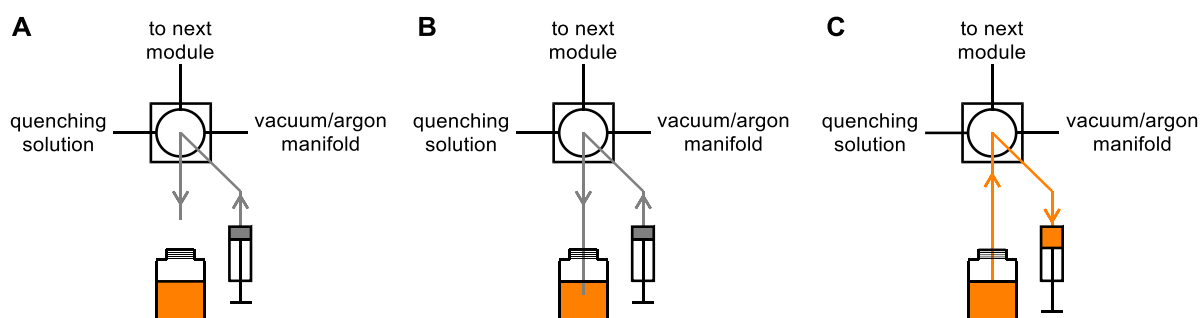
This module is important for SiF. It allows to load a reagent solution from a bottle or a Schlenk flask on a syringe. Then, the reagent solution can be loaded on a sample loop. Alternatively, the syringe can be pushed by a syringe pump to pump the reagent solution to another module or a reactor for flow reactions. This module allows also safe quenching or washing procedures.

Mode 1: idle



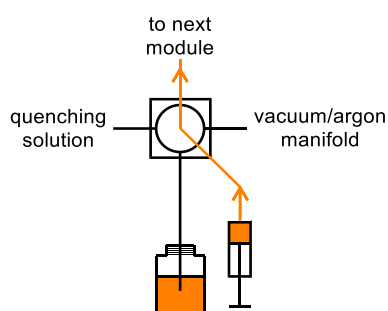
When the valve is switched to this position, the syringe is connected with the vacuum/argon manifold. Thus, the syringe can be evacuated and flushed with argon. In this way, argon can be loaded on the syringe.

Mode 2: loading



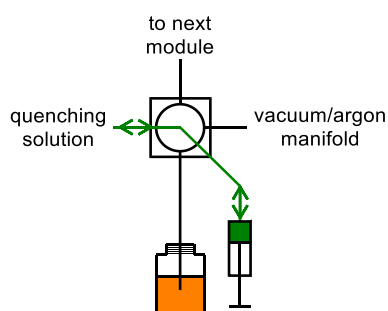
Left: In this position, argon from the syringe can be pushed through the tubes (grey) in order to remove oxygen and moisture from the tubes. **Center:** Then, the tube is connected to the reagent bottle or Schlenk flask under a flush of argon provided by the syringe. **Right:** The reagent solution is loaded on the syringe.

Mode 3: injection



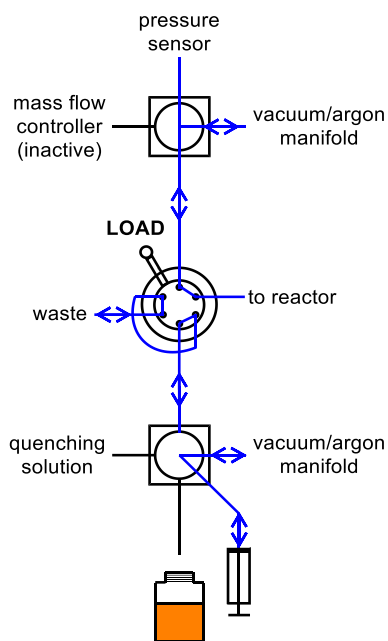
In this position, the reagent solution is injected in the next module.

Mode 4: quenching/washing



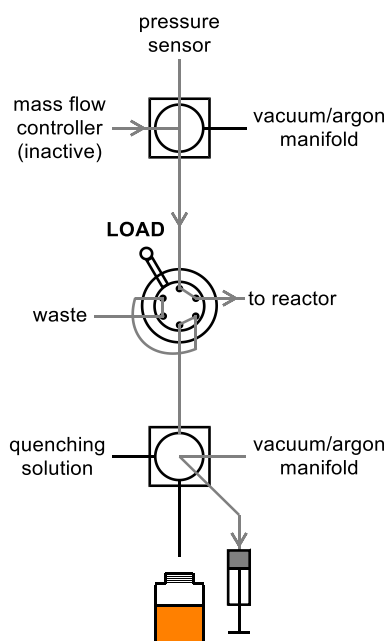
In this position, the syringe and the tubes can be quenched with a quenching solution. Afterwards, the syringe and the tubes can be washed with pure solvents. By removing the tube from the reagent solution bottle and switching to mode 3, the tube can be washed.

Step 2: warm-up period, drying of tubes



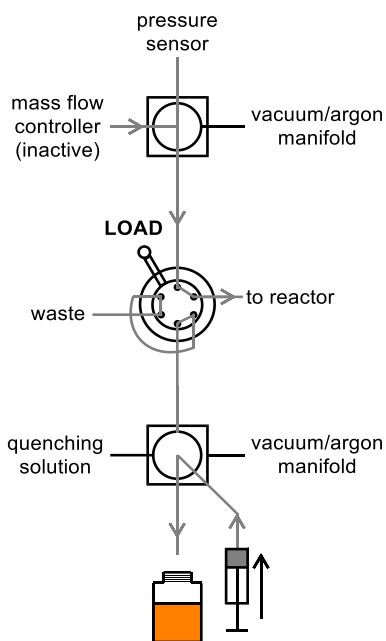
The MFC is switched to a flow rate of 0 mL/min. The 4-port-T-valve is switched, and the reactor is evacuated and flushed with argon. To do so, the end of the reactor is either sealed with plunger. Alternatively, the end of the reactor tube is equipped with a canula and the canula is introduced through a septum of a closed (Schlenk-)flask. It is also possible to connect the end of the reactor with a valve that switches between a plunger and an outlet in a collection flask.

Step 3: idle mode



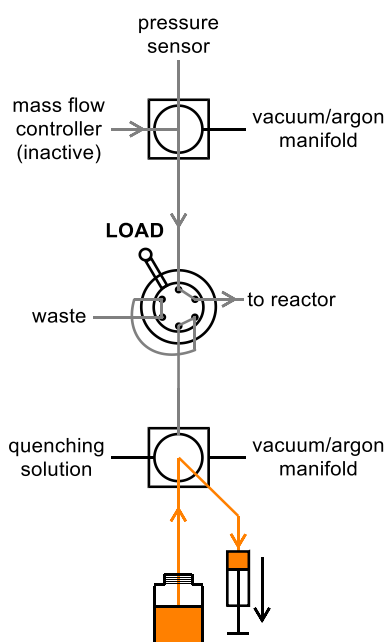
The 4-port-T-valve is switched and the MFC is switched to a flow rate of approximately 5 mL/min feeding argon through the reactor. The disposable syringe is loaded with argon.

Step 4: flushing of the reagent tubes



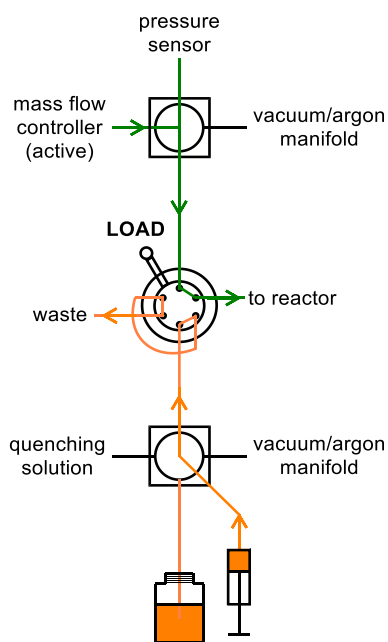
The 4-port selection valve is switched, and the disposable syringe is pushed to flush the argon inside of the syringe through the tube. In this way, the short tube between valve and reagent solution bottle is flushed with argon. Then, the 4-port selection valve is switched to the vacuum/argon manifold, the syringe loaded with argon, the 4-port selection valve is again switched to the reagent position and the argon inside the syringe pushed through the tubes. For very sensitive reagents, this procedure should be repeated an additional 1–3 times.

Step 5: loading of the reagent solution



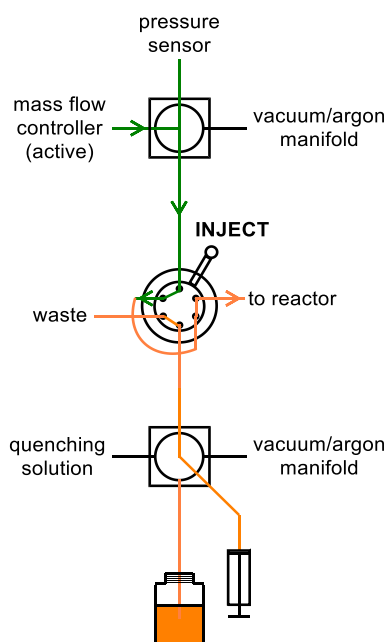
The reagent tube is introduced to the bottle of the reagent solution. The solution is loaded on the syringe.

Step 6: loading of the reagent solution on the sample loop



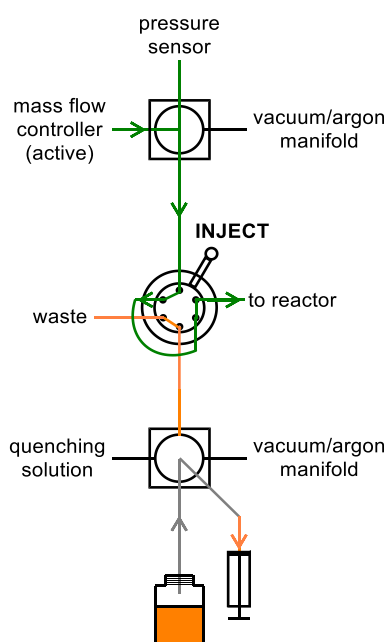
The 4-port selection valve is switched directing the reagent solution to the HPLC injection valve. The reagent solution is loaded on the sample loop by using the syringe.

Step 7: running a reaction



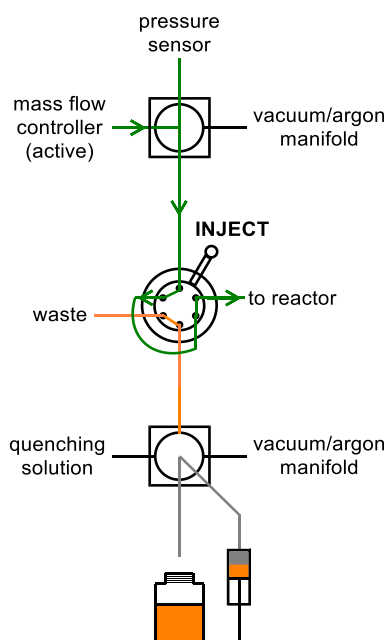
The reaction is started by switching the HPLC injection valve from the LOAD to the INJECTION position. The argon stream provided by the MFC is pumping the reagent solution from the sample loop to the reactor.

Step 8: removing remaining reagent solution I



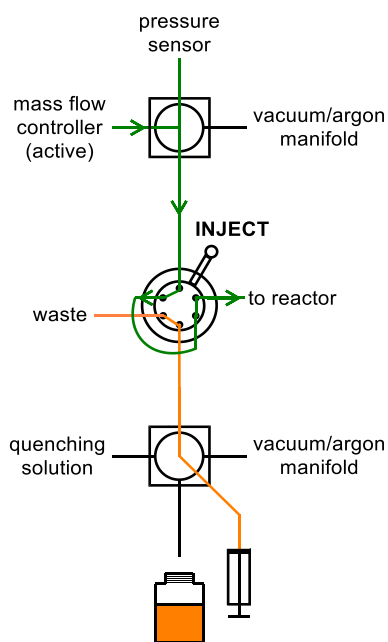
The 4-port selection valve is switched to the reagent solution and the canula reaching in the reagent solution is removed from the solution reaching in the gas space above the solution. The syringe is withdrawn to remove remaining reagent solution from the tubes.

Step 9: removing remaining reagent solution II



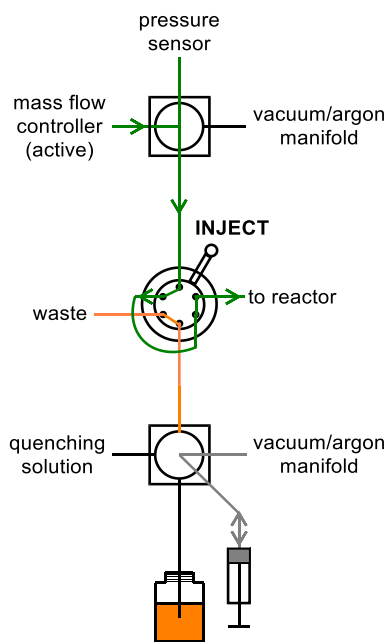
The canula is removed from the reagent solution.

Step 10: removing remaining reagent solution III



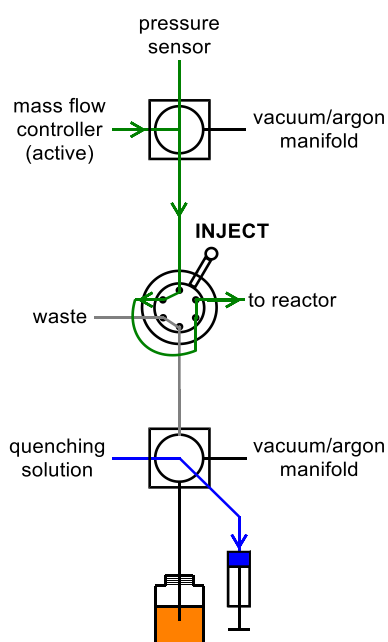
The reagent solution in the syringe is pumped to the waste by pushing the syringe.

Step 11: washing the system I



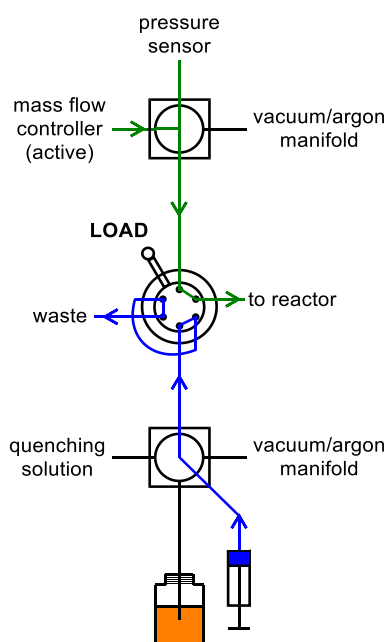
The 4-port selection valve is switched to the vacuum/argon manifold, the syringe loaded with argon, the 4-port selection valve is switched to the injection position and remaining reagent solution in the syringe and the tubes is pushed to the waste.

Step 12: washing the system II



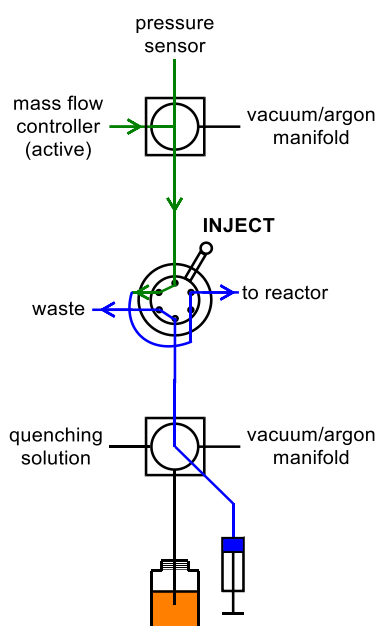
The 4-port selection valve is switched to the quenching solution and the solution is loaded on the syringe. The quenching solution can be e.g. *iso*-propanol for quenching organometallic reagents, but in most cases, it is recommended to use pure solvent, which should be the same as the one used for the reagent solution. When washing is performed with more “aggressive” solvents such as CH_2Cl_2 or tetrahydrofuran, at least one subsequent wash with *iso*-propanol or acetonitrile should be performed.

Step 13: washing the system III



The 4-port selection valve is switched to the quenching solution. The quenching solution is loaded on the syringe. The HPLC injection valve is switched to the LOAD position. The quenching solution is loaded on the sample loop by using the syringe.

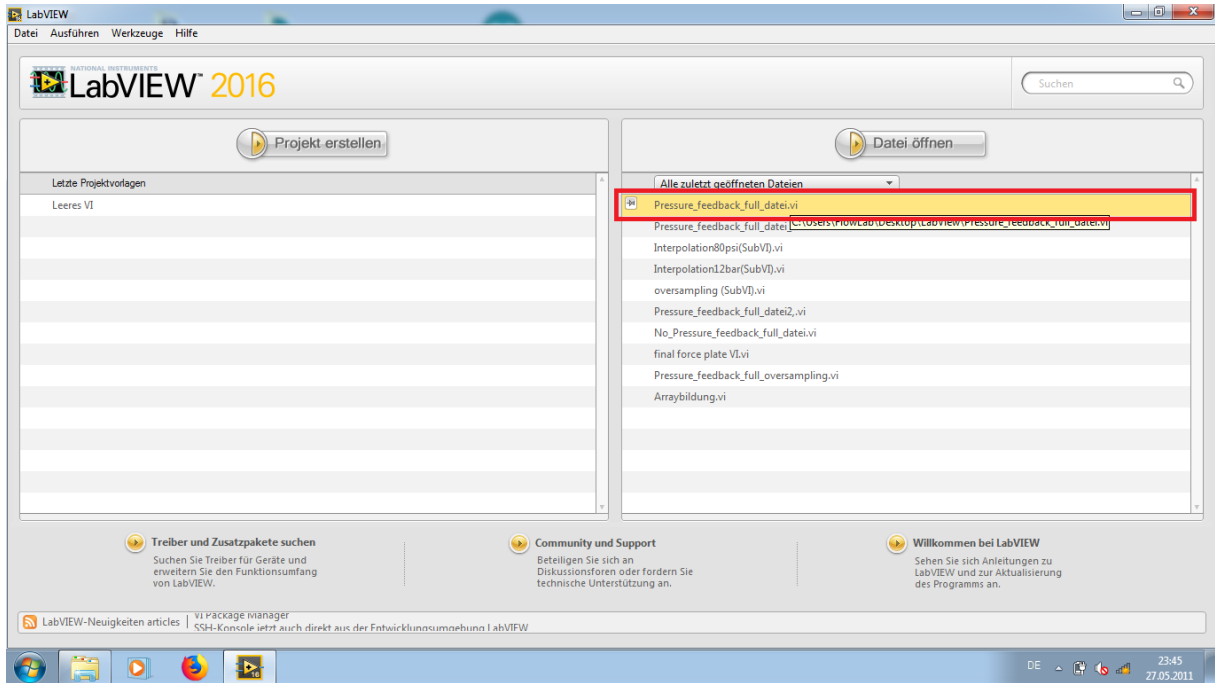
Step 14: washing the system IV



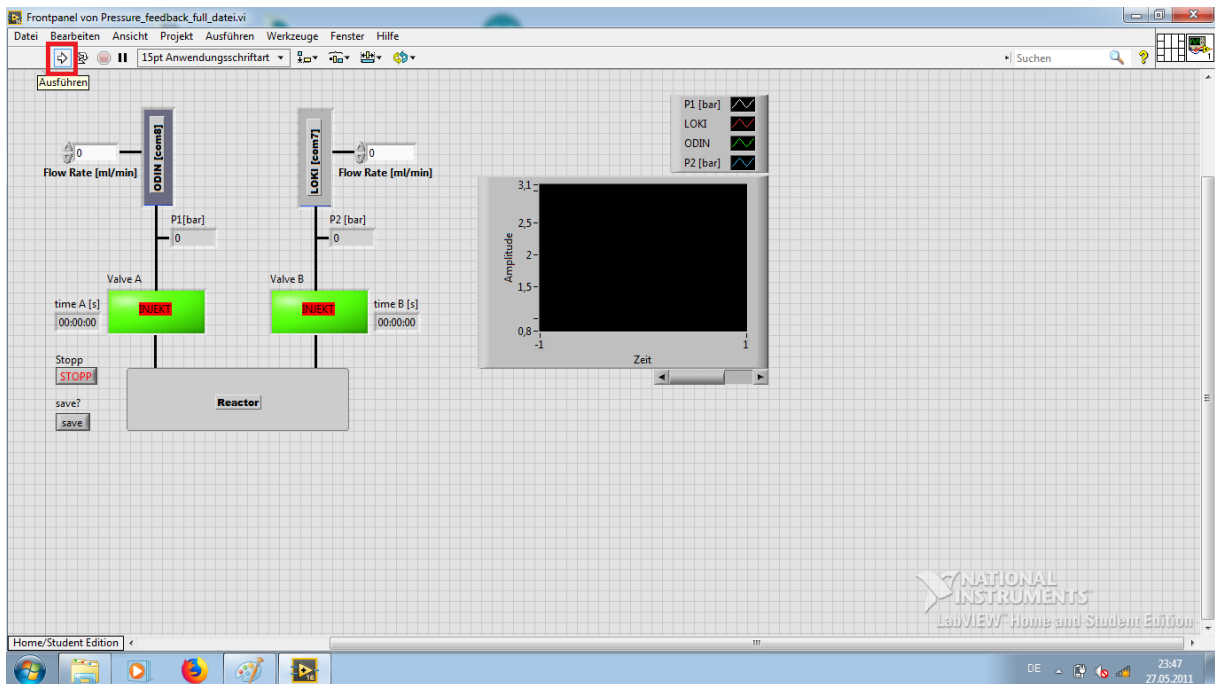
The HPLC injection valve is switched to the inject position and the quenching solution is pumped through the sample loop. Steps 12–14 are repeated at least two times.

3.3 Using the LabVIEW Interface

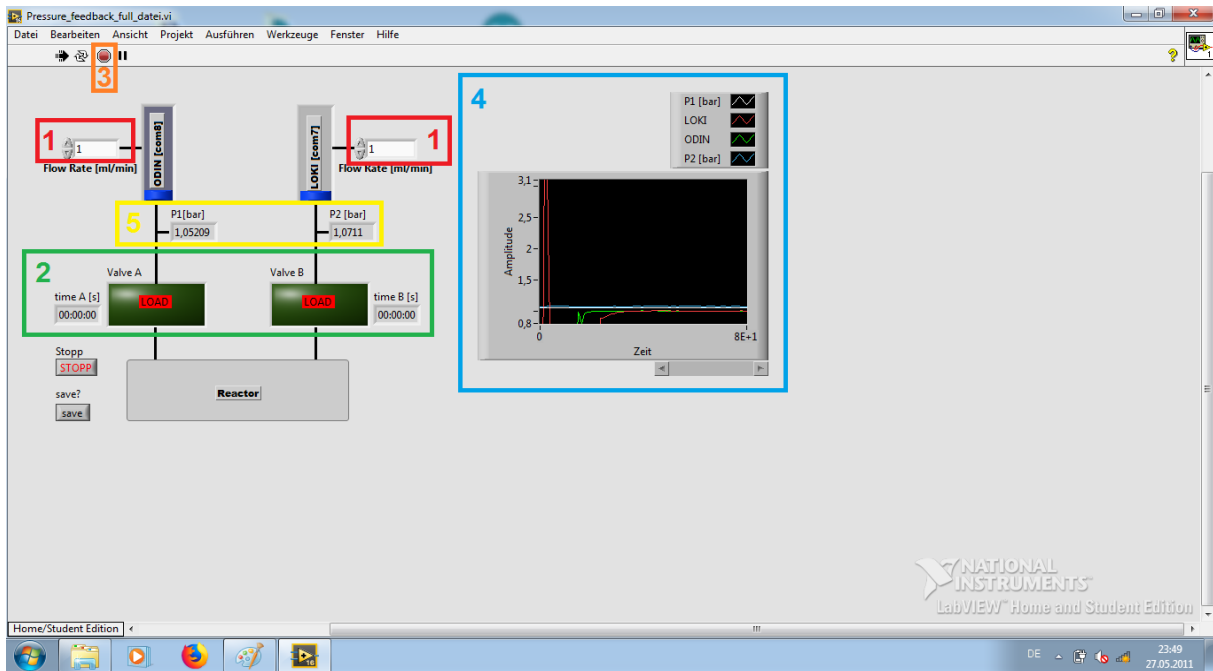
To control the MFCs and to monitor system pressure and time reading of the HPLC injection valves, a graphical user interface for the LabVIEW software (LabVIEW 2016) was written.



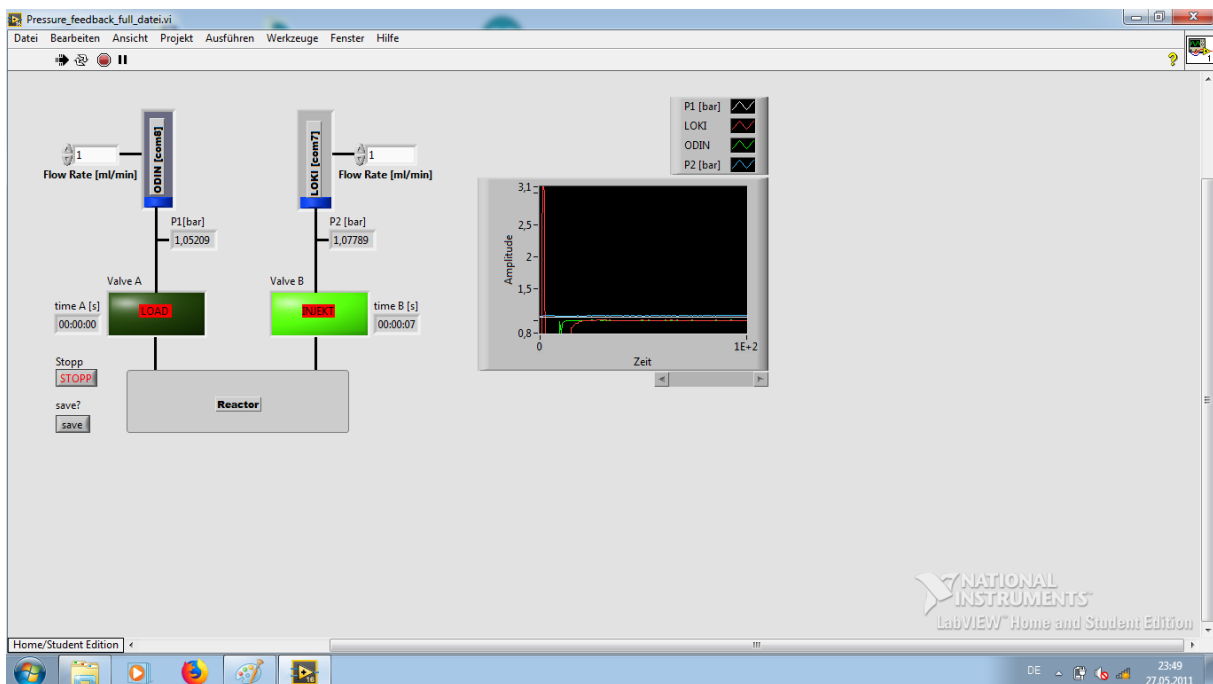
After opening LabVIEW, the script is started.



By clicking on the marked button (execute), the script is run.



The graphical user interface: 1. The flow rate is set by using the arrows or by entering the desired flow rate [x,y]. 2. The valve timers are starting when the valve is manually switched from load to inject, which is also displayed in the interface. The timer is reset by switching the valve back to load. 3. The LabVIEW Script is stopped by clicking this button. 4. This diagram shows the measured pressure (y-axis) versus the time (x-axis). In addition, the corrected flow rate for both MFCs is shown separately. 5. The current pressure measured on the outlets of both MFCs is displayed separately and updated every second.

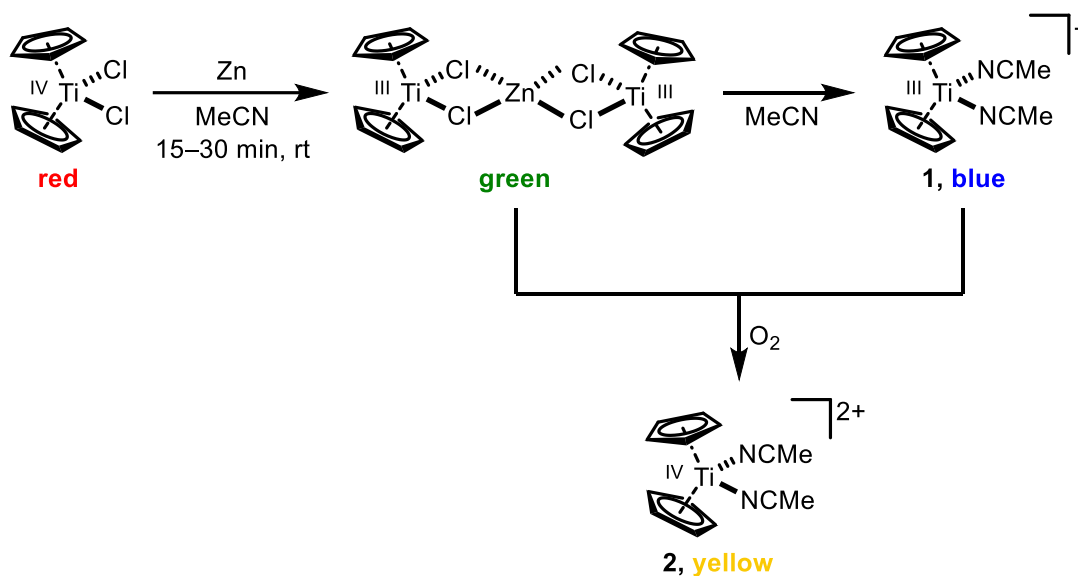


The counter of a HPLC injection valve is started by switching manually the corresponding HPLC valve from load to inject.

4. Experimental Procedures

4.1 Experiments to Check Oxygen-free Conditions Using SiF

To investigate the efficiency of SiF, the oxygen content of solutions in the flow system was monitored employing a commonly used titanium(III) metallocene complex as colorimetric indicator.^[9]

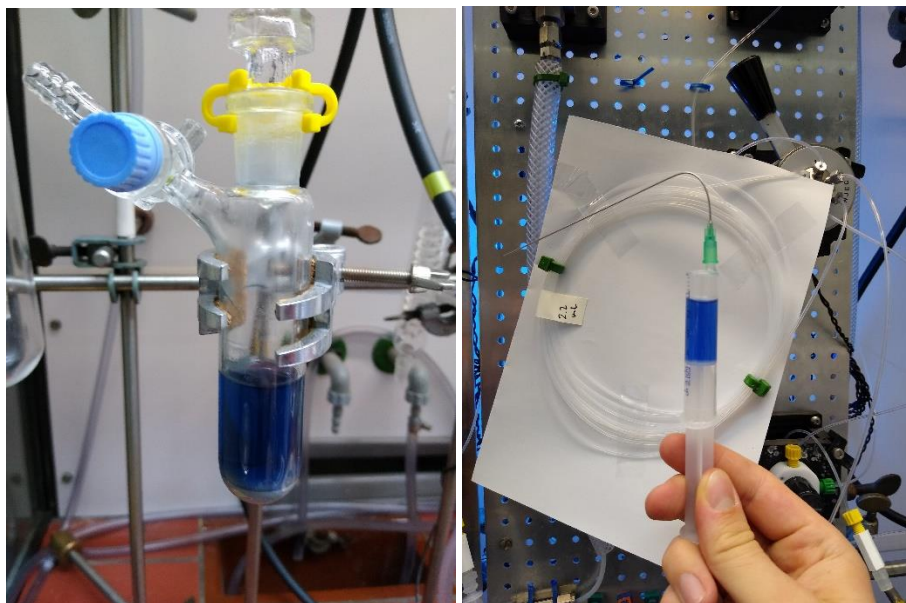


Scheme S1: Schematic presentation of the titanium(III) and titanium (IV) species formed in the colorimetric oxygen indicator solution. By reduction of titanocene dichloride (TiCp₂Cl₂) with zinc dust, the green Cl-bridged complex Cp₂Ti(μ-Cl)₂TiCp₂ is formed, which further reacts to blue Cp₂Ti(III)(NCMe)₂ (1). Both Cp₂Ti(μ-Cl)₂TiCp₂ and Cp₂Ti(III)(NCMe)₂ are readily oxidized by trace amounts of oxygen to give yellow Cp₂Ti(IV)(NCMe)₂ (2).^[9,10]

Procedure for preparing and using of the indicator solution:

A Schlenk tube was charged with MeCN (20 mL, HPLC grade) and the solvent was purged with argon for 5 min. Then, titanocene (II) dichloride (80–100 mg) and zinc dust (4–5 g) were added in an argon flush. The resulting red suspension was stirred with a large magnetic stirring bar until the suspension turned dark blue. The stirring was stopped to allow the solids to settle. The supernatant blue solution was loaded via syringe on a sample loop (V = 2.2 mL; FEP tube, outer diameter 1/16", inner diameter 1/32").

Experiment 1: Loading of a sample loop with SiF



Left: The colorimetric indicator solution in a Schlenk tube. **Right:** The indicator solution loaded on a syringe.



Left: The indicators solution ~30 seconds after loading on the sample loop. **Center:** After 30 min. **Right:** After 60 min.

This experiment indicates that the indicator solution can be loaded under exclusion of air and moisture on the sample load enabled by SiF. However, completely anaerobic conditions cannot be maintained over a longer period of time very probably due to the oxygen permeability of the tubes consisting of fluorinated polymers.^[11] Therefore, very oxygen-sensitive reactions should be set up and realized within minutes or by using tubes made from stainless steel 316L or comparable materials.

Experiment 2: Loading of a sample loop without SiF



Left: The indicator solution loaded on a syringe. **Center:** The indicator solution ~30 seconds after loading on the sample loop. **Right:** After 10 min.

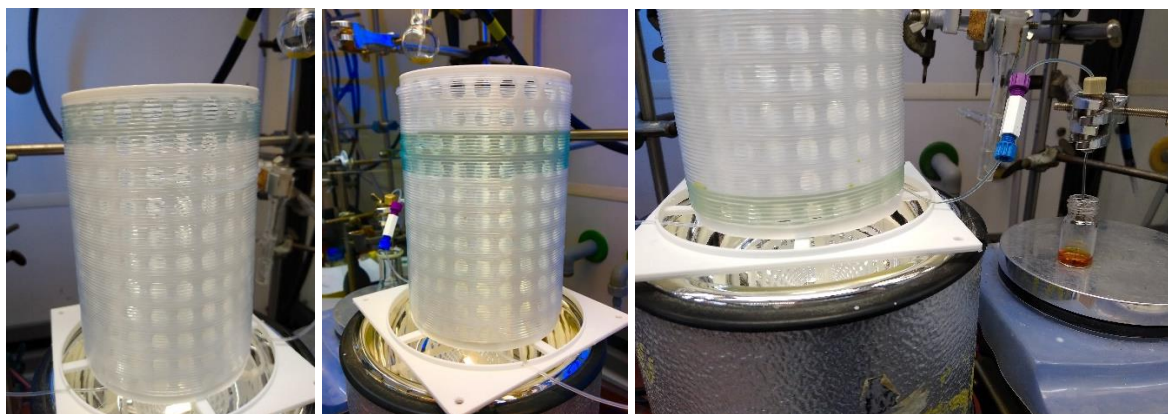
Experiment 3: Loading of a sample loop without SiF, flushing the tubes with argon for 5 min ($v_{\text{flow}} = 5 \text{ mL/min}$)



Left: The indicator solution ~30 seconds after loading on the sample loop. **Center:** After 10 min. **Right:** After 30 min.

Experiment 4: Passing a solution of indicator complex 1 through a 10 mL reactor using SiF

In another experiment, the indicator solution was loaded on the sample loop and pumped using a MFC ($v_{\text{flow}} = 1 \text{ mL/min}$) through a 10 mL tube reactor (FEP tube, outer diameter 1/16", inner diameter 1/32", 20 m length), which was previously deoxygenated using SiF.



Left: The indicators solution directly after entering the reactor. **Center:** After a residence time $t_r \approx 2$ min. **Right:** After a residence time $t_r \approx 10$ min, the reaction mixture is still green-blue while the solution leaving the reactor immediately colors orange.

4.2 Karl Fischer Titration Experiments

Experiments to investigate the efficiency of established anhydrous conditions

General procedure (GP01) for determining the drying efficiency of SiF:

Anhydrous THF (<5 ppm residual water) was obtained by distillation from sodium/benzophenone followed by storing over activated MS 3 Å for at least 72 h before use.^[12] Anhydrous THF was loaded on a sample loop (V = 5.0 mL; FEP tube, outer diameter 1/16", inner diameter 1/32"), using SiF. The sample loop was not washed with anhydrous THF prior use, as this could dry the sample loop. Then, the loaded THF was driven by an argon flow using MFCs with a flow rate of $v_{\text{flow}} = 1$ mL/min through a tube reactor (V = 4.0 mL, PTFE tube, outer diameter 1.6 mm, inner diameter 1 mm). At the end of the reactor, the THF was collected in a dry Schlenk tube. The collected THF was then directly analyzed by Karl Fischer titration. All experiments were performed twice, the collected THF was analyzed six times.

Table S1: Results of the Karl Fischer titration experiments.

Entry	Abbreviations from the general procedure GP01:	Residual water
1	none	12–15 ppm
2	Without SiF, tubes flushed with argon ^[a]	35–45 ppm
3	Without SiF, tubes flushed with argon ^[b]	19–24 ppm
4	After flushing the tubes with <i>i</i> PrOH, without SiF, tubes dried with THF (1 x 5 mL)	44–48 ppm
5	After flushing the tubes with <i>i</i> PrOH, without SiF, tubes dried with THF (2 x 5 mL)	18–20 ppm
6	After flushing the tubes with <i>i</i> PrOH, then SiF	16–18 ppm
7	After flushing the tubes with <i>i</i> PrOH, then flushing with argon ^[a]	68–101 ppm
8	After flushing the tubes with H ₂ O, then SiF	14–18 ppm
9	After flushing the tubes with H ₂ O, then flushing with argon ^[a]	>2000 ppm

[a] Flushing with argon was performed for 5 min using a flow rate of $v_{\text{flow}} = 5$ mL/min. [b] Flushing with argon was performed for 15 min using a flow rate of $v_{\text{flow}} = 5$ mL/min.

Control experiment 01

Anhydrous THF (5 mL) were placed in a dry Schlenk tube. The THF was transferred via a FEP tube (V = 5.0 mL) in another dry Schlenk tube using a positive pressure of argon. Prior transferring the THF, the tube was flushed with argon for 5 min.

Residual water: 12–13 ppm.

Control experiment 02

Anhydrous THF (5 mL) was loaded on a disposable 6 mL syringe. The THF was stored on the syringe for 1 min, then transferred in a dry Schlenk tube and analyzed.

Residual water: 90–106 ppm.

Control experiment 03

Anhydrous THF (5 mL) was loaded on a disposable 6 mL syringe. The THF was stored on the syringe for 1 min, then pushed through a tube FEP tube ($V = 1.0$ mL) and the outcoming THF (4 mL) was collected in a dry Schlenk tube and analyzed.

Residual water: 118–136 ppm.

Control experiment 04

A disposable 6 mL syringe was dried by pulling argon on the syringe and pushing it out for 3 times, as it is commonly done before using the syringe for moisture-sensitive applications. The THF was stored on the syringe for 1 min, then pushed through a tube FEP tube ($V = 1.0$ mL), which was prior flushed with argon for 5 min. The outcoming THF (4 mL) was collected in a dry Schlenk tube and analyzed.

Residual water: 16–20 ppm.

These experiments lead us to the following conclusions:

- The use of disposable syringes and FEP tubes for transfer processes lead to a slight increase of the residual water content (control experiments 01–04).
- Using SiF, sufficient anhydrous conditions can be realized (table S1, entries 1, 3, and 5).
- Even without using SiF, the residual water in the tubes is relatively small (table S1, entry 2). This is probably because the tubes are in any case flushed with argon by the MFCs (for comparison, see control experiments 03 and 04).
- When the tubes were wetted with *i*PrOH, the SiF provides better drying of the tubes (table S1, entry 3) compared to only flushing the tubes with argon (entry 4).
- When the tubes were wetted with H₂O, SiF still provides anhydrous conditions (table S1, entry 5), while flushing the tubes with argon fails in doing so (entry 6).

In summary, SiF provides anhydrous conditions reliably in the flow reactor and should be used when exclusion of moisture is important for the success of the reaction or when the tubes were previously washed with solvents such as *i*PrOH or H₂O.

4.3 Synthesis of Amides from Isocyanates and Grignard Reagents to Check Air- and Moisture Free Conditions

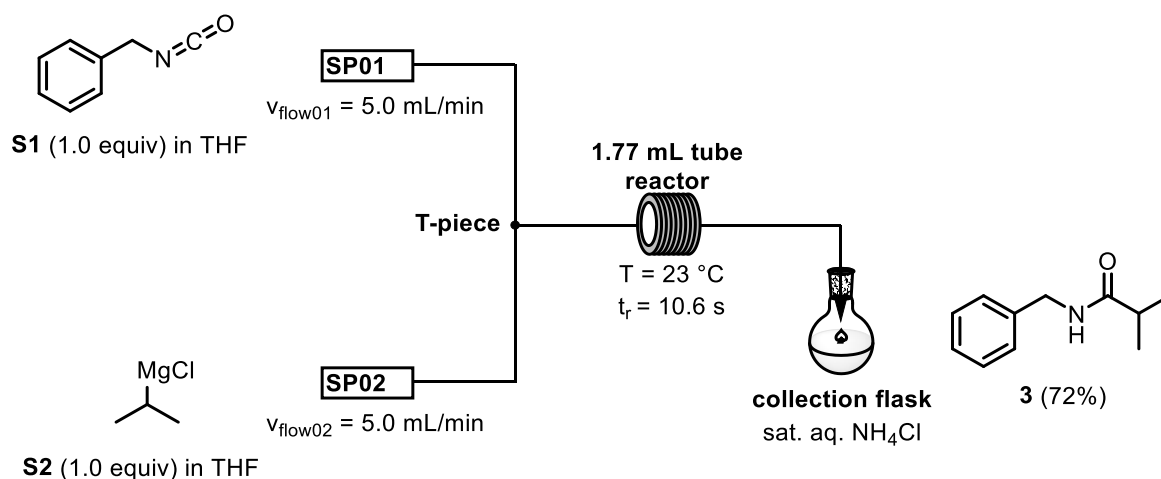
To prove that air- and moisture sensitive reactions can be performed in flow using SiF without wasting large amounts of solvents or reagents, a water-sensitive reaction involving a Grignard reagent was used as reference. For comparison, the reaction was performed one time according to the literature with a classical setup using syringe pumps. Drying and equilibration of the reactor is reached by discarding a prerun of three residence times, as it is typically done in flow chemistry.^[6] Then, the reaction was performed using our flow platform and SiF. With the syringe pump setup a yield of 72% (lit.: 76%)^[6] was obtained, while using our flow platform gave a comparable yield of 68%.

Using a syringe pump setup, a total amount of at least 8.85 mL anhydrous THF is used to dry the reactor. For the preparation of 1 mmol of product (based on a yield of 100%), in total 1.76 mmol of product are discarded due to prerun (equilibration period) and postrun (compensation of dead volume of the reactor) of the reaction. This means, that only 36% of the theoretically formed product is collected in this way. Based on the total amount of reagents that are employed in the flow reaction using a syringe pump setup, the corrected yield is only 28%.

Although the yield of product is slightly lower (68%) using our flow platform and SiF, the corrected yield involving all employed material is significantly higher (62% compared to 28%) as only small amounts of reagents are lost due to dead volume of tubes, connectors, valves etc.

It has to be noted, that the loss of reagents is only significant for small scale reactions, which are, however, quite important for natural product synthesis and late-stage applications. On multi-gram scale, the amount of reagents that are lost in drying and equilibration processes is comparably small and can sometimes be even neglected (see e.g. the multi-gram experiment in ref. 6).

Amide synthesis with a syringe pump setup



This procedure was performed according to the literature.^[6]

Directly prior use, the **1.77 mL tube reactor** was flushed with anhydrous THF (5 residence time, 8.9 mL).

In a dry Schlenk tube, anhydrous CuBr₂ (11.2 mg, 50.0 μmol) was placed and the tube was evacuated and backfilled with argon (3x). Then, benzyl isocyanate **S1** (666 mg, 5.00 mmol) and anhydrous THF were added to prepare 10 mL of a 0.5 M solution in THF. This solution was sonicated for 2 min, and then loaded on a gas tight syringe and placed on syringe pump 01 (**SP01**).

In another dry Schlenk tube, *i*PrMgCl **S2** (2.50 mL, 5.00 mmol; 2.0 M in THF) was placed and diluted with anhydrous THF (7.5 mL) to give 10 mL of a 0.5 M solution in THF. This solution was loaded on a gas tight syringe and placed on syringe pump 02 (**SP02**). Then, both solutions were mixed at 23 °C with a flow rate of $v_{\text{flow01}} = v_{\text{flow02}} = 5.0$ mL/min in a T-piece and pumped through the **1.77 mL tube reactor** (FEP tube, outer diameter 1/16", inner diameter 1/32") with a residence time $t_r = 10.6$ s. A prerun of three residence times (30 s, 5 mL) was discarded to allow drying and equilibration of the system. Then, a sample (24 s, 4 mL) of the reaction mixture was collected in a collection flask containing NH₄Cl (sat. aq., 10 mL). The mixture was diluted with EtOAc (10 mL) and NaCl (sat. aq., 10 mL) and the aqueous layer was separated and extracted with EtOAc (2x20 mL). The combined organic layers were dried (MgSO₄), filtered, and concentrated under reduced pressure. MPLC (cyclohexane/EtOAc 2:1) gave amide **S03** (128 mg, 722 μmol, 72% [lit.: 76%]^[6]) as a colorless solid.

The yield is based on the actual reacted reagent solutions: solution 1 (1.0 mL; benzyl isocyanate **S01** (134 mg, 1.00 mmol, 1.0 equiv) and CuBr₂ (2.2 mg, 0.10 μmol, 1 mol%)) and solution 2 (1.0 mL; *i*PrMgCl (1.00 mmol, 1.0 equiv)).

Calculation of solvent and product waste based on the reported procedure^[6]

Tube reactor with a reactor volume $V_R = 1.77$ mL; flow rates $v_1 = v_2 = 5.0$ mL/min. Residence time

$$t_r = \frac{V_R}{(v_1 + v_2)} = \frac{1.77 \text{ mL}}{10 \text{ mL/min}} = 0.177 \text{ min} \cong 10.62 \text{ s.}$$

“Prior to performing Grignard reactions, the system was flushed with dry THF, for at least 5 residence times.”

Thus, the amount of anhydrous THF used to flush the reactor can be calculated as:

$$5 \times V_R = (5 \times 1.77) \text{ mL} = 8.85 \text{ mL}$$

“An equilibration period of 3 residence times was allowed, then samples of 1 mmol (4 mL combined flow volume) were collected.”

This means that 1 mmol of product corresponds to a reaction volume of 4 mL (based on a theoretical yield of 100%). Therefore, in an equilibration period of 3 residence times, the theoretical amount of wasted product can be calculated as:

$$4 \text{ mL} \triangleq 1 \text{ mmol product}$$
$$3 \times V_R = (3 \times 1.77) \text{ mL} = 5.31 \text{ mL} \triangleq 1.32 \text{ mmol product}$$

As the reagents are not driven by gas or by pure solvent and the reactor has a dead volume of 1.77 mL, in addition a reaction mixture of at least 1.77 ml (corresponding to ≈ 0.44 mmol product) remains in the tube reactor (the dead volume of the mixing unit, syringes etc. was neglected). Therefore, the total loss of product is:

$$(1.32 + 0.44) \text{ mmol} = 1.76 \text{ mmol}$$

As according to the procedure 1 mmol of product is collected, the amount of collected product from the total amount of theoretically formed product, including equilibration period and dead volume, is:

$$\frac{1.00 \text{ mmol}}{(1.76 + 1.00) \text{ mmol}} = \frac{1.00}{2.76} \approx 36\%$$

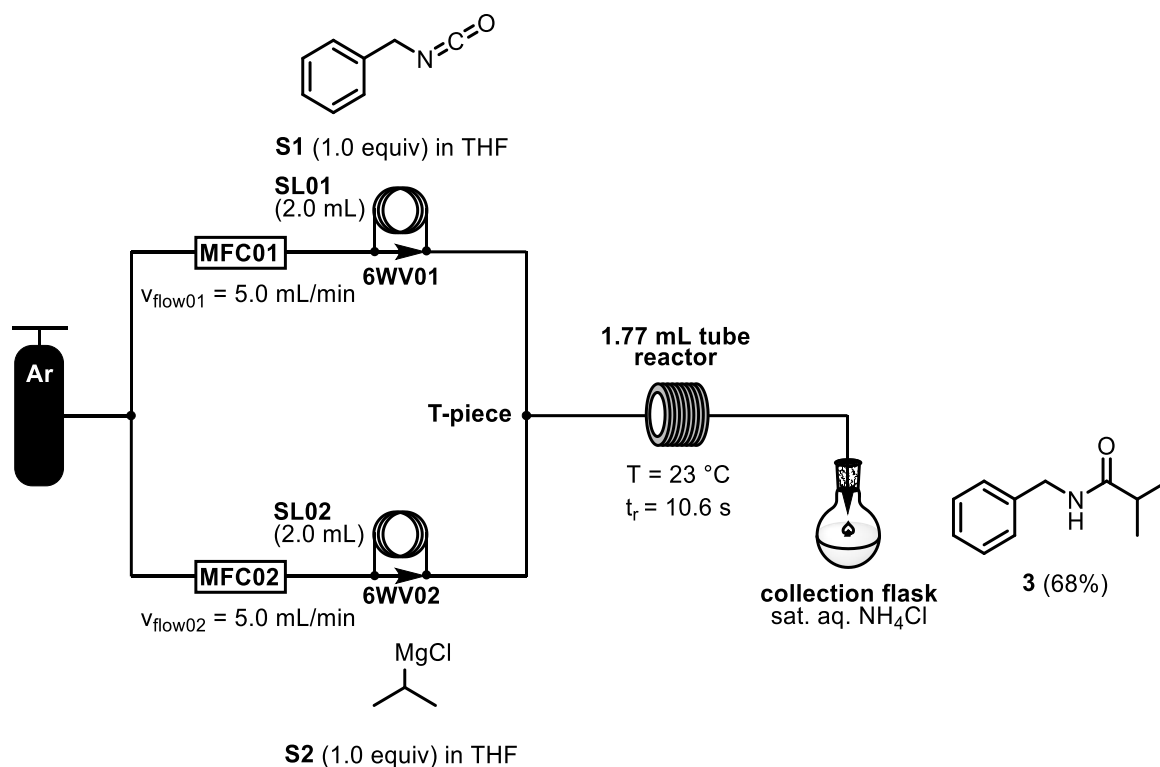
In conclusion, 8.85 mL of anhydrous THF and 1.76 mmol of product for the preparation of 1 mmol product are wasted, meaning that only 36% of the theoretically formed product can be isolated. The example reaction proceeds with a reported yield of 76%. Based on the amount of reagents that are actually employed in the reaction, the corrected yield can be calculated as:

$$0.36 \times 0.76 \approx 0.28 \triangleq 28\%$$

Thus, according to the reported procedure and based on the amount of reagents that are actually employed on a 1 mmol scale, the corrected yield is 28%.

The loss of reagents and solvents due to the dead volume of syringes, the mixing unit and connectors was neglected as it ranges typically below <0.5 mL (combined). Also, the waste of washing solutions and solvents that are used to clean the reactor, the mixing unit and the connectors were neglected.

Amide synthesis using the flow platform



In a dry Schlenk tube, anhydrous CuBr_2 (11.2 mg, 50.0 μmol) was placed and the tube was evacuated and backfilled with argon (3x). Then, benzyl isocyanate **S1** (666 mg, 5.00 mmol) and anhydrous THF were added to prepare a total of 10 mL of a 0.5 M solution in THF. This solution was sonicated for 2 min, and then loaded on sample loop 01 **SL01** ($V = 2.0 \text{ mL}$, FEP tube, outer diameter 1/16", inner diameter 1/32").

In another dry Schlenk tube, *i*PrMgCl **S2** (2.50 mL, 5.00 mmol; 2.0 M in THF) was placed and diluted with anhydrous THF (7.5 mL) to give 10 mL of a 0.5 M solution in THF. This solution was loaded on sample loop 02 **SL02** ($V = 2.0 \text{ mL}$, FEP tube, outer diameter 1/16", inner diameter 1/32"). Then, both solutions were mixed at 23 $^\circ\text{C}$ with a flow rate of $v_{\text{flow}01} = v_{\text{flow}02} = 5.0 \text{ mL/min}$ in a T-piece and pumped through the **1.77 mL tube reactor** (FEP tube, outer diameter 1/16", inner diameter 1/32") with a residence time $t_r = 10.6 \text{ s}$. The end of the reactor is equipped with a small canula and the reaction mixture was collected in a collection flask containing NH_4Cl (sat. aq., 10 mL). The mixture was diluted with EtOAc (10 mL) and NaCl (sat. aq., 10 mL) and the aqueous layer was separated and extracted with EtOAc (2x20 mL). The combined organic layers were dried (MgSO_4), filtered, and concentrated under reduced pressure. MPLC (cyclohexane/EtOAc 2:1) gave amide **S3** (121 mg, 683 μmol , 68%) as a colorless solid.

The yield is based on the actual reacted reagent solutions: solution 1 (2.0 mL; benzyl isocyanate **S01** (134 mg, 1.00 mmol, 1.0 equiv) and CuBr_2 (2.2 mg, 0.10 μmol , 1 mol%)) and solution 2 (2.0 mL; *i*PrMgCl (1.00 mmol, 1.0 equiv)).

$R_f = 0.28$ (cyclohexane/EtOAc 2:1)

^1H NMR (700 MHz, DMSO- d_6) δ [ppm] = 8.23 (t, $J = 6.1$ Hz, 1H), 7.33 – 7.30 (m, 2H), 7.24 – 7.21 (m, 3H), 4.25 (d, $J = 6.0$ Hz, 2H), 2.42 (hept, $J = 6.8$ Hz, 1H), 1.03 (d, $J = 6.9$ Hz, 6H).

^{13}C NMR (176 MHz, DMSO- d_6) δ [ppm] = 176.0, 139.8, 128.2, 127.0, 126.6, 41.8, 34.0, 19.6.

The spectroscopic data are consistent with those reported previously in the literature.^[6]

Calculation of solvent and product waste using our flow platform and SiF

No solvents are used to dry the reactor and neither a pre- nor a post-run are discarded. The tubes, connectors and syringes that are used to load a reagent solution on the sample loop have a dead volume of ~0.2 mL. Thus, for each reagent solution, 2.2 mL are employed from which 2.0 mL are actually reacted. So, for the preparation of 1 mmol product (corresponding to a combined volume of 4.0 mL), in total, 4.4 mL of reagent solutions are employed, which can be expressed as:

$$\frac{4.0 \text{ mL}}{4.4 \text{ mL}} \approx 0.91 \triangleq 91\%$$

As described above, the corrected yield for the amount of reagents that are actually employed is:

$$0.91 \times 0.68 \approx 0.62 \triangleq 62\%$$

The amount of consumed argon (typically a few hundred milliliters for each experiment) and the waste of washing solutions and solvents that are used to clean the reactor, the mixing unit etc. were neglected.

4.4 Aldol Reaction of the Key Intermediates Aldehyde **4** and Ester **5** of (+)-Darwinolide in Flow

Preliminary Screening of reaction conditions for the aldol reaction of deprotonated ester **5** and aldehyde **4**

In preliminary studies, ester **5** was deprotonated in batch. The deprotonated species and aldehyde **4** were then mixed in a flow reactor. It was found that when sodium bis(trimethylsilyl)amide was employed as base, the subsequent aldol coupling process was relatively slow leading to almost no conversion under the reaction conditions. When freshly prepared $\text{LiN}(i\text{Pr})_2$ was used as base, aldol coupling proceeded much faster, providing β -hydroxy ester **6** in acceptable yields. However, it has to be noted that increasing reaction times did not improve the yield. This is in accordance with our previous observations.^[1]

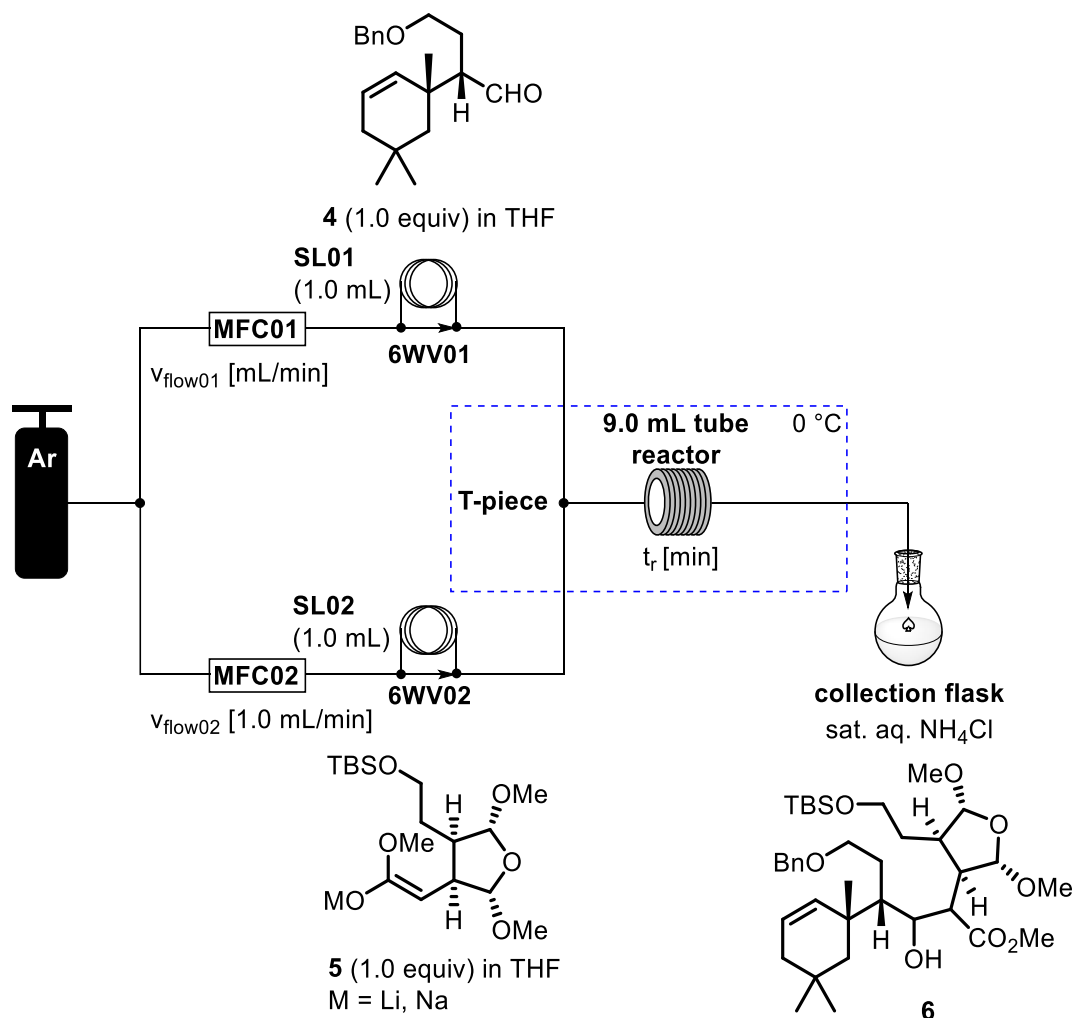


Table S2: Screening of different reaction conditions in flow.

Entry	Base	$V_{\text{flow_tot}}$ [mL/min] ^[a]	t_r [min]	Yield ^[b]
1	NaHMDS	2	4.5	n.d. ^[c]
2	LiN(<i>i</i> Pr) ₂	2	4.5	42%
3	LiN(<i>i</i> Pr) ₂	3	3	41%
4	LiN(<i>i</i> Pr) ₂	6	1.5	26%

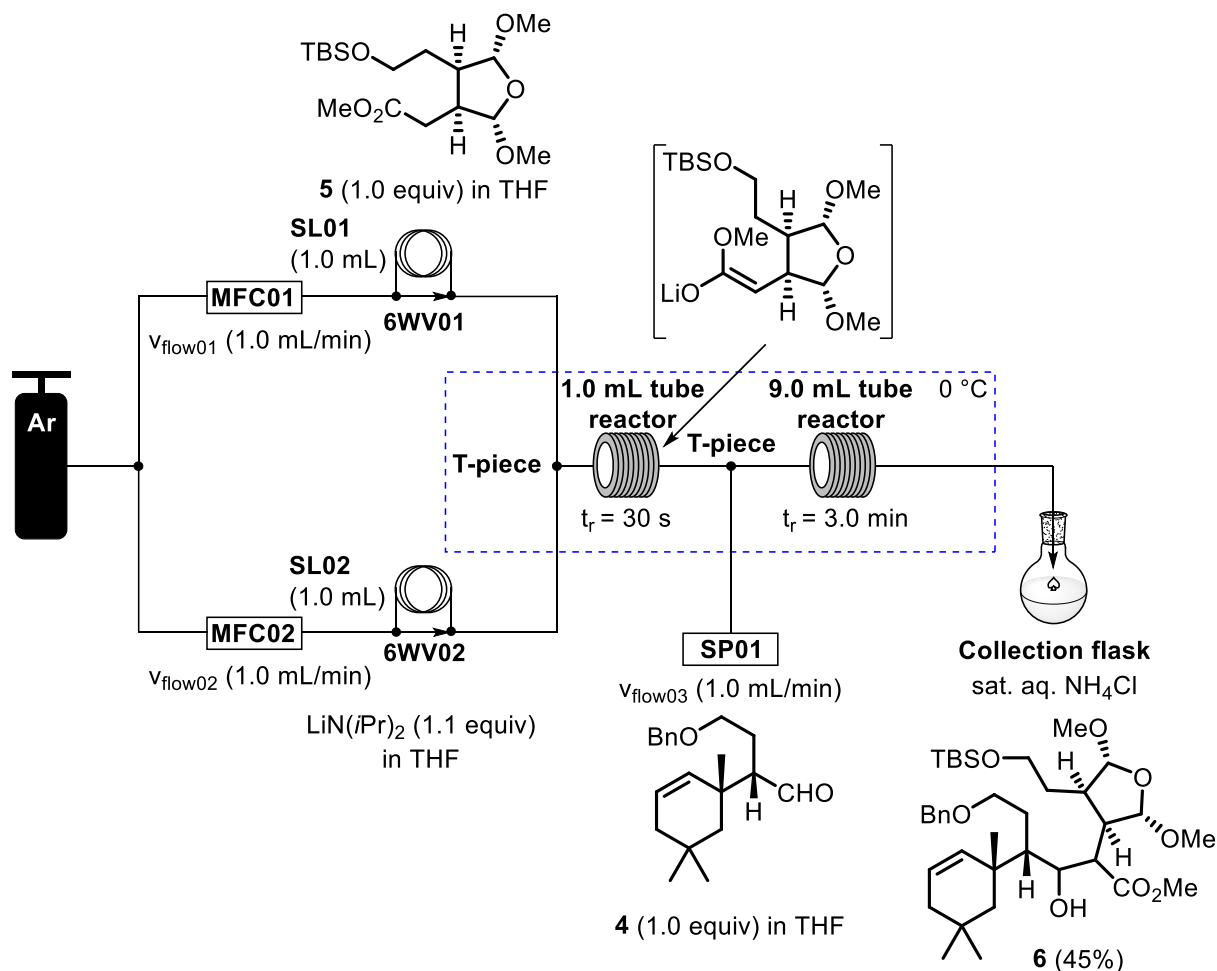
NaHMDS = sodium bis(trimethylsilyl)amide. LiN(*i*Pr)₂ was freshly prepared from HN(*i*Pr)₂ and *n*BuLi in THF at 0 °C. [a] $V_{\text{flow_tot}} = V_{\text{flow01}} + V_{\text{flow02}}$; $V_{\text{flow01}} = V_{\text{flow02}}$. [b] Isolated yield. [c] No conversion according to TLC.

In a dry Schlenk tube, a solution of ester **5** in THF (1.2 mL) was treated at 0 °C with base and stirred at this temperature for 5 min. Then, the reaction mixture was loaded on sample loop 01 (**SL01**, $V = 1.0$ mL, FEP tube, outer diameter 1/16", inner diameter 1/32").

In another dry Schlenk tube, 1.2 mL of a 0.083 M solution of aldehyde **4** (29.8 μ g, 100 μ mol) was prepared in THF and loaded on sample loop 02 **SL02** ($V = 1.0$ mL, FEP tube, outer diameter 1/16", inner diameter 1/32").

Then, both solutions were driven by an argon flow using **MFC01** (v_{flow01} [mL/min]) and **MFC02** (v_{flow01} [mL/min]). Both solutions were passed through a precooling tube (FEP tube, outer diameter 1/16", inner diameter 1/32", $V = 0.2$ mL), then mixed in a **T-piece** at 0 °C and pumped through a cooled **9.0 mL tube reactor** (FEP tube, outer diameter 1/16", inner diameter 1/32") at 0 °C with a residence time t_r [min]. At the end of this reactor, the reaction mixture was collected in a **collection flask** containing sat. aq. NH₄Cl (20 mL). The mixture was diluted with EtOAc (20 mL), the aqueous layer was separated, and extracted with EtOAc (2x20 mL). The combined organic layers were dried (MgSO₄), filtered, and concentrated under reduced pressure. Flash column chromatography (SiO₂, *n*pentane/Et₂O 3:1) gave β -hydroxy ester **6** as a colorless oil.

Deprotonation of ester **5** and aldol reaction with aldehyde **4** in flow



In a dry Schlenk tube, 6 mL of a 0.09 M solution of $\text{LiN}(i\text{Pr})_2$ in THF was prepared by addition of $n\text{BuLi}$ (220 μL , 546 μmol , 2.5 M in $n\text{hexane}$) to a solution of $\text{HN}(i\text{Pr})_2$ (60.0 mg, 84.0 μL , 600 μmol) in anhydrous THF (5.7 mL) at 0 °C followed by stirring at this temperature for 5 min. This solution was loaded on sample loop 02 (SL02, $V = 1.0$ mL, FEP tube, outer diameter 1/16", inner diameter 1/32").

In another dry Schlenk tube, 1.2 mL of a 0.083 M solution of ester **5** (36.0 mg, 100 μmol) was prepared in THF and loaded on sample loop 01 (SL01, $V = 1.0$ mL, FEP tube, outer diameter 1/16", inner diameter 1/32").

In a third dry Schlenk tube, 1.2 mL of a 0.083 M solution of aldehyde **4** (29.8 μg , 100 μmol) was prepared in THF and loaded on a gas tight syringe.

Then, both solutions were driven by an argon flow using MFC01 ($v_{\text{flow}01} = 1.0$ mL/min) and MFC02 ($v_{\text{flow}01} = 1.0$ mL/min). Both solutions were passed through a precooling tube (FEP tube, outer diameter 1/16", inner diameter 1/32", $V = 0.2$ mL), then mixed in a T-piece at 0 °C and pumped through a pre-cooled 1.0 mL tube reactor (FEP tube, outer diameter 1/16", inner diameter 1/32") at 0 °C with a residence time of $t_r = 30$ s. At the end of this reactor, the reaction stream was mixed with a solution of aldehyde **4** after passing through a precooling tube (FEP tube, outer diameter 1/16", inner diameter 1/32", $V = 0.2$ mL). The combined reaction stream was then pumped through a cooled 9.0 mL tube

reactor (FEP tube, outer diameter 1/16", inner diameter 1/32") at 0 °C with a residence time of $t_r = 3.0$ min. At the end of this reactor, the reaction mixture was collected in a **collection flask** containing sat. aq. NH_4Cl (20 mL). The mixture was diluted with EtOAc (20 mL), the aqueous layer was separated, and extracted with EtOAc (2x20 mL). The combined organic layers were dried (MgSO_4), filtered, and concentrated under reduced pressure. Flash column chromatography (SiO_2 , *n*-pentane/ Et_2O 3:1) gave β -hydroxy ester **6** (24.8 mg, 37.4 μmol , 45%) as a colorless oil along with reisolated aldehyde **4** (11.9 mg, 39.6 μmol , 48%) as colorless oil and ester **5** (13.8 mg, 38.1 μmol , 46%) as colorless oil.

The yield is based on the actual reacted reagent solutions loaded on **SL01** (ester **5** (30.0 mg, 83.0 μmol , 1.0 equiv)), **SL02** (1.0 mL; $\text{LiN}(i\text{Pr})_2$ 1.0 mL, 91.0 μmol , 1.1 equiv; 0.09 M in THF) and the solution of aldehyde **4** (24.9 mg, 83.0 μmol , 1.0 equiv) reaching the reaction stream (1.0 mL).

$R_f = 0.36$ (*n*-pentane/ Et_2O 3:1).

^1H NMR (700 MHz, CDCl_3) δ [ppm] = 7.34 – 7.31 (m, 5H), 5.63 (ddd, $J = 10.1, 6.0, 2.2$ Hz, 1H), 5.33 (ddd, $J = 10.1, 2.6, 1.4$ Hz, 1H), 4.90 (d, $J = 6.5$ Hz, 1H), 4.83 (s, 1H), 4.49 (d, $J = 12.1$ Hz, 1H), 4.45 (d, $J = 12.1$ Hz, 1H), 4.07 – 4.04 (m, 1H), 3.59 (s, 3H), 3.59 – 3.56 (m, 2H), 3.48 (s, 3H), 3.47 – 3.43 (m, 1H), 3.36 (s, 3H), 3.35 – 3.34 (m, 1H), 3.07 (dt, $J = 12.0, 6.5$ Hz, 1H), 2.75 (d, $J = 6.8$ Hz, 1H), 2.59 (dd, $J = 11.9, 3.8$ Hz, 1H), 2.26 (ddd, $J = 12.0, 6.6, 2.7$ Hz, 1H), 1.85 – 1.79 (m, 1H), 1.77 (dt, $J = 16.8, 2.6$, 1H), 1.69 (dddd, $J = 16.7, 6.0, 2.4, 0.9$ Hz, 1H), 1.59 (d, $J = 5.2$ Hz, 1H), 1.58 – 1.50 (m, 2H), 1.45 (td, $J = 5.0, 2.8$ Hz, 1H), 1.27 – 1.25 (m, 3H), 1.19 (ddd, $J = 14.1, 2.6, 1.3$ Hz, 1H), 1.07 (s, 3H), 0.95 (d, $J = 1.3$ Hz, 6H), 0.88 (s, 9H), 0.03 (s, 3H), 0.02 (s, 3H).

$^{13}\text{C}\{^1\text{H}\}$ NMR (151 MHz, CDCl_3) δ [ppm] = 173.1, 138.8, 134.6, 128.4, 127.8, 127.5, 125.3, 108.3, 107.8, 72.8, 71.6, 69.5, 61.8, 56.0, 54.8, 51.8, 51.1, 49.4, 45.5, 44.9, 44.8, 40.1, 38.5, 33.1, 30.1, 29.2, 28.5, 26.7, 26.0, 25.6, 18.4, –5.3, –5.3.

The spectroscopic data are consistent with those reported in the literature.^[1]

4.5 Ramberg Bäcklund Rearrangement of α -Chlorinated Sulfoxide **7** in Flow

Screening of different reaction conditions for the Ramberg-Bäcklund rearrangement of α -chlorinated sulfoxide **7** in flow

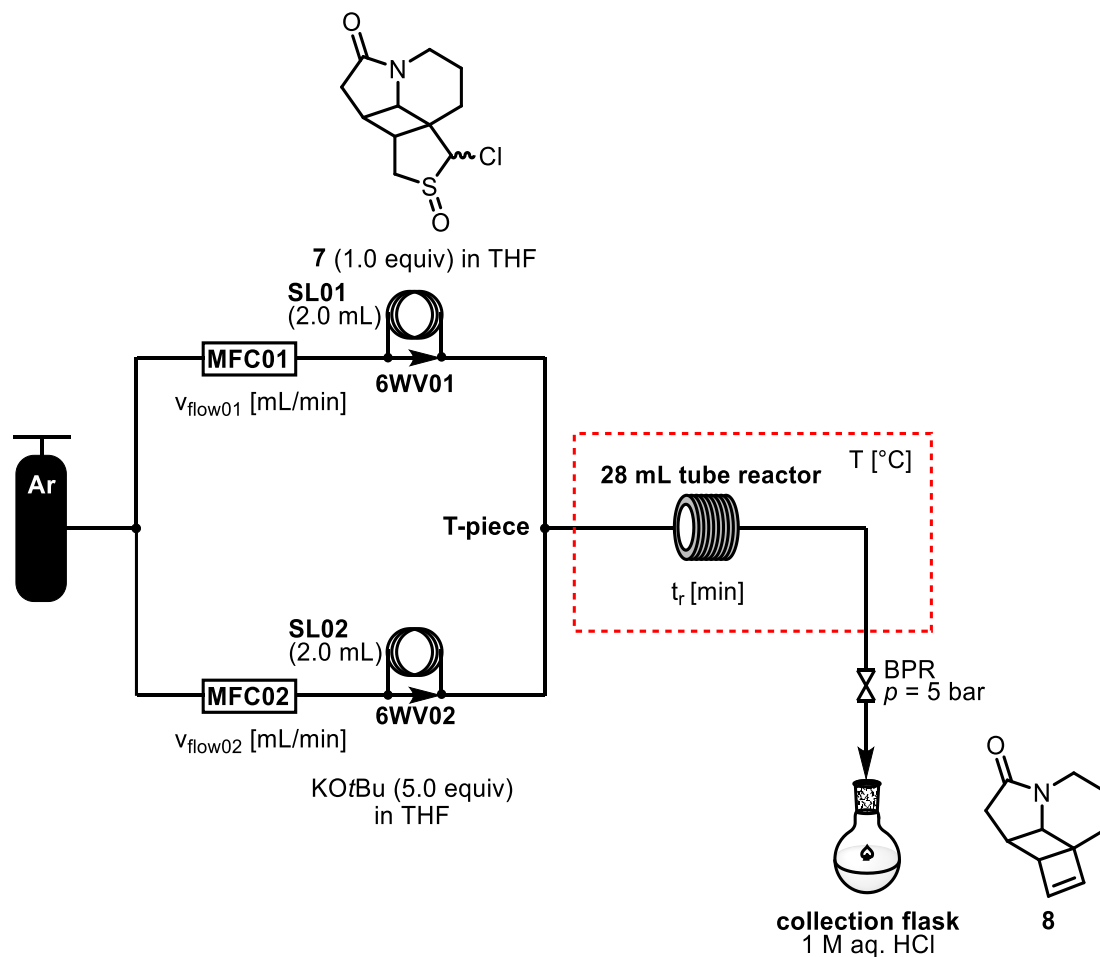


Table S3: Screening of different reaction conditions in flow.

Entry	T [°C]	t_r [min]	$V_{\text{flow_tot}}$ [mL/min] ^[a]	Yield [%] ^[b]
1	60	30	0.6	49
2	70	30	0.6	42
3	55	45	0.4	55
4	50	75	0.2	46

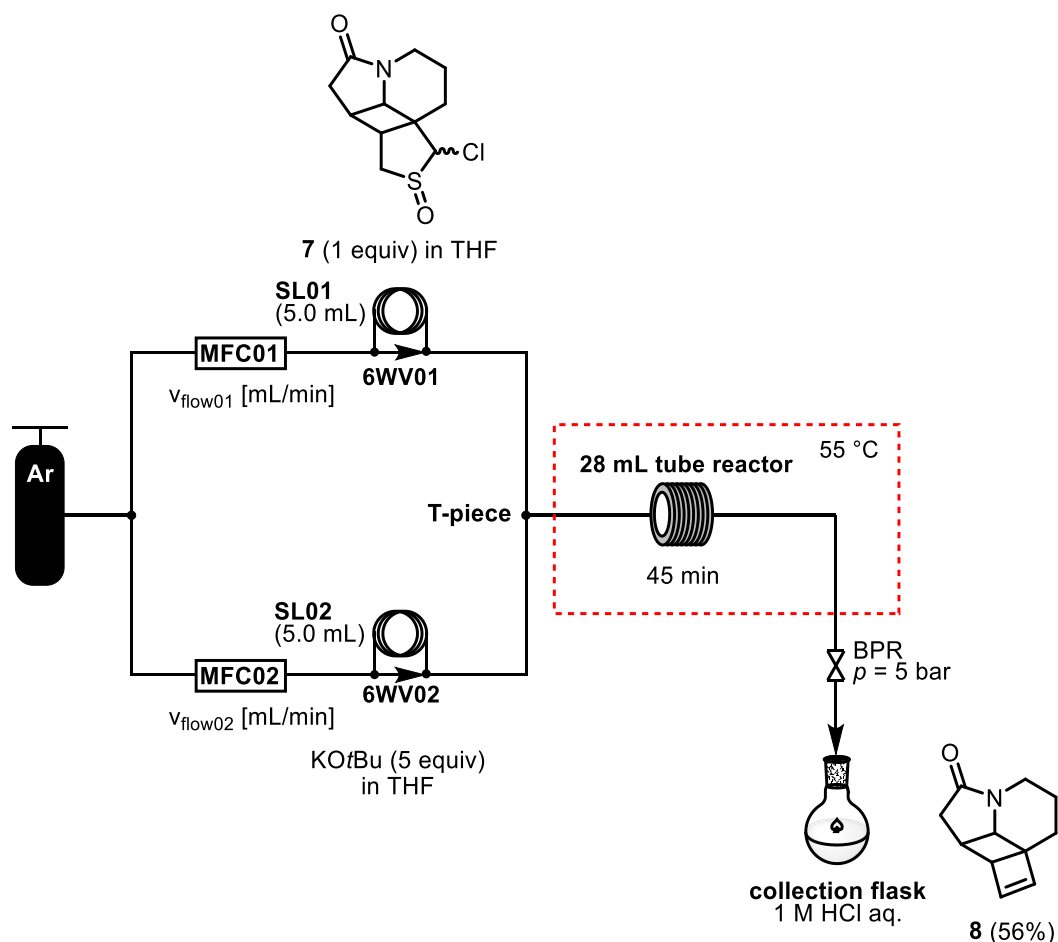
[a] $V_{\text{flow_tot}} = V_{\text{flow01}} + V_{\text{flow02}}$; $V_{\text{flow01}} = V_{\text{flow02}}$. [b] Isolated yield.

In a dry Schlenk tube, α -chlorinated sulfoxide **7** (12.5 mg, 48.1 μmol) was placed and the tube was evacuated and backfilled with argon (3x). Then, anhydrous and degassed THF (2.5 mL) was added. The resulting solution was loaded on sample loop **SL01** ($V = 2.0$ mL, FEP tube, outer diameter 1/16", inner diameter 1/32"). In another dry Schlenk tube, KO t Bu (27.0 mg, 241 μmol) was placed and the tube was

evacuated and backfilled with argon (3x). Then, anhydrous and degassed THF (2.5 mL) was added. The resulting solution was loaded on sample loop **SL02** ($V = 2.0$ mL, FEP tube, outer diameter 1/16", inner diameter 1/32"). Then, both solutions were driven by an argon flow using **MFC01** and **MFC02** with the flow rate ($v_{\text{flow_tot}} = v_{\text{flow01}} + v_{\text{flow02}}$; $v_{\text{flow01}} = v_{\text{flow02}}$) indicated. Both solutions were mixed in a **T-piece** and then pumped through a preheated **28 mL tube reactor** (PTFE tube, outer diameter 1/8", inner diameter 1/16") at the temperature indicated. At the end of the reactor, the reaction mixture was pressurized using a ZAIPUT back pressure regulator **BPR** (set to $p = 5$ bar) and then collected in a **50 mL collection flask** containing a stirred solution of HCl (1 M, aq., 10 mL). The mixture was diluted with EtOAc (20 mL). The aqueous layer was separated and extracted with EtOAc (2x20 mL). The combined organic layers were washed with NaHCO_3 (sat. aq., 25 mL), NaCl (sat. aq., 25 mL), dried (Na_2SO_4), filtered, and concentrated under reduced pressure. Flash column chromatography (cyclohexane/EtOAc 1:2) gave cyclobutene **8** as a yellow oil.

Yields are based on the actual reacted reagent solutions loaded on **SL01** (2.0 mL; α -chlorinated sulfoxide **7**, 10.0 mg, 38.0 μmol , 1.0 equiv) and **SL02** (2.0 mL; $\text{KO}t\text{Bu}$, 21.6 mg, 192 μmol , 5.0 equiv).

Ramberg Bäcklund rearrangement of α -chlorinated sulfoxide **7** under optimized conditions in flow



In a dry Schlenk tube, α -chlorinated sulfoxide **7** (30.0 mg, 115 μmol) was placed and the tube was evacuated and backfilled with argon (3x). Then, anhydrous and degassed THF (6.0 mL) was added. The resulting solution was loaded on sample loop **SL01** ($V = 5.0$ mL, FEP tube, outer diameter 1/16", inner diameter 1/32"). In another dry Schlenk tube, KO t Bu (64.8 mg, 577 μmol) was placed and the tube was evacuated and backfilled with argon (3x). Then, anhydrous and degassed THF (6.0 mL) was added. The resulting solution was loaded on sample loop **SL02** ($V = 5.0$ mL, FEP tube, outer diameter 1/16", inner diameter 1/32"). Then, both solutions were driven by an argon flow using **MFC01** ($v_{\text{flow}01} = 0.2$ mL/min) and **MFC02** ($v_{\text{flow}01} = 0.2$ mL/min). Both solutions were mixed in a **T-piece** and then pumped through a preheated **28 mL tube reactor** (PTFE tube, outer diameter 1/8", inner diameter 1/16") at 55 °C for 45 min. At the end of the reactor, the reaction mixture was pressurized using a ZAIPUT back pressure regulator **BPR** (set to $p = 5$ bar) and then collected in a **50 mL Erlenmeyer flask** containing a stirred solution of HCl (1 M, aq., 10 mL). The mixture was diluted with EtOAc (20 mL). The aqueous layer was separated and extracted with EtOAc (2x20 mL). The combined organic layers were washed with NaHCO₃ (sat. aq., 25 mL), NaCl (sat. aq., 25 mL), dried (Na₂SO₄), filtered and concentrated under reduced pressure. Flash column chromatography (cyclohexane/EtOAc 1:2) gave cyclobutene **8** (9.50 mg, 54.2 μmol , 56%) as a yellow oil.

The yield is based on the actual reacted reagent solutions loaded on **SL01** (5.0 mL; α -chlorinated sulfoxide **7** (25.0 mg, 96.0 μmol , 1.0 equiv)) and **SL02** (5.0 mL; KO t Bu (54.0 mg, 481 μmol , 5.0 equiv)).

$R_f = 0.40$ (cyclohexane/EtOAc 1:2).

¹H NMR (600 MHz, CDCl₃) δ [ppm] = 6.49 (d, $J = 2.5$ Hz, 1H), 6.09 (t, $J = 2.9$ Hz, 1H), 4.09 (ddt, $J = 13.0, 4.2, 1.8$ Hz, 1H), 3.93 (d, $J = 4.6$ Hz, 1H), 2.90 (dt, $J = 3.5, 1.8$ Hz, 1H), 2.71 (dd, $J = 17.4, 8.2$ Hz, 1H), 2.60 (td, $J = 12.4, 3.1$ Hz, 1H), 2.49 (ddd, $J = 7.6, 4.7, 1.8$ Hz, 1H), 2.27 (d, $J = 17.4$ Hz, 1H), 1.84 (ddd, $J = 15.0, 12.3, 5.6$ Hz, 1H), 1.75 (ddt, $J = 15.0, 4.4, 1.9$ Hz, 1H), 1.61 – 1.47 (m, 2H).

¹³C{¹H} NMR (151 MHz, CDCl₃) δ [ppm] = 175.0, 143.8, 138.8, 59.0, 55.9, 52.4, 39.9, 36.5, 34.6, 27.2, 23.2.

The spectroscopic data are consistent with those reported in the literature.^[2]

4.6 C–H Chlorination of (+)-Sclareolide in Flow

Screening of different reaction conditions for the C–H chlorination of (+)-sclareolide (**9**)

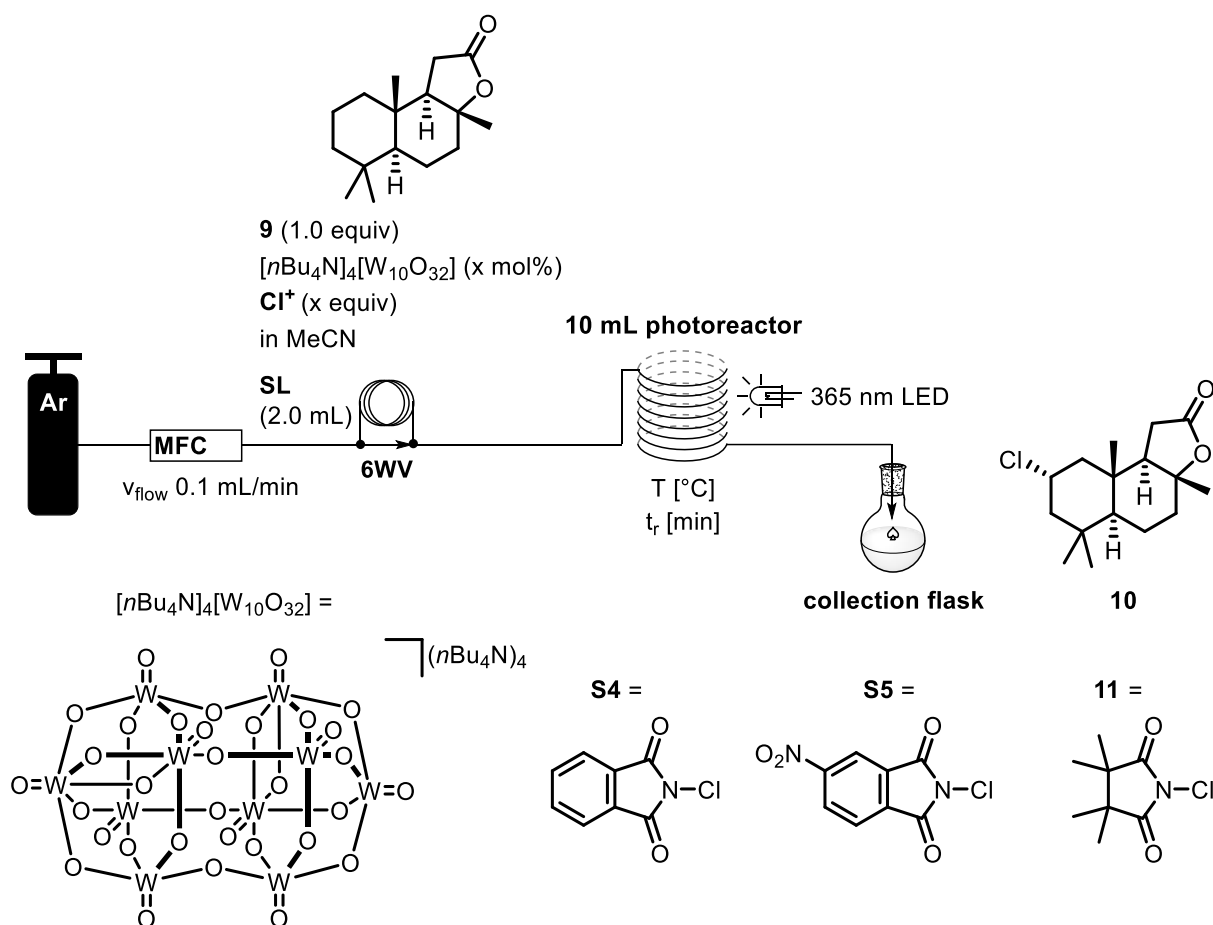


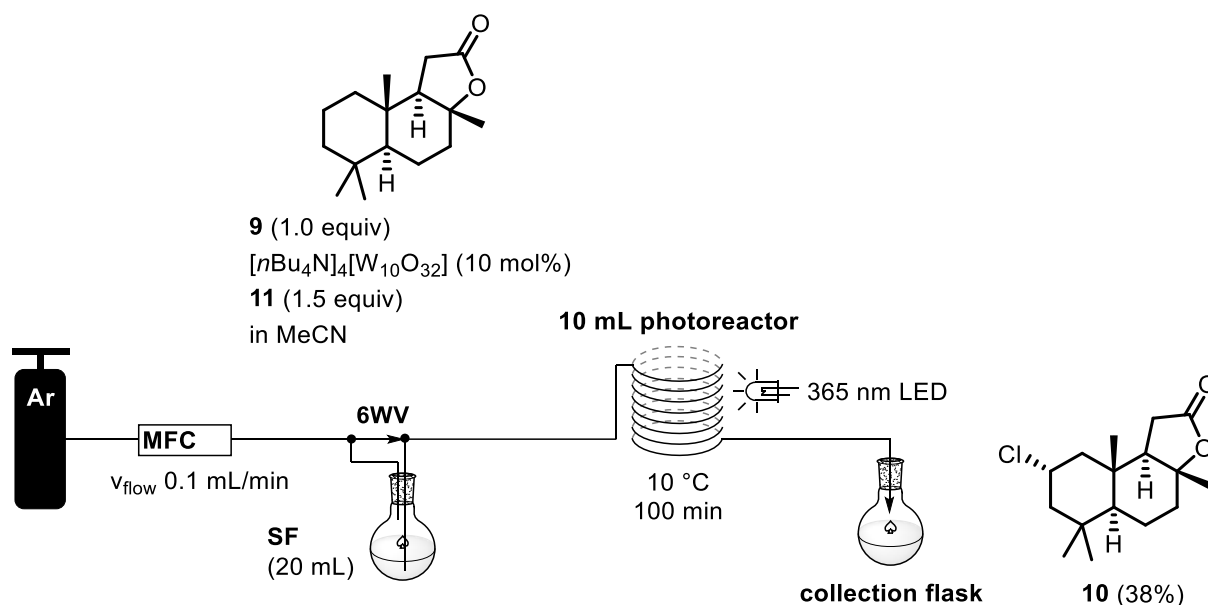
Table S4: Screening of reaction conditions.

Entry	Cl^+ (equiv)	mol%	conc. (9)	v_{flow} [min/mL] ^[a]	T [°C]	t_r [min]	Yield ^[b]
1	NCS (1.2)	5	0.1 M	0.1	30	100	11%
2	NCS (1.2)	5	0.2 M	0.1	30	100	17%
3	NCS (1.5)	7	0.2 M	0.1	30	100	24%
4	S4 (1.5)	10	0.2 M	0.1	30	100	19%
5	S5 (1.5) ^[c]	10	0.2 M	0.1	30	100	6%
6	11 (1.5)	10	0.2 M	0.1	30	100	29%
7 ^[d]	11 (1.5)	10	0.2 M	0.1	30	100	5%
8	11 (1.5)	10	0.2 M	0.2	30	50	20%
9	11 (1.5)	10	0.2 M	0.1	10	100	41%

[a] $V_{\text{flow_tot}} = V_{\text{flow01}} + V_{\text{flow02}}$; $V_{\text{flow01}} = V_{\text{flow02}}$. [b] Isolated yield. [c] Limited solubility of the Cl^+ source in MeCN. [d] 2-Methyl-2-butene (0.5 equiv) was used as additive.

In a vial, 2.5 mL of a solution of (+)-sclareolide (**9**, 1.0 equiv), $[n\text{Bu}_4\text{N}]_4[\text{W}_{10}\text{O}_{32}]$ and the Cl^+ source in MeCN (HPLC grade) were prepared. The solution was swirled, to achieve homogeneity and, if necessary, filtered through a plug of cotton in a Pasteur pipette. Then, the solution was purged with argon for 5 min and loaded on the sample loop **SL** ($V = 2.0$ mL; FEP tube, outer diameter 1/16", inner diameter 1/32"). Then, the solution was driven by an argon flow using the **MFC** with the flow rate v_{flow} indicated through a **10 mL photoreactor** (FEP tube, outer diameter 1/16", inner diameter 1/32") at the temperature indicated. At the end of the reactor, the reaction mixture was collected in a **collection flask**, diluted with EtOAc (10 mL) and loaded on Celite[®]. MPLC (cyclohexane/EtOAc 19:1 to 9:1) gave the title compound **10** as a colorless solid.

Gram scale C–H chlorination of (+)-sclareolide



In a vial, 20 mL of a solution of (+)-sclareolide (**9**, 1.00 g, 3.99 mmol, 1.0 equiv), [*n*Bu₄N]₄[W₁₀O₃₂] and 1-chloro-3,3,4,4-tetramethylpyrrolidine-2,5-dione (**11**, 1.14 g, 5.99 mmol, 1.5 equiv) in MeCN (HPLC grade) was prepared. The solution was swirled to achieve homogeneity and filtered through a plug of cotton using a Pasteur pipette in a 25 mL sample flask **SF** (V = 25 mL). The sample flask **SF** was sealed with a rubber septum, purged with argon for 5 min and connected with the 6-way valve **6WV** using two connection tubes with canulas. Then, the solution was driven by an argon flow using the **MFC** (*v*_{flow} = 0.1 mL/min) through a **10 mL photoreactor** (FEP tube, outer diameter 1/16", inner diameter 1/32") at 10 °C. At the end of the reactor, the reaction mixture was collected in a **collection flask**, diluted with MeCN (50 mL), and loaded onto Celite[®]. MPLC (cyclohexane/EtOAc 19:1 to 9:1) gave compound **10** (436 mg, 1.53 mmol, 38%) as a colorless solid.

*R*_f = 0.30 (cyclohexane/EtOAc 7:1).

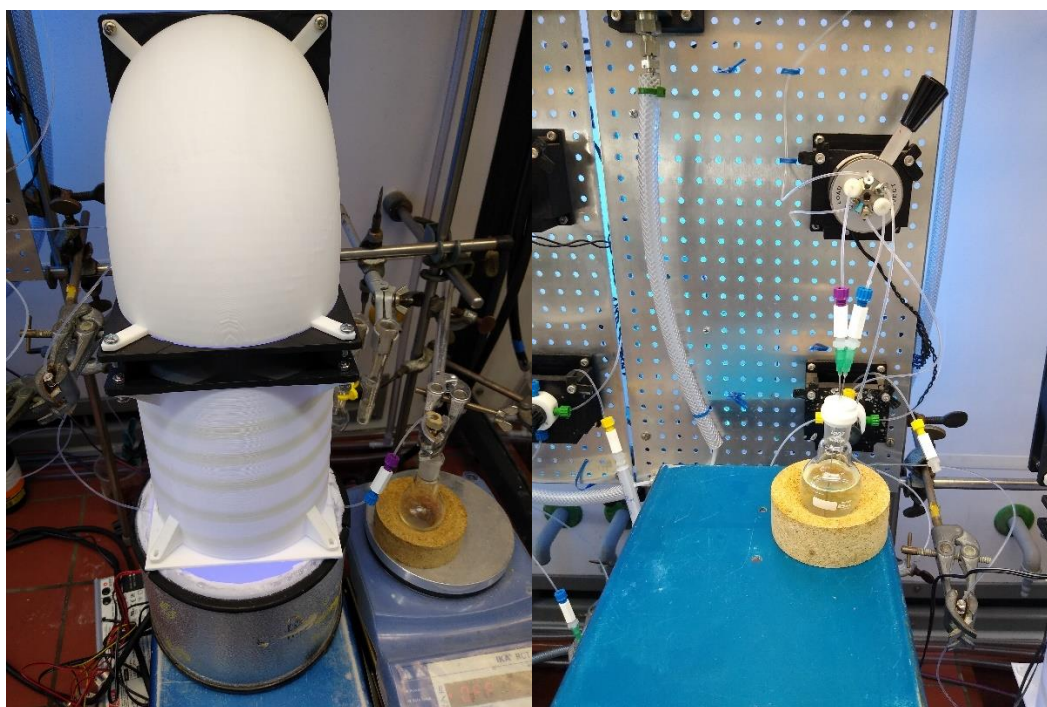
¹H NMR (600 MHz, CDCl₃) δ [ppm] = 4.23 (tt, *J* = 12.2, 4.2 Hz, 1H), 2.43 (dd, *J* = 16.2, 14.7 Hz, 1H), 2.28 (dd, *J* = 16.2, 6.5 Hz, 1H), 2.10 (dt, *J* = 12.0, 3.3 Hz, 1H), 2.05 – 1.97 (m, 3H), 1.93 – 1.87 (m, 1H), 1.74 – 1.67 (m, 1H), 1.53 (t, *J* = 12.7 Hz, 1H), 1.41 – 1.34 (m, 2H), 1.33 (d, *J* = 1.0 Hz, 3H), 0.97 (s, 3H), 0.96 (s, 3H), 0.89 (s, 3H).

¹³C NMR (151 MHz, CDCl₃) δ [ppm] = 176.3z, 86.0, 58.7, 55.9, 54.0, 52.5, 49.8, 38.5, 38.3, 36.0, 33.0, 28.7, 21.8, 21.5, 20.3, 15.9.

The spectroscopic data are consistent with those reported in the literature.^[13]

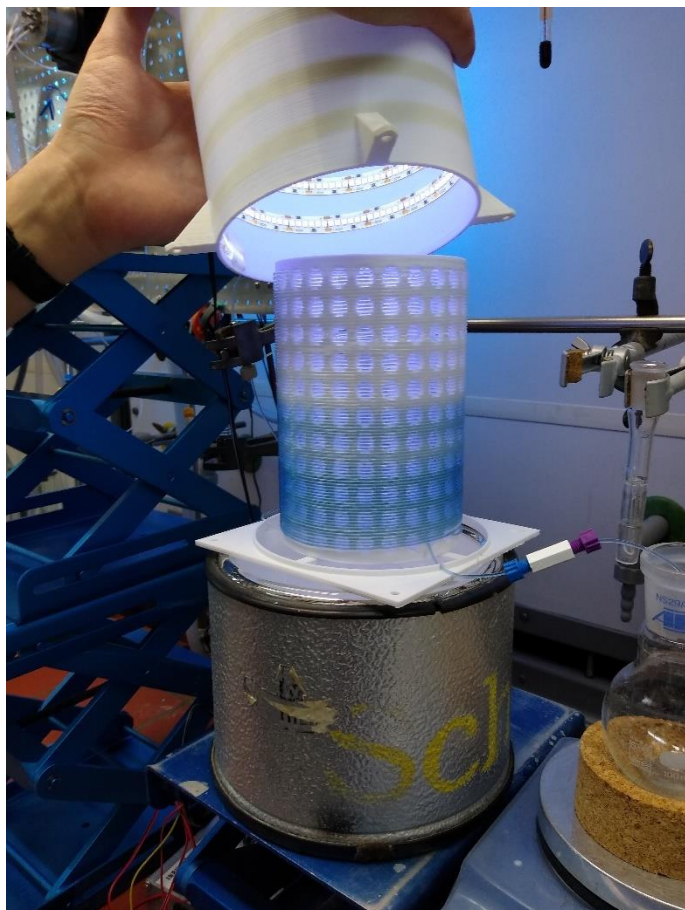


The flow setup for the photochemical gram scale C–H chlorination of (+)-sclareolide (9).



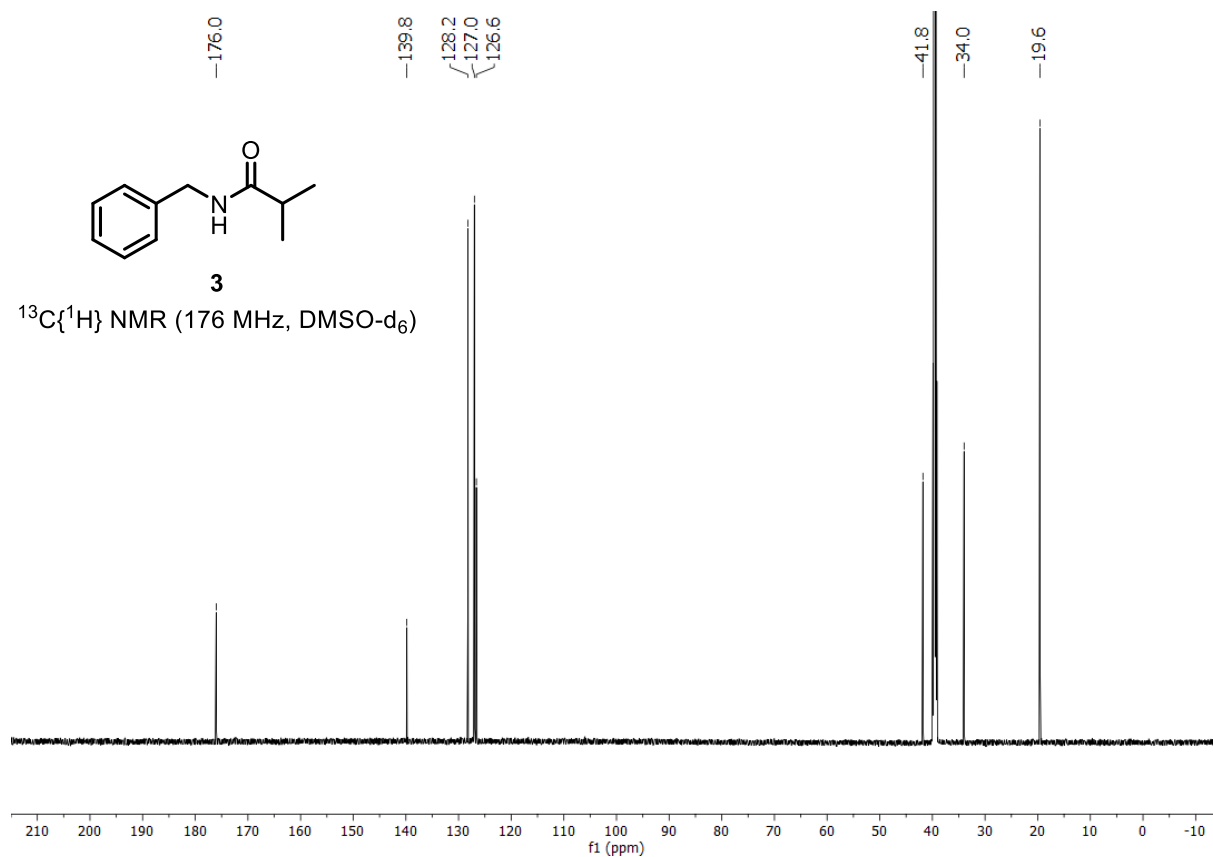
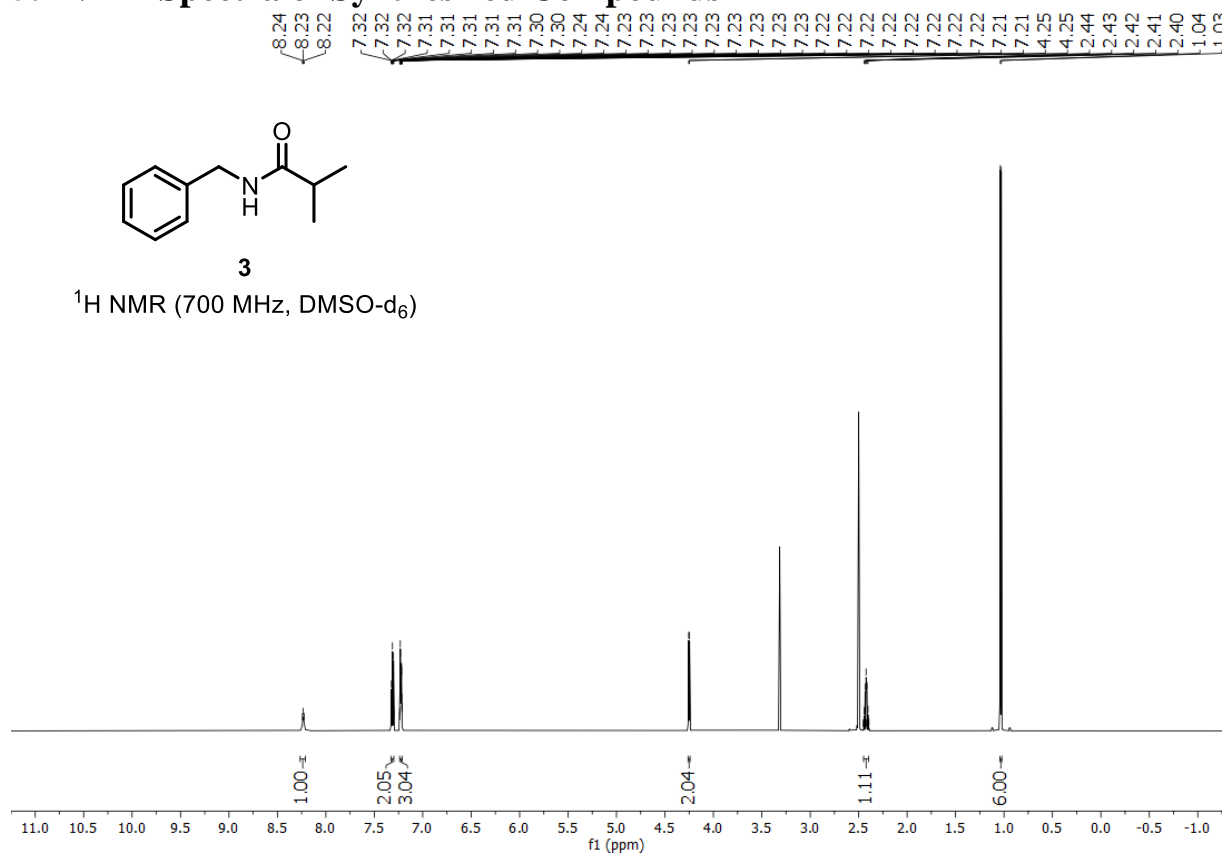
Left: The photoreaction was cooled by placing the photoreactor on a Dewar with liquid nitrogen. The evaporating nitrogen is drawn by two 140 mm PC fans through the photoreactor. The temperature is measured with a thermometer on the outlet of the photoreactor. By controlling the fan speed of the fans

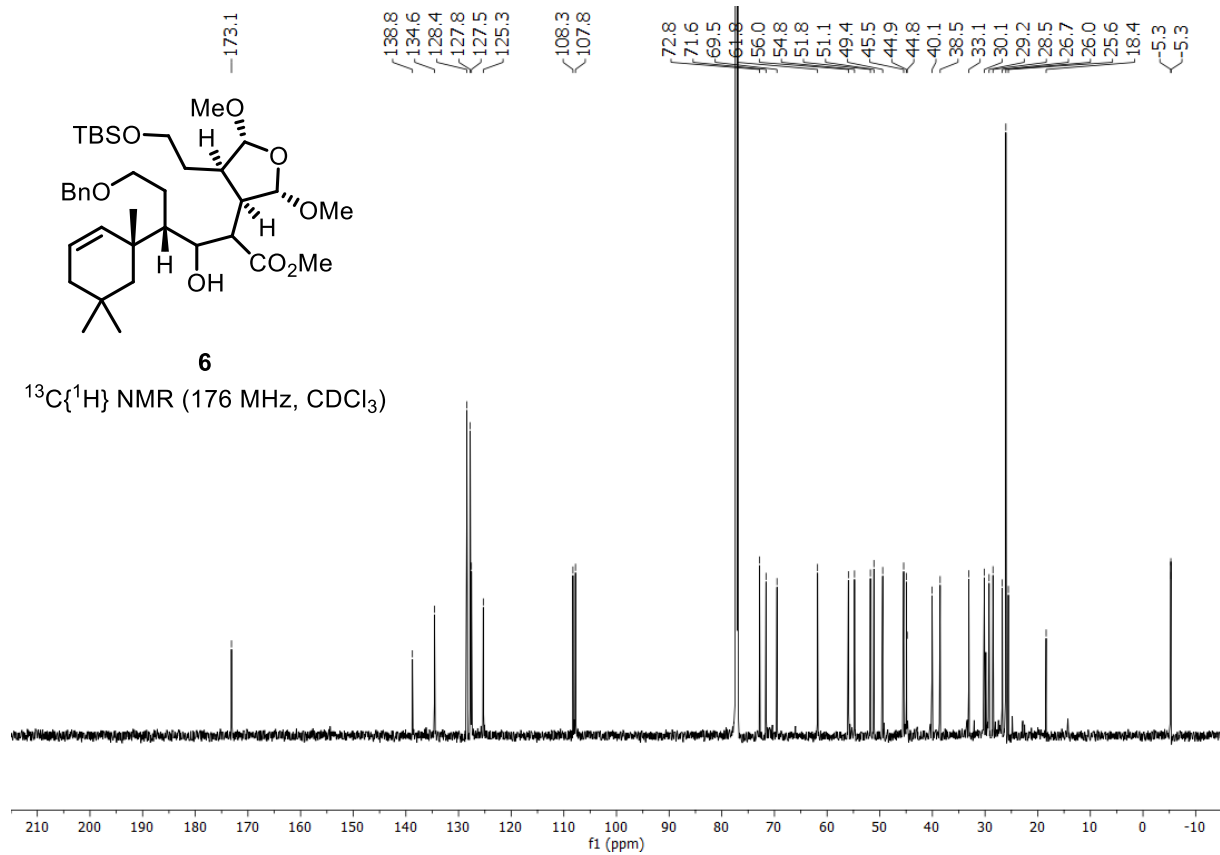
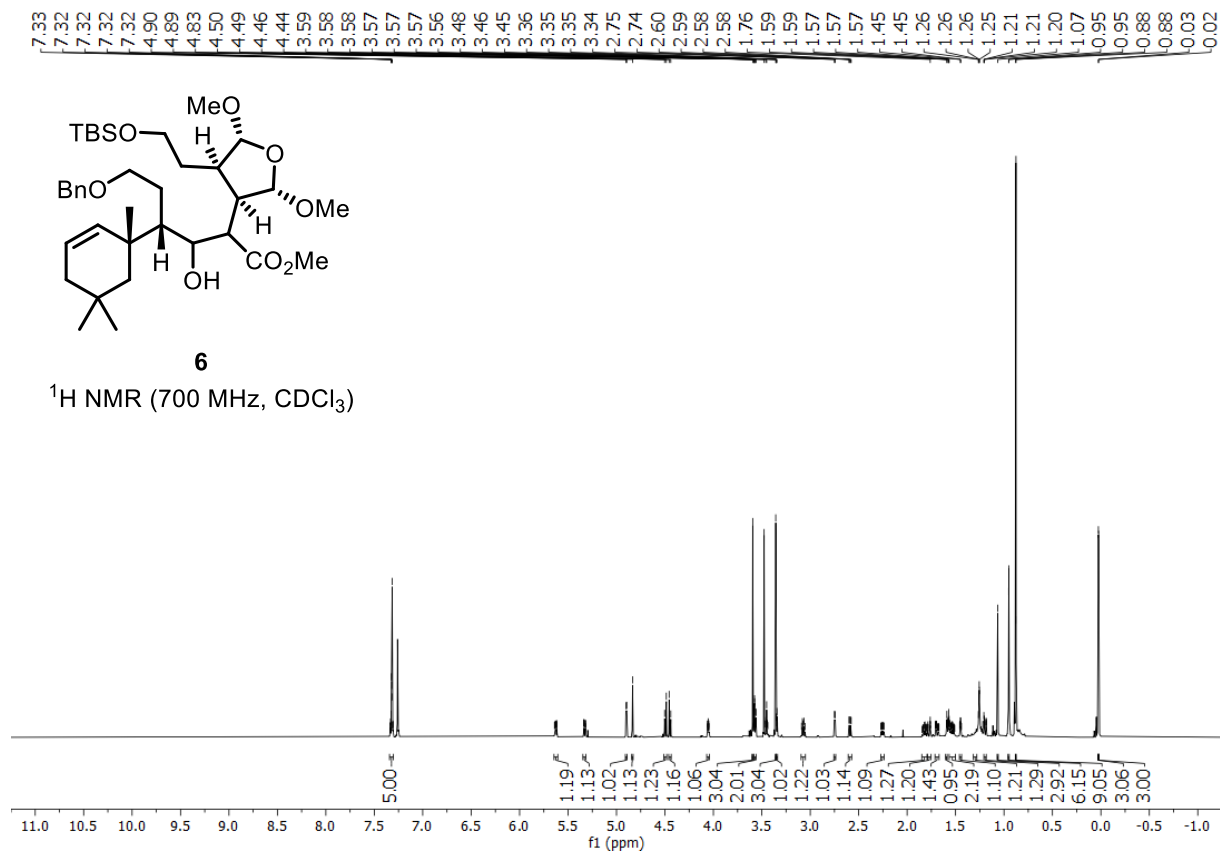
with a fan control, the temperature in the photoreactor can be controlled. **Right:** A 25 mL round bottom flask is used a sample flask equipped with a septum and canulas to provide a connection between the flask and the HPLC injection valve.

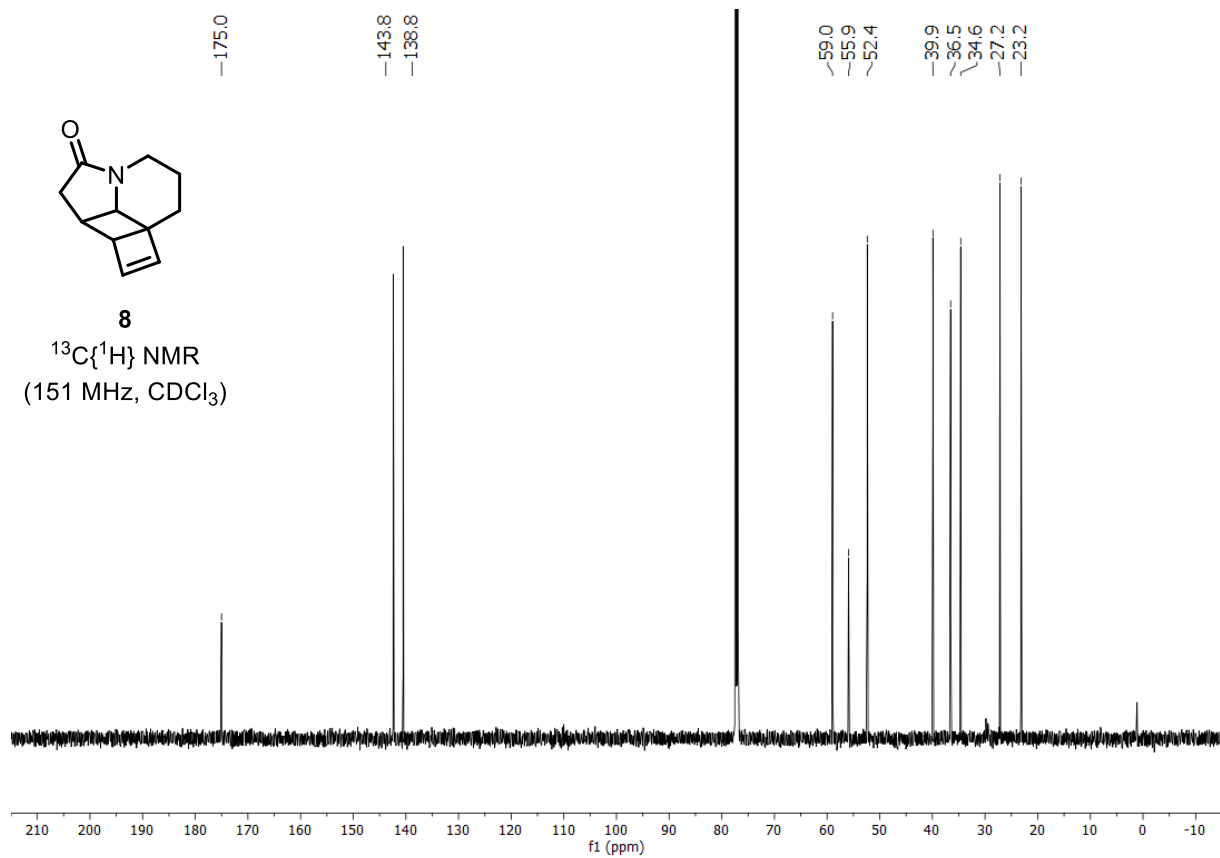
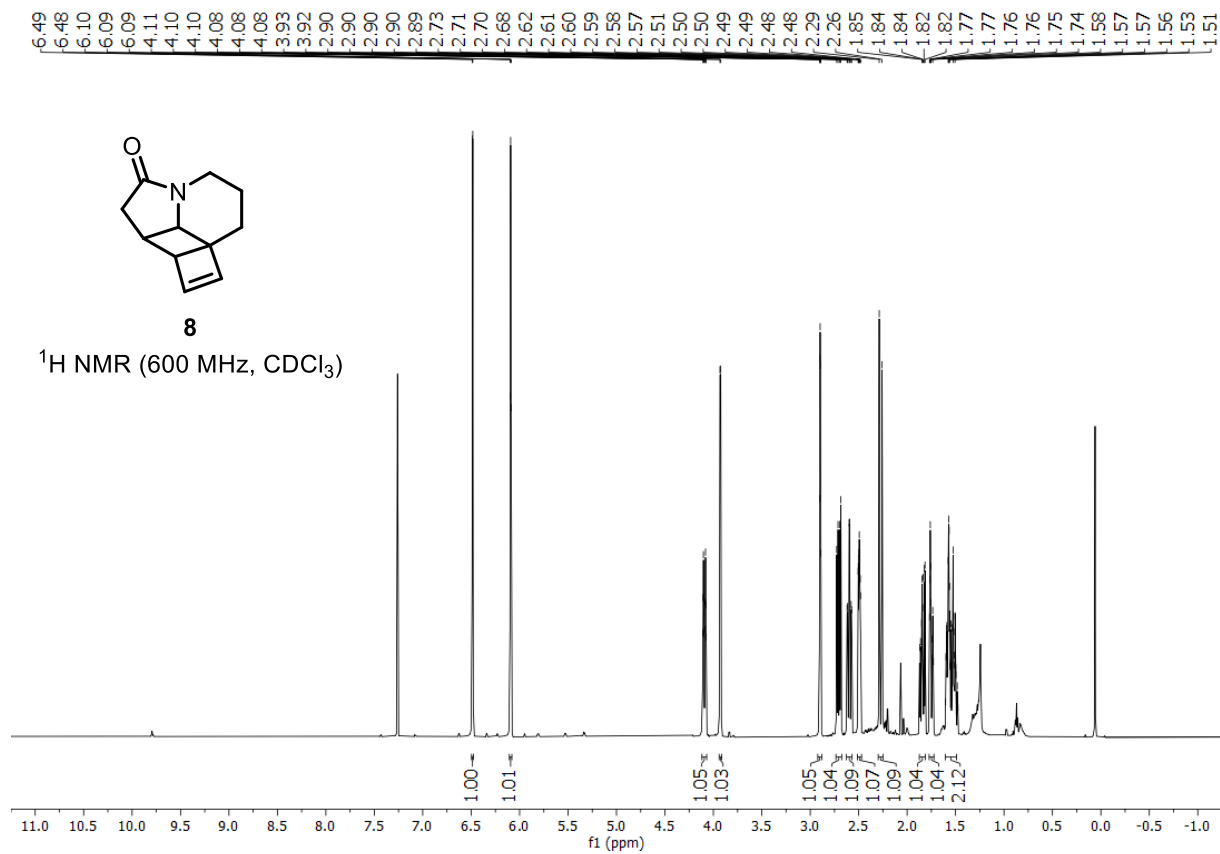


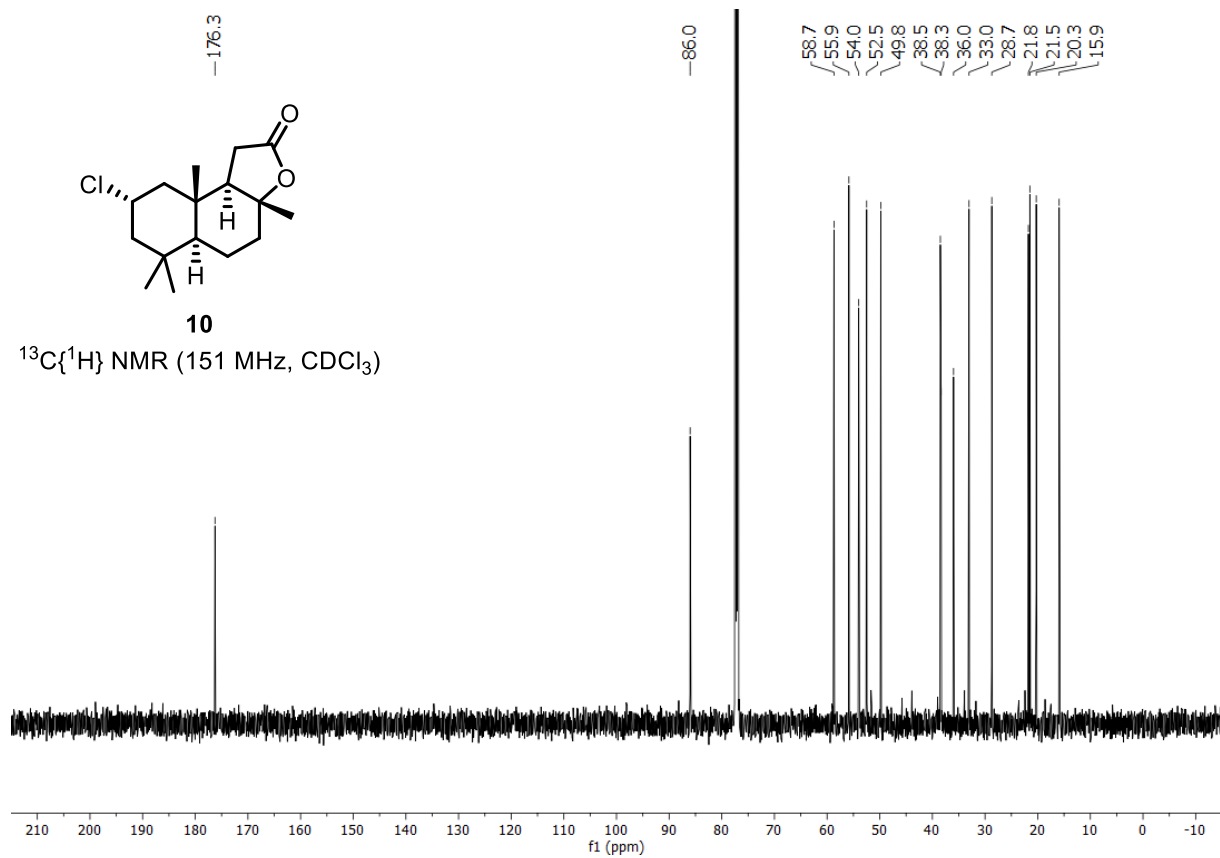
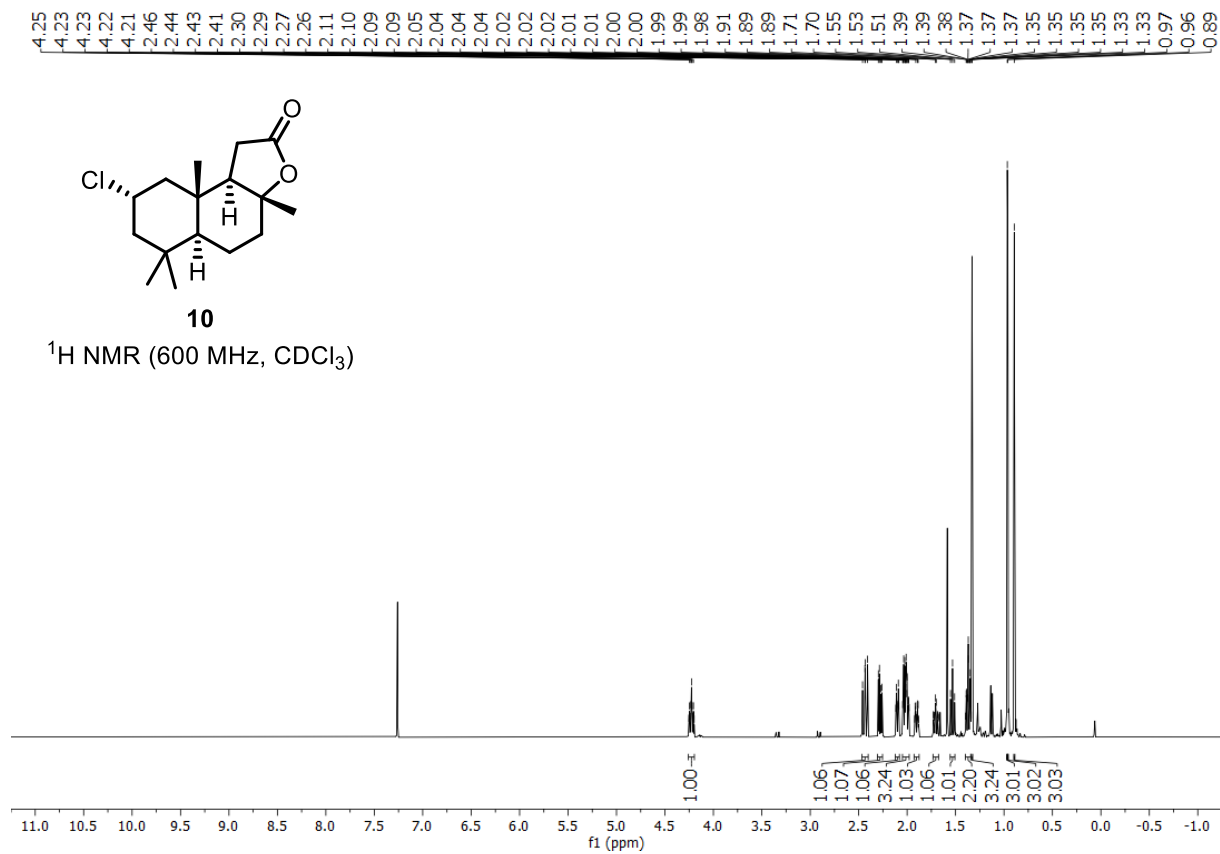
Over the course of the reaction (start on the top of the photoreactor, end on the bottom of the photoreactor), the chlorinating agent is continuously consumed. Thus, at the end of the reaction, the decatungstate deep blue anion $\text{H}^+[\text{W}_{10}\text{O}_{32}]^{5-}$ is not reoxidized to the colorless decatungstate $[\text{W}_{10}\text{O}_{32}]^{4-}$ anymore, resulting in a blue reaction mixture at the end of the reaction.

5. NMR Spectra of Synthesized Compounds









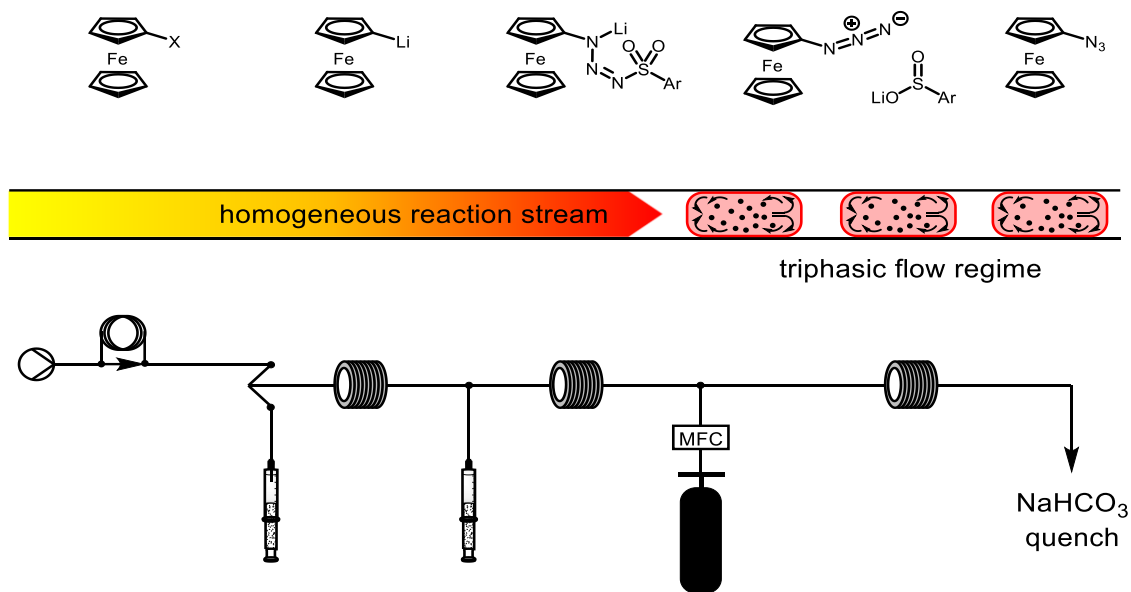
6. References

- [1] Siemon, T.; Steinhauer, S.; Christmann, M. Synthesis of (+)-Darwinolide, a Biofilm-Penetrating Anti-MRSA Agent. *Angew. Chem. Int. Ed.* **2019**, *58*, 1120–1122; *Angew. Chem.* **2019**, *131*, 1132–1134.
- [2] Reuß, F.; Heretsch, P. Synthesis of Aspidodispermine via Pericyclic Framework Reconstruction. *Org. Lett.* **2020**, *22*, 3956–3959.
- [3] Protti, S.; Ravelli, D.; Fagnoni, M.; Albini, A. Solar light-driven photocatalyzed alkylations. Chemistry on the window ledge. *Chem. Commun.* **2009**, 7351–7353.
- [4] Ponath, S.; Menger, M.; Grothues, L.; Weber, M.; Lentz, D.; Strohmam, C.; Christmann, M. Mechanistic Studies on the Organocatalytic α -Chlorination of Aldehydes: The Role and Nature of Off-Cycle Intermediates. *Angew. Chem. Int. Ed.* **2018**, *57*, 11683–11687; *Angew. Chem.* **2018**, *130*, 11857–11861.
- [5] Britton, J.; Jamison, T. F. The assembly and use of continuous flow systems for chemical synthesis. *Nature Prot.* **2017**, *12*, 2423–2446.
- [6] Williams, J. D.; Kerr, W. J.; Leach, S. G.; Lindsay, D. M. A Practical and General Amidation Method from Isocyanates Enabled by Flow Technology. *Angew. Chem. Int. Ed.* **2018**, *57*, 12126–12130; *Angew. Chem.* **2018**, *130*, 12302–12306.
- [7] https://www.buerkert.de/de/content/download/9318/335016/file/DE_Bestaendig_D.pdf
(09.11.2020)
- [8] Harding, M. J.; Brady, S.; O'Connor, H.; Lopez-Rodriguez, R.; Edwards, M. D.; Tracy, S.; Dowling, D.; Gibson, G.; Girard, K. P.; Ferguson, S. 3D printing of PEEK reactors for flow chemistry and continuous chemical processing. *React. Chem. Eng.* **2020**, *5*, 728–735.
- [9] Burgmayer, S. J. N. Use of a titanium metallocene as a colorimetric indicator for learning inert atmosphere techniques. *J. Chem. Educ.* **1998**, *75*, 460.
- [10] Yeung, D.; Penafiel, J.; Zijlstra, H. S.; McIndoe, J. S. Oxidation of Titanocene(III): The Deceptive Simplicity of a Color Change. *Inorg. Chem.* **2018**, *57*, 457–461.
- [11] Koros, W. J.; Wang, J.; Felder, R. M. Oxygen Permeation Through FEP Teflon and Kapton Polyimide. *J. Appl. Polym. Sci.* **1981**, *26*, 2805–2809.
- [12] Williams, D. B. G.; Lawton, M. Drying of Organic Solvents: Quantitative Evaluation of the Efficiency of Several Desiccants. *J. Org. Chem.* **2010**, *75*, 8351–8354.
- [13] Quinn, R. K.; Könst, Z. A.; Michalak, S. E.; Schmidt, Y.; Szklarski, A. R.; Flores, A. R.; Nam, S.; Horne, D. A.; Vanderwal, C. D.; Alexanian, E. J. Site-Selective Aliphatic C–H Chlorination Using *N*-Chloroamides Enables a Synthesis of Chlorolissoclimide. *J. Am. Chem. Soc.* **2016**, *138*, 696–702.

Appendix B

Scalable Synthesis of Functionalized Ferrocenyl Azides and Amines Enabled by Flow Chemistry

M. Kleoff, J. Schwan, L. Boeser, B. Hartmayer, M. Christmann, B. Sarkar, P. Heretsch



Institut für Chemie und Biochemie, Organische Chemie, Freie Universität Berlin, Takustraße 3,
14195 Berlin, Germany

This article is reproduced with permission from:

M. Kleoff, J. Schwan, L. Boeser, B. Hartmayer, M. Christmann, B. Sarkar, P. Heretsch, *Org. Lett.*
2020, *22*, 902–907.

<https://doi.org/10.1021/acs.orglett.9b04450>

© American Chemical Society

Author contributions: M. Kleoff and B. Sarkar designed the project. M. Kleoff and J. Schwan developed the flow setup. M. Kleoff, J. Schwan, L. Boeser, and B. Hartmayer carried out the experimental work. The analytical data were collected and analyzed by M. Kleoff. The manuscript was prepared by M. Kleoff and revised by J. Schwan, M. Christmann, and P. Heretsch.

Scalable Synthesis of Functionalized Ferrocenyl Azides and Amines Enabled by Flow Chemistry

Merlin Kleoff, Johannes Schwan, Lisa Boeser, Bence Hartmayer, Mathias Christmann,* Biprajit Sarkar,* and Philipp Heretsch*

Cite This: *Org. Lett.* 2020, 22, 902–907

Read Online

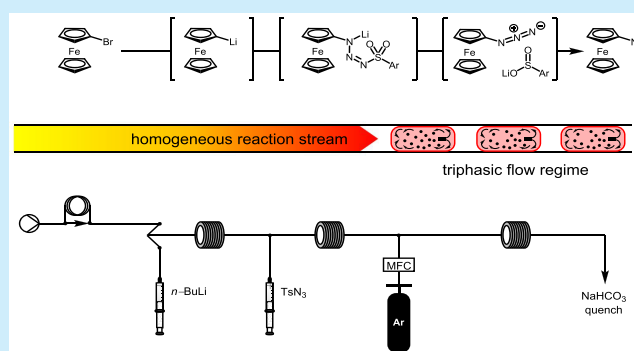
ACCESS |

Metrics & More

Article Recommendations

Supporting Information

ABSTRACT: A scalable access to functionalized ferrocenyl azides has been realized in flow. By halogen–lithium exchange of ferrocenyl halides and trapping with tosyl azide, a variety of functionalized ferrocenyl azides were obtained in high yields. To allow a scalable preparation of these potentially explosive compounds, a flow protocol was developed accelerating the reaction time to minutes and circumventing accumulation of potentially hazardous intermediates. The corresponding ferrocenyl amines were then prepared by a reliable reduction process.

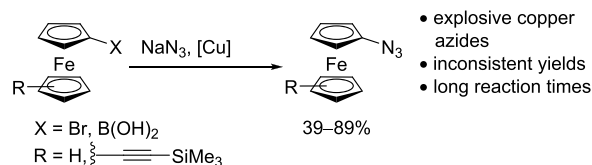


Since the discovery of ferrocene in 1951,¹ its derivatives have found innumerable applications in chemistry. The intriguing redox properties of ferrocenes led to applications in coordination chemistry,² inorganic materials,³ molecular wires and sensors.⁴ Their unique stability make ferrocenes useful in medicinal research⁵ and as privileged ligands in many catalysts.⁶ Frequently, these ferrocene based compounds are derived from ferrocenyl azides⁷ or amines.⁸ As organic azides can be readily reduced to the corresponding amines, ferrocenyl azides are the access hub to a large number of *N*-substituted ferrocenes. Owing to thermal lability and shock-sensitivity,⁹ the obvious synthetic potential of ferrocenyl azides has not been fully realized. For their preparation, copper mediated substitution of ferrocenyl bromides^{9a,10} and boronic acids¹¹ with sodium azide (Scheme 1A) was employed; however, this required the use of explosive copper azide. Alternatively, ferrocenyllithiums, prepared by lithiation of C–H bonds in ferrocenes, are reacted with aryl sulfonyl azides (Scheme 1B).^{6e,12} While for the former process inconsistent yields were reported, the latter suffers from low functional group tolerance.¹⁰ More recently, a single functionalized ferrocenyl azide was prepared by halogen–lithium exchange of the corresponding ferrocenyl halide.¹³ The azidation of aryl halides through bromine–lithium exchange and trapping with tosyl azide has been realized in flow very recently by Yoshida and Nagaki.^{14,15}

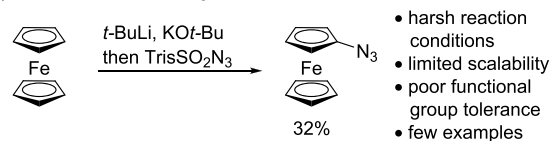
Fast chemical transformations immensely benefit from precise reaction control in a continuous flow setup.¹⁶ Enhanced heat and mass transfer has enabled organic reactions previously viewed impossible.^{14,15,17} Vice versa, slow reactions can be significantly accelerated by fast heating, frequently

Scheme 1. Synthesis of Functionalized Ferrocenyl Azides

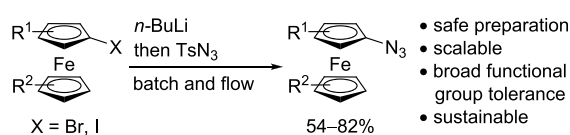
A) Copper-mediated substitution reaction



B) Azidation of ferrocenyllithiums



C) *this work*: Scalable synthesis of ferrocenyl azides in flow

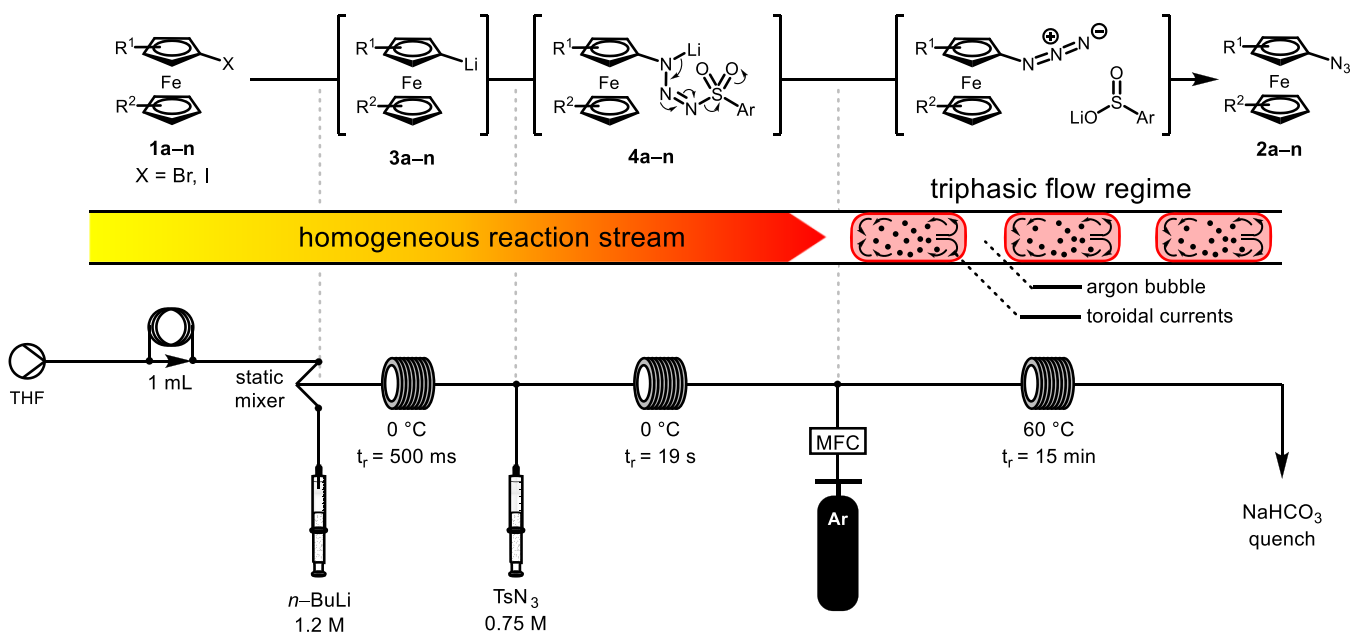


rendering a flow process more efficient and sustainable than a batch process.¹⁸ Herein, we describe the flow-enabled

Received: December 12, 2019

Published: January 15, 2020

Scheme 2. Optimized Setup for the Synthesis of Functionalized Ferrocenyl Azides in Flow



development of a general method for the safe and scalable synthesis of functionalized ferrocenyl azides (Scheme 1C) through azidation of ferrocenyllithiums.

In preliminary batch experiments we first investigated the propensity of halogen–metal exchange of iodoferrocene (**1a**), followed by trapping with arylsulfonyl azides under a variety of reaction conditions to give azidoferrocene (**2a**). Initially, *tert*-butyllithium was employed for iodine–lithium exchange at $-78\text{ }^{\circ}\text{C}$ for 30 min while different arylsulfonyl azides were screened (see Supporting Information). As a result, commercially available tosyl azide was identified to give the best yield (77%). To avoid the use of pyrophoric reagents, *n*-butyllithium was employed which also led to an increased yield (95%).¹⁹ To further improve the reaction parameters, we tested the iodine–lithium exchange and subsequent reaction with tosyl azide at $0\text{ }^{\circ}\text{C}$. Under these conditions, the yield dropped to 82% and handling of the exothermic reaction became a concern on a scale larger than 1 mmol.

With these general parameters established, our flow process was based on three reaction steps (Scheme 2): (1) halogen–lithium exchange of ferrocenyl halides of type **1** forming ferrocenyllithiums of type **3**, (2) trapping with tosyl azide leading to triazenes of type **4**, and finally, (3) thermal fragmentation of **4** to the desired ferrocenyl azides **2**. The combination of steps (1)/(2) with (3) in a continuous fashion immediately presented a general technological challenge for the reactor design: while halogen–lithium exchange of aryl halides and trapping with electrophiles can be performed at high flow rates within milliseconds,¹⁷ the fragmentation of triazene **4** is a slow reaction, necessitating, when performed in batch, warming from $-78\text{ }^{\circ}\text{C}$ to ambient temperatures over several hours. Thus, step (3) would translate into an extremely slow flow rate and require a steep decrease in flow rate of the incoming triazene stream. Although, triazene fragmentation can be promoted by thermolysis at temperatures of $120\text{--}130\text{ }^{\circ}\text{C}$,²⁰ this is usually avoided in batch due to safety considerations.²¹ Given the intrinsic properties of continuous flow, we deemed the thermal fragmentation a viable and

manageable reaction in a tube reactor, whereby fast heating of triazene **4** thermal strain is minimized significantly.^{16a,h}

We started to optimize the fast reactions and the slow fragmentation step separately. Thus, the iodine–lithium exchange of iodoferrocene (**1a**) and subsequent trapping with tosyl azide were conducted in a tube reactor. The resulting reaction mixture was collected in a flask and kept there for a prolonged time to complete fragmentation of triazene **4a** and determine the isolated yield of azidoferrocene (**2a**). As the intermediary ferrocenyllithium **3a** precipitated at temperatures below $0\text{ }^{\circ}\text{C}$, both reactions were performed at $0\text{ }^{\circ}\text{C}$ with precooled solutions of iodoferrocene (**1a**) and tosyl azide in tetrahydrofuran (THF) and *n*-butyllithium in *n*-hexane. A T-mixer was used for mixing the solutions of iodoferrocene and *n*-butyllithium with the result of the iodine–lithium exchange to take a relatively long time of 17 s, determined by complete conversion of starting material. When switching to a static mixer and a stainless-steel capillary reactor with an internal diameter of $250\text{ }\mu\text{m}$, full conversion was achieved in 500 ms.

We then focused our attention on the thermolytic fragmentation of triazene **4a** to azidoferrocene (**2a**). Thus, a solution of triazene **4a** in THF prepared in batch as described above was pumped through a tube reactor at elevated temperature. Upon fragmentation of triazene **4a** we observed precipitation of insoluble lithium *para*-toluenesulfonate, resulting in blockage of the tube reactor. Seeberger and Gilmore showed that suspensions can efficiently be kept in flow when a triphasic flow regime is used.²²

Thus, we merged the reaction mixture with an argon stream before entering the heated tube reactor. In the resulting gas–liquid flow, a strong toroidal current kept the precipitate in a floating state and blockage of the tubing was inhibited.²³ At a temperature of $60\text{ }^{\circ}\text{C}$, thermolysis of triazene **4a** was complete within 15 min providing azidoferrocene (**2a**) in a yield of 85%. In contrast, when a solution of triazene **4a** was heated from -78 to $60\text{ }^{\circ}\text{C}$ in batch, completion of the reaction required 30 min and gave a yield of only 70%, a limitation overcome by our flow process. Further accelerating the fragmentation by

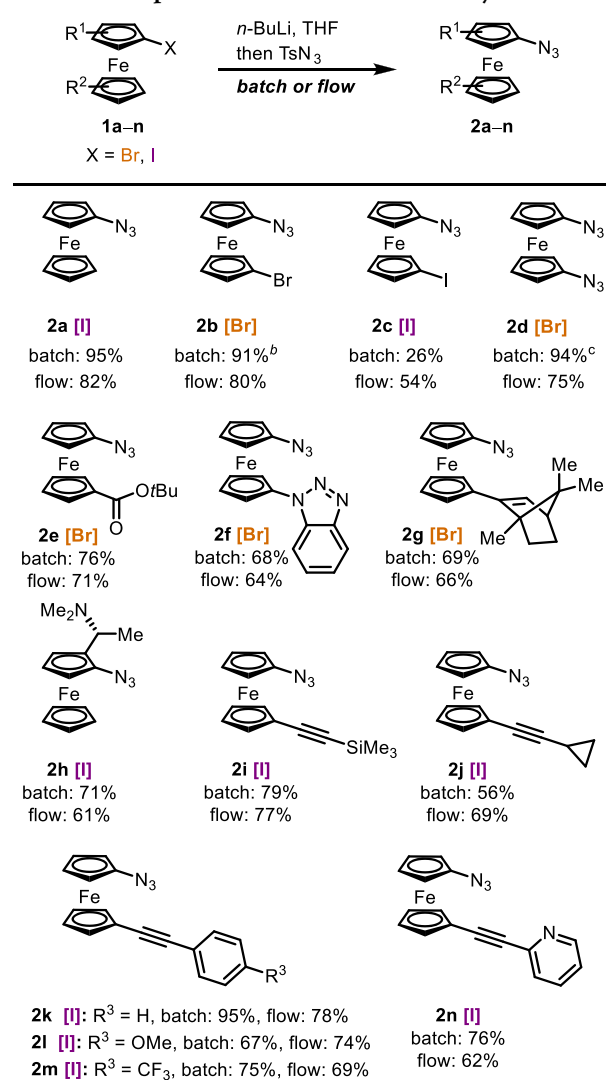
exceeding the boiling point of THF using back pressure regulators was only briefly contemplated, as blockage of the backpressure regulator by the suspension was expected.

We were now in the position to merge both processes into one continuous flow setup (Scheme 2). Some fine adjustment of flow rates and residence times was performed (see Supporting Information), and a mass flow controller providing a constant argon flow and a pumping system for solvent were employed to form a stable segmented flow regime. Iodoferrocene **1a** was introduced through an injection valve, while solutions of *n*-butyllithium in *n*-hexane and tosyl azide in THF were fed to the system by syringe pumps and mixed at 0 °C for 19 s. Finally, the reaction mixture was merged with an argon stream resulting in a segmented flow and warmed to 60 °C with a residence time of 15 min in a coiled tube reactor. Insoluble lithium *para*-toluenesulfinate precipitated from the reaction mixture resulting in a triphasic system of salt, liquid, and argon. The reaction mixture was eventually collected in a flask containing an aqueous sodium bicarbonate solution to quench any remaining reactive intermediates and remove inorganic byproducts. Using this flow setup, azidoferrocene (**2a**) was prepared in a yield of 82%. To showcase the practicality of our setup in the preparation of multigram quantities of azidoferrocenes, we performed a run with **1a** at a productivity of 4 g/h and achieved similar yields of **2a**.

We next applied our optimized flow conditions to a broad set of functionalized ferrocenyl halides **1b–n** (Scheme 3). The preparation of substrates **1e–1g** was achieved by selective bromine–lithium exchange of 1,1'-dibromoferrocene (see Supporting Information).¹⁰ Bromo-substituted ferrocenyl azide **2b** was obtained in an excellent yield. For the iodo-substituted compound **2c**, the yield dropped significantly to 26% in batch as the iodine–lithium exchange was less selective. However, in flow the selectivity could be enhanced providing **2c** in 54% yield. Double azidation of 1,1'-dibromoferrocene gave the valuable diazide **2d** in an improved yield of 94% compared to previously reported 59% in batch.^{9a} Due to its explosive nature, the preparation of this compound in flow (75% yield) benefited significantly from the better safety profile of our setup. Notably, the *tert*-butyl ester present in substrate **1e** was tolerated giving the corresponding azide **2e**, a precursor for ferrocene amino acids (*vide infra*). Camphor-derived ferrocenyl terpene **2g** was obtained in 66–69% yield. The planar chiral substrate **1h** was prepared by diastereoselective lithiation–iodination of enantioenriched Ugi's amine. Formation of the corresponding azide **2h** proceeded with retention of configuration. Heteroaromatic ferrocenyl azide **2f** could be obtained in good yield. As ethynyl-substituted ferrocene derivatives are frequently used in molecular wires,⁴ we prepared an array of ethynyl-substituted ferrocenyl azides (**2i–2n**). These compounds were obtained in good to excellent yields in batch and flow. Both, electron-donating (**2l**) and electron-withdrawing (**2m**) groups attached to the aromatic moiety were tolerated. Ethynyl azide **2i** was prepared in 77–79% yield presenting the opportunity for sequential click chemistry.^{11,24} For cyclopropyl-substituted azide **2j** the yield dropped slightly (56% in batch, 69% in flow). Generally, we assume that yields of ferrocenyl azides **2** are slightly lower in flow than in batch due to traces of water in the flow reactor resulting in hydrolysis of the intermediary ferrocenyllithiums **3**.

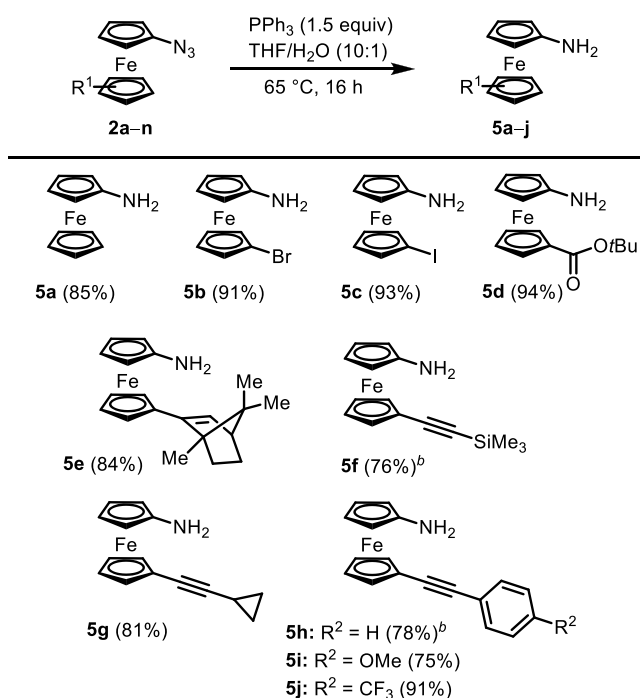
The reduction of ferrocenyl azides by palladium-catalyzed hydrogenation is well documented^{7c,25} but not suitable for ferrocenyl azides **2g** and **2i–n** containing olefin or alkyne

Scheme 3. Scope of Functionalized Ferrocenyl Azides^a



^aStarting from the corresponding ferrocenyl bromides [Br] or iodides [I]. Yields of isolated products are given. Batch reaction conditions: substrate (1 equiv), *n*-butyllithium (1.1 equiv), tosyl azide (1.2 equiv) in THF (0.05–0.16 M) at –78 °C, 30 min, warmed to 25 °C over 16 h. Flow reaction conditions: substrate (0.2 M in THF; $\nu = 2$ mL/min), *n*-butyllithium (1.2 M in *n*-hexane; $\nu = 0.4$ mL/min), tosyl azide (0.75 M in THF; $\nu = 0.8$ mL/min), argon ($\nu = 0.2$ mL/min), 0 to 60 °C, 15 min residence time. ^bBromine–lithium exchange was performed for 1 h. ^c*n*-Butyllithium (2.2 equiv) and tosyl azide (2.3 equiv) were used. For further details, see Supporting Information.

moieties. Treatment of ferrocenyl halides with ammonia in the presence of a copper/iron catalyst²⁶ would not allow the synthesis of halogenated ferrocenyl amines **5b** and **5c**. Thus, we decided to reduce ferrocenyl azides **2a–2n** to the corresponding amines **5a–5j** (Scheme 4) under Staudinger conditions. We found that treatment of ferrocenyl azides with triphenylphosphine (PPh₃) in a mixture of THF and water at 65 °C provided the corresponding amines **5a–5j** in consistently high yields. Among the products obtained, bromoferrocenyl amine **5b** is particularly valuable. A previous synthesis required five steps starting from 1,1'-dibromoferrocene and resulted in 31% yield.^{8e} We now prepared **5b** in two steps and 83% yield. The *tert*-butyl ester substituted ferrocenyl amine **5d** was obtained in 94% yield and is useful to access

Scheme 4. Scope of Functionalized Ferrocenyl Amines^a

^aYields of isolated products are given. Reaction conditions: Substrate (1 equiv), PPh_3 (1.5 equiv), THF/ H_2O (10:1), 65 °C, 16 h. ^b PPh_3 (3 equiv) was used.

conformationally restricted peptide mimetics.²⁷ Ethynyl-substituted ferrocenyl amines **5f–5j** were obtained in yields of 76–91%. Ferrocenyl azides **2d**, **f**, **h**, and **n** underwent decomposition under these reaction conditions, and the corresponding amines could not be obtained.

In conclusion, we have developed a general and scalable method for the functionalization of ferrocene derivatives in flow. By halogen–lithium exchange of ferrocenyl halides and subsequent trapping with tosyl azide, a variety of functionalized ferrocenyl azides were obtained. The application of flow chemistry accelerated the reaction over three distinct synthetic manipulations to minutes with an excellent safety and scalability profile, even on gram scale. In this process, a flow setup was designed that combined fast halogen–lithium exchange with a slow fragmentation step. The challenging precipitation of lithium *para*-toluenesulfonate was managed by employing a triphasic flow regime that prevented blockage of the tube reactor. In addition, a practical Staudinger protocol was developed for the reduction of functionalized ferrocenyl azides to the corresponding ferrocenyl amines in generally high yields.

■ ASSOCIATED CONTENT

Supporting Information

The Supporting Information is available free of charge at <https://pubs.acs.org/doi/10.1021/acs.orglett.9b04450>.

Experimental procedures and characterization data (PDF)

■ AUTHOR INFORMATION

Corresponding Authors

Mathias Christmann – *Organische Chemie, Freie Universität Berlin, Berlin, Germany*; orcid.org/0000-0001-9313-2392; Email: mathias.christmann@fu-berlin.de

Biprajit Sarkar – *Freie Universität Berlin, Berlin, Germany*; orcid.org/0000-0003-4887-7277; Email: biprajit.sarkar@fu-berlin.de

Philipp Heretsch – *Organische Chemie, Freie Universität Berlin, Berlin, Germany*; orcid.org/0000-0002-9967-3541; Email: philipp.heretsch@fu-berlin.de

Other Authors

Merlin Kleoff – *Organische Chemie, Freie Universität Berlin, Berlin, Germany*

Johannes Schwan – *Organische Chemie, Freie Universität Berlin, Berlin, Germany*

Lisa Boeser – *Organische Chemie, Freie Universität Berlin, Berlin, Germany*

Bence Hartmayer – *Organische Chemie, Freie Universität Berlin, Berlin, Germany*

Complete contact information is available at:

<https://pubs.acs.org/10.1021/acs.orglett.9b04450>

Notes

The authors declare no competing financial interest.

A version of this research was previously posted to ChemRxiv: Kleoff, Merlin; Schwan, Johannes; Boeser, Lisa; Hartmayer, Bence; Christmann, Mathias; Sarkar, Biprajit; Heretsch, Philipp (2019): Scalable Synthesis of Ferrocenyl Azides and Amines Enabled by Flow Chemistry. ChemRxiv. Preprint. Dec. 13, 2019. [10.26434/chemrxiv.11321975.v1](https://doi.org/10.26434/chemrxiv.11321975.v1).

■ ACKNOWLEDGMENTS

Financial support for this work was provided by Freie Universität Berlin (Forschungskommisionssmittel to P.H.). We are grateful to Dr. K. Gilmore (Max-Planck Institut für Kolloid- und Grenzflächenforschung, Potsdam), Dr. R. Zimmer, T. Siemon, and C. Hoyer for helpful discussions and to C. Groneberg for HPLC support (all Freie Universität Berlin). We acknowledge the assistance of the Core Facility BioSupraMol supported by the DFG.

■ REFERENCES

- (1) (a) Kealy, T. J.; Pauson, P. L. A New Type of Organo-Iron Compound. *Nature* **1951**, *168*, 1039–1040. (b) Miller, S. A.; Tebboth, J. A.; Tremaine, J. F. Dicyclopentadienyliron. *J. Chem. Soc.* **1952**, 632–635.
- (2) (a) Togni, A.; Hayashi, T. *Ferrocenes: Homogeneous Catalysis, Organic Synthesis, Materials Science*; Wiley: Weinheim, 2007. (b) Astruc, D. Why is Ferrocene so Exceptional? *Eur. J. Inorg. Chem.* **2017**, *2017*, 6–29. (c) Heinze, K.; Lang, H. Ferrocene – Beauty and Function. *Organometallics* **2013**, *32*, 5623–6164. (d) Siemeling, U.; Vor der Brüggen, J.; Vorfeld, U.; Neumann, B.; Stammler, H.-G.; Brockhinke, A.; Plessow, R.; Zanella, P.; Laschi, F.; de Biani, F. F.; Fontani, M.; Steenken, S.; Stapper, M.; Gurzadyan, G. Ferrocenyl-Functionalised Terpyridines and Their Transition-Metal Complexes: Syntheses, Structures and Spectroscopic and Electrochemical Properties. *Chem. Eur. J.* **2003**, *9*, 2819–2833.

(3) (a) Horikoshi, R.; Mochida, T. Ferrocene-Containing Coordination Polymers: Ligand Design and Assembled Structures. *Eur. J. Inorg. Chem.* **2010**, *2010*, 5355–5371. (b) Inkpen, M. S.; Scheerer, S.; Linseis, M.; White, A. J. P.; Winter, R. F.; Albrecht, T.; Long, N. J. Oligomeric ferrocene rings. *Nat. Chem.* **2016**, *8*, 825–830. (c) Hailes, R. L. N.; Oliver, A. M.; Gwyther, J.; Whittell, G. R.; Manners, I. Polyferrocenylsilanes: synthesis, properties, and applications. *Chem. Soc. Rev.* **2016**, *45*, 5358–5407. (d) Astruc, D. Electron-transfer processes in dendrimers and their implication in biology, catalysis, sensing and nanotechnology. *Nat. Chem.* **2012**, *4*, 255–267.

(4) (a) Pietschnig, R. Polymers with pendant ferrocenes. *Chem. Soc. Rev.* **2016**, *45*, 5216–5231. (b) Wilson, L. E.; Hassenrück, C.; Winter, R. F.; White, A. J. P.; Albrecht, T.; Long, N. J. Ferrocene- and Biferrocene-Containing Macrocycles towards Single-Molecule Electronics. *Angew. Chem., Int. Ed.* **2017**, *56*, 6838–6842. (c) Dong, T.-Y.; Lin, M.-C.; Chiang, M. Y.-N.; Wu, J.-Y. Development of Polynuclear Molecular Wires Containing Ruthenium(II) Terpyridine Complexes. *Organometallics* **2004**, *23*, 3921–3930. (d) Wilson, L. E.; Hassenrück, C.; Winter, R. F.; White, A. J. P.; Albrecht, T.; Long, N. J. Functionalised Biferrocene Systems towards Molecular Electronics. *Eur. J. Inorg. Chem.* **2017**, *2017*, 496–504. (e) Baumgardt, L.; Butenschön, H. 1,1'-Diaryl-Substituted Ferrocenes: Up to Three Hinges in Oligophenyleneethynylene-Type Molecular Wires. *Eur. J. Org. Chem.* **2010**, *2010*, 1076–1087. (f) Krauß, N.; Butenschön, H. Ferrocenes Bearing Highly Extended π Systems with Nitrile, Nitro, and Dimethylamino End Groups. *Eur. J. Org. Chem.* **2014**, *2014*, 6686–6695.

(5) (a) Jaouen, G.; Vessières, A.; Top, S. Ferrocifen type anticancer drugs. *Chem. Soc. Rev.* **2015**, *44*, 8802–8817. (b) Patra, M.; Gasser, G. The medicinal chemistry of ferrocene and its derivatives. *Nat. Rev. Chem.* **2017**, *1*, 0066. (c) Albada, B.; Metzler-Nolte, N. Organometallic–Peptide Bioconjugates: Synthetic Strategies and Medicinal Applications. *Chem. Rev.* **2016**, *116*, 11797–11839. (d) Mjos, K. D.; Orvig, C. Metallo drugs in Medicinal Inorganic Chemistry. *Chem. Rev.* **2014**, *114*, 4540–4563. (e) Hartinger, C. G.; Dyson, P. J. Bioorganometallic chemistry – from teaching paradigms to medicinal applications. *Chem. Soc. Rev.* **2009**, *38*, 391–401. (f) van Staveren, D. R.; Metzler-Nolte, N. Bioorganometallic chemistry of ferrocene. *Chem. Rev.* **2004**, *104*, 5931–5986.

(6) (a) Bandoli, G.; Dolmella, A. Ligating ability of 1,1'-bis(diphenylphosphino)ferrocene: a structural survey (1994–1998). *Coord. Chem. Rev.* **2000**, *209*, 161–196. (b) Atkinson, R. C. J.; Gibson, V. C.; Long, N. J. The syntheses and catalytic applications of unsymmetrical ferrocene ligands. *Chem. Soc. Rev.* **2004**, *33*, 313–328. (c) Dai, L.-X.; Tu, T.; You, S.-L.; Deng, W.-P.; Hou, X.-L. Asymmetric catalysis with chiral ferrocene ligands. *Acc. Chem. Res.* **2003**, *36*, 659–667. (d) Arrayás, R. G.; Adrio, J.; Carretero, C. Asymmetric catalysis with chiral ferrocene ligands. *Angew. Chem., Int. Ed.* **2006**, *45*, 7674–7715. (e) Haraguchi, R.; Hoshino, S.; Yamazaki, T.; Fukuzawa, S.-i. Chiral triazolylidene-Pd-PEPPSI: synthesis, characterization, and application in asymmetric Suzuki–Miyaura cross-coupling. *Chem. Commun.* **2018**, *54*, 2110–2113. (f) Steffen, P.; Unkelbach, C.; Christmann, M.; Hiller, W.; Strohmman, C. Catalytic and Stereoselective ortho-Lithiation of a Ferrocene Derivative. *Angew. Chem., Int. Ed.* **2013**, *52*, 9836–9840.

(7) (a) Klenk, S.; Rupf, S.; Suntrup, L.; van der Meer, M.; Sarkar, B. The Power of Ferrocene, Mesoionic Carbenes, and Gold: Redox-Switchable Catalysis. *Organometallics* **2017**, *36*, 2026–2035. (b) Romero, T.; Orenes, R. A.; Tárraga, A.; Molina, P. Preparation, Structural Characterization, Electrochemistry, and Sensing Properties toward Anions and Cations of Ferrocene-Triazole Derivatives. *Organometallics* **2013**, *32*, 5740–5753. (c) Chen, C.; Zhu, Y.-Z.; Zhao, H.-Y.; Zheng, J.-Y. Syntheses of N-bridged ferrocene/porphyrin-fullerene dyads and influence of iminofullerene isomers on the attached chromophores. *Tetrahedron Lett.* **2013**, *54*, 1607–1611. (d) Hettmanczyk, L.; Suntrup, L.; Klenk, S.; Hoyer, C.; Sarkar, B. Heteromultimetallic Complexes with Redox-Active Mesoionic Carbenes: Control of Donor Properties and Redox-Induced Catalysis. *Chem. Eur. J.* **2017**, *23*, 576–585.

(8) (a) Siemeling, U.; Auch, T.-C. 1,1'-Di(heteroatom)-functionalised ferrocenes as [N,N], [O,O] and [S,S] chelate ligands in transition metal chemistry. *Chem. Soc. Rev.* **2005**, *34*, 584–594. (b) Heinze, K.; Schlenker, M. Main Chain Ferrocenyl Amides from 1-Aminoferrocene-1'-carboxylic Acid. *Eur. J. Inorg. Chem.* **2004**, *2004*, 2974–2988. (c) Chang, Y.-W.; Huang, M.-J.; Lai, C.-C.; Chang, C.-C.; Huang, M.-P.; Liao, C.-Y.; Cheng, C.-H. A versatile ferrocene-containing material as a p-type charge generation layer for high-performance full color tandem OLEDs. *Chem. Commun.* **2016**, *52*, 14294–14297. (d) Wang, X.; Thevenon, A.; Brosmer, J. L.; Yu, L.; Khan, S. I.; Mehrkhodavandi, P.; Diaconescu, P. L. Redox Control of Group 4 Metal Ring-Opening Polymerization Activity toward 1-Lactide and ϵ -Caprolactone. *J. Am. Chem. Soc.* **2014**, *136*, 11264–11267. (e) Dey, S.; Quail, J. W.; Müller, J. [2]Ferrocenophanes with Nitrogen in Bridging Positions. *Organometallics* **2015**, *34*, 3039–3046. (f) Thie, C.; Bruhn, C.; Siemeling, U. Ferrocene-Based N-Heterocyclic Carbenes with Functionalised Benzyl Substituents. *Eur. J. Inorg. Chem.* **2015**, *2015*, 5457–5466. (g) Siemeling, U.; Färber, C.; Leibold, M.; Bruhn, C.; Mücke, P.; Winter, R. F.; Sarkar, B.; von Hopffgarten, M.; Frenking, G. Six-Membered N-Heterocyclic Carbenes with a 1,1'-Ferrocenediyl Backbone: Bulky Ligands with Strong Electron-Donor Capacity and Unusual Non-Innocent Character. *Eur. J. Inorg. Chem.* **2009**, *2009*, 4607–4612.

(9) (a) Shafir, A.; Power, M. P.; Whitener, G. D.; Arnold, J. Synthesis, Structure, and Properties of 1,1-Diamino- and 1,1-Diazidoferrocene. *Organometallics* **2000**, *19*, 3978–3982. (b) Steel, C.; Rosenblum, M.; Geyh, A. S. Kinetics of the thermal decomposition of ferrocenyl azide: Character of ferrocenyl nitrene. *Int. J. Chem. Kinet.* **1994**, *26*, 631–641. (c) Sutherland, R. G.; Abramovitch, R. A.; Azogu, C. I. Ferrocenyl radical and nitrene: formation of nitroferrocene with oxygen. *J. Chem. Soc. D* **1971**, 134–135.

(10) (a) Vanicek, S.; Jochriem, M.; Hassenrück, C.; Roy, S.; Kopacka, H.; Wurst, K.; Müller, T.; Winter, R. F.; Reiser, E.; Bildstein, B. Redox-Rich Metallocene Tetrazene Complexes: Synthesis, Structure, Electrochemistry, and Catalysis. *Organometallics* **2019**, *38*, 1361–1371. (b) Plázquez, D.; Rychlik, B.; Blauz, A.; Domagala, S. Synthesis, electrochemistry and anticancer activity of novel ferrocenyl phenols prepared via azide-alkyne 1,3-cycloaddition reaction. *J. Organomet. Chem.* **2012**, *715*, 102–112. (c) Tennyson, A. G.; Khramov, D. M.; Varnado, C. D., Jr.; Creswell, P. T.; Kamplain, J. W.; Lynch, V. M.; Bielawski, C. W. Indirectly Connected Bis(N-Heterocyclic Carbene) Bimetallic Complexes: Dependence of Metal–Metal Electronic Coupling on Linker Geometry. *Organometallics* **2009**, *28*, 5142–5147.

(11) Ilyashenko, G.; Al-Safadi, R.; Donnan, R.; Dubrovka, R.; Pancholi, J.; Watkinson, M.; Whiting, A. A synthesis of a 1,1'-desymmetrised ferrocene backbone and its facile one-pot double-“click” functionalization. *RSC Adv.* **2013**, *3*, 17081–17087.

(12) (a) Romero, T.; Orenes, R. A.; Espinosa, A.; Tárraga, A.; Molina, P. Synthesis, Structural Characterization, and Electrochemical and Optical Properties of Ferrocene–Triazole–Pyridine Triads. *Inorg. Chem.* **2011**, *50*, 8214–8224. (b) Tárraga, A.; Otón, F.; Espinosa, A.; Desamparados Velasco, M.; Molina, P.; Evans, D. J. Synthesis and properties of a new class of nitrogen-rich multinuclear [mn] ferrocenophanes. *Chem. Commun.* **2004**, 458–459. (c) Otón, F.; Espinosa, A.; Tárraga, A.; Ramírez de Arellano, C.; Molina, P. [3.3]Ferrocenophanes with Guanidine Bridging Units as Multi-signalling Receptor Molecules for Selective Recognition of Anions, Cations, and Amino Acids. *Chem. Eur. J.* **2007**, *13*, 5742–5752.

(13) Škoch, K.; Cisařová, I.; Schulz, J.; Siemeling, U.; Štěpnička, P. Synthesis and characterization of 1'-(diphenylphosphino)-1-isocyanoferrrocene, an organometallic ligand combining two different soft donor moieties, and its Group 11 metal complexes. *Dalton Trans.* **2017**, *46*, 10339–10354.

(14) Ichinari, D.; Ashikari, Y.; Mandai, K.; Aizawa, Y.; Yoshida, J.; Nagaki, A. A Novel Approach to Functionalization of Aryl Azides through the Generation and Reaction of Organolithium Species Bearing Masked Azides in Flow Microreactors. *Angew. Chem., Int. Ed.*

2019 DOI: 10.1002/anie.201912419. (b) Nagaki, A.; Ichinari, D.; Yoshida, J. Three-Component Coupling Based on Flash Chemistry. Carbolithiation of Benzynes with Functionalized Aryllithiums Followed by Reactions with Electrophiles. *J. Am. Chem. Soc.* **2014**, *136*, 12245–12248.

(15) (a) Bräse, S.; Banert, K., Eds. *Organic Azides: Synthesis and Applications*; Wiley: Chichester, West Sussex, 2010. (b) Bräse, S.; Gil, C.; Knepper, K.; Zimmermann, V. Organic Azides: An Exploding Diversity of a Unique Class of Compounds. *Angew. Chem., Int. Ed.* **2005**, *44*, 5188–5240. (c) Banert, K. The Chemistry of Unusually Functionalized Azides. *Synthesis* **2016**, *48*, 2361–2375. (d) Klahn, P.; Erhardt, H.; Kotthaus, A.; Kirsch, S. F. The Synthesis of α -Azidoesters and Geminal Triazides. *Angew. Chem., Int. Ed.* **2014**, *53*, 7913–7917. (e) Holzschneider, K.; Tong, M. L.; Mohr, F.; Kirsch, S. F. A Synthetic Route Toward Tetrazoles: The Thermolysis of Geminal Diazides. *Chem. Eur. J.* **2019**, *25*, 11725–11733.

(16) (a) Plutschack, M. B.; Pieber, B.; Gilmore, K.; Seeberger, P. H. The Hitchhiker's Guide to Flow Chemistry. *Chem. Rev.* **2017**, *117*, 11796–11893. (b) Movsisyan, M.; Delbeke, E. I. P.; Berton, J. K. E. T.; Battilocchio, C.; Ley, S. V.; Stevens, C. V. Taming hazardous chemistry by continuous flow technology. *Chem. Soc. Rev.* **2016**, *45*, 4892–4928. (c) Mallia, C. J.; Baxendale, I. R. The use of gases in flow synthesis. *Org. Process Res. Dev.* **2016**, *20*, 327–360. (d) Cambié, D.; Bottecchia, C.; Straathof, N. J. W.; Hessel, V.; Noël, T. Applications of continuous-flow photochemistry in organic synthesis, material science, and water treatment. *Chem. Rev.* **2016**, *116*, 10276–10341. (e) Noël, T.; Cao, Y.; Laudadio, G. The fundamentals behind the use of flow reactors in electrochemistry. *Acc. Chem. Res.* **2019**, *52*, 2858–2869. (f) Noël, T.; Buchwald, S. L. Cross-coupling in flow. *Chem. Soc. Rev.* **2011**, *40*, 5010–5029. (g) Gutmann, B.; Cantillo, D.; Kappe, C. O. Continuous-Flow Technology – A Tool for the Safe Manufacturing of Active Pharmaceutical Ingredients. *Angew. Chem., Int. Ed.* **2015**, *54*, 6688–6728. (h) Glasnov, T. N.; Kappe, C. O. Microwave-assisted synthesis under continuous-flow conditions. *Macromol. Rapid Commun.* **2007**, *28*, 395–410. (i) Ley, S. V.; Fitzpatrick, D. E.; Myers, R. M.; Battilocchio, C.; Ingham, R. J. Machine-assisted organic synthesis. *Angew. Chem., Int. Ed.* **2015**, *54*, 10122–10137.

(17) (a) Yoshida, J.; Kim, H.; Nagaki, A. "Impossible" chemistries based on flow and micro. *J. Flow Chem.* **2017**, *7*, 60–64. (b) Yoshida, J.; Nagaki, A.; Yamada, T. *Chem. Eur. J.* **2008**, *14*, 7450–7459. (c) Kim, H.; Nagaki, A.; Yoshida, J. A flow-microreactor approach to protecting-group-free synthesis using organolithium compounds. *Nat. Commun.* **2011**, *2*, 264. (d) Nagaki, A.; Moriwaki, Y.; Yoshida, J. Flow synthesis of arylboronic esters bearing electrophilic functional groups and space integration with Suzuki–Miyaura coupling without intentionally added base. *Chem. Commun.* **2012**, *48*, 11211–11213. (e) Williams, J. D.; Kerr, W. J.; Leach, S. G.; Lindsay, D. M. A Practical and General Amidation Method from Isocyanates Enabled by Flow Technology. *Angew. Chem., Int. Ed.* **2018**, *57*, 12126–12130. (f) Müller, S. T. R.; Hokamp, T.; Ehrmann, S.; Hellier, P.; Wirth, T. Ethyl lithiodiazoacetate: extremely unstable intermediate handled efficiently in flow. *Chem. - Eur. J.* **2016**, *22*, 11940–11942. (g) Weidmann, N.; Ketels, M.; Knochel, P. Sodiation of Arenes and Heteroarenes in Continuous Flow. *Angew. Chem., Int. Ed.* **2018**, *57*, 10748–10751.

(18) (a) Vaccaro, L. (Ed.), *Sustainable Flow Chemistry: Methods and Applications*; Wiley-VCH, Weinheim, 2017. (b) Gürsel, I. V.; Noël, T.; Wang, Q.; Hessel, V. Separation/recycling methods for homogeneous transition metal catalysts in continuous flow. *Green Chem.* **2015**, *17*, 2012–2026.

(19) The lower yield when using *tert*-butyllithium may be a result of undesired radical reactions, see: Ashby, E. C.; Pham, T. N. Single electron transfer in metal halogen exchange. The reaction of organolithium compounds with alkyl halides. *J. Org. Chem.* **1987**, *52*, 1291–1300.

(20) Ito, S. The Reaction of Benzenesulfonyl Azide with Phenylmagnesium Bromide. *Bull. Chem. Soc. Jpn.* **1966**, *39*, 635.

(21) Smith, P. A. S.; Rowe, C. D.; Bruner, L. B. Azides and amines from Grignard reagents and tosyl azide. *J. Org. Chem.* **1969**, *34*, 3430–3433.

(22) Pieber, B.; Shalom, M.; Antonietti, M.; Seeberger, P. H.; Gilmore, K. Continuous Heterogeneous Photocatalysis in Serial Micro-Batch Reactors. *Angew. Chem., Int. Ed.* **2018**, *57*, 9976–9979.

(23) This setup seemed more favorable to us in comparison to the alternative of keeping suspensions in flow by sonication, see: (a) Noël, T.; Naber, J. R.; Hartman, R. L.; McMullen, J. P.; Jensen, K. F.; Buchwald, S. L. Palladium-catalyzed amination reactions in flow: overcoming the challenges of clogging via acoustic irradiation. *Chem. Sci.* **2011**, *2*, 287–290. (b) Sedelmeier, J.; Ley, S. V.; Baxendale, I. R.; Baumann, M. KMnO_4 -Mediated Oxidation as a Continuous Flow Process. *Org. Lett.* **2010**, *12*, 3618–3621.

(24) (a) Rostovtsev, V. V.; Green, L. G.; Fokin, V. V.; Sharpless, K. B. A Stepwise Huisgen Cycloaddition Process: Copper(I)-Catalyzed Regioselective "Ligation" of Azides and Terminal Alkynes. *Angew. Chem., Int. Ed.* **2002**, *41*, 2596–2599. (b) Tornøe, C. W.; Christensen, C.; Meldal, M. Peptidotriazoles on Solid Phase: [1,2,3]-Triazoles by Regiospecific Copper(I)-Catalyzed 1,3-Dipolar Cycloadditions of Terminal Alkynes to Azides. *J. Org. Chem.* **2002**, *67*, 3057–3064. (c) Kolb, H. C.; Finn, M. G.; Sharpless, K. B. Click Chemistry: Diverse Chemical Function from a Few Good Reactions. *Angew. Chem., Int. Ed.* **2001**, *40*, 2004–2021.

(25) (a) Pauly, A. C.; Varnado, C. D., jr.; Bielawski, C. W.; Theato, P. Electrochromic Poly(acetylene)s with Switchable Visible/Near-IR Absorption Characteristics. *Macromol. Rapid Commun.* **2014**, *35*, 210–213. (b) Yao, W.; Zhu, J.; Zhou, X.; Jiang, R.; Wang, P.; Chen, W. Ferrocenophane-based bifunctional organocatalyst for highly enantioselective Michael reactions. *Tetrahedron* **2018**, *74*, 4205–4210.

(26) (a) Leonidova, A.; Joshi, T.; Nipkow, D.; Frei, A.; Penner, J.; Konatschnig, S.; Patra, M.; Gasser, G. An Environmentally Benign and Cost-Effective Synthesis of Aminoferrocene and Aminoruthenocene. *Organometallics* **2013**, *32*, 2037–2040. (b) Broomfield, L. M.; Wu, Y.; Martin, E.; Shafir, A. Phosphino-amine (PN) Ligands for Rapid Catalyst Discovery in Ruthenium-Catalyzed Hydrogen-Borrowing Alkylation of Anilines: A Proof of Principle. *Adv. Synth. Catal.* **2015**, *357*, 3538–3548.

(27) (a) Siebler, D.; Förster, C.; Heinze, K. Redox-responsive organometallic foldamers from ferrocene amino acid: Solid-phase synthesis, secondary structure and mixed-valence properties. *Dalton Trans* **2011**, *40*, 3558–3575. (b) Siebler, D.; Förster, C.; Gasi, T.; Heinze, K. Biferrocene Amino Acid, a Ferrocenylogue of Ferrocene Amino Acid: Synthesis, Cross-Linking, and Redox Chemistry. *Organometallics* **2011**, *30*, 313–327. (c) Beeren, S. R.; Sanders, J. K. M. Ferrocene-amino acid macrocycles as hydrazone-based receptors for anions. *Chem. Sci.* **2011**, *2*, 1560–1567.

Scalable Synthesis of Functionalized Ferrocenyl Azides and Amines Enabled by Flow Chemistry

Merlin Kleoff, Johannes Schwan, Lisa Boeser, Bence Hartmayer, Mathias Christmann,*
Biprajit Sarkar,* and Philipp Heretsch*

Supporting Information

1. General Information	156
2. Experimental Procedures.....	159
3. NMR Spectra of Synthesized Compounds.....	206
4. References	264

1. General Information

1.1. Materials and Methods

Unless otherwise noted, all reactions and workups were performed open to air. All substances sensitive to water and oxygen were handled under an argon atmosphere using standard Schlenk techniques and oil pump vacuum. Room temperature (rt) refers to 25 °C.

Anhydrous THF was distilled under an atmosphere of argon over sodium/benzophenone and stored over activated 3 Å mol sieves. Anhydrous *n*-hexane was obtained by storing over activated 3 Å mol sieves for 48 h. Anhydrous CH₂Cl₂, MeCN, and *n*-pentane were obtained from a solvent system MB SPS-800 from the company MBRAUN. Anhydrous HNiPr₂ and *n*-BuOH were distilled from KOH and stored over activated 3 Å mol sieves. TMEDA was distilled from CaH₂ and stored over activated 3 Å mol sieves in the dark at -18 °C.

EtOAc, *n*-pentane and *n*-hexane were purified by distillation on a rotary evaporator. All other solvents and commercially available reagents were used without further purification unless otherwise stated.

If necessary, *n*-BuLi was titrated before use in Et₂O with *n*-BuOH and 2,2'-bipyridine as indicator.

3 Å mol sieves were activated by drying over night at 100 °C in a drying cabinet followed by drying at 10⁻³ mbar for 30 min at 600 °C. ZnCl₂ was dried at 10⁻³ mbar for at least 15 min at 600 °C. ZnCl₂ solutions in THF were stored over 3 Å mol sieves. Tosyl azide was stored as a solution in THF over CaH₂ (for the preparation, see below).

The following compounds were prepared according to the literature: 2,4,6-Triisopropylbenzenesulfonyl azide^[1] and *para*-chlorobenzenesulfonyl azide.^[2]

Medium pressure liquid chromatography (MPLC) was performed with a TELEDYNE ISCO Combi-Flash Rf or a TELEDYNE ISCO Combi-Flash Rf200 using prepacked SiO₂-columns and cartridges from TELEDYNE. UV response was monitored at 254 nm and 280 nm. As eluents, cyclohexane (99.5%+ quality) and EtOAc (HPLC grade) were used.

High performance liquid chromatography (HPLC) was conducted on a modular KNAUER HPLC system with a UV detector at 254 nm and differential refractometer on a 4×250 mm column packed with Nucleosil 50-5 from MACHERY-NAGEL.

For column chromatography, silica 60 M (0.040-0.063 mm) from MACHERY-NAGEL or basic Aluminum oxide from ACROS or MACHERY-NAGEL were used. Basic aluminum oxide was deactivated prior use with 5 wt% water by adding the calculated amount of water to aluminum oxide followed by vigorously shaking for some minutes. Alternatively, after addition of water, the aluminum oxide was rotated at atmospheric pressure on a rotary evaporator for 15 min.

Unless otherwise stated, concentration under reduced pressure was performed by rotary evaporation at 40 °C and the appropriate pressure.

All reactions involving ferrocenyl azides were performed with additional care on a scale of less than 1 g and under modest exclusion of light. Concentration of solutions of ferrocenyl azides was performed by rotary evaporation at 38 °C and appropriate pressure. All ferrocenyl azides were stored as solids or oils, respectively, in the dark at 4 °C. When stored cold, most ferrocenyl azides were found to be relatively stable and decomposed very slowly over months. The decomposition products can easily be removed by filtration of a concentrated solution of the ferrocenyl azide in CH₂Cl₂ over a pad of basic Al₂O₃ (deactivated with 5 wt% H₂O). In solution, ferrocenyl azides decompose within a few days. Therefore, samples for NMR spectra in CDCl₃ were measured within minutes to hours after preparation.

1.2. Analysis

Reaction monitoring: Reactions were monitored by TLC carried out on Merck Silica Gel 50 F₂₅₄-plates and visualized by fluorescence quenching under UV-light ($\lambda = 254$ nm) or by using a stain of vanillin (6 g vanillin, 1.5 mL 96% H₂SO₄, 100 mL EtOH) and heat as developing agent.

NMR spectroscopy: All NMR spectra were acquired on a JEOL ECZ400 (400 MHz), a JEOL ECS400 (400 MHz), a JEOL ECX 400 (400 MHz), a JEOL ECP 500 (500 MHz), a Bruker Avance 500 (500 MHz), a Varian INOVA 600 (600 MHz) or a Bruker Avance 700 (700 MHz) in the reported deuterated solvents. Chemical shifts are reported in parts per million (ppm) with reference to the residual solvent peaks. The given multiplicities are phenomenological, thus, the actual appearance of the signals is stated and not the theoretically expected one. The following abbreviations were used to designate multiplicities: s = singlet, d = doublet, t = triplet, q = quartet, quint = quintet. In case no multiplicity could be identified, the chemical shift range of the signal is given (m = multiplet).

Infrared spectroscopy: Infrared (IR) spectra were measured on a NICOLET Nexus 670/870 FT-IR spectrometer or a JASCO FT/IR-4100 spectrometer. Wavenumbers $\tilde{\nu}$ are given in cm⁻¹ and intensities are as follows: s = strong, m = medium, w = weak.

High resolution mass spectrometry: High-resolution mass spectra (HRMS) were recorded using an AGILENT 6210 ESI-TOF spectrometer.

Optical Rotation: Optical rotations were measured on a JASCO P-2000 polarimeter at 589 nm using 100 mm cells and the solvent and concentration (g/100 mL) indicated.

1.3. Flow Equipment

All flow chemistry experiments were carried out using the following equipment:

Tubings, connectors and valves: FEP tubing (outer diameter 1/16", inner diameter 1/32") and PTFE tubing (outer diameter 1/8", inner diameter 1/16") were obtained from BOLA. T-mixers made from stainless steel 316L were provided by VICI. A static mixer with an internal volume of 2.2 μ L made from PEEK/UHMWPE was provided by UPCHURCH SCIENTIFIC. Tubings and mixers were connected using either coned 10-32 UNF fittings made from stainless steel 316L obtained from UPCHURCH SCIENTIFIC or flat bottom 1/4-28 UNF gripper fittings made from PP obtained from DIBAFIT. Adapters for 1/4-28 UNF systems were made from PP or PTFE and were provided from UPCHURCH SCIENTIFIC. Manual 6-way-valves made from stainless steel 316L were provided by KNAUER.

Gas delivery: A controlled stream of argon gas was delivered using a mass flow controller (EL-FLOW Prestige Series) from BRONKHORST. Connectors and adapters were provided from SWAGELOK.

Pumping systems: Liquids were delivered using 3D-printed syringe pumps based on a setup developed by M. Spano from the group of M. Croatt.^[3] Gas-tight Luer-Lock syringes made from glass were obtained from VWR. For solvent supply, a Waters 515 HPLC pump was used.

General remarks for performing flow experiments involving *n*-butyllithium:

Prior use, tubes were flushed with dry THF for at least 3 residence times. After performing reactions involving *n*-butyllithium, the tubes were washed with *i*PrOH (HPLC grade) for at least 3 residence times. Any blockages arising from solid formation were cleared using a solution of MeOH/H₂O/AcOH (10:1:1), followed by washing with *i*PrOH (HPLC grade) for at least 3 residence times.

2. Experimental Procedures

2.1. Optimization of Reaction Conditions for the Synthesis of Ferrocenyl Azides in Batch

Screening of different organolithiums and arylsulfonyl azides in batch

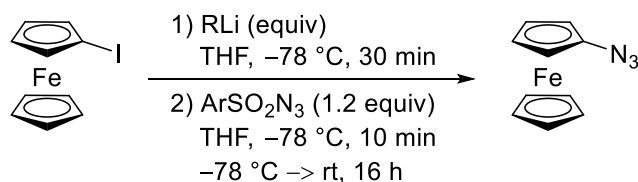


Table S1: Screening of different organolithiums (RLi) and arylsulfonyl azides (ArSO₂N₃)

Entry	RLi (equiv)	ArSO ₂ N ₃	Yield ^[a]
1	<i>t</i> -BuLi (2.1 equiv)	2,4,6- <i>(i</i> -Pr) ₃ C ₆ H ₂ SO ₂ N ₃	76%
2	<i>t</i> -BuLi (2.1 equiv)	4-Cl-C ₆ H ₄ SO ₂ N ₃	63%
3	<i>t</i> -BuLi (2.1 equiv)	TsN ₃	77%
4	<i>n</i> -BuLi (1.1 equiv)	TsN ₃	95%
5 ^[b]	<i>n</i> -BuLi (1.1 equiv)	TsN ₃	82%

[a] Isolated yield. [b] Iodine–lithium exchange was performed for 10 min at 0 °C (ice bath), TsN₃ was added dropwise at 0 °C and the reaction mixture was warmed to rt over 16 h.

In a dry Schlenk tube, iodoferrocene (100 mg, 0.321 mmol, 1.0 equiv) was placed and the Schlenk tube was evacuated and backfilled with argon (3×). Anhydrous THF (2 mL) was added and the resulting solution was cooled to -78 °C (acetone/dry ice). RLi was added dropwise and the mixture was stirred for 30 min. Then, ArSO₂N₃ (1.2 equiv; 1.0 M in THF) was added dropwise at -78 °C and the resulting dark red solution was stirred at this temperature for 10 min. The cooling bath was removed, the Schlenk tube was wrapped in aluminum foil and the mixture was stirred for 16 h at rt. After exposure to air, NaHCO₃ (sat. aq., 20 mL) and EtOAc (20 mL) were added. The aqueous layer was separated and extracted with EtOAc (2×20 mL). The combined organic layers were dried (Na₂SO₄), filtered, and concentrated under reduced pressure. Azidoferrocene (**2a**) was isolated by gravity column chromatography (basic Al₂O₃, activity grade I +5 wt% H₂O).

Initial attempts to accelerate the fragmentation of the triazene intermediate in batch.

As a preliminary investigation for the flow protocol, it was attempted to accelerate the fragmentation of the triazene species in batch at elevated temperature.

In a dry Schlenk tube, **1a** (100 mg, 0.321 mmol, 1.0 equiv) was placed and the Schlenk tube was evacuated and backfilled with argon (3×). Anhydrous THF (2 mL) was added and the resulting solution was cooled to -78 °C (acetone/dry ice). *n*-Butyllithium (0.141 mL, 0.353 mmol, 1.1 equiv; 2.5 M in *n*-hexane) was added dropwise and the mixture was stirred for 30 min. Tosyl azide (0.513 mL, 0.383 mmol, 1.2 equiv; 1.0 M in THF) was added dropwise at -78 °C. Then, the Schlenk tube was removed from the cooling bath and immersed in a preheated oil bath at the temperature stated. The solution was stirred at this temperature for the time indicated. The reaction progress was monitored by TLC. After exposure to air, NaHCO₃ (sat. aq., 20 mL) and EtOAc (20 mL) were added. The aqueous layer was separated and extracted with EtOAc (2×20 mL). The combined organic layers were dried (Na₂SO₄), filtered, and concentrated under reduced pressure. Azidoferrocene (**2a**) was isolated by gravity column chromatography (basic Al₂O₃, activity grade I +5 wt% H₂O, *n*-pentane).

Table S2. Fragmentation of the triazene species at elevated temperature in batch

Entry	Temperature (°C)	Time (min)	Yield ^[a]
1 ^[b]	50	10	62%
2 ^[b]	60	20	78%
3	60	30	70%

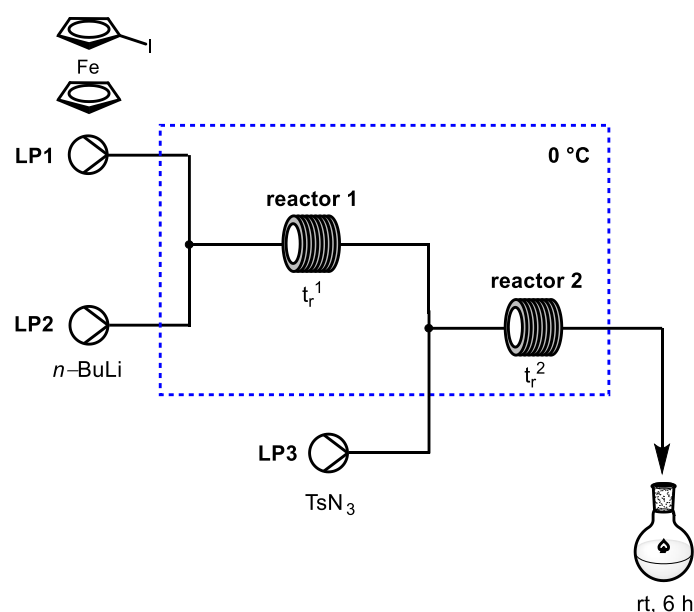
[a] Isolated yield. [b] Incomplete fragmentation of the triazene species.

These observations indicate that complete fragmentation of the triazene species requires approximately 30 min at 60 °C (entry 3). However, azidoferrocene (**2a**) can be isolated in a slightly higher yield although fragmentation was not complete when heating was performed only for 20 min (entry 2). This finding suggests that at 60 °C product **2a** starts to decompose resulting in lower yields.

2.2. Optimization of Reaction Conditions for the Synthesis of Ferrocenyl Azides in Flow

Attempts to perform iodine-lithium exchange and trapping with tosyl azide in a semi-batch procedure.

To find suitable reaction parameters for the iodine-lithium exchange and subsequent trapping with tosyl azide in flow, semi-batch experiments were conducted. The iodine-lithium exchange and the subsequent trapping with tosyl azide were performed in flow, while fragmentation of the triazene species was completed in batch.



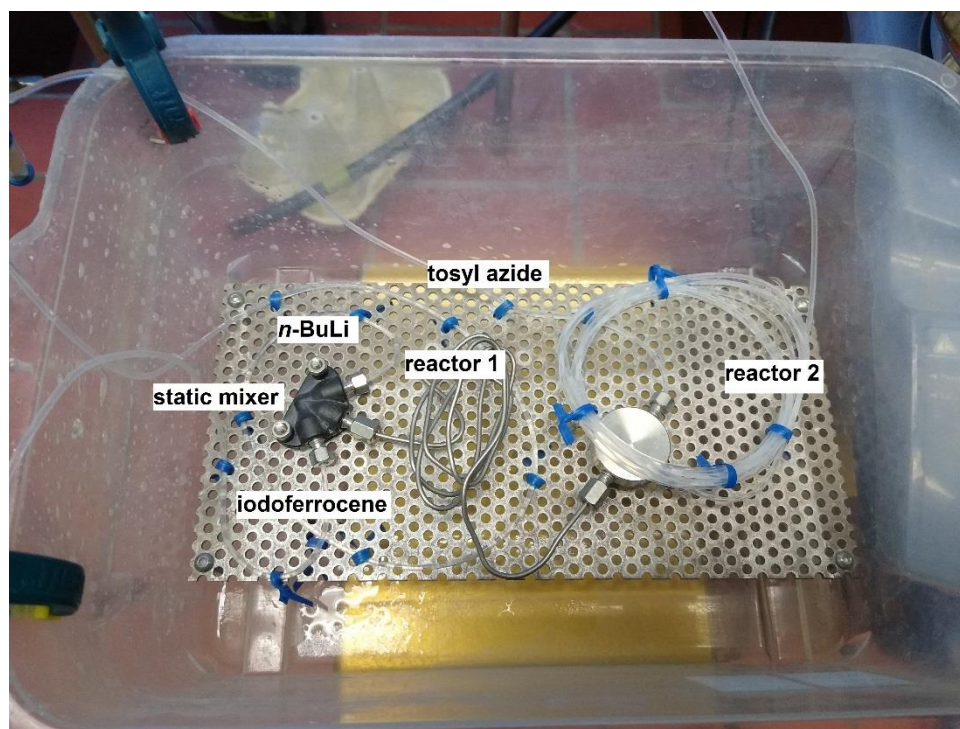
Syringe pumps (**LP1-LP3**) equipped with gas-tight 10 mL glass syringes were used to pump solutions of iodoferrocene (**1a**, 0.2 M in THF, v_{FcI}), *n*-butyllithium (1.2 M *n*-hexane, $v_{n\text{-BuLi}}$), and tosyl azide (0.75 M in THF, v_{TsN_3}). All solutions were pumped through precooling loops (FEP tube, outer diameter 1/16", inner diameter 1/32", $V = 0.15$ mL) before mixing. The solutions of iodoferrocene and *n*-butyllithium were merged in a T-mixer or a static mixer and pumped through tube **reactor 1** with t_r^1 . At the end of this reactor, the reaction stream was merged with a stream of tosyl azide in a T-mixer and pumped through tube **reactor 2** (FEP tube, outer diameter 1/16", inner diameter 1/32", $V = 1$ mL) with t_r^2 . The outlet of this tube reactor was connected to a flask or a dry Schlenk tube. **Reactor 1**, **reactor 2**, the mixing units and the precooling loops were cooled to 0 °C by immersion to an ice bath.

The syringe pumps were operated at the given flow rates. After an equilibration time of 3 residence times, a sample of 0.2 mmol was collected in a dry Schlenk tube. The collected reaction mixture was stirred at rt for 6 h. After exposure to air, NaHCO₃ (sat. aq., 20 mL) and EtOAc (20 mL) were added. The aqueous layer was separated and extracted with EtOAc (2×20 mL). The combined organic layers were dried (Na₂SO₄), filtered and concentrated under reduced pressure. Azidoferrocene (**2a**) was isolated by gravity column chromatography (basic Al₂O₃, activity grade I +5 wt% H₂O, *n*-pentane).

Table S3. Screening of parameters for iodine-lithium exchange and subsequent trapping with tosyl azide in a semi-batch procedure

Entry	v_{FcI} [mL/min]	$v_{n\text{-BuLi}}$ [mL/min]	v_{TsN_3} [mL/min]	t_{R^1} [s]	t_{R^2} [s]	Yield ^[e]
1 ^[a]	1.0	0.2	0.4	8	38	43%
2 ^[b]	1.0	0.2	0.4	17	38	67%
3 ^[b]	2.0	0.4	0.8	9	19	71%
4 ^[c]	2.0	0.4	0.8	0.5	19	82%
5 ^[c,d]	2.0	0.4	0.8	0.5	19	87%

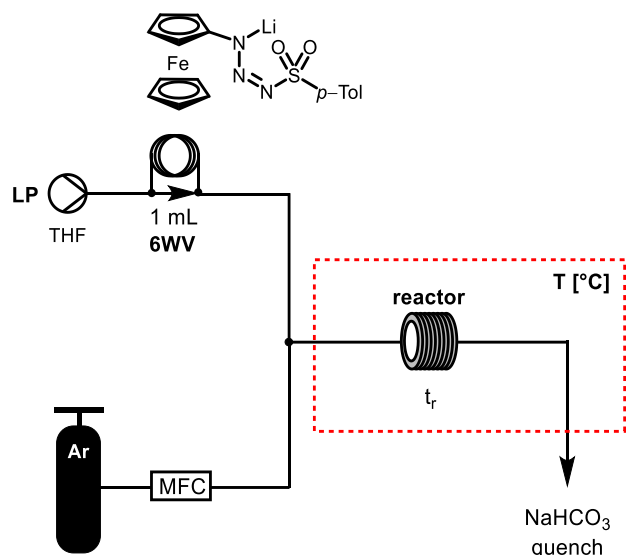
[a] **Reactor 1**: FEP tube (inner diameter 1/32", V = 0.15 mL) was used. [b] **Reactor 1**: FEP tube (inner diameter 1/32", V = 0.34 mL) was used. [c] **Reactor 1**: stainless steel capillary (inner diameter 250 μm , V = 20 μL) was used. [d] A static mixer with an internal volume of 20 μL was used for the iodine-lithium exchange. [e] Isolated yield.



Picture of the self-assembled reactor plate: Iodoferrocene and *n*-butyllithium are merged in the static mixer and then pumped through reactor 1. The reaction stream is merged with tosyl azide and then reacted in reactor 2.

Attempts to accelerate the fragmentation of the triazene intermediate in a semi-batch procedure.

In order to accelerate the fragmentation of the triazene intermediate in flow, semi-batch experiments were conducted. To prevent blocking of the tubings from precipitating salts, the reaction mixture was pumped as a segmented flow through a heated tube reactor resulting in a triphasic flow regime.^[4]



A HPLC pump (LP) to feed the solvent was connected to a HPLC injection valve (6WV) equipped with a 1 mL sample loop. The liquid supply was merged in a T-mixer with a stream of argon supplied by a mass flow controller (MFC). The resulting segmented flow was pumped through the tube reactor. The tube reactor with the volume V was immersed in a water bath at the given temperature. The reaction mixture was collected in a flask containing NaHCO₃ (sat. aq., 20 mL).

The pump and the reactor were washed with anhydrous THF for 2 residence times by pumping THF with the HPLC pump and simultaneously feeding argon using the MFC.

In a dry Schlenk tube, iodoferrocene **1a** (100 mg, 0.321 mmol, 1.0 equiv) was placed and the Schlenk tube was evacuated and backfilled with argon (3×). Anhydrous THF (1.1 mL) was added and the resulting solution was cooled to -78 °C (acetone/dry ice). *n*-Butyllithium (0.147 mL, 0.353 mmol, 1.1 equiv) was added dropwise and the mixture was stirred for 30 min. Then, tosyl azide (1.2 equiv; 1.0 M in THF) was added dropwise at -78 °C. Next, the solution was loaded on the sample loop of the HPLC injection valve. The solution was immediately injected by switching from the load to the inject position and the solution was pumped through the reactor at the given flow rate and temperature. The collected reaction mixture was diluted with EtOAc (20 mL). The aqueous layer was separated and extracted with EtOAc (2×20 mL). The combined organic layers were dried (Na₂SO₄), filtered and concentrated under reduced pressure. Azidoferrocene (**2a**) was isolated by gravity column chromatography (basic Al₂O₃, activity grade I +5 wt% H₂O, *n*-pentane).

Table S4. Fragmentation of the triazene species at elevated temperature in flow

Entry	v_{liquid} [mL/min]	v_{argon} [mL/min]	V [mL]	T [°C]	$t_{\text{R}}^{[a]}$ [min]	Yield ^[d]
1 ^[a,c]	0.4	0.4	10	50	10	49%
2 ^[a,c]	0.4	0.4	10	55	13	74%
3 ^[a,c]	0.2	0.2	10	60	15	85%
4 ^[b]	1.3	1.0	40	60	6	n.d.
5 ^[b]	3.0	0.3	40	60	15	85%

[a] A FEP tube reactor (inner diameter of 1/32") was used. [b] A PTFE tube reactor (inner diameter 1/16") was used. [c] Temporary blockage of the tube reactor was observed. [d] Isolated yield. N.d. = not determined.

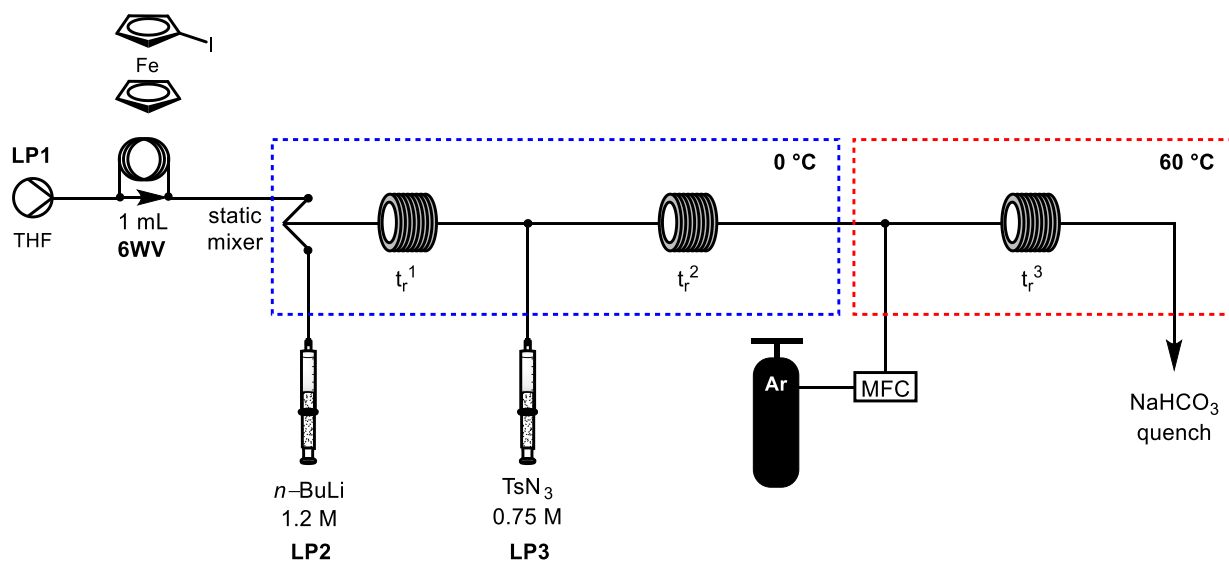
Due to expansion of the argon slugs and partial evaporation of the THF, the observed residence times are significantly lower than calculated.



Left: Picture of the tube reactor when the reaction mixture (red) is pumped through the reactor in a segmented flow; Right: Picture of the triphasic flow regime on the outlet of the reactor.

Optimization of parameters of the combined flow setup

Finally, the complete setup was constructed by combining both semi-batch procedures.



Syringe pumps (**LP2**, **LP3**) equipped with gastight 10 mL glass-syringes were used to pump solutions of *n*-butyllithium (1.2 M in *n*-hexane, $v_{n\text{-BuLi}}$) and tosyl azide (0.75 M in THF, v_{TsN_3}). Both solutions were passed through precooling loops (FEP tube, outer diameter 1/16", inner diameter 1/32", $V = 0.15$ mL) before mixing.

A HPLC pump (**LP1**) to feed the solvent was connected to a HPLC injection valve (**6WV**) equipped with a 1 mL sample loop. The liquid supply was passed through a precooled loop (FEP tube, outer diameter 1/16", inner diameter 1/32", $V = 0.15$ mL) and then merged in a static mixer (internal volume: 20 μL) with a solution of *n*-butyllithium (1.2 M in *n*-hexane, $v_{n\text{-BuLi}}$). The resulting reaction stream was pumped through tube **reactor1** (stainless steel capillary, inner diameter 250 μm , $V = 20$ μL) and then merged in a stainless steel T-mixer with a solution of tosyl azide. **Reactor1**, **reactor2**, the mixing units and the precooled loops were cooled to 0 °C by immersion to an ice bath.

The reaction stream was mixed in a T-mixer with argon provided by a mass flow controller (MFC) resulting in a segmented flow pattern. This stream was pumped through tube **reactor3** (PTFE tube, inner diameter 1/8", $V = 40$ mL) heated to 60 °C in a water bath. The resulting triphasic flow regime was collected in a flask containing NaHCO₃ (sat. aq., 50 mL).

The HPLC pump and the reactor were washed with anhydrous THF for 2 residence times by pumping THF with the HPLC pump and feeding argon using the MFC. A solution of iodoferrocene (**1a**) was loaded on the HPLC injection valve. The solutions of *n*-butyllithium and tosyl azide were pumped at the given flow rate for 15–20 s. Then, the solution of iodoferrocene (**1a**) was injected into the system by switching the HPLC valve to the "inject" position. The collected reaction mixture was diluted with EtOAc (50 mL). The aqueous layer was separated and extracted with EtOAc (2×50 mL). The combined organic layers were dried (Na₂SO₄), filtered, and concentrated under reduced pressure. Azidoferrocene

(2a) was isolated by gravity column chromatography (basic Al₂O₃, activity grade I +5 wt% H₂O, *n*-pentane).

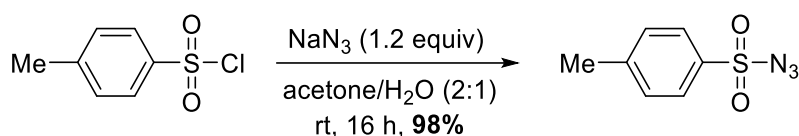
Table S5. Screening of parameters for the combined flow setup

Entry	V_{FcI}	V_{<i>n</i>-BuLi}	V_{TsN3}	V_{argon}	t_R¹	t_R²	t_R³	Yield^[c]
	[mL/min]	[mL/min]	[mL/min]	[mL/min]	[s]	[s]	[min]	
1^[a]	2.0	0.2	0.4	0.5	0.55	24	12	71
2^[a]	2.0	0.2	0.4	0.4	0.55	24	14	77
3^[b]	1.0	0.2	0.4	0.5	1	38	18	62
3^[b]	2.0	0.4	0.8	0.4	0.5	19	8	51
4^[b]	2.0	0.4	0.8	0.2	0.5	19	15	82

[a] A 0.1 M solution of iodoferrocene was employed. [b] A 0.2 M solution of iodoferrocene was employed. [c] Isolated yield.

2.3. Synthesis of Substrates

Synthesis of tosyl azide (S1)



In a 250 mL round bottom flask, tosyl chloride (10.0 g, 52.5 mmol, 1.0 equiv) was dissolved in acetone (80 mL). Under ice bath cooling, a solution of sodium azide (3.75 g, 57.7 mmol, 1.1 equiv) in H₂O (40 mL) was added over 10 min using a dropping funnel. The resulting suspension was stirred at rt for 1 h. Then, the suspension was diluted with NaCl (sat. aq., 50 mL) and EtOAc (50 mL). The aqueous layer was separated and extracted with EtOAc (2×100 mL). The combined organic layers were dried (Na₂SO₄), filtered, and concentrated under reduced pressure. The title compound **S1** (5.09 g, 25.8 mmol, 98%) was obtained without further purification as a colorless oil that solidified at 8 °C.

R_f = 0.49 (*n*-hexane/EtOAc 9:1).

¹H NMR (500 MHz, CDCl₃) δ [ppm] = 7.85 (d, *J* = 8.2 Hz, 2H), 7.41 (d, *J* = 8.2 Hz, 2H), 2.48 (s, 3H).

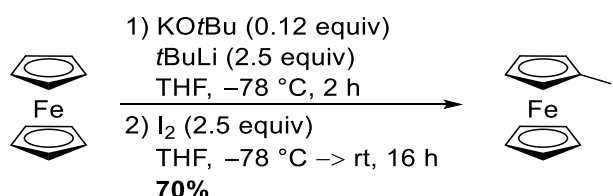
¹³C{¹H} NMR (126 MHz, CDCl₃) δ [ppm] = 146.3, 135.7, 130.4, 127.7, 21.9.

The spectroscopic data are consistent with those reported in the literature.^[2]

Preparation of a stock solution of tosyl azide in THF:

In a dry Schlenk tube, CaH₂ (~100 mg for 1 g of tosyl azide) was placed and the tube was evacuated and backfilled with argon (3×). A defined mass of tosyl azide was added as oil by using a Pasteur pipette. Then, a defined volume of anhydrous THF was added to give a concentration of 0.5-2.5 M. The resulting solution of tosyl azide in THF was dried over CaH₂ at least for 16 h prior use (gas evolution!). The solution was stored over CaH₂ at 8 °C in the dark and could be used for several months.

Synthesis of iodoferrocene (1a)



This compound was prepared according to a reported procedure with slight modifications.^[5]

In a dry 100 mL Schlenk tube, ferrocene (3.00 g, 16.1 mmol, 1.0 equiv) and potassium *tert*-butoxide (217 mg, 1.94 mmol, 0.12 equiv) were placed and the flask was evacuated and backfilled with argon (3×). Then, anhydrous THF (45 mL) was added and the resulting yellow solution was cooled to –

78 °C (acetone/dry ice). *tert*-Butyllithium (23.7 mL, 40.3 mmol, 2.5 equiv., 1.7 M in *n*-pentane) was added dropwise and the resulting orange mixture was stirred at –78 °C for 2 h. Then, solid iodine (10.2 g, 40.3 mmol, 2.5 equiv) was added portionwise over 10 min and the mixture was warmed to rt over 16 h by removing the cold bath. Then, the dark brown mixture was diluted with Na₂S₂O₃ (sat. aq., 100 mL) and EtOAc (50 mL). The aqueous layer was separated and extracted with EtOAc (3×100 mL). The combined organic layers were dried (MgSO₄), filtered, concentrated under reduced pressure, and loaded onto Celite®. Flash column chromatography (SiO₂, *n*-pentane) followed by removal of remaining ferrocene by sublimation at 60 °C/2 mbar on a rotary evaporator gave the title compound **1a** (3.52 g, 11.3 mmol, 70%) as a red oil that solidified upon standing.

If necessary, the product can be further purified by recrystallization from *n*-pentane at –78 °C.

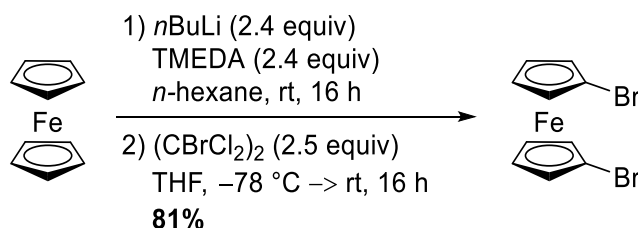
$R_f = 0.67$ (SiO₂; *n*-pentane; vis. vanillin).

¹H NMR (500 MHz, CDCl₃): δ [ppm] = 4.41 (t, $J = 1.9$ Hz, 2H), 4.19 (s, 5H), 4.15 (t, $J = 1.9$ Hz, 2H).

¹³C{¹H} NMR (126 MHz, CDCl₃): δ [ppm] = 74.6, 71.2, 69.0, 39.8.

The spectroscopic data are consistent with those reported in the literature.^[5]

Synthesis of 1,1'-dibromoferrocene (**1b**)



This compound was prepared according to a reported procedure with slight modifications.^[5]

In a dry 250 mL Schlenk flask equipped with a large, conical stirring bar, ferrocene (5.0 g, 27 mmol, 1.0 equiv) was placed and the flask was evacuated and backfilled with argon (3×). Then, anhydrous and degassed *n*-hexane (50 mL) and anhydrous tetramethylethylene diamine (9.7 mL, 65 mmol, 2.4 equiv) were added *via* syringe. While stirring, *n*-butyllithium (26 mL, 65 mmol, 2.4 equiv; 2.5 M in *n*-hexane) was added *via* syringe and the solution was stirred for 16 h at rt (gas evolution!). During this time, an orange precipitate was formed. The solution was removed *via* syringe and the precipitate was washed with anhydrous *n*-hexane (1×15 mL). The precipitate was dissolved in anhydrous THF (50 mL) and cooled to –78 °C (acetone/dry ice). 1,2-Dibromotetrachloroethane (22 g, 67 mmol, 2.5 equiv) was added as solid in portions over 10 min in a continuous argon stream and the resulting brown mixture was warmed to rt over 16 h. NH₄Cl (sat. aq., 50 mL) was added slowly and the resulting biphasic mixture was diluted with H₂O (50 mL). The organic layer was separated and the aqueous layer was extracted with CH₂Cl₂ (3×100 mL). The combined organic layers were dried (MgSO₄), filtered, concentrated under reduced pressure, and loaded onto SiO₂. Flash column chromatography (SiO₂; *n*-pentane/CH₂Cl₂

100:0 to 100:5) followed by removal of remaining ferrocene by sublimation at 60 °C and 2 mbar on a rotary evaporator gave the title compound **1b** (7.5 g, 22 mmol, 81%) as a red solid.

If necessary, the product can be further purified by recrystallization from *n*-pentane at -78 °C.

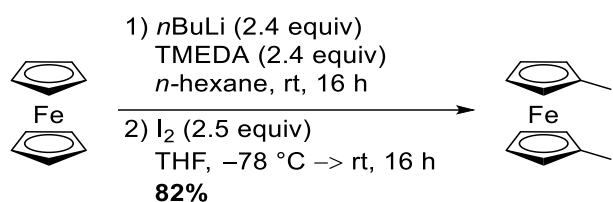
$R_f = 0.52$ (SiO₂; *n*-hexane; vis. vanillin).

¹H NMR (500 MHz, CDCl₃) δ [ppm] = 4.42 (t, $J = 1.9$ Hz, 4H), 4.17 (t, $J = 1.9$ Hz, 4H).

¹³C{¹H} NMR (126 MHz, CDCl₃) δ [ppm] = 78.4, 72.8, 70.1.

The spectroscopic data are consistent with those reported in the literature.^[5]

Synthesis of 1,1'-diiodoferrocene (**1c**):



This compound was prepared according to a reported procedure with slight modifications.^[5]

In a dry 250 mL Schlenk flask equipped with a large, conical stirring bar, ferrocene (5.0 g, 27 mmol, 1 equiv) was placed and the flask was evacuated and backfilled with argon (3×). Then, anhydrous *n*-hexane (50 mL) and anhydrous tetramethylethylene diamine (9.7 mL, 65 mmol, 2.4 equiv) were added *via* syringe. While stirring, *n*-butyllithium (26 mL, 65 mmol, 2.4 equiv; 2.5 M in *n*-hexane) was added *via* syringe and the solution was stirred for 16 h at rt (gas evolution!). During this time, an orange precipitate was formed. The solution was removed *via* syringe and the residue was washed with anhydrous *n*-hexane (1×15 mL). The precipitate was dissolved in anhydrous THF (50 mL) and cooled to -78 °C (acetone/dry ice). Iodine (17 g, 67 mmol, 2.5 equiv) was added in portions over 10 min in a continuous argon stream and the resulting dark brown mixture was warmed to rt over night. The mixture was diluted with Na₂S₂O₃ (sat. aq., 100 mL) and EtOAc (100 mL). The aqueous layer was separated and extracted with EtOAc (3×100 mL). The combined organic layers were dried (MgSO₄), filtered, concentrated under reduced pressure, and loaded onto SiO₂. Flash column chromatography (SiO₂; *n*-pentane/CH₂Cl₂ 100:0 to 100:5) followed by removal of remaining ferrocene by sublimation at 60 °C/2 mbar on a rotary evaporator gave the title compound **1c** (9.7 g, 22 mmol, 82%) as a brown oil.

If necessary, the product can be further purified by recrystallization from *n*-pentane at -78 °C.

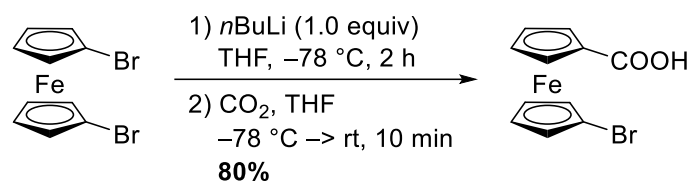
$R_f = 0.48$ (SiO₂; *n*-hexane; vis. vanillin).

¹H NMR (700 MHz, CDCl₃) δ [ppm] = 4.37 (t, $J = 1.9$ Hz, 4H), 4.18 (t, $J = 1.9$ Hz, 4H).

¹³C{¹H} NMR (176 MHz, CDCl₃) δ [ppm] = 77.7, 72.4, 40.4.

The spectroscopic data are consistent with those reported in the literature.^[5]

Synthesis of 1-bromo-1'-ferrocenylcarboxylic acid (**S2**)



In a dry 100 mL Schlenk tube, **1b** (1.0 g, 2.9 mmol, 1 equiv) was placed and the tube was evacuated and backfilled with argon (3×). Anhydrous THF (50 mL) was added and the resulting orange solution was cooled to -78 °C (acetone/dry ice). Then, *n*-butyllithium (1.2 mL, 2.9 mmol, 1.0 equiv; 2.5 M in *n*-hexane) was added dropwise at -78 °C and the resulting red solution was stirred at this temperature for 1 h. At -78 °C, a stream of dry CO₂ was bubbled through the solution for 10 min and the resulting yellow suspension was warmed to rt (gas evolution!). NH₄Cl (sat. aq., 10 mL) was added dropwise to the mixture. The solution was diluted with NH₄Cl (sat. aq., 50 mL) and EtOAc (20 mL). The aqueous layer was separated and extracted with EtOAc (4×50 mL). The combined organic layers were dried (MgSO₄), filtered, and loaded onto Celite®. Flash column chromatography (SiO₂, *n*-hexane/EtOAc 3:2 to 1:1) gave the title compound **S2** (0.72 g, 2.3 mmol, 80%) as a red solid.

$R_f = 0.35$ (SiO₂; *n*-hexane/EtOAc 3:2; vis. vanillin).

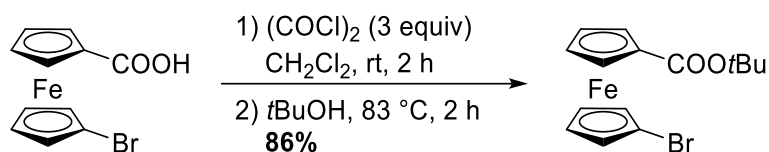
¹H NMR (500 MHz, CDCl₃) δ [ppm] = 4.91 (t, $J = 1.9$ Hz, 2H), 4.51 (t, $J = 1.9$ Hz, 2H), 4.49 (t, $J = 1.9$ Hz, 2H), 4.20 (t, $J = 1.9$ Hz, 2H).

¹³C{¹H} NMR (176 MHz, CDCl₃) δ [ppm] = 176.6, 78.2, 74.8, 72.8, 72.2, 72.0, 69.5.

HRMS (ESI-TOF) m/z calcd. for C₁₁H₁₀BrFeO₂⁺ ([M+H]⁺) 308.9208; found: 308.9209.

Note: A stream of CO₂ gas was provided as follows: A 50 mL flask was charged with a few chunks of dry ice and sealed with a septum equipped with a Teflon tube providing a continuous stream of CO₂ through the tube. A 25 mL flask was equipped with a septum and charged with conc. H₂SO₄ (10 mL). The septum was equipped with a transfer canula not reaching in the conc. H₂SO₄. The Teflon tube of the flask containing the dry ice was introduced through the septum and immersed in the conc. H₂SO₄. In this way, a continuous stream of CO₂-gas was bubbled through the conc. H₂SO₄ to dry the CO₂. Through the transfer canula, a continuous stream of anhydrous CO₂ is provided. After some minutes of flushing the system with CO₂, the transfer canula was introduced into the reaction mixture.

Synthesis of 1-bromo-1'-ferrocenylcarboxylic acid *tert*-butyl ester (**1e**)



In a dry 25 mL Schlenk flask, **S2** (600 mg, 1.94 mmol, 1.0 equiv) was placed and the flask was evacuated and backfilled with argon (3×). Anhydrous CH₂Cl₂ (10 mL) was added. To the resulting red suspension, oxalyl chloride (500 μL, 5.83 mmol, 3.0 equiv) was added *via* syringe in one portion under water bath cooling. The resulting red solution was stirred at rt until no more gas evolution was observed (1-2 h). The red solution was concentrated under reduced pressure and under exclusion of moisture. Then, *t*BuOH (10 mL) was added and the resulting red solution was heated to 83 °C. The mixture was diluted with NaHCO₃ (sat. aq., 50 mL) and EtOAc (50 mL). The aqueous layer was separated and extracted with EtOAc (3×50 mL). The combined organic layers were dried (MgSO₄), filtered, and concentrated under reduced pressure, and loaded onto Celite[®]. Flash column chromatography (SiO₂, *n*-hexane/EtOAc 10:1) gave the title compound **1e** (607 mg, 1.66 mmol, 86%) as a red oil.

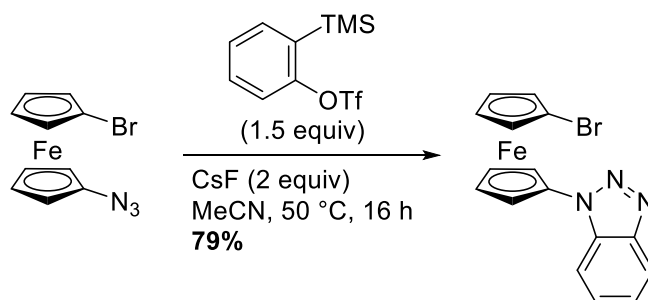
*R*_f = 0.49 (SiO₂; *n*-hexane/EtOAc 9:1; vis. vanillin).

¹H NMR (700 MHz, CDCl₃) δ [ppm] = 4.75 (t, *J* = 2.0 Hz, 2H), 4.41 (t, *J* = 1.9 Hz, 2H), 4.39 (t, *J* = 2.0 Hz, 2H), 4.14 (t, *J* = 1.9 Hz, 2H), 1.57 (s, 9H).

¹³C{¹H} NMR (176 MHz, CDCl₃) δ [ppm] = 170.0, 80.6, 78.1, 75.2, 73.7, 72.7, 71.8, 68.9, 28.5.

HRMS (ESI-TOF) *m/z* calcd. for C₁₅H₁₇BrFeO₂Na⁺ ([M+Na]⁺) 386.9653; found: 386.9659.

Synthesis of 1-(1*H*-benzo[*d*][1,2,3]triazole)-1'-bromoferrocene (**1f**)



In a dry 20 mL Schlenk tube, finely powdered cesium fluoride (99.3 mg, 0.654 mmol, 2.0 equiv) was placed and the cesium fluoride was dried at 10⁻³ mbar at 300 °C for 10 min. After cooling to rt, 1-azido-1'-bromoferrocene (**2b**, 100 mg, 0.327 mmol, 1.0 equiv) was added and the tube was evacuated and backfilled with argon (3×). Then, anhydrous MeCN (4 mL) was added and to the resulting orange solution, 2-(trimethylsilyl)phenyl trifluoromethanesulfonate (0.120 mL, 0.491 mmol, 1.5 equiv) was added. The Schlenk tube was sealed and the mixture was stirred at 50 °C for 16 h. After cooling to rt, the mixture was diluted with NaHCO₃ (sat. aq., 50 mL) and CH₂Cl₂ (50 mL). The organic layer was separated and the aqueous layer was extracted with CH₂Cl₂ (3×50 mL). The combined organic layers

were dried (Na_2SO_4), filtered, and loaded onto Celite. Flash column chromatography (SiO_2 , n -hexane/EtOAc 5:1) gave the title compound **1f** (98.6 mg, 0.258 mmol, 79%) as an orange solid.

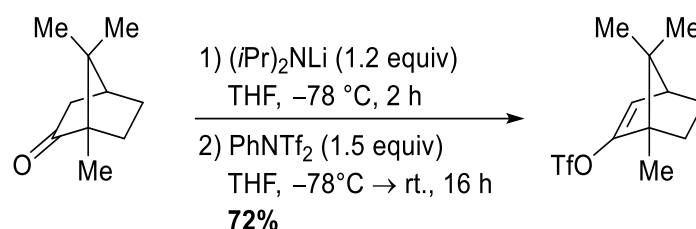
$R_f = 0.37$ (SiO_2 , n -hexane/EtOAc 5:1).

^1H NMR (400 MHz, CDCl_3) δ [ppm] = 4.20 (t, $J = 1.9$ Hz, 2H), 4.42 (t, $J = 2.0$ Hz, 2H), 4.51 (t, $J = 1.9$ Hz, 2H), 5.04 (t, $J = 2.0$ Hz, 2H), 7.43 (ddd, $J = 8.4, 7.0, 1.0$ Hz, 1H), 7.58 (ddd, $J = 8.4, 7.0, 1.0$ Hz, 1H), 7.87 (dt, $J = 8.4, 0.9$ Hz, 1H), 8.12 (dt, $J = 8.4, 0.9$ Hz, 1H).

$^{13}\text{C}\{^1\text{H}\}$ NMR (100 MHz, CDCl_3) δ [ppm] = 146.6, 133.0, 128.0, 124.4, 120.5, 110.9, 95.2, 78.5, 72.0, 69.6, 69.3, 64.5.

HRMS (ESI-TOF) m/z calcd. for $\text{C}_{16}\text{H}_{13}\text{BrFeN}_3^+$ ($[\text{M}+\text{H}]^+$) 381.9637; found: 381.9648.

Synthesis of (1*S*, 4*S*)-1,7,7-trimethylbicyclo[2.2.1]hept-2-enyl trifluoromethanesulfonate (**S3**)



This compound was prepared according to a reported procedure with slight modifications.^[6]

In a dry 20 mL Schlenk tube, anhydrous diisopropylamine (0.33 mL, 2.4 mmol, 1.2 equiv) was placed and anhydrous THF (2 mL) was added. The solution was cooled to -78°C (acetone/dry ice). Then, n -butyllithium (1.1 mL, 2.4 mmol, 1.2 equiv; 2.5 M in n -hexane) was added dropwise and the solution was warmed to 0°C over 30 min by exchanging the cooling bath to an ice bath. After cooling back to -78°C (acetone/dry ice), a solution of (-)-camphor (0.30 g, 2.0 mmol, 1.0 equiv) in anhydrous THF (2 mL) was added and the resulting solution was stirred at -78°C for 2 h. Then, N -phenylbis(trifluoromethanesulfonimide) (0.92 g, 2.4 mmol, 1.2 equiv) was added and the solution was warmed to rt by changing the cooling bath to a water bath. The solution was diluted with NH_4Cl (sat. aq., 20 mL) and EtOAc (20 mL). The aqueous layer was separated and extracted with EtOAc (3×20 mL). The combined organic layers were dried (Na_2SO_4), filtered, and concentrated under reduced pressure. Flash column chromatography (SiO_2 , n -pentane) gave the title compound **S3** (0.40 g, 1.4 mmol, 72%) as a colorless oil.

$R_f = 0.71$ (SiO_2 ; n -pentane; vis. vanillin).

^1H NMR (500 MHz, CDCl_3) δ [ppm] = 5.66 (d, $J = 3.8$ Hz, 1H), 2.45 (t, $J = 3.8$ Hz, 1H), 1.93 (ddt, $J = 12.2, 8.5, 3.7$ Hz, 1H), 1.65 (dddd, $J = 12.2, 8.6, 3.7, 0.7$ Hz, 1H), 1.33 (ddd, $J = 12.5, 9.2, 3.7$ Hz, 1H), 1.15 (ddd, $J = 12.5, 9.1, 3.7$ Hz, 1H), 1.03 (s, 3H), 0.92 (s, 3H), 0.79 (s, 3H).

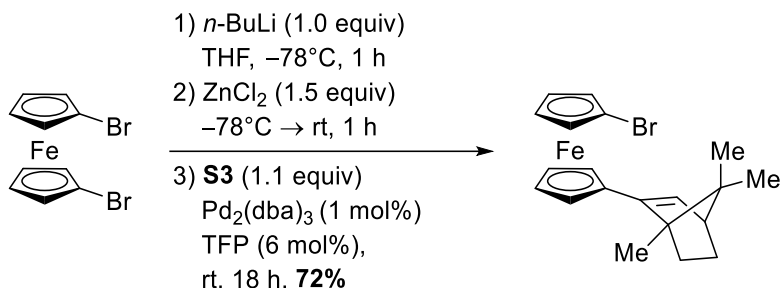
$^{13}\text{C}\{^1\text{H}\}$ NMR (176 MHz, CDCl_3) δ [ppm] = 155.4, 119.6 (q, $J = 315.3$ Hz), 117.8, 57.1, 54.0, 50.3, 31.0, 25.5, 19.9, 19.1, 9.6.

^{19}F NMR (565 MHz, CDCl_3) δ [ppm] = -73.5 .

The spectroscopic data are consistent with those reported in the literature.^[6]

Note: The title compound is volatile. Concentration at a pressure of less than 100 mbar/ 40 °C can lead to significant loss of product.

Synthesis of 1-bromo-1'-[(1S, 4S)-1,7,7-trimethylbicyclo[2.2.1]hept-2-enyl]ferrocene (**1g**)



In a dry 100 mL Schlenk tube, **1b** (0.44 g, 1.3 mmol 1.0 equiv) was placed and the flask was evacuated and backfilled with argon (3 \times). Anhydrous THF (22 mL) was added *via* syringe and the resulting orange solution was cooled to -78°C (acetone/dry ice). Then, *n*-butyllithium (0.51 mL, 1.3 mmol, 1.0 equiv; 2.5 M in *n*-hexane) was added dropwise over 15 min and the resulting red solution was stirred at -78°C for 1 h. A solution of ZnCl_2 (0.26 g, 1.9 mmol, 1.5 equiv) in anhydrous THF (2 mL) was added and the resulting yellow solution was stirred at -78°C for 30 min and then warmed to rt over 30 min by removing the cooling bath. A solution of **S3** (0.40 g, 1.4 mmol, 1.1 equiv.) in anhydrous THF (2 mL), tris(dibenzylideneacetone)dipalladium(0) (12 mg, 13 μmol , 1 mol%) and tri(2-furyl)phosphine (18 mg, 77 μmol , 6 mol%) were added in a continuous argon stream. The Schlenk tube was sealed and the orange suspension was stirred at rt for 18 h. The resulting red solution was diluted with NH_4Cl (sat. aq., 30 mL) and EtOAc (30 mL). The aqueous layer was separated and extracted with EtOAc (3 \times 60 mL). The combined organic layers were dried (Na_2SO_4), filtered, concentrated under reduced pressure, and loaded onto silica. Flash column chromatography (SiO_2 , *n*-pentane) gave the title compound **1g** (0.37 g, 0.94 mmol, 73%) essentially pure as an orange solid. An analytically pure sample was obtained by HPLC (Phenomenex 21.2 \times 250 mm RP Gemini NX 5 μm C18; 0.7 L/min; t_r 8.5 min).

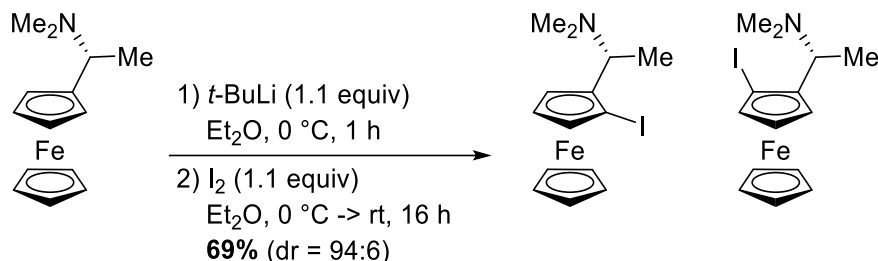
R_f = 0.56 (SiO_2 ; *n*-pentane; vis. vanillin).

^1H NMR (500 MHz, CDCl_3) δ [ppm] = 6.06 (d, J = 3.3 Hz, 1H), 4.37 – 4.28 (m, 4H), 4.25 (tdd, J = 3.8, 2.4, 1.9 Hz, 2H), 4.08 (t, J = 1.9 Hz, 2H), 2.31 (t, J = 3.5 Hz, 1H), 1.90 (ddt, J = 12.3, 8.7, 3.7 Hz, 1H), 1.60 (ddd, J = 11.8, 8.7, 3.5 Hz, 1H), 1.26 (s, 3H), 1.26 – 1.14 (m, 1H), 1.03 (ddd, J = 12.3, 9.1, 3.6 Hz, 1H), 0.91 (s, 3H), 0.82 (s, 3H).

$^{13}\text{C}\{^1\text{H}\}$ NMR (126 MHz, CDCl_3) δ [ppm] = 144.7, 130.8, 84.7, 78.0, 71.2, 71.2, 71.0, 71.0, 69.2, 68.6, 68.4, 68.4, 56.9, 55.2, 51.7, 32.1, 25.8, 20.2, 19.8, 13.4.

HRMS (ESI-TOF) m/z calcd. for $C_{20}H_{23}BrFe^+$ ($[M]^+$) 398.0333; found: 398.0333.

(S)-1-Iodo-2-[3-(*R*)-(N,N-dimethylamino)ethyl]ferrocene (1h**)**



This compound was prepared according to a reported procedure.^[7]

In a dry 25 mL Schlenk tube, (*R*)-*N,N*-dimethyl-1-ferrocenylethylamine (0.26 g, 1.0 mmol, 1.0 equiv) was placed. Anhydrous Et₂O (6 mL) was added and the resulting solution was cooled to 0 °C (ice bath). *tert*-Butyllithium (0.66 mL, 1.1 mmol, 1.1 equiv.; 1.7 M in *n*-pentane) was added dropwise and the reaction mixture was stirred at 0 °C for 1 h. Then, a solution of iodine (0.31 g, 1.2 mmol, 1.2 equiv) in Et₂O (7.5 mL) was added dropwise. The reaction mixture was slowly warmed to rt. Then, the mixture was diluted with Na₂S₂O₃ (sat. aq., 10 mL) and Et₂O (10 mL), the aqueous layer was separated and extracted with Et₂O (3×10 mL). The combined organic layers were washed with H₂O (20 mL), NaCl (sat. aq., 20 mL), dried (MgSO₄), filtered, and concentrated under reduced pressure. Flash column chromatography (SiO₂, CH₂Cl₂/Et₂O 1:1 + 0.5% NEt₃) gave the title compound **1h** (0.27 g, 0.70 mmol, 69%, dr 94:6 [¹H NMR]) as an orange oil.

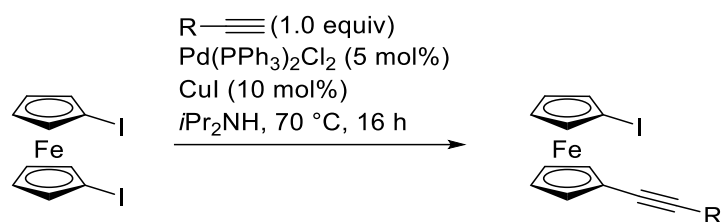
R_f = 0.30 (SiO₂, CH₂Cl₂/Et₂O 1:1 + 0.5% NEt₃, vis. vanillin).

¹H NMR (500 MHz, CDCl₃): δ [ppm] = 4.46 (dd, *J* = 2.5, 1.3 Hz, 1H), 4.24 (pt, *J* = 2.5 Hz, 1H), 4.15 (dd, *J* = 2.5, 1.3 Hz, 1H), 4.12 (s, 5H), 3.62 (q, *J* = 6.8 Hz, 1H), 2.14 (s, 6H), 1.50 (d, *J* = 6.8 Hz, 3H).

¹³C{¹H} NMR (126 MHz, CDCl₃): δ [ppm] = 90.3, 74.5, 71.8, 68.3, 65.7, 57.7, 45.6, 41.3, 16.1.

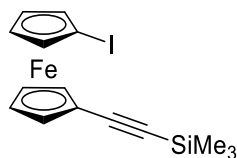
The spectroscopic data are consistent with those reported in the literature.^[7]

General Procedure 1 (GP1) for the Sonogashira coupling of 1,1'-diiodoferrocene with various acetylenes



In a dry Schlenk tube, **1c** (1.0 equiv) was placed and the flask was evacuated and backfilled with argon (3×). Anhydrous (*i*-Pr)₂NH (ca. 0.15 M) was added *via* syringe. To the resulting orange solution, the corresponding acetylene (1.0 equiv), bis(triphenylphosphine)palladium(II) dichloride (5 mol%) and copper(I) iodide (10 mol%) were added in a continuous stream of argon. The schlenk tube was sealed and the orange suspension was stirred at 70 °C for 16 h. After cooling to rt, the red suspension was diluted with EtOAc, filtered over a pad of Celite[®], and eluted with EtOAc (3×). The filtrate was concentrated and loaded onto Celite[®]. Flash column chromatography gave the ethynyl-substituted ferrocenes **1i** – **1n**.

Synthesis of 1-iodo-1'-(trimethylsilylethynyl)ferrocene (**1i**)



According to **GP1**, the title compound was prepared from **1c** (700 mg, 1.60 mmol, 1.0 equiv), *i*Pr₂NH (10 mL), trimethylsilylacetylene (221 μL, 1.60 mmol, 1.0 equiv), bis(triphenylphosphine)palladium(II) dichloride (56.0 mg, 80 μmol, 5 mol%), and copper(I) iodide (30.4 mg, 160 μmol, 10 mol%). Flash column chromatography (SiO₂, *n*-pentane/CH₂Cl₂ 100:0 to 50:1 to 10:1) gave the title compound **1i** (299 mg, 733 μmol, 46%) as a red oil.

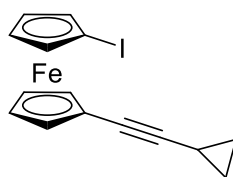
*R*_f = 0.30 (SiO₂; *n*-hexane; vis. vanillin).

¹H NMR (700 MHz, CDCl₃) δ [ppm] = 4.39 (dt, *J* = 8.5, 1.9 Hz, 4H), 4.19 (dt, *J* = 7.9, 1.9 Hz, 4H), 0.24 (s, 9H).

¹³C{¹H} NMR (176 MHz, CDCl₃) δ [ppm] = 102.9, 92.0, 76.7, 74.6, 72.2, 71.4, 67.2, 40.6, 0.4.

The spectroscopic data are consistent with those reported in the literature.^[8]

Synthesis of 1-iodo-1'-(cyclopropylethynyl)ferrocene (**1j**)



According to **GP1**, the title compound was prepared from **1c** (0.50 g, 1.4 mmol, 1.0 equiv), cyclopropylacetylene (0.12 mL, 1.4 mmol, 1.2 equiv), bis(triphenylphosphine)-palladium(II) dichloride (40 mg, 57 μ mol, 1.5 mol%), and CuI (22 mg, 0.11 mmol, 3 mol%) in *i*Pr₂NH (6 mL). The mixture was stirred at 50 °C for 48 h. Flash column chromatography (SiO₂, *n*-pentane/CH₂Cl₂ 100:0 to 20:1) gave the title compound **1j** (0.13 g, 0.34 mmol, 31%) as an orange oil.

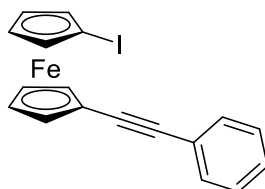
R_f = 0.19 (SiO₂; *n*-pentane, vis. vanillin).

¹H NMR (500 MHz, CDCl₃) δ [ppm] = 4.38 (t, J = 1.8 Hz, 2H), 4.31 (t, J = 1.9 Hz, 2H), 4.17 (t, J = 1.8 Hz, 2H), 4.14 (t, J = 1.9 Hz, 2H), 1.36 (tt, J = 8.3, 5.0 Hz, 1H), 0.83 (ddt, J = 8.3, 5.7, 3.0 Hz, 2H), 0.77 (ddd, J = 7.6, 5.2, 2.8 Hz, 2H).

¹³C{¹H} NMR (126 MHz, CDCl₃) δ [ppm] = 90.9, 76.3, 74.1, 72.4, 71.6, 71.0, 68.8, 41.1, 8.7, 0.5.

HRMS (ESI-TOF) m/z calcd. for C₁₅H₁₃FeI⁺ ([M]⁺) 375.9411; found: 375.9411.

Synthesis of 1-iodo-1'-(phenylethynyl)ferrocene (**1k**)



According to **GP1**, the title compound was prepared from **1c** (500 mg, 1.14 mmol, 1.0 equiv), phenylacetylene (125 μ L, 1.14 mmol, 1.0 equiv), bis(triphenylphosphine)palladium(II) dichloride (40.0 mg, 570 μ mol, 5 mol%), and CuI (22.0 mg, 114 μ mol, 10 mol%) in anhydrous *i*Pr₂NH (10 mL). Flash column chromatography (SiO₂, *n*-pentane/CH₂Cl₂ 100:0 to 10:1) followed by recrystallization from *n*-pentane at -78 °C gave the title compound **1k** (208 mg, 505 μ mol, 44%) as an orange powder.

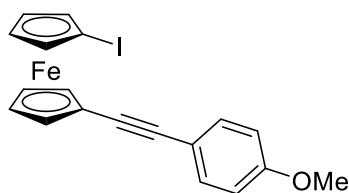
R_f = 0.23 (SiO₂; *n*-pentane; vis. vanillin).

¹H NMR (700 MHz, CDCl₃) δ [ppm] = 7.52 (dd, J = 7.6, 2.0 Hz, 2H), 7.33–7.32 (m, 3H), 4.48 (t, J = 1.9 Hz, 2H), 4.45 (t, J = 1.8 Hz, 2H), 4.26 (t, J = 1.9 Hz, 2H), 4.24 (t, J = 1.8 Hz, 2H).

¹³C{¹H} NMR (176 MHz, CDCl₃) δ [ppm] = 131.6, 128.4, 128.0, 123.9, 87.1, 87.1, 76.5, 74.2, 72.2, 71.1, 67.8, 41.3.

The spectroscopic data are consistent with those reported in the literature.^[9]

Synthesis of 1-iodo-1'-(1-ethynyl-4-methoxybenzene)ferrocene (**1l**)



According to **GP1**, the title compound was prepared from **1c** (250 mg, 571 μmol , 1.0 equiv), 1-ethynyl-4-methoxybenzene (75.8 mg, 571 μmol , 1.0 equiv), bis(triphenylphosphine)-palladium(II) dichloride (20.0 mg, 29.0 μmol , 5 mol%), and CuI (10.9 mg, 57.0 μmol , 10 mol%) in anhydrous *i*Pr₂NH (4 mL). Flash column chromatography (SiO₂, *n*-pentane/CH₂Cl₂ 8:1) gave the title compound **1l** (94.0 mg, 213 μmol , 37%) as a red solid.

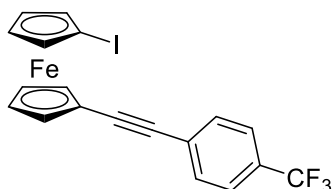
R_f = 0.25 (SiO₂; *n*-pentane/CH₂Cl₂ 8:1; vis. vanillin).

¹H NMR (700 MHz, CDCl₃) δ [ppm] = 7.46 (d, J = 8.8 Hz, 2H), 6.86 (d, J = 8.8 Hz, 2H), 4.45 (dt, J = 6.9, 1.8 Hz, 4H), 4.23 (dt, J = 10.3, 1.9 Hz, 4H), 3.83 (s, 3H).

¹³C{¹H} NMR (176 MHz, CDCl₃) δ [ppm] = 159.5, 133.1, 116.1, 114.1, 86.9, 85.5, 76.4, 74.1, 72.0, 71.0, 68.3, 55.5, 41.4.

HRMS (ESI-TOF) m/z calcd. for C₁₉H₁₆FeIO⁺ ([M+H]⁺) 442.9590; found: 442.9605.

Synthesis of 1-iodo-1'-(1-ethynyl-4-trifluoromethylbenzene)ferrocene (**1m**)



According to **GP1**, the title compound was prepared from **1c** (310 mg, 708 μmol , 1.0 equiv), 1-ethynyl-4-trifluoromethylbenzene (121 mg, 708 μmol , 1.0 equiv), bis(triphenylphosphine)-palladium(II) dichloride (24.8 mg, 35.0 μmol , 5 mol%) and CuI (13.5 mg, 71.0 μmol , 10 mol%) in *i*Pr₂NH (10 mL). Flash column chromatography (SiO₂, *n*-pentane/CH₂Cl₂ 100:0 to 20:1) gave the title compound **1m** (111 mg, 231 μmol , 33%) as a red solid.

R_f = 0.55 (SiO₂; *n*-pentane, vis. vanillin).

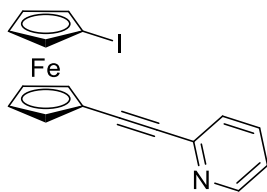
¹H-NMR (500 MHz, CDCl₃): δ [ppm] = 7.61 (d, J = 8.3 Hz, 2H), 7.58 (d, J = 7.7 Hz, 2H), 4.50 (pt, J = 2.0 Hz, 2H), 4.46 (pt, J = 2.0 Hz, 2H), 4.30 (pt, J = 2.0 Hz, 2H), 4.24 (pt, J = 2.0 Hz, 2H).

¹³C{¹H} NMR (176 MHz, CDCl₃) δ [ppm] = 131.7, 129.6 (q, J = 32.5 Hz), 127.8, 125.4 (q, J = 3.8 Hz), 124.2 (J = 272.2 Hz), 90.2, 85.9, 76.6, 74.4, 72.4, 71.0, 70.2, 66.9.

¹⁹F NMR (471 MHz, CDCl₃): δ [ppm] = 62.6.

HRMS (ESI-TOF) m/z calcd. for C₁₉H₁₂F₃FeI⁺ ([M]⁺) 479.9285; found: 479.9290.

Synthesis of 1-iodo-1'-(pyridylethynyl)ferrocene (**1n**)



According to **GP1**, the title compound was prepared from **1c** (250 mg, 571 μmol , 1.0 equiv), 2-ethynylpyridine (63.3 μL , 58.9 mg, 571 μmol , 1.0 equiv), bis(triphenylphosphine)-palladium(II) dichloride (20.0 mg, 29.0 μmol , 5 mol%), and CuI (10.9 mg, 57.0 μmol , 10 mol%) in anhydrous *i*Pr₂NH (4 mL). Flash column chromatography (SiO₂, *n*-hexane/EtOAc 5:1) gave the title compound **1n** (101 mg, 245 μmol , 43%) as a red solid.

R_f = 0.28 (SiO₂; *n*-hexane/EtOAc 5:1; vis. vanillin).

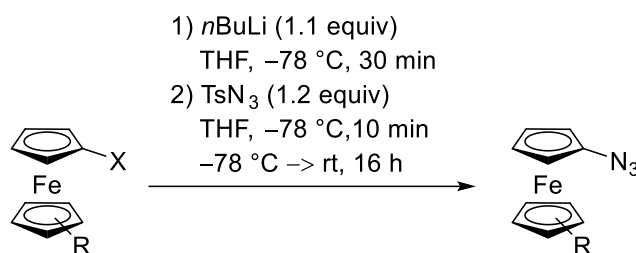
¹H NMR (500 MHz, CDCl₃) δ [ppm] = 8.65–8.55 (m, 1H), 7.65 (td, J = 7.7, 1.7 Hz, 1H), 7.50 (d, J = 7.8 Hz, 1H), 7.22 (dd, J = 7.8, 4.7 Hz, 1H), 4.55 (t, J = 1.9 Hz, 2H), 4.46 (t, J = 1.9 Hz, 2H), 4.28 (t, J = 1.9 Hz, 2H), 4.25 (t, J = 1.9 Hz, 2H).

¹³C{¹H} NMR (126 MHz, CDCl₃) δ [ppm] = 150.1, 144.0, 136.2, 127.0, 122.5, 88.0, 86.6, 76.5, 74.5, 72.8, 71.4, 66.2, 40.9.

The spectroscopic data are consistent with those reported in the literature.^[10]

2.4. Synthesis of Ferrocenyl Azides in Batch

General Procedure 2 (GP2) for the synthesis of ferrocenyl azides in batch



In a dry Schlenk tube, the ferrocenyl halide (1.0 equiv) was placed and the Schlenk tube was evacuated and backfilled with argon (3×). THF (0.05-0.32 M) was added and the resulting solution was cooled to -78 °C (acetone/dry ice). *n*-Butyllithium (1.1 equiv) was added dropwise and the mixture was stirred for 30 min. Then, tosyl azide (1.2 equiv) was added dropwise at -78 °C and the resulting dark red solution was stirred at this temperature for 1 h. The cooling bath was removed, the Schlenk tube was wrapped in aluminum foil and the mixture was stirred for 16 h at rt. After exposure to air, NaHCO₃ (sat. aq.) and EtOAc were added. The aqueous layer was separated and extracted with EtOAc. The combined organic layers were dried (Na₂SO₄), filtered, and concentrated under reduced pressure. Gravity column chromatography (basic Al₂O₃, activity grade I +5 wt% H₂O) gave the ferrocenyl azide. If necessary, further purification was performed by recrystallization from *n*-pentane at -78 °C.

Note 1: Drying with MgSO₄ instead of Na₂SO₄ gave lower yields.

Note 2: For column chromatography, the crude product was suspended in a small amount of the eluent and the resulting suspension was directly loaded onto the column using a Pasteur pipette.

Note 3: In some cases, flash column chromatography was possible, but in general, gravity column chromatography gave better separations.

Graphical Guide for the Synthesis of Ferrocenyl Azides in Batch



Left: Schlenk tube with ferrocenyl iodide. Center: Solution of ferrocenyl iodide in tetrahydrofuran at $-78\text{ }^{\circ}\text{C}$. Right: Reaction mixture after adding *n*-butyllithium.



Left: Reaction mixture after adding tosyl azide. Center: Reaction mixture after removing the cold bath. Right: Reaction mixture stirred under exclusion of light.

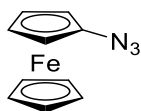


Left: Reaction mixture after stirring at room temperature over night. Center: Aqueous work-up of the reaction mixture. Right: TLC of the reaction mixture after aqueous workup (left lane: starting material, middle lane: co-spot; right lane: crude product; vis. vanillin).



Left: Removal of the drying agent by filtration. Center: Gravity column chromatography of the crude product. Right: Pure product.

Synthesis of Azidoferrocene (2a)



According to **GP2**, the title compound was prepared from **1a** (0.50 g, 1.6 mmol, 1.0 equiv), *n*-butyllithium (0.71 mL, 1.8 mmol, 1.1 equiv; 2.5 M in *n*-hexane), and tosyl azide (0.77 mL, 1.9 mmol, 2.5 equiv; 0.75 M in THF) in THF (10 mL). Gravity column chromatography (basic Al₂O₃, activity grade I+5 wt% H₂O; *n*-pentane) gave the title compound **2a** (0.35 g, 1.5 mmol, 95%) as a red oil that solidified upon standing at -18 °C.

$R_f = 0.41$ (SiO₂, *n*-hexane, vis. vanillin).

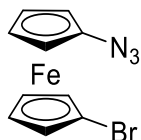
¹H NMR (400 MHz, CDCl₃) δ [ppm] = 4.28 (s, 5H), 4.26 (t, $J = 1.9$ Hz, 2H), 4.04 (t, $J = 1.9$ Hz, 2H).

¹³C{¹H} NMR (100 MHz, CDCl₃) δ [ppm] = 99.3, 69.3, 65.4, 60.7.

FT-IR (neat) $\tilde{\nu}$ [cm⁻¹] = 3109 (w), 3090 (w), 2323 (m), 2196 (m), 2113 (s), 2107 (m), 1712 (w), 1451 (s), 1408 (m), 1373 (m), 1350 (m), 1282 (s), 1222 (m), 1104 (s), 1058 (m), 1021 (m), 1000 (s), 915 (m), 892 (m), 850 (m), 843 (m), 819 (s), 738 (m), 618 (w), 590 (w).

HRMS (ESI-TOF) m/z calcd. for C₁₀H₉FeN₃⁺ ([M]⁺) 227.0146; found: 227.0136.

Synthesis of 1-azido-1'-bromoferrocene (2b)



According to **GP1**, to a solution of **1b** (300 mg, 0.873 mmol, 1.0 equiv) in anhydrous THF (15 mL), *n*-butyllithium (0.349 mL, 0.873 mmol, 1.0 equiv; 2.5 M in *n*-hexane) was added dropwise over 10 min at -78 °C (acetone/dry ice). During the addition and for another 1 h, the reaction mixture was carefully maintained below -70 °C while 1-lithio-1'-bromoferrocene partially precipitated. Then, tosyl azide (1.40 mL, 1.05 mmol, 1.2 equiv; 0.75 M in THF) was added dropwise at -78 °C over 10 min and the resulting dark red solution was stirred at this temperature for 1 h. The cooling bath was removed, the Schlenk tube was wrapped in aluminum foil and the mixture was stirred for 16 h at rt. The mixture was diluted with NaHCO₃ (sat. aq., 50 mL) and EtOAc (40 mL) and the aqueous layer was separated and extracted with EtOAc (2×50 mL). The combined organic layers were dried (Na₂SO₄), filtered, and concentrated under reduced pressure. Gravity column chromatography (basic Al₂O₃, activity grade I+5 wt% H₂O; *n*-pentane) gave the title compound **2b** (242 mg, 0.791 mmol, 91%) as a red oil that solidified upon standing.

$R_f = 0.32$ (SiO₂, *n*-pentane, vis. vanillin).

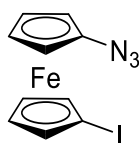
^1H NMR (500 MHz, CDCl_3) δ [ppm] = 4.52 (t, J = 1.9 Hz, 2H), 4.27 (t, J = 2.0 Hz, 2H), 4.20 (t, J = 1.9 Hz, 2H), 4.12 (t, J = 2.0 Hz, 2H).

$^{13}\text{C}\{^1\text{H}\}$ NMR (126 MHz, CDCl_3) δ [ppm] = 100.7, 78.7, 71.5, 68.3, 68.0, 62.9.

FT-IR (neat) $\tilde{\nu}$ [cm^{-1}] = 2924 (s), 2854 (s), 2111 (s), 1716 (w), 1459 (m), 1410 (w), 1374 (w), 1287 (m), 1260 (w), 1153 (w), 1098 (w), 1022 (m), 918 (w), 873 (m), 807 (m), 741 (w), 699 (w).

HRMS (ESI-TOF) m/z calcd. for $\text{C}_{10}\text{H}_8\text{BrFeN}_3^+$ ($[\text{M}]^+$) 304.9251; found: 304.9243.

Synthesis of 1-azido-1'-iodoferrocene (2c)



According to **GP2**, the title compound was prepared from **1c** (131 mg, 299 μmol , 1.0 equiv), *n*-butyllithium (110 μL , 299 μmol , 1.0 equiv; 2.7 M in *n*-hexane), and tosyl azide (142 μL , 359 μmol , 1.2 equiv; 2.5 M in THF) in THF (5 mL). Gravity column chromatography (basic Al_2O_3 , activity grade I +5 wt% H_2O ; *n*-pentane) gave the title compound **2c** (27.0 mg, 77.0 μmol , 26%) as a brown oil.

R_f = 0.39 (SiO_2 , *n*-pentane, vis. vanillin).

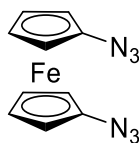
^1H NMR (400 MHz, CDCl_3) δ [ppm] = 4.51 (t, J = 1.8 Hz, 2H), 4.25 (t, J = 1.8 Hz, 2H), 4.22 (t, J = 2.0 Hz, 2H), 4.08 (t, J = 2.0 Hz, 2H).

$^{13}\text{C}\{^1\text{H}\}$ NMR (100 MHz, CDCl_3) δ [ppm] = 100.7, 75.9, 70.0, 68.5, 63.3, 40.9.

FT-IR (neat) $\tilde{\nu}$ [cm^{-1}] = 3098 (w), 2961 (w), 2208 (w), 2107 (s), 1631 (w), 1457 (w), 1403 (2), 1378 (m), 1344 (s), 1285 (w), 1261 (m), 1143 (m), 1105 (w), 1051 (w), 1020 (s), 916 (w), 864 (s), 805 (s), 585 (w).

HRMS (ESI-TOF) m/z calcd. for $\text{C}_{10}\text{H}_8\text{FeIN}_3^+$ ($[\text{M}]^+$) 352.9112; found: 352.9121.

Synthesis of 1,1'-diazidoferrocene (2d)



According to **GP2**, the title compound was prepared from **1b** (200 mg, 0.582 mmol, 1.0 equiv), *n*-butyllithium (0.512 mL, 1.28 mmol, 2.2 equiv; 2.5 M in *n*-hexane), and tosyl azide (1.81 mL, 1.34 mmol, 2.3 equiv; 0.75 M in THF) in THF (5 mL). Gravity column chromatography (basic Al_2O_3 , activity grade I +5 wt% H_2O ; *n*-pentane) gave the title compound **2d** (147 mg, 0.548 mmol, 94%) as an orange oil that solidified upon standing.

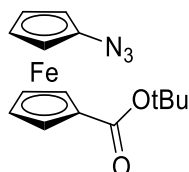
R_f = 0.29 (SiO_2 , *n*-hexane, vis. vanillin).

^1H NMR (700 MHz, CDCl_3) δ [ppm] = 4.35 (t, J = 2.0 Hz, 4H), 4.15 (t, J = 2.0 Hz, 4H).

$^{13}\text{C}\{^1\text{H}\}$ NMR (176 MHz, CDCl_3) δ [ppm] = 100.5, 66.5, 61.6.

The spectroscopic data are consistent with those reported in the literature.^[11]

Synthesis of 1-azido-1'-ferrocenylcarboxylic acid *tert*-butyl ester (**2e**)



According to **GP2**, the title compound was prepared from **1e** (200 mg, 548 μmol , 1.0 equiv), *n*-butyllithium (241 μL , 603 μmol , 1.1 equiv; 2.5 M in *n*-hexane) and tosyl azide (877 μL , 657 μmol , 1.2 equiv; 0.75 M in THF) in THF (5 mL). Gravity column chromatography (basic Al_2O_3 , activity grade I +5 wt% H_2O ; *n*-pentane/ Et_2O 20:1) gave the title compound **2e** (136 mg, 416 μmol , 76%) as a red oil. R_f = 0.40 (SiO_2 , *n*-pentane/ Et_2O = 20:1, vis. vanillin).

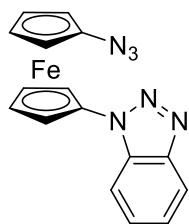
^1H NMR (400 MHz, CDCl_3) δ [ppm] = 4.83 (t, J = 2.0 Hz, 2H), 4.43 (t, J = 2.0 Hz, 2H), 4.25 (t, J = 2.0 Hz, 2H), 4.07 (t, J = 1.9 Hz, 2H), 1.56 (s, 9H).

$^{13}\text{C}\{^1\text{H}\}$ NMR (100 MHz, CDCl_3) δ [ppm] = 170.2, 100.6, 80.5, 74.9, 72.0, 71.2, 67.0, 61.8, 28.4.

FT-IR (neat) $\tilde{\nu}$ [cm^{-1}] = 2976 (w), 2927 (w), 2854 (w), 2443 (w), 2319 (w), 2204 (w), 2111 (s), 1709 (s), 1458 (s), 1393 (w), 1367 (m), 1288 (s), 1256 (w), 1181 (w), 1137 (s), 1025 (w), 917 (w), 814 (w), 778 (w), 741 (w).

HRMS (ESI): m/z calcd. for $\text{C}_{15}\text{H}_{16}\text{FeN}_3\text{NaO}_2^+$ ($[\text{M}+\text{Na}]^+$) 350.0562; found: 350.0566.

Synthesis of 1-azido-1'-(1*H*-benzo[*d*][1,2,3]triazole)ferrocene (**2f**)



According to **GP2**, the title compound was prepared from **1f** (39 mg, 0.10 mmol, 1.0 equiv), *n*-butyllithium (49 μL , 0.12 mmol, 1.2 equiv.; 2.5 M in *n*-hexane), and tosyl azide (50 μL , 0.12 mmol, 1.2 equiv.; 2.5 M in THF) in anhydrous THF (2 mL). Gravity column chromatography (basic Al_2O_3 , activity grade I +5 wt% H_2O ; *n*-hexane/ EtOAc 4:1) followed by recrystallization from *n*-pentane at -78 $^\circ\text{C}$ gave the title compound **2f** (24 mg, 69 μmol , 68%) as a yellow solid.

R_f = 0.30 (SiO_2 , *n*-hexane/ EtOAc 4:1).

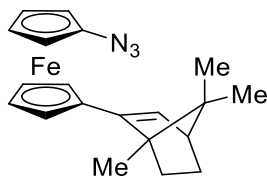
^1H NMR (400 MHz, CDCl_3) δ [ppm] = 8.11 (d, $J = 8.4$ Hz, 1H), 7.81 (d, $J = 8.4$ Hz, 1H), 7.57 (t, $J = 7.7$ Hz, 1H), 7.42 (t, $J = 7.7$ Hz, 1H), 5.08 (t, $J = 2.0$ Hz, 2H), 4.47 (t, $J = 2.0$ Hz, 2H), 4.33 (t, $J = 2.0$ Hz, 2H), 4.15 (t, $J = 2.0$ Hz, 2H).

$^{13}\text{C}\{^1\text{H}\}$ NMR (100 MHz, CDCl_3) δ [ppm] = 146.5, 133.0, 128.0, 124.4, 120.5, 110.7, 101.0, 94.8, 67.9, 67.4, 63.6, 62.2.

FT-IR (neat) $\tilde{\nu}$ [cm^{-1}] = 3126 (w), 3104 (w), 3074 (w), 2363 (w), 2333 (w), 2103 (s), 2031 (m), 1610 (w), 1588 (w), 1515 (m), 1462 (m), 1450 (m), 1372 (w), 1297 (m), 1282 (m), 1250 (w), 1219 (w), 1204 (w), 1168 (w), 1147 (w), 1125 (w), 1074 (m), 1058 (m), 1029 (m), 992 (w), 924 (m), 917 (m), 868 (m), 885 (m), 831 (w), 807 (w), 781 (w), 744 (m).

HRMS (ESI): m/z calcd. for $\text{C}_{16}\text{H}_{12}\text{FeN}_6^+$ ($[\text{M}]^+$) 344.0473; found: 344.0467.

Synthesis of 1-azido-1'-[(1S, 4S)-1,7,7-trimethylbicyclo[2.2.1]hept-2-enyl]ferrocene (2g)



According to **GP2**, the title compound was prepared from **1g** (200 mg, 501 μmol , 1.0 equiv), *n*-butyllithium (220 μL , 551 μmol , 1.1 equiv.; 2.5 M in *n*-hexane), and tosyl azide (802 μL , 601 μmol , 1.2 equiv.; 0.75 M in THF) in anhydrous THF (5 mL). Gravity column chromatography (basic Al_2O_3 , activity grade I +5 wt% H_2O ; *n*-pentane) gave the title compound **2g** (125 mg, 346 μmol , 69%) as an orange oil.

$R_f = 0.42$ (SiO_2 ; *n*-pentane; vis. vanillin).

^1H NMR (400 MHz, CDCl_3) δ [ppm] = 6.04 (d, $J = 3.3$ Hz, 1H), 4.39 (dq, $J = 11.2, 1.8$ Hz, 2H), 4.32 (t, $J = 1.9$ Hz, 2H), 4.18 (dq, $J = 8.8, 1.8$ Hz, 2H), 4.01 (t, $J = 2.0$ Hz, 2H), 2.30 (t, $J = 3.5$ Hz, 1H), 1.88 (ddt, $J = 12.2, 8.7, 3.7$ Hz, 1H), 1.58 (ddd, $J = 12.0, 8.7, 3.5$ Hz, 1H), 1.25 (s, 3H), 1.17 (ddd, $J = 12.1, 9.1, 3.6$ Hz, 1H), 1.01 (ddd, $J = 12.3, 9.1, 3.5$ Hz, 1H), 0.89 (s, 3H), 0.80 (s, 3H).

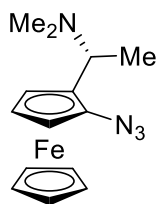
$^{13}\text{C}\{^1\text{H}\}$ NMR (100 MHz, CDCl_3) δ [ppm] = 144.8, 130.7, 99.5, 84.5, 77.4, 69.2, 69.1, 67.9, 66.9, 66.6, 61.6, 61.5, 56.9, 55.2, 51.7, 32.2, 25.8, 20.1, 19.8, 13.3.

FT-IR (neat) $\tilde{\nu}$ [cm^{-1}] = 2949 (m), 2870 (m), 2104 (s), 2024 (w), 1456 (s), 1384 (m), 1372 (m), 1363 (m), 1336 (w), 1285 (m), 1221 (w), 1163 (m), 1132 (w), 1105 (m), 1065 (m), 1023 (m), 917 (m), 878 (m), 818 (s), 804 (s), 740 (m), 708 (w), 699 (w).

HRMS (ESI): m/z calcd. for $\text{C}_{20}\text{H}_{23}\text{FeN}_3^+$ ($[\text{M}]^+$) 361.1241; found: 361.1242.

$[\alpha]_{\text{D}}^{21} = -36.5$ ($c = 0.86$, CHCl_3).

Synthesis of (S)-1-Azido-2-[3-(R)-(N,N-dimethylamino)ethyl]ferrocen (2h)



According to **GP2**, the title compound was prepared from **1h** (0.10 g, 0.26 mmol, 1.0 equiv), *n*-butyllithium (0.12 mL, 0.29 mmol, 1.1 equiv.; 2.4 M in *n*-hexane), and tosyl azide (0.42 mL, 0.31 mmol, 1.2 equiv.; 0.75 M in THF) in anhydrous THF (3 mL). Gravity column chromatography (basic Al₂O₃, activity grade I +5 wt% H₂O; CH₂Cl₂/EtOAc 100:0 to 5:1) gave the title compound **2h** (55 mg, 0.19 mmol, 71%; d.r. = 96:4 [¹H NMR]) as a brown oil.

R_f = 0.50 (SiO₂, CH₂Cl₂/MeOH 9:1, vis. vanillin).

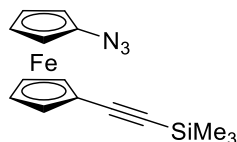
¹H NMR (600 MHz, CDCl₃): δ [ppm] = 4.36 (dd, *J* = 2.6, 1.4 Hz, 1H), 4.23 (s, 5H), 4.04 (t, *J* = 2.6 Hz, 1H), 4.02 (dd, *J* = 2.7, 1.4 Hz, 1H), 3.76 (q, *J* = 6.9 Hz, 1H), 2.10 (s, 6H), 1.44 (d, *J* = 6.9 Hz, 3H).

¹³C{¹H} NMR (151 MHz, CDCl₃): δ [ppm] = 98.0, 81.8, 69.8, 65.2, 63.3, 59.5, 55.3, 40.8, 15.1.

HRMS (ESI): *m/z* calcd. for C₁₄H₁₉FeN₄⁺ ([M+H]⁺) 299.0954; found: 299.0965.

The spectroscopic data are consistent with those reported in the literature.^[11]

Synthesis of 1-azido-1'-(trimethylsilylethynyl)ferrocene (2i)



According to **GP2**, the title compound was prepared from **1i** (100 mg, 0.245 mmol, 1.0 equiv), *n*-butyllithium (99.8 μL, 0.270 mmol, 1.1 equiv; 2.7 M in *n*-hexane), and tosyl azide (118 μL, 0.294 mmol, 1.2 equiv; 2.5 M in THF) in anhydrous THF (3 mL). Gravity column chromatography (basic Al₂O₃, activity grade I +5 wt% H₂O; *n*-pentane) gave the title compound **2i** (63.0 mg, 0.195 mmol, 79%) as an orange oil.

R_f = 0.57 (SiO₂; *n*-pentane/CH₂Cl₂ 9:1; vis. vanillin).

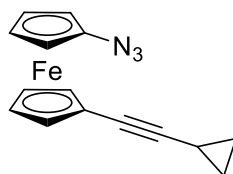
¹H NMR (400 MHz, CDCl₃) δ [ppm] = 4.54 (t, *J* = 1.9 Hz, 2H), 4.26 (dt, *J* = 3.3, 1.9 Hz, 4H), 4.07 (t, *J* = 2.0 Hz, 2H), 0.22 (s, 9H).

¹³C{¹H} NMR (100 MHz, CDCl₃) δ [ppm] = 103.0, 100.3, 92.0, 73.0, 69.8, 66.8, 67.4, 62.3, 0.21.

FT-IR (neat) $\tilde{\nu}$ [cm⁻¹] = 2958 (w), 2148 (m), 2109 (s), 1459 (m), 1369 (w), 1287 (m), 1249 (m), 1163 (w), 1026 (w), 927 (m), 842 (s), 759 (m), 741 (w), 726 (w), 699 (w).

HRMS (ESI-TOF) *m/z* calcd. for C₁₅H₁₈FeN₃Si⁺ ([M+H]⁺) 324.0614; found: 324.0601.

Synthesis of 1-azido-1'-(ethynylcyclopropyl)ferrocene (**2j**)



According to **GP2**, the title compound was prepared from **1j** (76 mg, 0.20 mmol, 1.0 equiv), *n*-butyllithium (90 μ L, 0.22 mmol, 1.1 equiv; 2.4 M in *n*-hexane), and tosyl azide (0.33 mL, 0.24 mmol, 1.2 equiv; 0.75 M in THF) in THF (2.5 mL). Gravity column chromatography (basic Al₂O₃, activity grade I +5 wt% H₂O; *n*-pentane) gave the title compound **2j** (33 mg, 0.11 mmol, 56%) as a brown oil.

R_f = 0.23 (SiO₂; *n*-pentane/CH₂Cl₂ 10:1; vis. vanillin).

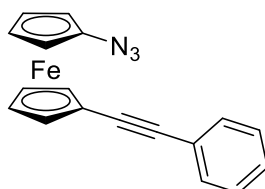
¹H NMR (700 MHz, CDCl₃) δ [ppm] = 4.45 (s, 2H), 4.24 (s, 2H), 4.21 (s, 2H), 4.05 (s, 2H), 1.34 (tt, J = 8.3, 4.8 Hz, 1H), 0.81 (dq, J = 7.2, 4.0 Hz, 2H), 0.76 (dq, J = 7.6, 4.9, 4.3 Hz, 2H).

¹³C{¹H} NMR (176 MHz, CDCl₃) δ [ppm] = 99.9, 90.7, 72.5, 69.3, 68.4, 67.1, 62.0, 8.5, 0.5. One resonance is missing presumably due to solvent overlap.

FT-IR (neat) $\tilde{\nu}$ [cm⁻¹] = 3091 (w), 3009 (w), 2923 (w), 2852 (w), 2442 (w), 2321 (w), 2201 (w), 2105 (s), 2204 (m), 1457 (s), 1370 (m), 1285 (s), 1260 (m), 1223 (w), 1204 (w), 1162 (m), 1116 (w), 1089 (w), 1051 (m), 1024 (s), 966 (w), 918 (m), 897 (s), 808 (s), 768 (w), 741 (m).

HRMS (ESI-TOF) m/z calcd. for C₁₅H₁₃FeN₃H⁺ ([M+H⁺]) 292.0532; found: 292.0544.

Synthesis of 1-azido-1'-phenylferrocene (**2k**)



According to **GP2**, the title compound was prepared from **1k** (41 mg, 0.10 mmol, 1.0 equiv), *n*-butyllithium (44 μ L, 0.11 mmol, 1.1 equiv; 2.5 M in *n*-hexane), and tosyl azide (48 μ L, 0.12 mmol, 1.2 equiv; 2.5 M in THF) in THF (2 mL). Gravity column chromatography (basic Al₂O₃, activity grade I +5 wt% H₂O, *n*-pentane) gave the title compound **2k** (31 mg, 0.095 mmol, 95%) as an orange solid.

R_f = 0.38 (SiO₂; *n*-pentane/CH₂Cl₂ 9:1, vis. vanillin).

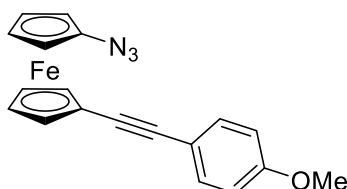
¹H NMR (400 MHz, CDCl₃) δ [ppm] = 7.52 – 7.48 (m, 2H), 7.36 – 7.29 (m, 3H), 4.62 (t, J = 1.9 Hz, 2H), 4.33 (t, J = 1.9 Hz, 2H), 4.31 (t, J = 2.0 Hz, 2H), 4.12 (t, J = 2.0 Hz, 2H).

¹³C{¹H} NMR (100 MHz, CDCl₃) δ [ppm] = 131.6, 128.4, 127.9, 123.9, 100.2, 87.2, 86.9, 77.4, 72.7, 69.9, 67.2, 62.2.

FT-IR (neat) $\tilde{\nu}$ [cm⁻¹] = 3084 (w), 3057 (w), 2442 (w), 2321 (w), 2206 (w), 2106 (s), 2024 (w), 1599 (w), 1571 (w), 1497 (m), 1458 (s), 1442 (m), 1369 (w), 1285 (m), 1223 (w), 1204 (w), 1162 (m), 1070 (w), 1026 (m), 924 (m), 916 (m), 812 (m), 755 (s), 740 (m), 690 (m).

HRMS (ESI-TOF) m/z calcd. for C₁₈H₁₃FeN₃⁺ ([M]⁺) 328.0532; found: 328.0535.

Synthesis of 1-azido-1'-(1-ethynyl-4-methoxybenzene)ferrocene (**2l**)



According to **GP2**, the title compound was prepared from **1l** (87 mg, 0.20 mmol, 1 equiv), *n*-butyllithium (0.18 mL, 0.22 mmol, 1.1 equiv; 1.2 M in *n*-hexane), and tosyl azide (0.32 mL, 0.24 mmol, 1.2 equiv; 0.75 M in THF) in THF (2 mL). Gravity column chromatography (basic Al₂O₃, activity grade I +5 wt% H₂O; *n*-pentane/CH₂Cl₂ 5:1) followed by recrystallization from *n*-hexane at -78 °C gave the title compound **2l** (47 mg, 0.13 mmol, 67%) as an orange solid.

R_f = 0.36 (SiO₂, *n*-pentane/CH₂Cl₂ 4:1; vis. vanillin).

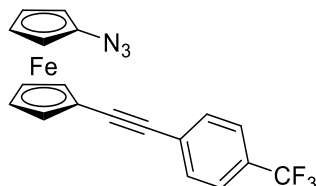
¹H NMR (700 MHz, CDCl₃) δ [ppm] = 7.43 (d, J = 8.8 Hz, 2H), 6.86 (d, J = 8.8 Hz, 2H), 4.59 (t, J = 1.9 Hz, 2H), 4.31 (t, J = 1.8 Hz, 2H), 4.31 – 4.30 (m, 2H), 4.11 (t, J = 2.0 Hz, 2H), 3.82 (s, 3H).

¹³C{¹H} NMR (176 MHz, CDCl₃) δ [ppm] = 159.4, 133.0, 116.0, 114.1, 100.2, 86.8, 85.5, 72.5, 69.7, 67.8, 67.2, 62.1, 55.4.

FT-IR (neat) $\tilde{\nu}$ [cm⁻¹] = 3090 (w), 3001 (w), 2920 (w), 2837 (w), 2441 (w), 2360 (m), 2341 (m), 2203 (w), 2108 (s), 2205 (w), 1718 (w), 1604 (m), 1568 (w), 1513 (m), 1458 (m), 1441 (w), 1370 (w), 1284 (m), 1246 (s), 1164 (m), 1106 (w), 1027 (m), 925 (w), 830 (m), 813 (m), 733 (m), 668 (m).

HRMS (ESI-TOF) m/z calcd. for C₁₉H₁₅FeN₃ONa⁺ ([M+Na]⁺) 380.0457; found: 380.0441.

Synthesis of 1-azido-1'-(1-ethynyl-4-trifluoromethylbenzene)ferrocene (**2m**)



According to **GP2**, the title compound was prepared from **1m** (47 mg, 98 μ mol, 1.0 equiv), *n*-butyllithium (40 μ L, 0.11 mmol, 1.1 equiv; 2.4 M in *n*-hexane), and tosyl azide (0.16 mL, 0.12 mmol, 1.2 equiv; 0.75 M in THF) in THF (1.5 mL). Gravity column chromatography (basic Al₂O₃, activity grade I +5 wt% H₂O, *n*-pentane) gave the title compound **2m** (29 mg, 74 μ mol, 75%) as an orange solid.

$R_f = 0.26$ (SiO₂; *n*-pentane, vis. vanillin).

¹H NMR (700 MHz, CDCl₃) δ [ppm] = 7.58 (s, 4H), 4.64 (t, $J = 1.8$ Hz, 2H), 4.37 (t, $J = 1.8$ Hz, 2H), 4.32 (t, $J = 1.9$ Hz, 2H), 4.13 (t, $J = 1.9$ Hz, 2H).

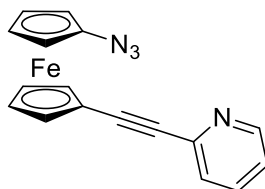
¹³C{¹H} NMR (176 MHz, CDCl₃) δ [ppm] = 131.7, 129.5 (q, $J = 32.4$ Hz), 127.7, 125.4 (d, $J = 3.7$ Hz), 124.2 (q, $J = 272.2$ Hz), 100.3, 90.2, 85.7, 72.9, 70.3, 67.3, 66.4, 62.2.

¹⁹F NMR (565 MHz, CDCl₃) δ [ppm] = -62.6.

FT-IR (neat): $\tilde{\nu}$ [cm⁻¹] = 2961 (w), 2923 (w), 2361 (w), 2205 (w), 2110 (s), 1607 (m), 1460 (m), 1406 (m), 1371 (w), 1321 (s), 1288 (m), 1261 (m), 1161 (s), 1117 (s), 1103 (s), 1065 (s), 1029 (s), 1016 (s), 918 (m), 838 (s), 802 (s), 745 (m).

HRMS (ESI-TOF) m/z calcd. for C₁₉H₁₂F₃FeN₃⁺ ([M]⁺) 395.0333; found: 395.0321.

Synthesis of 1-azido-1'-(ethynylpyridyl)ferrocene (**2n**)



According to **GP2**, the title compound was prepared from **1n** (70 mg, 0.17 mmol, 1.0 equiv), *n*-butyllithium (75 μ L, 0.19 mmol, 1.1 equiv; 2.4 M in *n*-hexane), and tosyl azide (0.27 mL, 0.20 mmol, 1.2 equiv; 0.75 M in THF) in THF (3.5 mL). Gravity column chromatography (basic Al₂O₃, activity grade I +5 wt% H₂O; *n*-hexane/EtOAc 10:1) gave the title compound **2n** (42 mg, 0.13 mmol, 76%) without further purification as a brown oil.

$R_f = 0.27$ (SiO₂; *n*-hexane/EtOAc 4:1; vis. vanillin).

¹H NMR (700 MHz, CDCl₃) δ [ppm] = 8.58 (dt, $J = 4.7, 1.5$ Hz, 1H), 7.64 (td, $J = 7.7, 1.8$ Hz, 1H), 7.46 (dt, $J = 7.8, 1.1$ Hz, 1H), 7.21 (ddd, $J = 7.6, 4.9, 1.2$ Hz, 1H), 4.68 (t, $J = 1.9$ Hz, 2H), 4.37 (t, $J = 1.9$ Hz, 2H), 4.32 (t, $J = 2.0$ Hz, 2H), 4.13 (t, $J = 2.0$, 2H).

¹³C{¹H} NMR (176 MHz, CDCl₃) δ [ppm] = 150.1, 144.0, 136.2, 126.9, 122.4, 100.4, 88.1, 86.4, 73.1, 70.4, 67.6, 65.7, 62.2.

FT-IR (neat) $\tilde{\nu}$ [cm⁻¹] = 3078 (w), 2920 (w), 2849 (w), 2454 (w), 2206 (m), 2106 (s), 2027 (m), 1578 (s), 1560 (m), 1477 (m), 1460 (s), 1423 (m), 1366 (w), 1292 (s), 1227 (w), 1174 (w), 1164 (w), 1153 (w), 1091 (w), 1024 (s), 987 (m), 918 (m), 807 (s), 772 (s), 736 (s).

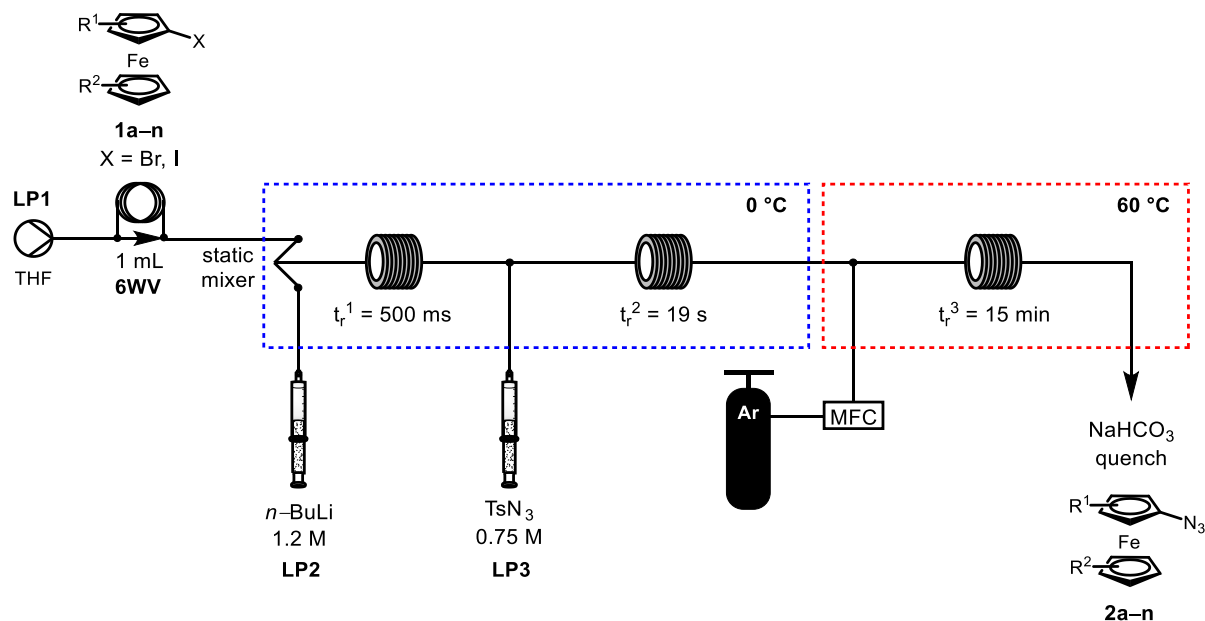
HRMS (ESI-TOF) m/z calcd. for C₁₇H₁₂FeN₄K⁺ ([M+K]⁺) 367.0043; found: 367.0061.

2.5. Synthesis of Ferrocenyl Azides in Flow

Preparation of a stock solution of *n*-butyllithium in *n*-hexane

In a dry Schlenk tube, a stock solution of *n*-butyllithium in *n*-hexane with a concentration of 1.2 M was prepared. This solution was stored in the dark at 8 °C and could be used for several months without changes in yield. However, it is recommended to titrate this stock solution from time to time.

General Procedure 3 (GP3) for the synthesis of ferrocenyl azides in flow



Syringe pumps (**LP2**, **LP3**) equipped with gas-tight 10 mL glass-syringes were used to pump solutions of *n*-butyllithium (1.2 M *n*-hexane) and tosyl azide (0.75 M in THF). Both solutions were passed through precooling loops (FEP tube, outer diameter 1/16", inner diameter 1/32", V = 0.15 mL) before mixing. A HPLC pump (**LP1**) to feed the solvent was connected to a HPLC injection valve (**6WV**) equipped with a 1 mL sample loop. The liquid supply was passed through a pre-cooled loop (FEP tube, outer diameter 1/16", inner diameter 1/32", V = 0.15 mL) and then merged in a static mixer (internal volume: 20 μL) with a solution of *n*-butyllithium (1.2 M *n*-hexane). The resulting reaction stream was pumped through tube **reactor1** (stainless steel capillary, inner diameter 250 μm, V = 20 μL) and then merged in a stainless steel T-mixer with a solution of tosyl azide. **Reactor1**, **reactor2**, the mixing units, and the pre-cooled loops were cooled to 0 °C by immersion into an ice bath.

The reaction stream was mixed in a T-mixer with argon provided by a mass flow controller (MFC) resulting in a segmented flow pattern. This stream was pumped through tube **reactor3** (PTFE tube, inner diameter 1/8", V = 40 mL) heated to 60 °C in a water bath. The resulting triphasic flow regime was collected in a flask containing NaHCO₃ (sat. aq., 50 mL).

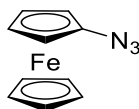
The HPLC pump and the reactor were washed with anhydrous THF for 2 residence times by pumping THF with the HPLC pump and feeding argon using the MFC ($v_{\text{argon}} = 0.2 \text{ mL/min}$) until a steady state was achieved. A solution of the ferrocenyl halide (**1a–1n**, 0.2 M in THF) was loaded on the HPLC injection valve. The solutions of *n*-butyllithium ($v_{n\text{-BuLi}} = 0.4 \text{ mL/min}$) and tosyl azide ($v_{\text{TsN}_3} = 0.8 \text{ mL/min}$) were pumped at the given flow rate for 15–20 s. Then, the solution of the ferrocenyl halide (**1a–1n**) was injected ($v_{\text{FcX}} = 2.0 \text{ mL/min}$) into the system by switching the HPLC valve to the “inject” position. The collected reaction mixture was diluted with EtOAc (50 mL). The aqueous layer was separated and extracted with EtOAc (2×50 mL). The combined organic layers were dried (Na_2SO_4), filtered, and concentrated under reduced pressure. The corresponding ferrocenyl azide (**2a–2n**) was isolated by gravity column chromatography.

Note 1: Drying with MgSO_4 instead of Na_2SO_4 gave lower yields.

Note 2: For column chromatography, the crude product was suspended in a small amount of the eluent and the resulting suspension was directly loaded onto the column using a Pasteur pipette.

Note 3: In some cases, flash column chromatography was possible, but in general, gravity column chromatography gave better separations.

Synthesis of azidoferrocene (**2a**)



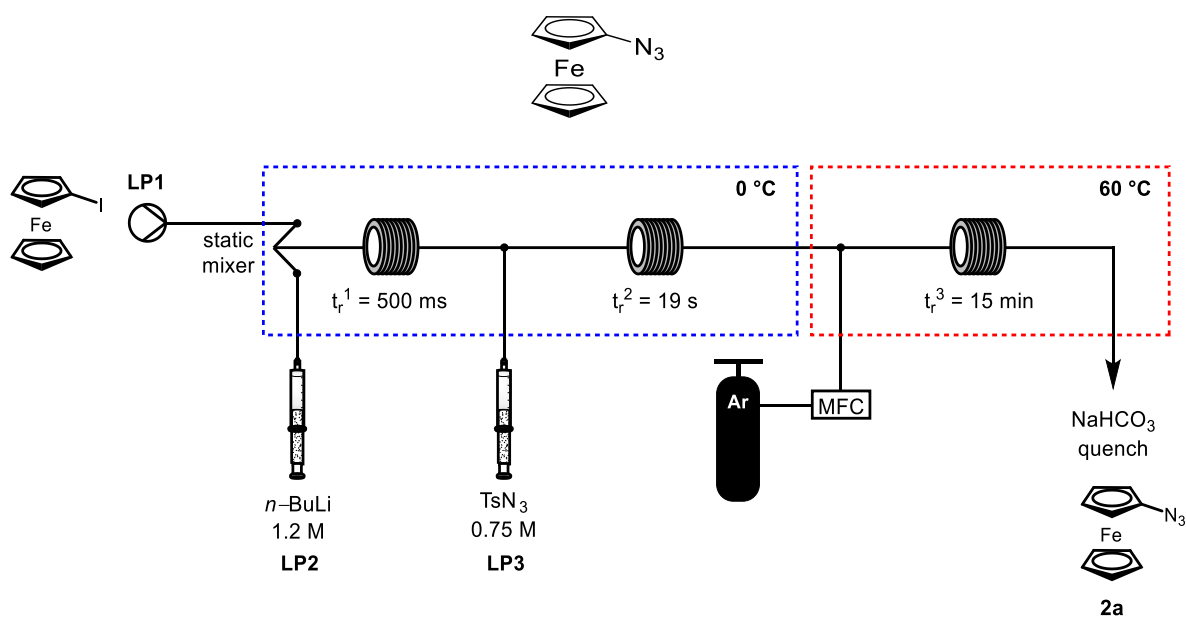
According to **GP3**, the title compound was prepared from **1a** (62 mg, 0.20 mmol). Gravity column chromatography (basic Al_2O_3 , activity grade I +5 wt% H_2O ; *n*-pentane) gave the title compound **2a** (37 mg, 0.16 mmol, 82%) as a red oil that solidified upon standing at $-18 \text{ }^\circ\text{C}$.

$R_f = 0.41$ (SiO_2 , *n*-hexane, vis. vanillin).

$^1\text{H NMR}$ (700 MHz, CDCl_3) δ [ppm] = 4.28 (s, 5H), 4.26 (t, $J = 1.9 \text{ Hz}$, 2H), 4.04 (t, $J = 1.9 \text{ Hz}$, 2H).

$^{13}\text{C}\{^1\text{H}\}$ NMR (176 MHz, CDCl_3) δ [ppm] = 99.3, 69.3, 65.5, 60.7.

Synthesis of azidoferrocene (**2a**) on gram scale



Syringe pumps (**LP2**, **LP3**) equipped with gas-tight 10 mL glass-syringes were used to pump solutions of *n*-butyllithium (1.2 M *n*-hexane) and tosyl azide (0.75 M in THF). Both solutions were passed through precooling loops (FEP tube, outer diameter 1/16", inner diameter 1/32", V = 0.15 mL) before mixing. A solution of iodoferrocene **1a** (0.2 M in THF) was provided by a HPLC pump (**LP1**) and was passed through a pre-cooled loop (FEP tube, outer diameter 1/16", inner diameter 1/32", V = 0.15 mL) and then merged in a static mixer (internal volume: 20 μ L) with a solution of *n*-butyllithium (1.2 M *n*-hexane). The resulting reaction stream was pumped through tube **reactor1** (stainless steel capillary, inner diameter 250 μ m, V = 20 μ L) and then merged in a stainless steel T-mixer with a solution of tosyl azide. **Reactor1**, **reactor2**, the mixing units, and the pre-cooled loops were cooled to 0 °C by immersion into an ice bath.

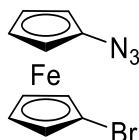
The reaction stream was mixed in a T-mixer with argon provided by a mass flow controller (MFC) resulting in a segmented flow pattern. This stream was pumped through tube **reactor3** (PTFE tube, inner diameter 1/8", V = 40 mL) heated to 60 °C in a water bath. The resulting triphasic flow regime was collected in a flask containing NaHCO₃ (sat. aq., 50 mL).

The HPLC pump and the reactor were washed with anhydrous THF for 2 residence times by pumping THF with the HPLC pump and feeding argon using the MFC ($v_{\text{argon}} = 0.2$ mL/min) until a steady state was achieved. The solutions of *n*-butyllithium ($v_{n\text{-BuLi}} = 0.4$ mL/min) and tosyl azide ($v_{\text{TsN}_3} = 0.8$ mL/min) were pumped at the given flow rate for 15–20 s. Then, a solution of iodoferrocene **1a** was pumped by the HPLC pump into the system. After a steady state has been reached, the reaction mixture was collected for 15 min. Then, the reaction mixture was diluted with EtOAc (50 mL). The aqueous layer was separated and extracted with EtOAc (2 \times 50 mL). The combined organic layers were dried (Na₂SO₄), filtered, and concentrated under reduced pressure. Gravity column chromatography

(basic Al₂O₃, activity grade I +5 wt% H₂O; *n*-pentane) gave the title compound **2a** (37 mg, 0.16 mmol, 82%) as a red oil that solidified upon standing at -18 °C. Gravity column chromatography (basic Al₂O₃, activity grade I +5 wt% H₂O; *n*-pentane) gave the title compound **2a** (0.96 g, 4.2 mmol, 69%) as a red oil that solidified upon standing at -18 °C.

The spectroscopic data are consistent with those reported above.

Synthesis of 1-azido-1'-bromoferrocene (**2b**)



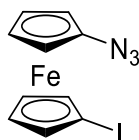
According to **GP3**, the title compound was prepared from **1b** (83 mg, 0.24 mmol). Gravity column chromatography (basic Al₂O₃, activity grade I +5 wt% H₂O; *n*-pentane) gave the title compound **2b** (59 mg, 0.19 mmol, 80%) as a red oil that solidified upon standing.

*R*_f = 0.32 (SiO₂, *n*-pentane, vis. vanillin).

¹H NMR (700 MHz, CDCl₃) δ [ppm] = 4.52 (t, *J* = 1.9 Hz, 2H), 4.27 (t, *J* = 1.9 Hz, 2H), 4.20 (t, *J* = 1.9 Hz, 2H), 4.12 (t, *J* = 1.9 Hz, 2H).

¹³C{¹H} NMR (176 MHz, CDCl₃) δ [ppm] = 100.7, 78.7, 71.5, 68.3, 67.9, 62.8.

Synthesis of 1-azido-1'-iodoferrocene (**2c**)



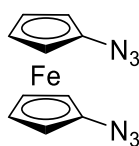
According to **GP3**, the title compound was prepared from **1c** (105 mg, 0.240 mmol). Gravity column chromatography (basic Al₂O₃, activity grade I +5 wt% H₂O; *n*-pentane) gave the title compound **2c** (45.9 mg, 0.130 mmol, 54%) as a brown oil.

*R*_f = 0.39 (SiO₂, *n*-pentane, vis. vanillin).

¹H NMR (600 MHz, CDCl₃) δ [ppm] = 4.51 (t, *J* = 1.8 Hz, 2H), 4.25 (t, *J* = 1.8 Hz, 2H), 4.22 (t, *J* = 2.0 Hz, 2H), 4.08 (t, *J* = 2.0 Hz, 2H).

¹³C{¹H} NMR (151 MHz, CDCl) δ [ppm] = 100.6, 75.9, 70.0, 68.5, 63.3, 40.9.

Synthesis of 1,1'-diazidoferrocene (**2d**)



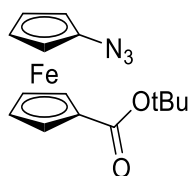
According to **GP3**, the title compound was prepared from **1b** (34 mg, 0.10 mmol). Gravity column chromatography (basic Al₂O₃, activity grade I +5 wt% H₂O; *n*-pentane) gave the title compound **2d** (20 mg, 0.075 mmol, 75%) as a brown oil.

*R*_f = 0.29 (SiO₂, *n*-hexane, vis. vanillin).

¹H NMR (600 MHz, CDCl₃) δ [ppm] = 4.35 (s, 4H), 4.15 (s, 4H).

¹³C{¹H} NMR (151 MHz, CDCl₃) δ [ppm] = 100.4, 66.5, 61.6.

Synthesis of 1-azido-1'-ferrocenylcarboxylic acid *tert*-butyl ester (**2e**)



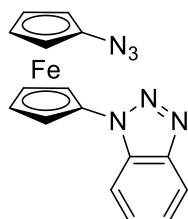
According to **GP3**, the title compound was prepared from **1e** (73 mg, 0.20 mmol). Gravity column chromatography (basic Al₂O₃, activity grade I + 5 wt% H₂O; *n*-pentane/Et₂O 20:1) gave the title compound **2e** (47 mg, 0.14 mmol, 71%) as a red oil.

*R*_f = 0.40 (SiO₂, *n*-pentane/Et₂O= 20:1, vis. vanillin).

¹H NMR (700 MHz, CDCl₃) δ [ppm] = 4.84 (t, *J* = 1.9 Hz, 2H), 4.44 (t, *J* = 1.9 Hz, 2H), 4.26 (t, *J* = 1.9 Hz, 2H), 4.08 (t, *J* = 1.9 Hz, 2H), 1.57 (s, 9H).

¹³C{¹H} NMR (176 MHz, CDCl₃) δ [ppm] = 170.3, 100.6, 80.6, 75.0, 72.1, 71.2, 67.1, 61.8, 28.4.

Synthesis of 1-azido-1'-(1*H*-benzo[*d*][1,2,3]triazole)ferrocene (**2f**)



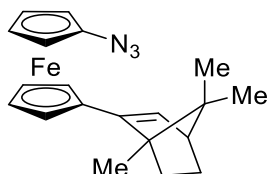
According to **GP3**, the title compound was prepared from **1f** (76 mg, 0.20 mmol). Gravity column chromatography (basic Al₂O₃, activity grade I +5 wt% H₂O; *n*-hexane/EtOAc 4:1) gave the title compound **2f** (44 mg, 0.13 mmol, 64%) as a brown solid.

*R*_f = 0.30 (SiO₂, *n*-hexane/EtOAc 4:1).

^1H NMR (600 MHz, CDCl_3) δ [ppm] = 8.12 (d, J = 8.3 Hz, 1H), 7.82 (d, J = 8.4 Hz, 1H), 7.57 (t, J = 7.7 Hz, 1H), 7.42 (t, J = 7.8 Hz, 1H), 5.08 (s, 2H), 4.48 (s, 2H), 4.34 (s, 2H), 4.15 (s, 2H).

$^{13}\text{C}\{^1\text{H}\}$ NMR (151 MHz, CDCl_3) δ [ppm] = 146.5, 133.0, 128.0, 124.4, 120.5, 110.7, 100.9, 94.7, 67.8, 67.4, 63.6, 62.1.

Synthesis of 1-azido-1'-[(1S, 4S)-1,7,7-trimethylbicyclo[2.2.1]hept-2-enyl]ferrocene (2g)



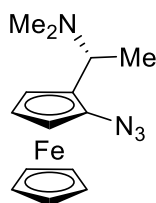
According to **GP3**, the title compound was prepared from **1g** (80 mg, 0.20 mmol). Gravity column chromatography (basic Al_2O_3 , activity grade I +5 wt% H_2O ; *n*-hexane) gave the title compound **2g** (48 mg, 0.13 mmol, 66%) as an orange oil.

R_f = 0.42 (SiO_2 ; *n*-pentane; vis. vanillin).

^1H NMR (600 MHz, CDCl_3) δ [ppm] = 6.04 (d, J = 3.3 Hz, 1H), 4.39 (d, J = 14.3 Hz, 2H), 4.31 (s, 2H), 4.18 (d, J = 12.4 Hz, 2H), 4.01 (s, 2H), 2.30 (t, J = 3.3 Hz, 1H), 1.88 (td, J = 8.6, 3.8 Hz, 1H), 1.58 (ddd, J = 11.9, 8.4, 3.6 Hz, 1H), 1.24 (s, 3H), 1.17 (ddd, J = 11.7, 8.9, 3.5 Hz, 1H), 1.01 (ddd, J = 12.3, 9.1, 3.4 Hz, 1H), 0.89 (s, 3H), 0.80 (s, 3H).

$^{13}\text{C}\{^1\text{H}\}$ NMR (151 MHz, CDCl_3) δ [ppm] = 144.9, 130.7, 99.5, 84.5, 69.2, 69.1, 67.9, 66.9, 66.6, 61.6, 61.5, 56.9, 55.2, 51.7, 32.2, 25.8, 20.1, 19.8, 13.3. One resonance is missing due solvent overlap.

Synthesis of (S)-1-Azido-2-[3-(R)-(N,N-dimethylamino)ethyl]ferrocen (2h)



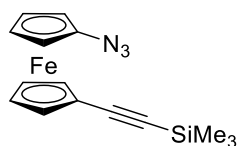
According to **GP3**, the title compound was prepared from **1h** (76 mg, 0.20 mmol). Gravity column chromatography (basic Al_2O_3 , activity grade I +5 wt% H_2O ; $\text{CH}_2\text{Cl}_2/\text{EtOAc}$ 100:0 to 5:1) gave the title compound **2h** (36 mg, 0.12 mmol, 61%; d.r. = 96:4 [^1H NMR]) as a brown oil.

R_f = 0.50 (SiO_2 , $\text{CH}_2\text{Cl}_2/\text{MeOH}$ 9:1, vis. vanillin).

^1H NMR (500 MHz, CDCl_3) δ [ppm] = 4.36 (dd, J = 2.6, 1.5 Hz, 1H), 4.23 (s, 5H), 4.04 (t, J = 2.6 Hz, 1H), 4.02 (dd, J = 2.8, 1.4 Hz, 1H), 3.75 (q, J = 6.9 Hz, 1H), 2.09 (s, 6H), 1.44 (d, J = 6.9 Hz, 3H).

$^{13}\text{C}\{^1\text{H}\}$ NMR (126 MHz, CDCl_3) δ [ppm] = 97.9, 81.8, 69.8, 65.2, 63.3, 59.5, 55.2, 40.8, 15.2.

Synthesis of 1-azido-1'-(trimethylsilylethynyl)ferrocene (**2i**)



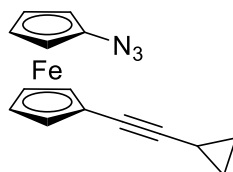
According to **GP3**, the title compound was prepared from **1i** (82 mg, 0.20 mmol). Gravity column chromatography (basic Al₂O₃, activity grade I +5 wt% H₂O; *n*-pentane) gave the title compound **2i** (50 mg, 0.15 mmol, 77%) as a red oil.

*R*_f = 0.57 (SiO₂; *n*-pentane/CH₂Cl₂ 9:1; vis. vanillin).

¹H NMR (700 MHz, CDCl₃) δ [ppm] = 4.54 (t, *J* = 1.9 Hz, 2H), 4.26 (t, *J* = 1.9 Hz, 2H), 4.25 (t, *J* = 1.9 Hz, 2H), 4.07 (t, *J* = 2.0 Hz, 2H), 0.22 (s, 9H).

¹³C{¹H} NMR (176 MHz, CDCl₃) δ [ppm] = 103.0, 100.3, 92.0, 73.0, 69.8, 67.4, 66.9, 62.4, 0.22.

Synthesis of 1-azido-1'-(ethinylcyclopropyl)ferrocene (**2j**)



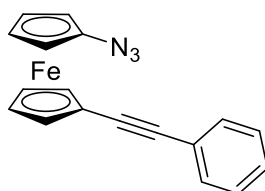
According to **GP3**, the title compound was prepared from **1j** (75mg, 0.20 mmol). Gravity column chromatography (basic Al₂O₃, activity grade I +5 wt% H₂O; *n*-pentane) gave the title compound **2j** (40 mg, 0.14 mmol, 69%) as a red oil.

*R*_f = 0.23 (SiO₂; *n*-pentane/CH₂Cl₂ 10:1; vis. vanillin).

¹H NMR (600 MHz, CDCl₃) δ [ppm] = 4.45 (t, *J* = 1.9 Hz, 2H), 4.24 (t, *J* = 1.9 Hz, 2H), 4.21 (t, *J* = 1.9 Hz, 2H), 4.05 (t, *J* = 2.0 Hz, 2H), 1.34 (tt, *J* = 8.2, 5.0 Hz, 1H), 0.83 – 0.79 (m, 2H), 0.77 – 0.74 (m, 2H).

¹³C{¹H} NMR (151 MHz, CDCl₃) δ [ppm] = 99.9, 90.7, 72.5, 69.2, 68.4, 67.0, 62.0, 8.5, 0.5. One resonance is missing presumably due to solvent overlap.

Synthesis of 1-azido-1'-phenylferrocene (**2k**)



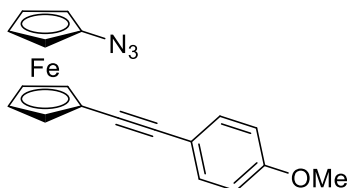
According to **GP3**, the title compound was prepared from **1k** (82 mg, 0.20 mmol). Gravity column chromatography (basic Al₂O₃, activity grade I +5 wt% H₂O, *n*-pentane) gave the title compound **2k** (51 mg, 0.16 mmol, 78%) as an orange solid.

$R_f = 0.38$ (SiO₂; *n*-pentane/CH₂Cl₂ 9:1, vis. vanillin).

¹H NMR (700 MHz, CDCl₃) δ [ppm] = 7.51–7.47 (m, 2H), 7.34–7.29 (m, 3H), 4.62 (t, $J = 1.9$ Hz, 2H), 4.33 (t, $J = 1.9$ Hz, 2H), 4.31 (t, $J = 2.0$ Hz, 2H), 4.12 (t, $J = 1.9$ Hz, 2H).

¹³C{¹H} NMR (176 MHz, CDCl₃) δ [ppm] = 131.6, 128.4, 127.9, 123.9, 100.2, 87.2, 86.9, 72.7, 69.9, 67.3, 62.2. One resonance is missing due solvent overlap.

Synthesis of 1-azido-1'-(1-ethynyl-4-methoxybenzene)ferrocene (**2l**)



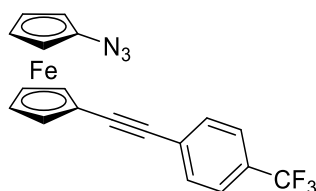
According to **GP3**, the title compound was prepared from **1k** (89 mg, 0.20 mmol). Gravity column chromatography (basic Al₂O₃, activity grade I +5 wt% H₂O; *n*-pentane/CH₂Cl₂ 10:1) gave the title compound **2l** (53 mg, 0.15 mmol, 74%) as an orange solid.

$R_f = 0.36$ (SiO₂, *n*-pentane/CH₂Cl₂ 4:1; vis. vanillin).

¹H NMR (700 MHz, CDCl₃) δ [ppm] = 7.43 (d, $J = 8.7$ Hz, 2H), 6.86 (d, $J = 8.7$ Hz, 2H), 4.59 (t, $J = 1.9$ Hz, 2H), 4.31 (dt, $J = 6.0, 1.9$ Hz, 4H), 4.11 (t, $J = 2.0$ Hz, 2H), 3.82 (s, 3H).

¹³C{¹H} NMR (176 MHz, CDCl₃) δ [ppm] = 159.4, 133.0, 116.0, 114.1, 100.2, 86.8, 85.5, 72.5, 69.7, 67.8, 67.2, 62.2, 55.4.

Synthesis of 1-azido-1'-(1-ethynyl-4-trifluoromethylbenzene)ferrocene (**2m**)



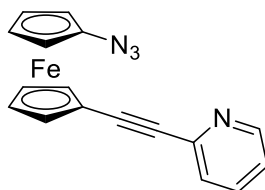
According to **GP3**, the title compound was prepared from **1m** (96 mg, 0.20 mmol). Gravity column chromatography (basic Al₂O₃, activity grade I +5 wt% H₂O, *n*-pentane) gave the title compound **2m** (55 mg, 0.14 mmol, 69%) as an orange solid.

*R*_f = 0.26 (SiO₂; *n*-pentane, vis. vanillin).

¹H NMR (600 MHz, CDCl₃) δ [ppm] = 7.58 (s, 4H), 4.64 (t, *J* = 1.9 Hz, 2H), 4.37 (t, *J* = 1.9, 2H), 4.32 (t, *J* = 2.0 Hz, 2H), 4.13 (t, *J* = 2.0 Hz, 2H).

¹³C{¹H} NMR (151 MHz, CDCl₃) δ [ppm] = 131.7, 129.6, 129.4, 127.7, 125.4, 100.3, 90.2, 85.7, 72.9, 70.3, 67.3, 66.4, 62.2. Due to poor resolution of the spectrum, the C-F couplings could not be detected.

Synthesis of 1-azido-1'-(pyridylethynyl)ferrocene (**2n**)



According to **GP3**, the title compound was prepared from **1n** (82 mg, 0.20 mmol). Gravity column chromatography (basic Al₂O₃, activity grade I +5 wt% H₂O; *n*-hexane/EtOAc 10:1) gave the title compound **2n** (40 mg, 0.12 mmol, 62%) as a brown oil.

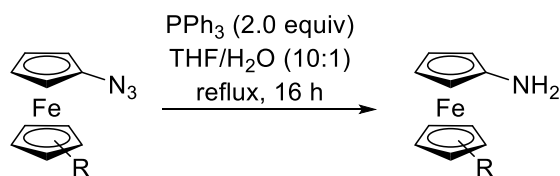
*R*_f = 0.27 (SiO₂; *n*-hexane/EtOAc 4:1; vis. vanillin).

¹H NMR (600 MHz, CDCl₃) δ [ppm] = 8.58 (d, *J* = 4.8 Hz, 1H), 7.63 (t, *J* = 7.6 Hz, 1H), 7.46 (d, *J* = 7.9 Hz, 1H), 7.20 (dd, *J* = 7.6, 4.8 Hz, 1H), 4.68 (s, 2H), 4.37 (s, 2H), 4.32 (s, 2H), 4.13 (s, 2H).

¹³C{¹H} NMR (151 MHz, CDCl₃) δ [ppm] = 150.1, 143.9, 136.2, 126.9, 122.4, 100.4, 88.1, 86.4, 73.1, 70.4, 67.5, 65.7, 62.2.

2.6. Synthesis of Ferrocenyl Amines

General Procedure 5 (GP5) for the Staudinger reduction of ferrocenyl azides

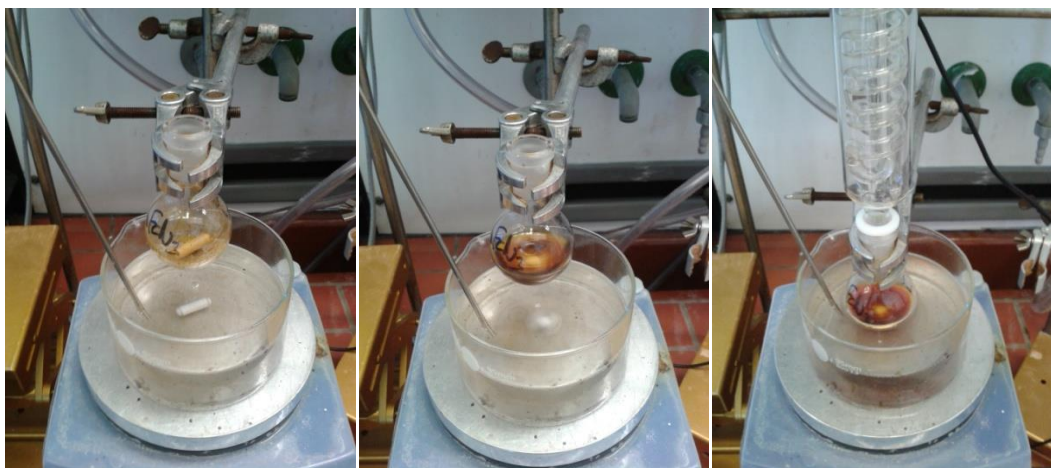


A round bottom flask was charged with ferrocenyl azide (1.0 equiv). THF (10 mL/mmol) and H₂O (1 mL/mmol) were added. To the resulting solution, powdered triphenylphosphine (2.0 equiv) was added in one portion and the mixture was stirred at rt for 10 min. Then, the mixture was heated to reflux for 16 h using a reflux condenser. After cooling to rt, the mixture was concentrated under reduced pressure. The residue was dissolved in CH₂Cl₂ and loaded onto Celite[®]. Flash column chromatography gave the corresponding amine.

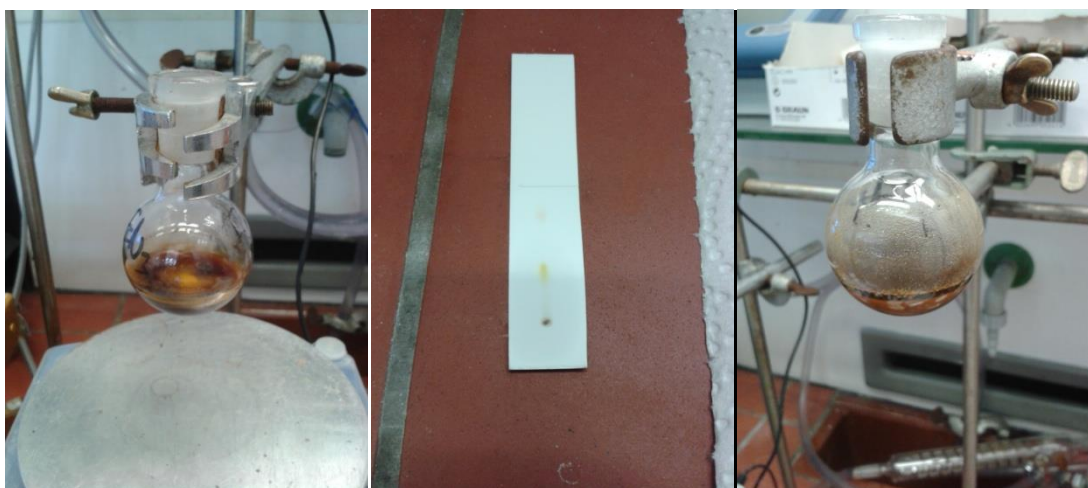
Note 1: Ferrocenyl amines decompose slowly in contact with air and should be stored in the dark under argon at 8 °C.

Note 2: CDCl₃ was neutralized by passing it through a small pad of Na₂CO₃ prior use.

Graphical Guide for the Synthesis of Ferrocenyl Amines



Left: Round bottom flask with ferrocenyl azide. Center: Solution of ferrocenyl azide before the addition of triphenyl phosphine. Right: Reaction mixture after addition of triphenyl phosphine.

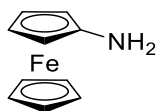


Left: Reaction mixture after refluxing for 16 h. Center: TLC of the crude product. Right: Crude product after addition of Celite®.



Left: Flash column chromatography of the crude product. Right: Pure product.

Synthesis of aminoferrocene (5a)



According to **GP5**, the title compound was prepared from **2a** (175 mg, 771 μmol , 1.0 equiv) and triphenylphosphine (303 mg, 1.16 mmol, 1.5 equiv) in THF (5 mL) and H₂O (0.5 mL). Flash column chromatography (SiO₂; *n*-hexane/EtOAc 1:1) gave the title compound **5a** (131 mg, 651 μmol , 85%) as a brown solid.

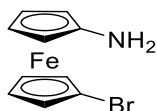
R_f = 0.42 (SiO₂; *n*-hexane /EtOAc 1:1; vis. vanillin).

¹H NMR (700 MHz, CDCl₃) δ [ppm] = 4.10 (s, 5H), 4.00 (s, 2H), 3.85 (s, 2H), 2.59 (s, 2H).

¹³C{¹H} NMR (176 MHz, CDCl₃) δ [ppm] = 105.5, 69.0, 63.6, 58.0.

The spectroscopic data are consistent with those reported in the literature.^[13]

Synthesis of 1-amino-1'-bromoferrocene (5b)



According to **GP5**, the title compound was prepared from **2b** (100 mg, 0.327 mmol, 1.0 equiv) and triphenylphosphine (129 mg, 0.490 mmol, 1.5 equiv) in THF (7 mL) and H₂O (0.7 mL). Flash column chromatography (SiO₂; *n*-hexane/EtOAc 3:2) gave the title compound **5b** (83.0 mg, 0.297 mmol, 91%) as a yellow solid.

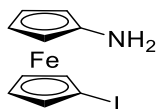
R_f = 0.51 (SiO₂; *n*-hexane/EtOAc 3:2; vis. vanillin).

¹H NMR (700 MHz, C₆D₆) δ [ppm] = 4.13 (s, 2H), 3.72 (s, 2H), 3.69 (s, 2H), 3.59 (s, 2H), 2.09 (s, 2H).

¹³C{¹H} NMR (176 MHz, C₆D₆) δ [ppm] = 108.0, 79.9, 71.1, 67.6, 65.8, 60.1.

The spectroscopic data are consistent with those reported in the literature.^[14]

Synthesis of 1-amino-1'-iodoferrocene (5c)



According to **GP5**, the title compound was prepared from **2c** (50 mg, 0.14 mmol, 1.0 equiv) and triphenylphosphine (56 mg, 0.21 mmol, 1.5 equiv) in THF (2 mL) and H₂O (0.2 mL). MPLC (SiO₂; cyclohexane/EtOAc 100:0 to 70:30 to 80:20) gave the title compound **5c** (43 mg, 0.13 mmol, 93%) as a yellow solid.

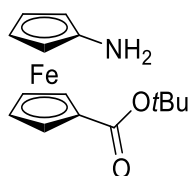
$R_f = 0.45$ (SiO₂; *n*-hexane/EtOAc 2:1; vis. vanillin).

¹H NMR (500 MHz, CDCl₃) δ [ppm] = 4.31 (t, $J = 1.9$ Hz, 2H), 4.08 (t, $J = 1.8$ Hz, 2H), 3.91 (t, $J = 1.9$ Hz, 2H), 3.87 (t, $J = 1.9$ Hz, 2H), 2.72 (s, 2H).

¹³C{¹H} NMR (126 MHz, CDCl₃) δ [ppm] = 106.7, 75.3, 69.0, 66.1, 60.7, 44.8.

HRMS (ESI): m/z calcd. for C₁₀H₁₀FeIN ([M]⁺) 326.9207; found: 326.9204.

Synthesis of 1-amino-1'-ferrocenylcarboxylic acid *tert*-butyl ester (**5d**)



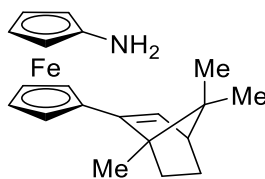
According to **GP5**, the title compound was prepared from **2e** (150 mg, 458 μ mol, 1.0 equiv) and triphenylphosphine (180 mg, 688 μ mol, 1.5 equiv) in THF (3 mL) and H₂O (0.3 mL). MPLC (cyclohexane/EtOAc 100:0 to 70:30) gave the title compound **5d** (130 mg, 432 μ mol, 94%) as a red oil. $R_f = 0.29$ (SiO₂; *n*-hexane/EtOAc 3:1; vis. vanillin).

¹H NMR (500 MHz, CDCl₃) δ [ppm] = 4.66 (t, $J = 1.9$ Hz, 2H), 4.29 (t, $J = 1.9$ Hz, 2H), 3.96 (t, $J = 1.9$ Hz, 2H), 3.87 (t, $J = 1.9$ Hz, 2H), 2.65 (s, 2H), 1.55 (s, 9H).

¹³C{¹H} NMR (126 MHz, CDCl₃) δ [ppm] = 170.7, 106.6, 80.0, 74.1, 71.6, 71.0, 65.1, 59.6, 28.6.

HRMS (ESI-TOF) m/z calcd. for C₁₉H₁₅F₃FeN⁺ ([M+H]⁺) 370.0501; found: 370.0519.

Synthesis of 1-amino-1'-[(1*S*, 4*S*)-1,7,7-trimethylbicyclo[2.2.1]hept-2-enyl]ferrocene (**5e**)



According to **GP5**, the title compound was prepared from **2g** (50 mg, 0.14 mmol, 1.0 equiv) and triphenylphosphine (54 mg, 0.21 mmol, 1.5 equiv) in THF (5 mL) and H₂O (0.5 mL). MPLC (SiO₂; cyclohexane/EtOAc 100:0 to 70:30) gave the title compound **5e** (39 mg, 0.12 mmol, 84%) as an orange solid.

$R_f = 0.31$ (SiO₂; *n*-hexane/EtOAc 10:3; vis. vanillin).

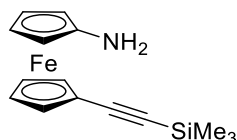
¹H NMR (600 MHz, CDCl₃) δ [ppm] = 5.95 (d, $J = 3.2$ Hz, 1H), 4.21 (s, 2H), 4.12 (q, $J = 2.3$ Hz, 2H), 3.92 (d, $J = 10.6$ Hz, 2H), 3.83 (s, 2H), 2.55 (s, 2H), 2.29 (t, $J = 3.5$ Hz, 1H), 1.88 (ddd, $J = 12.2, 8.5, 3.8$ Hz, 1H), 1.57 (ddd, $J = 12.0, 8.6, 3.6$ Hz, 1H), 1.25 (s, 3H), 1.17 (ddd, $J = 12.2, 9.1, 3.7$ Hz, 1H), 1.00 (ddd, $J = 12.3, 9.1, 3.5$ Hz, 1H), 0.90 (s, 3H), 0.80 (s, 3H).

$^{13}\text{C}\{^1\text{H}\}$ NMR (151 MHz, CDCl_3) δ [ppm] = 145.7, 129.3, 105.5, 83.0, 69.2, 67.7, 66.8, 64.8, 59.7, 56.8, 55.2, 51.6, 32.2, 29.8, 26.0, 20.2, 19.8, 13.4.

HRMS (ESI-TOF) m/z calcd. for $\text{C}_{20}\text{H}_{25}\text{FeN}^+$ ($[\text{M}]^+$) 335.1336; found: 335.1339.

$[\alpha]_{\text{D}}^{24} = -9.0$ ($c = 1.00$, CHCl_3).

Synthesis of 1-amino-1'-(trimethylsilylethynyl)ferrocene (**5f**)



According to **GP5**, the title compound was prepared from **2i** (20 mg, 0.062 mmol, 1.0 equiv) and triphenylphosphine (49 mg, 0.19 mmol, 3.0 equiv) in THF (1.5 mL) and H_2O (0.15 mL). Flash column chromatography (SiO_2 ; n -pentane/EtOAc/ Et_3N 150:10:1) gave the title compound **5f** (14 mg, 0.047 mmol, 76%) as a dark yellow solid.

$R_f = 0.31$ (SiO_2 ; n -pentane/EtOAc/ Et_3N 90:10:1; vis. vanillin).

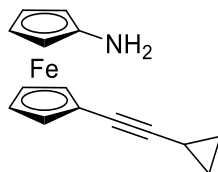
^1H NMR (400 MHz, CDCl_3) δ [ppm] = 4.38 (t, $J = 1.9$ Hz, 2H), 4.14 (t, $J = 1.9$ Hz, 2H), 3.93 (t, $J = 1.9$ Hz, 2H), 3.87 (t, $J = 1.9$ Hz, 2H), 2.74 (s, 2H), 0.22 (s, 9H).

$^{13}\text{C}\{^1\text{H}\}$ NMR (100 MHz, CDCl_3) δ [ppm] = 104.1, 104.0, 91.2, 72.7, 69.1, 66.0, 65.4, 60.1, 0.3.

HRMS (ESI): m/z calcd. for $\text{C}_{15}\text{H}_{19}\text{FeNSi}$ ($[\text{M}]^+$) 297.0636; found: 297.0637.

Note: For TLC and column chromatography, the silica was deactivated prior to use with the stated eluent containing Et_3N .

Synthesis of 1-amino-1'-(ethynylcyclopropyl)ferrocene (**5g**)



According to **GP5**, the title compound was prepared from **2j** (30 mg, 0.10 mmol, 1.0 equiv) and triphenylphosphine (41 mg, 0.16 mmol, 3.0 equiv) in THF (2 mL) and H_2O (0.2 mL). Flash column chromatography (SiO_2 ; n -hexane/EtOAc 10:3) gave the title compound **5g** (22 mg, 0.080 mmol, 81%) as a brown solid.

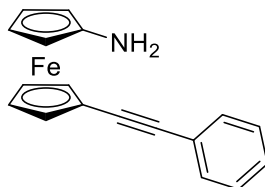
$R_f = 0.33$ (SiO_2 ; n -hexane/EtOAc 10:3; vis. vanillin).

^1H NMR (500 MHz, CDCl_3) δ [ppm] = 4.29 (s, 2H), 4.07 (s, 2H), 3.93 (s, 2H), 3.85 (s, 2H), 2.75 (s, 2H), 1.36 (dt, $J = 8.4, 5.2$, 1H), 0.83 (dt, $J = 7.0, 3.5$, 2H), 0.72 (dd, $J = 5.1, 2.3$, 2H).

$^{13}\text{C}\{^1\text{H}\}$ NMR (126 MHz, CDCl_3) δ [ppm] = 104.5, 90.6, 73.2, 72.2, 68.6, 67.3, 65.1, 60.2, 8.7, 0.4.

HRMS (ESI-TOF) m/z calcd. for $C_{15}H_{16}FeN^+$ ($[M+H]^+$) 266.0627; found: 266.0635.

Synthesis of 1-amino-1'-(phenylethynyl)ferrocene (**5h**)



According to **GP5**, the title compound was prepared from **2k** (25 mg, 0.076 mmol, 1.0 equiv) and triphenylphosphine (60 mg, 0.23 mmol, 3.0 equiv) in THF (2 mL) and H₂O (0.2 mL). Flash column chromatography (SiO₂; *n*-hexane/EtOAc 7:3) followed by recrystallization from *n*-pentane at -78 °C gave the title compound **5h** (18 mg, 0.060 mmol, 78%) as an orange solid.

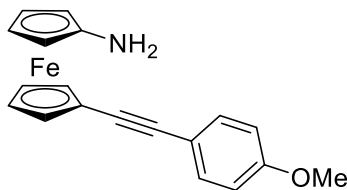
R_f = 0.36 (SiO₂; *n*-hexane/EtOAc 7:3; vis. vanillin).

¹H NMR (400 MHz, CDCl₃) δ [ppm] = 7.49 – 7.45 (m, 2H), 7.36 – 7.29 (m, 3H), 4.46 (t, J = 1.9 Hz, 2H), 4.20 (t, J = 1.9 Hz, 2H), 4.00 (t, J = 1.9 Hz, 2H), 3.90 (t, J = 1.9 Hz, 2H), 2.74 (s, 2H).

¹³C{¹H} NMR (100 MHz, CDCl₃) δ [ppm] = 131.4, 128.6, 127.9, 123.9, 105.4, 88.1, 86.9, 72.4, 69.3, 66.3, 65.3, 60.1.

HRMS (ESI): m/z calcd. for $C_{18}H_{15}FeN^+$ ($[M]^+$) 301.0554; found: 301.0555.

Synthesis of 1-amino-1'-(ethinylcyclopropyl)ferrocene (**5i**)



According to **GP5**, the title compound was prepared from **2l** (40 mg, 0.11 mmol, 1.0 equiv) and triphenylphosphine (38 mg, 0.17 mmol, 1.5 equiv) in THF (2 mL) and H₂O (0.2 mL). Flash column chromatography (SiO₂; *n*-hexane/EtOAc 3:1) gave the title compound **5i** (28 mg, 0.085 mmol, 75%) as an orange solid.

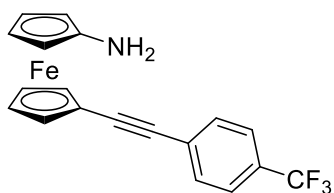
R_f = 0.30 (SiO₂; *n*-hexane/EtOAc 3:1; vis. vanillin).

¹H NMR (600 MHz, CDCl₃) δ [ppm] = 7.40 (d, J = 8.7 Hz, 2H), 6.85 (d, J = 8.7 Hz, 2H), 4.44 (s, 2H), 4.18 (s, 2H), 4.00 (s, 2H), 3.90 (s, 2H), 3.82 (s, 3H), 2.74 (s, 2H).

¹³C{¹H} NMR (151 MHz, CDCl₃) δ [ppm] = 159.4, 132.8, 116.0, 114.2, 105.2, 86.7, 86.2, 72.2, 69.1, 66.8, 65.3, 60.1, 55.5.

HRMS (ESI-TOF) m/z calcd. for $C_{19}H_{18}FeNO^+$ ($[M+H]^+$) 332.0733; found: 332.0733.

Synthesis of 1-amino-1'-[(4-trifluoromethyl)phenylethynyl]ferrocene (**5j**)



According to **GP5**, the title compound was prepared from **2m** (100 mg, 253 μmol , 1.0 equiv) and triphenylphosphine (85.9 mg, 380 μmol , 1.5 equiv) in THF (5 mL) and H₂O (0.5 mL). MPLC (cyclohexane/EtOAc 90:10 to 70:3) gave the title compound **5j** (85.0 mg, 230 μmol , 91%) as an orange solid.

R_f = 0.41 (SiO₂; *n*-hexane/EtOAc 3:1; vis. vanillin).

¹H NMR (500 MHz, CD₂Cl₂) δ [ppm] = 7.59 (s, 4H), 4.48 (t, J = 1.9 Hz, 2H), 4.24 (t, J = 1.9 Hz, 2H), 3.99 (t, J = 1.9 Hz, 2H), 3.90 (t, J = 1.9 Hz, 2H), 2.72 (s, 2H).

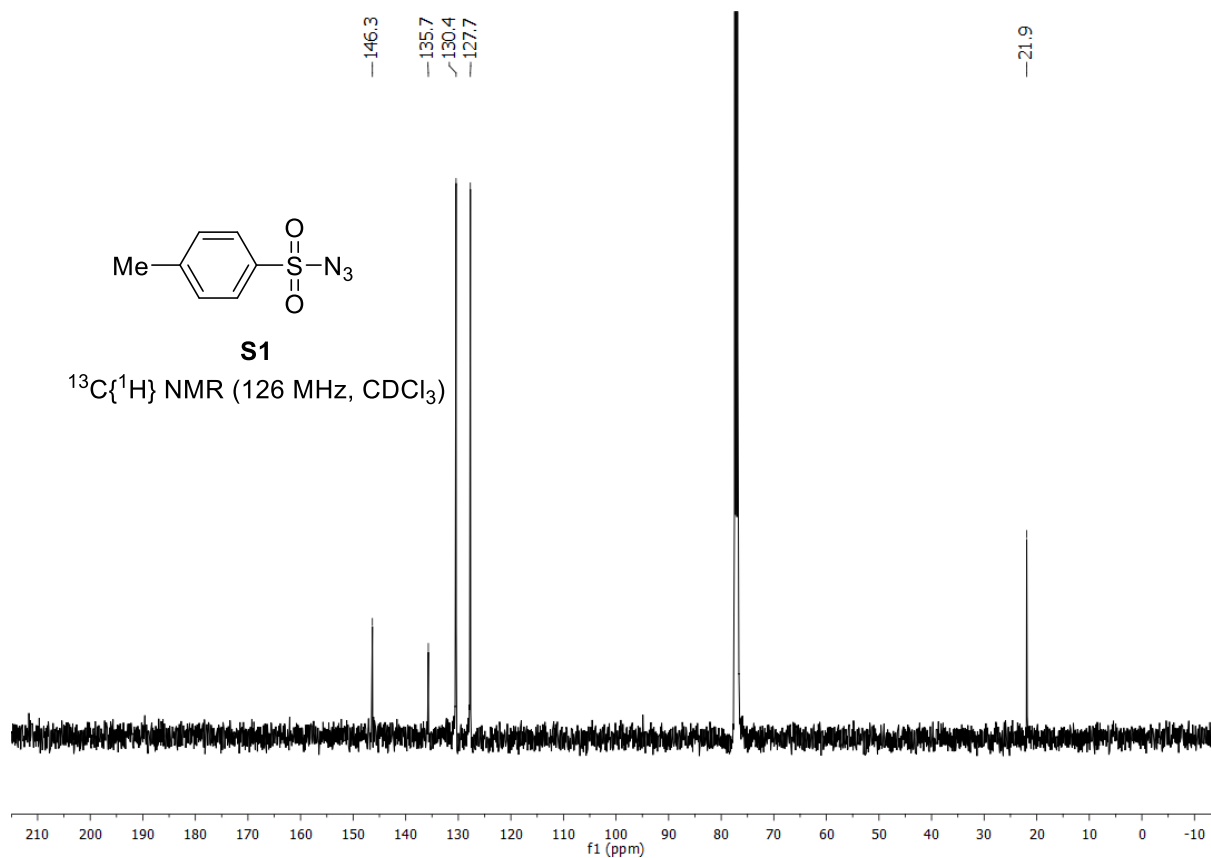
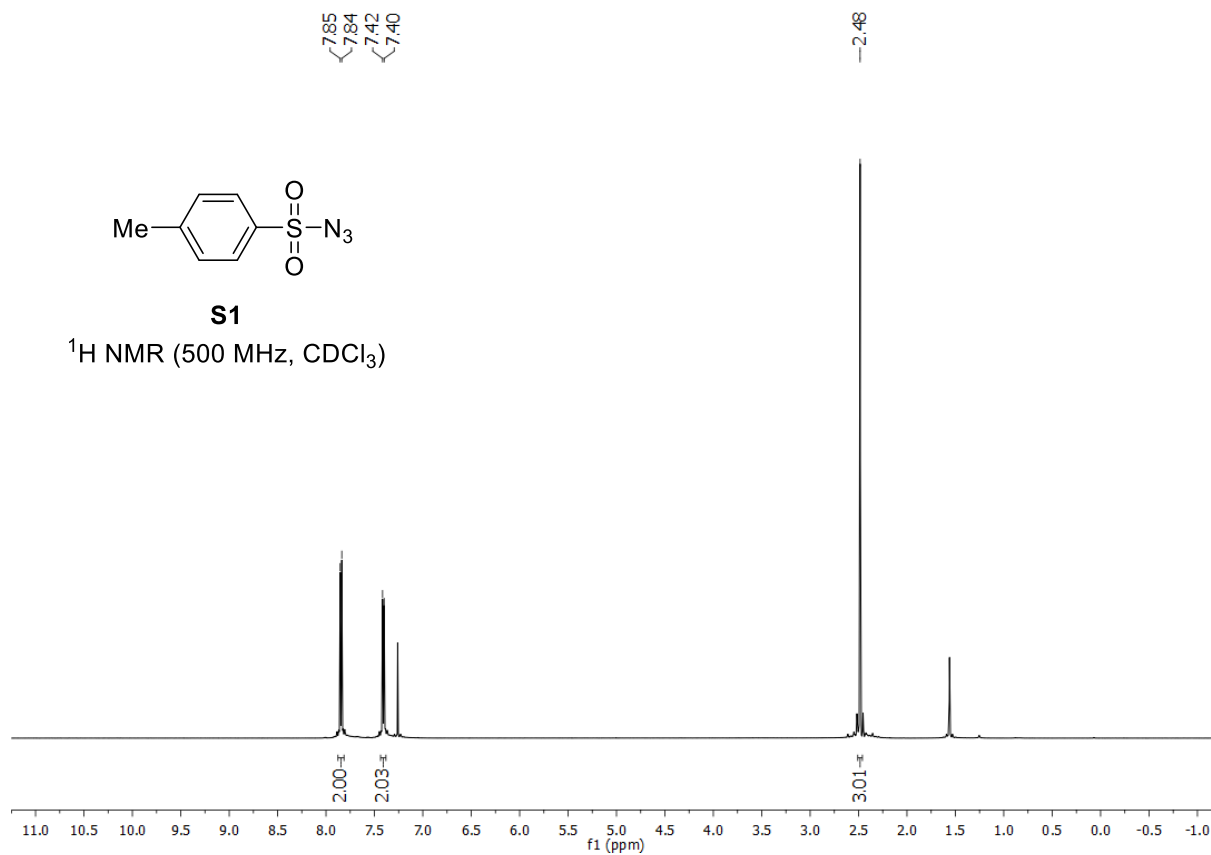
¹³C{¹H} NMR (126 MHz, CD₂Cl₂) δ [ppm] = 131.9, 129.5 (q, J = 32.5 Hz), 128.6, 125.9 (q, J = 3.8 Hz), 123.7, 107.1, 92.1, 85.7, 73.0, 70.3, 65.8, 65.5, 60.0. Due to poor resolution of the spectrum, one C-F coupling could not be detected.

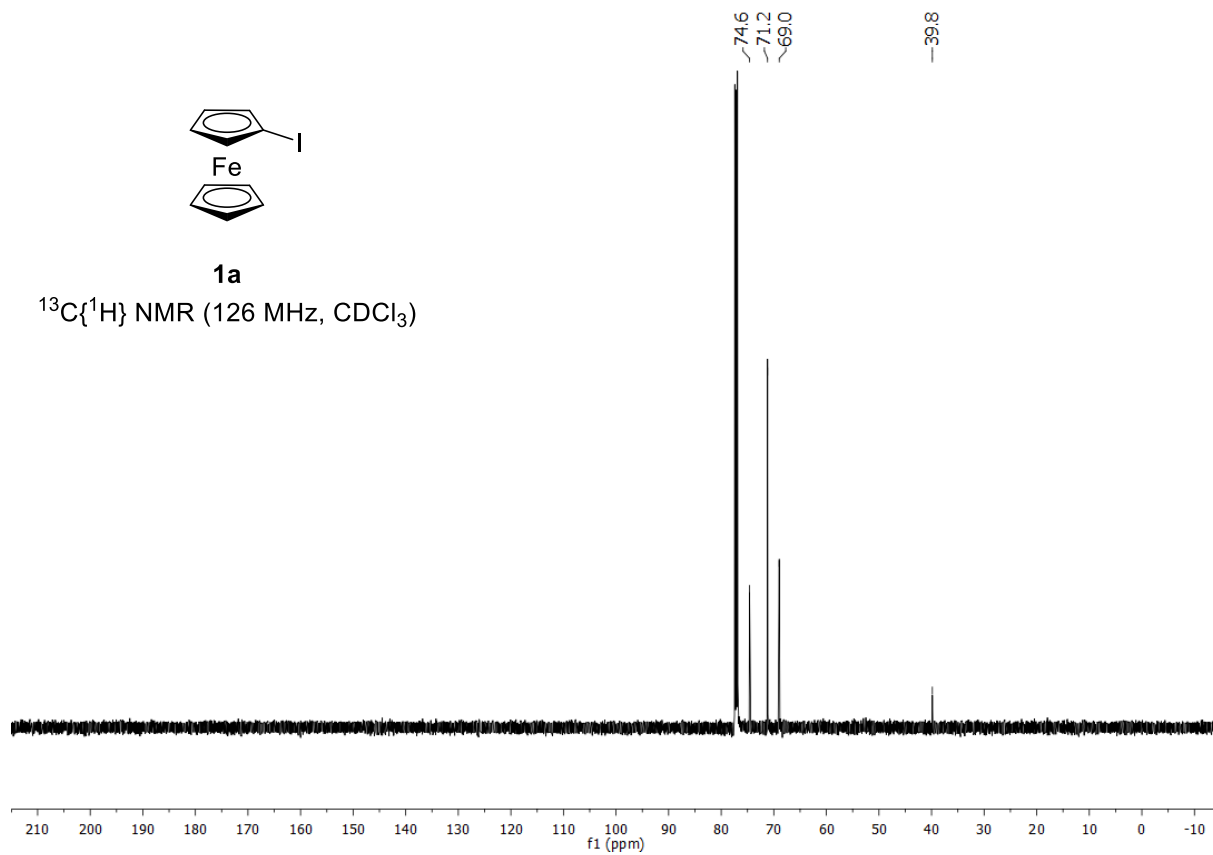
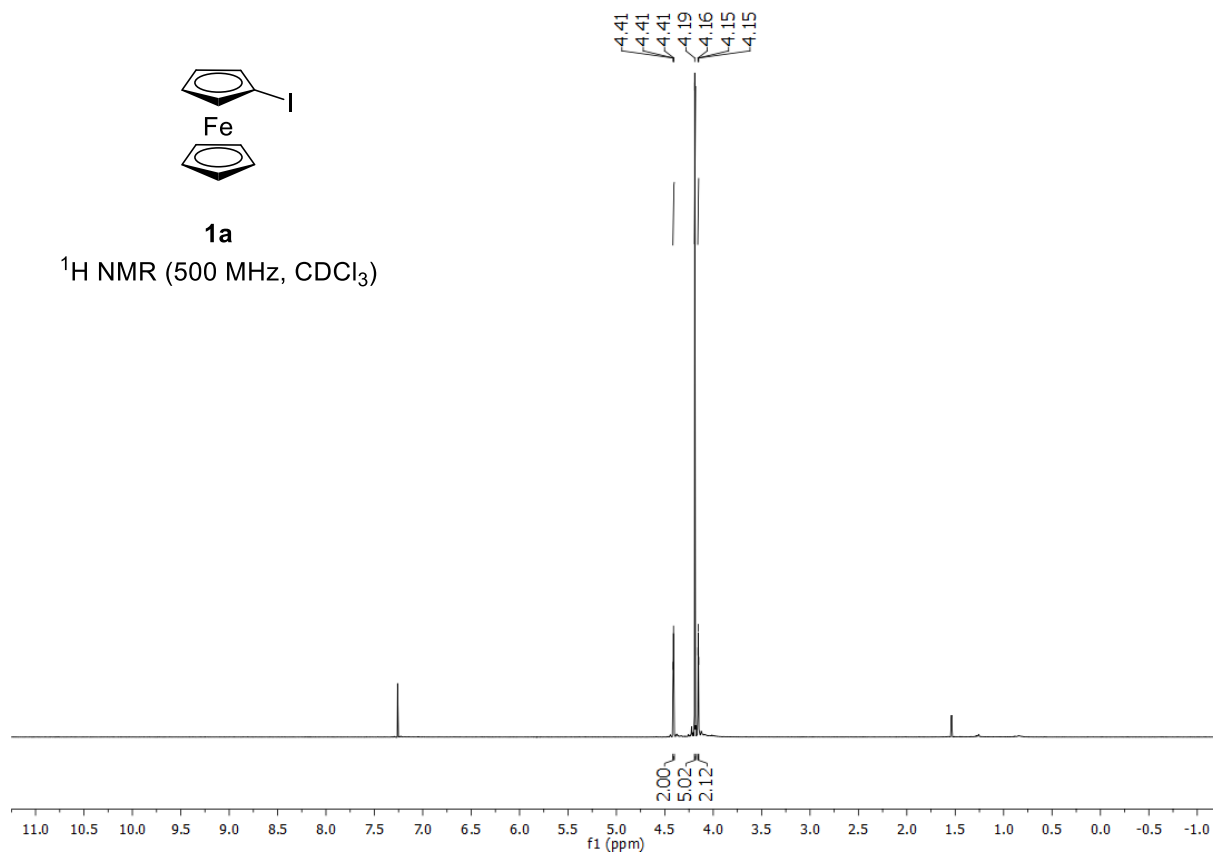
¹⁹F NMR (471 MHz, CD₂Cl₂) δ [ppm] = -62.9.

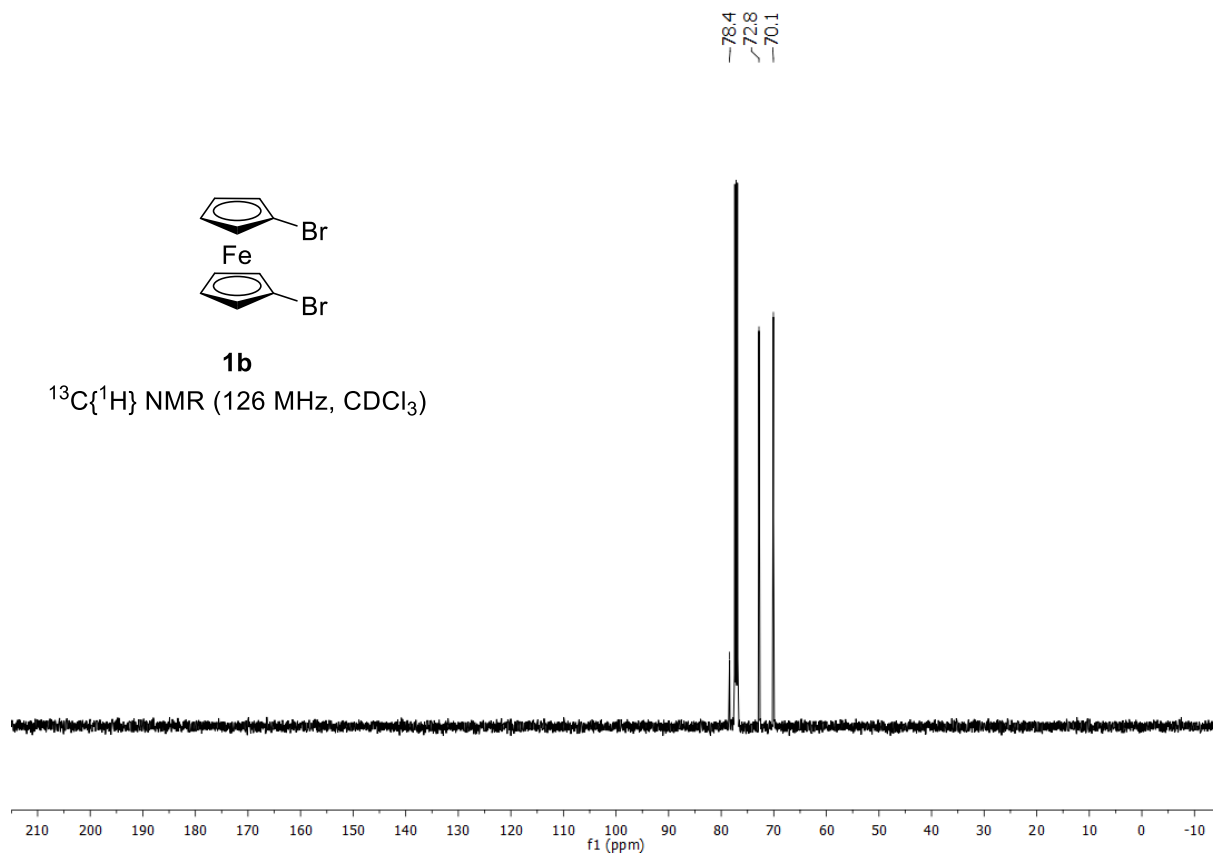
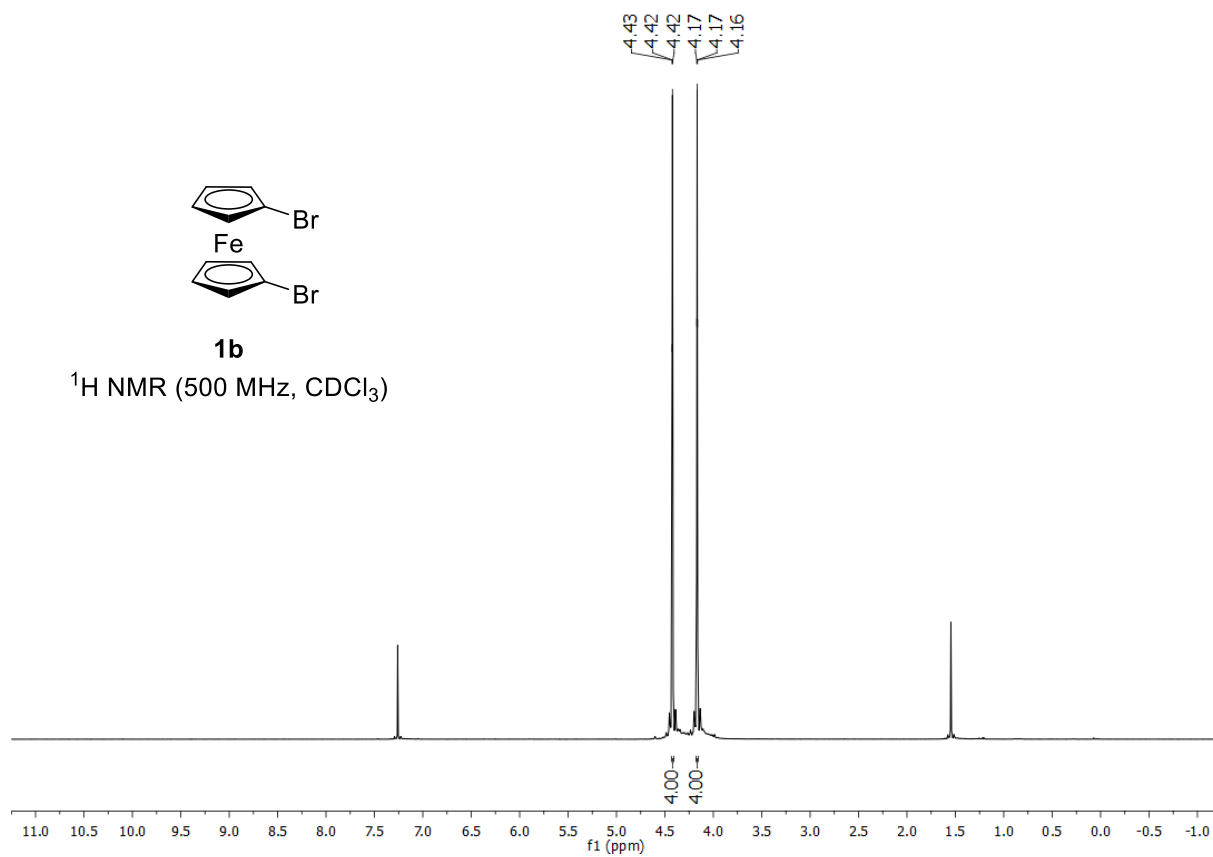
HRMS (ESI-TOF) m/z calcd. for C₁₉H₁₅F₃FeN⁺ ([M+H]⁺) 370.0501; found: 370.0519.

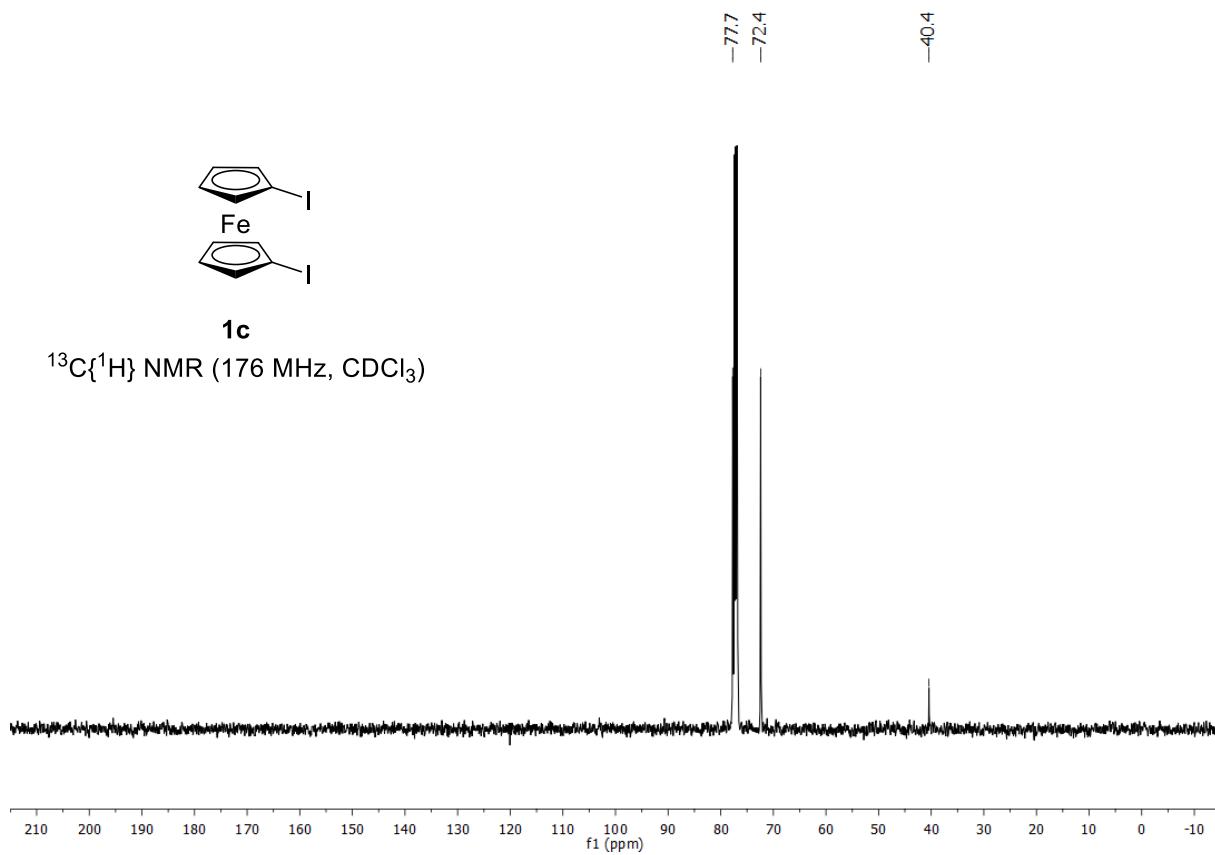
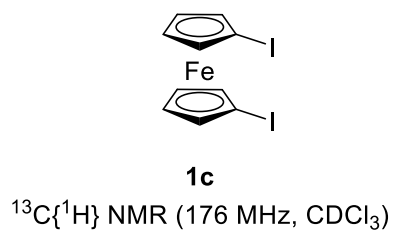
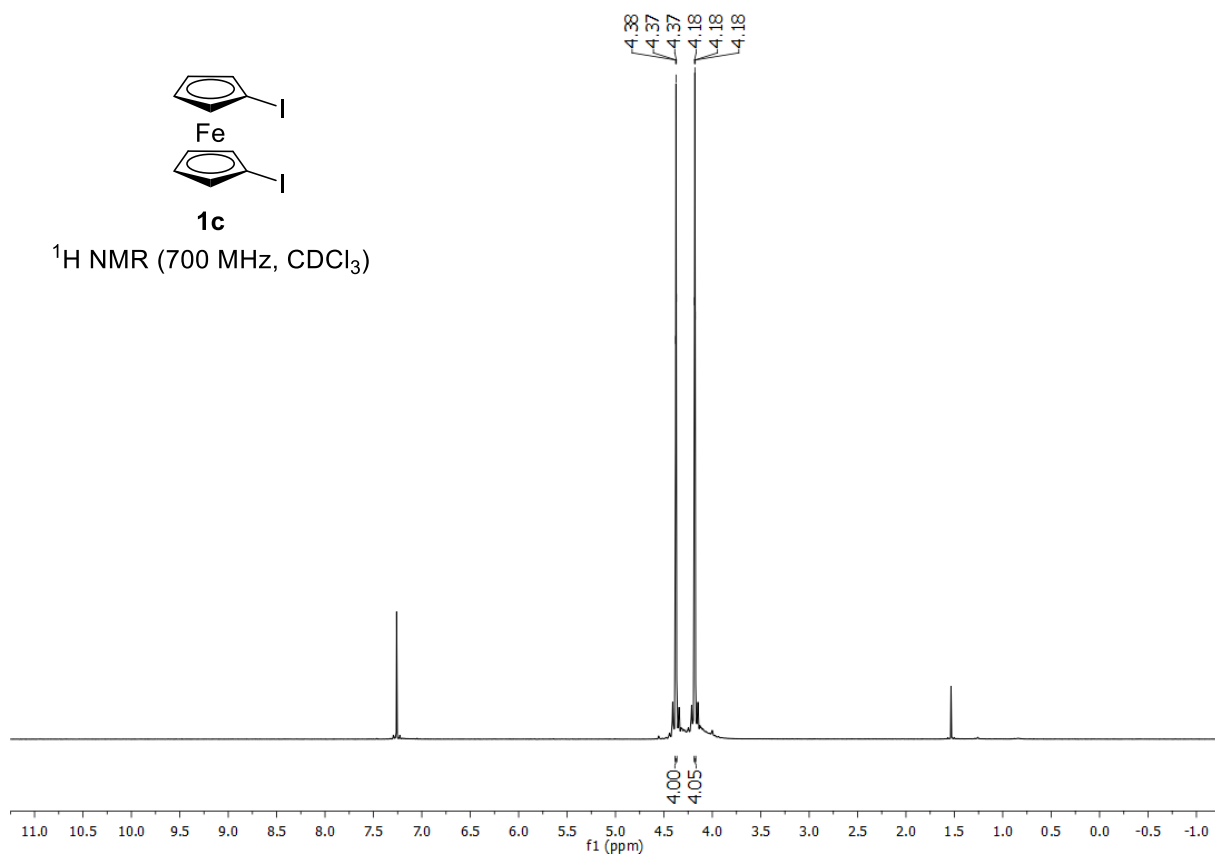
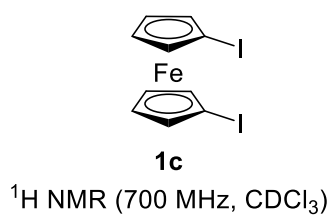
3. NMR Spectra of Synthesized Compounds

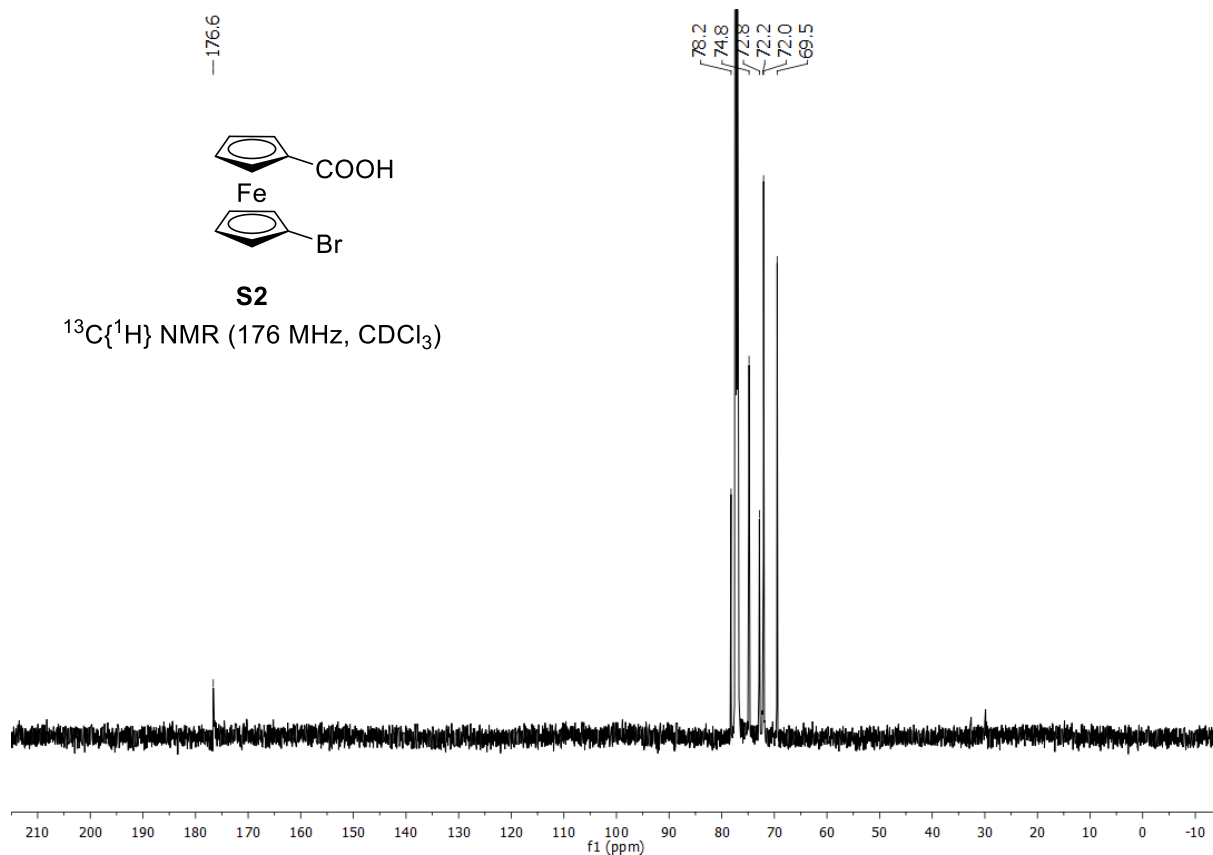
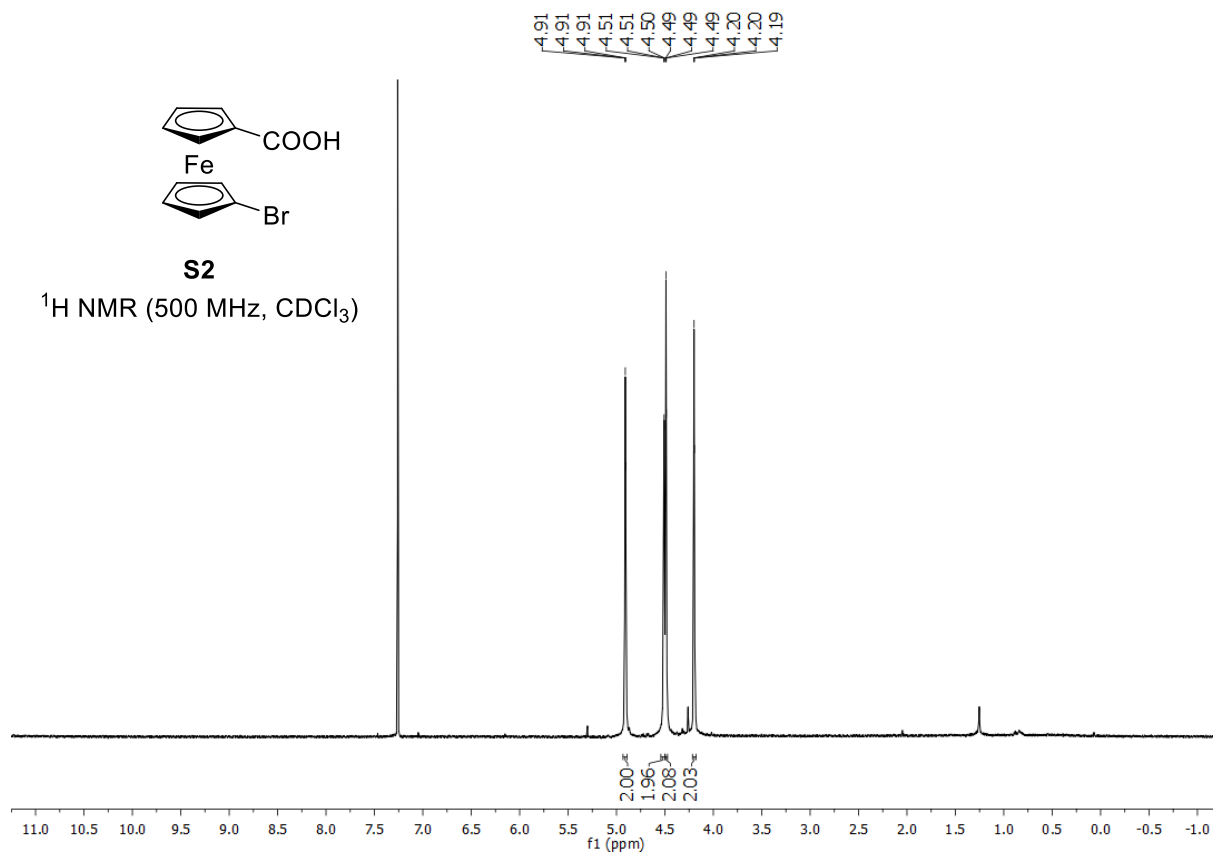
3.1 NMR Spectra of Compounds Synthesized in Batch

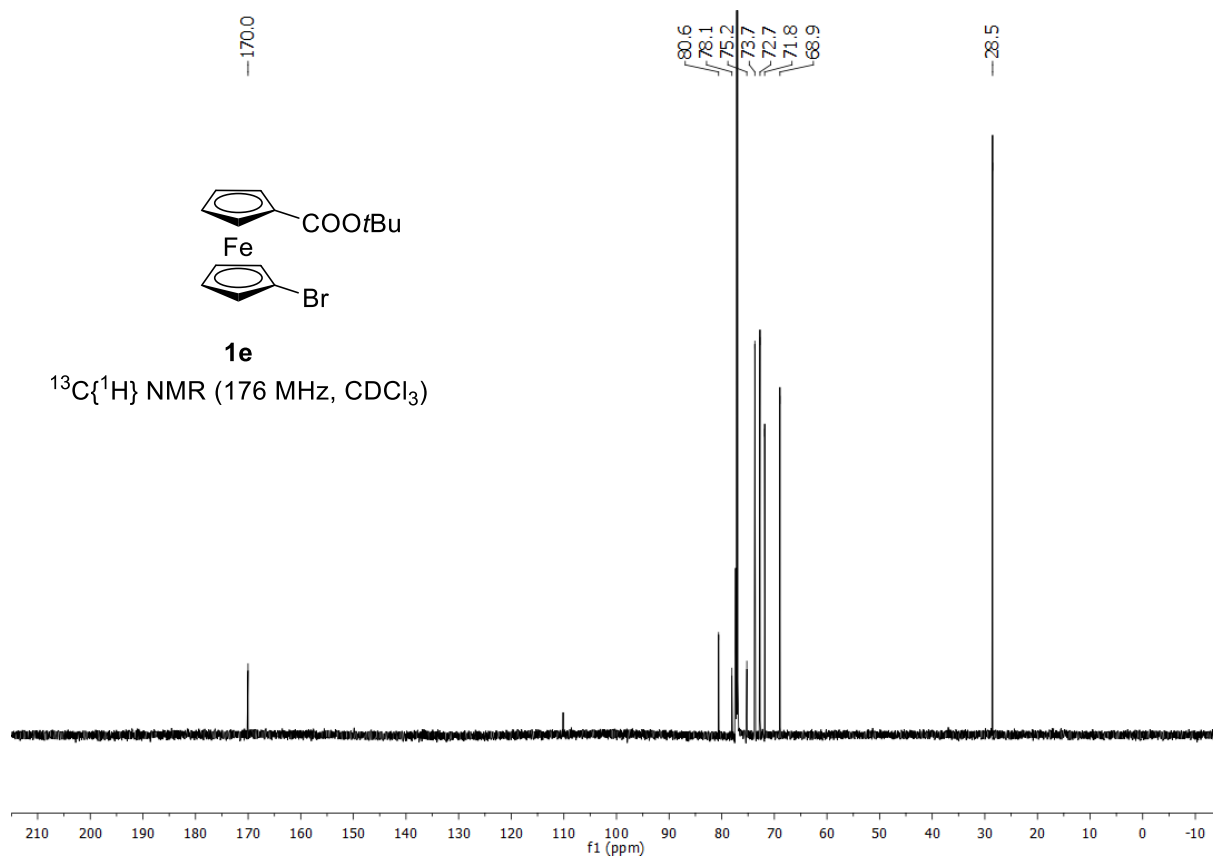
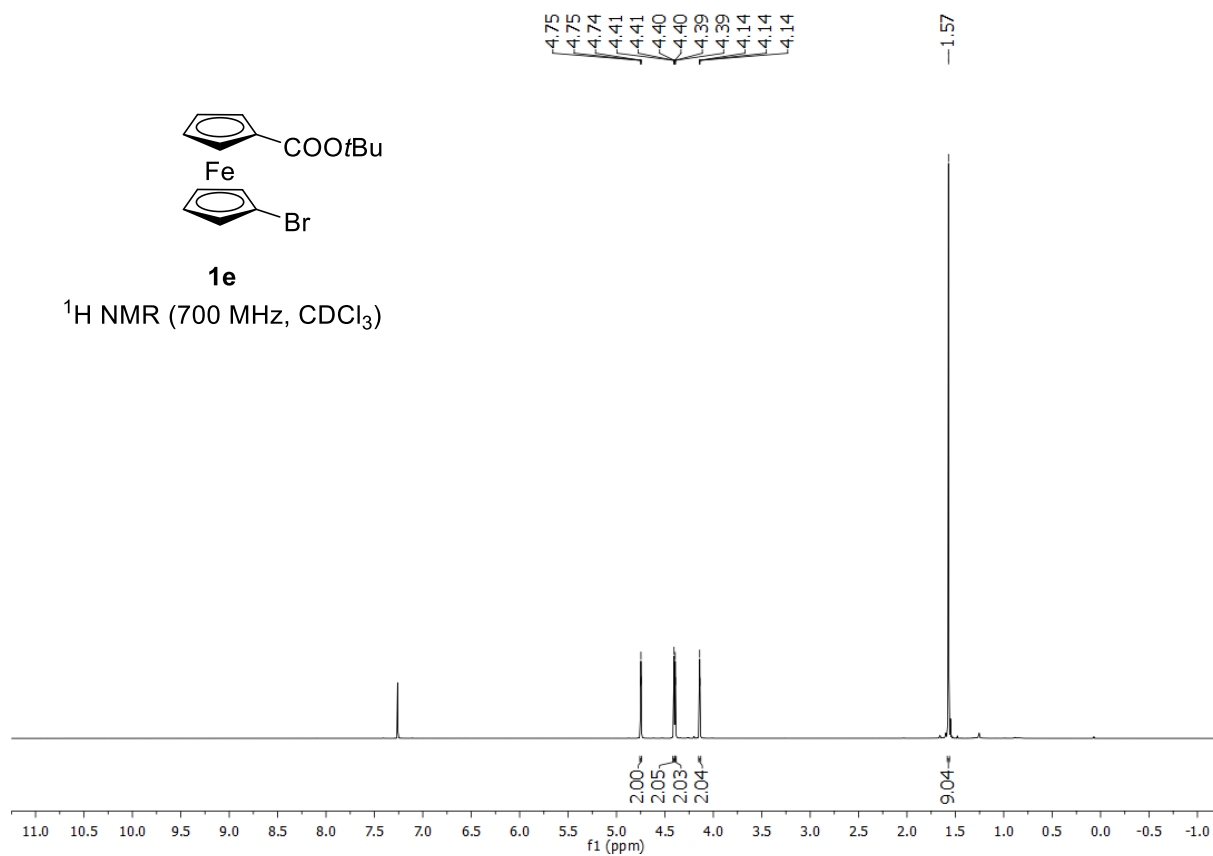


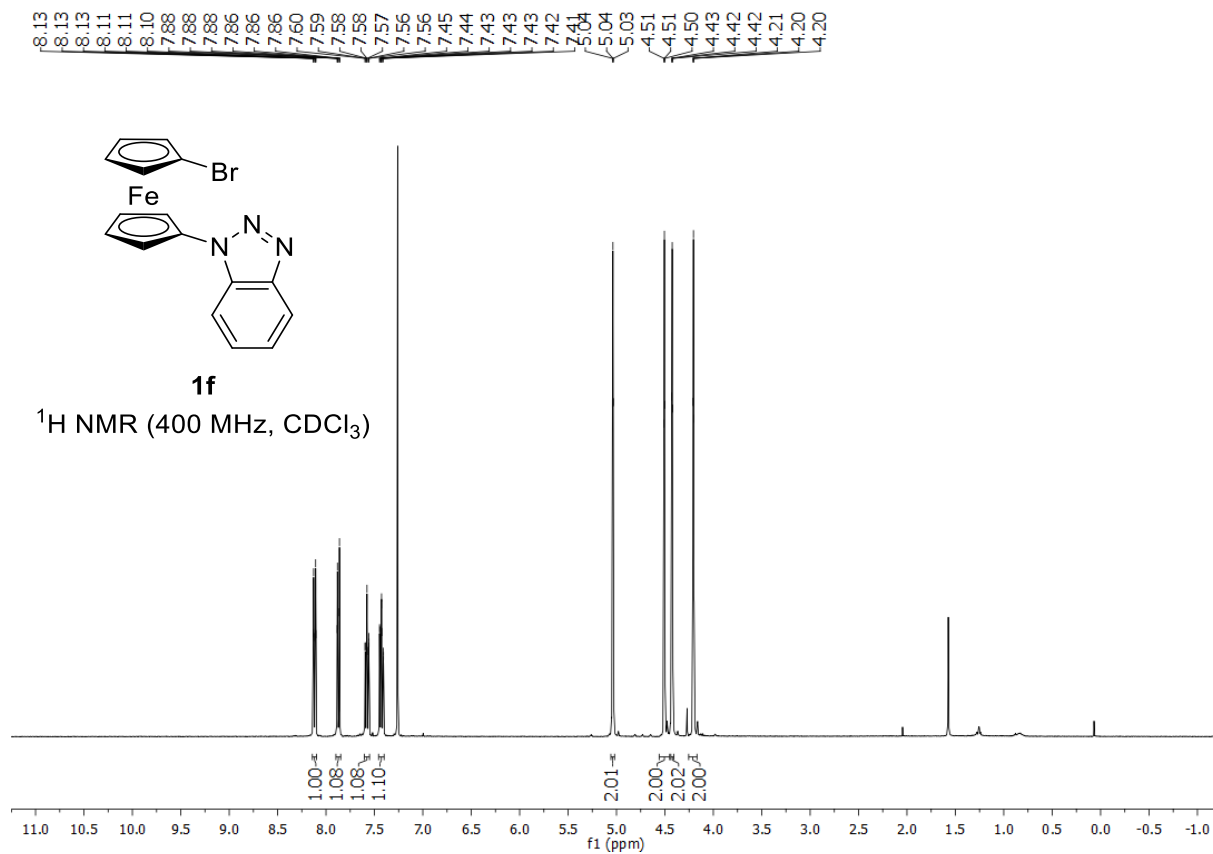




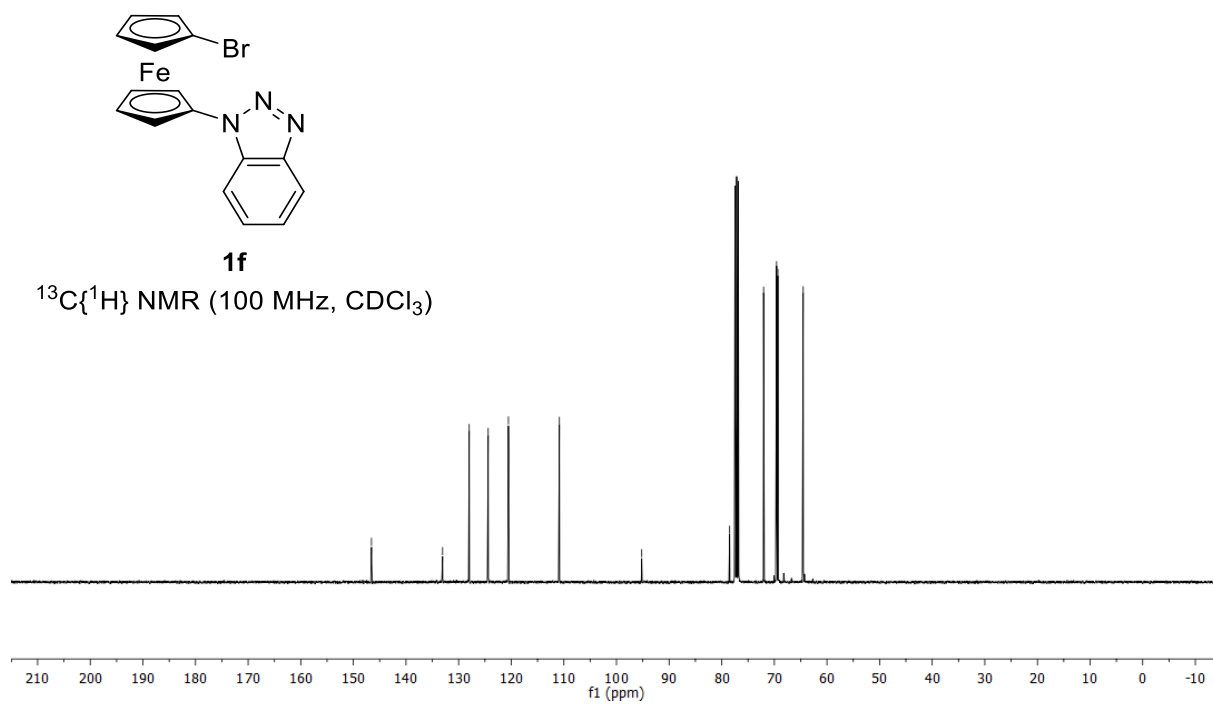


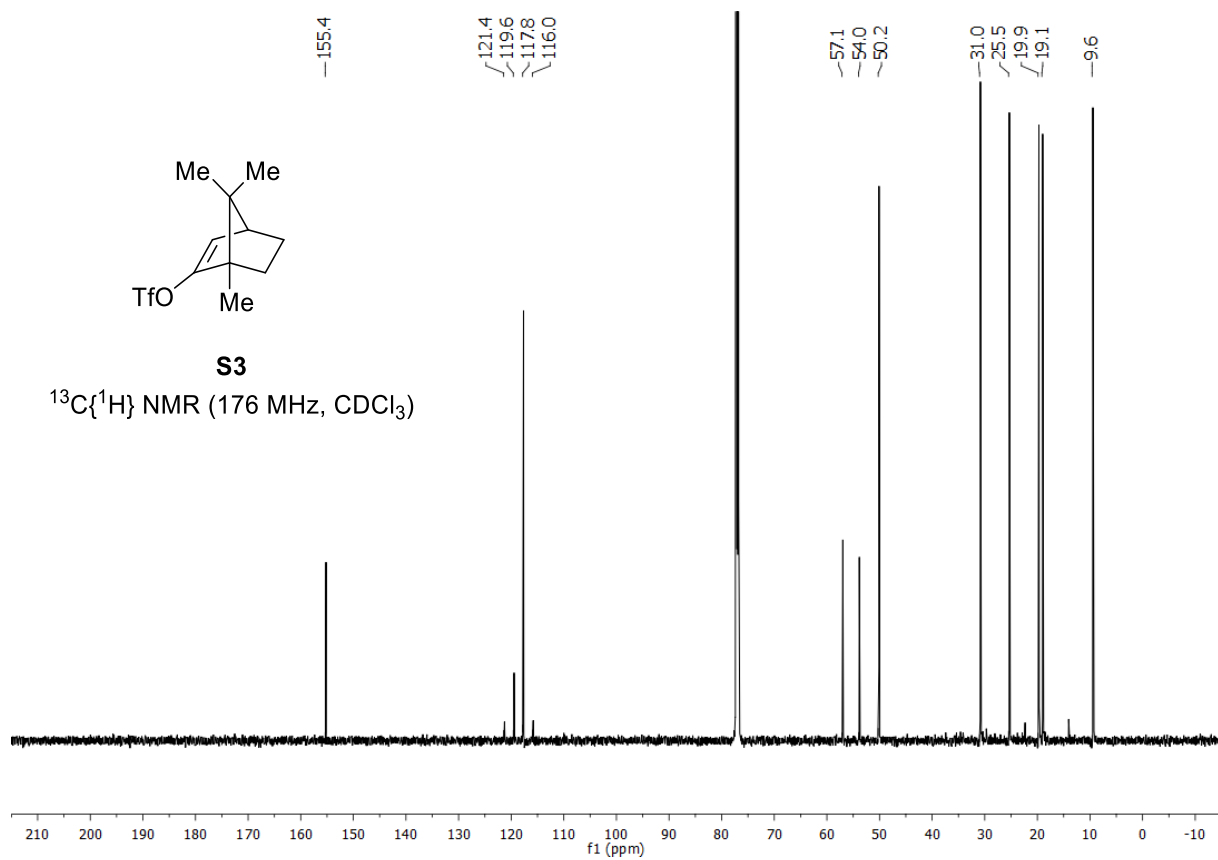
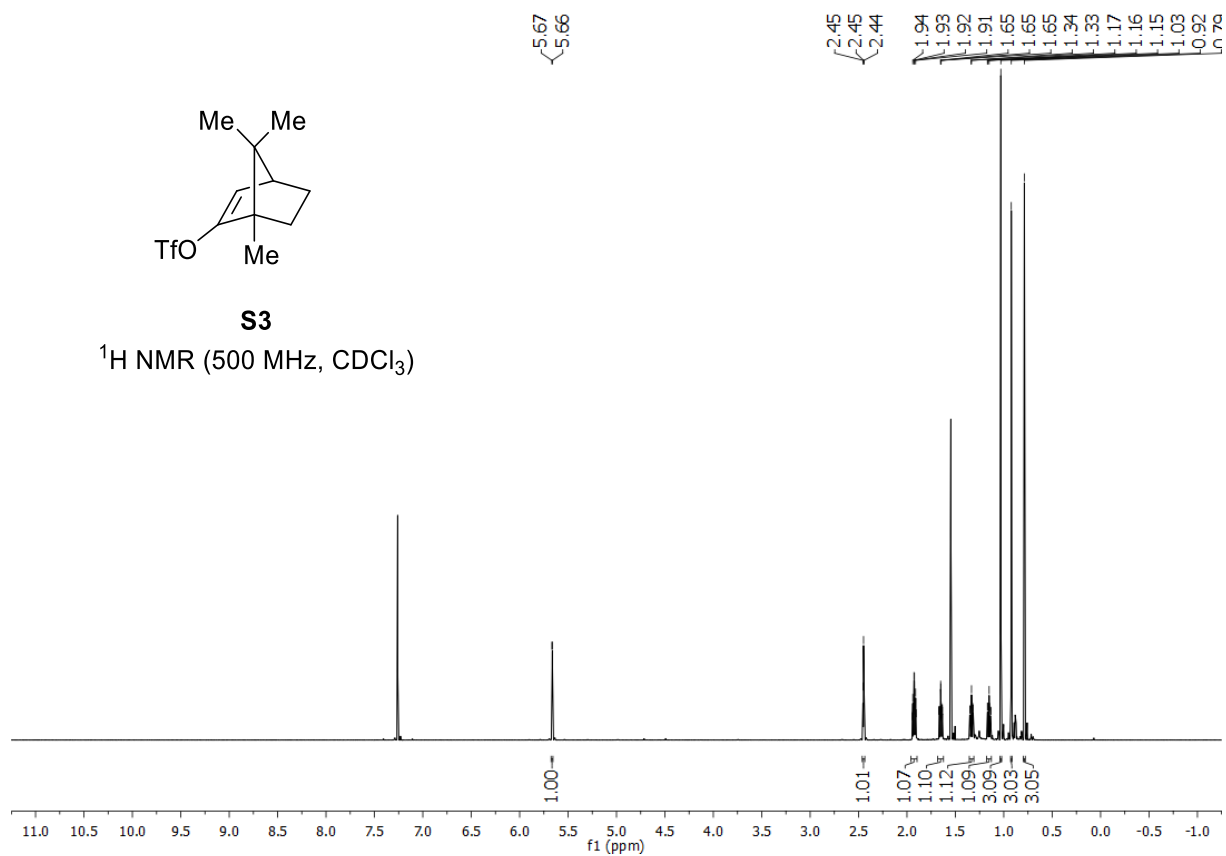


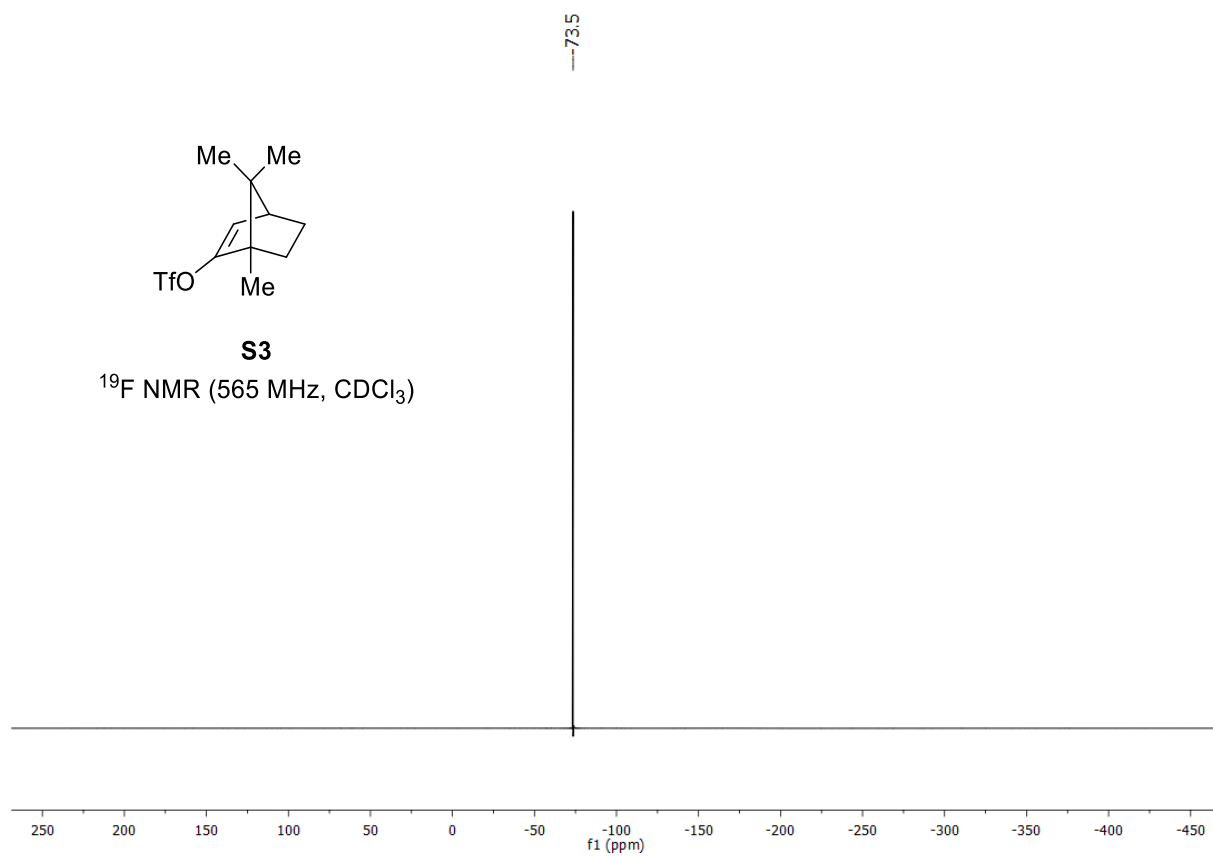


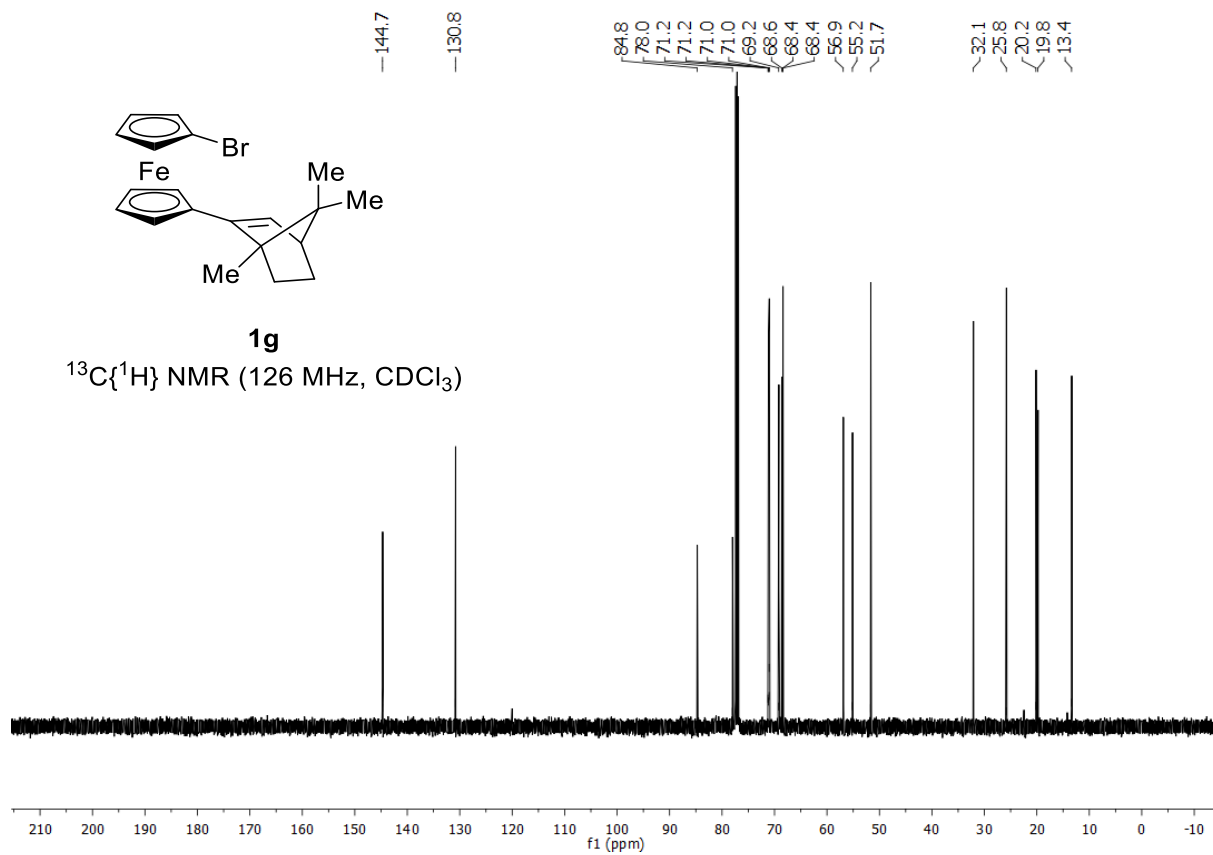
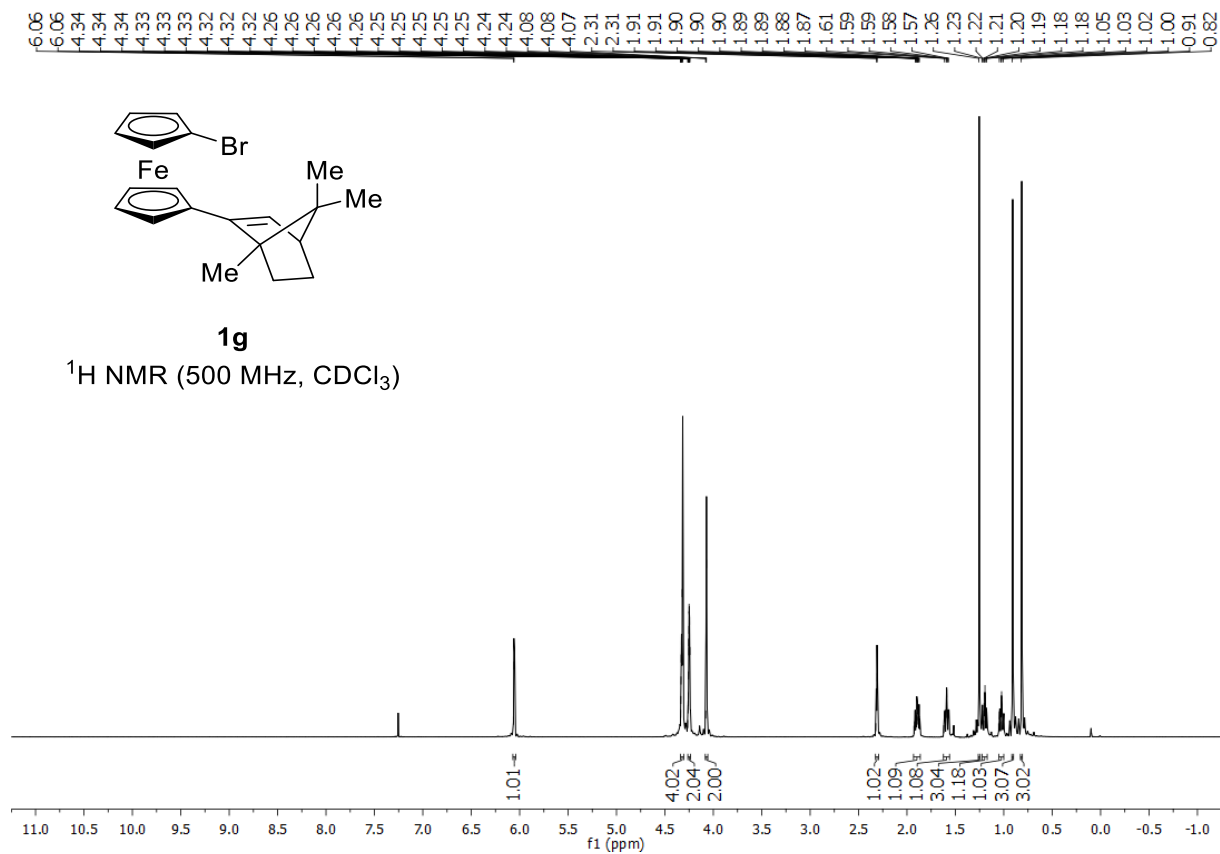


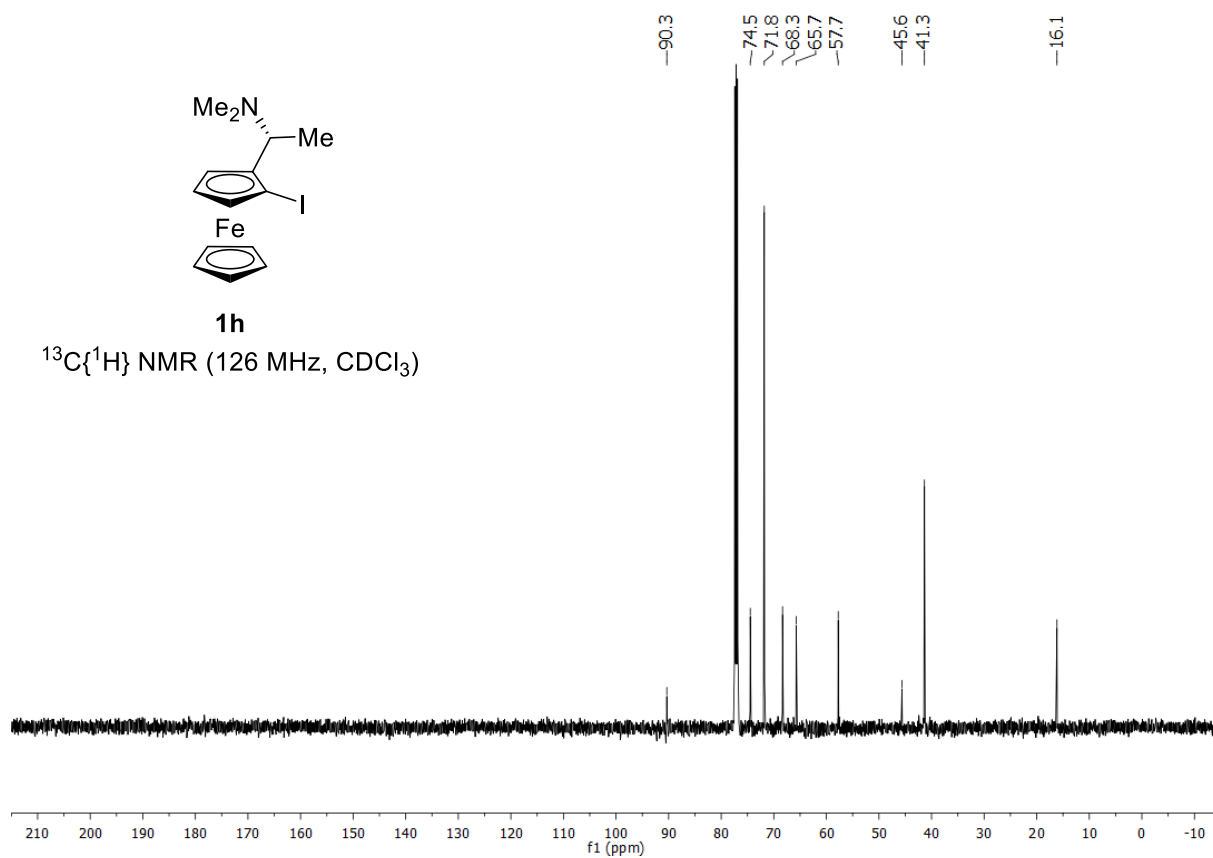
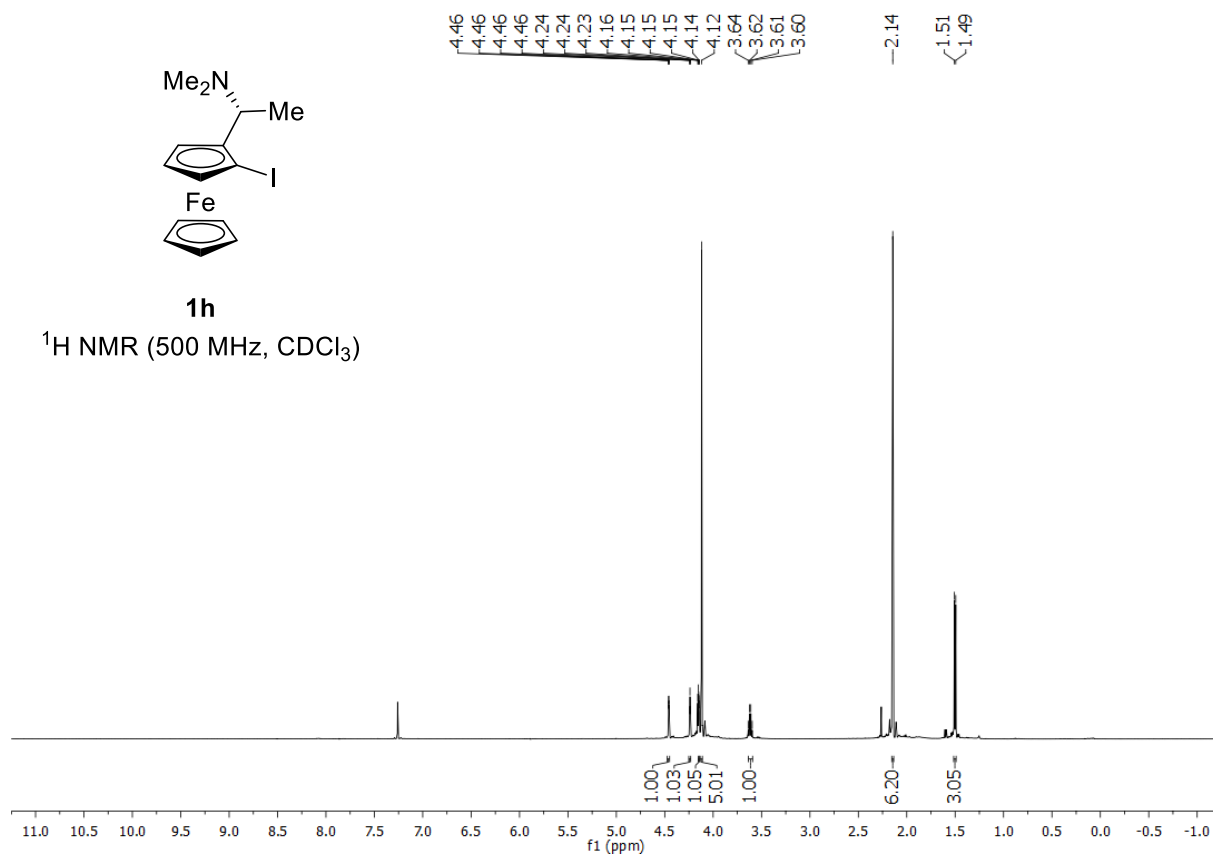
-146.6
-133.0
-128.0
-124.4
-120.5
-110.8
-95.2
78.5
72.0
69.6
69.3
64.5

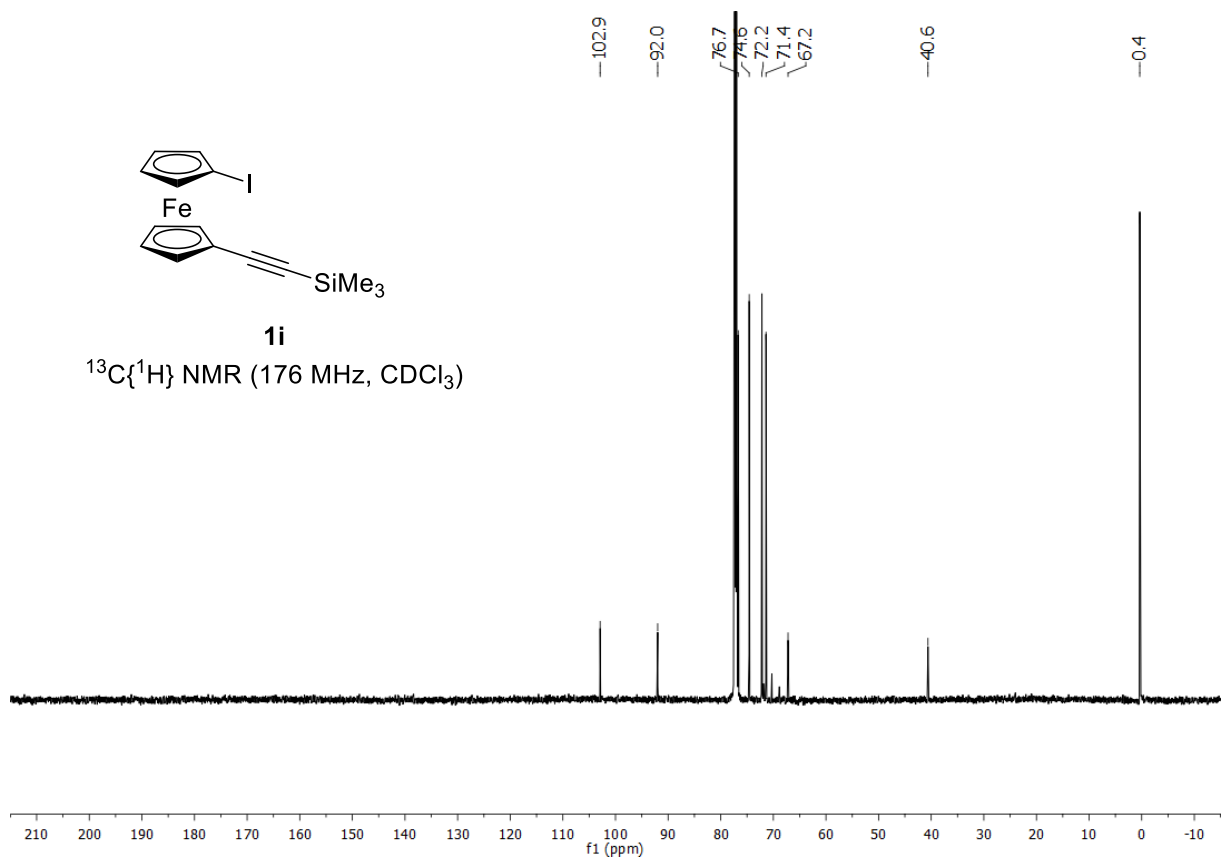
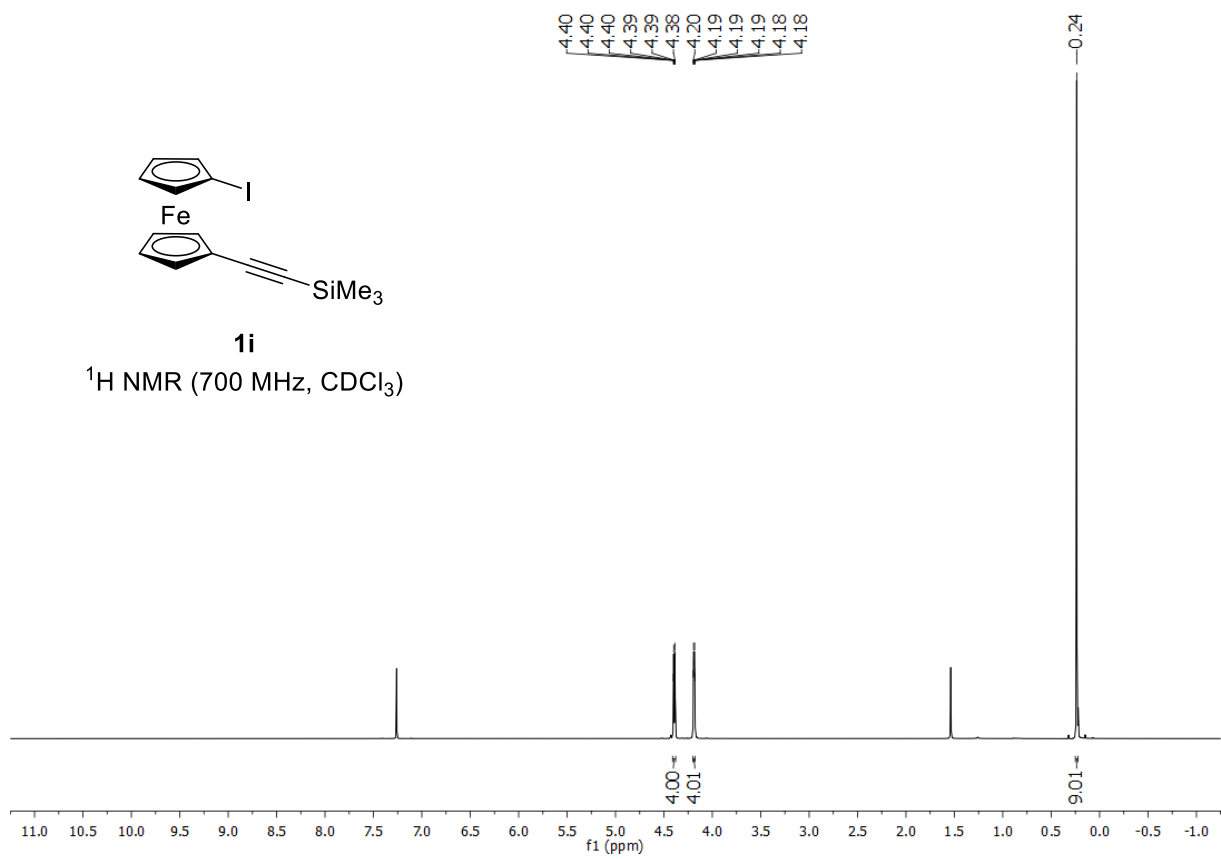


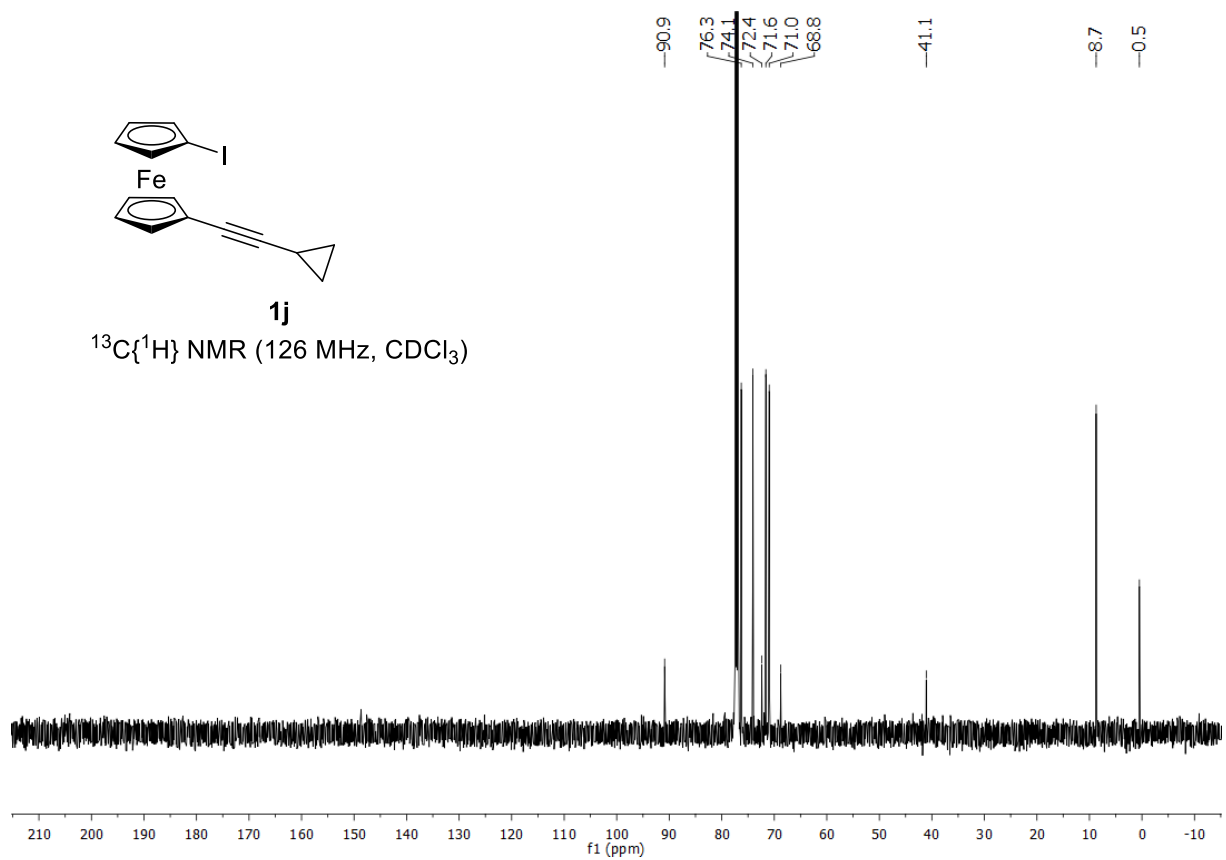
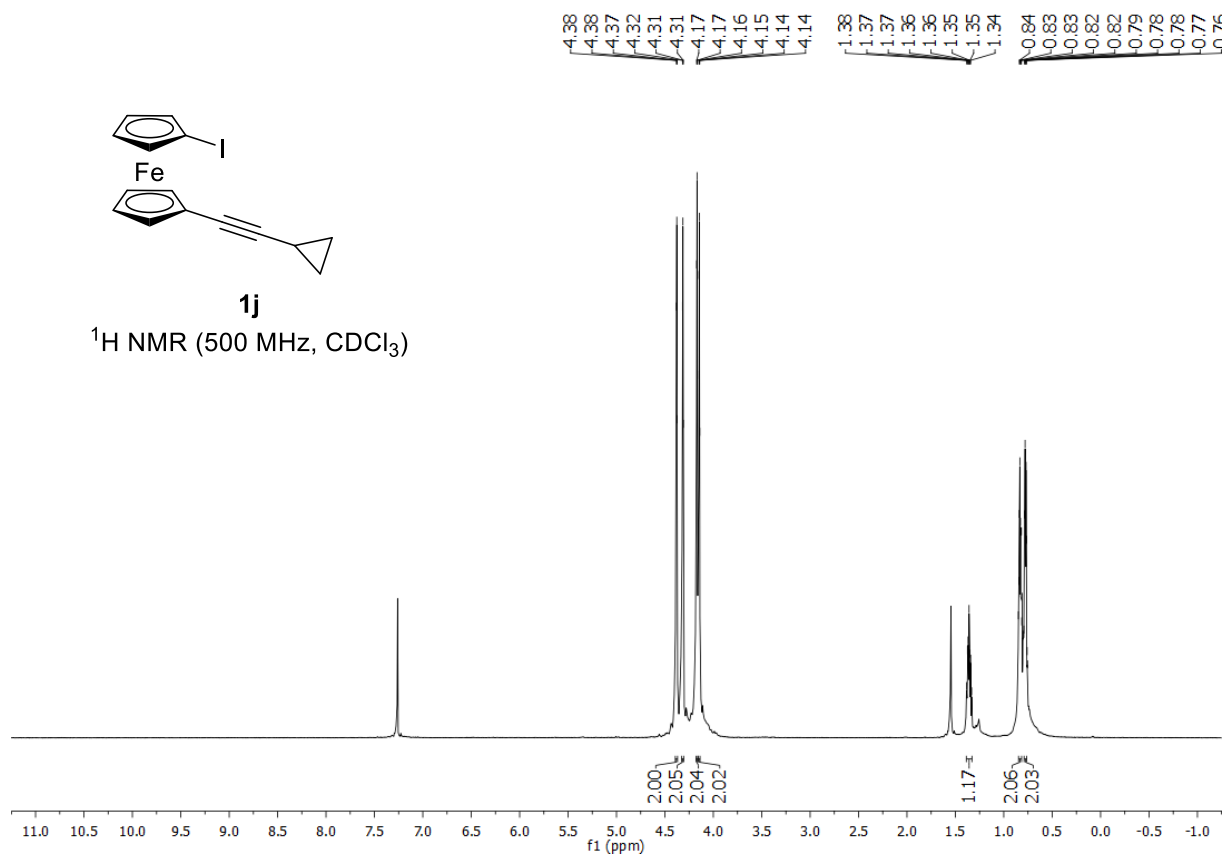


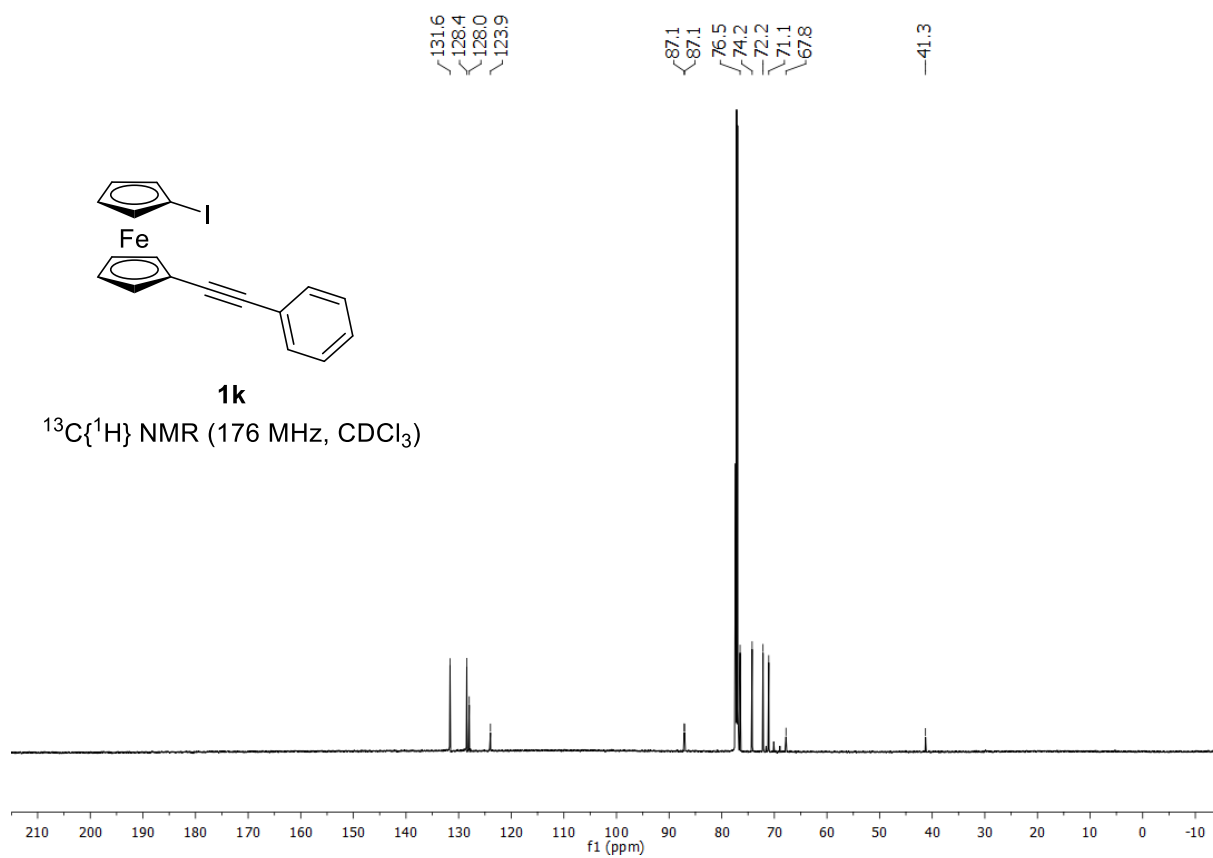
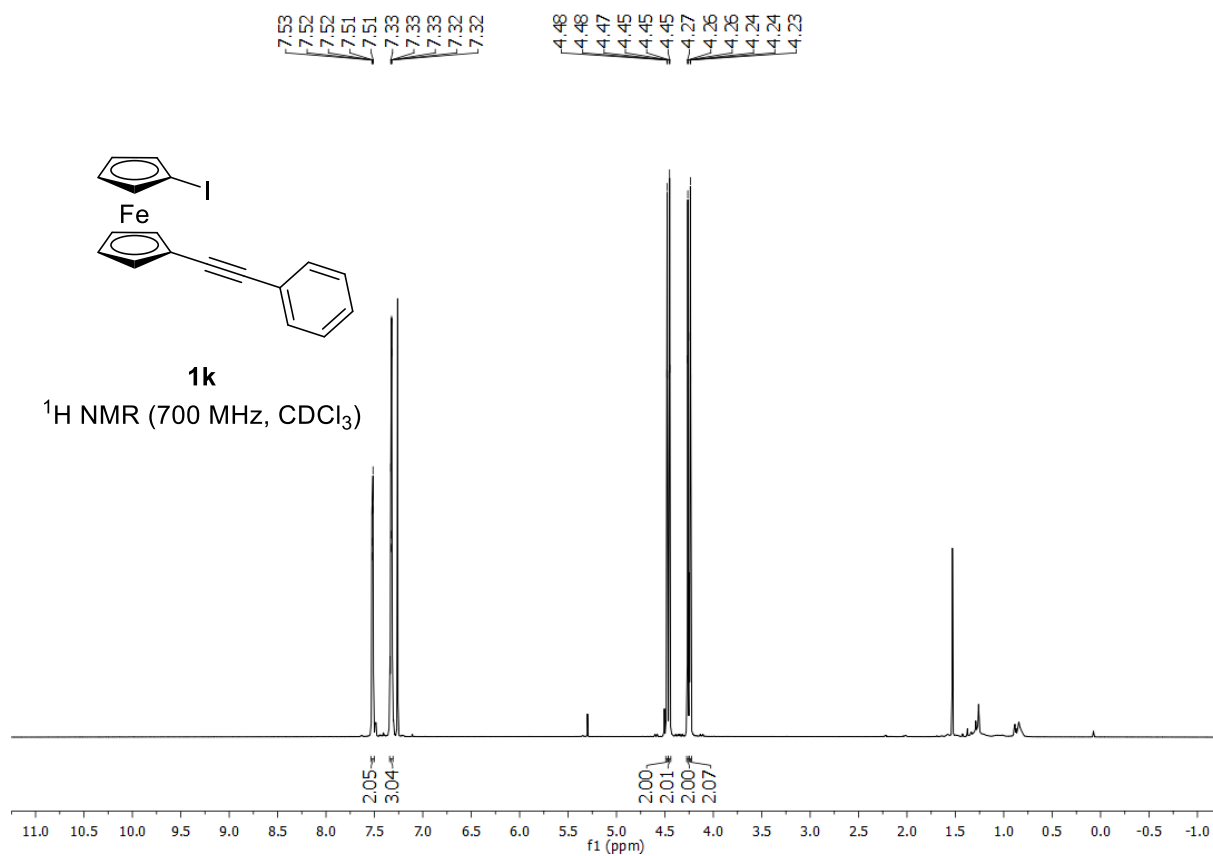


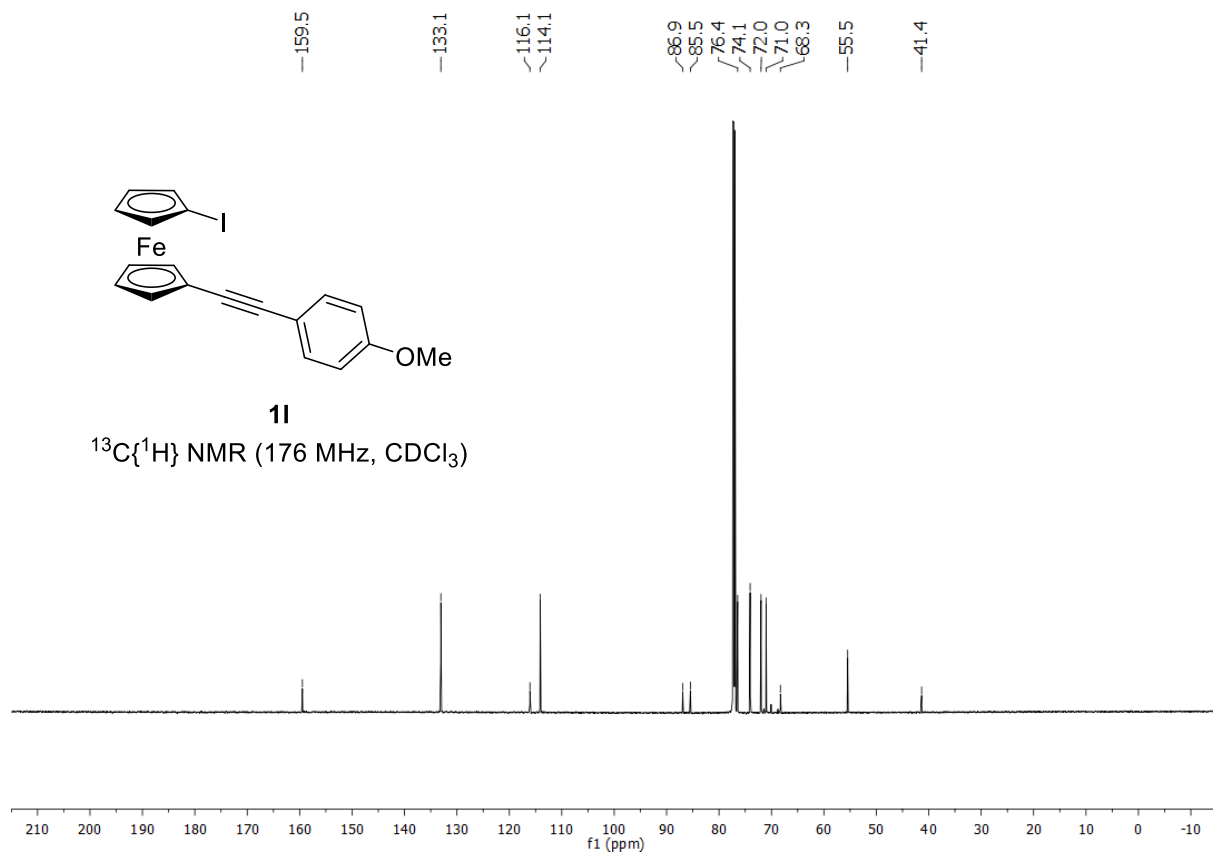
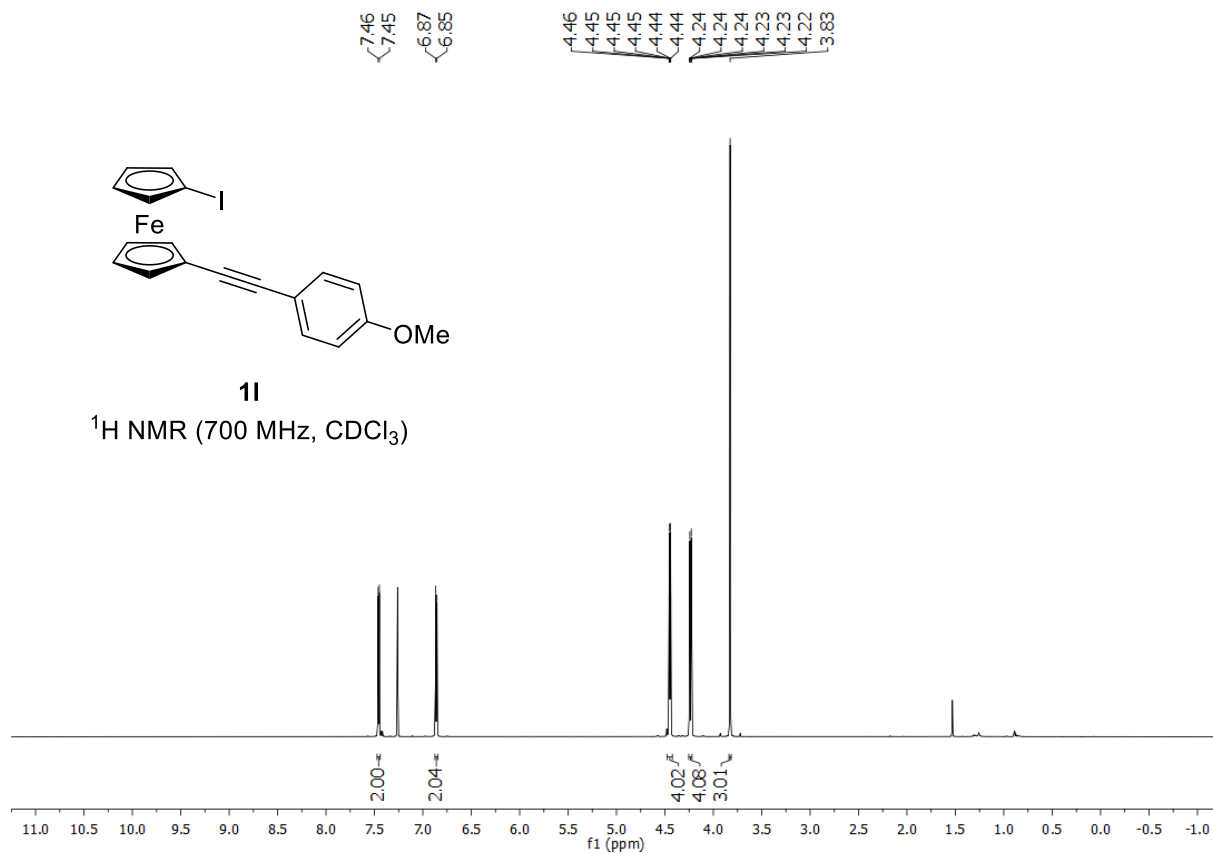


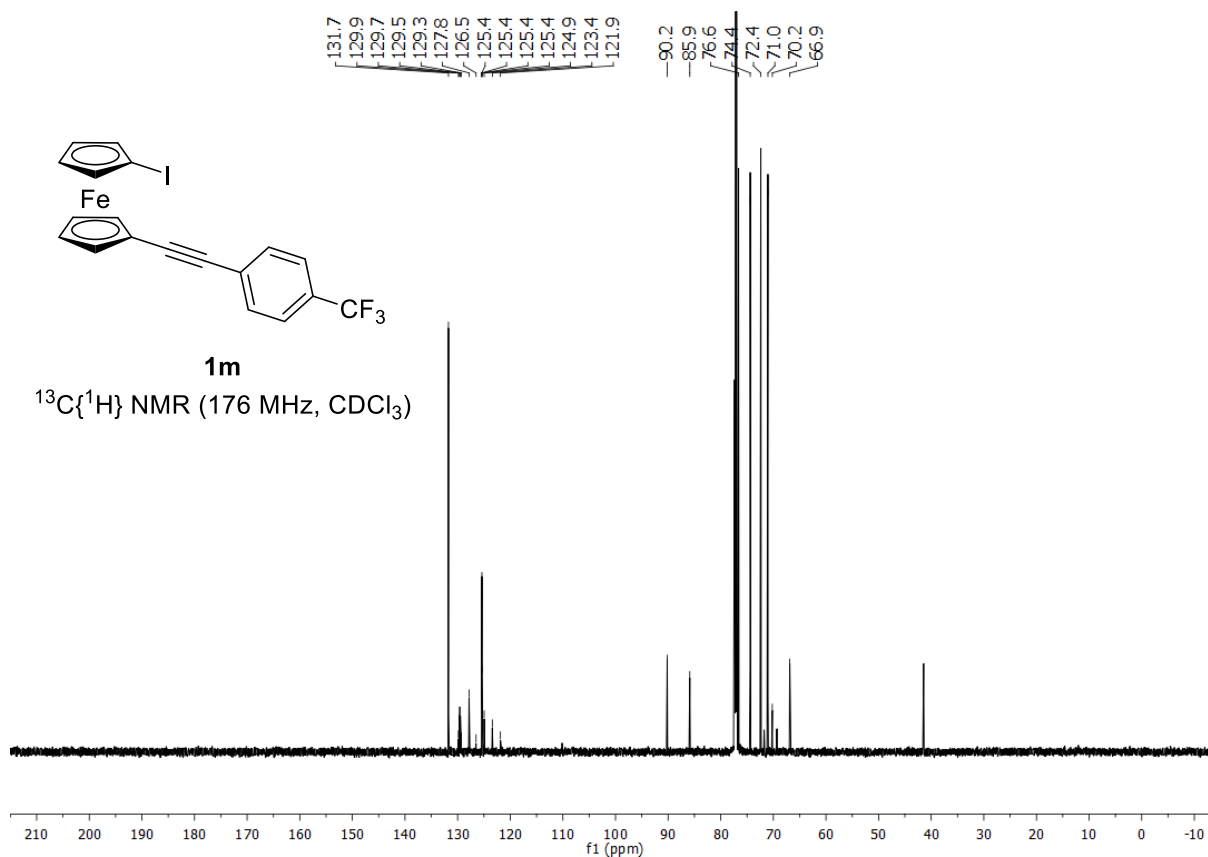
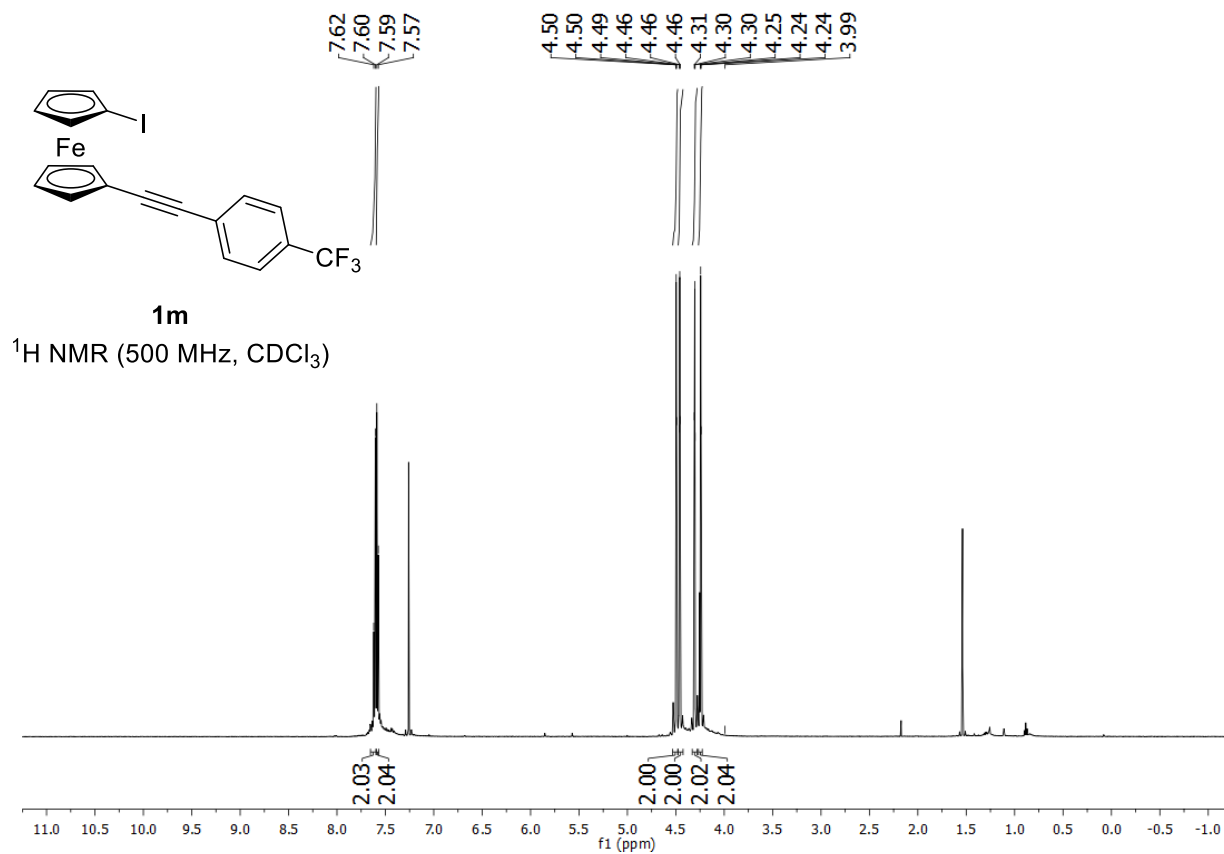


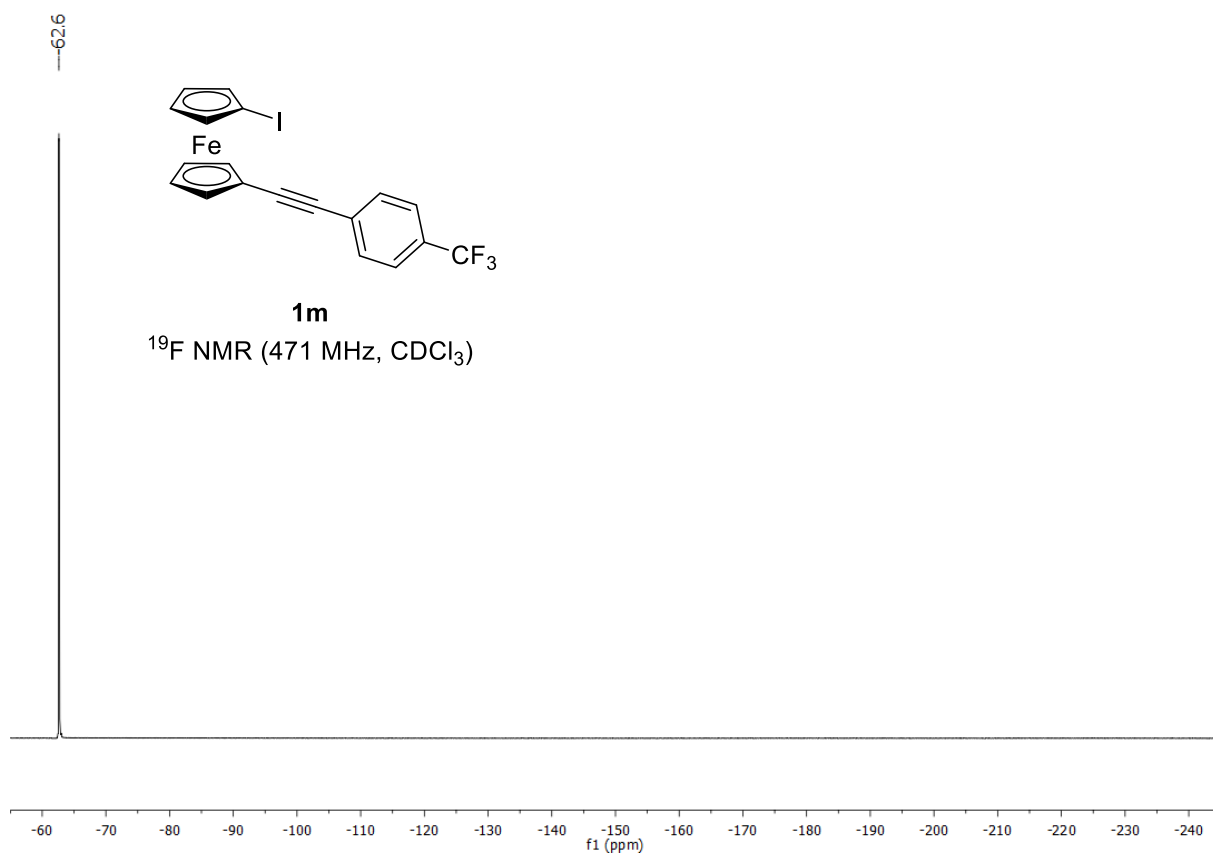


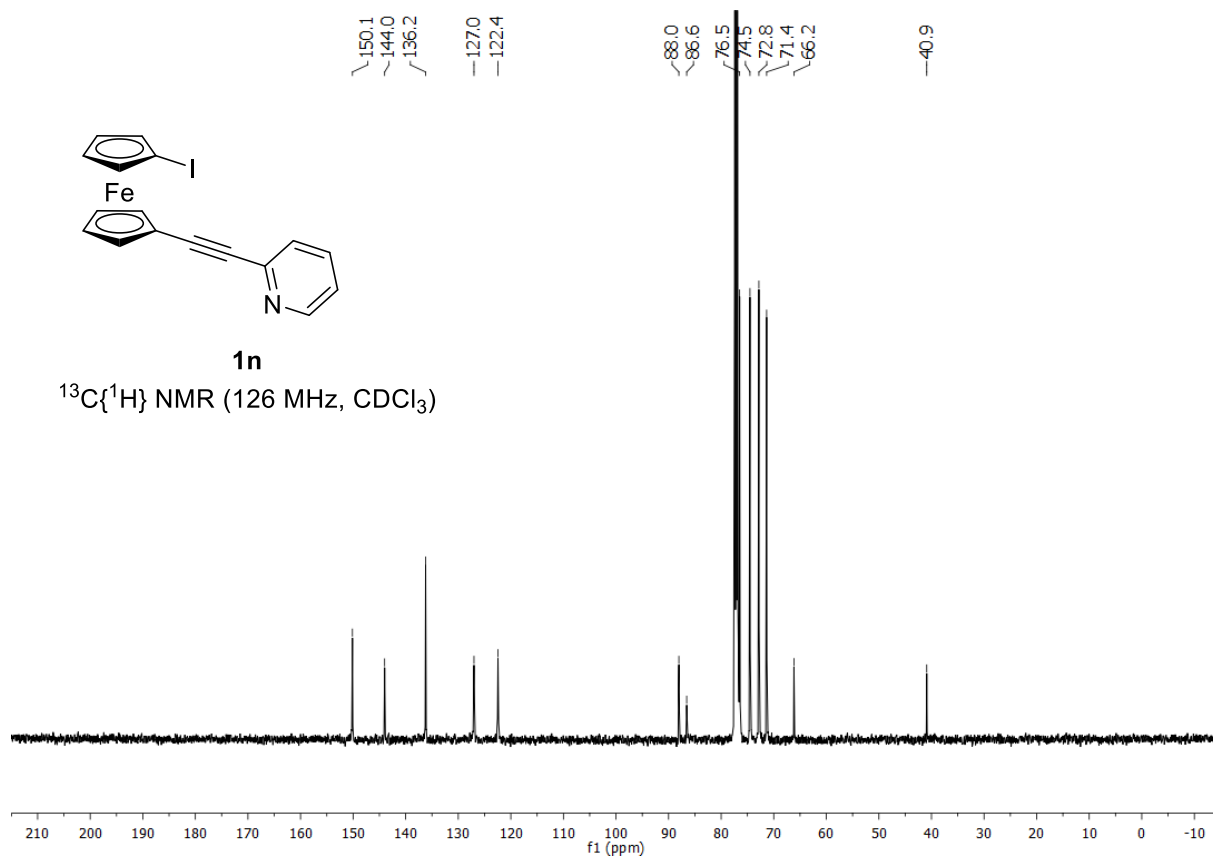
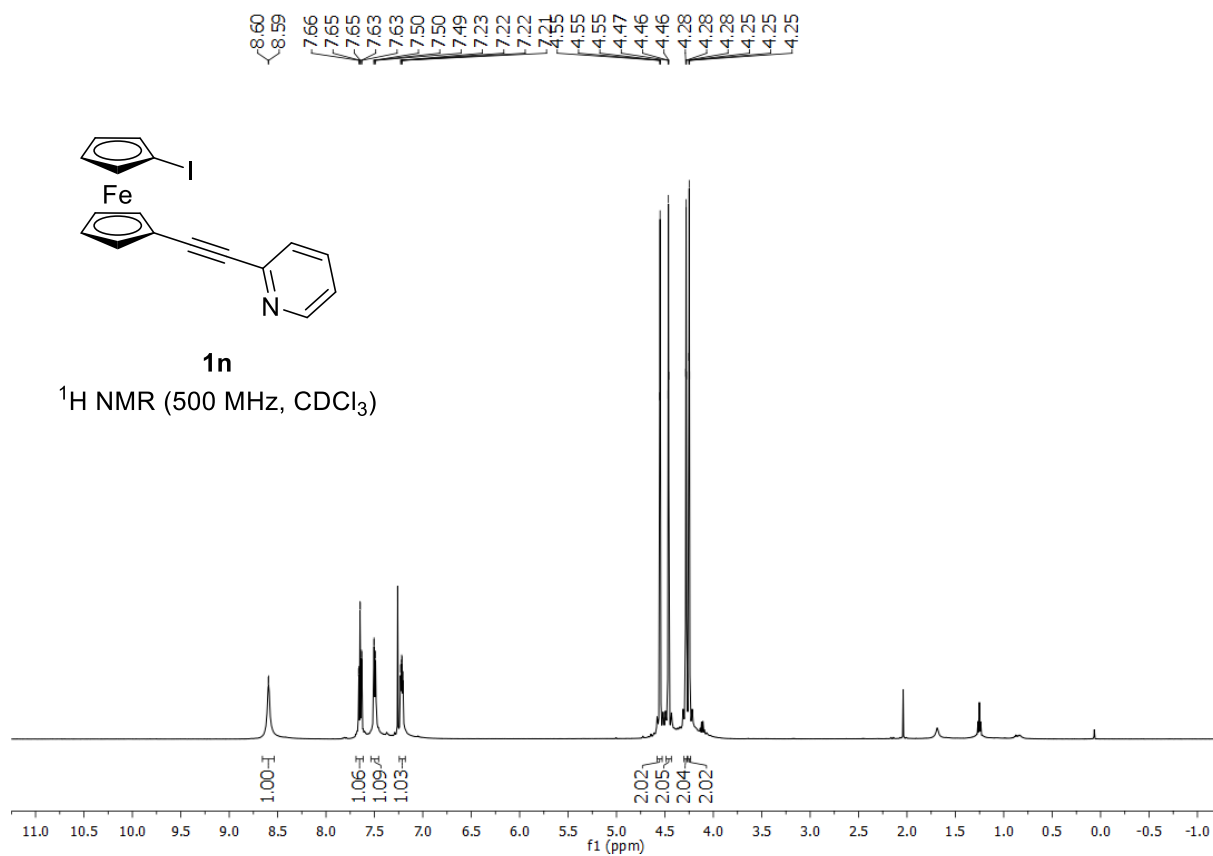


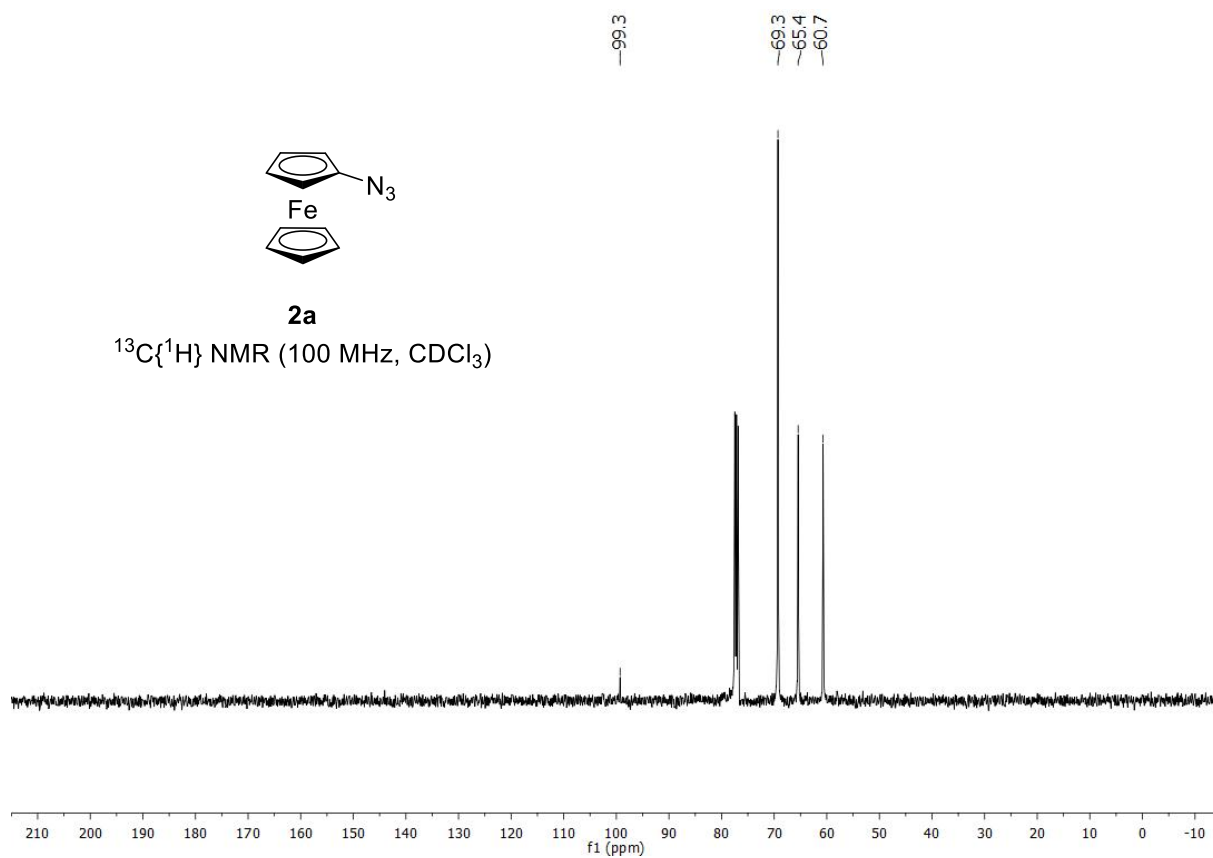
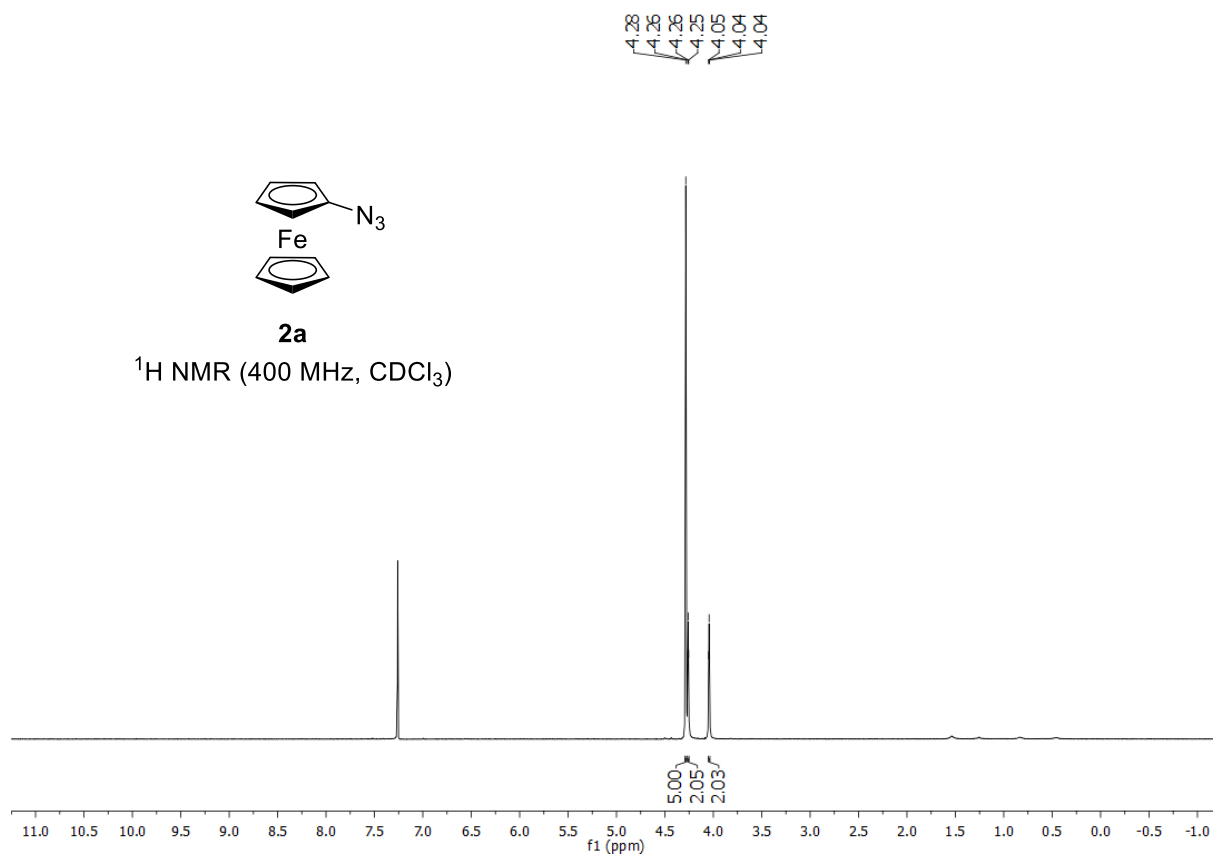


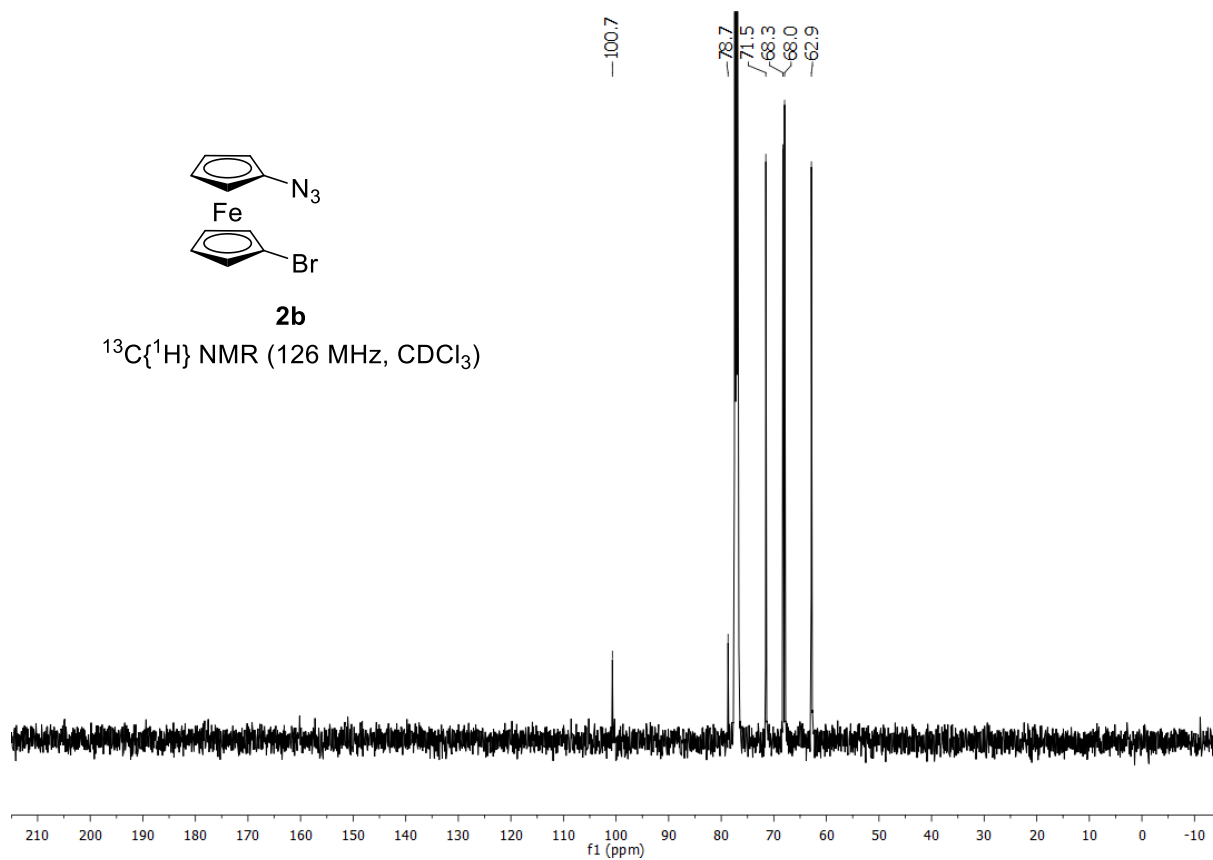
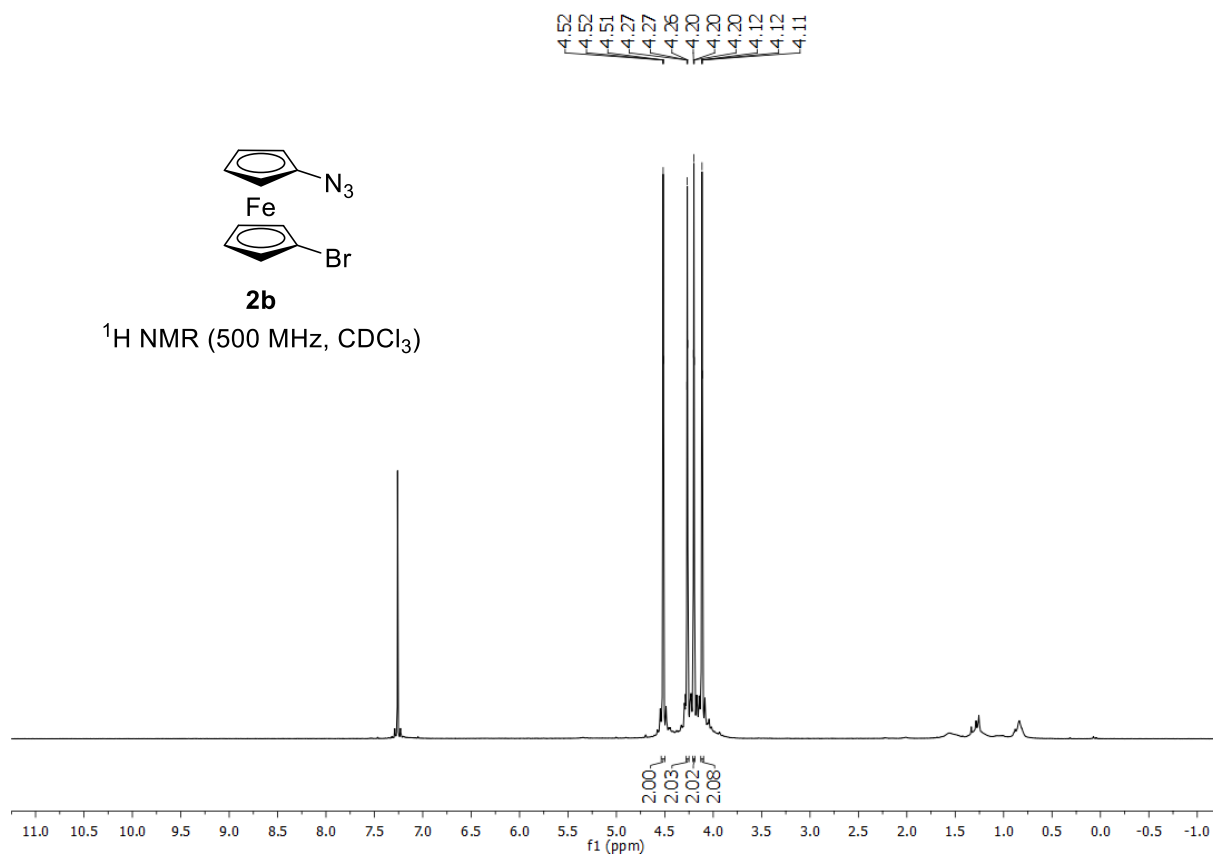


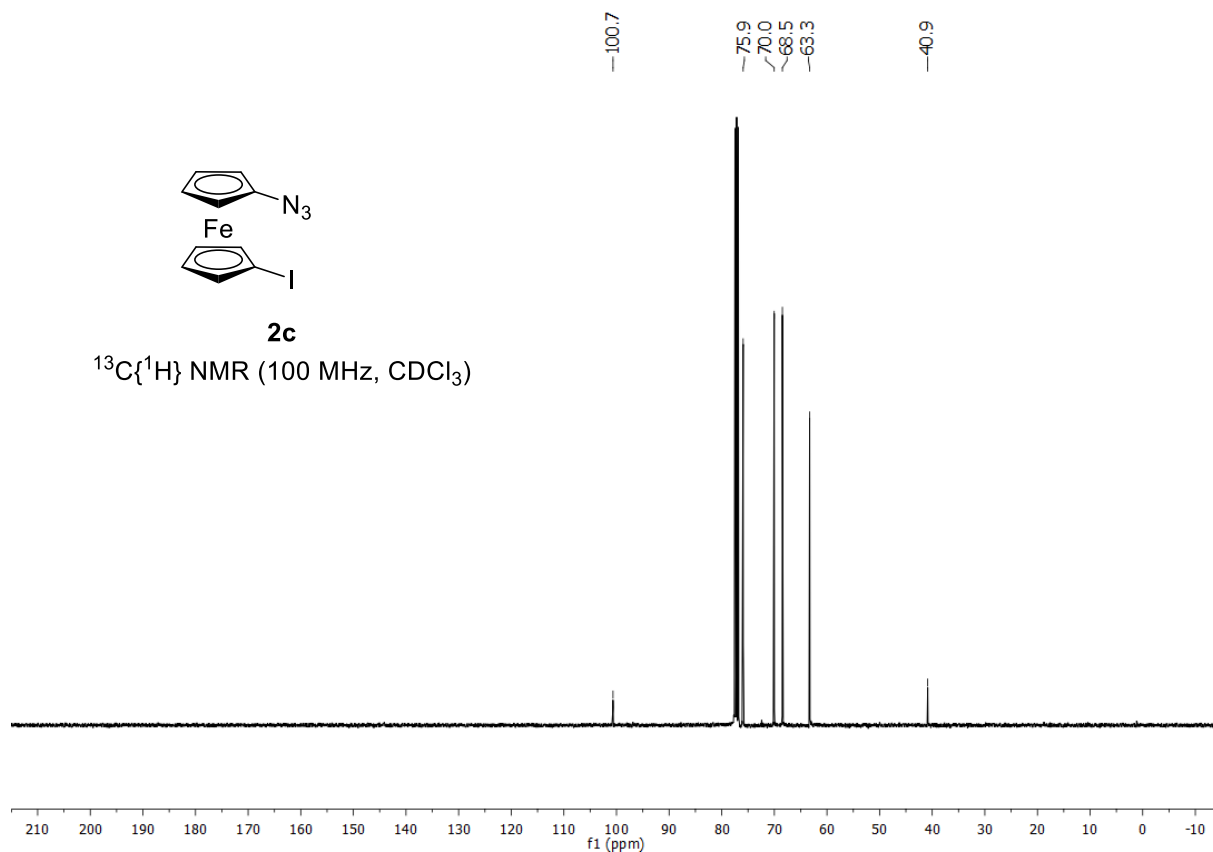
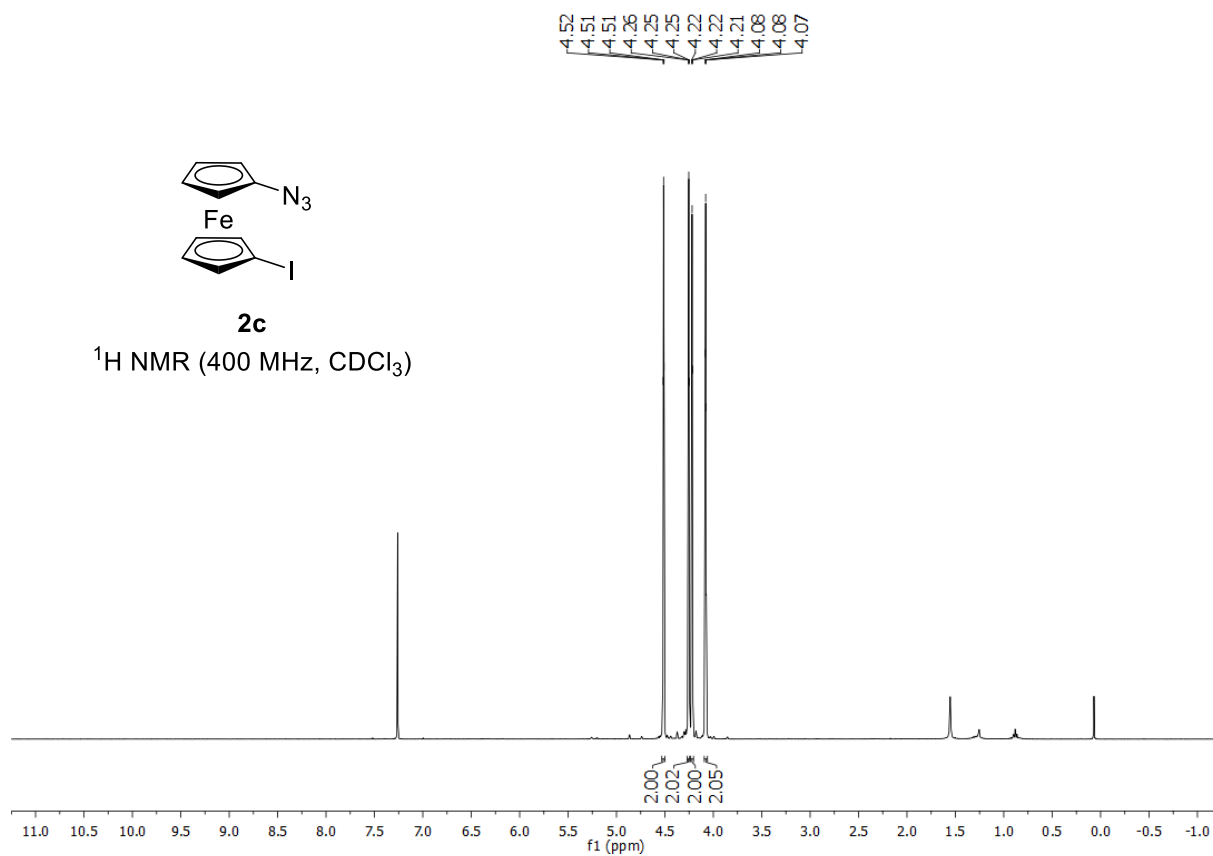


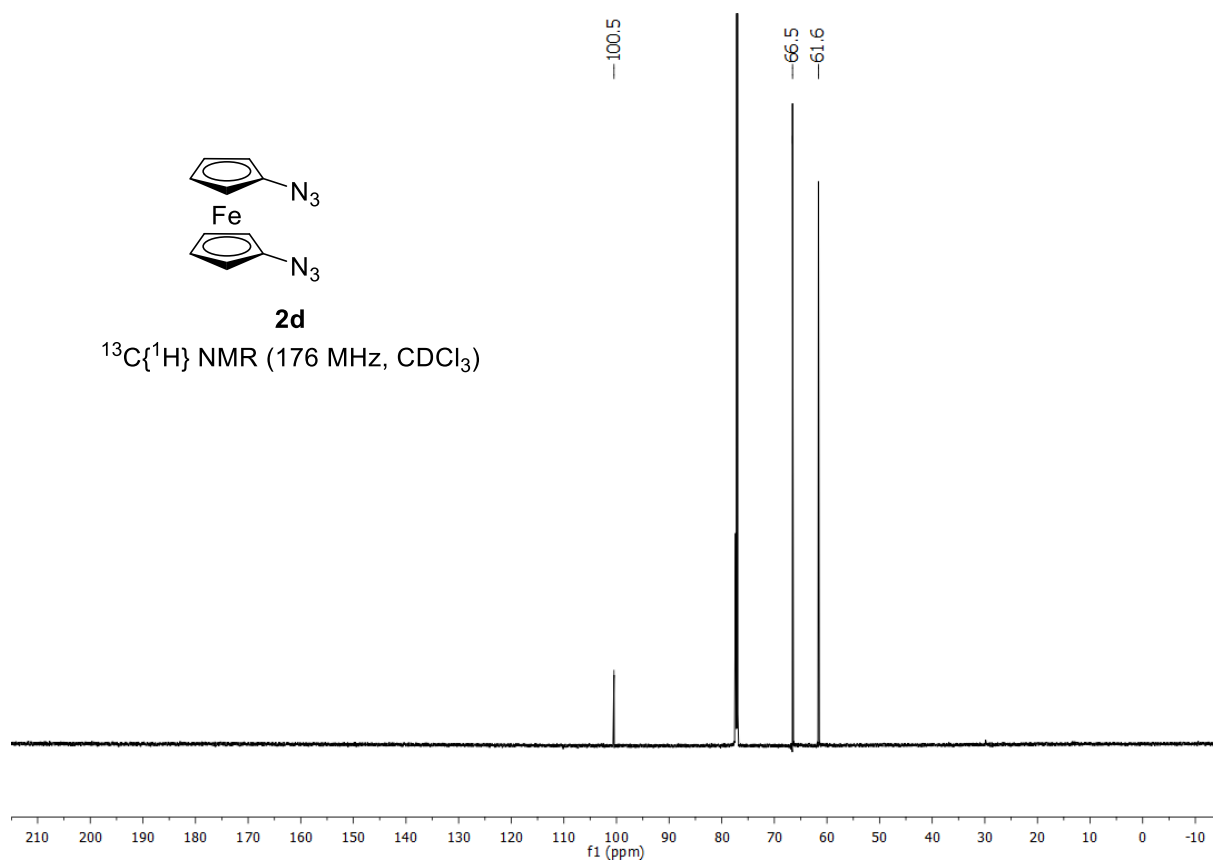
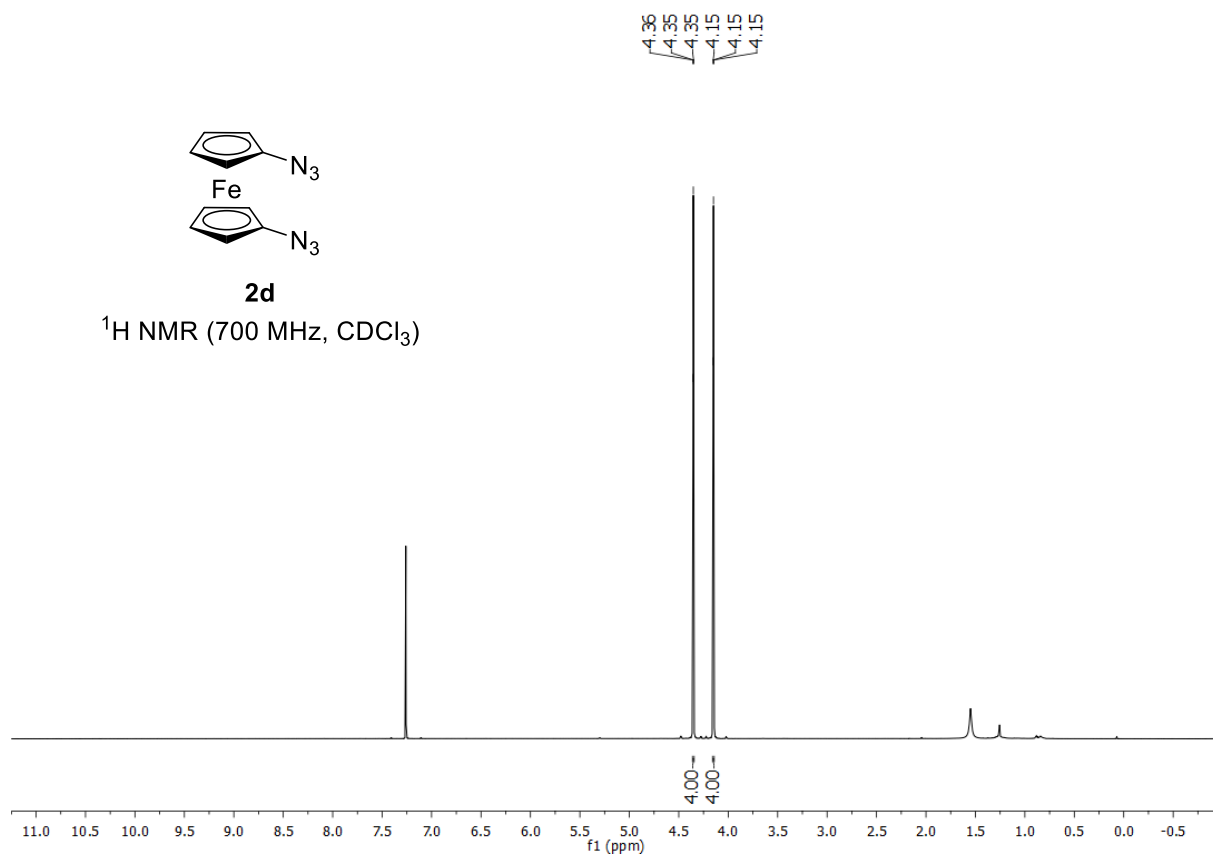


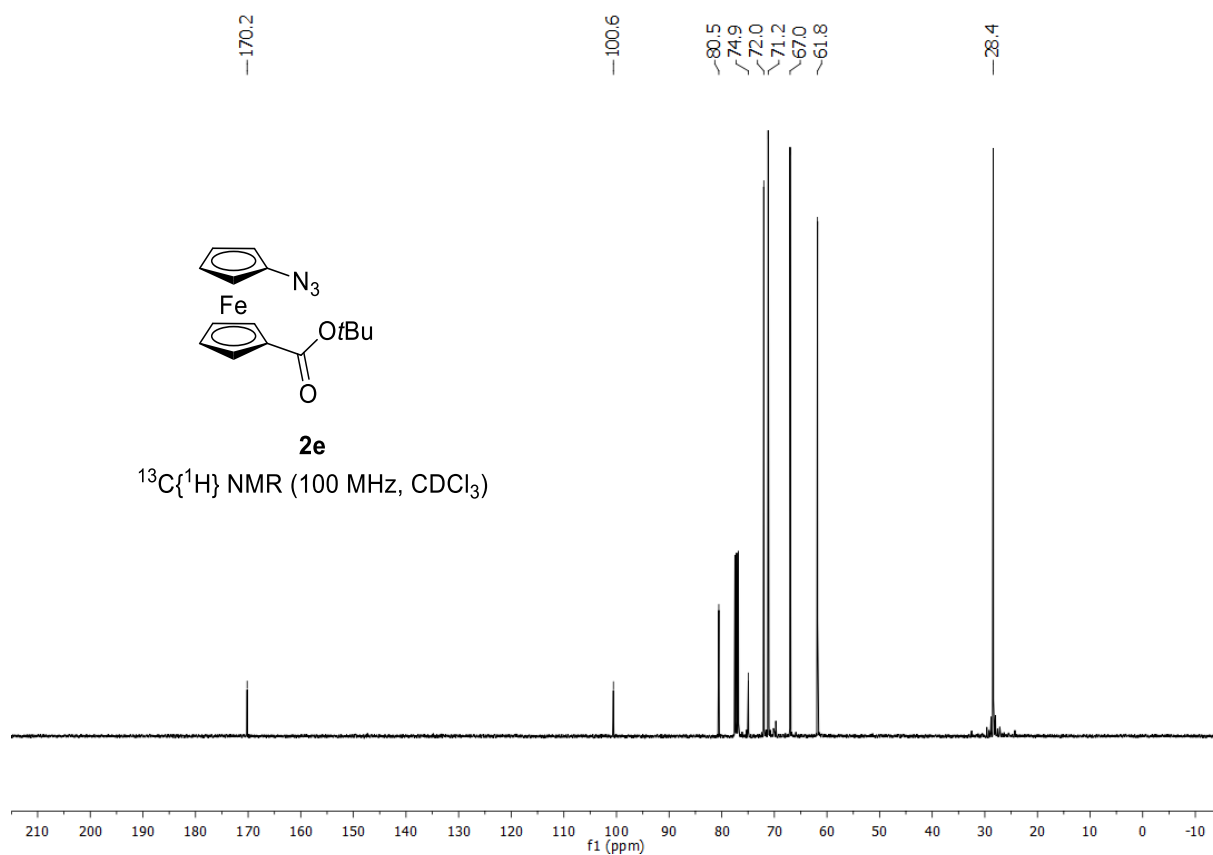
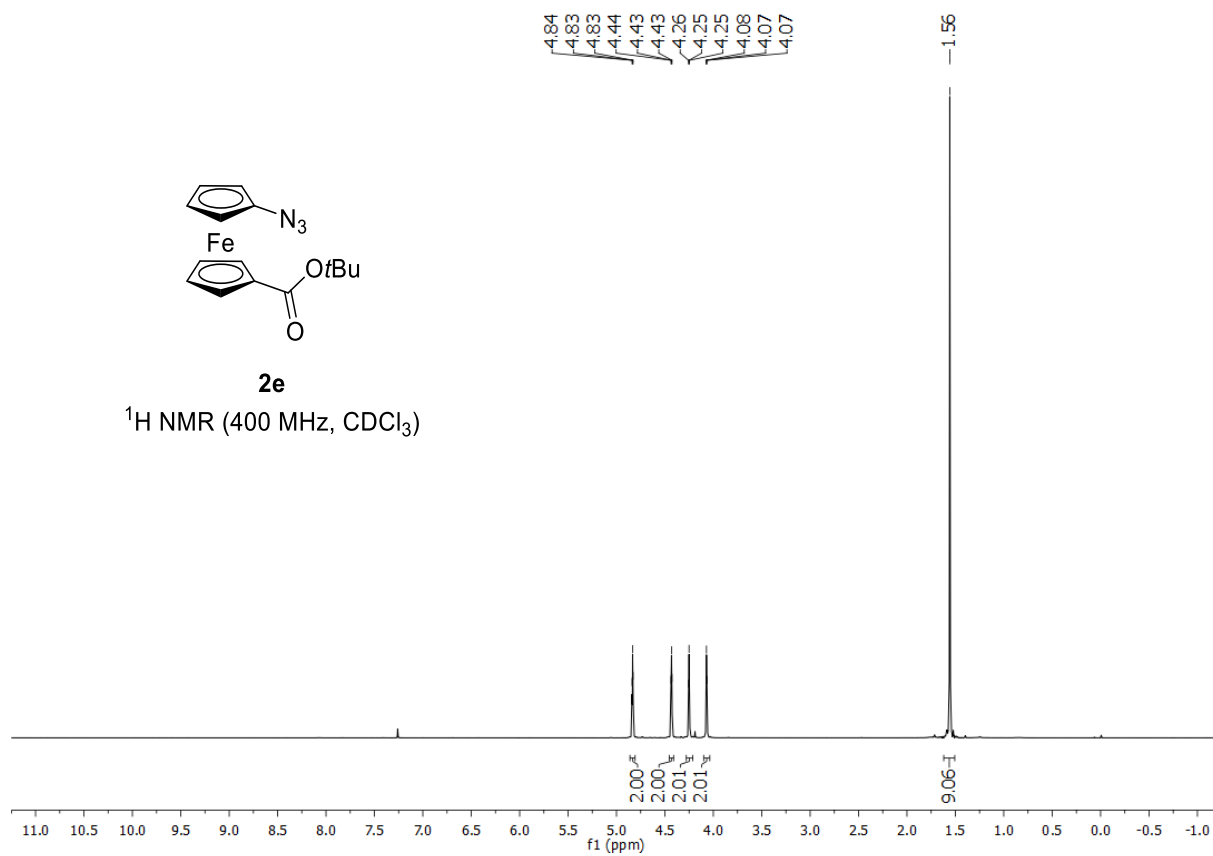


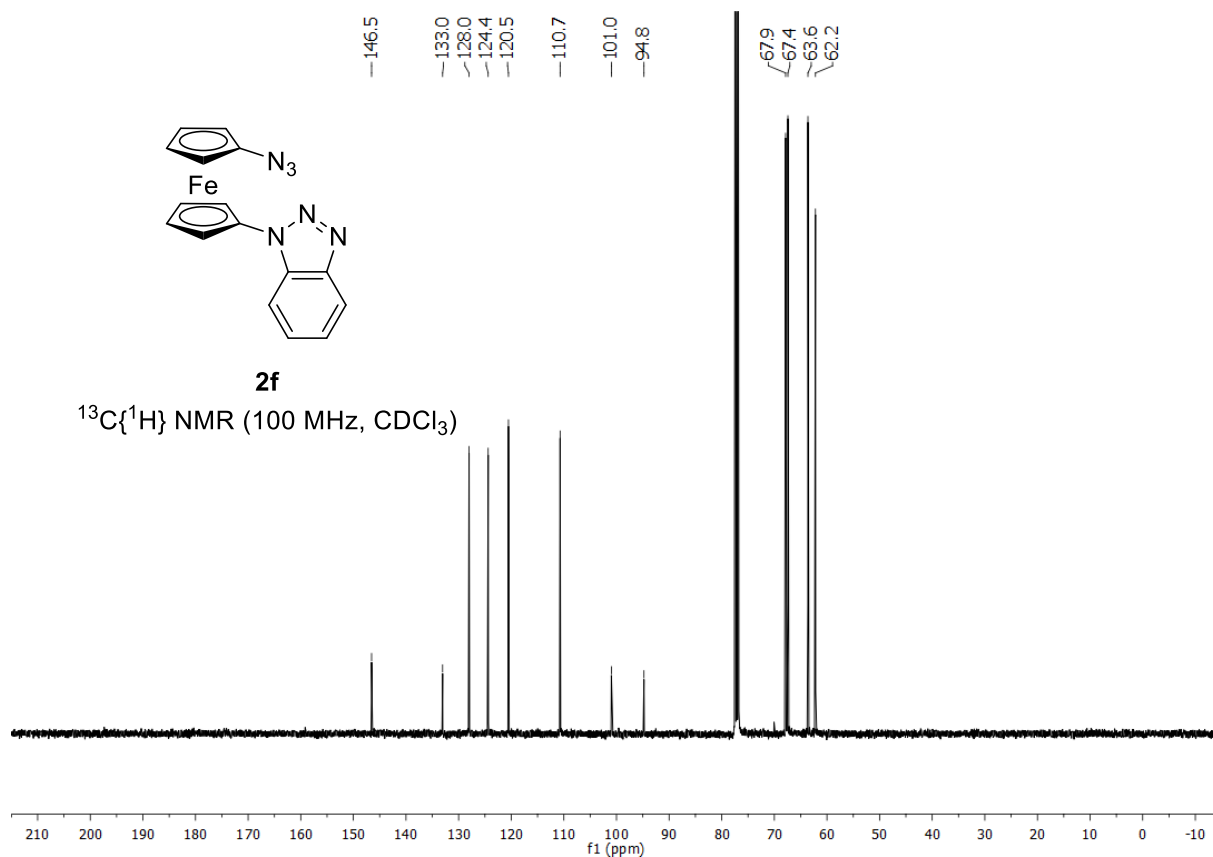
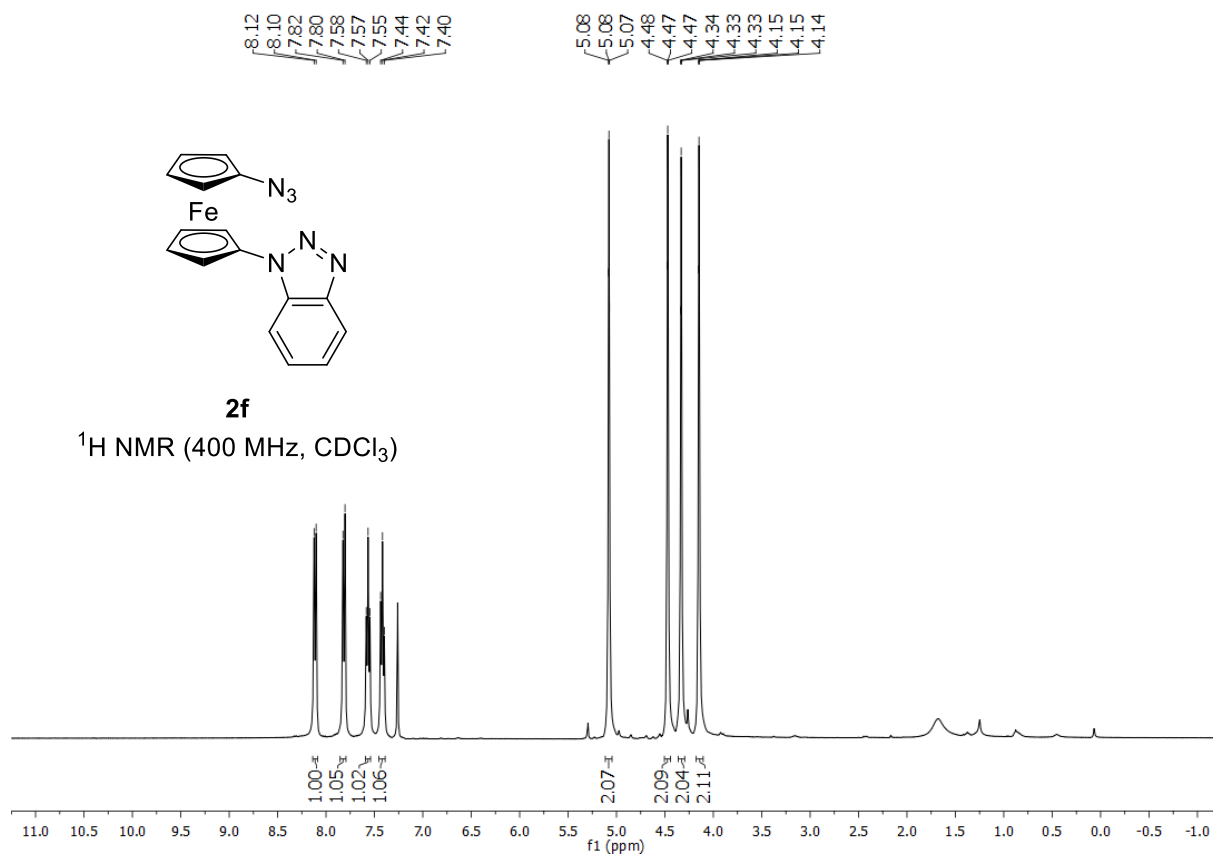


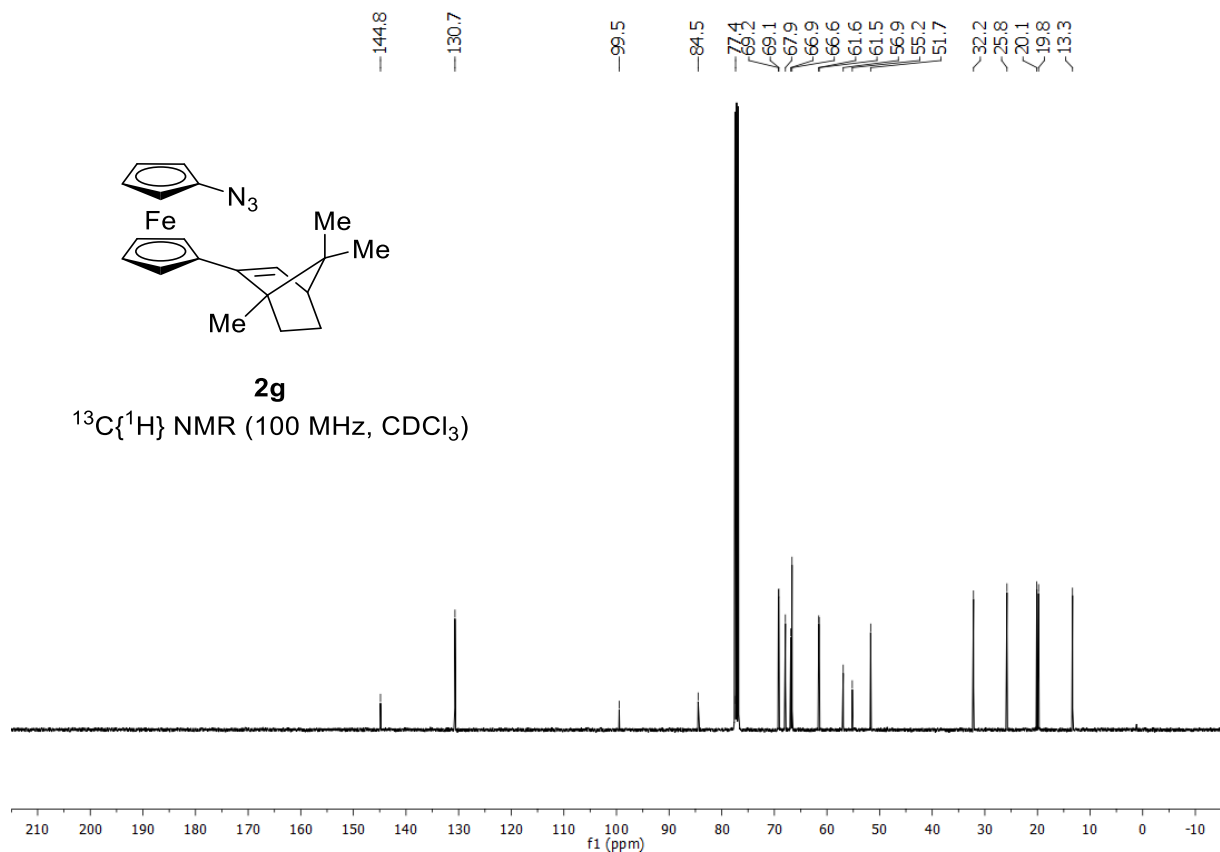
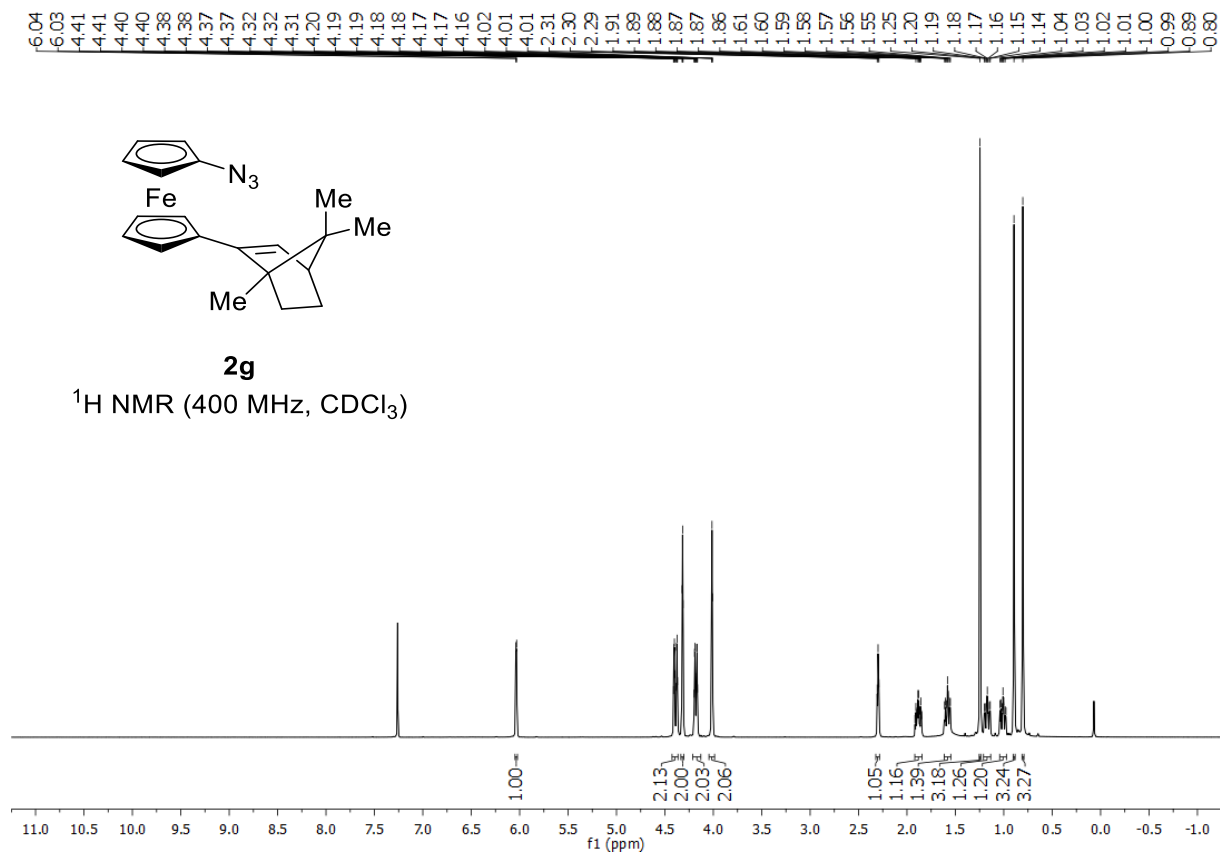


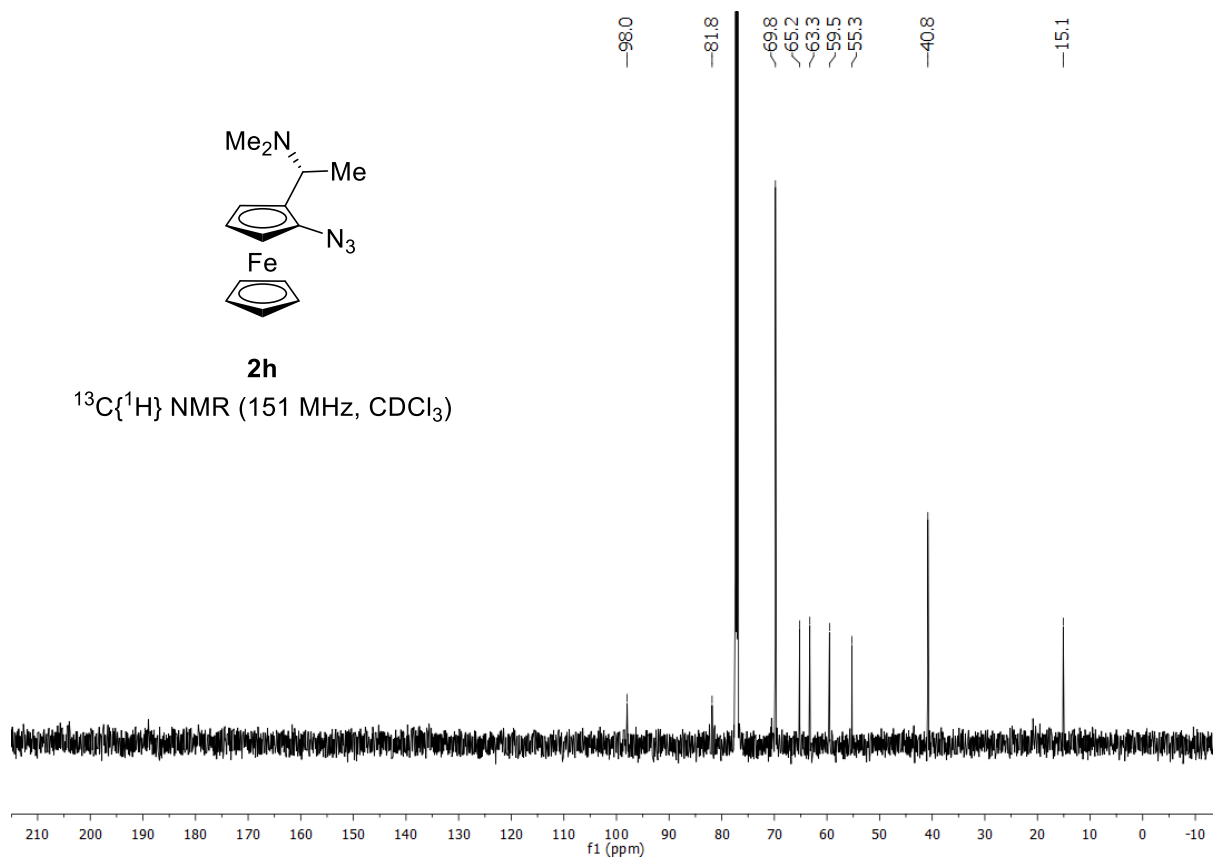
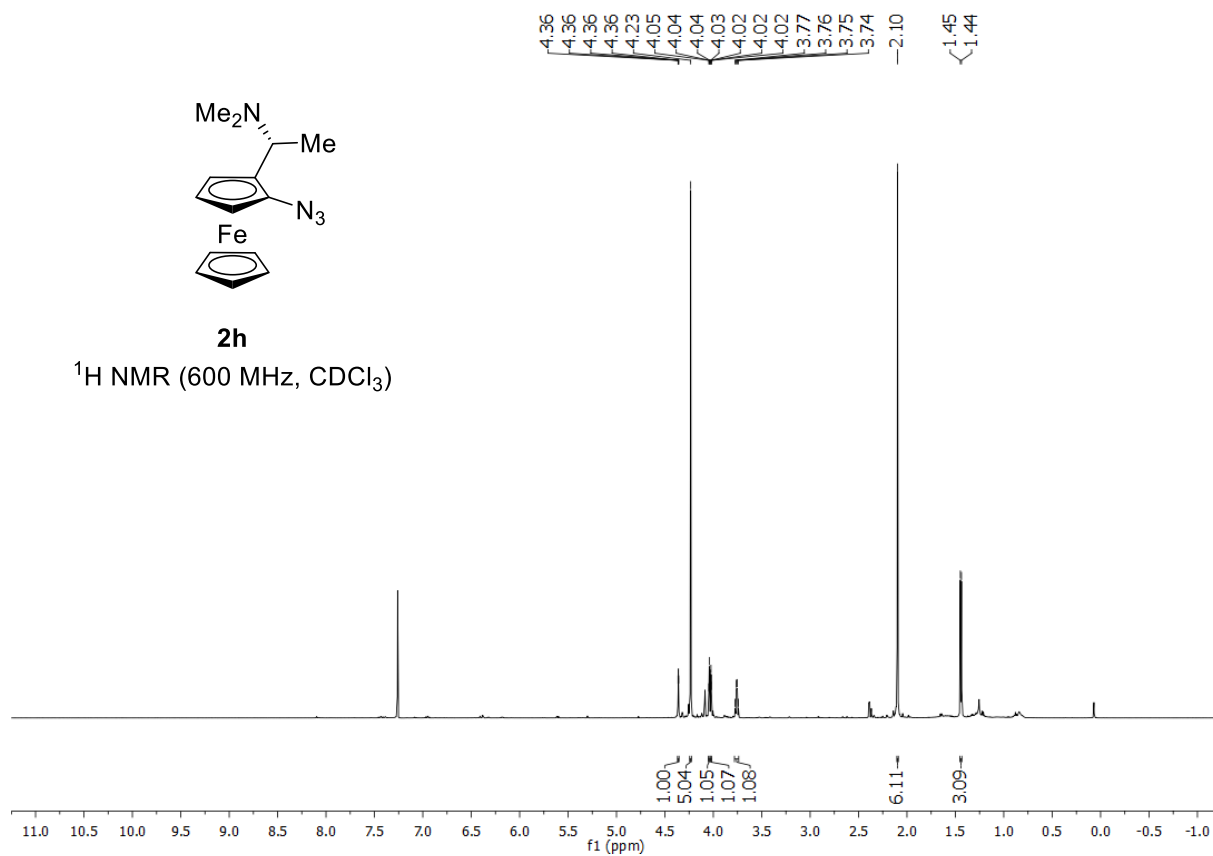


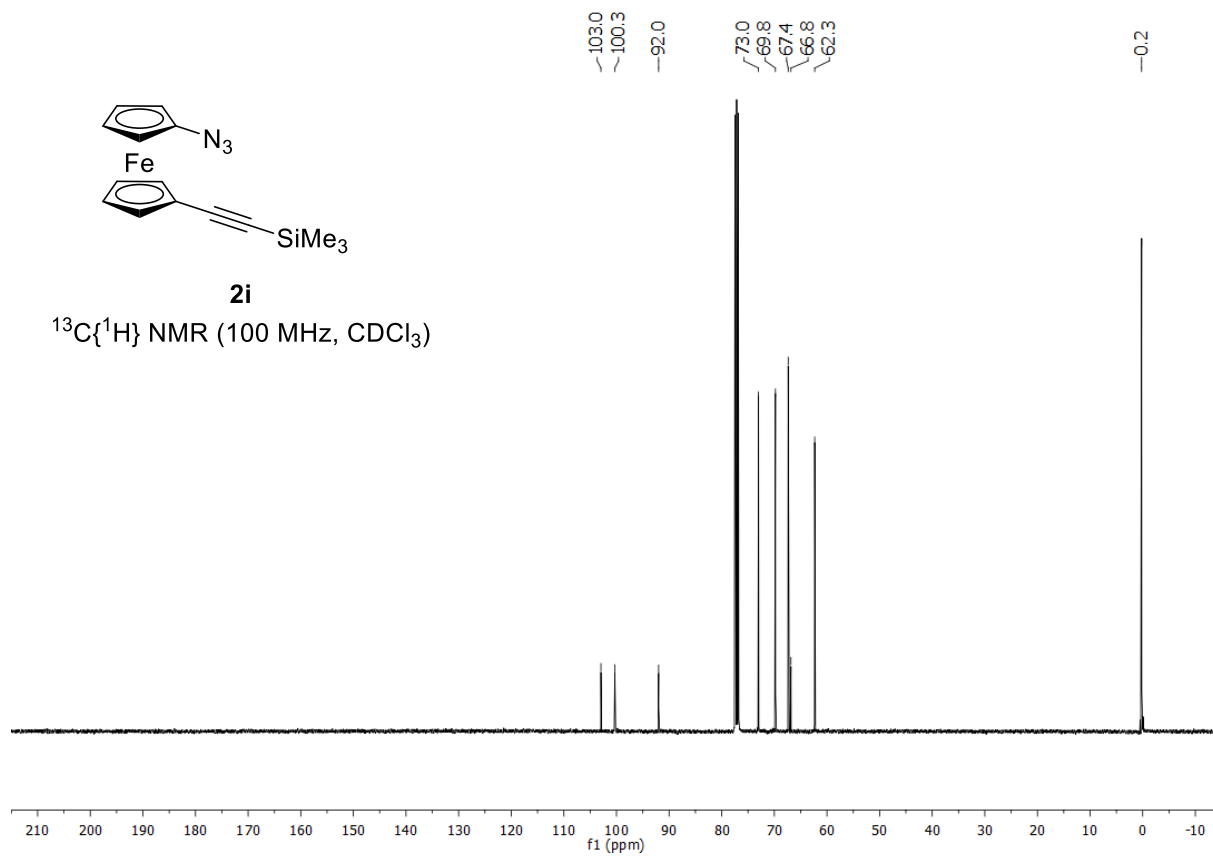
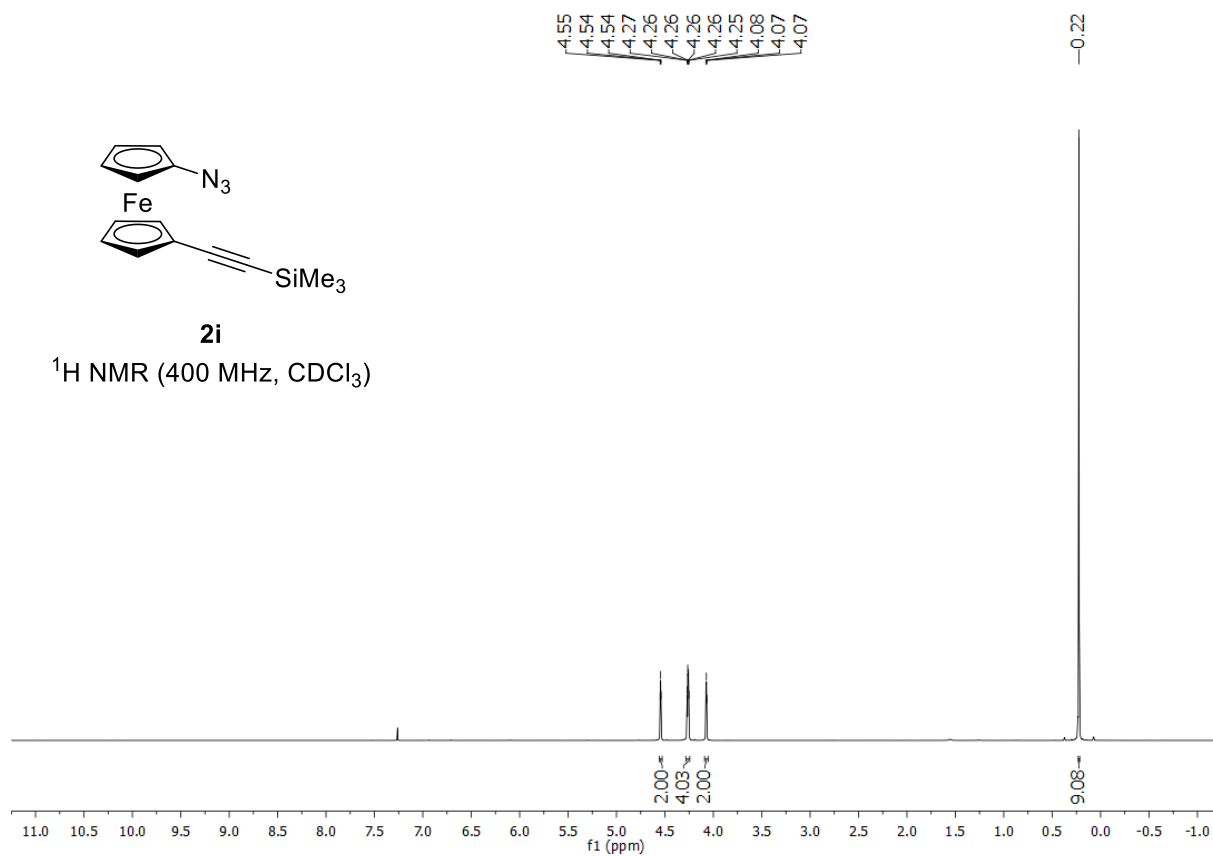


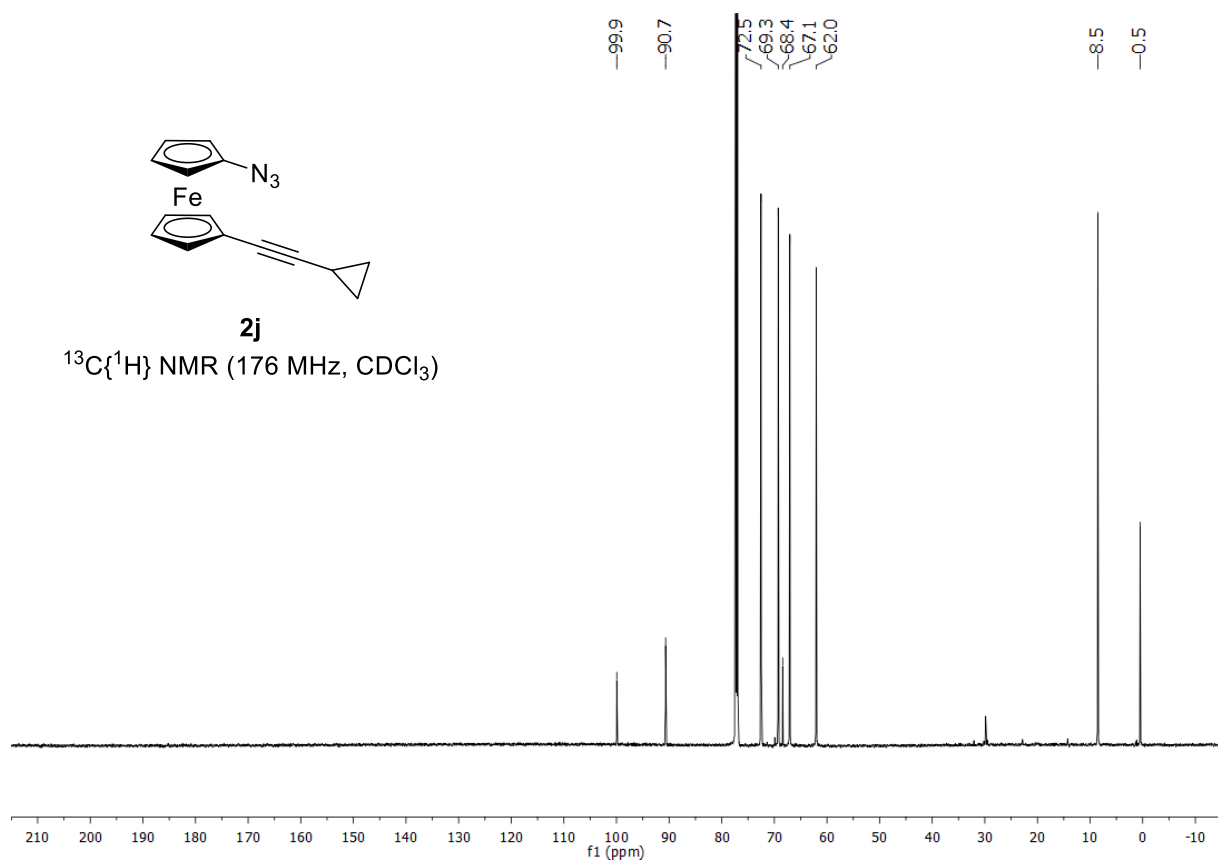
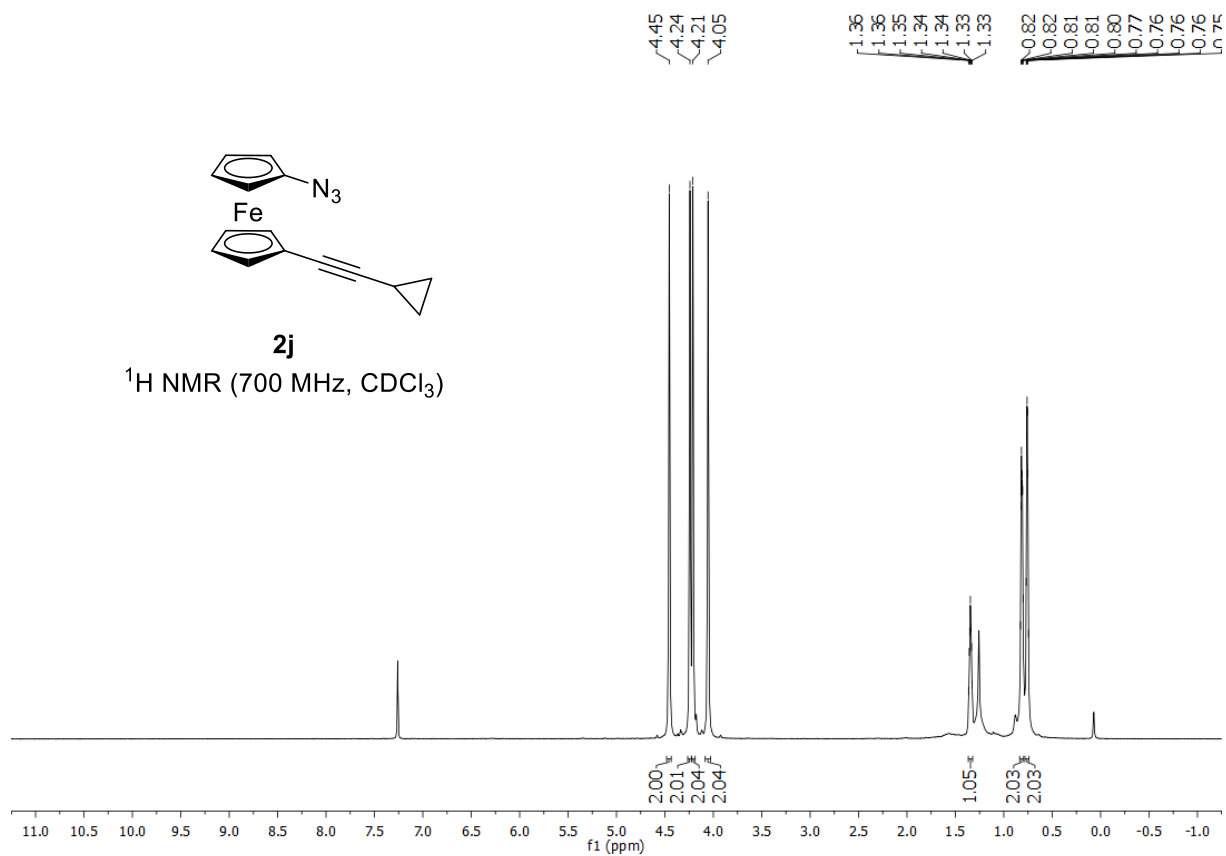


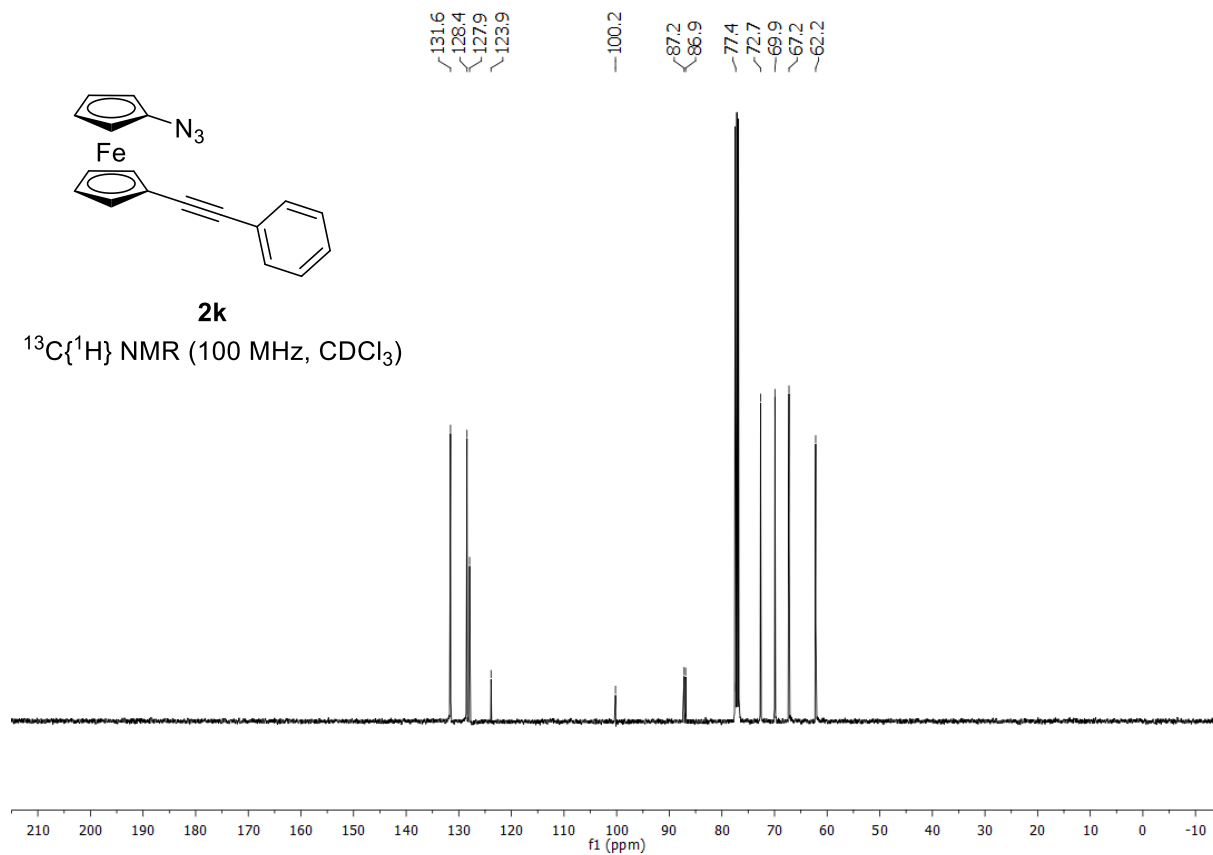
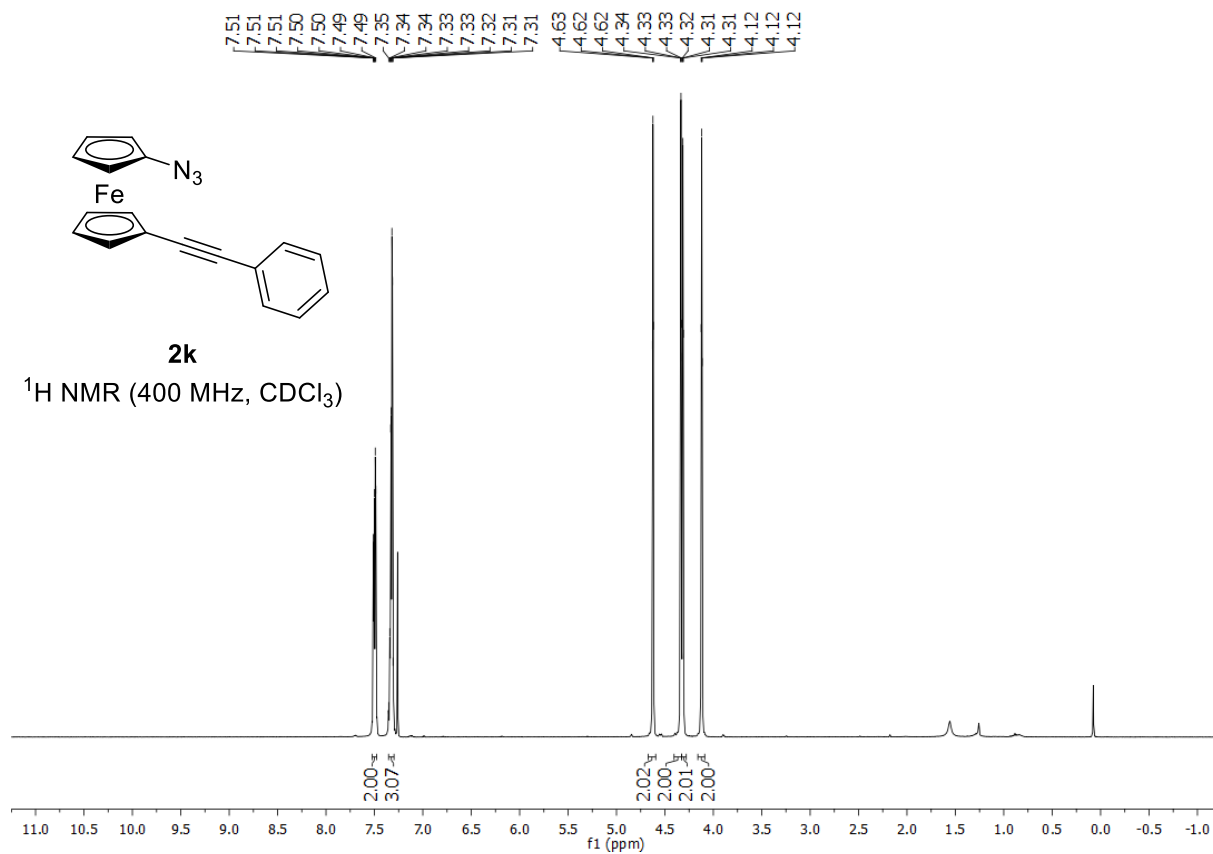


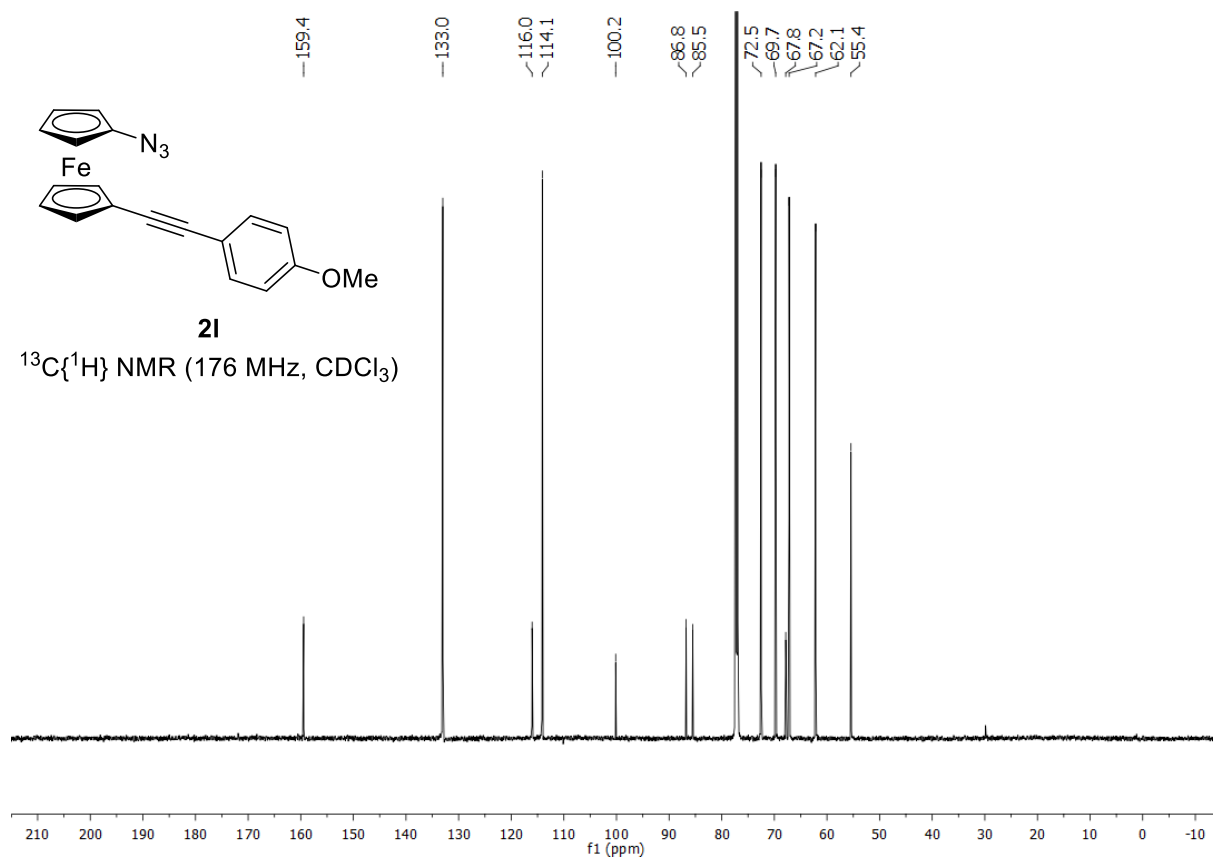
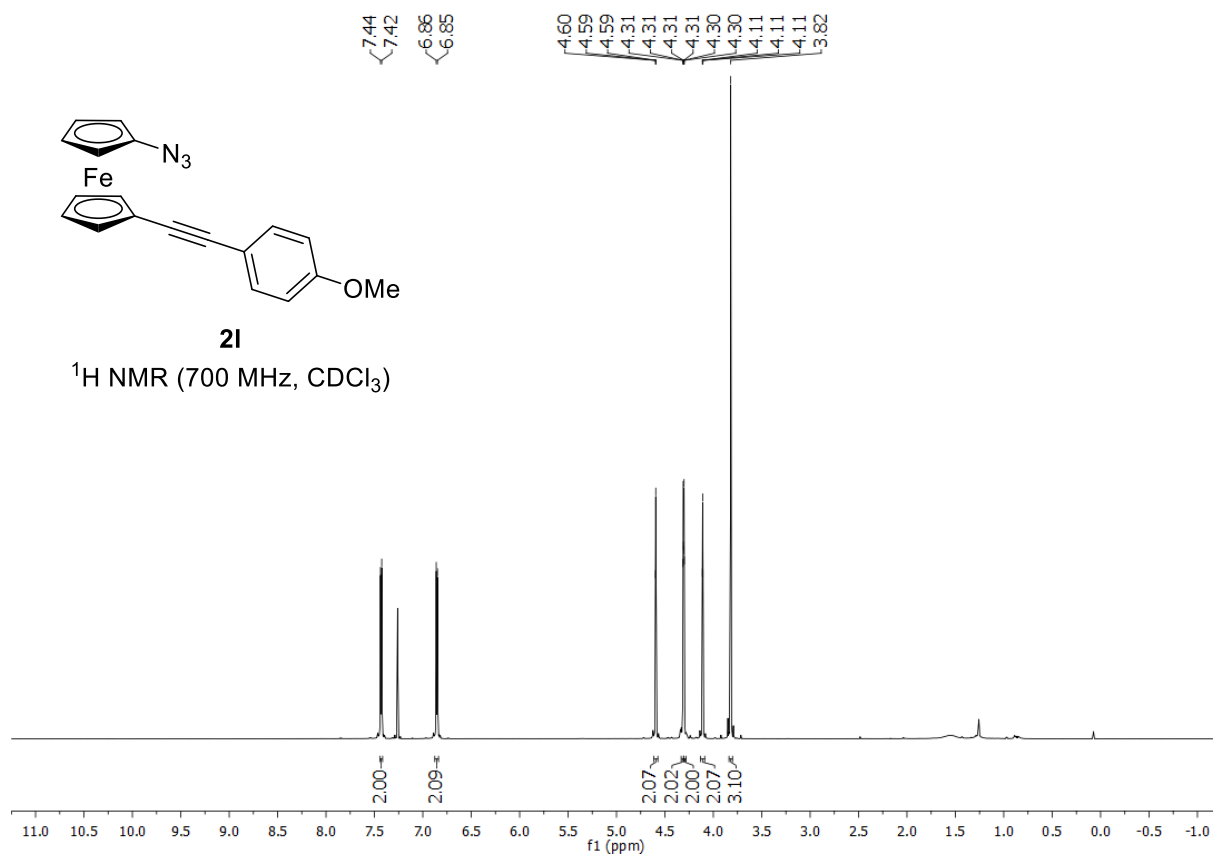


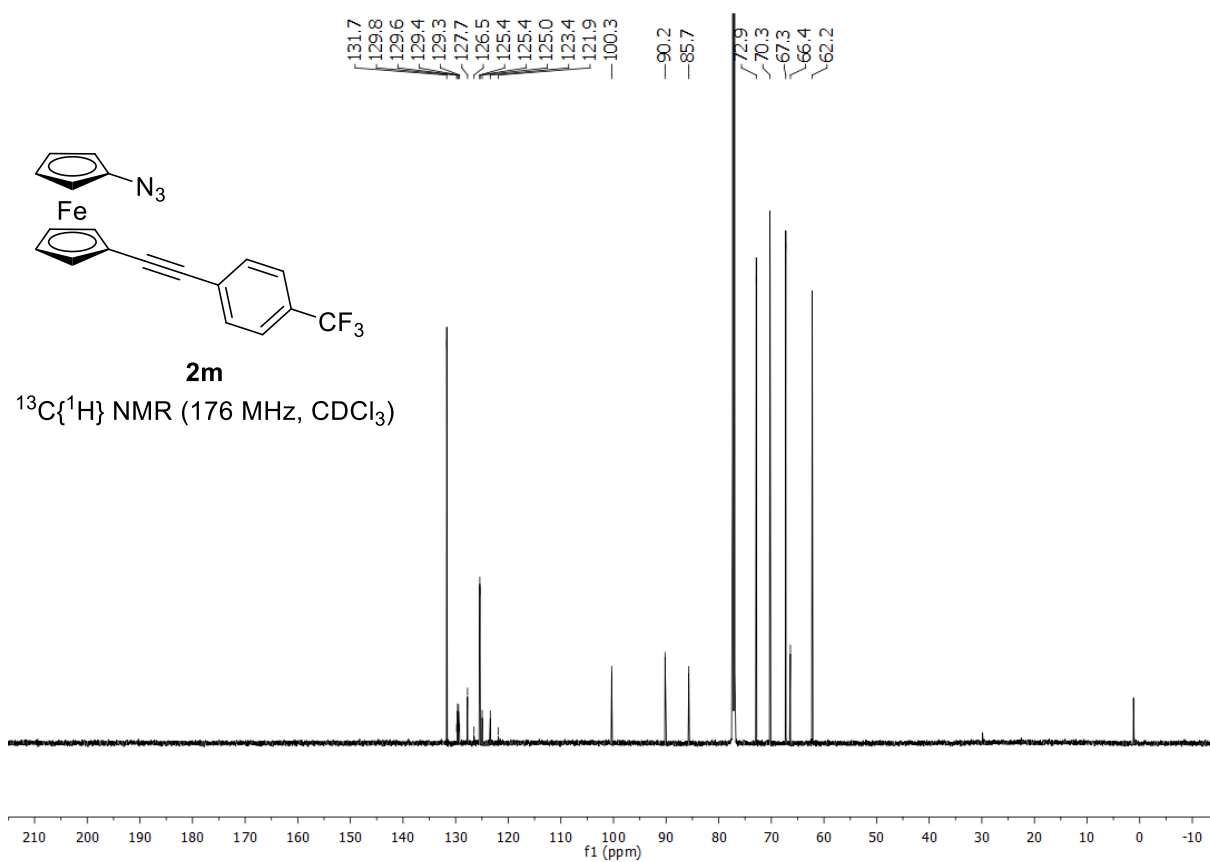
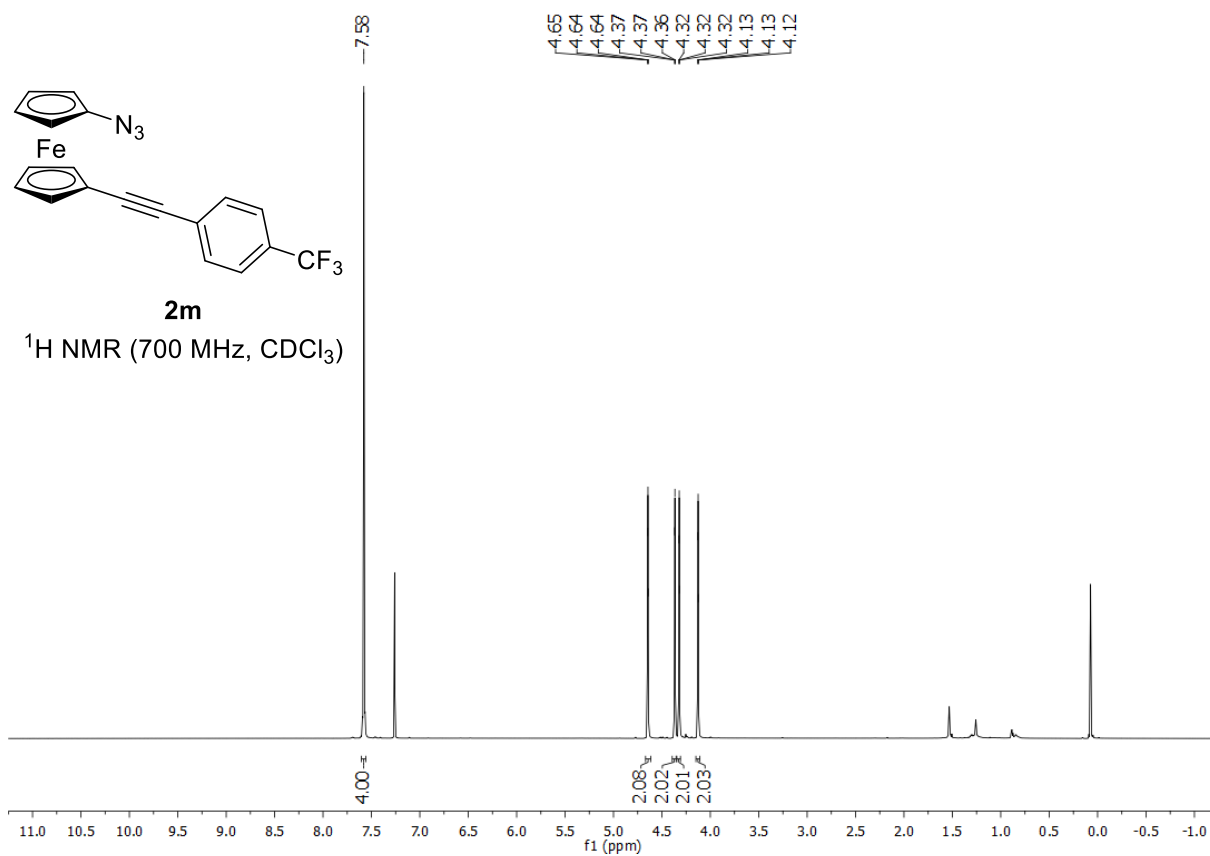


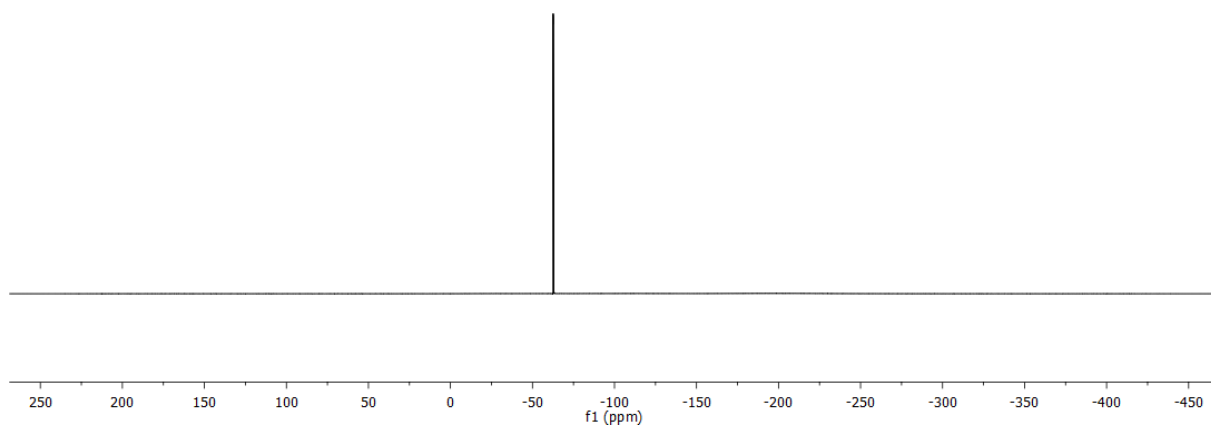
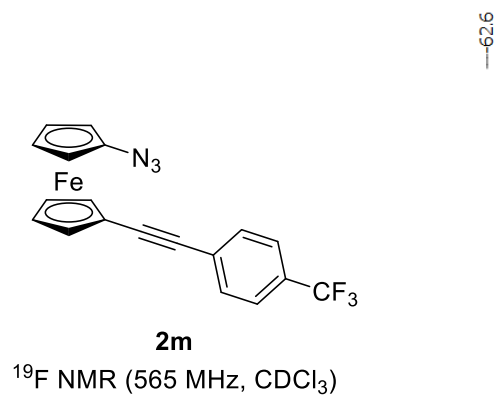


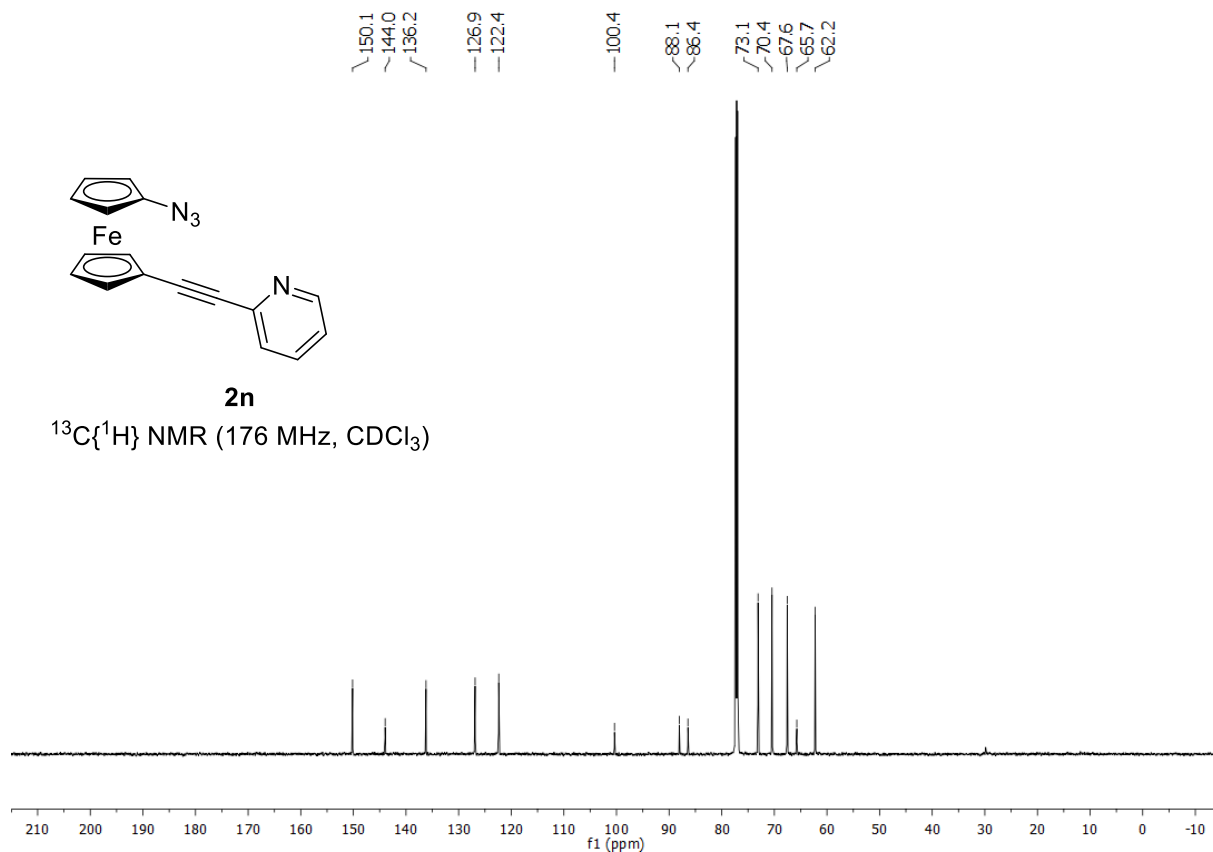
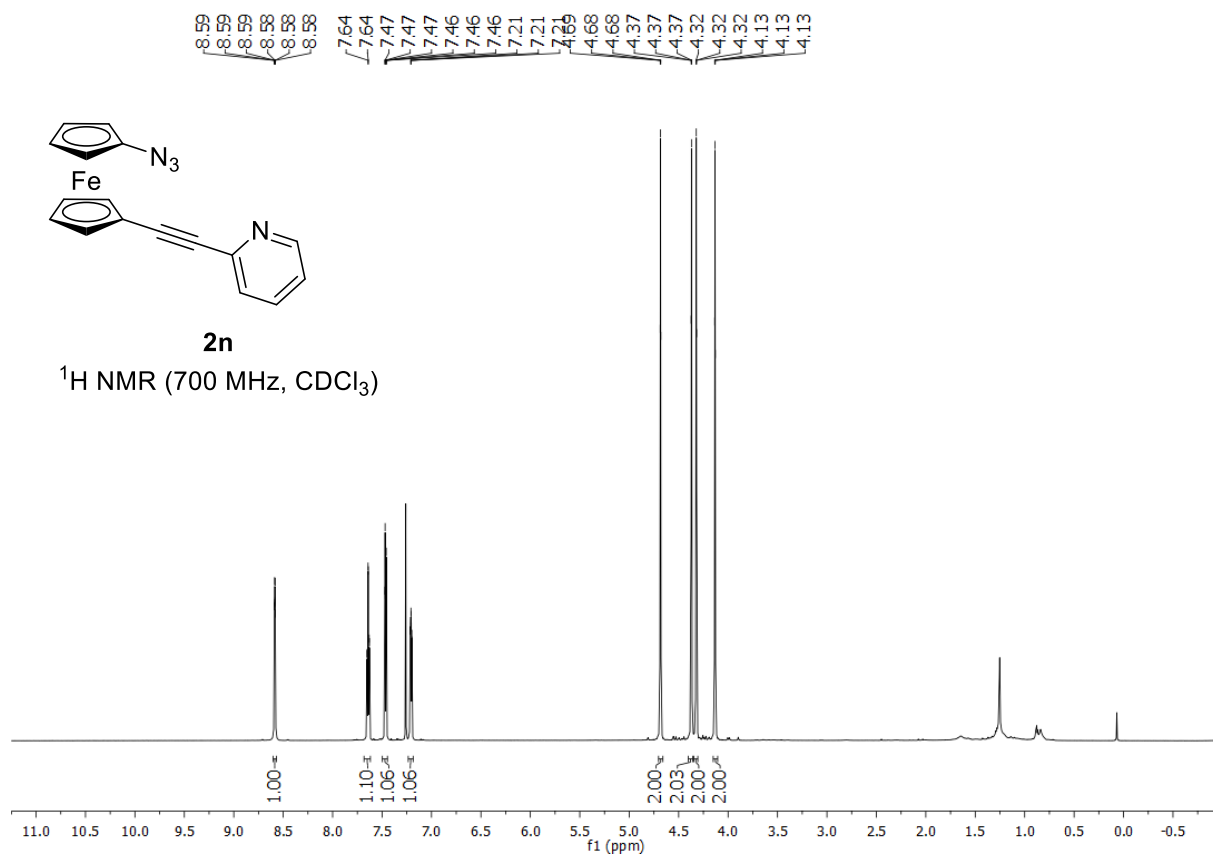


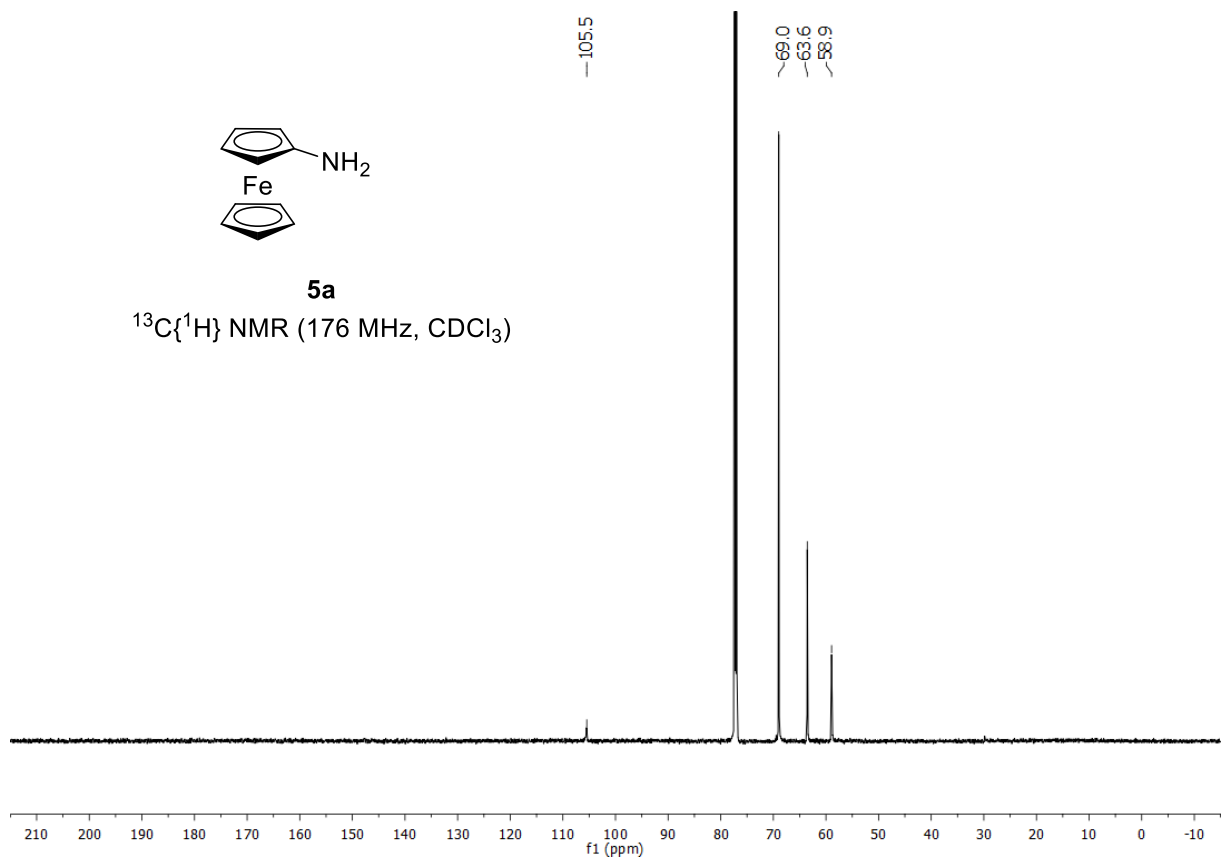
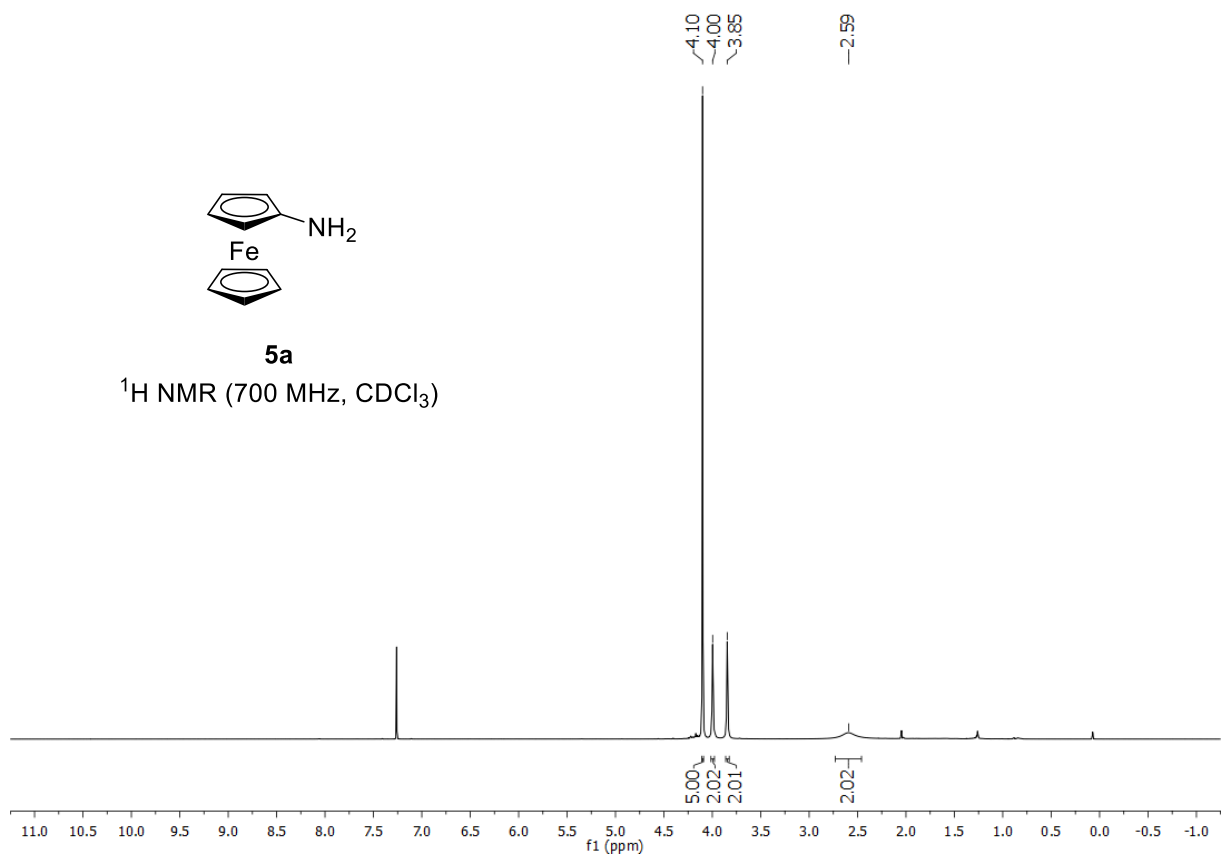


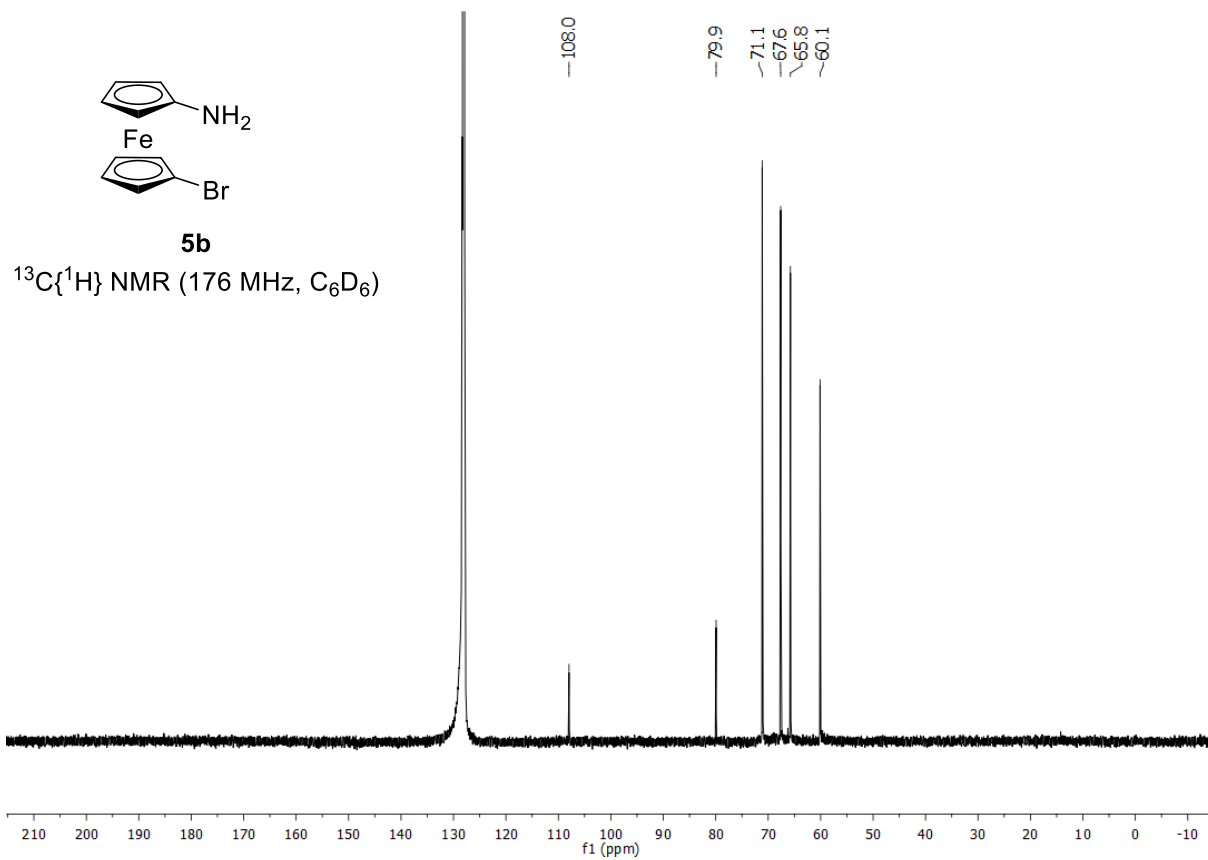
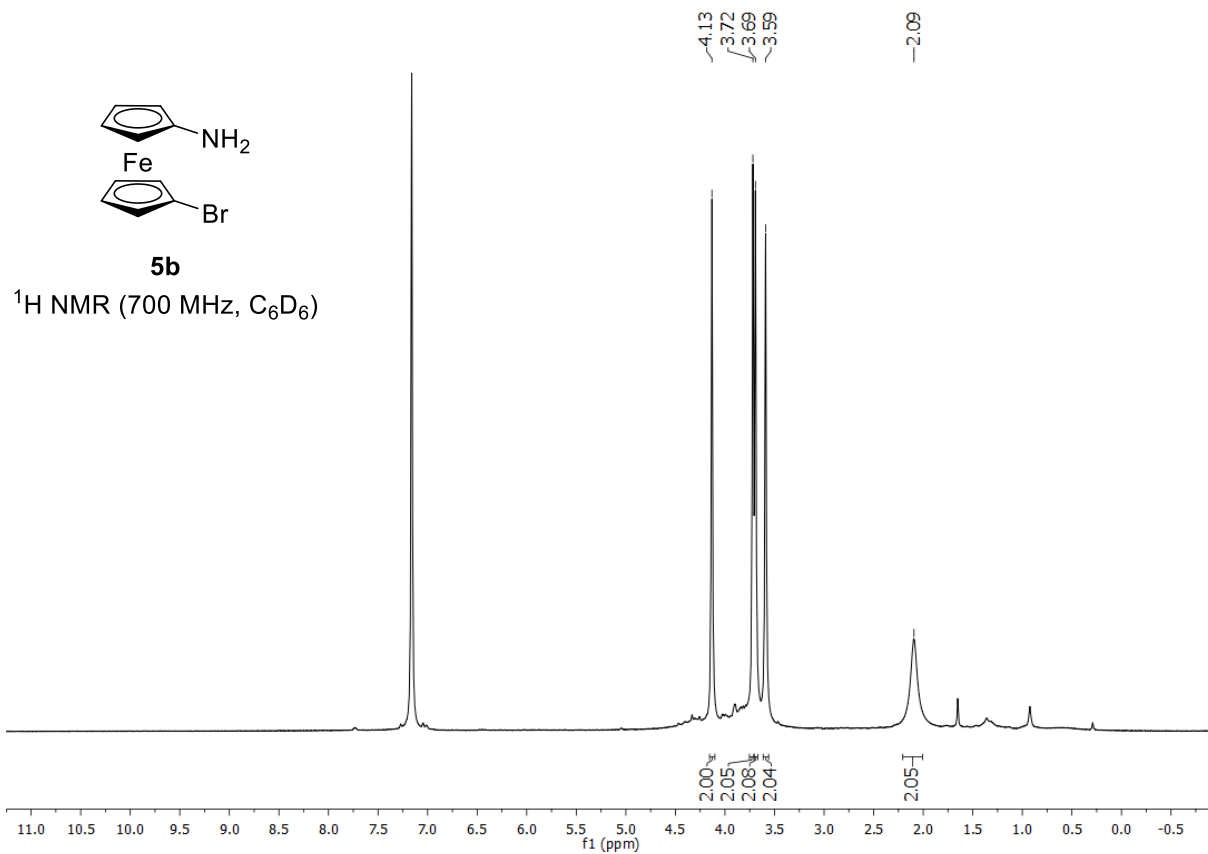


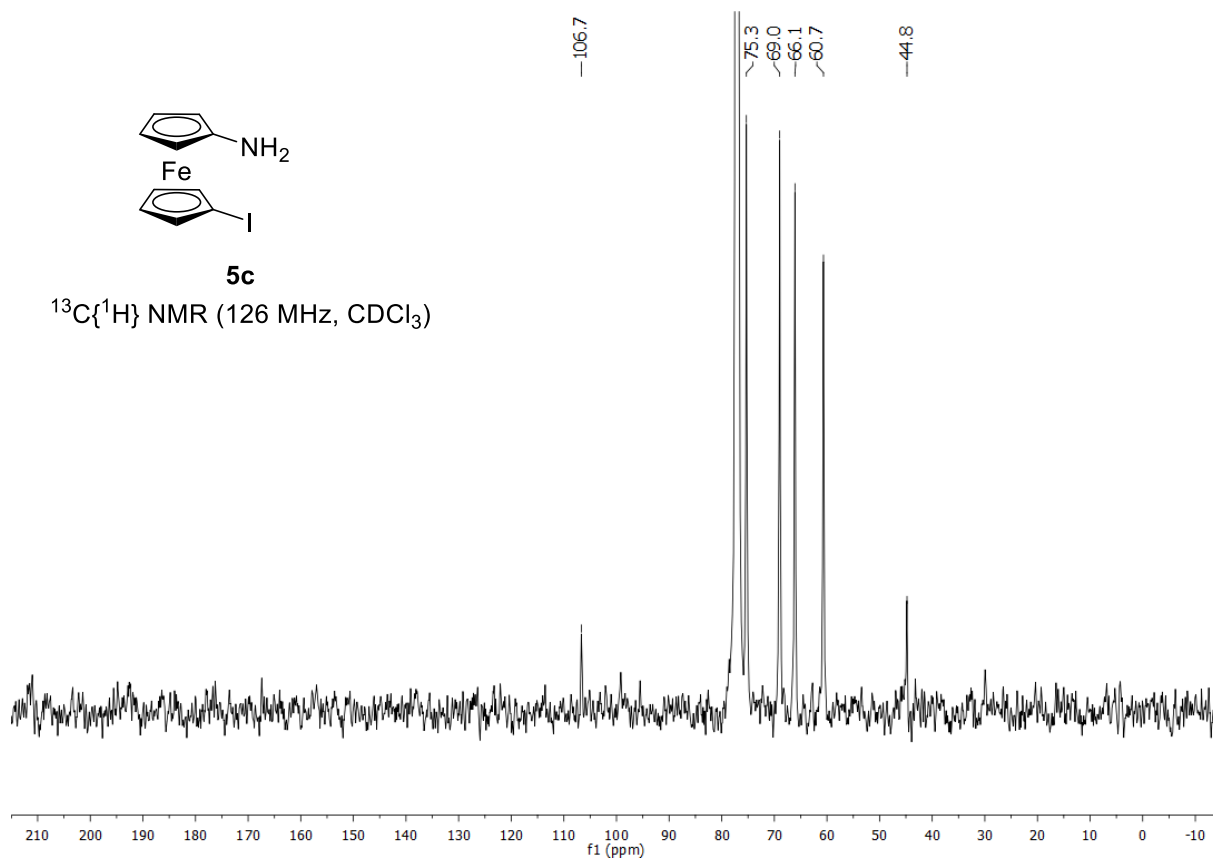
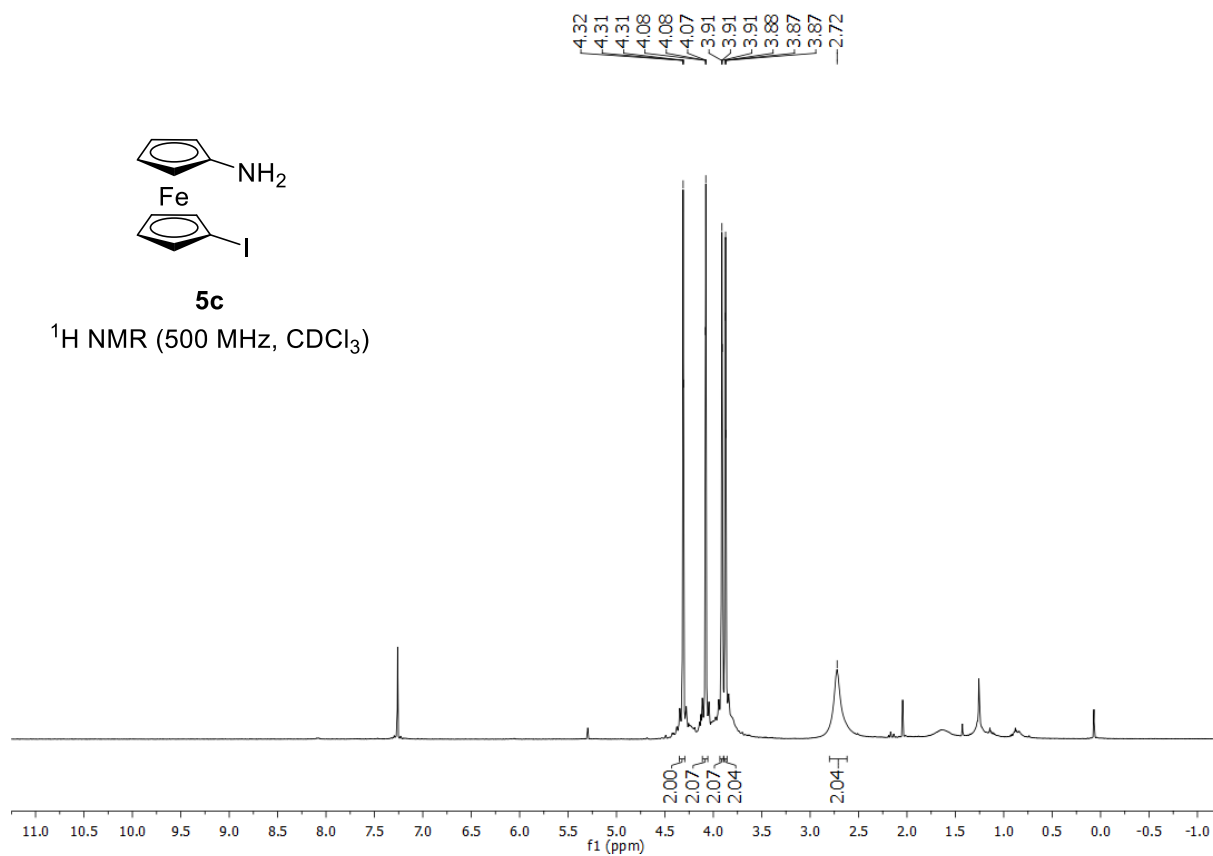


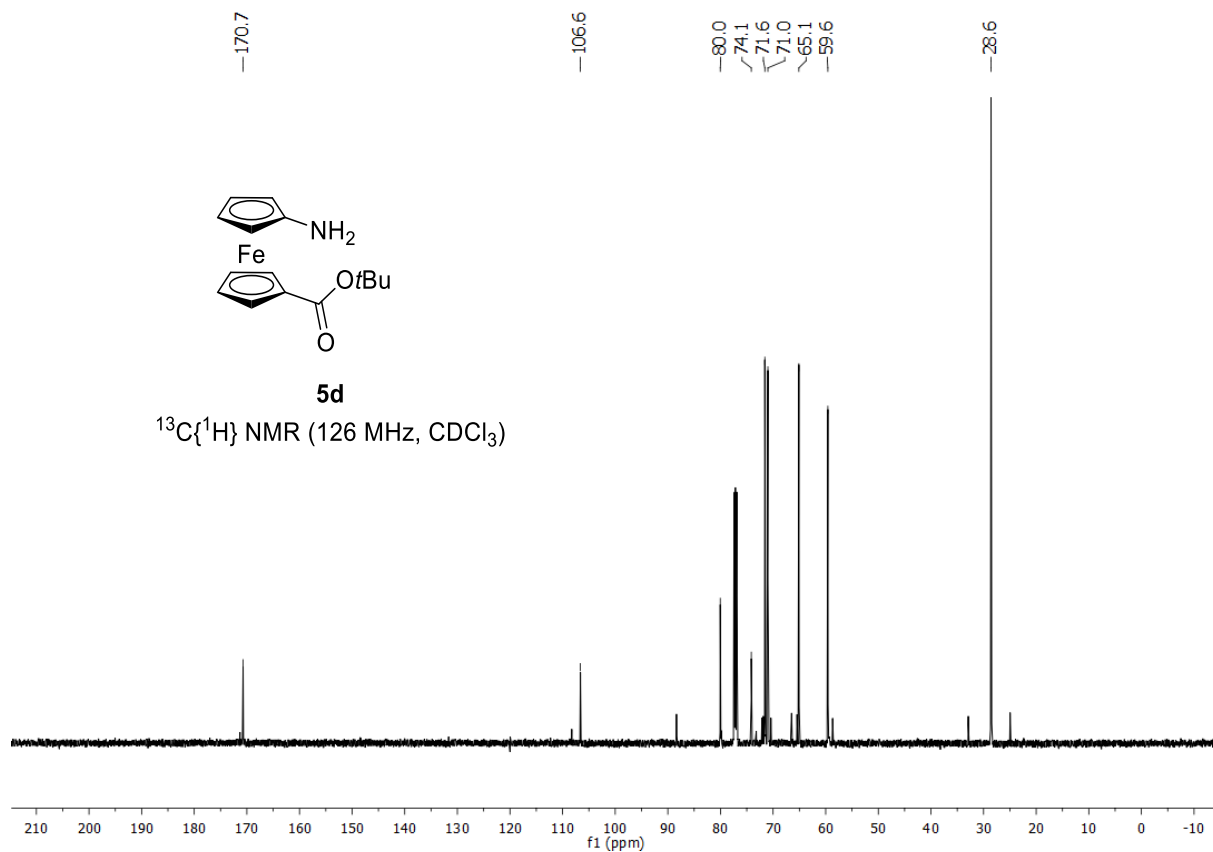
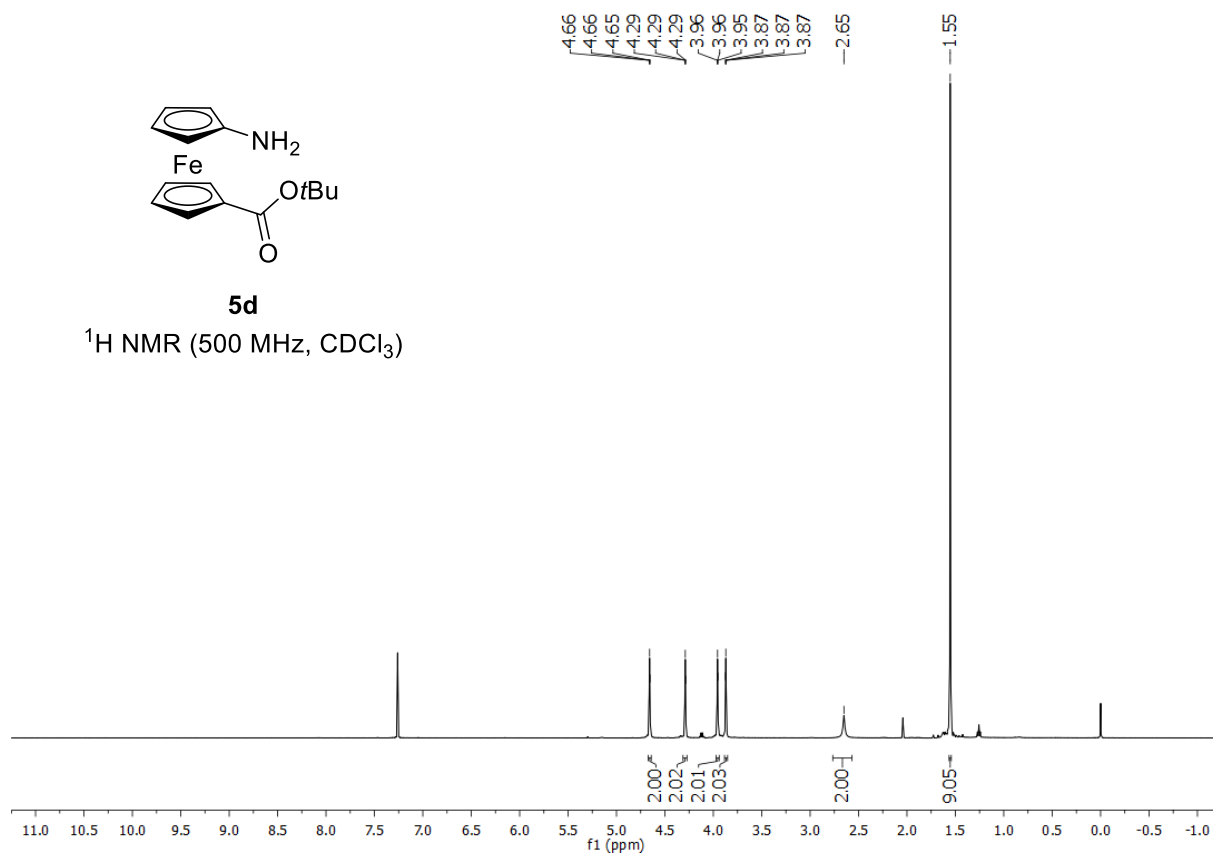


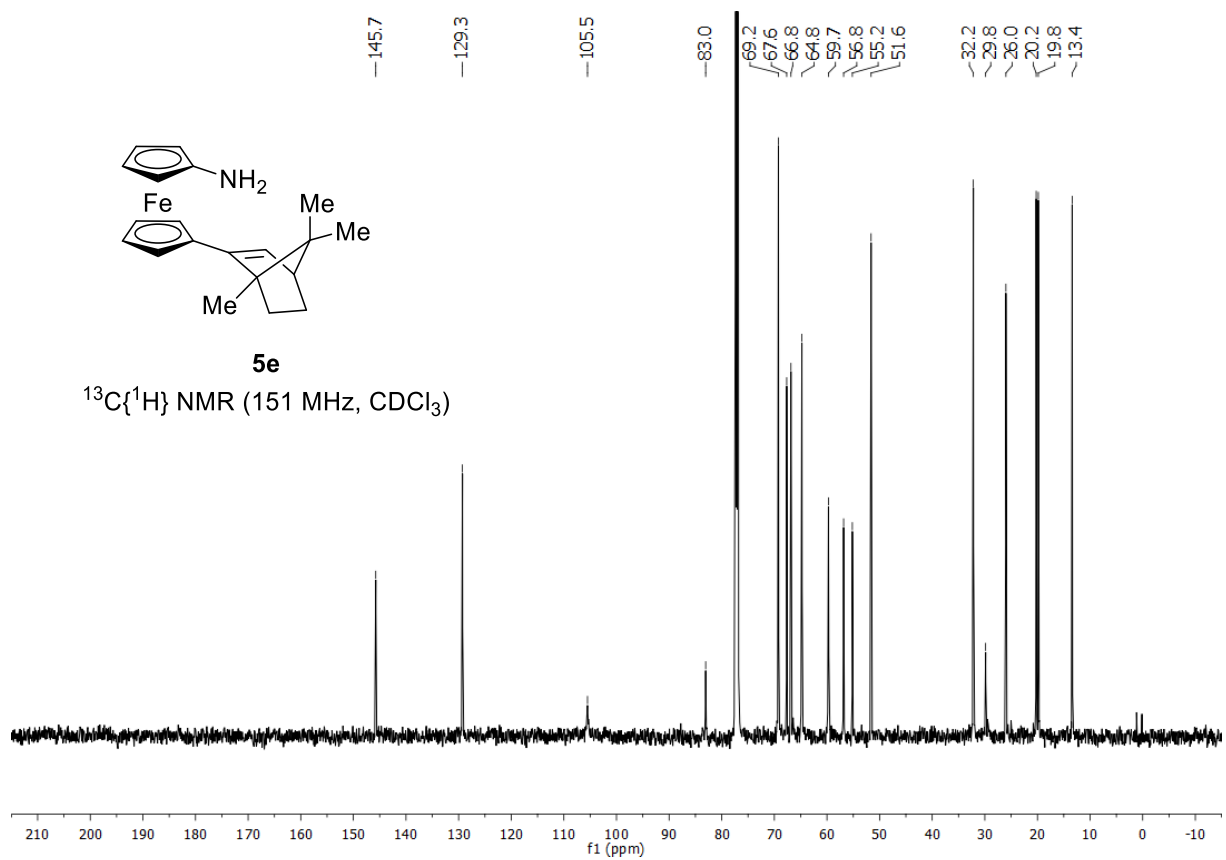
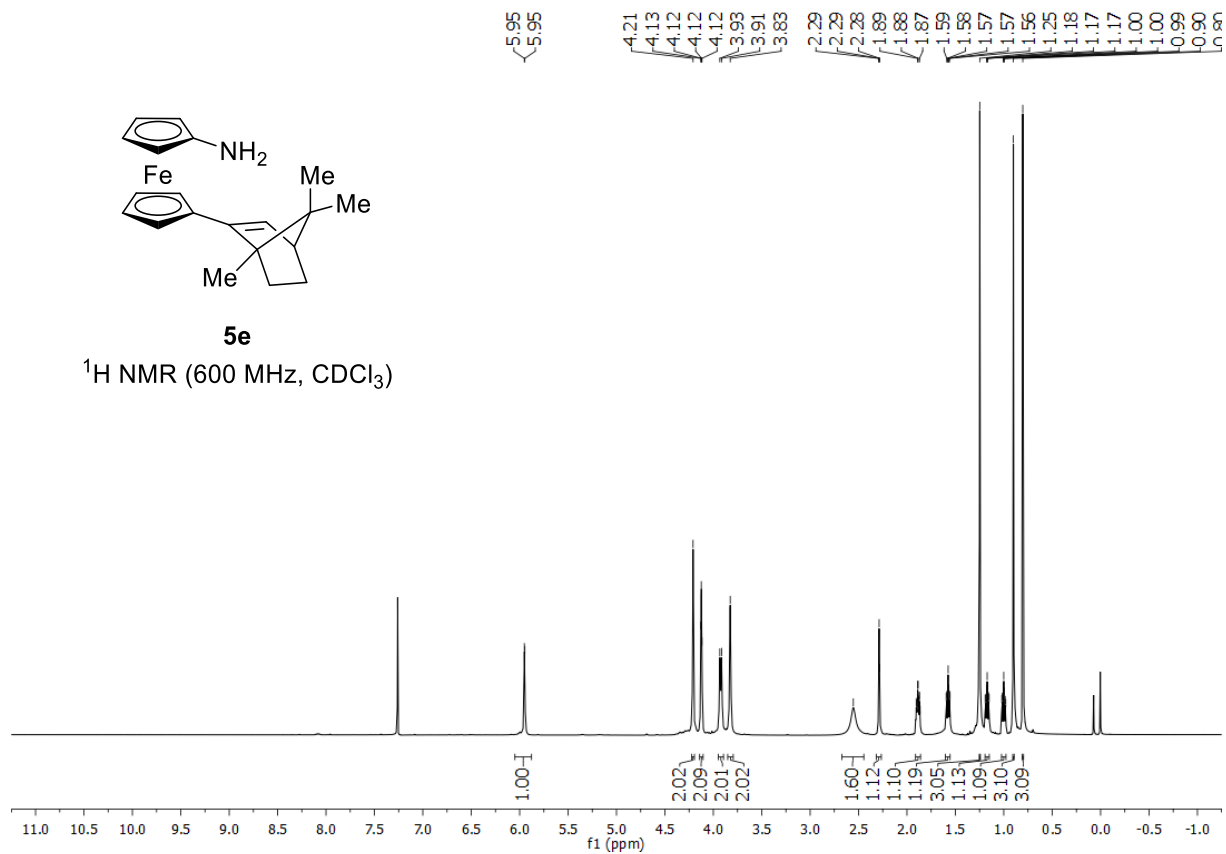


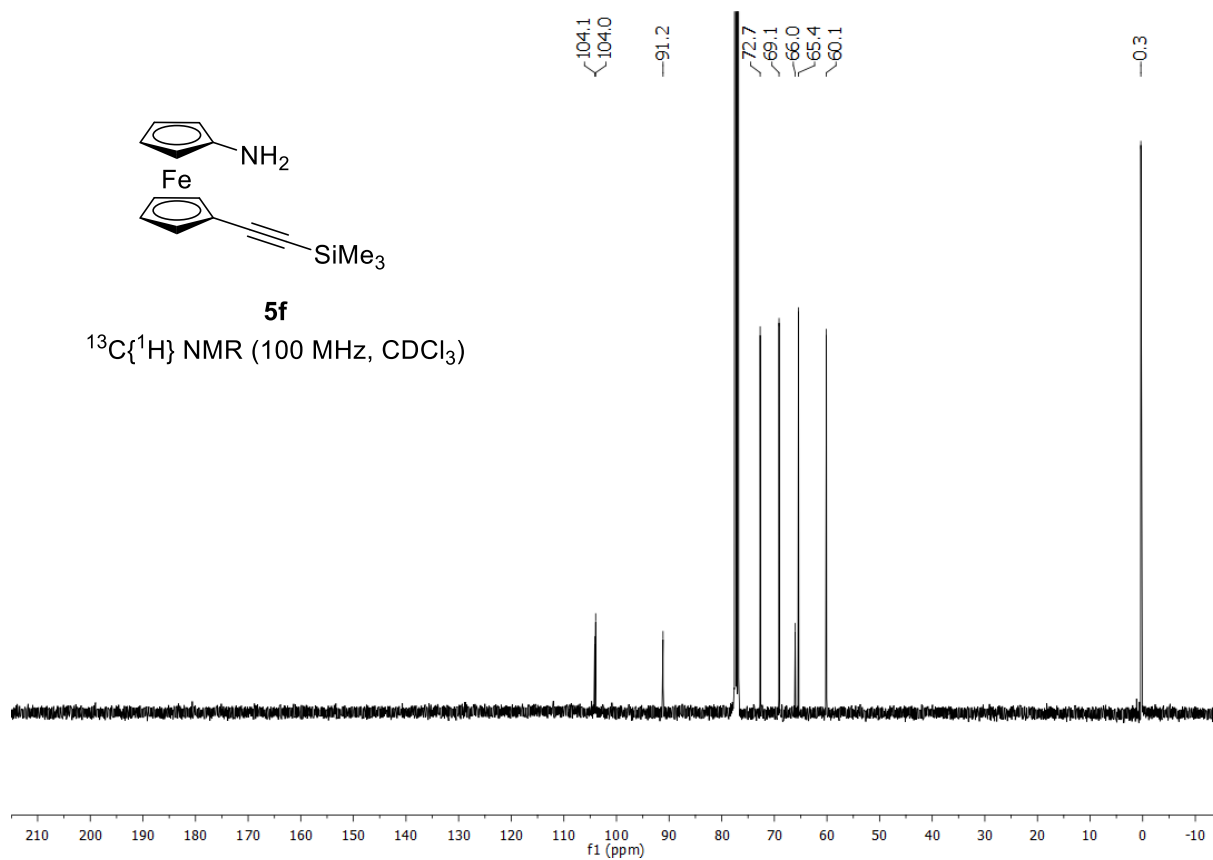
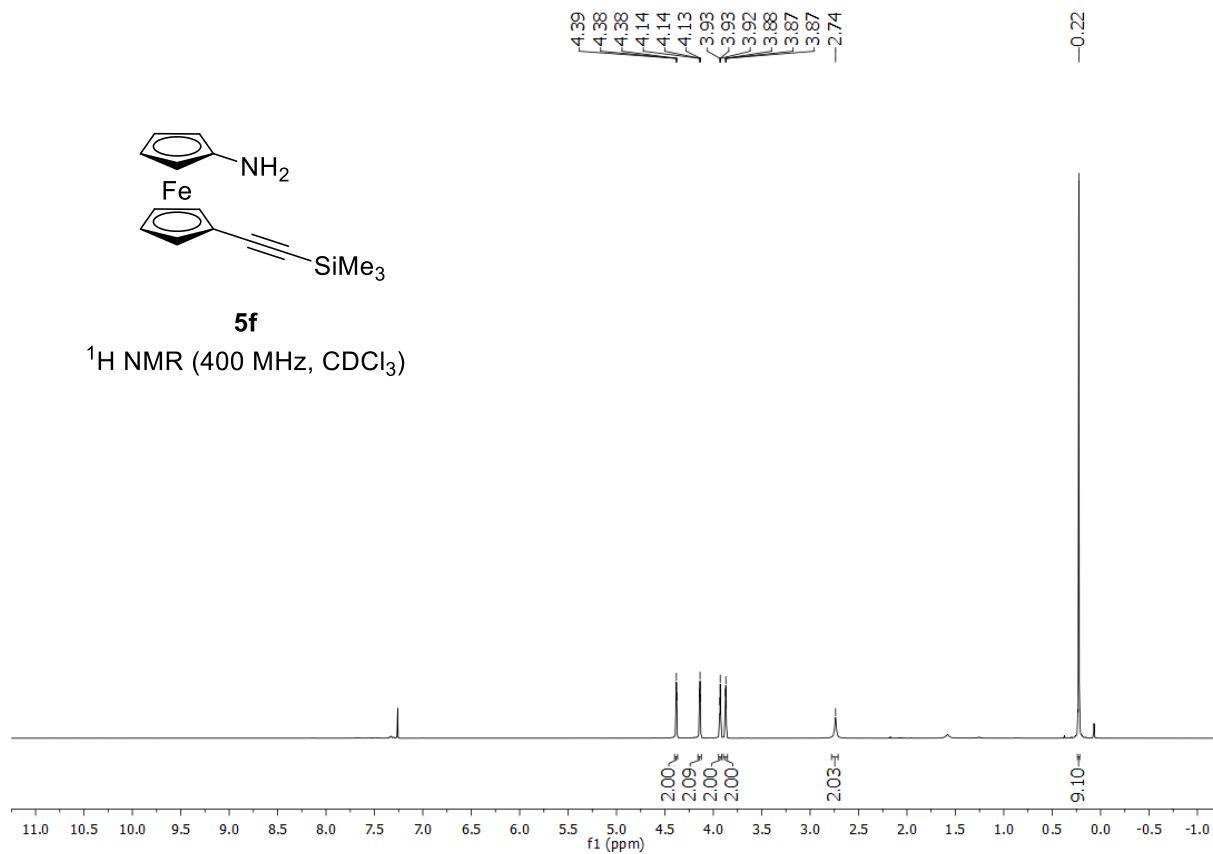


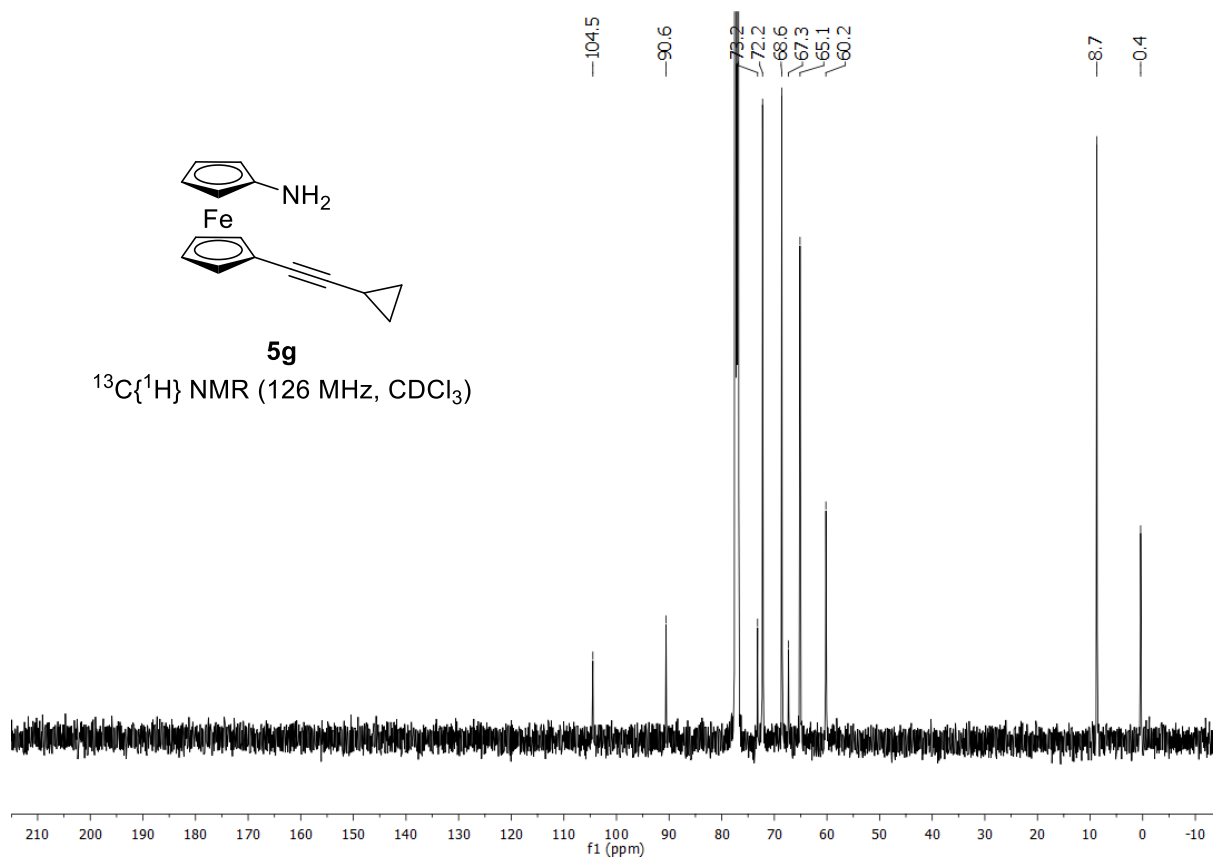
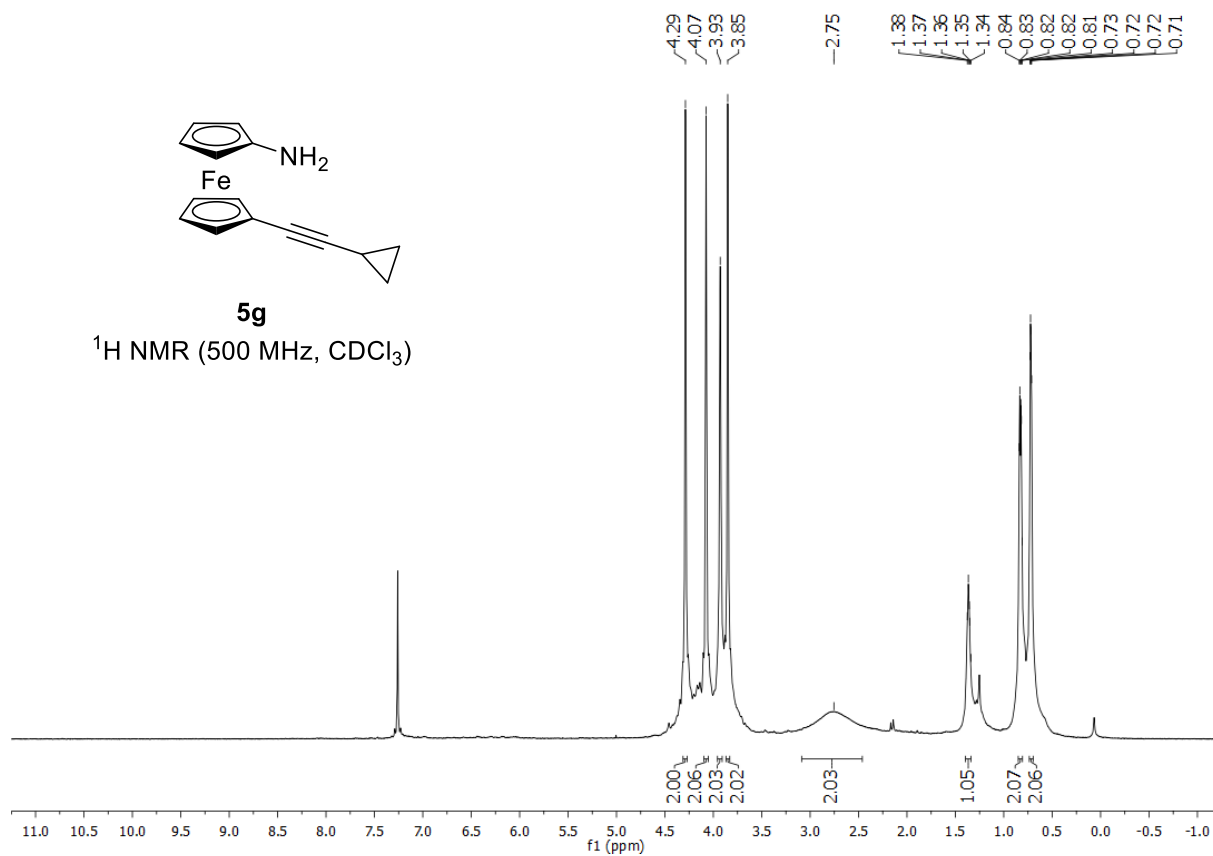


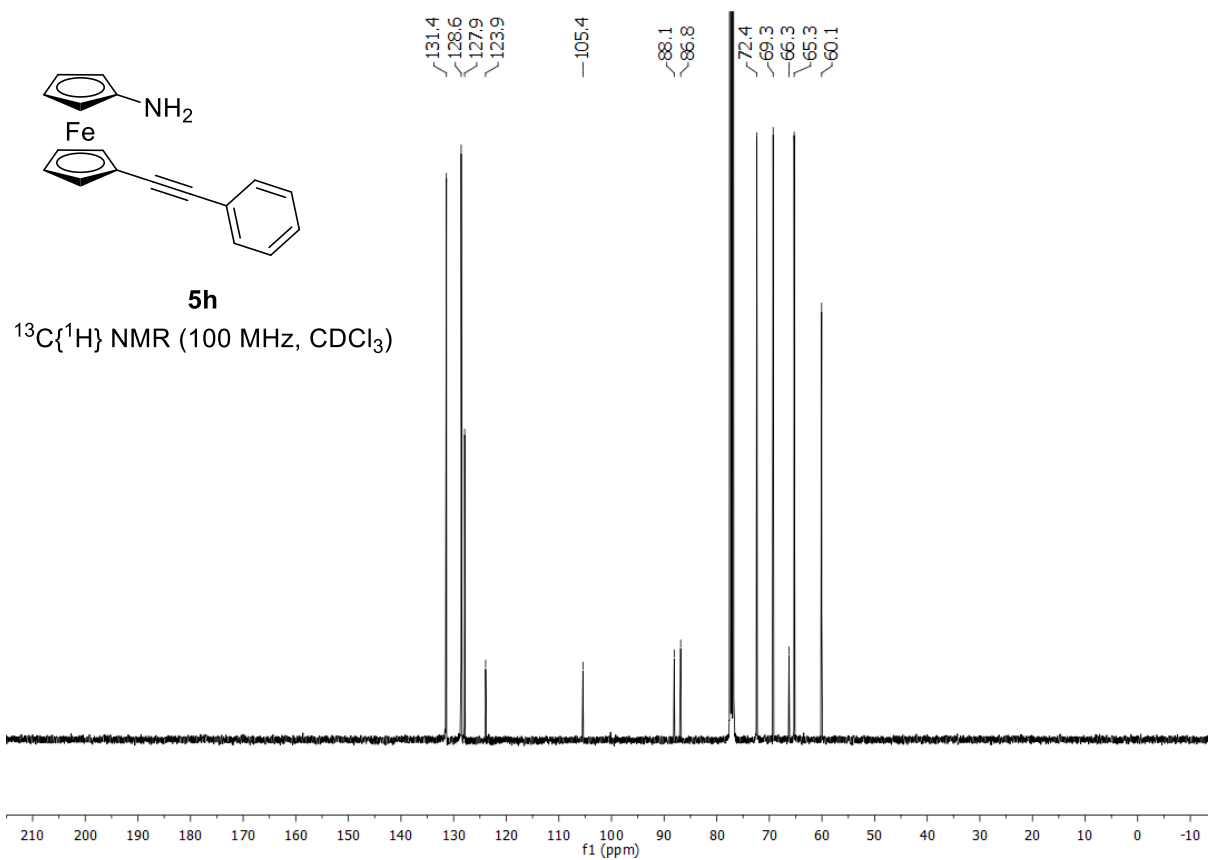
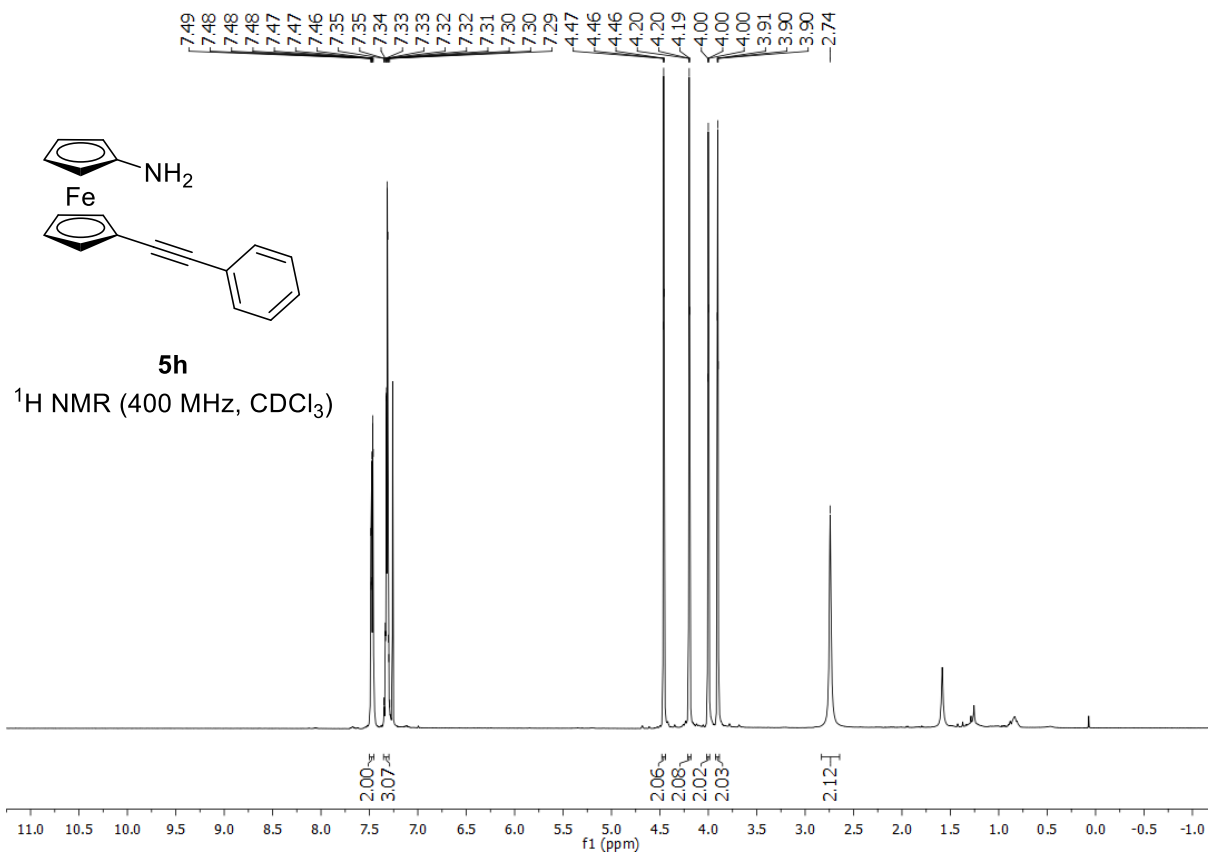


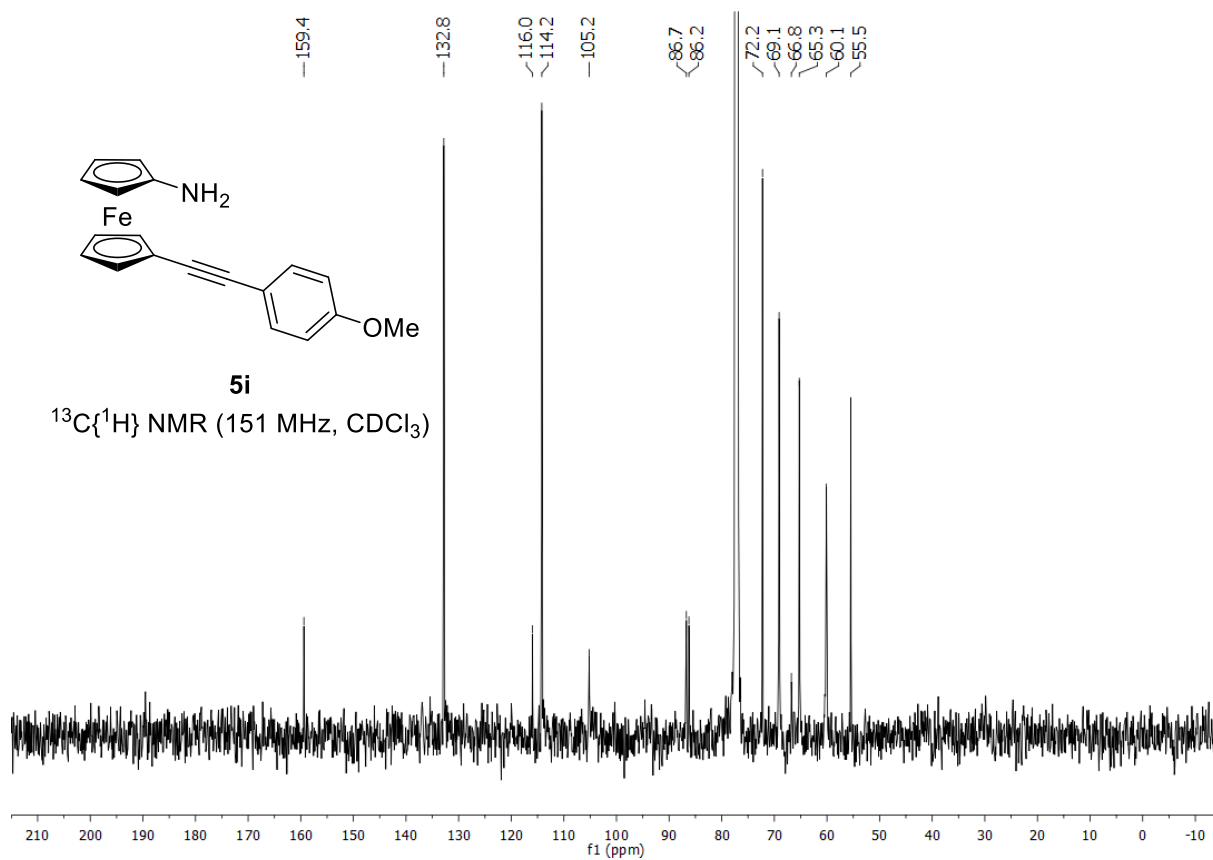
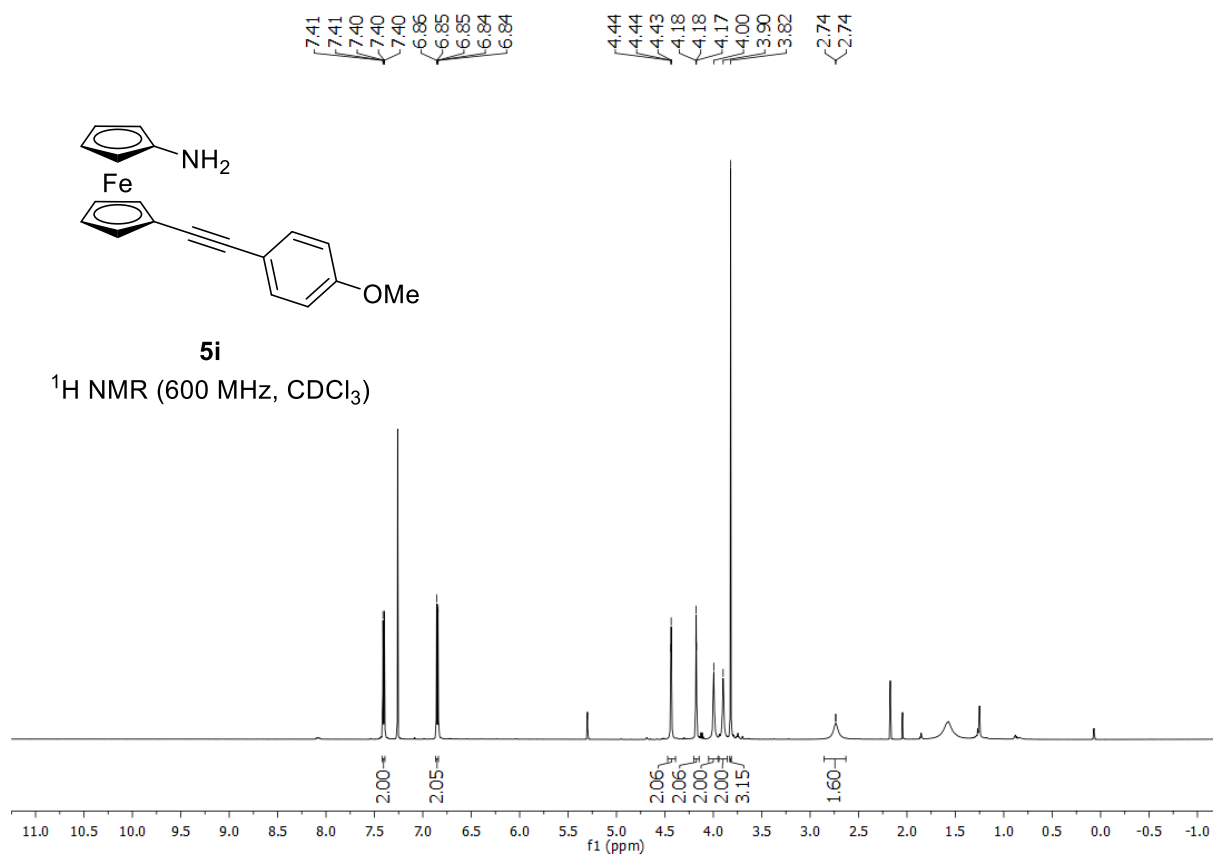


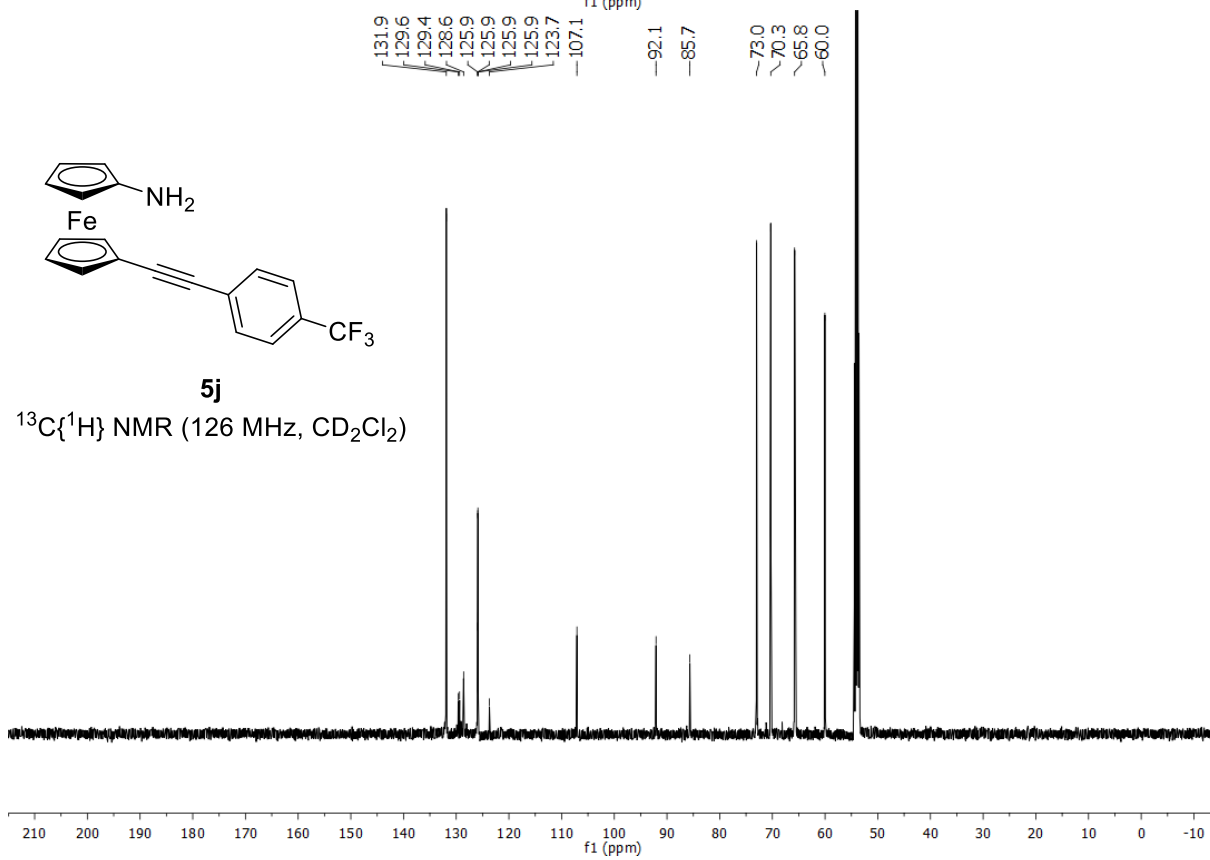
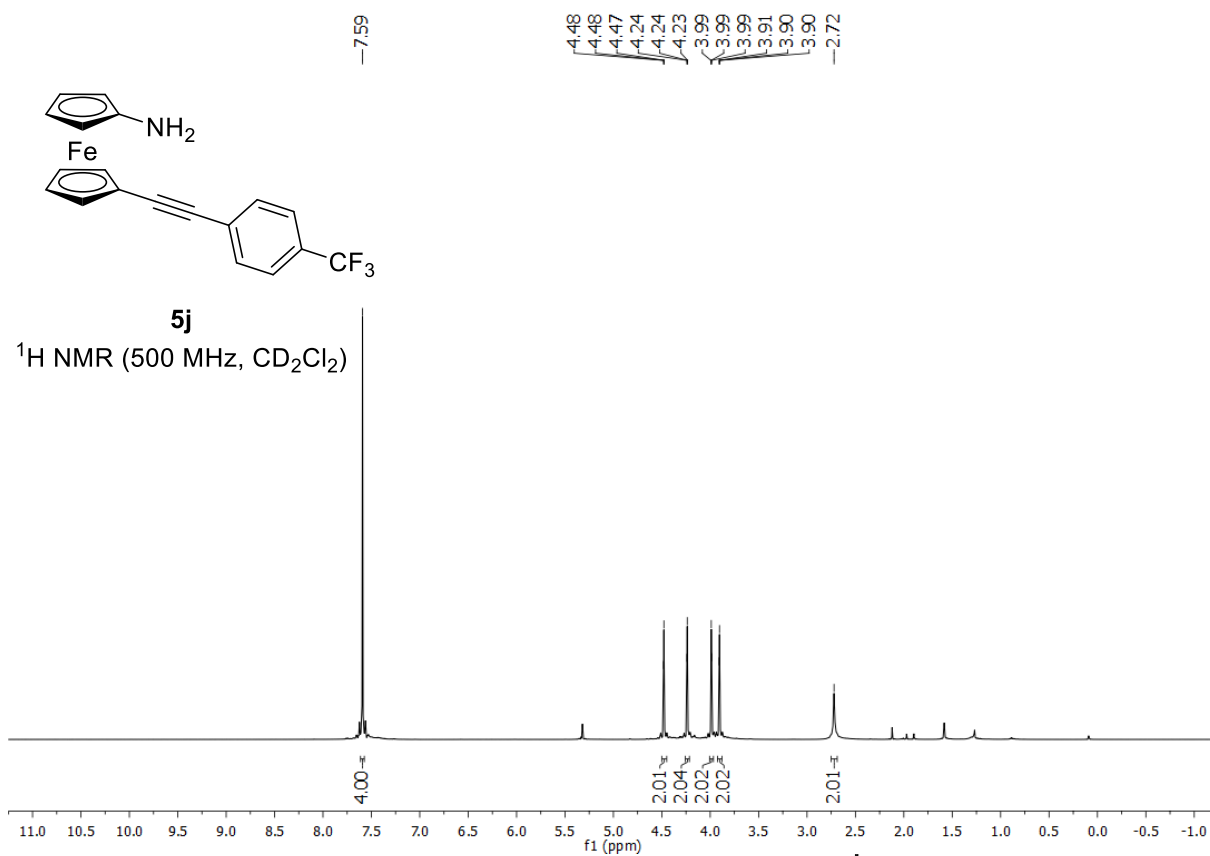


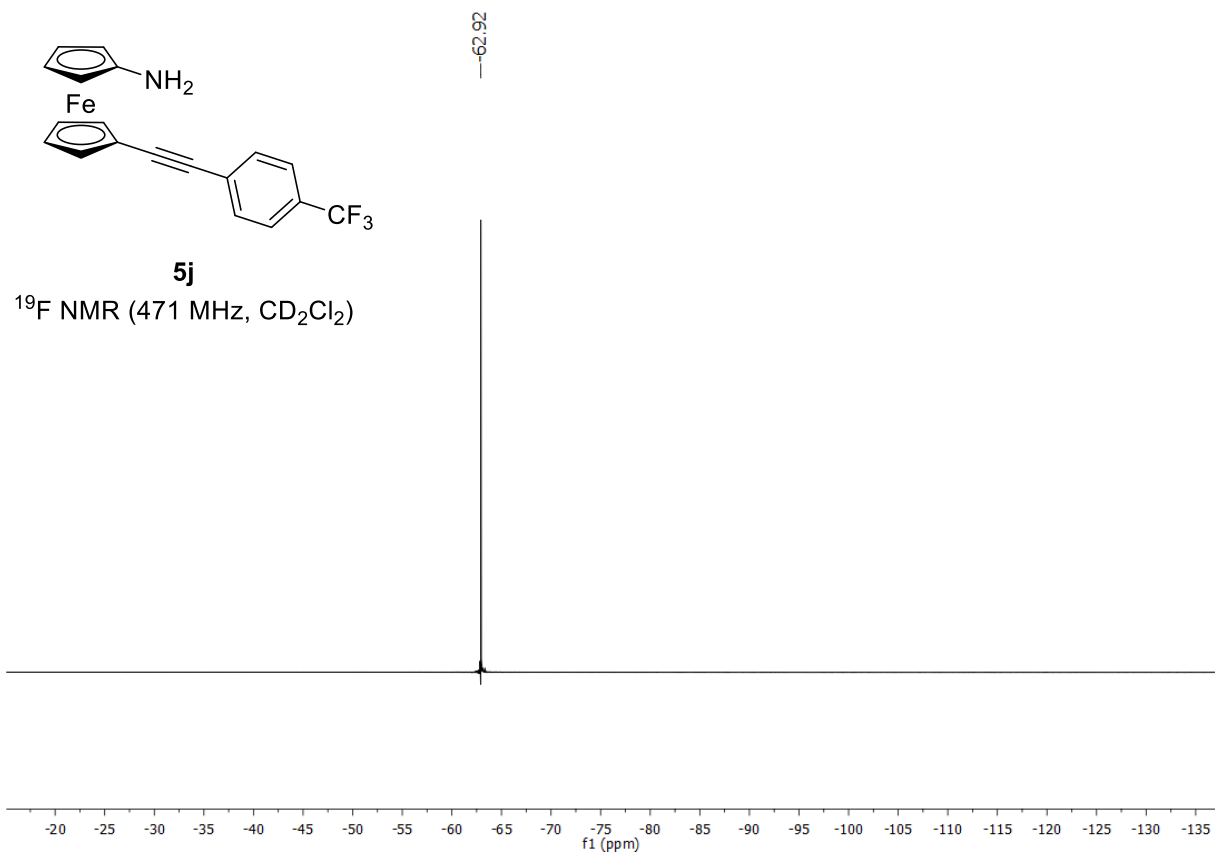




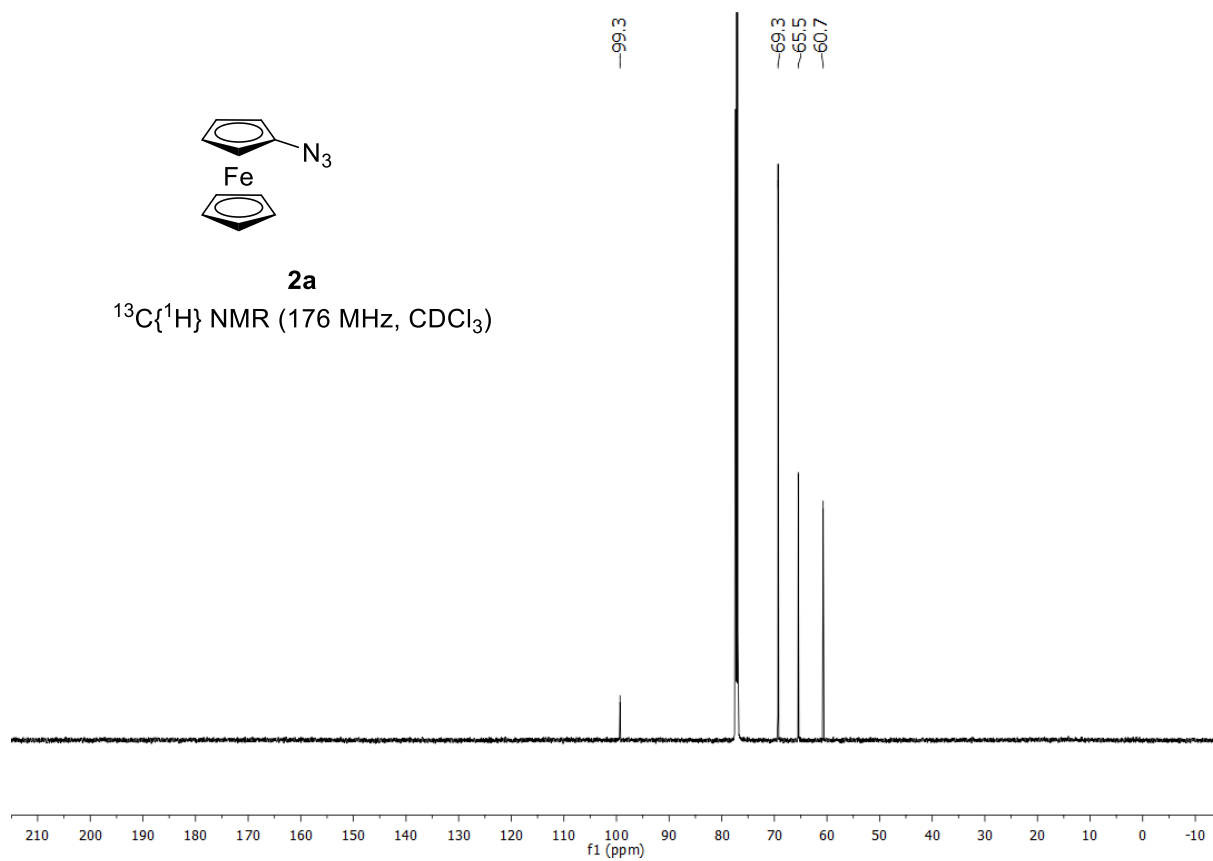
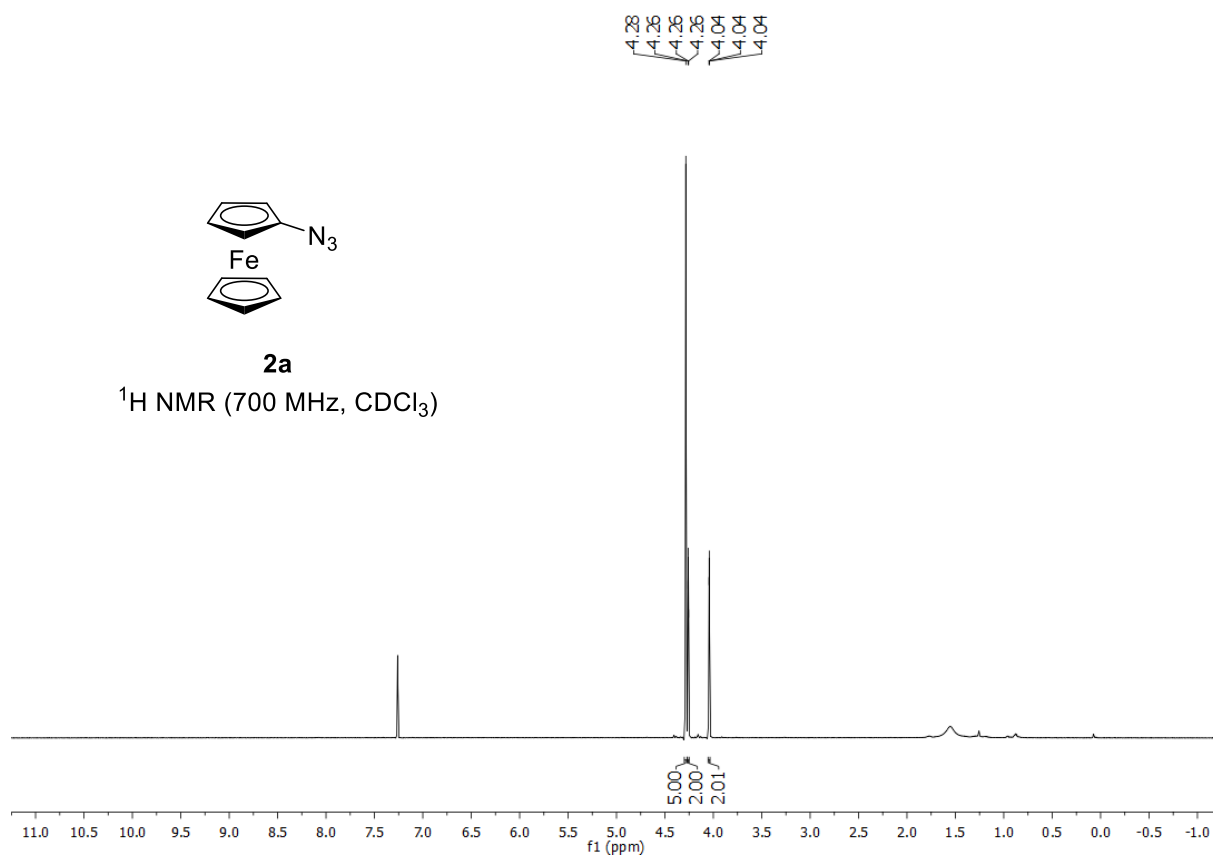


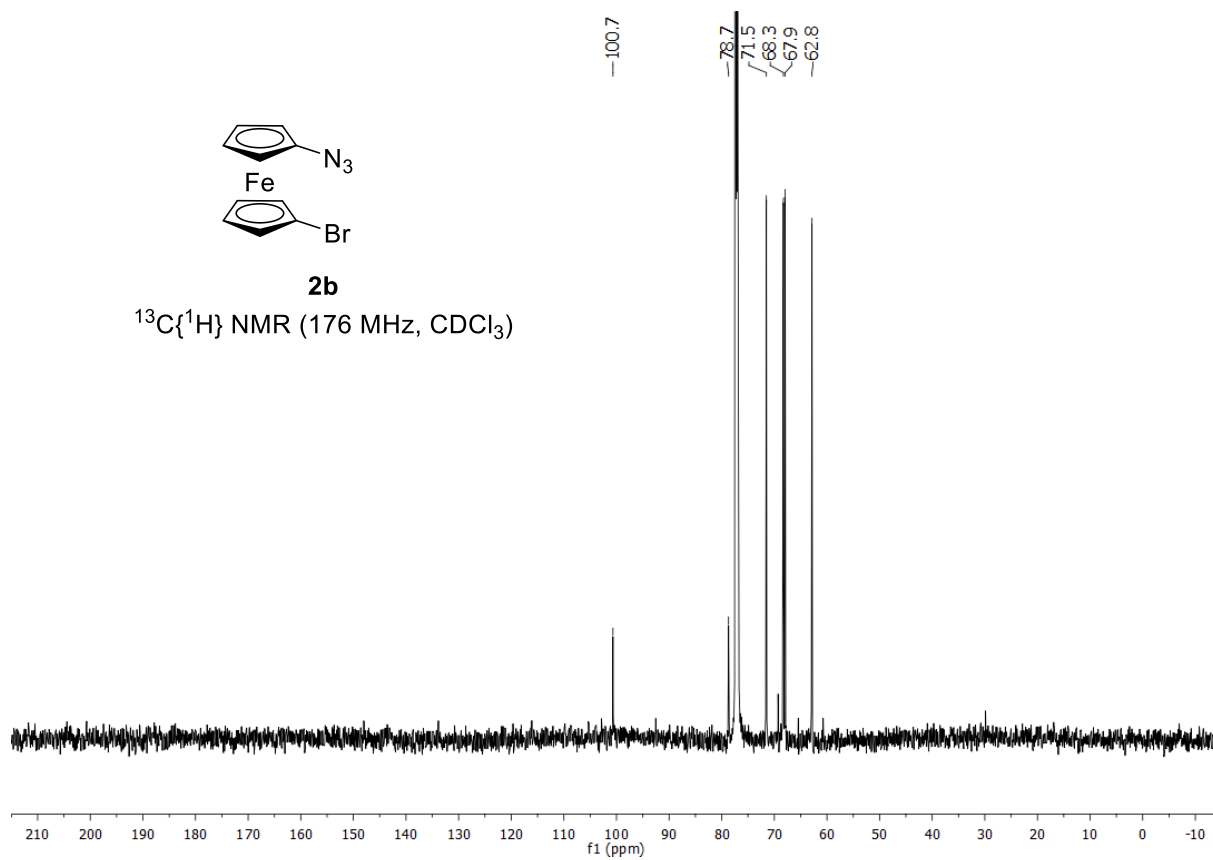
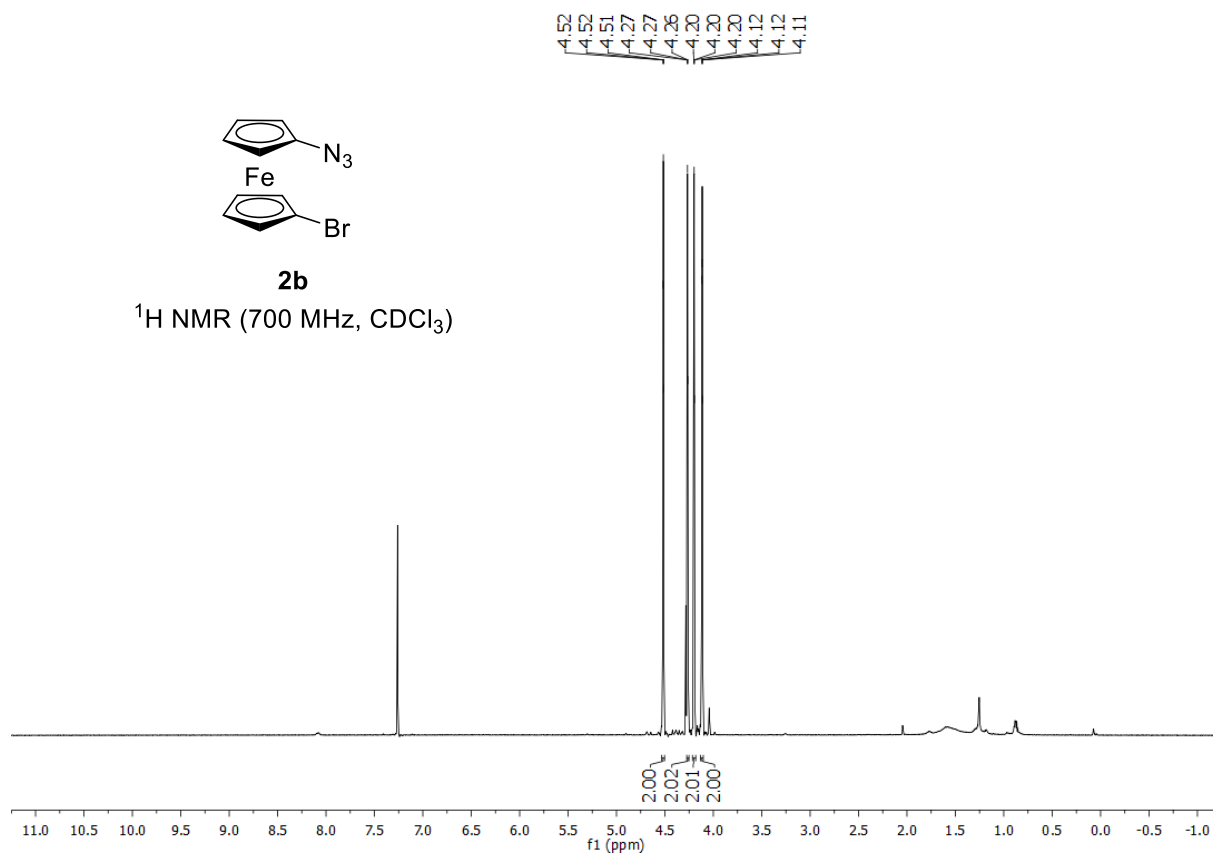


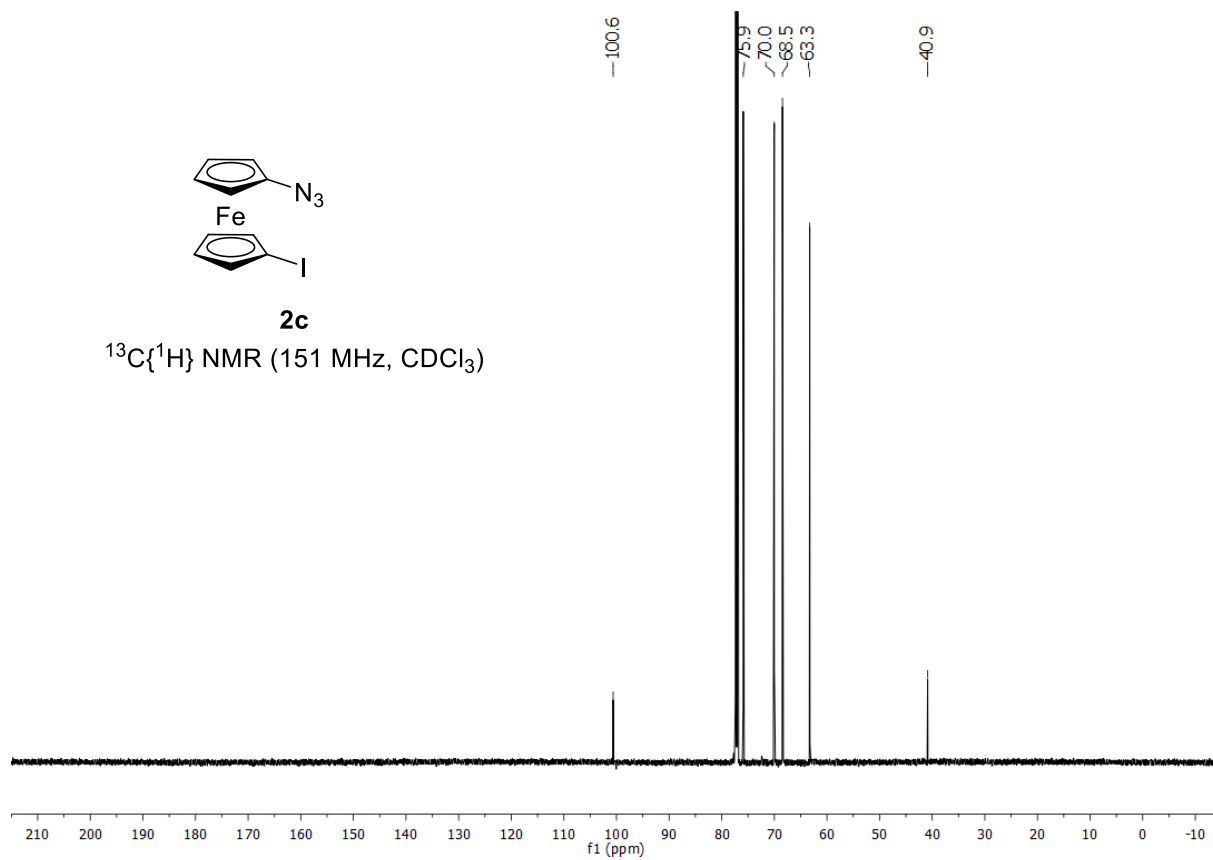
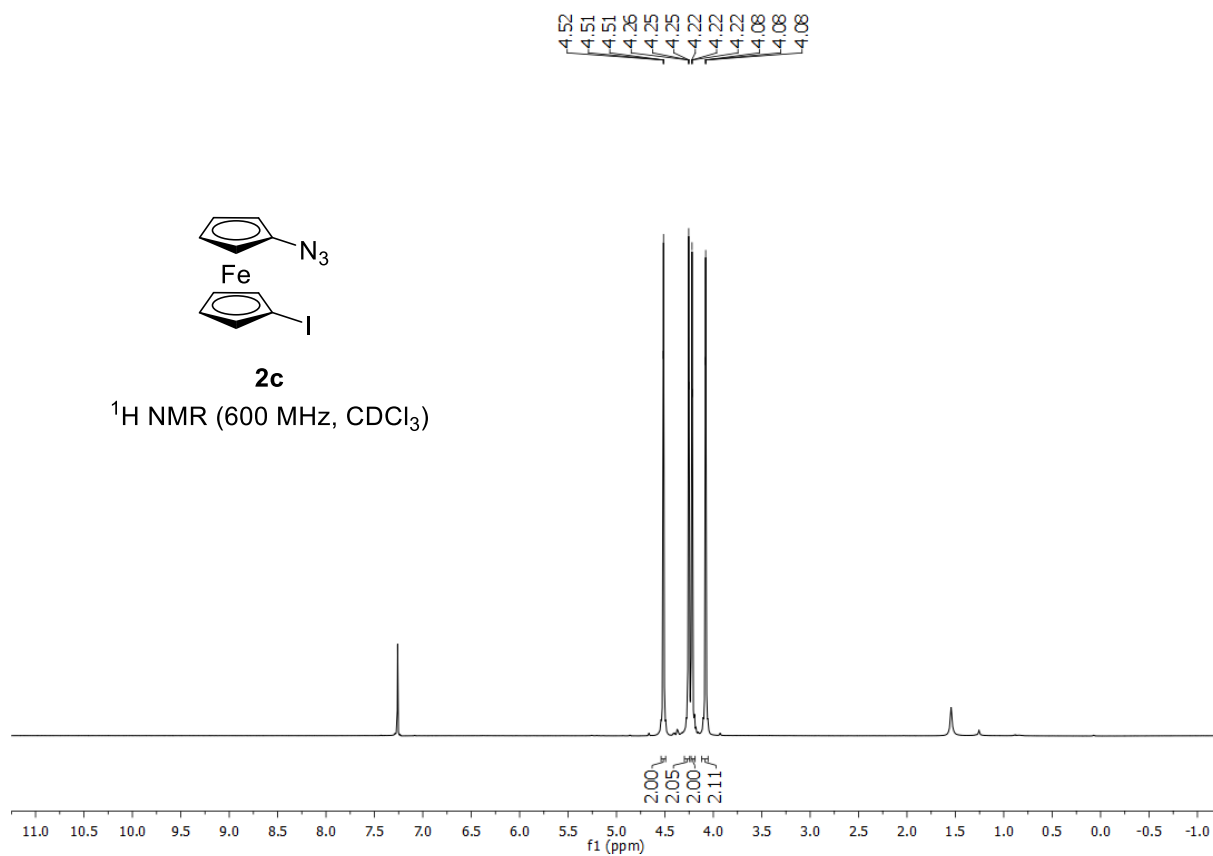


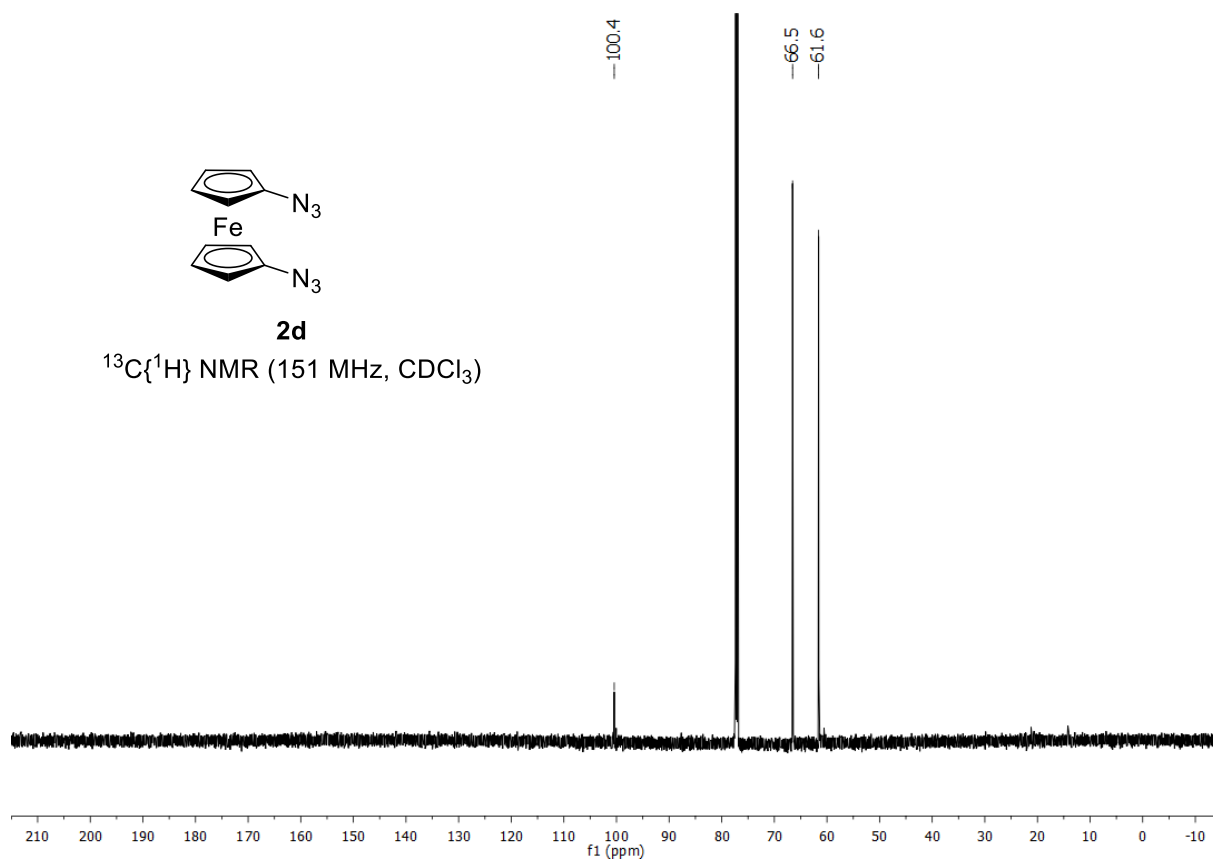
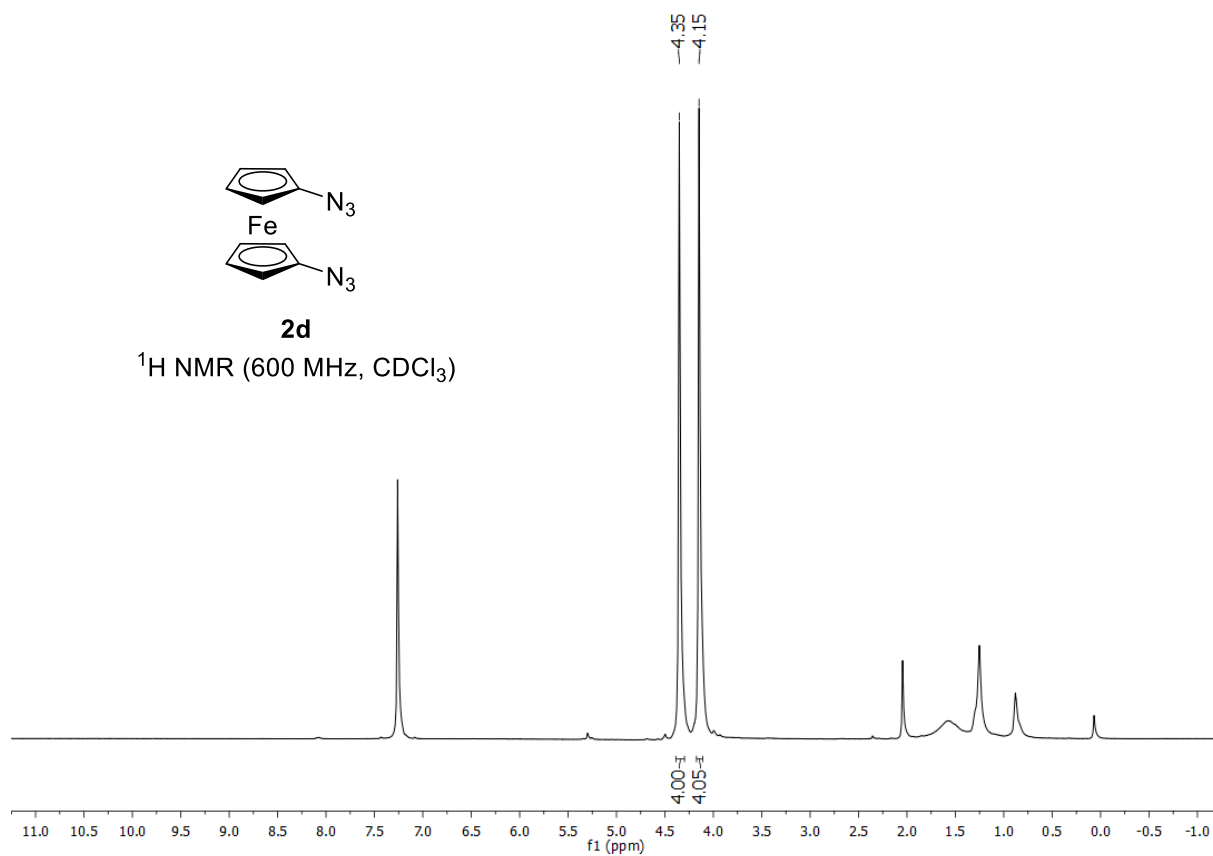


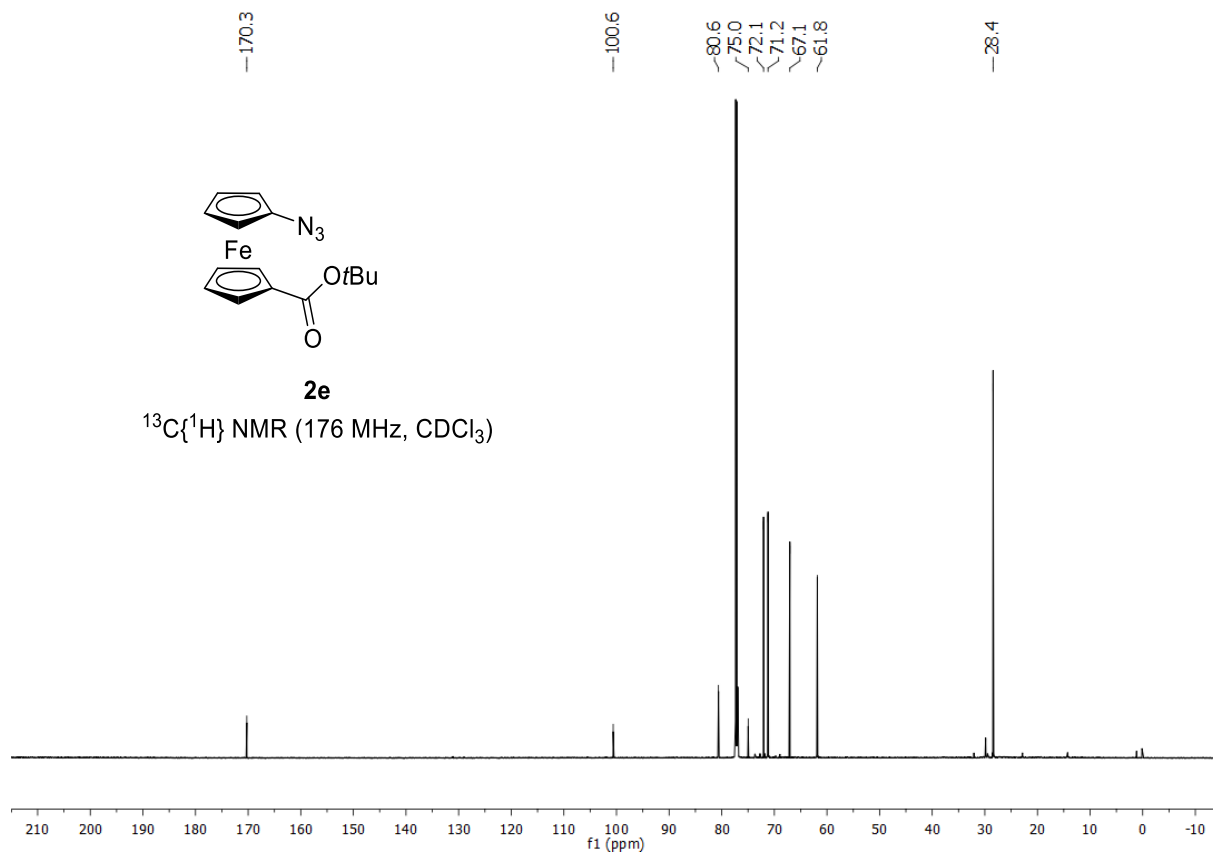
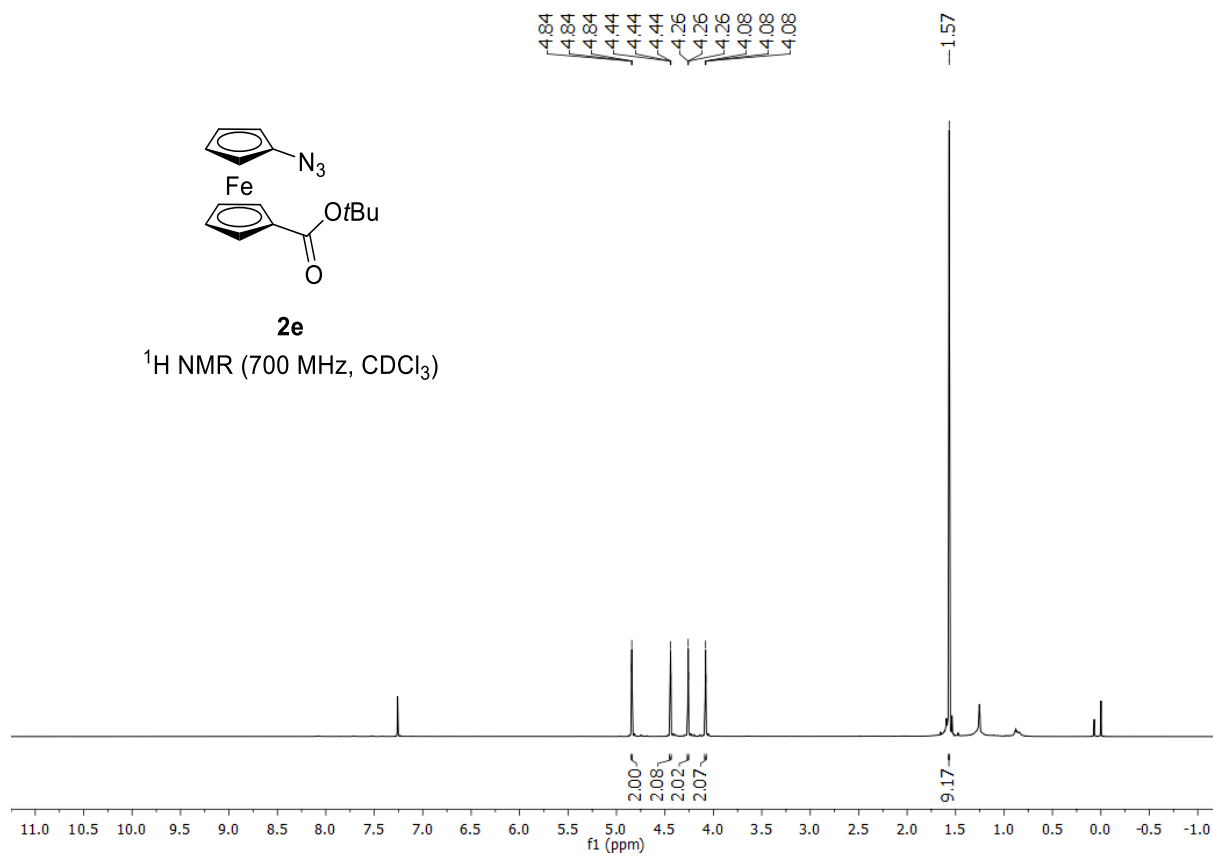
3.2 NMR Spectra of Compounds Synthesized in Flow

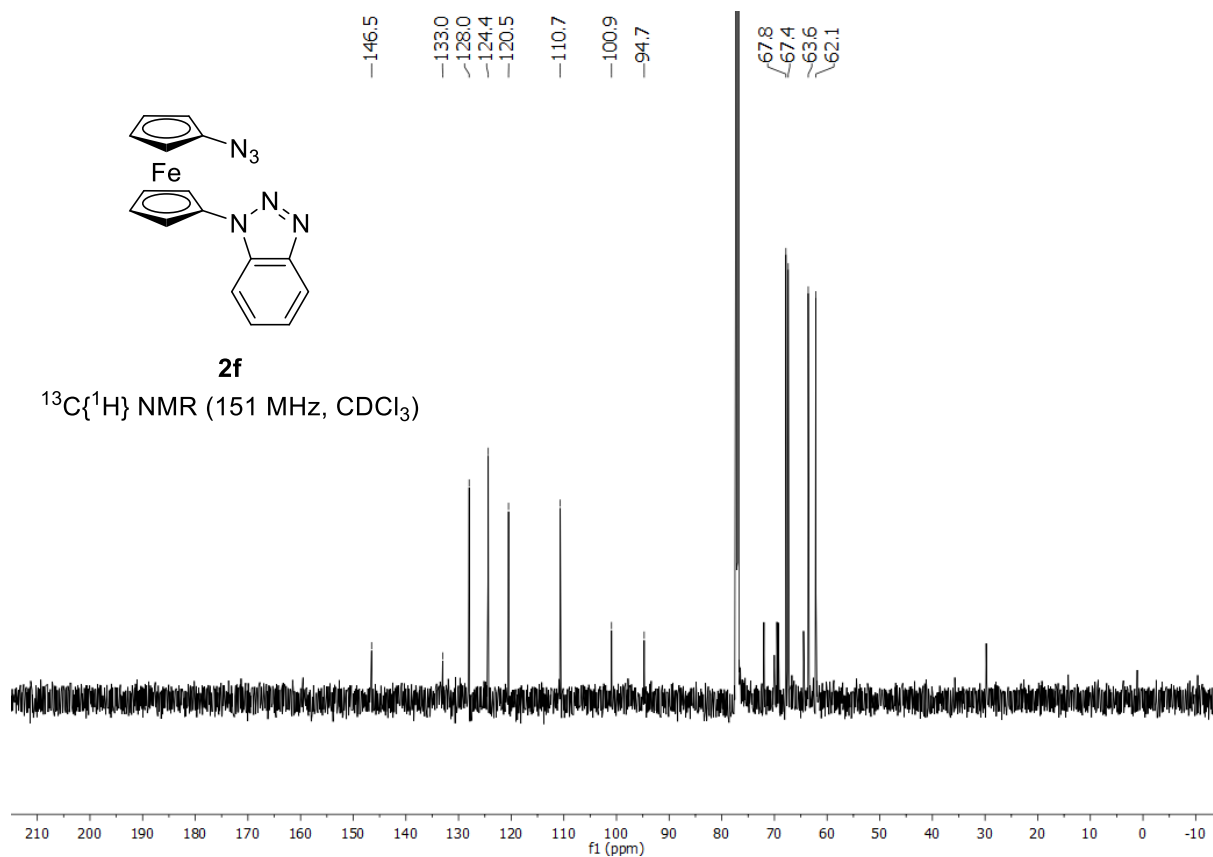
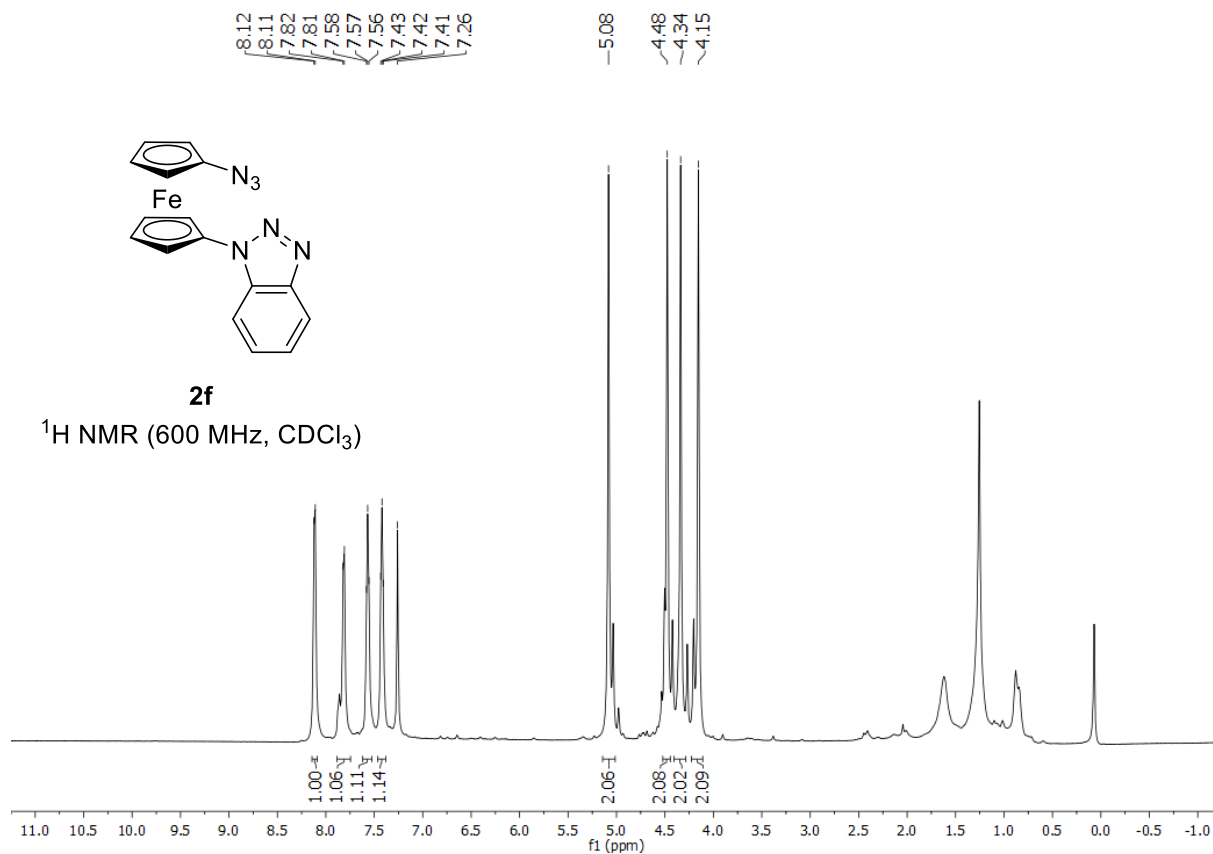


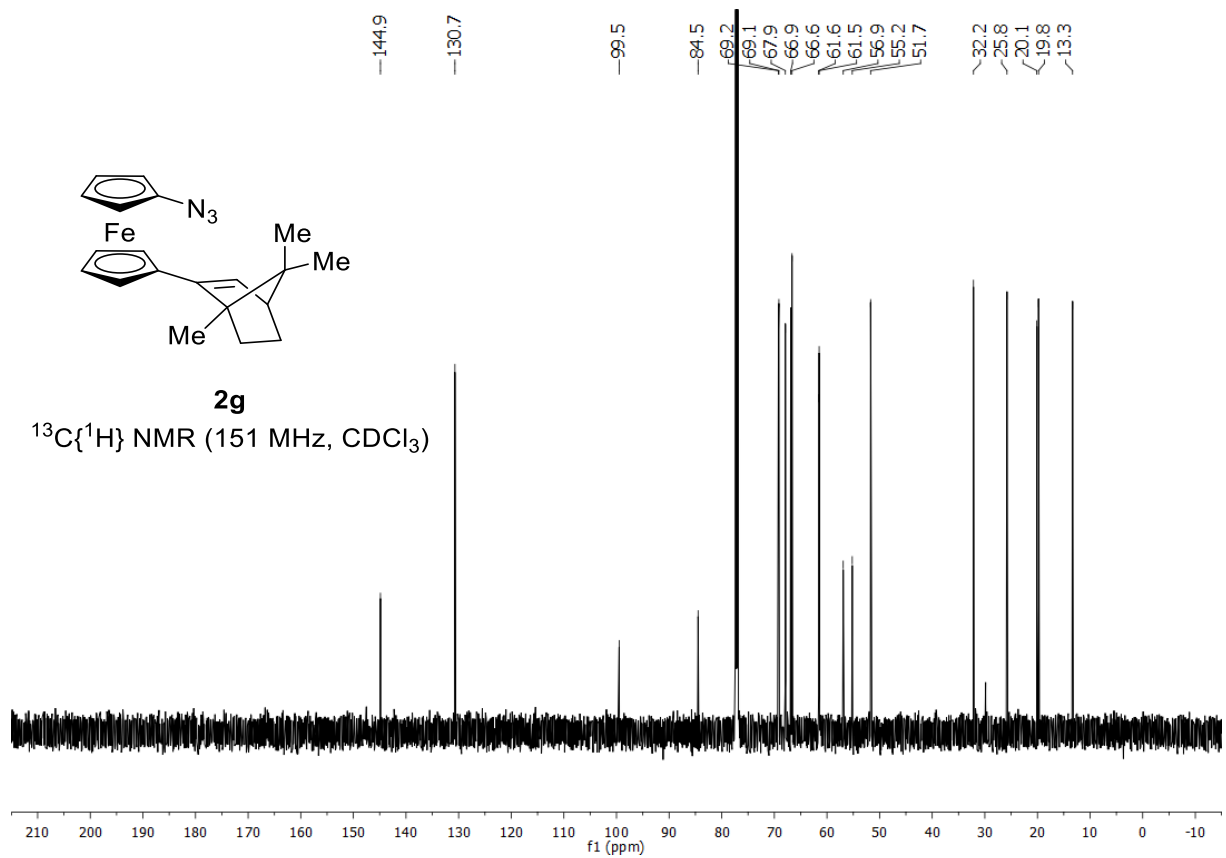
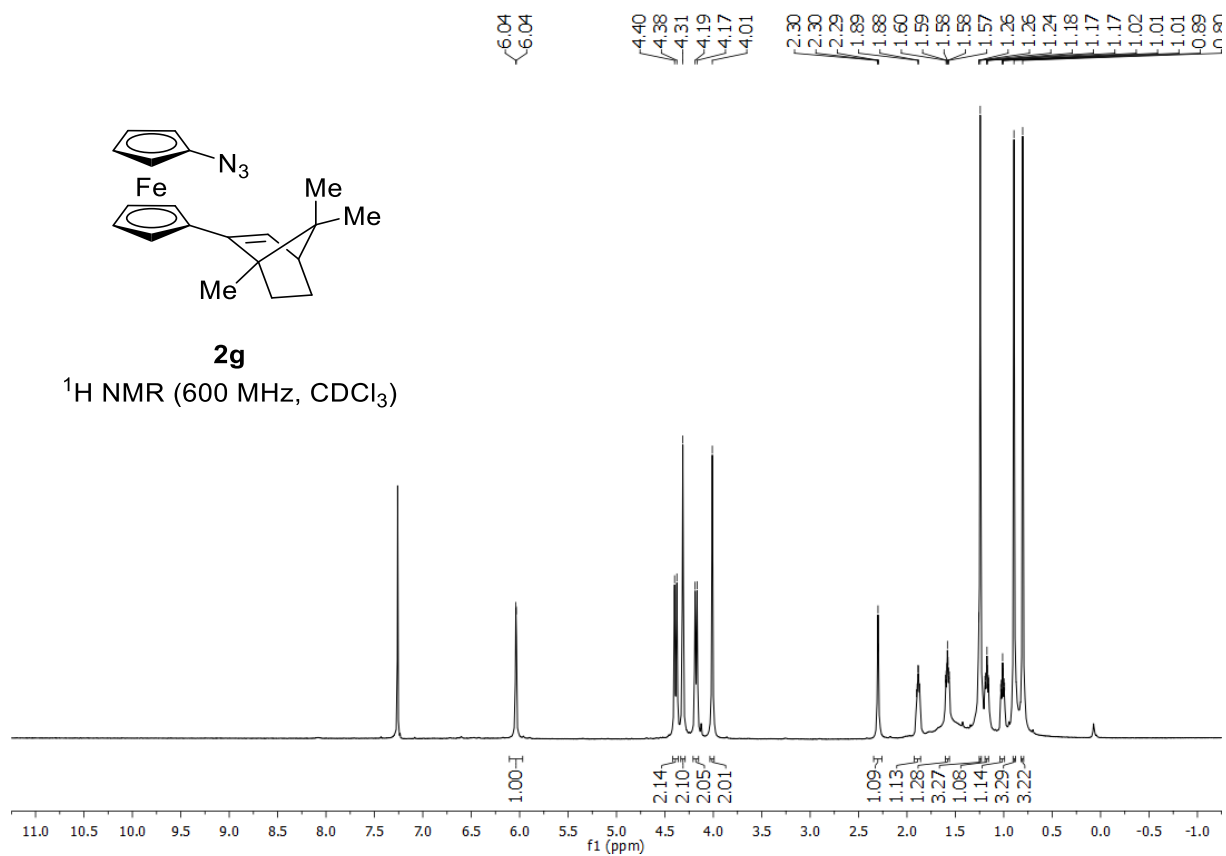


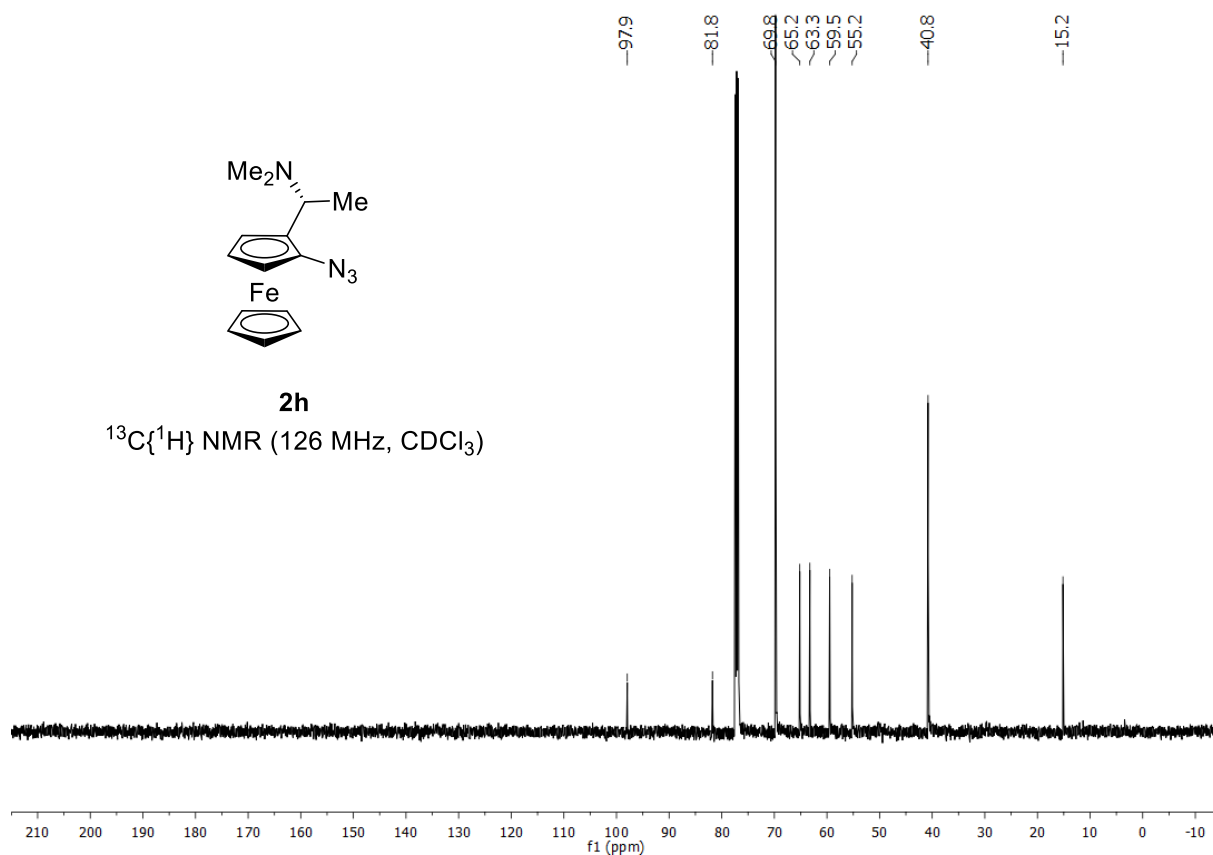
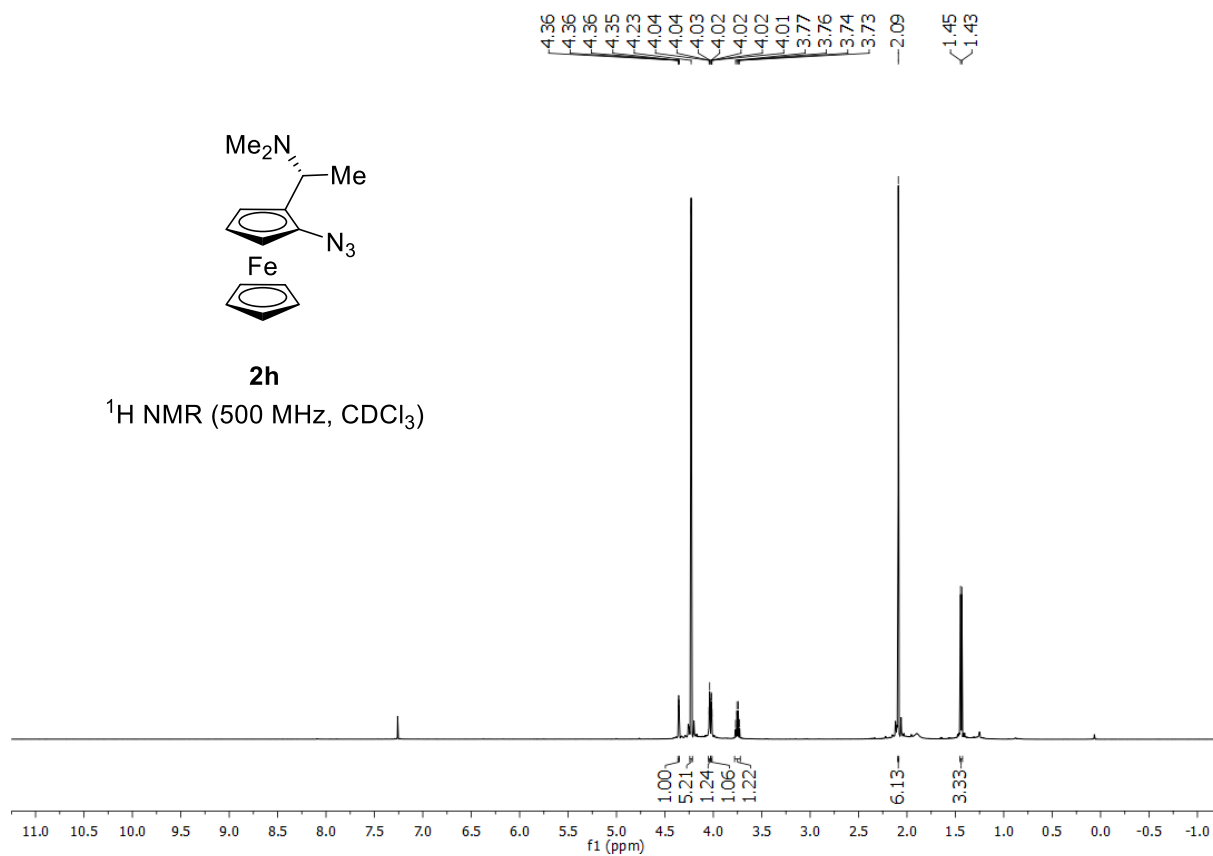


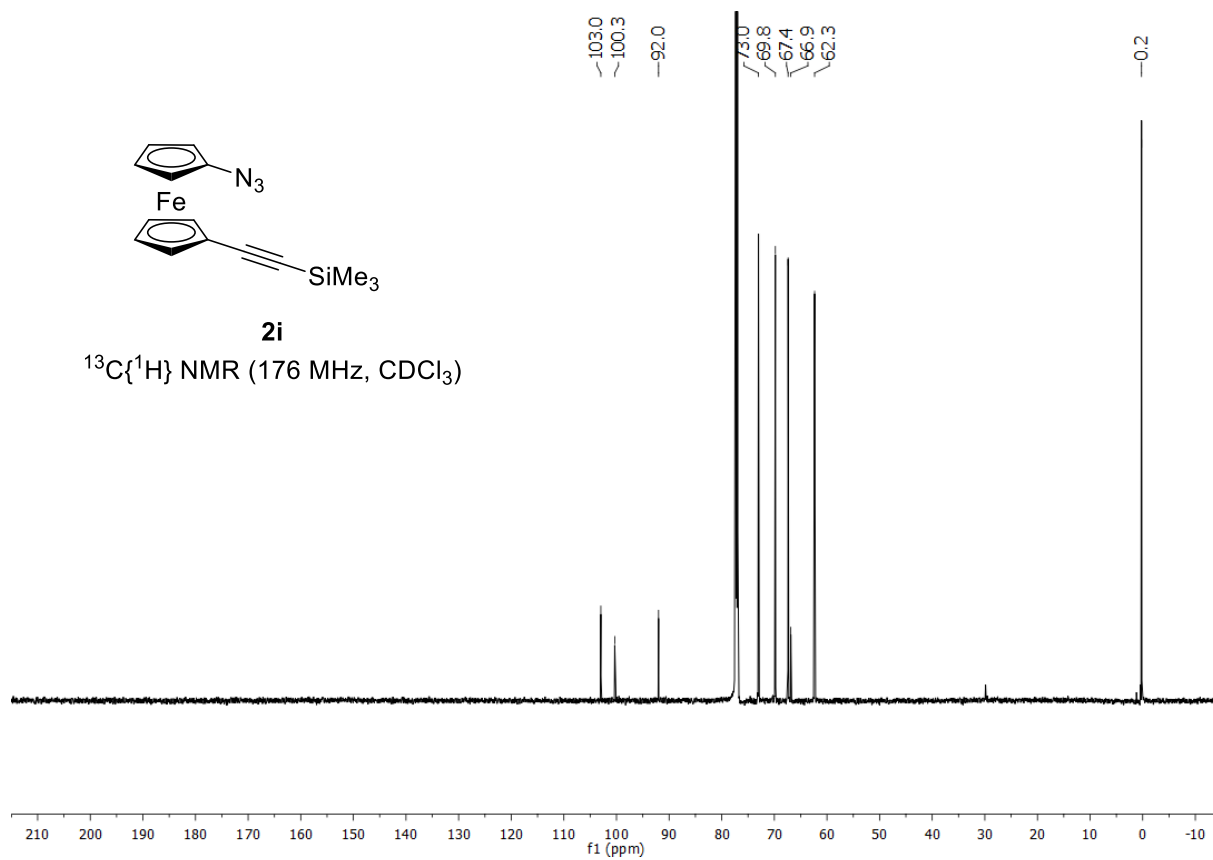
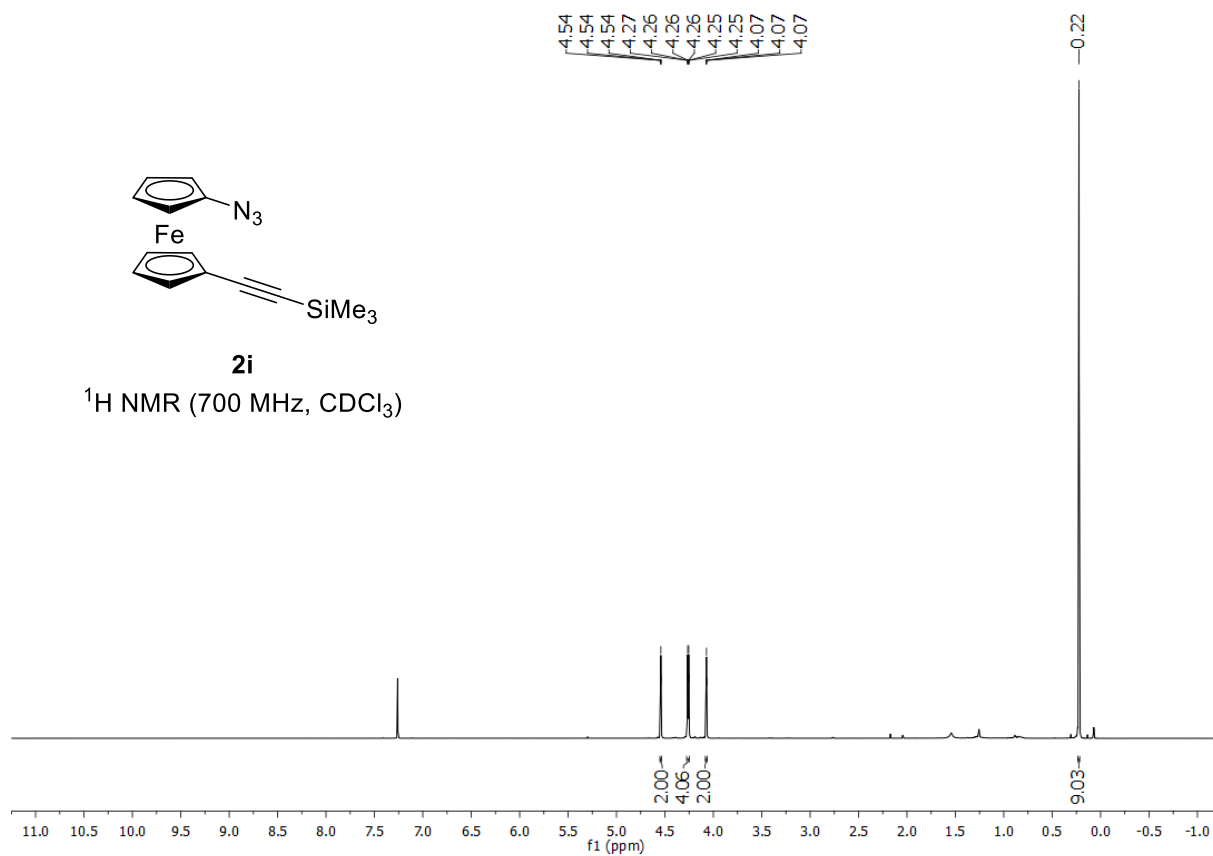


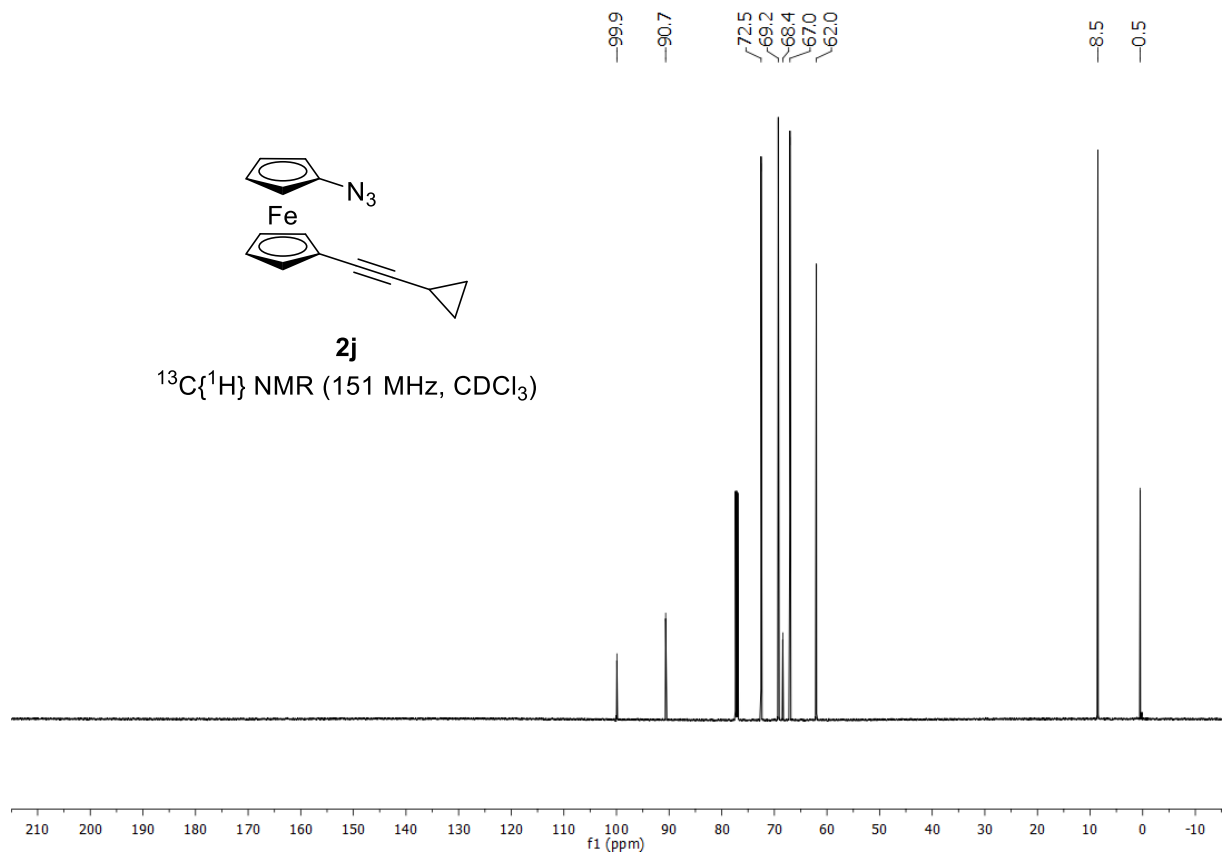
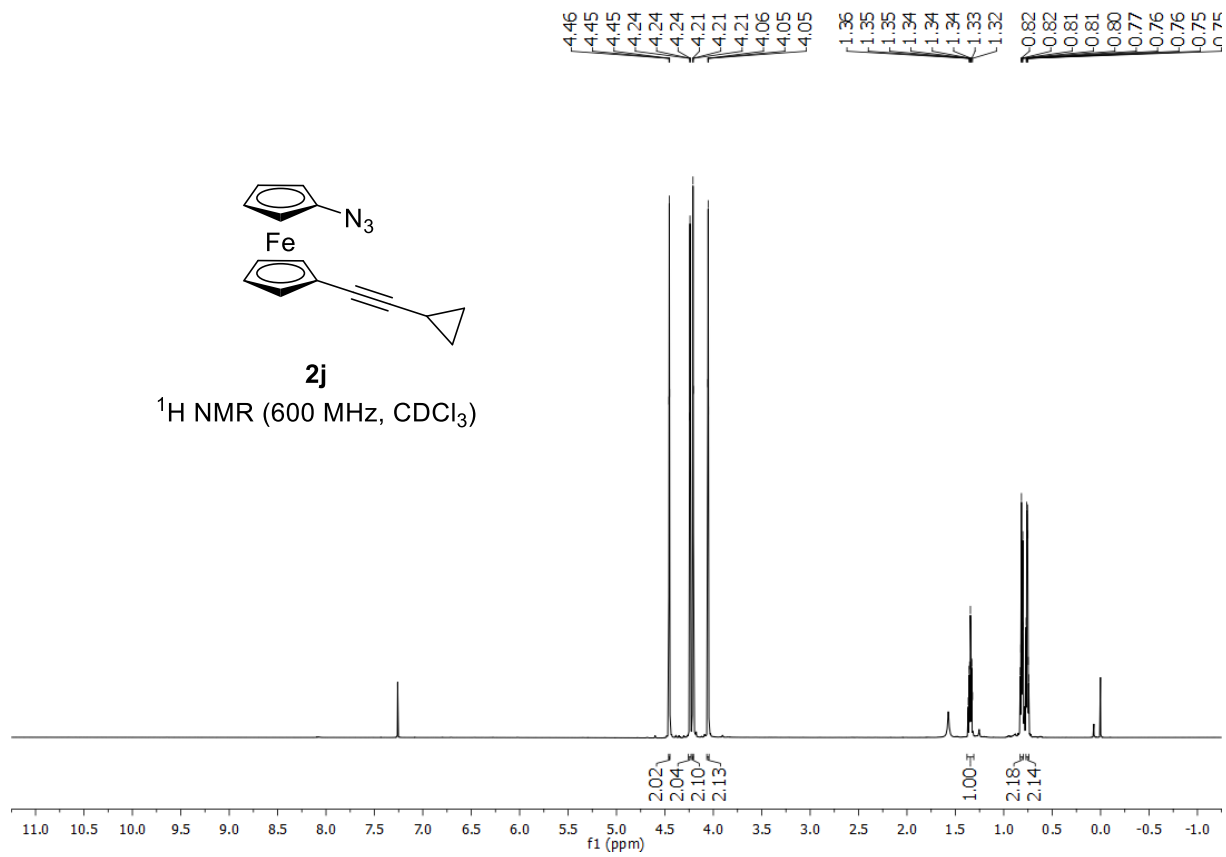


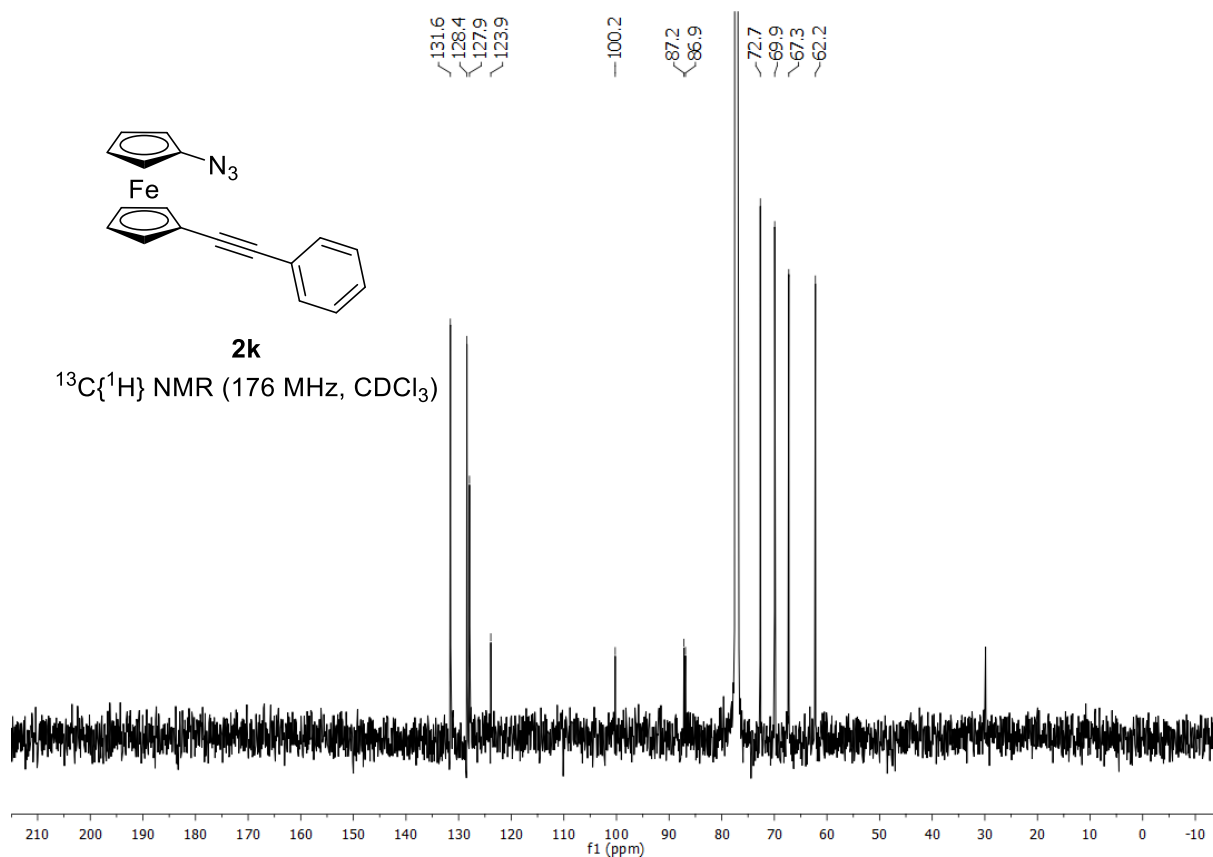
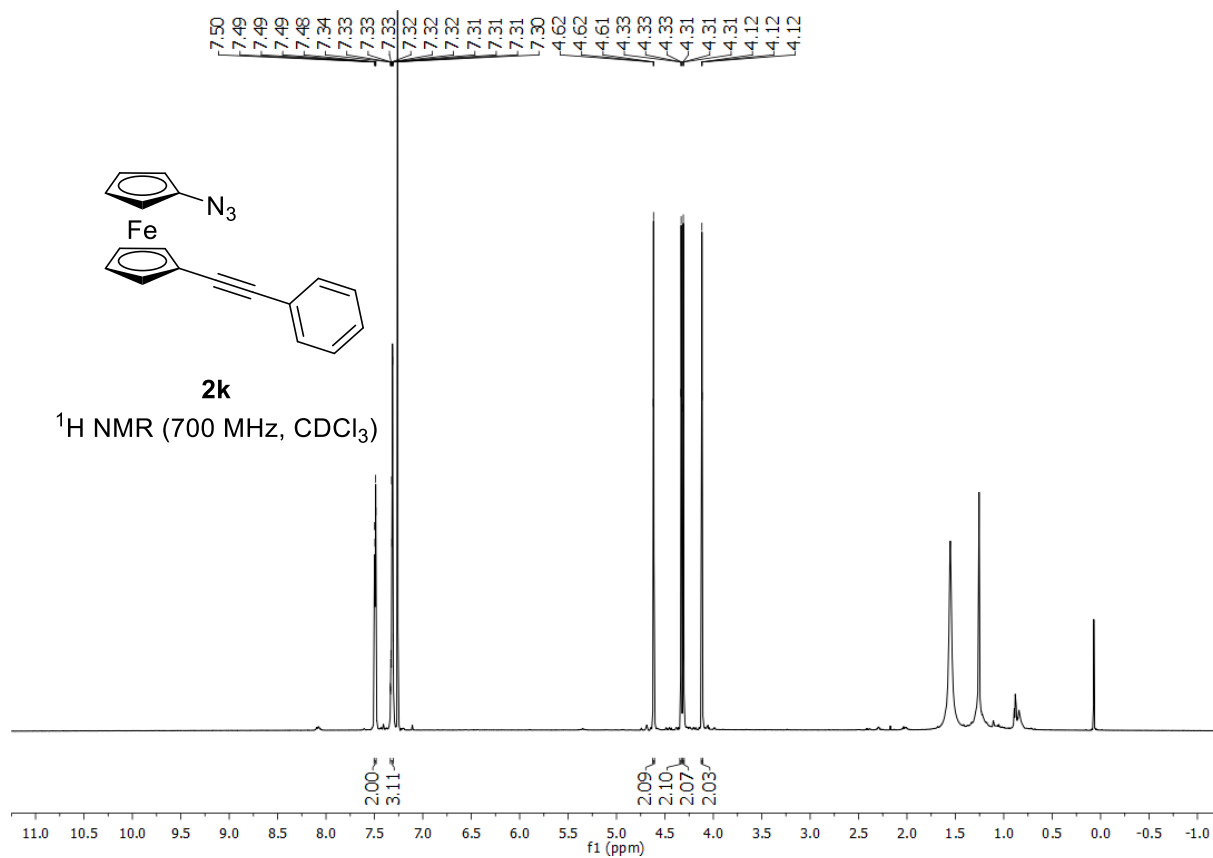


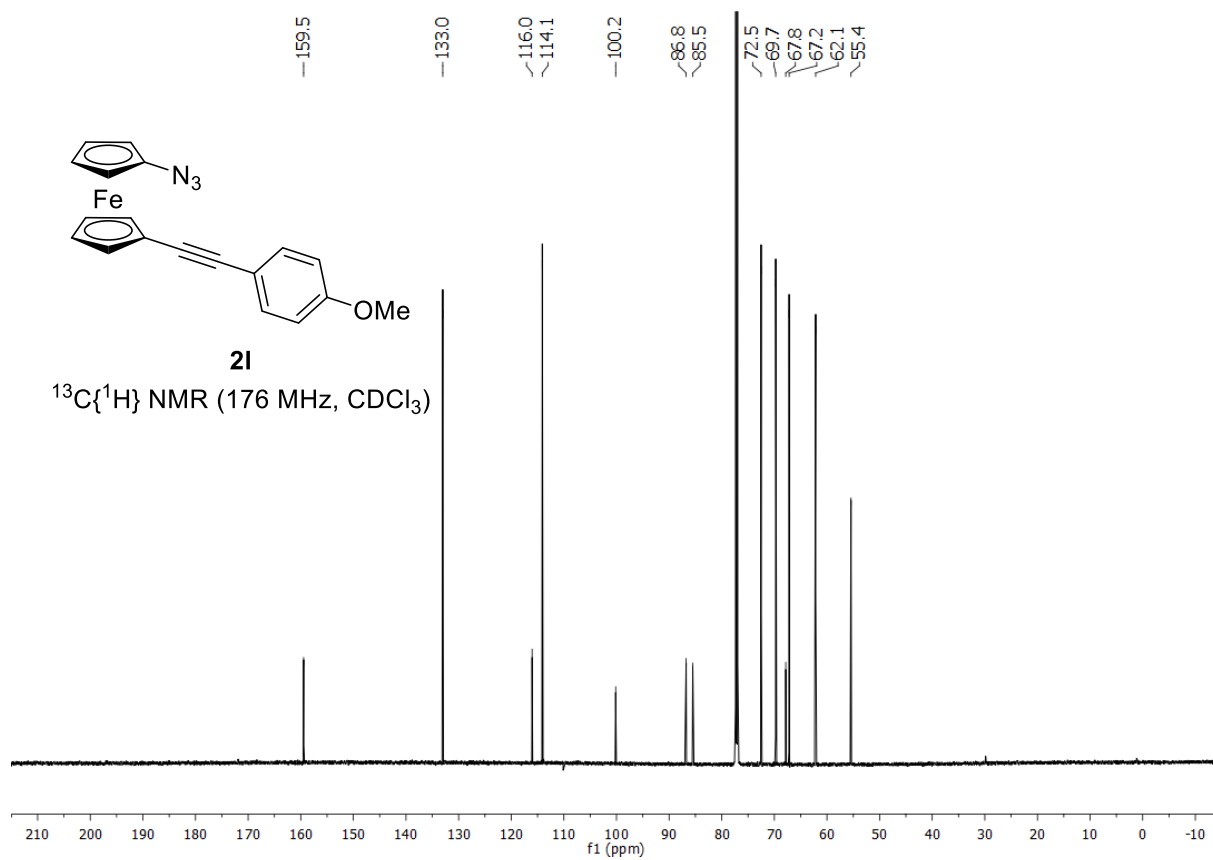
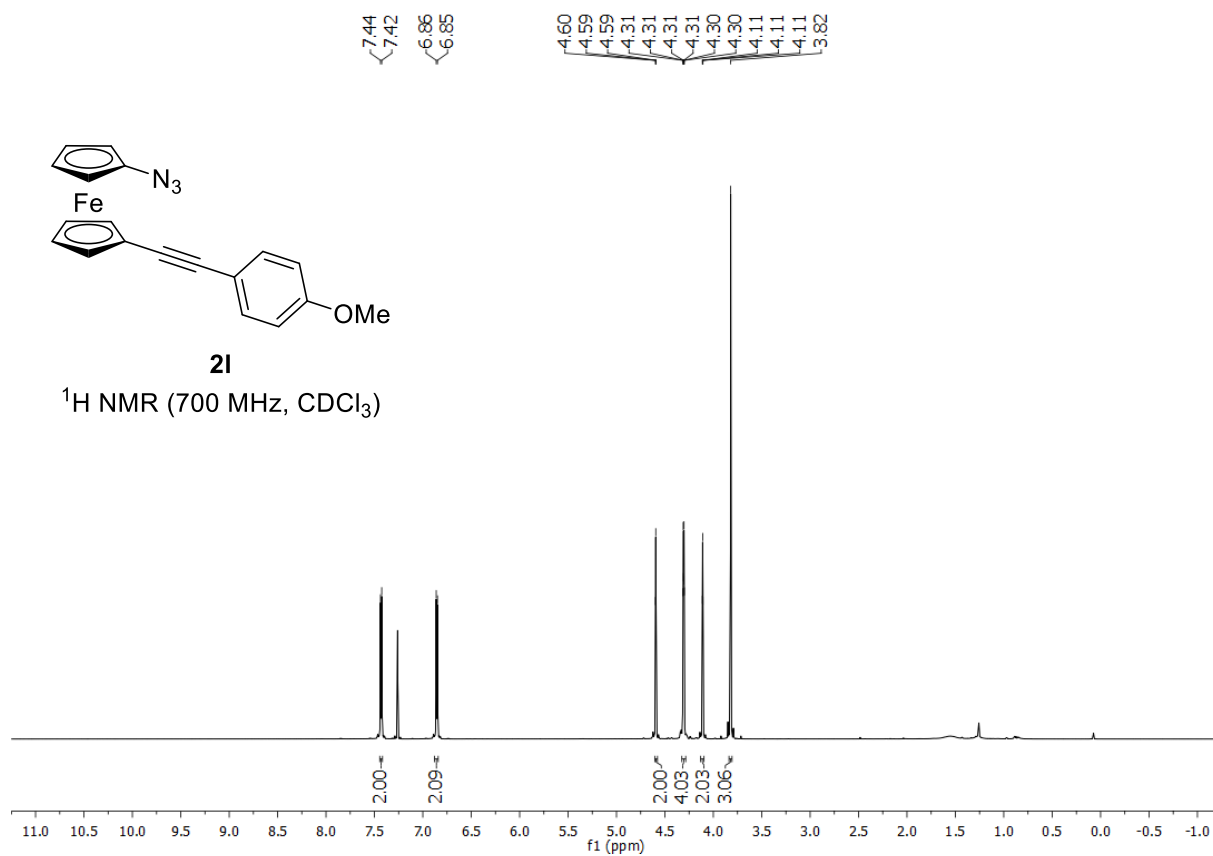


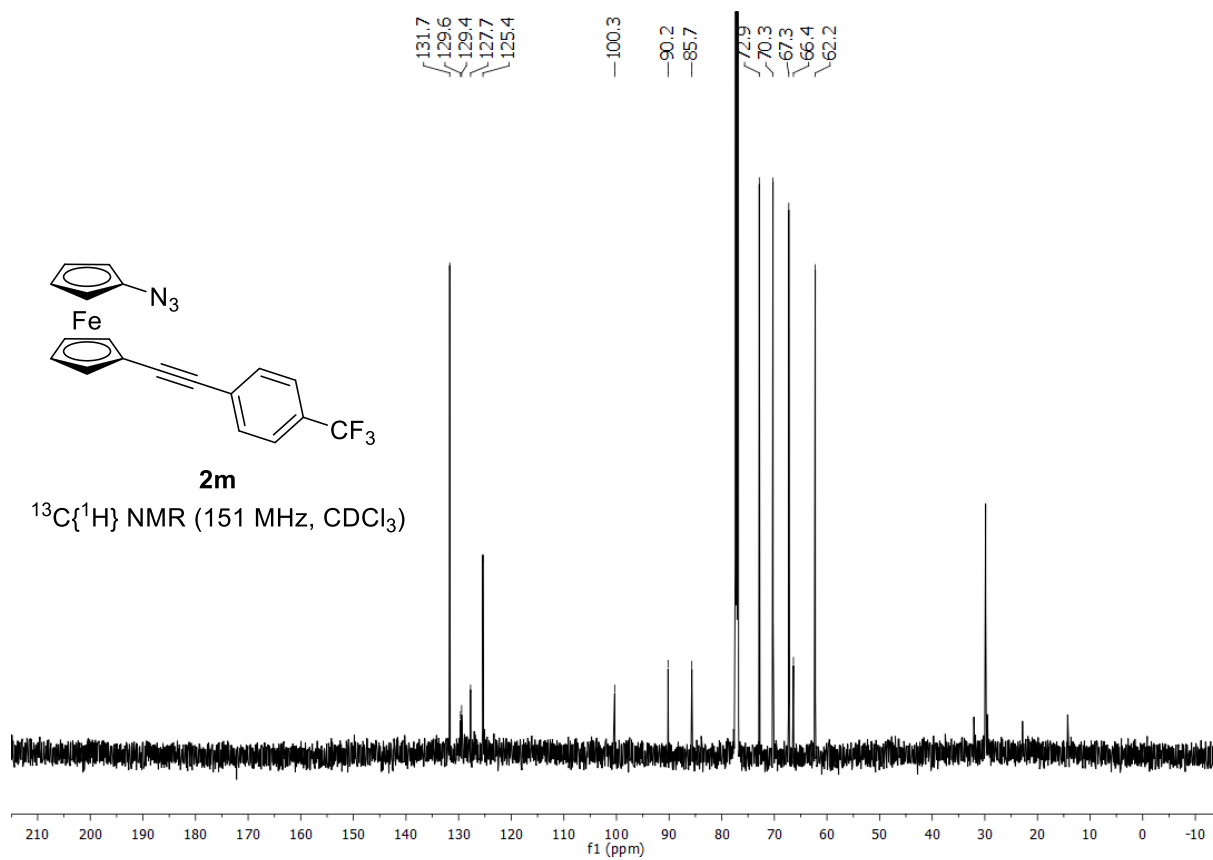
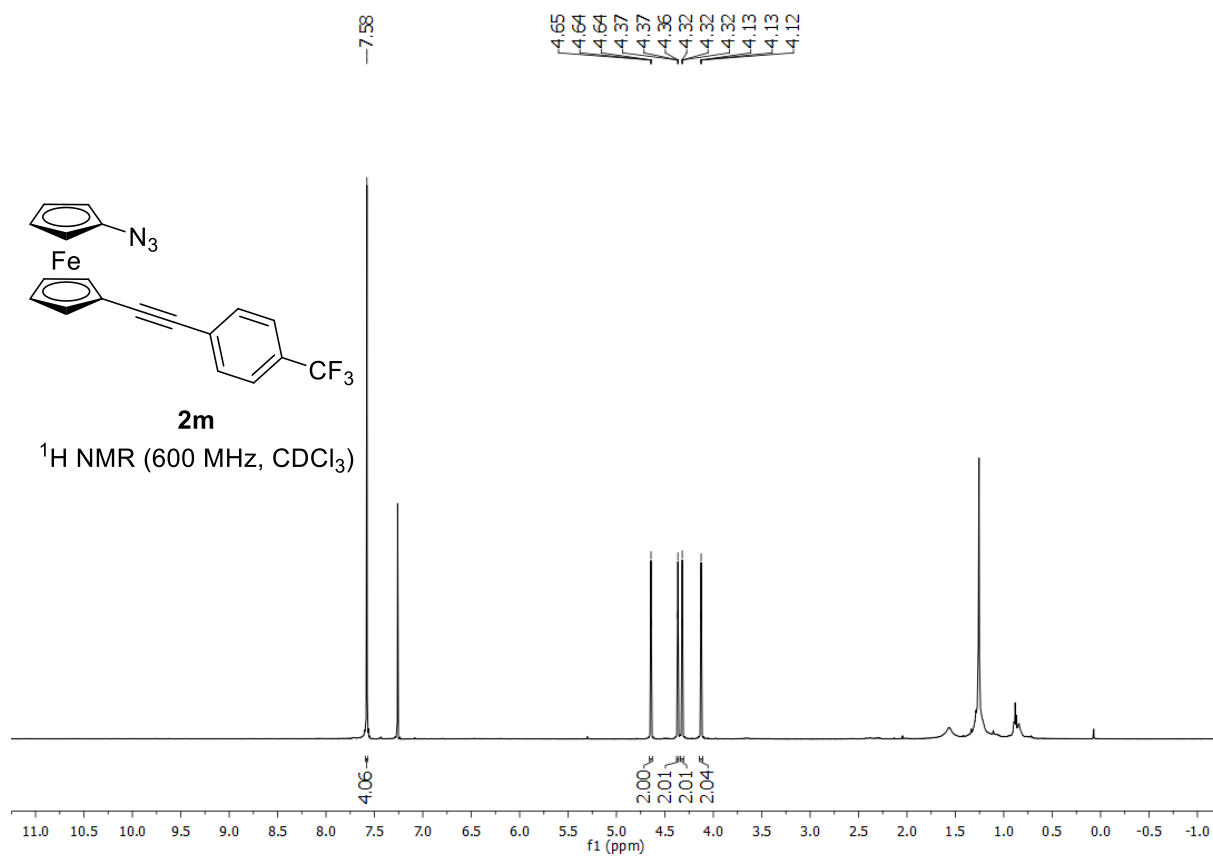


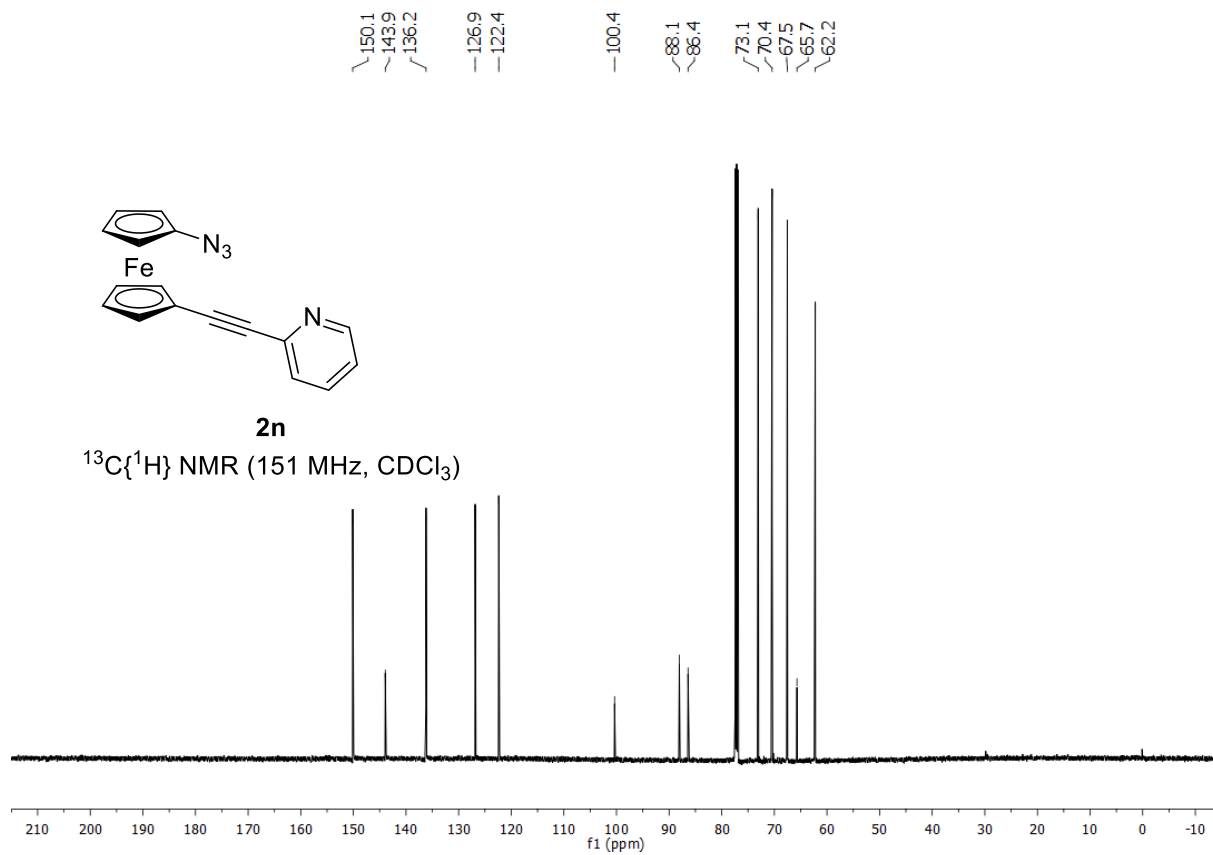
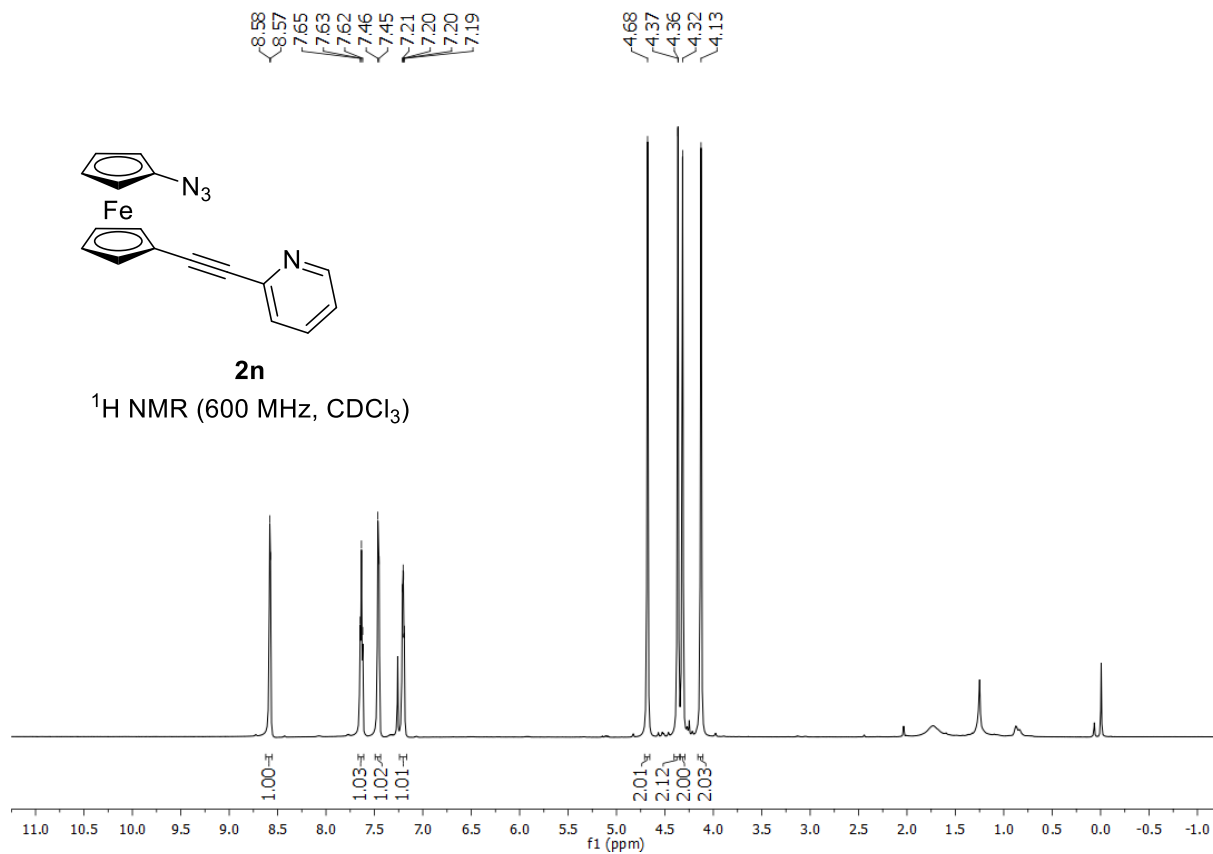












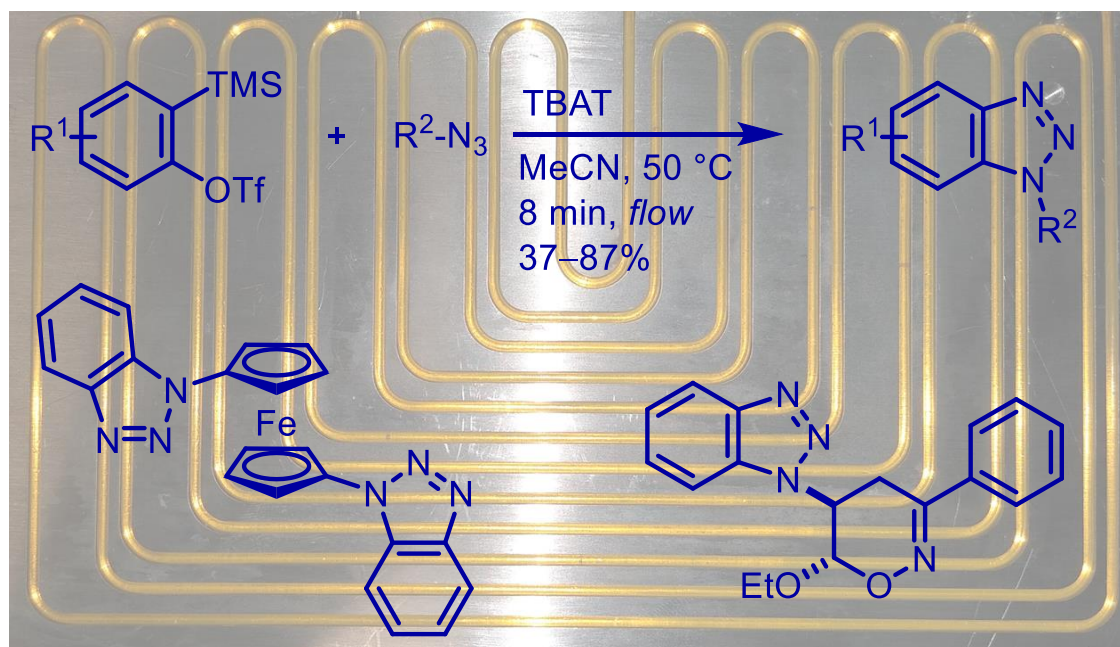
4. References

- [1] S. Diethelm, C. S. Schindler, E. M. Carreira, *Chem. Eur. J.* **2014**, *20*, 6071–6080.
- [2] N. N. Bhuvan Kumar, O. A. Mukhina, A. G. Kutateladze, *J. Am. Chem. Soc.* **2013**, *135*, 9608–9611.
- [3] The original setup was developed by M. Spano from the Croatt research group, is open source and can be found on: <https://chem.uncg.edu/croatt/flow-chemistry/> (25.02.19). For a recent application of this setup, see: L. Fakhouri, C. D. Cook, M. H. Al-Huniti, L. M. Console-Bram, D. P. Hurst, M. B. S. Spano, D. J. Nasrallah, M. G. Caron, L. S. Barak, P. H. Reggio, M. Abood, M. P. Croatt, *Biorg. Med. Chem.* **2017**, *25*, 4355–4367.
- [4] B. Pieber, M. Shalom, M. Antonietti, P. H. Seeberger, K. Gilmore, *Angew. Chem. Int. Ed.* **2018**, *57*, 9976–9979; *Angew. Chem.* **2018**, *130*, 10127–10131.
- [5] D. A. Khobragade, S. G. Mahamulkar, L. Pospíšil, I. Císařova, L. Rulíšek, U. Jahn, *Chem. Eur. J.* **2012**, *18*, 12267–12277.
- [6] T. Okitsu, K. Sato, K. Iwatsuka, N. Sawada, K. Nakagawa, T. Okano, S. Yamada, H. Kakuta, A. Wada, *Bioorg. Med. Chem.* **2011**, *19*, 2939–2949.
- [7] K. Tappe, P. Knochel, *Tetrahedron: Asymmetry* **2004**, *15*, 91–102.
- [8] T.-Y. Dong, S. W. Chang, S.-F. Lin, M.-C. Lin, Y.-S. Wen, L. Lee *Organometallics* **2006**, *25*, 2018–2024.
- [9] L. E. Wilson, C. Hassenrück, R. F. Winter, A. J. P. White, T. Albrecht, N. J. Long, *Eur. J. Inorg. Chem.* **2017**, 496–504.
- [10] C. Engrakul, L. R. Sita, *Organometallics* **2008**, *27*, 927–937.
- [11] A. Shafir, M. P. Power, G. D. Whitener, J. Arnold, *Organometallics* **2000**, *19*, 3978–3982.
- [12] W. Yao, M. Chen, X. Liu, R. Jiang, S. Zhang, W. Chen, *Catal. Sci. Technol.* **2014**, *4*, 1726–1729.
- [13] P. Srinivas, S. Prabhakar, F. Chevallier, E. Nassar, W. Erb, V. Dorcet, V. Jouikov, P. R. Krishna, F. Mongin, *New. J. Chem.* **2016**, *40*, 9441–9447.
- [14] S. Dey, J. W. Quail, J. Müller, *Organometallics* **2015**, *34*, 3039–3046.

Appendix C

Scalable Synthesis of Benzotriazoles via [3+2] Cycloaddition of Azides and Arynes in Flow

M. Kleoff, L. Boeser, L. Baranyi, P. Heretsch



Institut für Chemie und Biochemie, Organische Chemie, Freie Universität Berlin, Takustraße 3,
14195 Berlin, Germany

This article is reproduced with permission from:

M. Kleoff, L. Boeser, L. Baranyi, P. Heretsch, *Eur. J. Org. Chem.* **2021**, 979–982.

<https://doi.org/10.1002/ejoc.202001543>

© 2021 The Authors. Published by Wiley-VCH Verlag GmbH & Co. KGaA.

License No.: 5092980110246

Author contributions: M. Kleoff designed the project. M. Kleoff, L. Boeser, and L. Baranyi carried out the experimental work. The analytical data were collected and analyzed by M. Kleoff and L. Boeser. The manuscript was prepared by M. Kleoff and revised by L. Boeser and P. Heretsch.

Special
Collection

Scalable Synthesis of Benzotriazoles via [3 + 2] Cycloaddition of Azides and Arynes in Flow

Merlin Kleoff,^[a] Lisa Boeser,^[a] Linda Baranyi,^[a] and Philipp Heretsch*^[a]

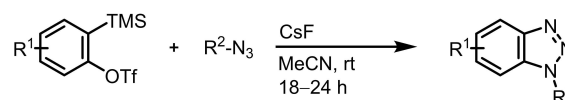
A method for the metal-free synthesis of benzotriazoles in flow is reported. Using azides and in situ generated arynes, benzotriazoles are formed in a [3 + 2] cycloaddition within minutes. Employing different substitution patterns of the azide and aryne coupling partners, a modular access to benzotriazoles is provided. Thermal strain of hazardous azides and accumulation of reactive intermediates is minimized by short reaction times in flow, improving the safety profile of the process. The scalability of the reaction is demonstrated.

The copper(I)-catalyzed [3 + 2] cycloaddition of azides and alkynes (CuAAC) has affected chemistry, biology, and medicinal research alike.^[1] In biological systems, azides and alkynes serve as bioorthogonal linkers allowing conjugation between two molecules by the formation of 1,2,3-triazoles.^[1f,h,2] Owing to the toxicity of copper for living cells, copper-free [3 + 2] cycloadditions are of great interest.^[3] Thus, the metal-free reaction of azides with arynes to substituted 1,2,3-benzotriazoles could allow further applications.^[4,5]

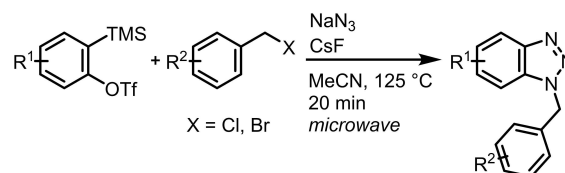
With the appearance of pathogens resistant to commonazole-based pharmaceuticals, benzotriazoles emerged as valuable substitutes and since have been employed for antibacterial, antifungal, and antiviral agents with remarkable potency.^[4c-f,6] Therefore, rapid and scalable access to a broad range of functionalized benzotriazoles could further support medicinal studies.

As described by Larock^[7a] and others,^[7b-f] reaction of *ortho*-trimethylsilyl triflates with fluoride ions generates arynes which undergo [3 + 2] cycloaddition with azides (Scheme 1A). The resulting benzotriazoles were obtained after reaction times of up to 24 hours. To accelerate the reaction, a microwave protocol was developed for the synthesis of benzyl substituted

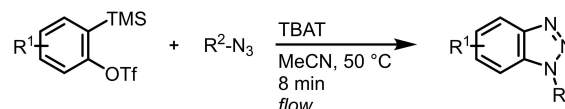
A) [3+2] Cycloaddition of arynes and azides in batch (Larock)



B) Microwave-assisted three component reaction (Biehl)



C) This work: Scalable synthesis of benzotriazoles in flow



Scheme 1. A) Synthesis of benzotriazoles via [3 + 2] cycloaddition of arynes and azides in batch at room temperature. B) Microwave-assisted reaction of arynes with in situ formed benzyl azides. C) Expedient and scalable synthesis of benzotriazoles in flow. TBAT: tetrabutylammonium triphenyldifluorosilylate; Tf: trifluoromethanesulfonyl; TMS: trimethylsilyl.

benzotriazoles but required a reaction temperature of 125 °C (Scheme 1B).^[8]

As heating of organic azides and highly reactive aryne intermediates poses the danger of an explosion, upscaling is problematic.^[9] In recent years, flow chemistry has evolved as an alternative to overcome these limitations.^[10] Given the superior heat and mass transfer in microreactors, various reactions can be significantly accelerated while offering an improved safety and sustainability profile.^[10-12]

We have recently developed a flow platform for the synthesis of natural products and their analogs. Reagents are driven with argon instead of solvent to reduce solvent and reagent waste from drying and equilibration procedures.^[13,14] Using this flow platform, we here describe a scalable method for the efficient preparation of benzotriazoles by [3 + 2] cycloaddition of arynes and azides in flow (Scheme 1C).

At the outset, we screened conditions for the reaction of benzyne precursor **1a** with benzyl azide (**2a**) leading to benzotriazole **3a** (Table 1). To streamline the process and minimize thermal strain of organic azides, we aimed for a short residence time in a heated tube reactor.

Initially, tetrabutylammonium fluoride (TBAF) was used as a fluoride source since the limited solubility of cesium fluoride in

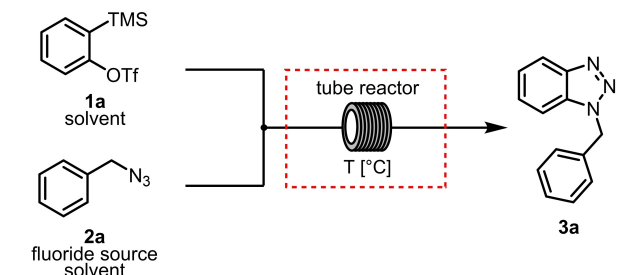
[a] M. Kleoff, L. Boeser, L. Baranyi, Prof. Dr. P. Heretsch
Institut für Chemie und Biochemie
Freie Universität Berlin
Takustraße 3, 14195 Berlin, Germany
E-mail: philipp.heretsch@fu-berlin.de
www.chemie.fu-berlin.de/heretsch

Supporting information for this article is available on the WWW under
<https://doi.org/10.1002/ejoc.202001543>

Part of the "YourJOC Talents" Special Collection.

© 2020 The Authors. European Journal of Organic Chemistry published by Wiley-VCH GmbH. This is an open access article under the terms of the Creative Commons Attribution Non-Commercial NoDerivs License, which permits use and distribution in any medium, provided the original work is properly cited, the use is non-commercial and no modifications or adaptations are made.

Table 1. Optimization of the [3+2] cycloaddition of benzyne and benzyl azide in a flow reactor.^[a]



Entry	Fluoride source	Solvent	T [°C]	Yield [%]
1	TBAF	THF	50	30
2	TBAF	PhCF ₃	50	33
3	TBAF	MeCN	50	53
4	KF/18-c-6	MeCN	50	3
5	TBAT	MeCN	50	74
6	TBAT	MeCN	40	68
7	TBAT	MeCN	55	72
8	TBAT	MeCN	60	66
9 ^[b]	TBAT	MeCN	50	64
10 ^[c]	TBAT	MeCN	50	87

[a] Yields of isolated product are given. Reaction conditions: **1a** (0.3 mmol, 0.15 M, 1.5 equiv), **2a** (0.2 mmol, 0.1 M, 1.0 equiv), TBAT (0.32 mmol, 0.16 M, 1.6 equiv); flow rate: 0.4 mL, 8 min. [b] Performed with a residence time of 4 min. [c] Performed with 1.7 equiv. of **1a** and 1.8 equiv. of TBAT. 18-c-6: 1,4,7,10,13,16-hexaoxacyclooctadecane; THF: tetrahydrofuran.

acetonitrile precluded its use in our flow process. At 50 °C and with a residence time of 8 minutes, different solvents (entries 1–3) were screened. While tetrahydrofuran (THF) and benzonitrile resulted in low yields, employing acetonitrile as solvent, **3a** was isolated with a moderate yield of 53%. When potassium fluoride and 18-crown-6 were used, almost no product was obtained (entry 4). Switching to tetrabutylammonium triphenyldifluorosilicate (TBAT) as a fluoride source gave smooth conversion to benzotriazole **3a** and an improved yield of 74% (entry 5). Further investigation of parameters revealed a residence time of 8 min at 40 °C led to an incomplete reaction (68% yield, entry 6). At higher temperatures, complete consumption of starting material was observed, but lower yields were obtained (entries 7 and 8).

Employing higher flow rates and a shorter residence time of 4 minutes at 50 °C, incomplete conversion of starting material was observed along with a lower yield of 64% (entry 9). Eventually, when 1.7 equivalents of benzyne precursor **1a** and 1.8 equivalents of TBAT were used, the yield of benzotriazole **3a** could be increased to 87% (entry 10). In accordance with our previous studies, the reaction could be performed without exclusion of air and moisture.^[13a]

With the optimized flow protocol in hand, the scope of the [3+2] cycloaddition of benzyne with various azides was investigated (Scheme 2). Despite the intriguing properties of ferrocenyl benzotriazoles,^[4d] they have not been prepared from arynes and ferrocenyl azides, thus far.^[13b] This may be attributed



Merlin Kleoff was born in Berlin, Germany, in 1994 and studied chemistry at Freie Universität Berlin where he received his B.Sc. in 2015. During his Master studies, he worked with Prof. Dr. H.-U. Reißig on the preparation of super Lewis basic terpyridine ligands. In 2018, he completed his M.Sc. with a thesis on the synthesis of new ferrocene building blocks in the group of Prof. Dr. B. Sarkar. He then joined the group of Prof. Dr. P. Heretsch for his PhD where he is currently working on synthetic applications of flow chemistry.



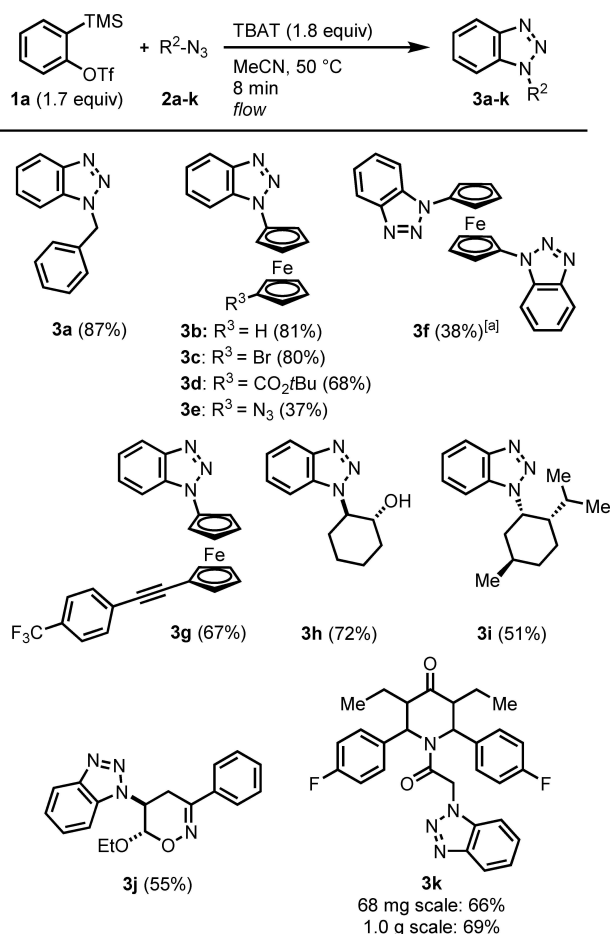
Lisa Boeser was born in Berlin, Germany, in 1998 and studied chemistry at Freie Universität Berlin. She completed her B. Sc. with a thesis on the scalable synthesis of ferrocenyl azides in flow in the group of Prof. Dr. P. Heretsch in 2019. Currently, she is conducting her master studies at Freie Universität Berlin.



Linda Baranyi was born in 1993 in Furth im Wald, Germany. She studied chemistry at the Humboldt-Universität zu Berlin where she received her B.Sc. in 2018. Currently, she is conducting her master studies in chemistry at Freie Universität Berlin.



Philipp Heretsch was born in Lippstadt, Germany, in 1982. He obtained his PhD degree from Universität Leipzig (supervisor: Prof. Dr. A. Giannis) in 2009. After a postdoctoral stay with K.C. Nicolaou at The Scripps Research Institute, La Jolla, California, and at Rice University, Houston, Texas, he was appointed assistant professor at Freie Universität Berlin in 2015. His group is interested in framework manipulation strategies in the context of abeo-steroid and alkaloid synthesis as well as application of flow chemistry in natural product synthesis.



Scheme 2. Scope of benzotriazoles **3a–k** for the reaction of benzyne with organic azides **2**. Yields of isolated product are given. Reaction conditions: **1a** (0.34 mmol, 0.17 M, 1.7 equiv), **2a–k** (0.2 mmol, 0.1 M, 1.0 equiv), TBAT (0.36 mmol, 0.18 M, 1.8 equiv), 50 °C, 8 min. For further details, see the supporting information. [a] Employing **1a** (0.34 mmol, 0.17 M, 3.4 equiv), **2e** (0.1 mmol, 0.05 M, 1.0 equiv), and TBAT (0.36 mmol, 0.18 M, 3.6 equiv).

to the potential explosiveness and thermal lability of ferrocenyl azides, hampering their use in reactions at elevated temperatures.^[15]

Employing our flow protocol, the reaction of azidoferrocene **2b** provided the corresponding ferrocenyl benzotriazole **3b** in a good yield of 81%. Also, the bromo- (**3c**, 80% yield) and the ester-functionalized ferrocenyl benzotriazoles (**3d**, 68% yield) could be obtained.

1,1'-Diazidoferrocene **2e** is a valuable building block for redox-switchable catalysts and sensors.^[15,16] Due to the explosiveness of **2e** at temperatures above 56 °C,^[15] synthetic applications are limited, especially on a larger scale. However, in flow, azide **2e** could be used without safety concerns. When 1.7 equivalents of benzyne precursor **1a** were employed, monobenzotriazole **3e** was isolated in a moderate yield of 37%. Using 3.4 equivalents of benzyne precursor **1a** and 3.6 equivalents of TBAT, dibenzotriazole **3f** was obtained in 38% yield. The alkynyl substituted ferrocenyl benzotriazole **3g** was isolated in 67% yield. Although, alcohols can react as nucleophiles with arynes, the [3 + 2] cycloaddition of alcohol

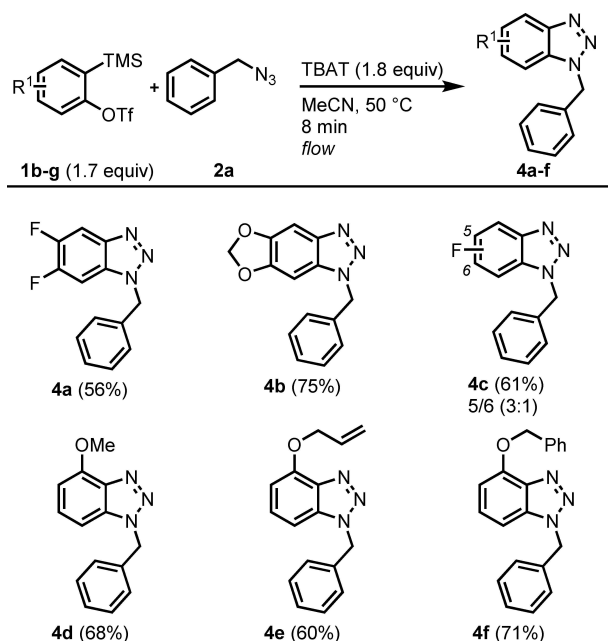
substituted azide **2h** gave benzotriazole **3h** with a good yield of 72%. The enantioenriched benzotriazole **3i** (51% yield) was derived from the corresponding menthyl azide under retention of the stereoconfiguration.

Eventually, heterocyclic azides were tested as substrates. The 5,6-dihydro-2-oxazine **2j** was prepared by aza-Michael addition of 6*H*-1,2-oxazine with sodium azide in protic solvents (see the supporting information).^[17] Cycloaddition with benzyne gave the corresponding benzotriazole **3j** in a yield of 55%.

As benzotriazole substituted piperidone **3k** shows promising antibacterial and antifungal activity,^[6] we aimed for its rapid and scalable synthesis. Employing our method, we prepared **3k** in a yield of 66%. To demonstrate the scalability of our flow protocol, we synthesized **3k** also on a gram scale corresponding to a theoretical productivity of 0.33 g/h in a similar yield of 69% with the same reactor setup.

Finally, we investigated the scope of arynes by using functionalized aryne precursors **1b–g** (Scheme 3). When electron-deficient aryne precursor **1b** was employed, difluorinated benzotriazole **4a** was isolated in 56% yield. The sesamol-derived aryne precursor **1c** reacted smoothly to benzotriazole **4b** in a good yield of 75%. Using fluorinated aryne precursor **1d**, an inseparable mixture of the 5- and 6-fluoro isomers of benzotriazole **4c** (61% yield) was obtained in a 3:1 ratio. In contrast, reaction with *ortho*-substituted precursors **1e–g** selectively gave the 4-functionalized benzotriazoles **4d–f** (60–71% yield), as assigned by nOe spectroscopic analysis.

In conclusion, we have developed a flow protocol for the metal-free synthesis of benzotriazoles by [3 + 2] cycloaddition of azides and in situ generated arynes. Due to the short residence time of 8 minutes, thermal strain is minimized



Scheme 3. Scope of benzotriazoles **4a–f** for the reaction of various arynes **1b–g** with benzyl azide **2a**. Yields of isolated product are given. Reaction conditions: **1b–g** (0.34 mmol, 0.17 M, 1.7 equiv), **2a** (0.2 mmol, 0.1 M, 1.0 equiv), TBAT (0.36 mmol, 0.18 M, 1.8 equiv), 50 °C, residence time: 8 min.

enhancing the safety and efficiency of this protocol. A variety of functionalized azides and arynes have been employed to provide the corresponding benzotriazoles, including the gram-scale preparation of an antibacterial benzotriazole.

Acknowledgements

Financial support for this work was provided by the Boehringer Ingelheim Stiftung. We are grateful to Dr. Johannes Schwan, Dr. Reinhold Zimmer, and Nicole Fouquet (all Freie Universität Berlin) for preparative support. We acknowledge the assistance of the Core Facility BioSupraMol supported by the DFG. Open access funding enabled and organized by Projekt DEAL.

Conflict of Interest

The authors declare no conflict of interest.

Keywords: Arynes · Click chemistry · Cycloaddition · Flow chemistry · Nitrogen heterocycles

- [1] a) H. C. Kolb, M. G. Finn, K. B. Sharpless, *Angew. Chem. Int. Ed.* **2001**, *40*, 2004–2021; *Angew. Chem.* **2001**, *113*, 2056–2075; b) V. V. Rostovtsev, L. G. Green, V. V. Fokin, K. B. Sharpless, *Angew. Chem. Int. Ed.* **2002**, *41*, 2596–2599; *Angew. Chem.* **2002**, *114*, 2708–2711; c) C. W. Tornøe, C. Christensen, M. Meldal, *J. Org. Chem.* **2002**, *67*, 3057–3064; d) M. Meldal, C. W. Tornøe, *Chem. Rev.* **2008**, *108*, 2952–3015; e) D. Schweinfurth, L. Hettmanczyk, L. Suntrup, B. Sarkar, *Z. Allg. Anorg. Chem.* **2017**, *643*, 554–584; f) P. Thirumurugan, D. Matosiuk, K. Jozwiak, *Chem. Rev.* **2013**, *113*, 4905–4979; g) P. L. Golas, K. Matyjaszewski, *Chem. Soc. Rev.* **2010**, *39*, 1338–1354; h) A. H. El-Sagheer, T. Brown, *Chem. Soc. Rev.* **2009**, *39*, 1388–1405.
- [2] a) E. M. Sletten, C. R. Bertozzi, *Angew. Chem. Int. Ed.* **2009**, *48*, 6984–6998; *Angew. Chem.* **2009**, *121*, 7108–7133; b) C. P. Glindemann, A. Backenköhler, M. Strieker, U. Wittstock, P. Klahn, *ChemBioChem* **2019**, *20*, 2341–2345.
- [3] a) J. C. Jewett, C. R. Bertozzi, *Chem. Soc. Rev.* **2010**, *39*, 1272–1279; b) X. Hou, C. Ke, J. F. Stoddart, *Chem. Soc. Rev.* **2016**, *45*, 3766–3780; c) E. Kim, H. Koo, *Chem. Sci.* **2019**, *10*, 7835–7851; d) H. B. Jalani, A. C. Karagöz, S. B. Tsogoeva, *Synthesis* **2017**, *49*, 29–41; e) J. Escorihuela, A. T. M. Marcelis, H. Zuñihof, *Adv. Mater. Interfaces* **2015**, *2*, 1500135.
- [4] For selected reviews concerning benzotriazoles, see: a) A. R. Katritzky, S. Rachwal, *Chem. Rev.* **2010**, *110*, 1564–1610; b) A. R. Katritzky, S. Rachwal, *Chem. Rev.* **2011**, *111*, 7063–7120; c) I. Briguglio, S. Piras, P. Corona, E. Gavini, M. Nieddu, G. Boatto, A. Carta, *Eur. J. Med. Chem.* **2015**, *97*, 612–648; d) Y. Ren, L. Zhang, C.-H. Zhou, R.-X. Geng, *Med. Chem.* **2014**, *4*, 640–662; e) X. M. Peng, G.-X. Cai, C.-H. Zhou, *Curr. Top. Med. Chem.* **2013**, *13*, 1963–2010; f) R. R. Kale, V. Prasad, P. P. Mohapatra, V. K. Tiwari, *Monatsh. Chem.* **2010**, *141*, 1159–1182; g) E. Loukopoulos, G. E. Kostakis, *Coord. Chem. Rev.* **2019**, *395*, 193–229.
- [5] For selected reviews concerning arynes, see: a) A. Bhunia, S. R. Yetra, A. T. Biju, *Chem. Soc. Rev.* **2012**, *41*, 3140–3152; b) J. García-Lopez, M. F. Greaney, *Chem. Soc. Rev.* **2016**, *45*, 6766–6798; c) J. Shi, Y. Li, Y. Li, *Chem. Soc. Rev.* **2017**, *46*, 1707–1719; d) A. V. Dubrovskiy, N. A. Markina, R. C. Larock, *Org. Biomol. Chem.* **2013**, *11*, 191–218; e) R. Karmakar, D. Lee, *Chem. Soc. Rev.* **2016**, *45*, 4459–4470; f) D. B. Werz, A. T. Biju, *Angew. Chem. Int. Ed.* **2020**, *59*, 3385–3398; *Angew. Chem.* **2020**, *132*, 3410–3420; g) H. Takikawa, A. Nishii, T. Sakai, K. Suzuki, *Chem. Soc. Rev.* **2018**, *47*, 8030–8056; h) A. E. Goetz, T. K. Shah, N. K. Garg, *Chem. Commun.* **2015**, *51*, 34–45.
- [6] R. Ramachandran, M. Rani, S. Senthana, Y. T. Jeong, S. Kabilan, *Eur. J. Med. Chem.* **2011**, *46*, 1926–1934.
- [7] For selected examples, see: a) F. Shi, J. P. Waldo, Y. Chen, R. C. Larock, *Org. Lett.* **2008**, *10*, 2409–2412; b) L. Campbell-Verduyn, P. H. Elsinga, L. Mirfeizi, R. A. Dierckx, B. L. Feringa, *Org. Biomol. Chem.* **2008**, *6*, 3461–3463; c) S. Chandrasekhar, M. Seenaiyah, C. L. Rao, C. R. Reddy, *Tetrahedron* **2008**, *64*, 11325–11327; d) D. J. Atkinson, J. Sperry, M. A. Brimble, *Synlett* **2011**, 99–103; e) F. Zhang, J. E. Moses, *Org. Lett.* **2009**, *11*, 1587–1590; f) G. Singh, R. Kumar, J. Swett, B. Zajc, *Org. Lett.* **2013**, *15*, 4086–4089.
- [8] H. Ankati, E. Biehl, *Tetrahedron Lett.* **2009**, *50*, 4677–4682.
- [9] a) S. Bräse, K. Banert (Eds.), *Organic Azides: Synthesis and Applications*, Wiley: Chichester, West Sussex, 2010; b) S. Bräse, C. Gil, K. Knepper, V. Zimmermann, *Angew. Chem. Int. Ed.* **2005**, *44*, 5188–5240; *Angew. Chem.* **2005**, *117*, 5320–5374; c) P. Klahn, H. Erhardt, A. Kotthaus, S. F. Kirsch, *Angew. Chem. Int. Ed.* **2014**, *53*, 7913–7917; *Angew. Chem.* **2014**, *126*, 8047–8051.
- [10] a) M. B. Plutschack, B. Pieber, K. Gilmore, P. H. Seeberger, *Chem. Rev.* **2017**, *117*, 11796–11893; b) M. Movsisyan, E. I. P. Delbeke, J. K. E. T. Berton, C. Battilocchio, S. V. Ley, C. V. Stevens, *Chem. Soc. Rev.* **2016**, *45*, 4892–4928; c) C. J. Mallia, I. R. Baxendale, *Org. Process Res. Dev.* **2016**, *20*, 327–360; d) D. Cambié, C. Bottecchia, N. J. W. Straathof, V. Hessel, T. Noël, *Chem. Rev.* **2016**, *116*, 10276–10341; e) T. Noël, S. L. Buchwald, *Chem. Soc. Rev.* **2011**, *40*, 5010–5029; f) B. Gutmann, D. Cantillo, C. O. Kappe, *Angew. Chem. Int. Ed.* **2015**, *54*, 6688–6728; *Angew. Chem.* **2015**, *127*, 6788–6832; g) C. Empel, R. M. Koenigs, *J. Flow Chem.* **2020**, *10*, 157–160; h) S. T. R. Müller, T. Wirth, *ChemSusChem* **2015**, *8*, 245–250; i) M. Elsherbini, T. Wirth, *Acc. Chem. Res.* **2019**, *52*, 3287–3296.
- [11] C. Wiles, P. Watts, *Green Chem.* **2014**, *14*, 38–54.
- [12] Benzotriazoles have been prepared in flow, for example, from chloronitrobenzenes and amines, see: M. Chen, S. L. Buchwald, *Angew. Chem. Int. Ed.* **2013**, *52*, 4247–4250; *Angew. Chem.* **2013**, *125*, 4341–4344.
- [13] a) J. Schwan, M. Kleoff, B. Hartmayer, P. Heretsch, M. Christmann, *Org. Lett.* **2018**, *20*, 7661–7664; b) M. Kleoff, J. Schwan, L. Boeser, B. Hartmayer, M. Christmann, B. Sarkar, P. Heretsch, *Org. Lett.* **2020**, *22*, 902–907.
- [14] M. Kleoff, J. Schwan, M. Christmann, P. Heretsch, *ChemRxiv* **2020**, DOI: 10.26434/chemrxiv.13266260.v1.
- [15] A. Shafir, M. P. Power, G. D. Whitener, J. Arnold, *Organometallics* **2000**, *19*, 3978–3982.
- [16] a) J. Wei, P. L. Diaconescu, *Acc. Chem. Res.* **2019**, *52*, 415–424; b) F. Zapata, A. Caballero, P. Molina, *Eur. J. Inorg. Chem.* **2016**, 237–241.
- [17] K. Homann, J. Angermann, M. Collas, R. Zimmer, H.-U. Reissig, *J. Prakt. Chem.* **1998**, *340*, 649–655.

Manuscript received: November 25, 2020
Revised manuscript received: December 14, 2020
Accepted manuscript online: December 15, 2020

European Journal of Organic Chemistry

Supporting Information

Scalable Synthesis of Benzotriazoles via [3 + 2] Cycloaddition of Azides and Arynes in Flow

Merlin Kleoff, Lisa Boeser, Linda Baranyi, and Philipp Heretsch*

1. General Information	272
2. Experimental Procedures.....	275
3. NMR Spectra of Synthesized Compounds.....	298
4. References	326

1. General Information

1.1. Materials and Methods

Unless otherwise noted, all reactions and workups were performed open to air. All substances sensitive to water and oxygen were handled under an argon atmosphere using standard Schlenk techniques and oil pump vacuum. Room temperature (rt) refers to 23 °C.

Anhydrous THF was distilled under an atmosphere of argon over sodium/benzophenone and stored over activated 3 Å mol sieves. Anhydrous CH₂Cl₂ and PhMe were obtained from a solvent system MB SPS-800 from the company MBRAUN. Anhydrous DMF was obtained from Acros and stored over 3 Å mol sieves.

EtOH, EtOAc, *n*-pentane and *n*-hexane were purified by distillation on a rotary evaporator. All other solvents and commercially available reagents were used without further purification unless otherwise stated.

3 Å mol sieves were activated by drying in an oven at 250 °C and 10⁻³ mbar for 2–3 h.

Medium pressure liquid chromatography (MPLC) was performed with a TELEDYNE ISCO Combi-Flash Rf or a TELEDYNE ISCO Combi-Flash Rf200 using prepacked SiO₂-columns and cartridges from TELEDYNE. UV response was monitored at 254 nm and 280 nm. As eluents, cyclohexane (99.5%+ quality) and EtOAc (HPLC grade) were used.

For flash column chromatography, SiO₂ 60 M (0.040-0.063 mm) from MACHEREY-NAGEL or basic Al₂O₃ from ACROS or MACHEREY-NAGEL were used. Basic Al₂O₃ was deactivated prior use with 5 wt% H₂O by adding the calculated amount of H₂O to activated Al₂O₃ followed by vigorous shaking for some minutes.

Concentration under reduced pressure was performed by rotary evaporation at 40 °C and the appropriate pressure.

Organic azides should be prepared and handled with additional care and should be stored cold and in the dark.

The following compounds were prepared according to the literature: **1b**,^[1] **1c**,^[1] **1d**,^[2] **1f**,^[3] **1g**,^[3] **2a**,^[4] **2b–g**,^[5] **2h**,^[6] **2i**.^[7]

1.2. Analysis

Reaction monitoring: Reactions were monitored by TLC carried out on Merck Silica Gel 50 F₂₅₄-plates and visualized by fluorescence quenching under UV-light ($\lambda = 254$ nm) or by using a stain of vanillin (6 g vanillin, 1.5 mL 96% aq. H₂SO₄, 100 mL EtOH) and heat as developing agent.

NMR spectroscopy: All NMR spectra were acquired on a JEOL ECP 500 (500 MHz), a BRUKER Avance 500 (500 MHz), a VARIAN Inova 600 (600 MHz), or a BRUKER Avance 700 (700 MHz) in the reported deuterated solvents. Chemical shifts are reported in parts per million (ppm) with reference to the residual solvent peaks. The given multiplicities are phenomenological; thus, the actual appearance of the signals is stated and not the theoretically expected one. The following abbreviations were used to designate multiplicities: s = singlet, d = doublet, t = triplet, q = quartet, p = pentet. In case no multiplicity could be identified, the chemical shift range of the signal is given (m = multiplet).

Infrared spectroscopy: Infrared (IR) spectra were measured on a NICOLET Nexus 670/870 FT-IR spectrometer or a JASCO FT/IR-4100 spectrometer. Wavenumbers $\tilde{\nu}$ are given in cm⁻¹ and intensities are as follows: s = strong, m = medium, w = weak.

High resolution mass spectrometry: High-resolution mass spectra (HRMS) were recorded using an AGILENT 6210 ESI-TOF spectrometer.

Optical rotation: Optical rotations were measured on a JASCO P-2000 polarimeter at 589 nm using 100 mm cells and the solvent and concentration (g/100 mL) indicated.

Melting points: Melting points were recorded with a BÜCHI Melting Point B-545 and are uncorrected.

1.3. Flow Equipment

All flow experiments were carried out using a self-assembled flow platform as previously reported.^[8]

Tubes, connectors, and valves: FEP tube (outer diameter 1/16", inner diameter 1/32") and PTFE tube (outer diameter 1/16", inner diameter 1/32") were obtained from BOLA. T-mixers made from stainless steel 316L were provided by VICI. Tubes and mixers were connected using either coned 10-32 UNF fittings made from stainless steel 316L obtained from UPCHURCH SCIENTIFIC or flat bottom 1/4-28 UNF gripper fittings made from PP obtained from DIBAFIT. Adapters for 1/4-28 UNF systems were made from PP or PTFE and were provided from UPCHURCH SCIENTIFIC. Manual 6-way-valves made from stainless steel 316L were provided by KNAUER.

Reactor: A 4 mL reactor plate consisting of aluminum was provided from THALES NANO (article number: THS-I0000). The reactor plate was equipped with coiled PTFE tube (outer diameter 1/16",

inner diameter 1/32"). The reactor plate was placed on a magnetic stirrer with heat function from IKA and heated until the required temperature was constant.

Gas delivery: A controlled stream of argon gas was delivered using a mass flow controller (EL-FLOW Prestige Series) from BRONKHORST. Connectors and adapters were provided from SWAGELOK.

2. Experimental Procedures

2.1. Optimization of Reaction Conditions in Flow

Screening of different reaction conditions for the [3+2]-cycloaddition of benzyne with benzyl azide **2a** in flow

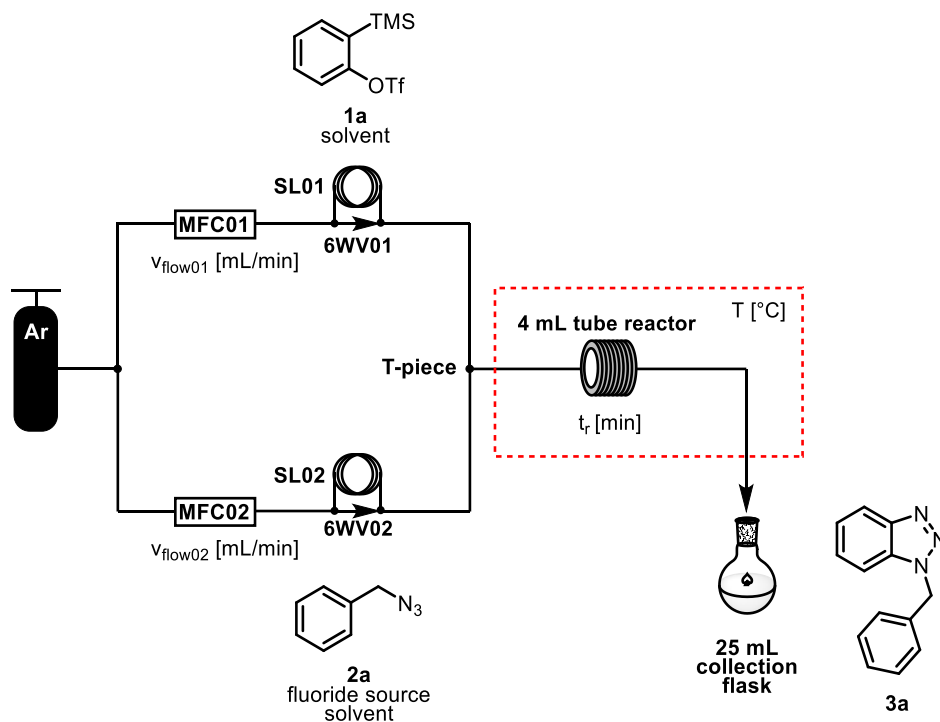


Table S1: Screening of different reaction conditions in flow.

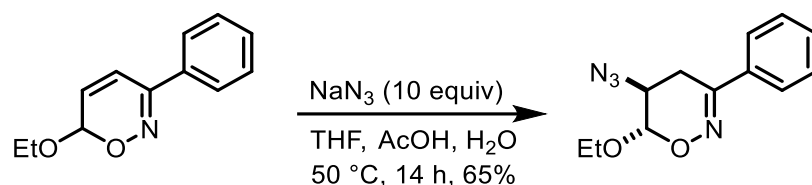
Entry	Fluoride source	Solvent	T [°C]	t _r [min]	V _{flow_tot} [min/mL]	Yield [%] ^[a]
1 ^[b,c]	TBAF	THF	50	7	0.4	30
2 ^[b]	TBAF	PhCF ₃	50	8	0.4	33
3 ^[b]	TBAF	MeCN	50	8	0.4	53
4	KF/18-c-6	MeCN	50	8	0.4	3
5	TBAT	MeCN	50	8	0.4	74
6	TBAT	MeCN	40	8	0.4	68
7	TBAT	MeCN	55	8	0.4	72
8 ^[c]	TBAT	MeCN	60	7	0.4	66
9 ^[d]	TBAT	MeCN	50	4	0.8	64
10 ^[e]	TBAT	MeCN	50	8	0.4	87
11 ^[f]	TBAT	MeCN	50	8	0.4	83

TBAF = tetrabutylammonium fluoride, TBAT = tetrabutylammonium triphenyldifluorosilicate, 18-c-6 = 1,4,7,10,13,16-hexaoxacyclooctadecane. [a] Isolated yield. [b] TBAF was added as a 1.0 M solution in THF. Thus, the solvent of the reaction is a mixture of THF and the indicated solvent. [c] The residence time t_r is slightly shorter than calculated due to partial evaporation of the solvent leading to higher flow rates. [d] Performed at higher flow rates: $v_{\text{flow}01} = v_{\text{flow}02} = 0.4$ mL/min resulting in $v_{\text{flow_tot}} = 0.8$ mL/min. [e] 1.7 equiv of the benzyne-precursor and 1.8 equiv of TBAT were used. [f] A solution of the fluoride source was pumped to a solution of benzyl azide and the benzyne precursor.

Open to air, in a small vial, 2.5 mL of a solution of 2-(trimethylsilyl)phenyl trifluoromethanesulfonate (**1a**) was prepared in the solvent indicated and loaded on sample loop **SL01** ($V = 2$ mL). In another vial, 2.5 mL of a solution of benzyl azide (**2a**, 0.1 M) and the fluoride source indicated was prepared in the solvent indicated and loaded on sample loop **SL02** ($V = 2$ mL). Then, both solutions were driven by an argon flow using mass flow controllers **MFC01** and **MFC02** with the flow rate ($v_{\text{flow_tot}} = v_{\text{flow}01} + v_{\text{flow}02}$; $v_{\text{flow}01} = v_{\text{flow}02}$) indicated. Both solutions were mixed in a **T-piece** and then pumped through a preheated **4 mL tube reactor** at the temperature indicated. At the end of the reactor, the reaction mixture was collected in a **25 mL collection flask**, diluted with EtOAc (10 mL) and loaded on Celite[®]. MPLC (cyclohexane/EtOAc 100:0 to 80:20) gave benzotriazole **3a** as a colorless solid.

2.2. Synthesis of Substrates

Synthesis of 5-azido-6-ethoxy-3-phenyl-5,6-dihydro-4H-1,2-oxazine (S1)



In a pressure tube, 6-ethoxy-3-phenyl-6H-1,2-oxazine^[9] (43 mg, 0.21 mmol, 1.0 equiv) and NaN_3 (0.13 g, 2.1 mmol, 10 equiv) were placed. Anhydrous THF (0.60 mL), AcOH (0.18 mL) and H_2O (0.31 mL) were added, the pressure tube was sealed, and the resulting solution was stirred at 50 °C for 14 h. After cooling to rt, the mixture was diluted with NaHCO_3 (sat. aq., 10 mL) and CH_2Cl_2 (10 mL). The organic layer was separated, and the aqueous layer was extracted with CH_2Cl_2 (3×10 mL). The combined organic layers were dried (Na_2SO_4), filtered, concentrated under reduced pressure, and loaded on Celite[®]. MPLC (cyclohexane/EtOAc 100:0 to 80:20) gave the title compound **S1** (34 mg, 0.14 mmol, 65%) as a colorless solid.

$R_f = 0.33$ (SiO_2 , *n*-hexane/EtOAc 15:1).

^1H NMR (600 MHz, CDCl_3) δ [ppm] = 7.71 – 7.68 (m, 2H), 7.44 – 7.39 (m, 3H), 5.02 (d, $J = 3.4$, 1H), 3.97 (dq, $J = 9.7, 7.1$ Hz, 1H), 3.88 (dt, $J = 6.4, 3.2$ Hz, 1H), 3.71 (dq, $J = 9.7, 7.1$ Hz, 1H), 2.99 (dd, $J = 18.2, 6.2$ Hz, 1H), 2.61 (dd, $J = 18.2, 3.1$ Hz, 1H), 1.23 (t, $J = 7.1$ Hz, 3H).

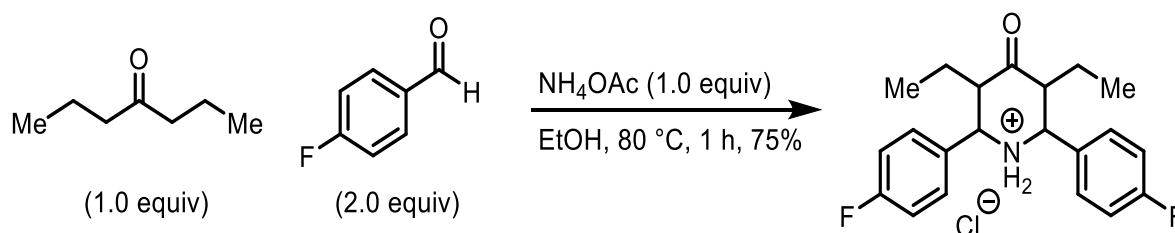
$^{13}\text{C}\{^1\text{H}\}$ NMR (151 MHz, CDCl_3) δ [ppm] = 154.4, 135.1, 130.2, 128.8, 125.6, 96.0, 64.7, 52.6, 24.1, 15.1.

FT-IR (neat) $\tilde{\nu}$ [cm^{-1}] = 2979 (w), 2926 (w), 2902 (w), 2113 (s), 2090 (s), 1496 (w), 1444 (w), 1415 (w), 1379 (w), 1339 (w), 1253 (s), 1176 (m), 1112 (s), 1091 (s), 1076 (m), 1036 (m), 990 (m), 929 (w), 891 (s), 836 (m), 759 (s), 736 (w).

HRMS (ESI-TOF) m/z calcd. for $\text{C}_{12}\text{H}_{14}\text{N}_4\text{NaO}_2^+$ ($[\text{M}+\text{Na}]^+$) 269.1009; found: 269.1006.

M.p. = 84–85 °C (EtOAc).

Synthesis of 3,5-diethyl-2,6-bis(4-fluorophenyl)-4-oxopiperidin-1-ium chloride (S2)



In a 100 mL round bottom flask, NH_4OAc (3.37 g, 43.8 mmol, 1.0 equiv) was dissolved in EtOH (25 mL). 4-Heptanone (6.10 mL, 43.8 mmol, 1.0 equiv) and 4-fluorobenzaldehyde (9.37 mL, 87.6 mmol, 2.0 equiv; freshly distilled prior use) were added and the colorless solution was stirred at 80 °C for 1 h.

After cooling to rt, the yellow solution was poured into stirring Et₂O (300 mL). While stirring, a weak stream of gaseous HCl (note 1) was introduced with a PTFE tube for 10 min until no precipitate was formed anymore. The resulting colorless precipitate was filtered off, washed with Et₂O (3x50 mL) and *n*-pentane (3x50 mL), affording the title compound **S2** (12.4 g, 32.6 mmol, 75%), essentially pure, as a colorless solid.

Further purification can be performed by recrystallization from boiling EtOH/H₂O.

Note 1: Gaseous HCl was generated by adding HCl (aq., 37%) with a pressure-equalizing dropping funnel to stirred H₂SO₄ (aq., 96%) in a round bottom flask under water bath cooling. The pressure-equalizing dropping funnel was sealed with a rubber septum containing a PTFE tube (1/8" outer diameter, 1/16" inner diameter) that was introduced to the ethereal solution.

¹H NMR (600 MHz, DMSO-*d*₆) δ [ppm] = 11.01 (s, 1H), 10.03 (s, 1H), 7.92 (s, 4H), 7.30 (t, *J* = 8.6 Hz, 4H), 4.72 (s, 2H), 3.68 (s, 2H), 1.33 (dq, *J* = 14.6, 7.2 Hz, 2H), 1.29 – 1.20 (m, 2H), 0.71 (t, *J* = 7.3 Hz, 6H).

¹³C{¹H} NMR (151 MHz, DMSO-*d*₆) δ [ppm] = 204.5, 162.6 (d, *J* = 246.4 Hz), 131.8, 130.7, 115.5 (d, *J* = 21.5 Hz), 62.5, 52.2, 17.9, 10.9.

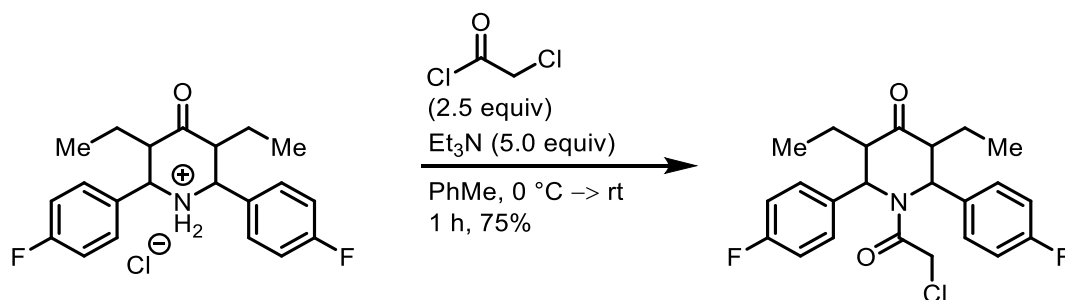
¹⁹F NMR (565 MHz, DMSO-*d*₆) δ [ppm] = -111.8.

FT-IR (neat) $\tilde{\nu}$ [cm⁻¹] = 3444 (very broad), 3276 (w), 2251 (w), 2125 (w), 1660 (w), 1609 (w), 1514 (w), 1455 (w), 1227 (w), 1160 (w), 1052 (s), 1024 (s), 887 (w), 822 (m), 759 (m).

HRMS (ESI-TOF) *m/z* calcd. for C₂₁H₂₄F₂NO⁺ ([M]⁺) 344.1815; found: 344.1830.

M.p. = 261–263 °C (*n*-pentane).

Synthesis of 1-(2-chloroacetyl)-3,5-diethyl-2,6-bis(4-fluorophenyl)piperidin-4-one (**S3**)



S2 (10.0 g, 26.4 mmol, 1.0 equiv) was placed in a 250 mL Schlenk flask with a large conical stirring bar. The Schlenk flask was evacuated and backfilled with argon (3x). Anhydrous PhMe (100 mL) was added. Anhydrous Et₃N (18.4 mL, 132 mmol, 5.0 equiv) was added under ice bath cooling and the suspension was stirred at 0 °C for 5 min. Then, 2-chloroacetyl chloride (5.25 mL, 66.0 mmol, 2.5 equiv; freshly distilled prior use) was added slowly at this temperature via syringe over 10 min. After stirring for 10 min, the ice bath was switched to a water bath and the brown suspension was stirred for additional 40 min. The mixture was filtered over a pad of silica (h = 5 cm) and the silica pad was washed with

EtOAc (5x50 mL). The filtrate was washed with NaHCO₃ (sat. aq., 200 mL) and NaCl (sat. aq., 200 mL), dried (Na₂SO₄), filtered, and concentrated under reduced pressure. After recrystallization from boiling *n*-hexane, the title compound **S3** (5.12 g, 12.2 mmol, 46%) was obtained as a colorless solid.

*R*_f = 0.30 (SiO₂, *n*-hexane/EtOAc 8:1).

¹H NMR (600 MHz, CDCl₃) δ [ppm] = 7.14 (s, 4H), 7.02 (t, *J* = 8.5 Hz, 4H), 5.62 (s, 2H), 3.90 (s, 2H), 2.85 (s, 2H), 1.65 (ddd, *J* = 13.9, 7.5, 6.2 Hz, 2H), 1.43 (d, *J* = 14.1 Hz, 2H) 0.93 (t, *J* = 7.4 Hz, 6H).

¹³C{¹H} NMR (151 MHz, CDCl₃) δ [ppm] = 209.2, 169.4, 162.4 (d, *J* = 248.6 Hz), 136.9 (d, *J* = 3.4 Hz), 129.3, 116.2 (d, *J* = 21.7 Hz), 116.1, 52.5, 42.8, 20.4, 11.1.

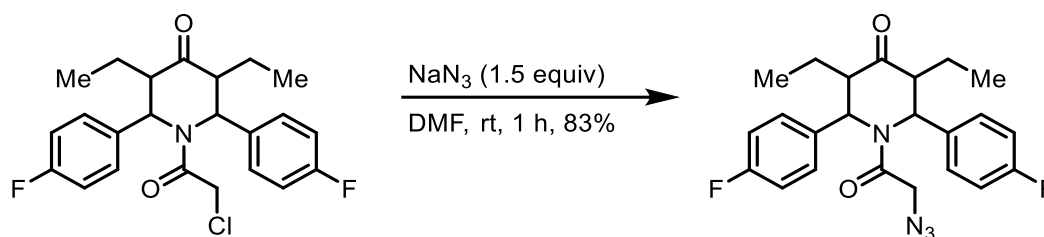
¹⁹F NMR (565 MHz, CDCl₃) δ [ppm] = -113.0.

FT-IR (neat) $\tilde{\nu}$ [cm⁻¹] = 3077 (w), 3014 (w), 2969 (m), 2937 (m), 2878 (w), 1898 (w), 1714 (s), 1650 (s), 1604 (s), 1509 (s), 1459 (w), 1385 (s), 1337 (w), 1226 (s), 1160 (s), 1137 (w) 1100 (w), 1014 (w), 927 (w), 854 (s), 836 (m), 792 (w), 781 (w), 752 (s).

HRMS (ESI-TOF) *m/z* calcd. for C₂₃H₂₄ClF₂NNaO₂⁺ ([M+Na]⁺) 442.1356; found: 442.1374.

M.p. = 112–114 °C (*n*-hexane).

Synthesis of 1-(2-azidoacetyl)-3,5-diethyl-2,6-bis(4-fluorophenyl)piperidin-4-one (**2k**)



S3 (4.00 g, 9.53 mmol, 1.0 equiv) and NaN₃ (929 mg, 14.3 mmol, 1.5 equiv) were placed in a 100 mL Schlenk flask. The flask was evacuated and backfilled with argon (3x). Then, anhydrous DMF (40 mL) was added. The brown solution was stirred at rt for 1 h. Then, the mixture was diluted with EtOAc (50 mL) and H₂O (100 mL). The organic layer was separated and the aqueous layer was extracted with EtOAc (3x50 mL). The combined organic layers were washed with NaCl (sat. aq, 3x100 mL), dried (MgSO₄), filtered, concentrated under reduced pressure, and loaded onto Celite[®]. MPLC (cyclohexane/EtOAc 100:0 to 85:15) gave the title compound **2k** (3.36 g, 7.88 mmol, 83%) as a colorless solid.

*R*_f = 0.25 (SiO₂, *n*-hexane/EtOAc 8:1).

¹H NMR (600 MHz, CDCl₃) δ [ppm] = 7.11 (s, 4H), 7.02 (t, *J* = 8.4 Hz, 4H), 5.45 (s, 2H), 3.68 (s, 2H), 2.85 (q, *J* = 6.2 Hz, 2H), 1.67 – 1.54 (m, 2H), 1.44 (dt, *J* = 14.6, 7.3 Hz, 2H), 0.92 (t, *J* = 7.4 Hz, 6H).

¹³C{¹H} NMR (151 MHz, CDCl₃) δ [ppm] = 209.0, 170.4, 162.3 (d, *J* = 248.6 Hz), 136.6 (d, *J* = 3.4 Hz), 129.4 (d, *J* = 8.1 Hz), 116.1 (d, *J* = 21.5 Hz), 57.2, 52.4, 52.0, 20.8, 11.1.

¹⁹F NMR (565 MHz, CDCl₃) δ [ppm] = -112.9.

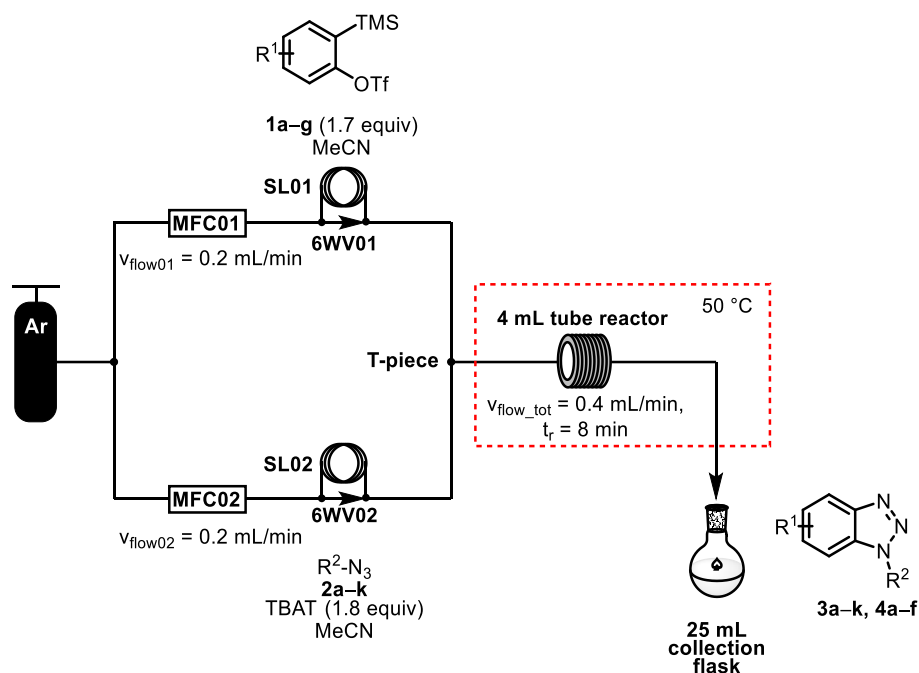
FT-IR (neat) $\tilde{\nu}$ [cm⁻¹] = 3016 (w), 2970 (m), 2938 (w), 2879 (w), 2105 (s), 1714 (s), 1655 (s), 1605 (m), 1509 (s), 1458 (w), 1387 (m), 1362 (w), 1256 (s), 1227 (s), 1161 (s), 1135 (w), 1097 (w), 1070 (w), 1050 (w), 1014 (w), 989 (w), 923 (w), 895 (w), 854 (s), 829 (m), 750 (s).

HRMS (ESI-TOF) m/z calcd. for C₂₃H₂₄F₂N₄NaO₂⁺ ([M+Na]⁺) 449.1759; found: 449.1779.

M.p. = 124–125 °C (EtOAc).

2.3. Synthesis of Benzotriazoles in Flow

General procedure (GP1) for the synthesis of benzotriazoles in flow



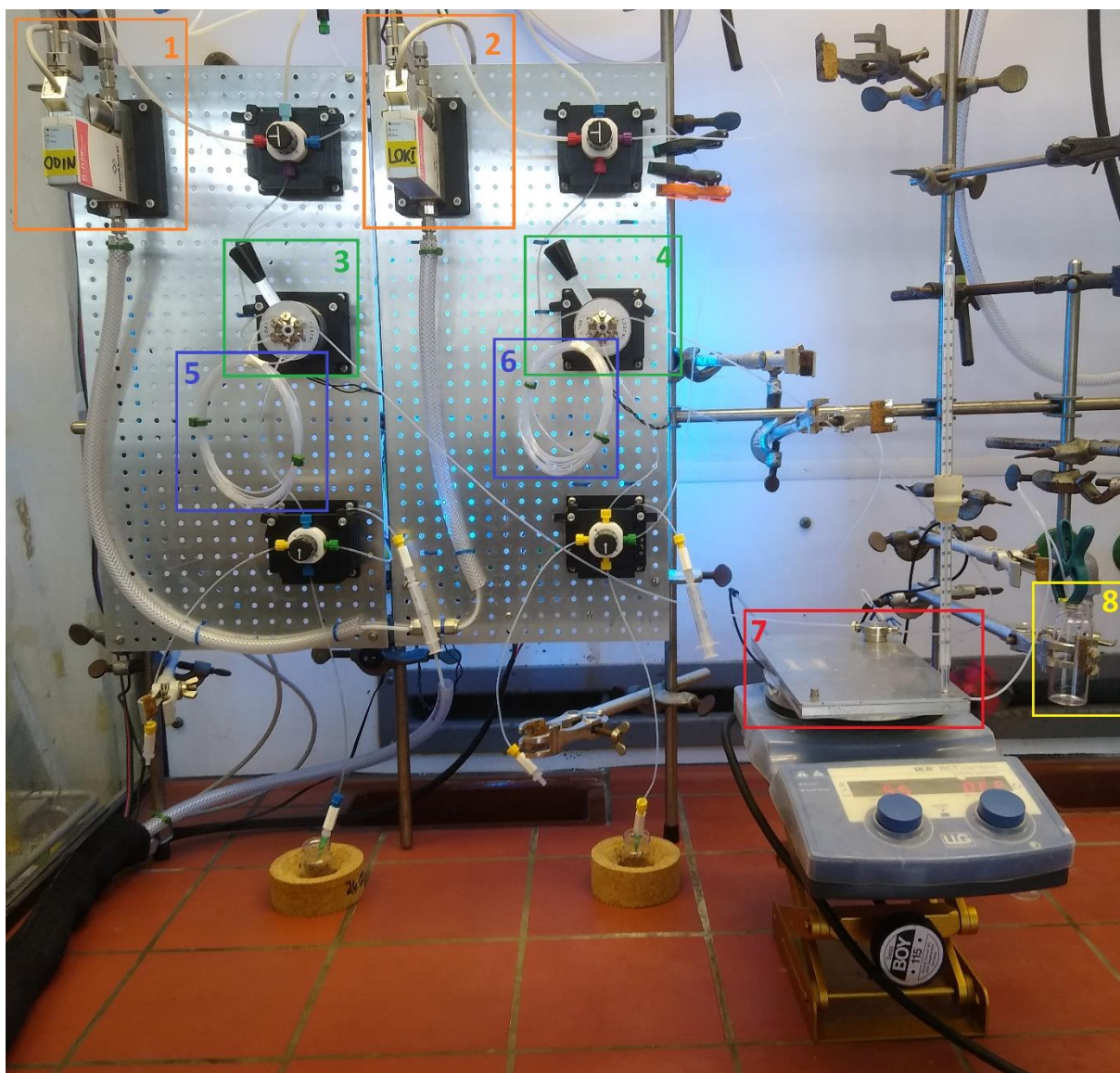
In a small vial, open to air, 2.5 mL of a solution of the aryne precursor **1a-g** (425 μmol , 1.7 equiv, 0.17 M) indicated were prepared in MeCN and loaded on sample loop **SL01** ($V = 2 \text{ mL}$). In another vial, 2.5 mL of a solution of the azide **2a-k** (250 μmol , 1.0 equiv, 0.1 M) and TBAT (243 mg, 450 μmol , 1.8 equiv, 0.18 M) were prepared in MeCN and loaded on sample loop **SL02** ($V = 2 \text{ mL}$). Then, both solutions were driven by an argon flow using mass flow controllers **MFC01** and **MFC02** with a flow rate of $V_{\text{flow}01} = V_{\text{flow}02} = 0.2 \text{ mL/min}$. Both solutions were mixed in a **T-piece** and then pumped through a preheated **4 mL tube reactor** at $50 \text{ }^\circ\text{C}$. At the end of the reactor, the reaction mixture was collected in a **25 mL collection flask**, diluted with EtOAc (10 mL) and loaded on Celite[®]. MPLC (cyclohexane/EtOAc) gave the corresponding benzotriazoles **3a-k** and **4a-f**.

Note 1: Although all reactions can be performed without exclusion of air and moisture, MeCN containing too much water can lead to solubility problems.

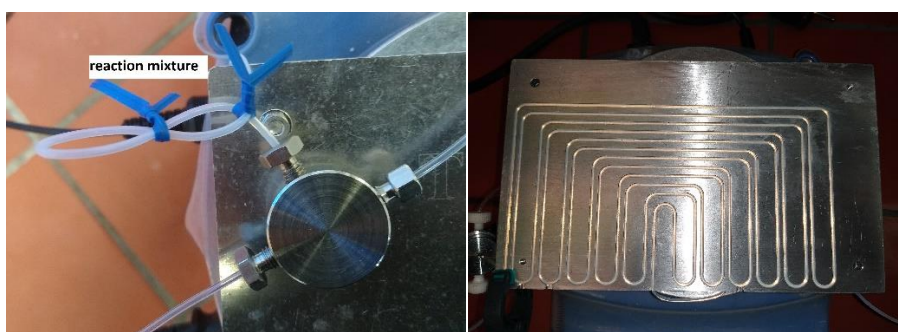
Note 2: In order to solubilize the reactants in MeCN, sonication of the solutions can be performed.

Note 3: In the reaction, Ph_3SiF is formed as byproduct. Although this compound is quite non-polar, it tends to stick to the column. To remove it by column chromatography, a relatively long non-polar pre-run (cyclohexane/EtOAc 100/0 to 90/10) should be performed before polarity of the eluent is increased.

Note 4: Further purification of benzotriazoles can be performed by recrystallization from *n*-hexane/ CHCl_3 .

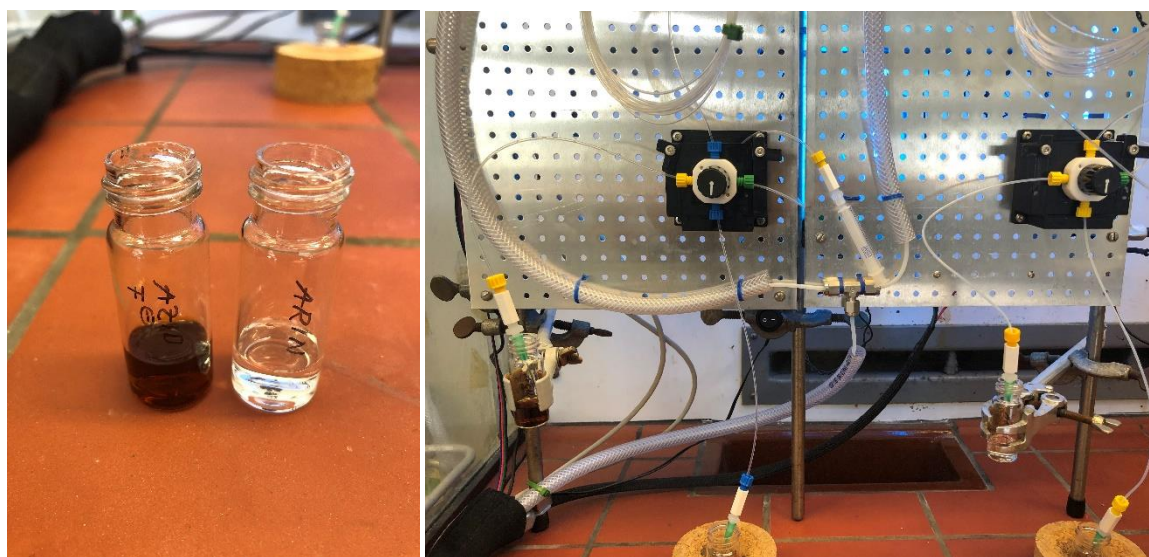


Flow-setup: 1. Mass flow controller 01. 2. Mass flow controller 02. 3. 6-Way valve 01. 4. 6-Way valve 02. 5. Sample Loop 01. 6. Sample Loop 02. 7. Tube reactor with T-piece. 8. Collection vial.

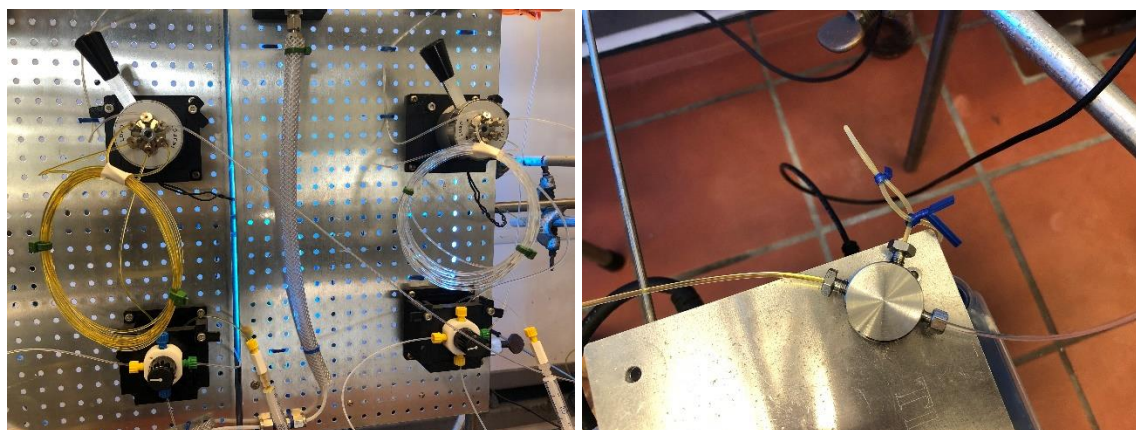


Left: The T-piece mixing the reactant solutions before the reaction mixture enters the heated tube reactor. To further enhance mixing, the tube was coiled and secured with cable fixer. Right: Inside view in the tube reactor from THALES NANO. The tube is embedded in an aluminum housing.

Graphical Guide for the Synthesis of Benzotriazoles in Flow (example: compound 3b)



Left: Stock solutions of ferrocenyl azide **2b** and TBAT (left) and benzyne precursor **1a** (right) in MeCN.
Right: The stock solutions are connected with the load valves of the flow platform.

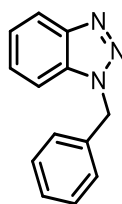


Left: The sample loops ($V = 2$ mL; SL01 and SL02) of the injection valves (6WV01 and 6WV02) are loaded with the solutions. Right: The T-piece while mixing the solutions.



Left: The crude product solution after passing through the heated tube reactor. **Right:** The isolated product **3b**.

Synthesis of 1-benzyl-1*H*-benzo[*d*][1,2,3]triazole (**3a**)



According to **GP1**, the title compound was prepared from **1a** (0.10 g, 0.35 mmol, 1.7 equiv), **2a**^[4] (27 mg, 0.20 mmol, 1.0 equiv), and TBAT (0.19 g, 0.36 mmol, 1.8 equiv). MPLC (cyclohexane/EtOAc 100:0 to 80:20) gave the title compound **3a** (37 mg, 0.18 mmol, 87%) as a colorless solid.

$R_f = 0.21$ (SiO₂, *n*-hexane/EtOAc 7:1).

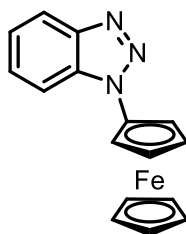
¹H NMR (600 MHz, CDCl₃) δ [ppm] = 8.07 (d, $J = 8.3$ Hz, 1H), 7.43 – 7.25 (m, 8H), 5.85 (s, 2H).

¹³C{¹H} NMR (151 MHz, CDCl₃) δ [ppm] = 146.5, 134.9, 132.9, 129.1, 128.6, 127.7, 127.5, 124.1, 120.2, 109.9, 52.4.

FT-IR (neat) $\tilde{\nu}$ [cm⁻¹] = 3087 (w), 3065 (w), 3031 (w), 2923 (w), 2923 (w), 2852 (w), 1739 (w), 1615 (w), 1589 (w), 1496 (m), 1475 (w), 1456 (m), 1441 (m), 1419 (w), 1365 (w), 1323 (m), 1306 (w), 1276 (w), 1263 (m), 1244 (w), 1224 (s), 1204 (w), 1180 (w), 1162 (m), 1137 (w), 1095 (84), 1070 (m), 1027 (w), 1002 (w), 948 (m), 916 (w), 907 (w), 821 (w), 805 (w), 790 (m), 774 (m), 744 (s), 721 (s).

The spectroscopic data are consistent with those reported in the literature.^[10]

Synthesis of 1-(1*H*-benzo[*d*][1,2,3]triazole)-ferrocene (**3b**)



According to **GP1**, the title compound was prepared from **1a** (0.10 g, 0.35 mmol, 1.7 equiv), **2b**^[5] (46 mg, 0.20 mmol, 1.0 equiv), and TBAT (0.19 g, 0.36 mmol, 1.8 equiv). MPLC (cyclohexane/EtOAc 100:0 to 80:20) gave the title compound **3b** (50 mg, 0.17 mmol, 81%) as a yellow solid.

$R_f = 0.40$ (SiO₂, *n*-hexane/EtOAc 5:1).

¹H NMR (600 MHz, CDCl₃) δ [ppm] = 8.11 (d, $J = 8.4$ Hz, 1H), 7.85 (d, $J = 8.3$ Hz, 1H), 7.56 (t, $J = 7.6$ Hz, 1H), 7.41 (t, $J = 7.6$ Hz, 1H), 4.98 (t, $J = 1.9$ Hz, 2H), 4.36 (t, $J = 1.9$ Hz, 2H), 4.27 (s, 5H).

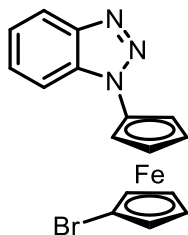
¹³C{¹H} NMR (151 MHz, CDCl₃) δ [ppm] = 146.6, 133.2, 127.8, 124.3, 120.5, 110.9, 93.9, 70.1, 66.7, 62.7.

FT-IR (neat) $\tilde{\nu}$ [cm⁻¹] = 2952 (w), 2919 (s), 2850 (m), 1737 (s), 1511 (s), 1376 (w), 1277 (s), 1206 (s), 1120 (s), 1072 (s), 1000 (m), 922 (w), 874 (m), 742 (s).

HRMS (ESI-TOF) m/z calcd. for C₁₆H₁₃FeN₃Na⁺ ([M+Na]⁺) 326.0351; found: 326.0364.

M.p. = 108–109 °C (EtOAc).

Synthesis of 1-(1*H*-benzo[*d*][1,2,3]triazole)-1'-bromoferrocene (**3c**)



According to **GP1**, the title compound was prepared from **1a** (0.10 g, 0.35 mmol, 1.7 equiv), **2c**^[5] (60 mg, 0.20 mmol, 1.0 equiv), and TBAT (0.19 g, 0.36 mmol, 1.8 equiv). MPLC (cyclohexane/EtOAc 100:0 to 85:15) gave the title compound **3c** (60 mg, 0.16 mmol, 80%) as a yellow solid.

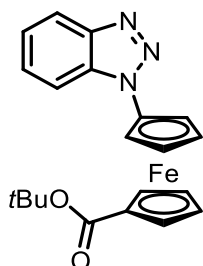
$R_f = 0.29$ (SiO₂, *n*-hexane/EtOAc 5:1).

¹H NMR (600 MHz, CDCl₃) δ [ppm] = 8.12 (d, $J = 8.3$ Hz, 1H), 7.87 (d, $J = 8.4$ Hz, 1H), 7.58 (t, $J = 7.6$, 1H), 7.43 (t, $J = 7.6$ Hz, 1H), 5.04 (t, $J = 2.1$ Hz, 2H), 4.50 (t, $J = 2.0$ Hz, 2H), 4.42 (t, $J = 2.0$ Hz, 2H), 4.20 (t, $J = 2.0$ Hz, 2H).

¹³C{¹H} NMR (151 MHz, CDCl₃) δ [ppm] = 146.5, 133.0, 128.0, 124.4, 120.5, 110.9, 95.2, 78.5, 72.0, 69.6, 69.3, 64.5.

The spectroscopic data are consistent with those reported in the literature.^[5]

Synthesis of 1-(1*H*-benzo[*d*][1,2,3]triazole)-1'-ferrocenylcarboxylic acid *tert*-butyl ester (**3d**)



According to **GP1**, the title compound was prepared from **1a** (0.10 g, 0.35 mmol, 1.7 equiv), **2d** (68 mg, 0.20 mmol, 1.0 equiv), and TBAT (0.19 g, 0.36 mmol, 1.8 equiv). MPLC (cyclohexane /EtOAc 100:0 to 90:10) gave the title compound **3d** (55 mg, 0.14 mmol, 68%) as an orange oil.

$R_f = 0.26$ (SiO₂, *n*-hexane/EtOAc 6:1).

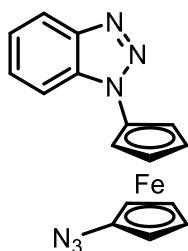
¹H NMR (600 MHz, CDCl₃) δ [ppm] = 8.11 (d, $J = 8.4$ Hz, 1H), 7.86 (d, $J = 8.4$ Hz, 1H), 7.58 (t, $J = 7.6$ Hz, 1H), 7.43 (t, $J = 7.7$ Hz, 1H), 4.99 (s, 2H), 4.82 (s, 2H), 4.42 (s, 2H), 4.40 (s, 2H), 1.46 (s, 9H).

¹³C{¹H} NMR (151 MHz, CDCl₃) δ [ppm] = 169.9, 146.5, 132.9, 128.0, 124.4, 120.5, 110.8, 94.8, 80.7, 75.0, 73.0, 71.9, 68.4, 63.7, 28.3.

FT-IR (neat) $\tilde{\nu}$ [cm⁻¹] = 3094 (w), 2922 (w), 1612 (m), 1516 (m), 1449 (w), 1406 (w), 1323 (s), 1281 (w), 1165 (m), 1124 (m), 1105 (m), 1066 (m), 1031 (w), 923 (w), 874 (w), 842 (m), 814 (w), 783 (w), 746 (m), 714 (w).

HRMS (ESI-TOF) m/z calcd. for C₂₁H₂₁FeN₃NaO₂⁺ ([M+Na]⁺) 426.0875; found: 426.0881.

Synthesis of 1-(1*H*-benzo[*d*][1,2,3]triazole)-1'-azidoferrocene (**3e**)



Caution! 1,1'-Diazidoferrocene is potentially explosive and should be handled with care!

According to **GP1**, the title compound was prepared from **1a** (0.10 g, 0.35 mmol, 1.7 equiv), **2e**^[5] (53 mg, 0.20 mmol, 1.0 equiv), and TBAT (0.19 g, 0.36 mmol, 1.8 equiv). Gravity column chromatography (basic Al₂O₃ +5 wt% H₂O; *n*-hexane/EtOAc 4:1) gave the title compound **3e** (25 mg, 73 μmol, 37%) as a brown solid.

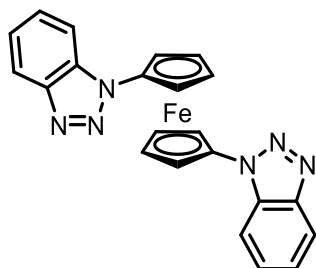
*R*_f = 0.30 (SiO₂, *n*-hexane/EtOAc 4:1).

¹H NMR (700 MHz, CDCl₃) δ [ppm] = 8.11 (dt, *J* = 8.3, 0.9 Hz, 1H), 7.81 (dt, *J* = 8.4, 0.9 Hz, 1H), 7.56 (ddd, *J* = 8.2, 6.9, 1.0 Hz, 1H), 7.42 (ddd, *J* = 8.4, 6.9, 0.9 Hz, 1H), 5.08 (t, *J* = 2.0 Hz, 2H), 4.47 (t, *J* = 2.0 Hz, 2H), 4.34 (t, *J* = 2.0 Hz, 2H), 4.15 (t, *J* = 2.0 Hz, 2H).

¹³C NMR (176 MHz, CDCl₃) δ [ppm] = 146.6, 133.1, 128.0, 124.4, 120.5, 110.7, 101.0, 94.8, 67.9, 67.4, 63.6, 62.2.

The spectroscopic data are consistent with those reported in the literature.^[5]

Synthesis of 1,1'-bis(1*H*-benzo[*d*][1,2,3]triazole)ferrocene (**3f**)



Caution! 1,1'-Diazidoferrocene is potentially explosive and should be handled with care!

According to **GP1**, the title compound was prepared from **1a** (0.10 g, 0.34 mmol, 3.4 equiv), **2e**^[5] (27 mg, 0.10 mmol, 1.0 equiv, 0.05 M), and TBAT (0.19 g, 0.36 mmol, 3.6 equiv). MPLC (cyclohexane /EtOAc 100:0 to 60:40) gave the title compound **3f** (16 mg, 38 μmol, 38%) as an orange solid.

*R*_f = 0.34 (SiO₂, *n*-hexane/EtOAc 2:1).

¹H NMR (600 MHz, CDCl₃) δ [ppm] = 7.96 (d, *J* = 8.3 Hz, 2H), 7.48 (d, *J* = 8.2 Hz, 2H), 7.37 (t, *J* = 7.6 Hz, 2H), 7.31 (t, *J* = 7.6 Hz, 2H), 5.10 (t, *J* = 2.0 Hz, 4H), 4.49 (t, *J* = 2.0 Hz, 4H).

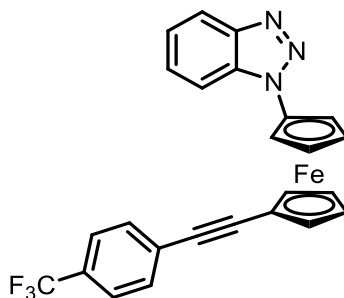
¹³C{¹H} NMR (151 MHz, CDCl₃) δ [ppm] = 147.3, 132.6, 128.1, 124.3, 118.7, 109.2, 96.3, 68.6, 64.0.

FT-IR (neat) $\tilde{\nu}$ [cm⁻¹] = 2954 (m), 2917 (s), 2849 (m), 1737 (s), 1510 (m), 1446 (m), 1375 (s), 1277 (m), 1217 (s), 1203 (s), 1073 (m), 1050 (m), 1033 (m), 923 (m), 872 (m), 818 (m), 782 (s), 738 (s).

HRMS (ESI-TOF) m/z calcd. for C₂₂H₁₆FeN₆Na⁺ ([M+Na]⁺) 443.0678; found: 443.0670.

M.p. = 218–220 °C (EtOAc).

Synthesis of 1-(1*H*-benzo[*d*][1,2,3]triazole)-1'-(1-ethynyl-4-trifluoromethylbenzene)ferrocene (**3g**)



According to **GP1**, the title compound was prepared from **1a** (0.10 g, 0.34 mmol, 1.7 equiv), **2g**^[5] (80 mg, 0.20 mmol, 1.0 equiv), and TBAT (0.19 g, 0.36 mmol, 1.8 equiv). MPLC (cyclohexane/EtOAc 100:0 to 85:15) gave the title compound **3g** (64 mg, 0.14 mmol, 67%) as an orange solid.

R_f = 0.26 (SiO₂, *n*-hexane/EtOAc 7:1).

¹H NMR (500 MHz, CDCl₃) δ [ppm] = 7.92 (dd, J = 11.4, 8.4 Hz, 2H), 7.51 (d, J = 8.3 Hz, 3H), 7.30 (d, J = 7.6 Hz, 3H), 5.11 (s, 2H), 4.62 (s, 2H), 4.44 (s, 2H), 4.38 (s, 2H).

¹³C{¹H} NMR (151 MHz, CDCl₃) δ [ppm] = 146.3, 132.8, 131.5, 129.5 (q, J = 32.6 Hz), 127.8, 127.1, 125.2 (q, J = 7.6 Hz), 124.2, 124.1 (q, J = 272.1 Hz), 120.4, 110.9, 95.4, 89.3, 85.8, 73.3, 71.0, 68.4, 66.9, 63.5.

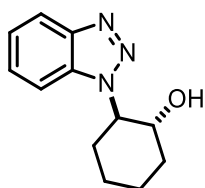
¹⁹F NMR (565 MHz, CDCl₃) δ [ppm] = -62.6.

FT-IR (neat) $\tilde{\nu}$ [cm⁻¹] = 3004 (w), 2970 (m), 2937 (w), 1738 (s), 1715 (s), 1517 (w), 1456 (94), 1367 (s), 1290 (s), 1228 (s), 1217 (s), 1141 (s), 1074 (w), 1056 (m), 1028 (w), 920 (m), 781 (w), 743 (m), 732 (m).

HRMS (ESI-TOF) m/z calcd. for C₂₅H₁₆F₃FeN₃Na⁺ ([M+Na]⁺) 494.0538; found: 494.0532.

M.p. = 135–137 °C (EtOAc).

Synthesis of 2-(1*H*-benzo[*d*][1,2,3]triazol-1-yl)cyclohexan-1-ol (**3h**)



According to **GP1**, the title compound was prepared from **1a** (0.10 g, 0.35 mmol, 1.7 equiv), **2h**^[6] (29 mg, 0.20 mmol, 1.0 equiv), and TBAT (0.19 g, 0.36 mmol, 1.8 equiv). MPLC (cyclohexane/EtOAc 100:0 to 50:50) gave the title compound **3h** (32 mg, 0.15 mmol, 72%) as a colorless solid.

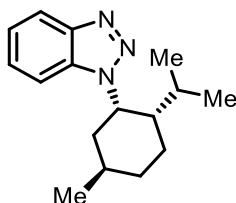
$R_f = 0.25$ (SiO₂, *n*-hexane/EtOAc 3:2).

¹H NMR (600 MHz, CDCl₃) δ [ppm] = 7.70 (d, $J = 8.3$ Hz, 1H), 7.57 (d, $J = 8.3$ Hz, 1H), 7.41 (t, $J = 7.5$ Hz, 1H), 7.21 (t, $J = 7.5$ Hz, 1H), 4.41 (q, $J = 4.8, 4.3$ Hz, 2H), 3.21 (s, 1H), 2.34 – 2.24 (m, 1H), 2.15 (qd, $J = 10.3, 8.9, 4.3$ Hz, 2H), 1.96 – 1.89 (m, 2H), 1.64 – 1.44 (m, 3H).

¹³C{¹H} NMR (151 MHz, CDCl₃) δ [ppm] = 145.4, 133.7, 127.1, 124.1, 119.4, 110.0, 72.6, 65.5, 34.2, 31.5, 25.2, 24.4.

The spectroscopic data are consistent with those reported in the literature.^[10]

Synthesis of 1-((1*S*,2*S*,5*R*)-2-isopropyl-5-methylcyclohexyl)-1*H*-benzo[*d*][1,2,3]triazole (**3i**)



According to **GP1**, the title compound was prepared from **1a** (0.10 g, 0.34 mmol, 1.7 equiv), **2i**^[7] (36 mg, 0.20 mmol, 1.0 equiv), and TBAT (0.19 g, 0.36 mmol, 1.8 equiv). MPLC (cyclohexane/EtOAc 100:0 to 95:5) gave the title compound **3i** (26 mg, 0.10 mmol, 51%) as a colorless oil.

$R_f = 0.19$ (SiO₂, *n*-hexane/EtOAc 80:1).

¹H NMR (600 MHz, CDCl₃) δ [ppm] = 8.07 (dt, $J = 8.4, 0.9$ Hz, 1H), 7.50 (d, $J = 8.3$ Hz, 1H), 7.46 (ddd, $J = 8.2, 6.9, 1.0$ Hz, 1H), 7.35 (ddd, $J = 8.1, 6.7, 1.1$ Hz, 1H), 5.13 (q, $J = 3.8$ Hz, 1H), 2.41 (qd, $J = 13.2, 3.8$ Hz, 1H), 2.03 – 1.85 (m, 4H), 1.59 – 1.48 (m, 2H), 1.31 (dp, $J = 9.1, 6.6$ Hz, 1H), 1.13 – 1.05 (m, 1H), 0.81 (d, $J = 6.6$ Hz, 3H), 0.79 (d, $J = 6.8$ Hz, 3H), 0.68 (d, $J = 6.6$ Hz, 3H).

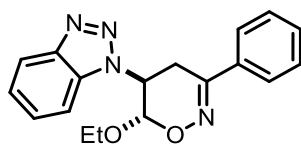
¹³C{¹H} NMR (151 MHz, CDCl₃) δ [ppm] = 145.0, 133.8, 127.0, 123.8, 120.0, 109.5, 56.1, 47.3, 40.9, 35.1, 29.2, 26.1, 25.6, 22.2, 21.3, 20.9.

FT-IR (neat) $\tilde{\nu}$ [cm⁻¹] = 2950 (s), 2924 (s), 2870 (m), 2847 (m), 1733 (w), 1454 (s), 1269 (m), 1225 (m), 1164 (m), 1062 (m), 785 (m), 769 (w), 745 (s), 727 (w).

HRMS (ESI-TOF) m/z calcd. for C₁₆H₂₃N₃Na⁺ ([M+Na]⁺) 280.1784; found: 280.1787.

$[\alpha]_D^{27} = -27.1$ ($c = 1.00$, CHCl₃).

Synthesis of 5-(1*H*-benzo[*d*][1,2,3]triazol-1-yl)-6-ethoxy-3-phenyl-5,6-dihydro-4*H*-1,2-oxazine (3j)



According to **GP1**, the title compound was prepared from **1a** (0.10 g, 0.34 mmol, 1.7 equiv), **2j** (49 mg, 0.20 mmol, 1.0 equiv), and TBAT (0.19 g, 0.36 mmol, 1.8 equiv). MPLC (cyclohexane/EtOAc 100:0 to 50:50) gave the title compound **3j** (35 mg, 0.11 mmol, 55%) as a colorless solid.

$R_f = 0.33$ (SiO₂, *n*-hexane/EtOAc 3:1).

¹H NMR (600 MHz, CDCl₃) δ [ppm] = 8.09 (t, $J = 5.4$ Hz, 1H), 7.82 – 7.79 (m, 2H), 7.61 (t, $J = 5.6$ Hz, 1H), 7.51 (t, $J = 7.6$ Hz, 1H), 7.47 – 7.43 (m, 3H), 7.40 (t, $J = 8.0$ Hz, 1H), 5.30 – 5.21 (m, 2H), 3.98 (ddd, $J = 13.8, 8.2, 4.5$ Hz, 1H), 3.64 (dddd, $J = 16.7, 14.3, 6.1, 3.9$ Hz, 2H), 3.45 (dd, $J = 18.4, 7.5$ Hz, 1H), 1.14 (t, $J = 7.0$ Hz, 3H).

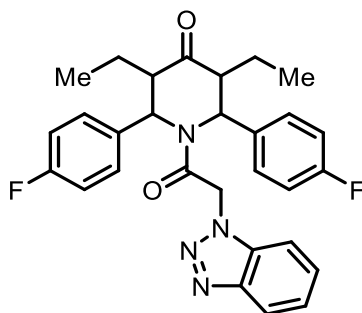
¹³C{¹H} NMR (151 MHz, CDCl₃) δ [ppm] = 154.2, 143.6, 134.5, 133.5, 131.4, 128.9, 127.9, 126.0, 123.6, 119.0, 109.7, 97.4, 63.5, 54.7, 23.1, 12.7.

FT-IR (neat) $\tilde{\nu}$ [cm⁻¹] = 3063 (w), 2977 (m), 2926 (m), 1711 (m), 1614 (w), 1493 (m), 1454 (s), 1444 (s), 1357 (m), 1295 (m), 1278 (m), 1219 (s), 1162 (m), 1098 (s), 1077 (m), 1036 (m), 995 (s), 893 (s), 837 (w), 784 (m), 762 (s), 747 (s).

HRMS (ESI-TOF) m/z calcd. for C₁₈H₁₈N₄O₂Na⁺ ([M+Na]⁺) 345.1322; found: 345.1333.

M.p. = 126–127 °C (EtOAc).

Synthesis of 1-(2-(1*H*-benzo[*d*][1,2,3]triazol-1-yl)acetyl)-3,5-diethyl-2,6-bis(4-fluorophenyl)-piperidin-4-one (3k)



According to **GP1**, the title compound was prepared from **1a** (81 mg, 0.27 mmol, 1.7 equiv, 0.14 M), **2k** (68 mg, 0.16 mmol, 1.0 equiv, 0.08 M), and TBAT (0.16 g, 0.29 mmol, 1.8 equiv, 0.15 M). MPLC (cyclohexane/EtOAc 100:0 to 80:20) gave the title compound **3k** (53 mg, 0.11 mmol, 66%) as a colorless solid.

Note: Higher concentrations of the reagents were not practical due to limited solubility of **2k** in MeCN.

$R_f = 0.22$ (SiO₂, *n*-hexane/EtOAc 4:1).

^1H NMR (600 MHz, CDCl_3) δ [ppm] = 8.07 (d, J = 8.3 Hz, 1H), 7.51 – 7.48 (m, 1H), 7.41 – 7.37 (m, 2H), 7.21 (s, 4H), 7.07 (t, J = 8.5 Hz, 4H), 5.67 (d, J = 16.0 Hz, 2H), 5.28 (s, 2H), 2.85 (q, J = 6.1 Hz, 2H), 1.59 (s, 2H), 1.35 (dt, J = 12.7, 6.5 Hz, 2H), 0.83 (t, J = 7.4 Hz, 6H).

$^{13}\text{C}\{^1\text{H}\}$ NMR (151 MHz, CDCl_3) δ [ppm] = 208.8, 168.3, 162.4 (d, J = 248.8 Hz), 146.1, 136.7, 133.6, 129.5 (d, J = 7.7 Hz), 128.2, 124.4, 120.3, 116.3 (d, J = 21.6 Hz), 109.9, 52.3, 51.0, 20.5, 10.9.

One carbon is missing probably due to signal overlap.

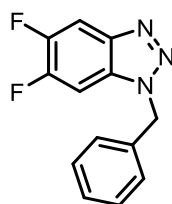
^{19}F NMR (565 MHz, CDCl_3) δ [ppm] = -112.6.

FT-IR (neat) $\tilde{\nu}$ [cm^{-1}] = 3067 (w), 2968 (m), 2937 (m), 2878 (w), 1715 (s), 1662 (s), 1604 (m), 1509 (s), 1456 (m), 1420 (w), 1389 (m), 1348 (w), 1313 (w), 1265 (m), 1227 (s), 1162 (s), 1095 (m), 855 (s), 829 (s), 780 (w), 744 (s).

HRMS (ESI-TOF) m/z calcd. for $\text{C}_{29}\text{H}_{28}\text{F}_2\text{N}_4\text{O}_2\text{Na}^+$ ($[\text{M}+\text{Na}]^+$) 525.2072; found: 525.2087.

M.p. = 192–193 °C (EtOAc).

Synthesis of 1-benzyl-5,6-difluoro-1H-benzo[*d*][1,2,3]triazole (4a)



According to **GP1**, the title compound was prepared from **1b**^[11] (0.11 g, 0.34 mmol, 1.7 equiv), **2a** (26 mg, 0.20 mmol, 1.0 equiv), and TBAT (0.19 g, 0.36 mmol, 1.8 equiv). MPLC (cyclohexane/EtOAc 100:0 to 85:15) gave the title compound **4a** (27 mg, 0.11 mmol, 56%) as a colorless solid. Analytically pure samples were obtained by recrystallization (*n*-hexane/PhMe).

R_f = 0.33 (SiO_2 , *n*-hexane/EtOAc 6:1).

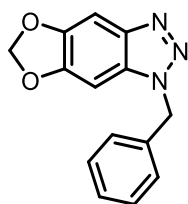
^1H NMR (600 MHz, CDCl_3) δ [ppm] = 7.81 (t, J = 8.0 Hz, 1H), 7.42 – 7.32 (m, 3H), 7.30 – 7.22 (m, 2H), 7.07 (t, J = 7.5 Hz, 1H), 5.80 (s, 2H).

$^{13}\text{C}\{^1\text{H}\}$ NMR (151 MHz, CDCl_3) δ [ppm] = 151.6 (dd, J = 253.2, 16.9 Hz), 149.2 (dd, J = 248.2, 16.1 Hz), 141.6 (d, J = 9.5 Hz), 134.0, 129.4, 129.0, 128.7 (d, J = 11.3 Hz), 127.7, 106.7 (d, J = 20.0 Hz), 97.3 (d, J = 23.4 Hz), 52.9.

^{19}F NMR (565 MHz, CDCl_3) δ [ppm] = -131.7 (dt, J = 18.2, 8.0 Hz), -138.0 (dt, J = 17.5, 8.1 Hz).

The spectroscopic data are consistent with those reported in the literature.^[11]

Synthesis of 1-benzyl-1*H*-[1,3]dioxolo[4',5':4,5]benzo[1,2-*d*][1,2,3]triazole (**4b**)



According to **GP1**, the title compound was prepared from **1c**^[11] (0.11 g, 0.34 mmol, 1.7 equiv), **2a** (26 mg, 0.20 mmol, 1.0 equiv), and TBAT (0.19 g, 0.36 mmol, 1.8 equiv). MPLC (cyclohexane/EtOAc 100:0 to 75:25) gave the title compound **4b** (37 mg, 0.15 mmol, 75%) as a colorless solid.

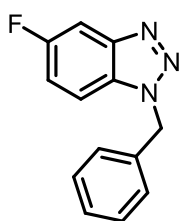
$R_f = 0.27$ (SiO₂, *n*-hexane/EtOAc 4:1).

¹H NMR (500 MHz, CDCl₃) δ [ppm] = 7.32 – 7.27 (m, 4H), 7.22 – 7.19 (m, 2H), 6.57 (d, $J = 0.6$ Hz, 1H), 5.98 (s, 2H), 5.68 (s, 2H).

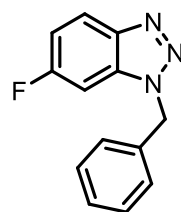
¹³C NMR (126 MHz, CDCl₃) δ [ppm] = 149.8, 147.1, 142.3, 134.7, 129.6, 129.2, 128.6, 127.6, 102.3, 97.3, 88.5, 52.5.

The spectroscopic data are consistent with those reported in the literature.^[11]

Synthesis of 1-benzyl-5(6)-fluoro-1*H*-benzo[*d*][1,2,3]triazole (**4c**)



5-fluoro isomer



6-fluoro isomer

According to **GP1**, the title compound was prepared from **1d**^[2] (0.11 g, 0.34 mmol, 1.7 equiv), **2a** (26 mg, 0.20 mmol, 1.0 equiv), and TBAT (0.19 g, 0.36 mmol, 1.8 equiv). MPLC (cyclohexane/EtOAc 100:0 to 85:15) gave the title compounds **4c** (27 mg, 0.12 mmol, 61%; inseparable mixture of the 5- and 6-isomers in a ratio of 3:1 [¹⁹F NMR]) as a pale brown solid. Analytically pure samples were obtained by recrystallization (*n*-hexane/PhMe).

$R_f = 0.36$ (SiO₂, *n*-hexane/EtOAc 6:1).

NMR Data of the 5-fluoro isomer (major):

¹H NMR (600 MHz, CDCl₃) δ = 7.69 (dd, $J = 8.3, 2.3$ Hz, 1H), 7.34 (d, $J = 6.9$ Hz, 3H), 7.30 – 7.25 (m, 3H), 7.18 (td, $J = 8.9, 2.3$ Hz, 1H), 5.84 (s, 2H).

¹³C{¹H} NMR (151 MHz, CDCl₃) δ [ppm] = 159.0, 146.8, 134.5, 130.0, 129.3, 128.8, 127.7, 117.6 (d, $J = 27.7$ Hz), 110.9 (d, $J = 10.3$ Hz), 104.7 (d, $J = 24.3$ Hz), 52.8.

¹⁹F NMR (565 MHz, CDCl₃) δ [ppm] = -117.7 (q, $J = 7.6$ Hz).

NMR Data of the 6-fluoro isomer (minor):

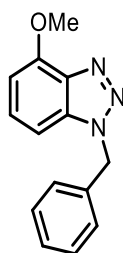
^1H NMR (600 MHz, CDCl_3) δ = 8.02 (dd, J = 9.1, 4.6 Hz, 1H), 7.38 – 7.32 (m, 3H), 7.30 – 7.25 (m, 3H), 7.11 (td, J = 9.1, 2.2 Hz, 1H), 6.97 (dd, J = 7.9, 2.2 Hz, 1H), 5.80 (s, 2H).

$^{13}\text{C}\{^1\text{H}\}$ NMR (151 MHz, CDCl_3) δ [ppm] = 160.6, 134.4, 129.3, 128.8, 127.7, 121.7 (d, J = 10.9 Hz), 114.1 (d, J = 26.8 Hz), 95.7 (d, J = 27.6 Hz), 52.5. Two carbons are not resolved.

^{19}F NMR (565 MHz, CDCl_3) δ [ppm] = -111.5 (q, J = 8.0, 7.3 Hz).

The spectroscopic data for both isomers are consistent with those reported in the literature.^[11]

Synthesis of 1-benzyl-4-methoxy-1H-benzo[*d*][1,2,3]triazole (4d)



According to **GP1**, the title compound was prepared from **1e** (0.11 g, 0.34 mmol, 1.7 equiv), **2a** (26 mg, 0.20 mmol, 1.0 equiv), and TBAT (0.19 g, 0.36 mmol, 1.8 equiv). MPLC (cyclohexane/EtOAc 100:0 to 75:25) gave the title compound **4d** (32 mg, 0.13 mmol, 68%) as a colorless solid.

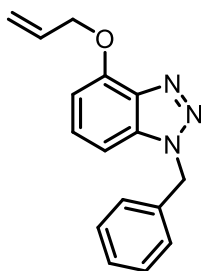
R_f = 0.25 (SiO_2 , *n*-hexane/EtOAc 5:1).

^1H NMR (600 MHz, CDCl_3) δ [ppm] = 7.34 – 7.24 (m, 6H), 6.90 (d, J = 8.3 Hz, 1H), 6.66 (d, J = 7.7 Hz, 1H), 5.81 (s, 2H), 4.10 (s, 3H).

$^{13}\text{C}\{^1\text{H}\}$ NMR (151 MHz, CDCl_3) δ [ppm] = 151.9, 138.4, 134.9, 134.9, 129.1, 128.8, 128.5, 127.7, 103.4, 102.0, 56.4, 52.4.

The spectroscopic data are consistent with those reported in the literature.^[10]

Synthesis of 4-(allyloxy)-1-benzyl-1H-benzo[*d*][1,2,3]triazole (4e)



According to **GP1**, the title compound was prepared from **1f**^[3] (0.12 g, 0.34 mmol, 1.7 equiv), **2a** (26 mg, 0.20 mmol, 1.0 equiv), and TBAT (0.19 g, 0.36 mmol, 1.8 equiv). Flash column chromatography (*n*-pentane/ CH_2Cl_2 1:1 to *n*-pentane/EtOAc 90:10) gave the title compound **4e** (31 mg, 0.12 mmol, 60%) as a colorless oil.

R_f = 0.26 (SiO_2 , *n*-hexane/EtOAc 6:1).

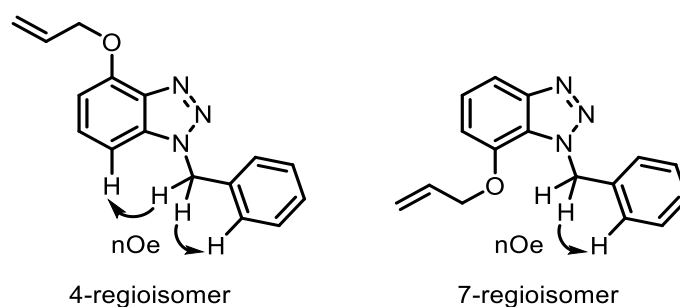
^1H NMR (700 MHz, CDCl_3) δ [ppm] = 7.35 – 7.30 (m, 3H), 7.30 – 7.27 (m, 2H), 6.91 (d, J = 8.3 Hz, 1H), 6.69 (d, J = 7.7 Hz, 1H), 6.18 (ddt, J = 17.3, 10.7, 5.4 Hz, 1H), 5.82 (s, 2H), 5.51 (dd, J = 17.2, 1.6 Hz, 1H), 5.34 (dq, J = 10.5, 1.4 Hz, 1H), 4.95 (dt, J = 5.5, 1.5 Hz, 2H).

^{13}C NMR (176 MHz, CDCl_3) δ [ppm] = 150.8, 138.5, 135.1, 134.9, 133.0, 129.1, 128.7, 128.5, 127.6, 118.3, 105.3, 102.0, 70.3, 52.4.

FT-IR (neat) $\tilde{\nu}$ [cm^{-1}] = 2954 (m), 2919 (s), 2850 (m), 1738 (s), 1600 (m), 1509 (m), 1455 (m), 1365 (s), 1231 (s), 1217 (s), 1094 (m), 1059 (m), 984 (w), 926 (w), 784 (m), 739 (s).

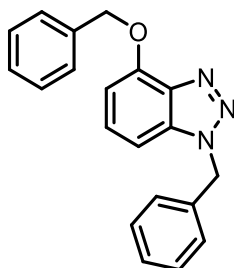
HRMS (ESI-TOF) m/z calcd. for $\text{C}_{16}\text{H}_{15}\text{N}_3\text{ONa}^+$ ($[\text{M}+\text{Na}]^+$) 288.1107; found: 288.1108.

Structure assignment:



The position of the ether group was assigned by a 1D GOESY experiment. The benzylic protons show excitation of two aromatic protons which is only possible for the 4-regioisomer.

Synthesis of 4-(benzyloxy)-1-benzyl-1H-benzo[*d*][1,2,3]triazole (**4f**)



According to **GPI**, the title compound was prepared from **1g**^[31] (0.13 g, 0.33 mmol, 1.7 equiv), **2a** (26 mg, 0.20 mmol, 1.0 equiv), and TBAT (0.19 g, 0.36 mmol, 1.8 equiv). MPLC (cyclohexane/EtOAc 100:0 to 85:15) gave the title compound **4f** (44 mg, 0.14 mmol, 71%) as a colorless solid.

R_f = 0.26 (SiO_2 , *n*-hexane/EtOAc 5:1).

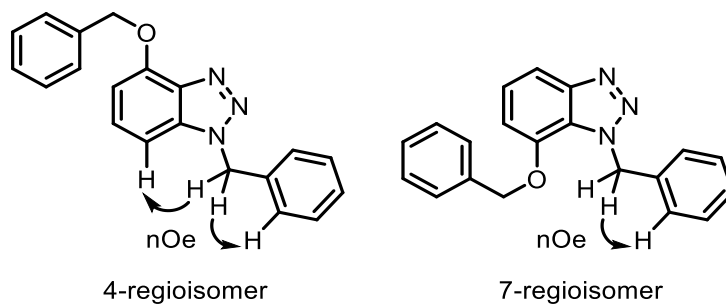
^1H NMR (700 MHz, CDCl_3) δ [ppm] = 7.57 – 7.54 (m, 2H), 7.40 (dd, J = 8.4, 6.9 Hz, 2H), 7.37 – 7.31 (m, 4H), 7.30 – 7.27 (m, 3H), 6.92 (d, J = 8.3 Hz, 1H), 6.73 (d, J = 7.7 Hz, 1H), 5.84 (s, 2H), 5.53 (s, 2H).

^{13}C NMR (176 MHz, CDCl_3) δ [ppm] = 150.9, 138.6, 136.7, 135.1, 134.9, 129.1, 128.7, 128.7, 128.5, 128.2, 127.7, 127.7, 105.8, 102.1, 71.4, 52.4.

FT-IR (neat) $\tilde{\nu}$ [cm^{-1}] = 3056 (w), 2925 (m), 1714 (s), 1665 (s), 1604 (s), 1509 (s), 1456 (m), 1391 (m), 1264 (s), 1229 (m), 1162 (m), 1095 (m), 1059 (m), 855 (w), 829 (w), 781 (w), 731 (s).

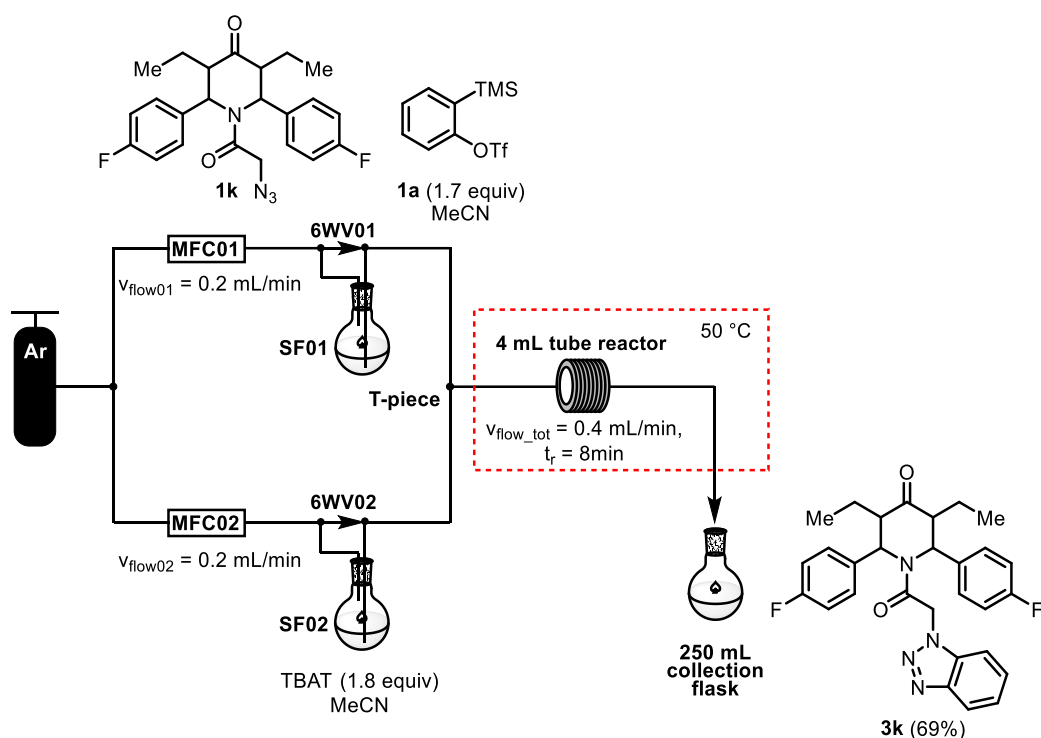
HRMS (ESI-TOF) m/z calcd. for $C_{20}H_{17}N_3ONa^+$ ($[M+Na]^+$) 338.1264; found: 338.1266.

Structure assignment:



The position of the ether group was assigned by a 1D GOESY experiment. The benzylic protons (N - CH_2 -C) show excitation of two aromatic protons which is only possible for the 4-regioisomer.

Procedure for the gram scale preparation of benzotriazole **3k**

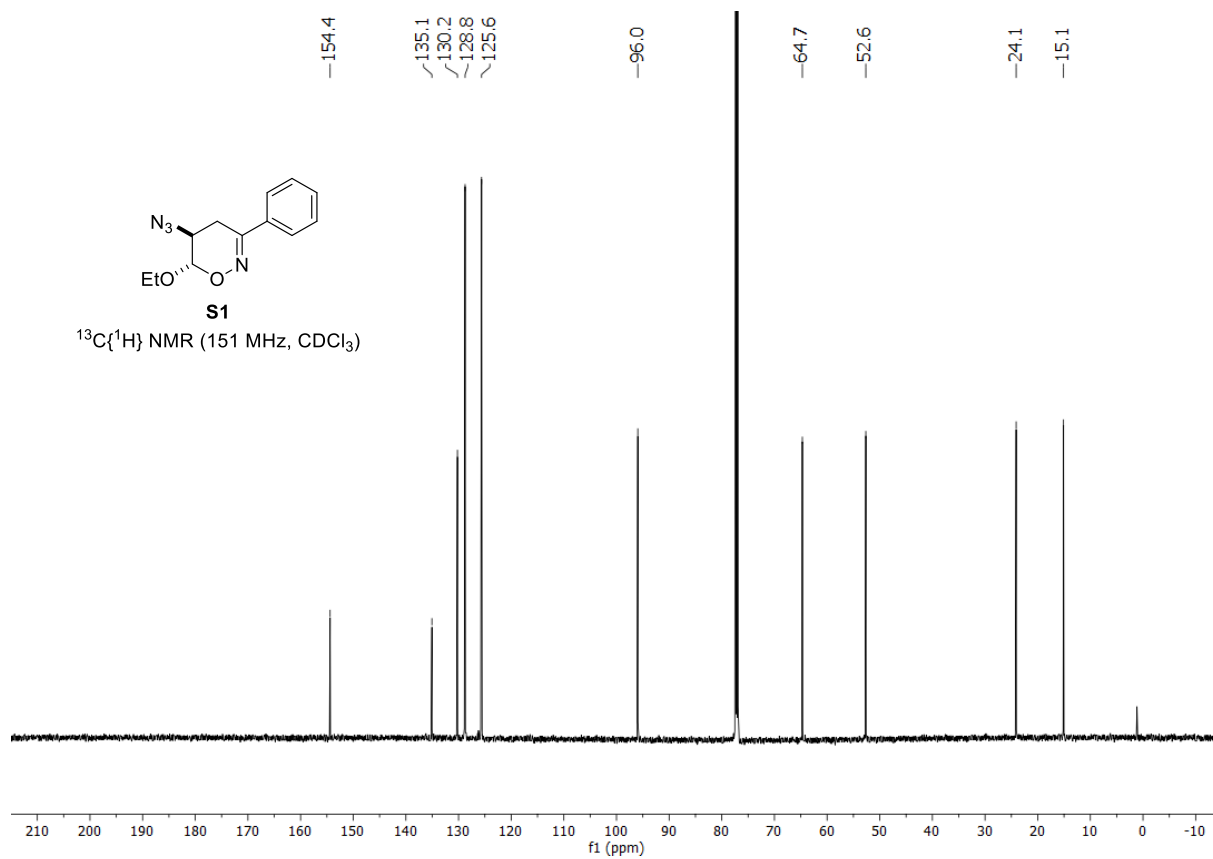
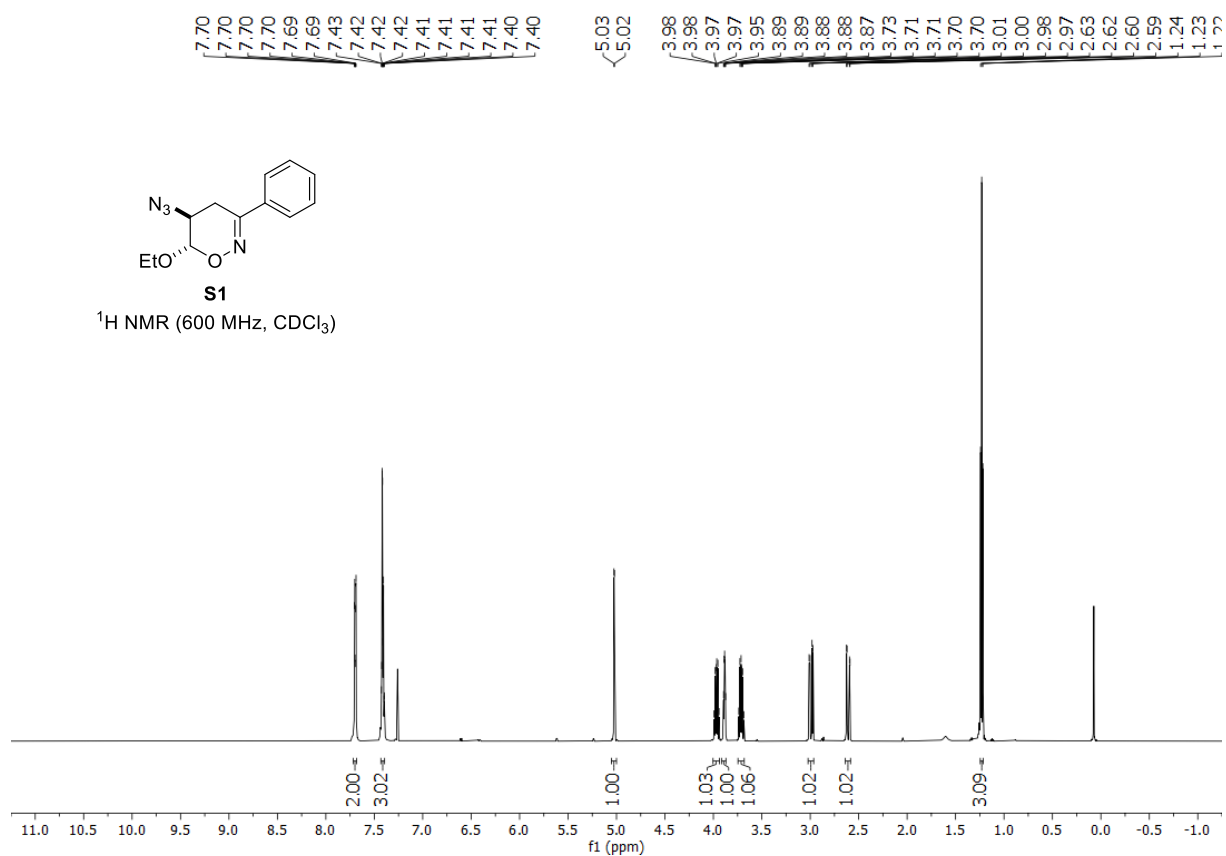


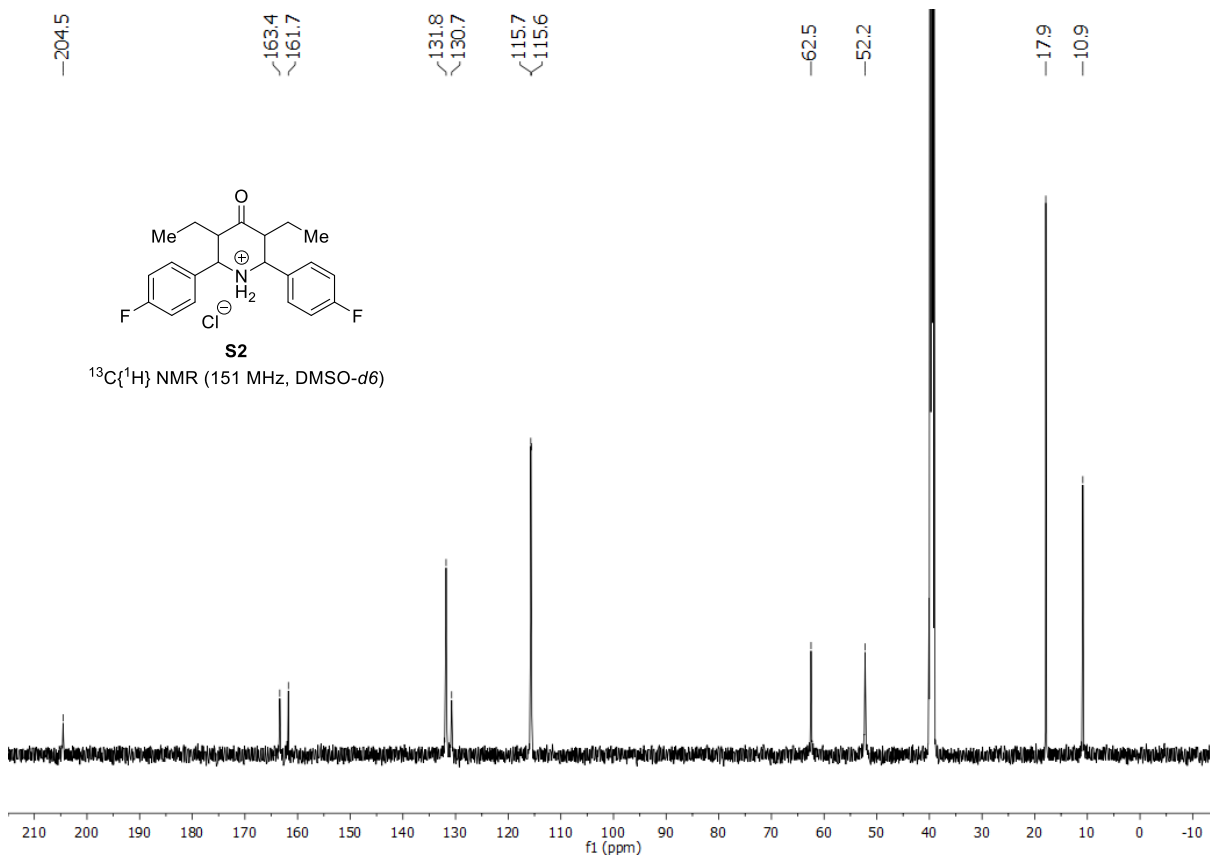
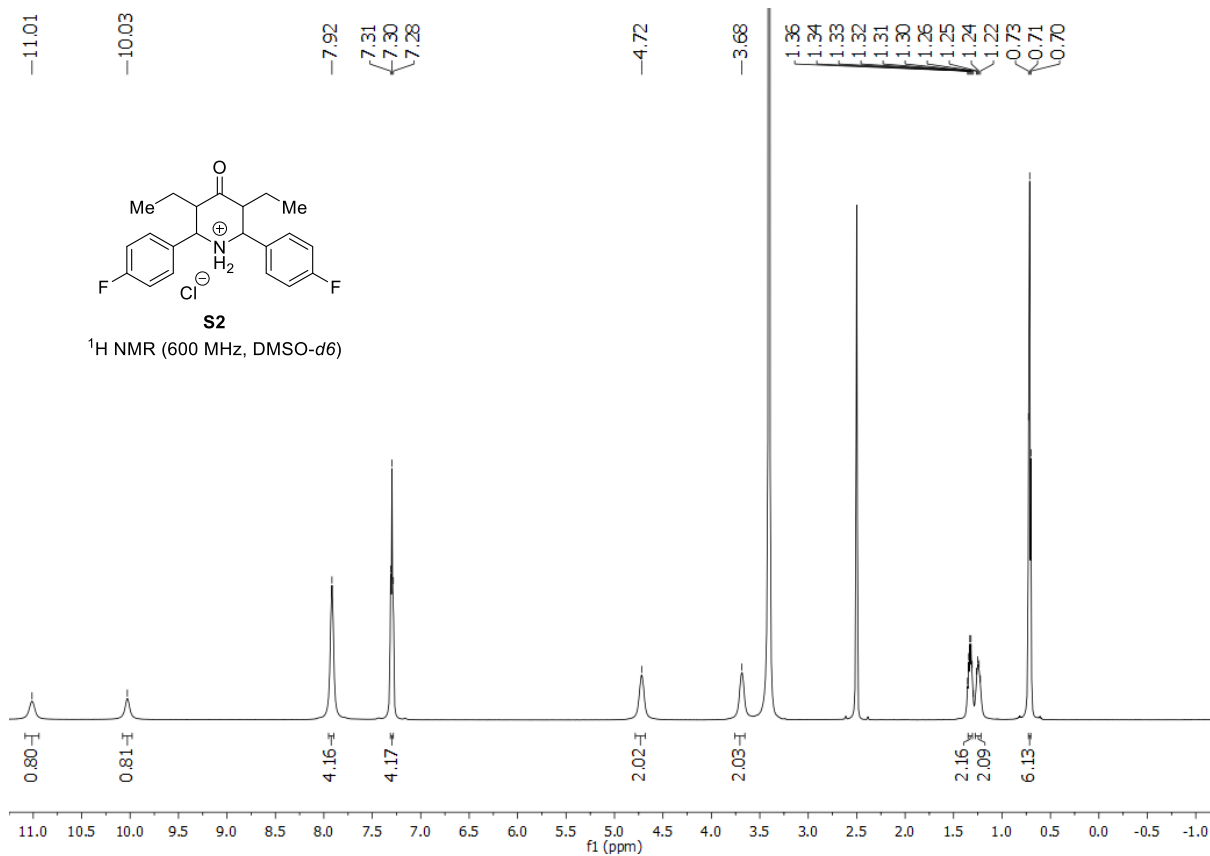
Open to air, in a 50 mL round bottom flask, 30 mL of a solution of azide **2k** (1.02 g, 2.40 mmol, 1.0 equiv, 0.08 M) and benzyne precursor **1a** (0.989 mL, 1.22 g, 4.08 mmol, 1.7 equiv, 0.14 M) were prepared in MeCN. The sample flask (**SF01**) was sealed with a rubber septum and connected with the 6-way valve 01 (**6WV01**) using two cannulas in such a way that the argon stream provided by **MFC01** drives the solution in the 6-way valve 01 (**6WV01**). In another 50 mL round bottom flask, 30 mL of a solution of TBAT (2.33 g, 4.32 mmol, 1.8 equiv, 0.14 M) were prepared in MeCN. The sample flask (**SF02**) was sealed with a rubber septum and connected with the 6-way valve 02 (**6WV02**) using two cannulas in such a way that the argon stream provided by **MFC02** drives the solution in the 6-way valve 02 (**6WV02**). Then, both solutions were driven by an argon flow using mass flow controllers **MFC01** and **MFC02** with a flow rate of $v_{\text{flow01}} = v_{\text{flow02}} = 0.2$ mL/min. Both solutions were mixed in a **T-piece** and then pumped through a preheated **4 mL tube reactor** at 50 °C. At the end of the reactor, the reaction mixture was collected in a **250 mL collection flask** and loaded on Celite[®]. MPLC (cyclohexane/EtOAc 100:0 to 80:20) gave benzotriazole **3k** (834 mg, 1.66 mmol, 69%) as a colorless solid.

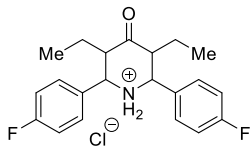


Flow-setup: 1. Mass flow controller 01. 2. Mass flow controller 02. 3. 6-Way valve 01. 4. 6-Way valve 02. 5. Sample Flask 01. 6. Sample Flask 02. 7. Tube reactor with T-piece. 8. Collection flask.

3. NMR Spectra of Synthesized Compounds

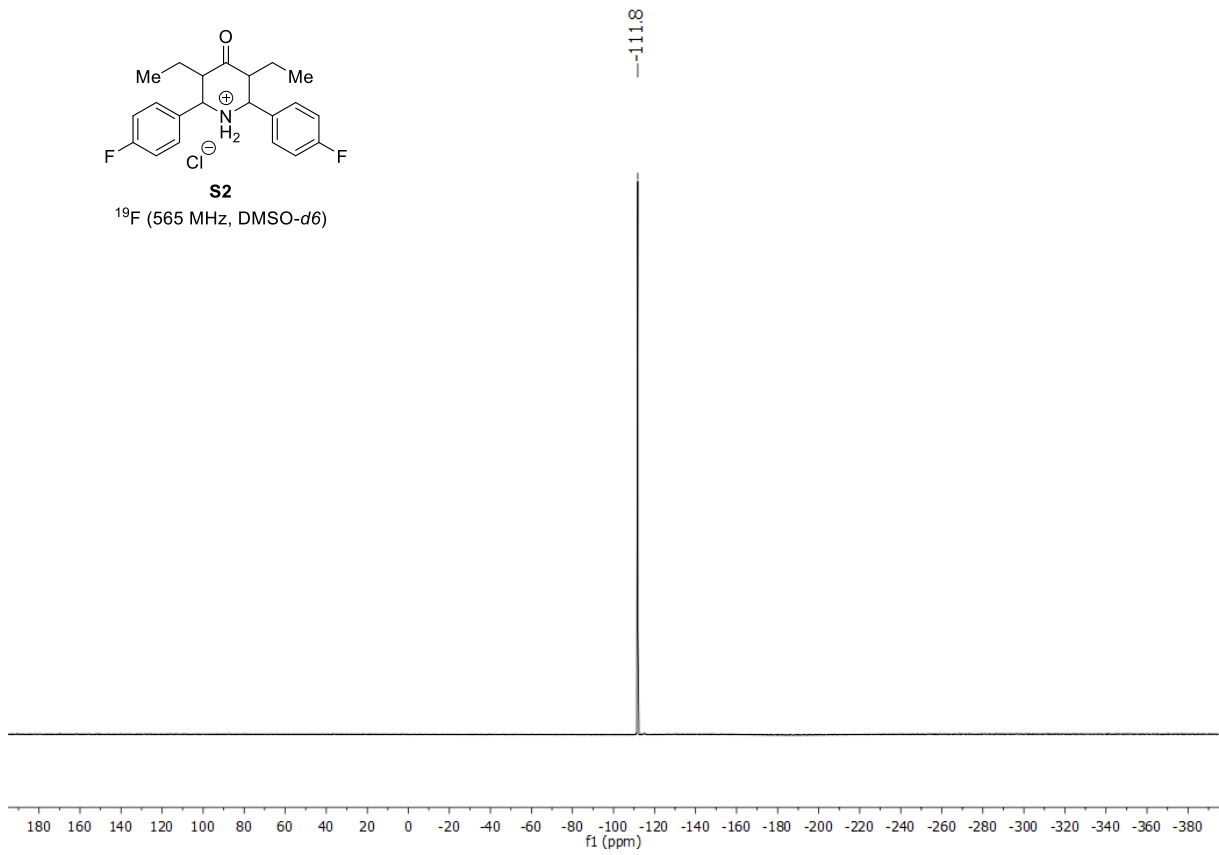


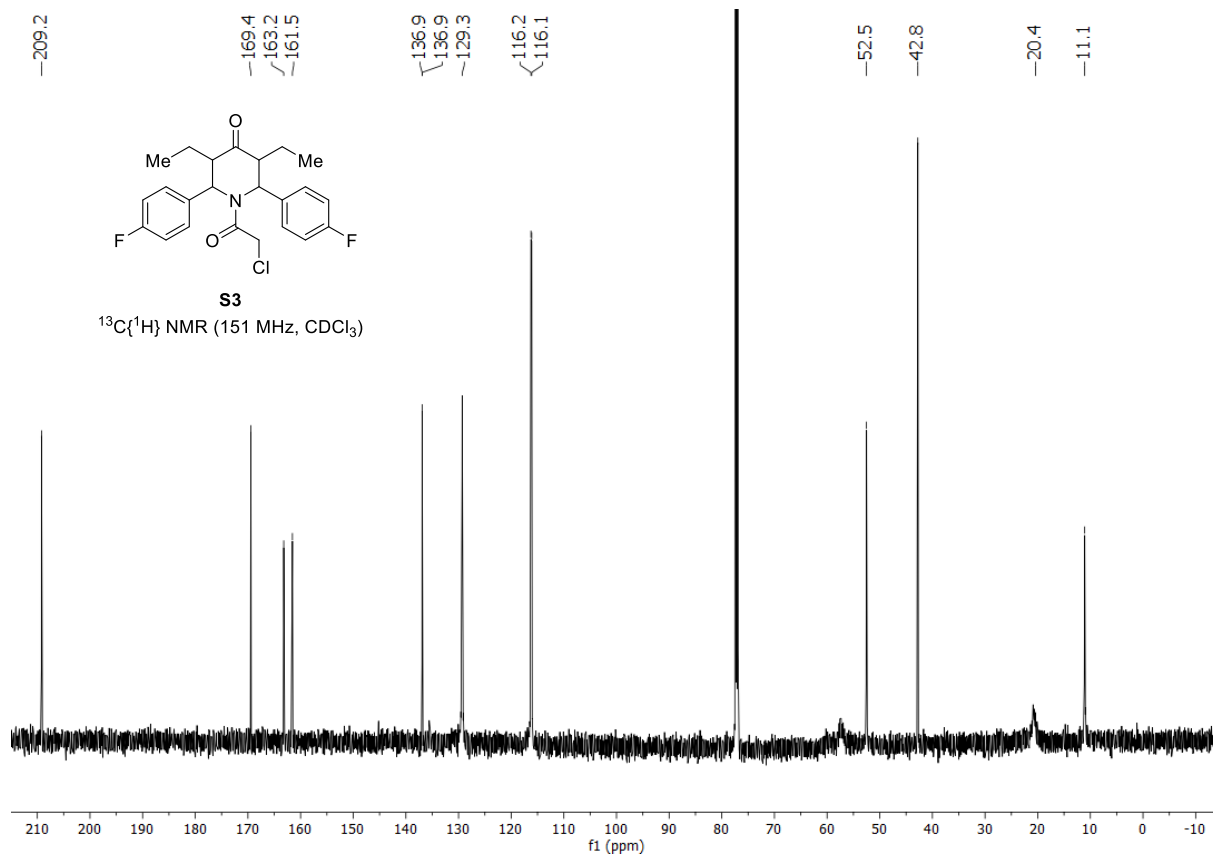
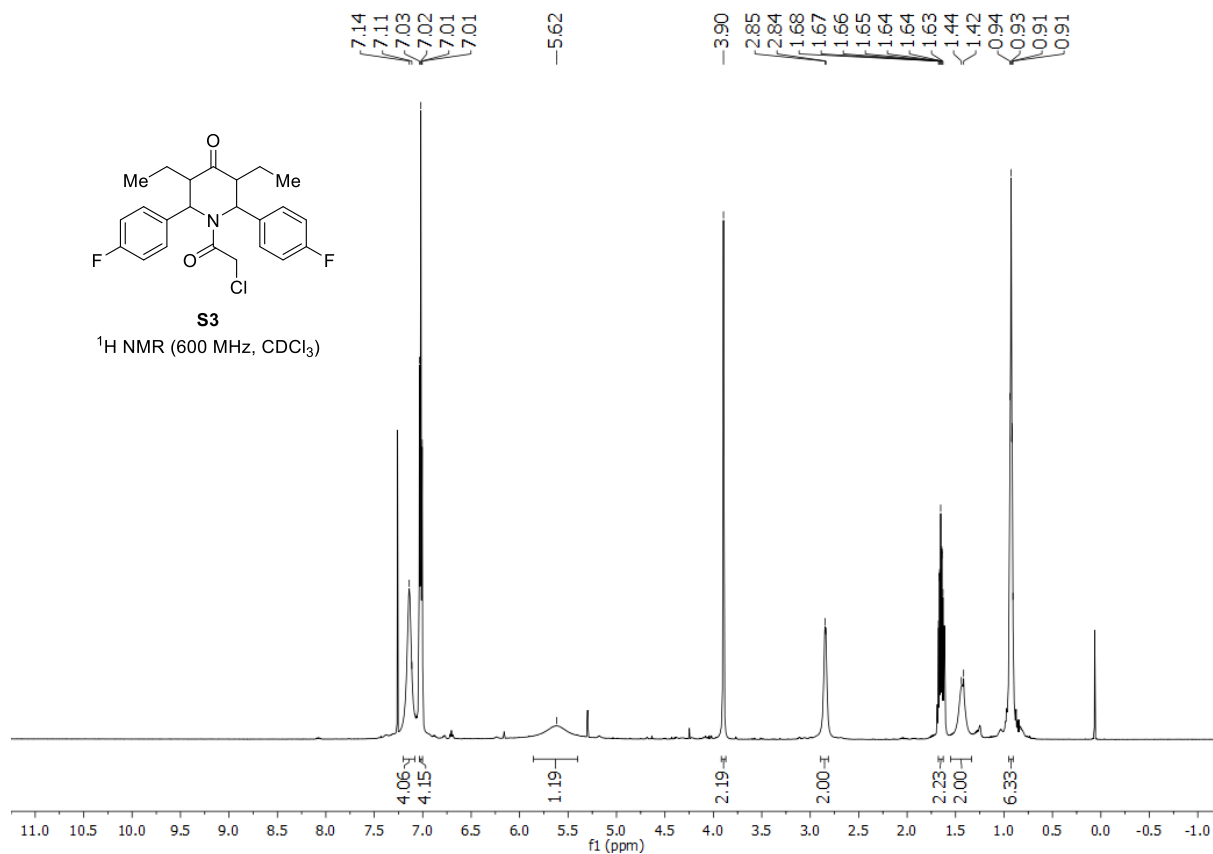


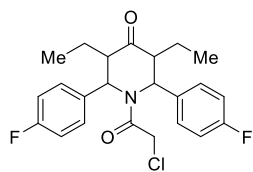


S2

¹⁹F (565 MHz, DMSO-*d*₆)

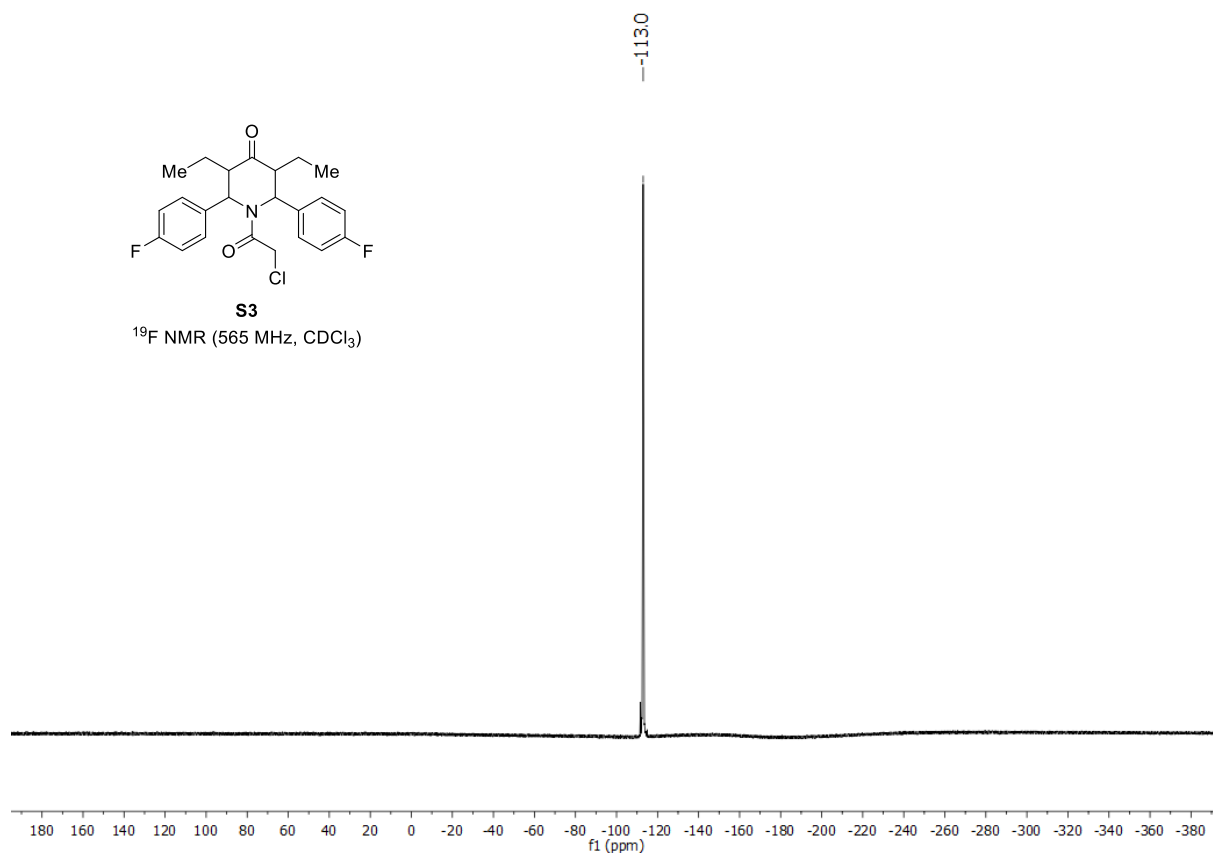


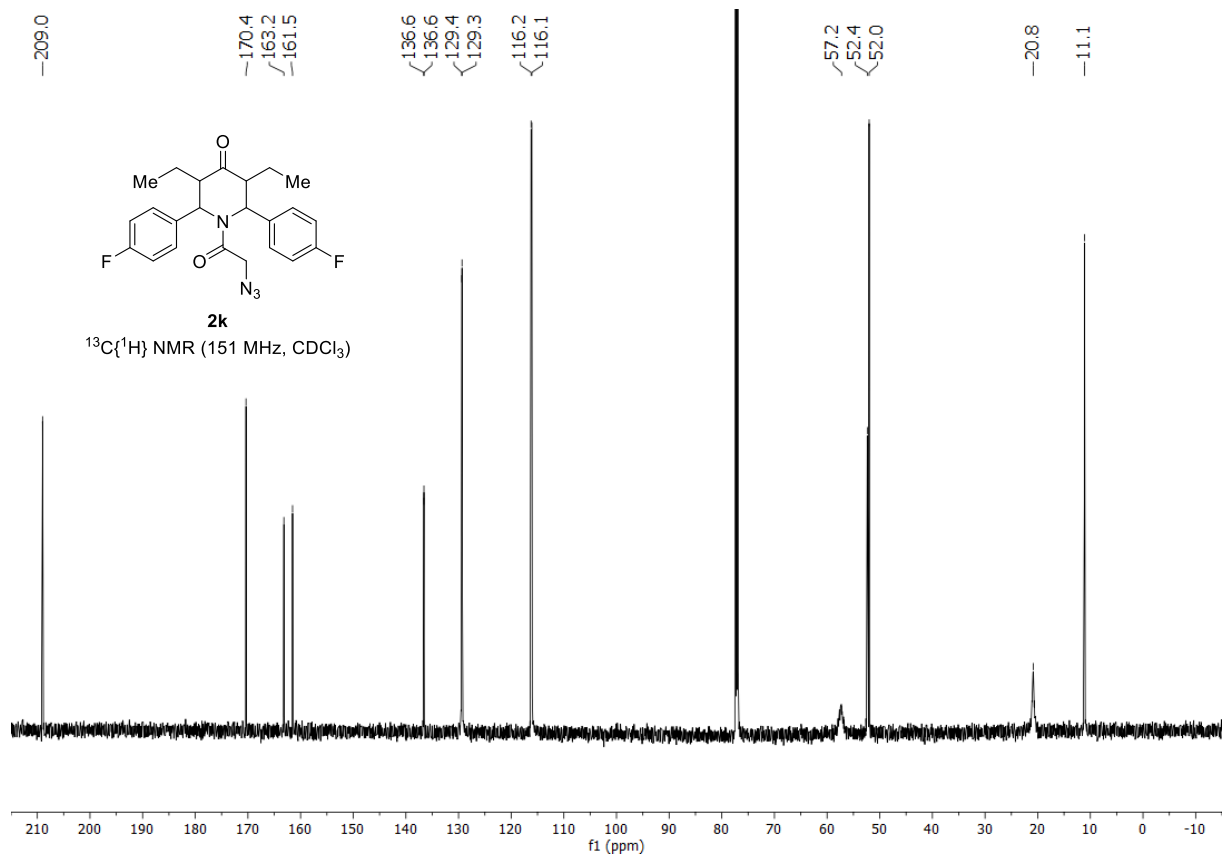
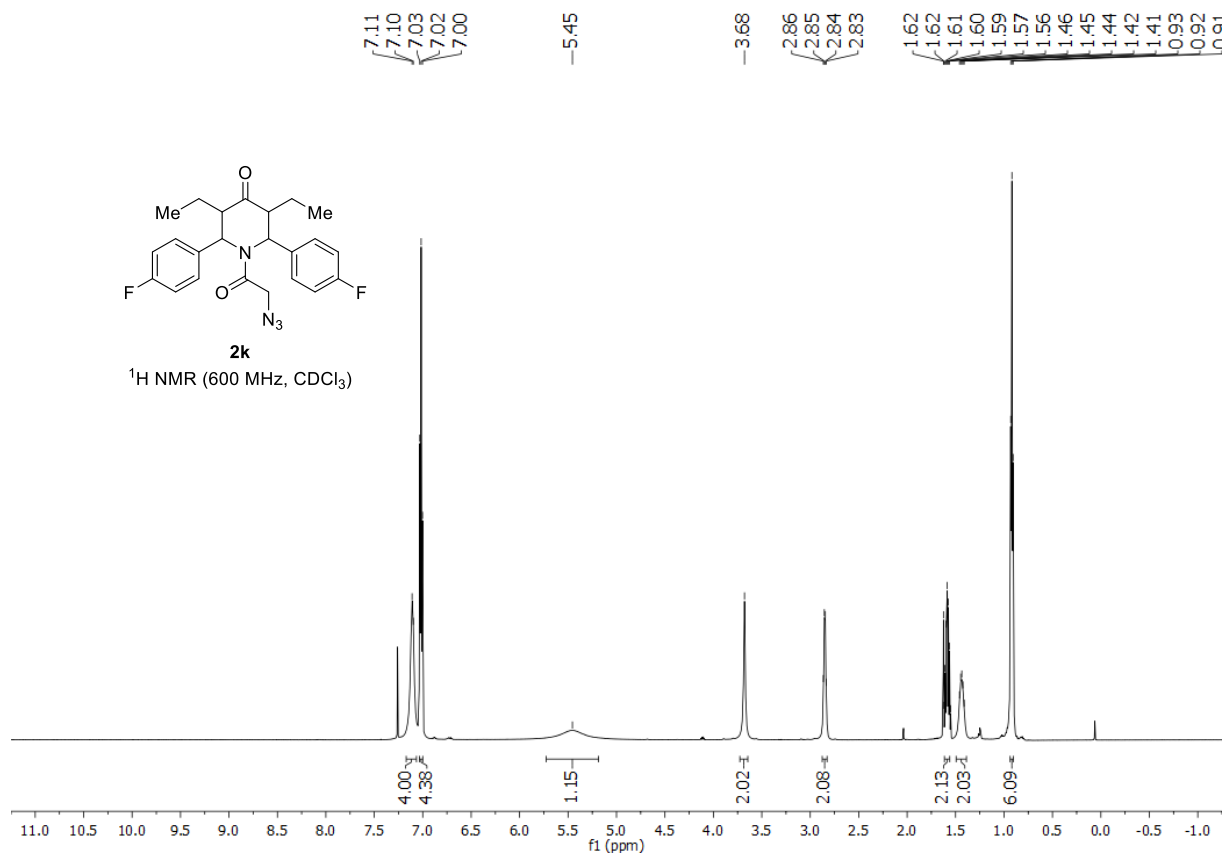


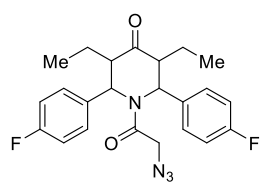


S3

¹⁹F NMR (565 MHz, CDCl₃)

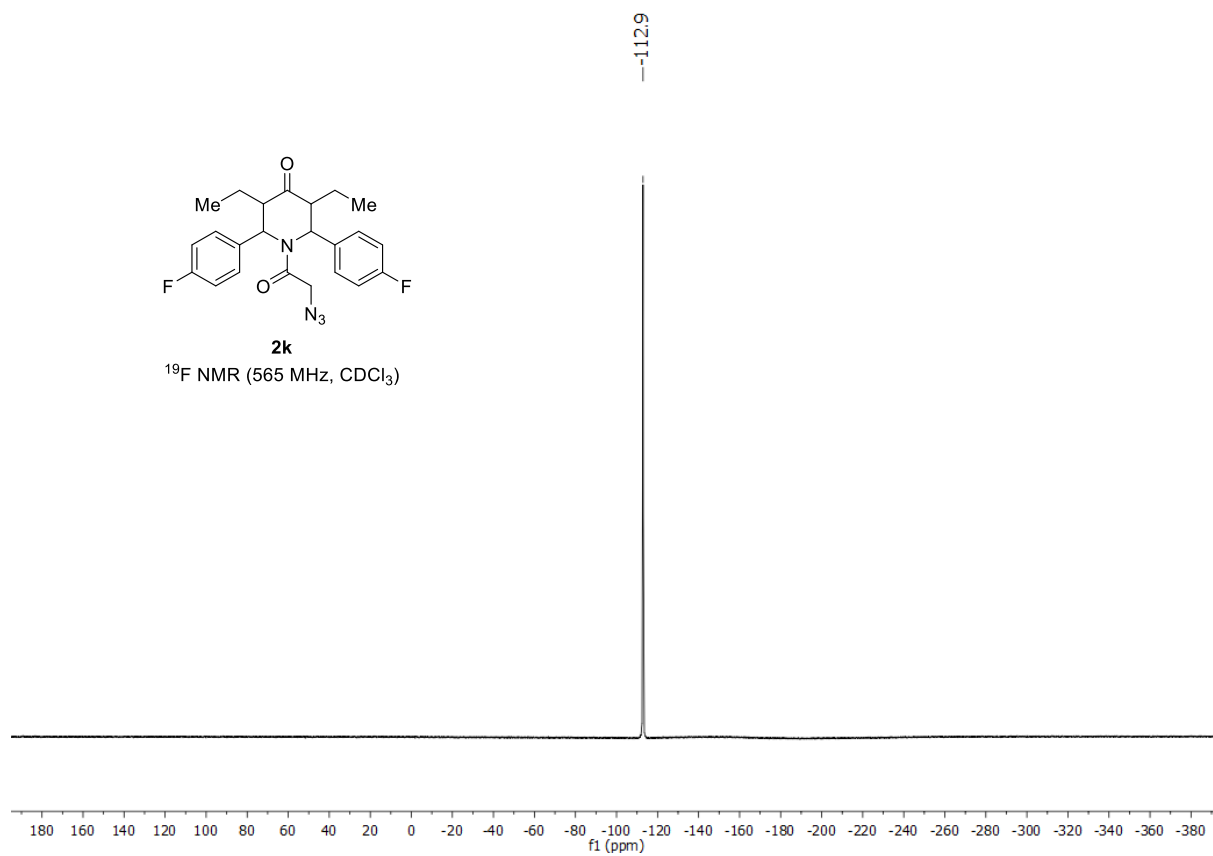


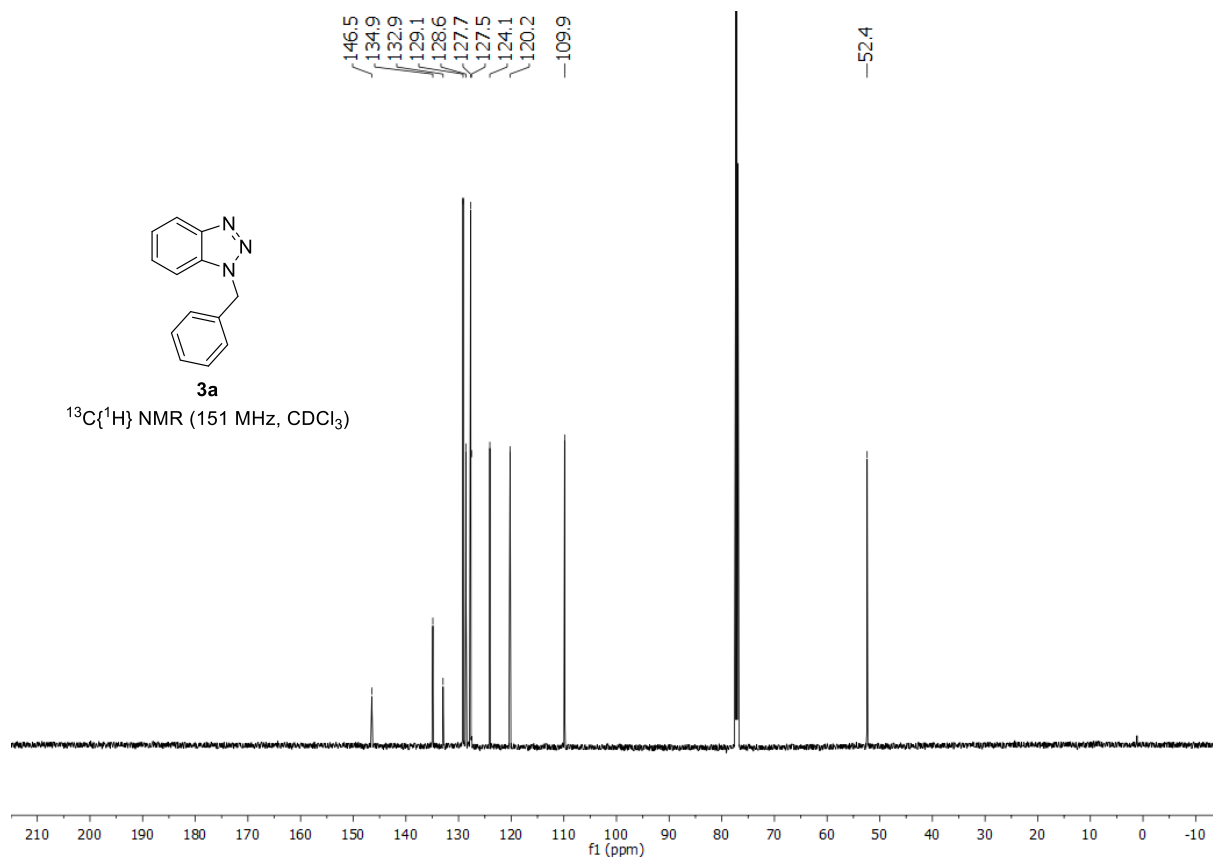
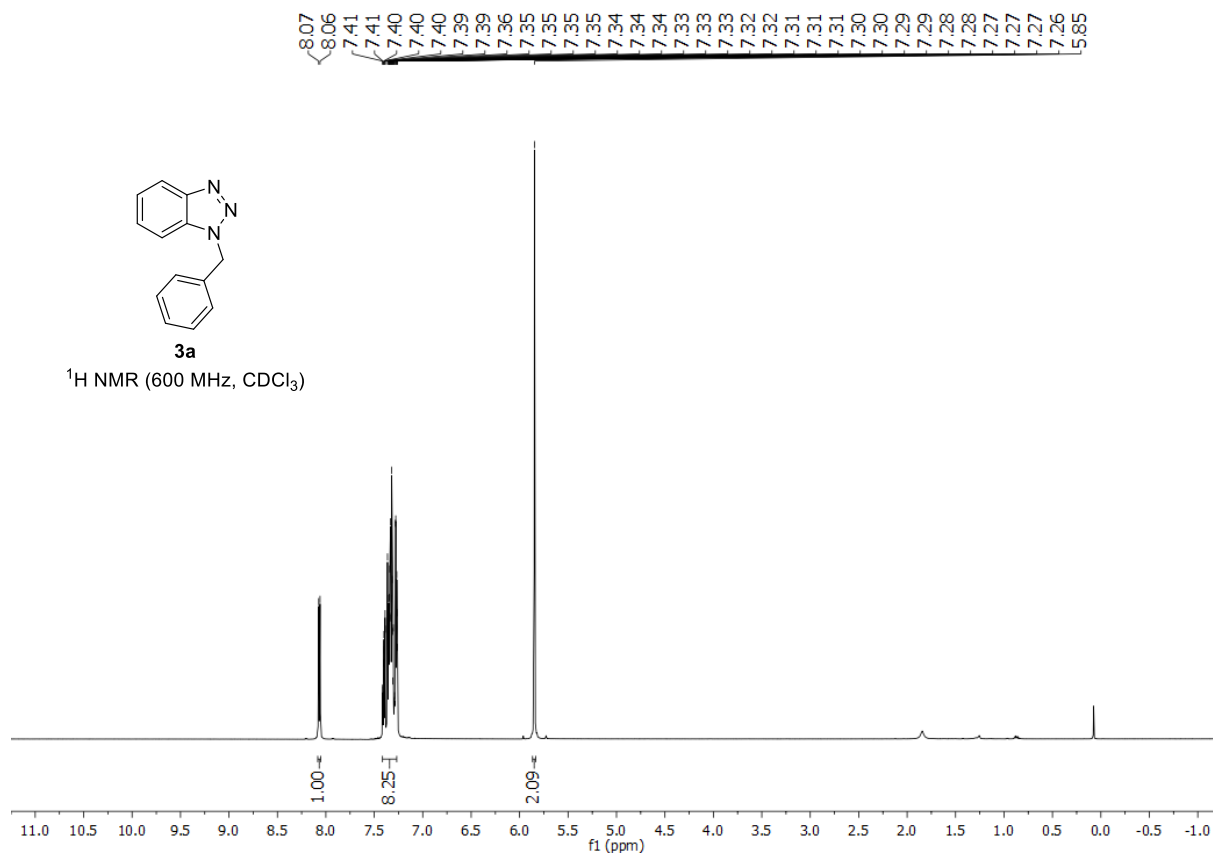


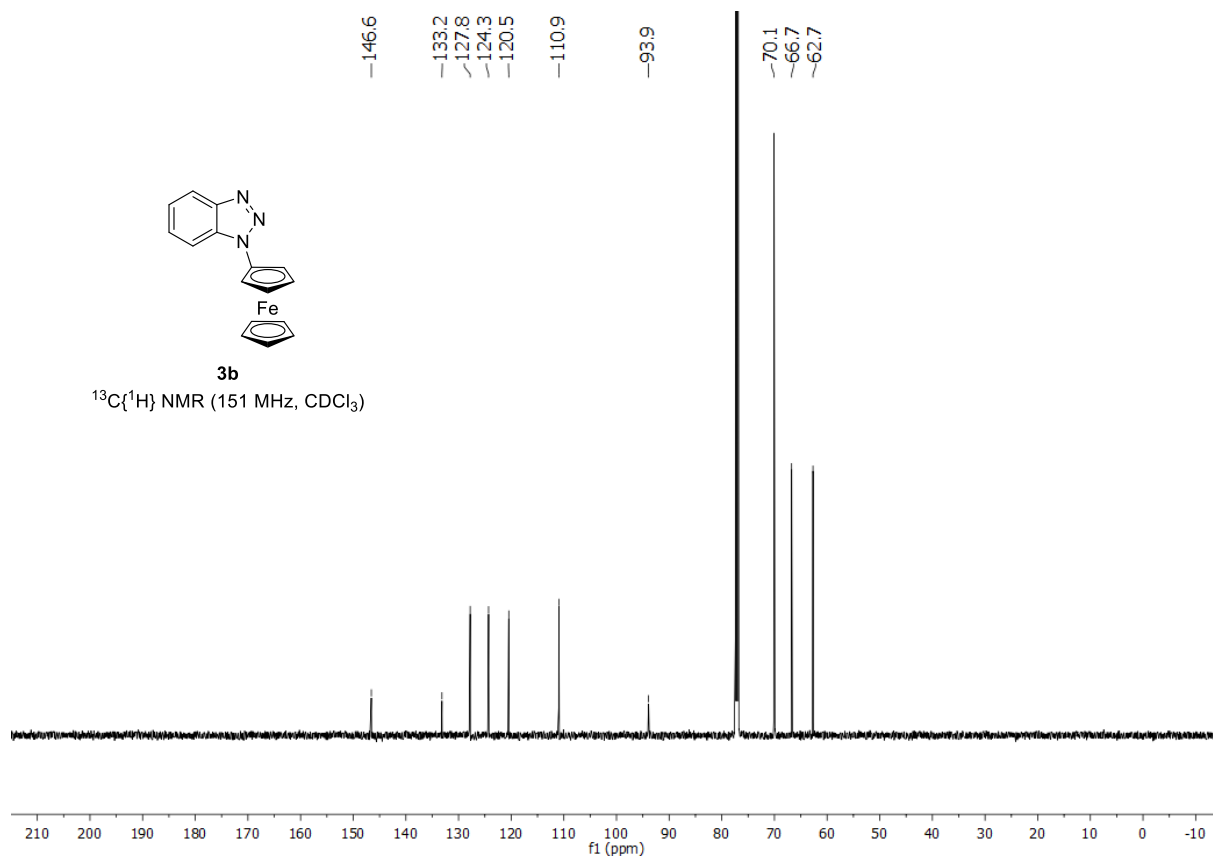
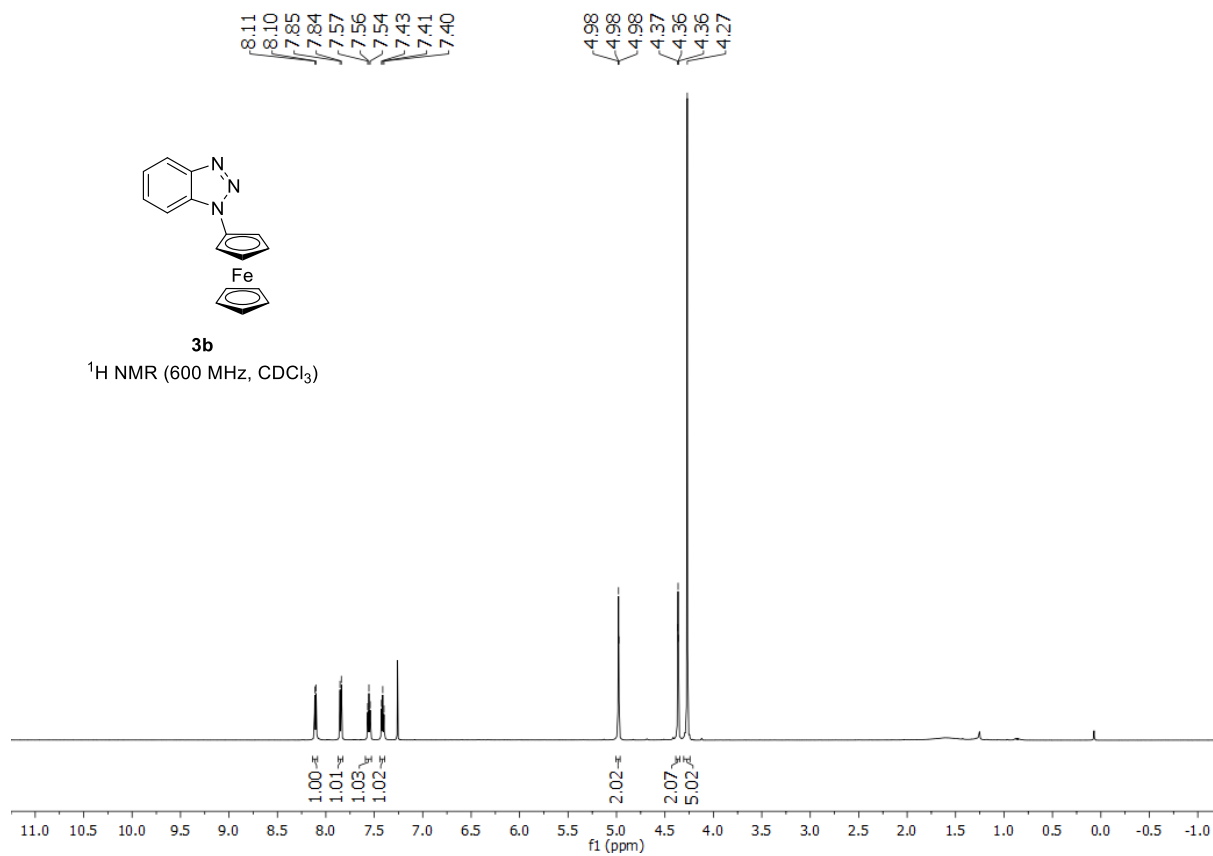


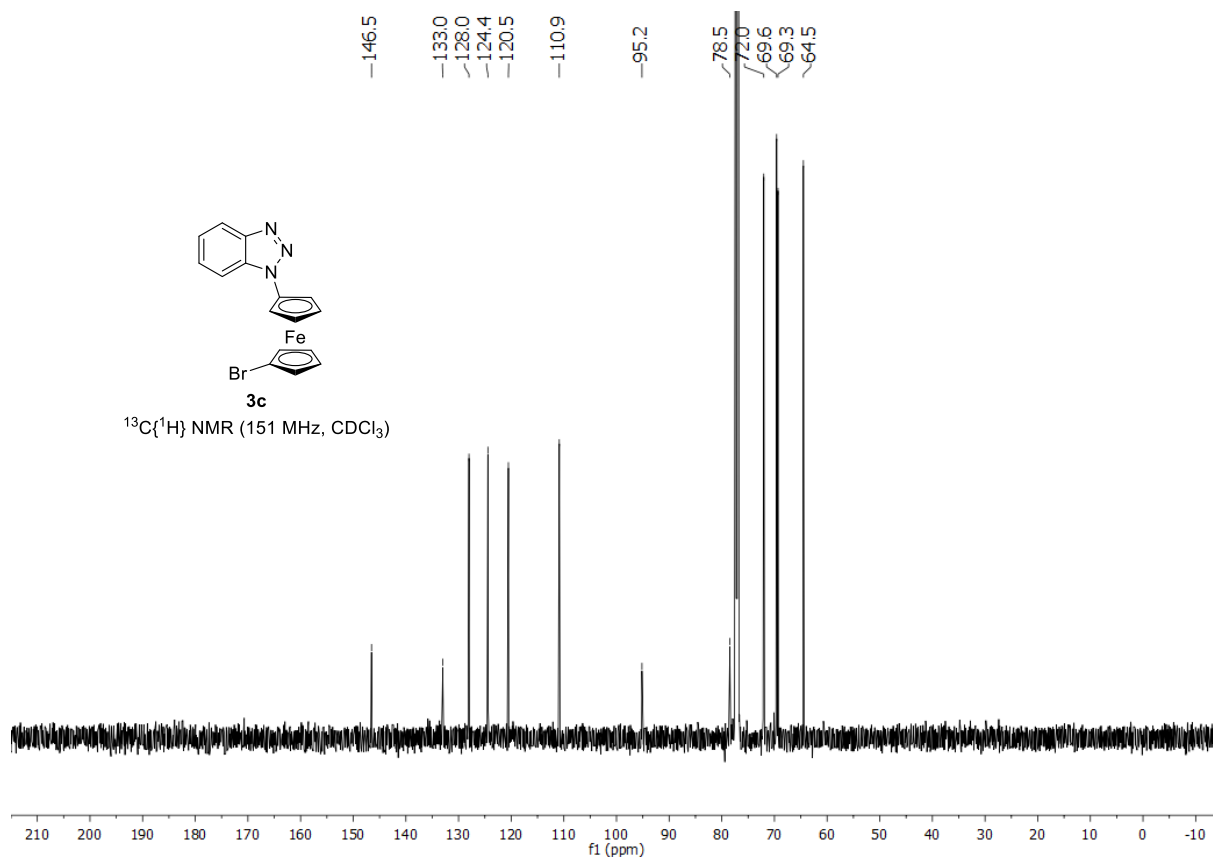
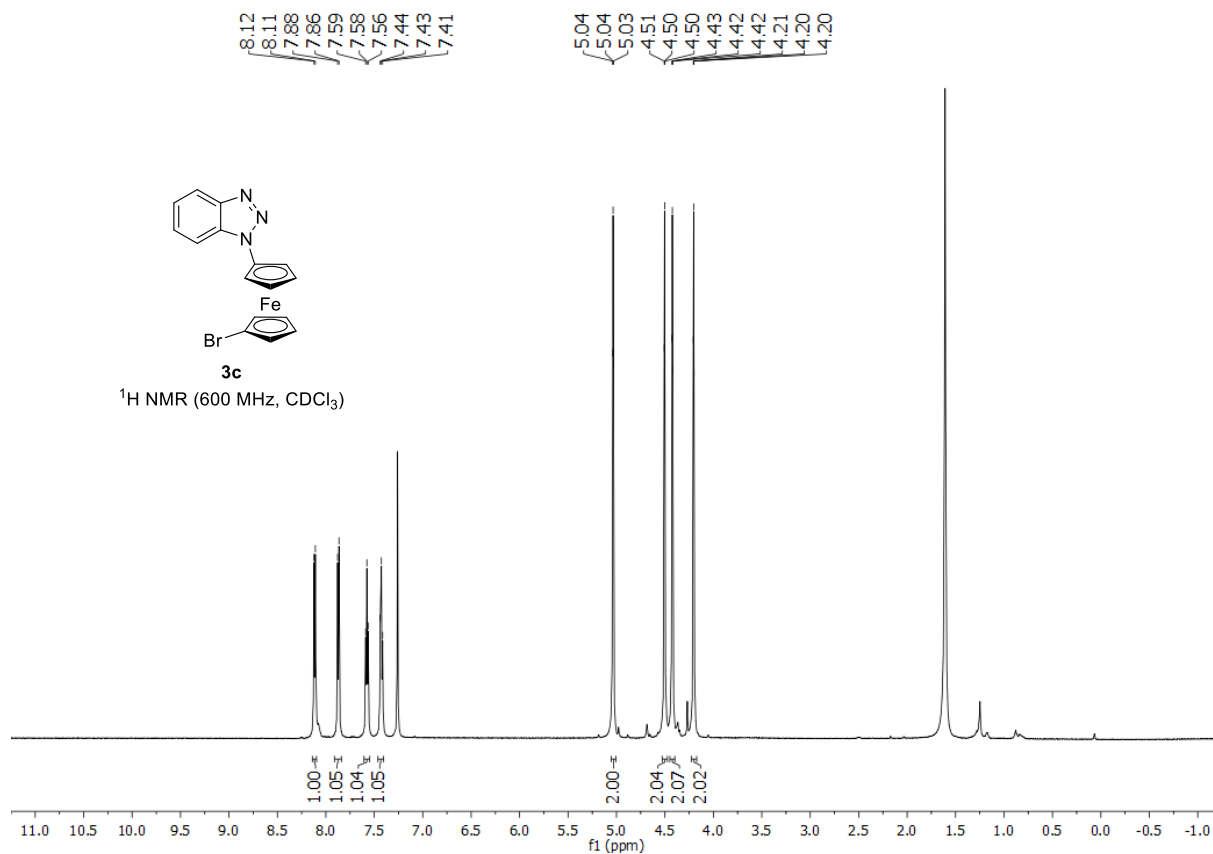
2k

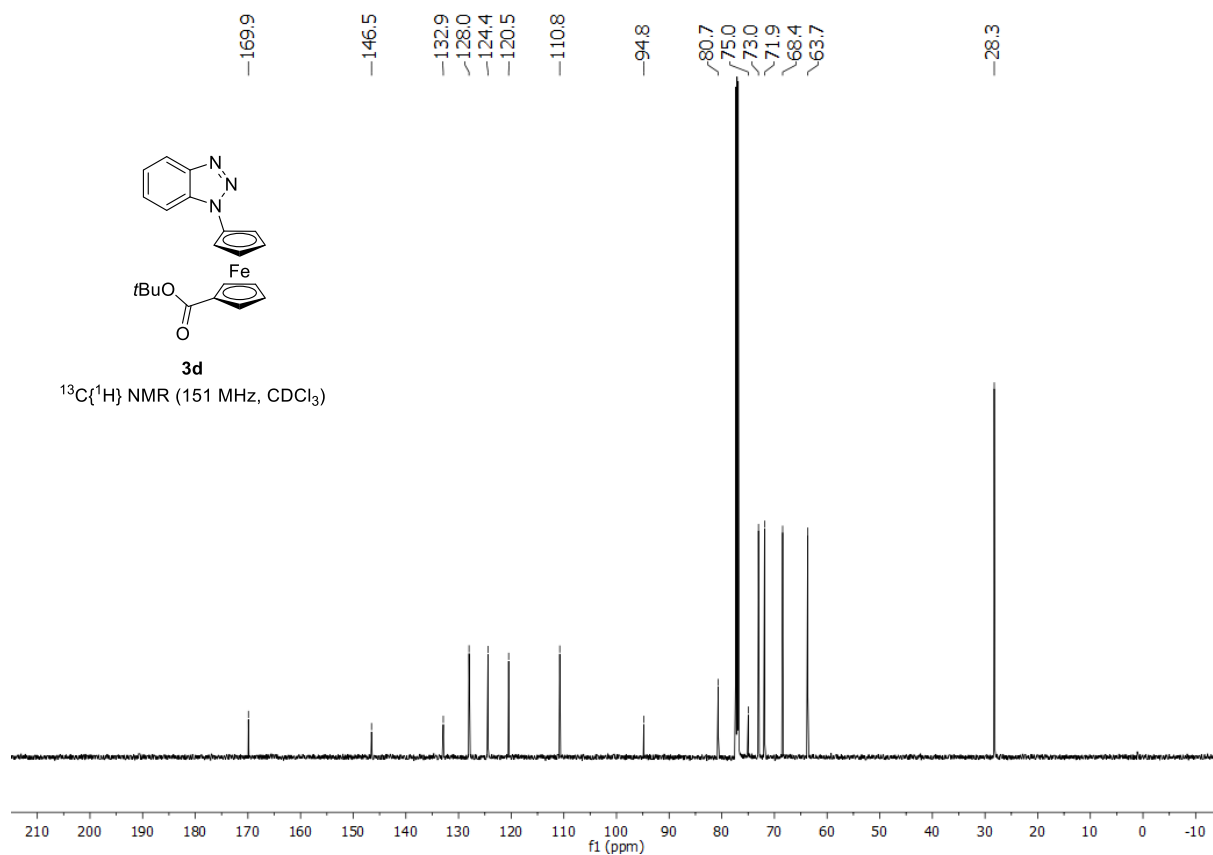
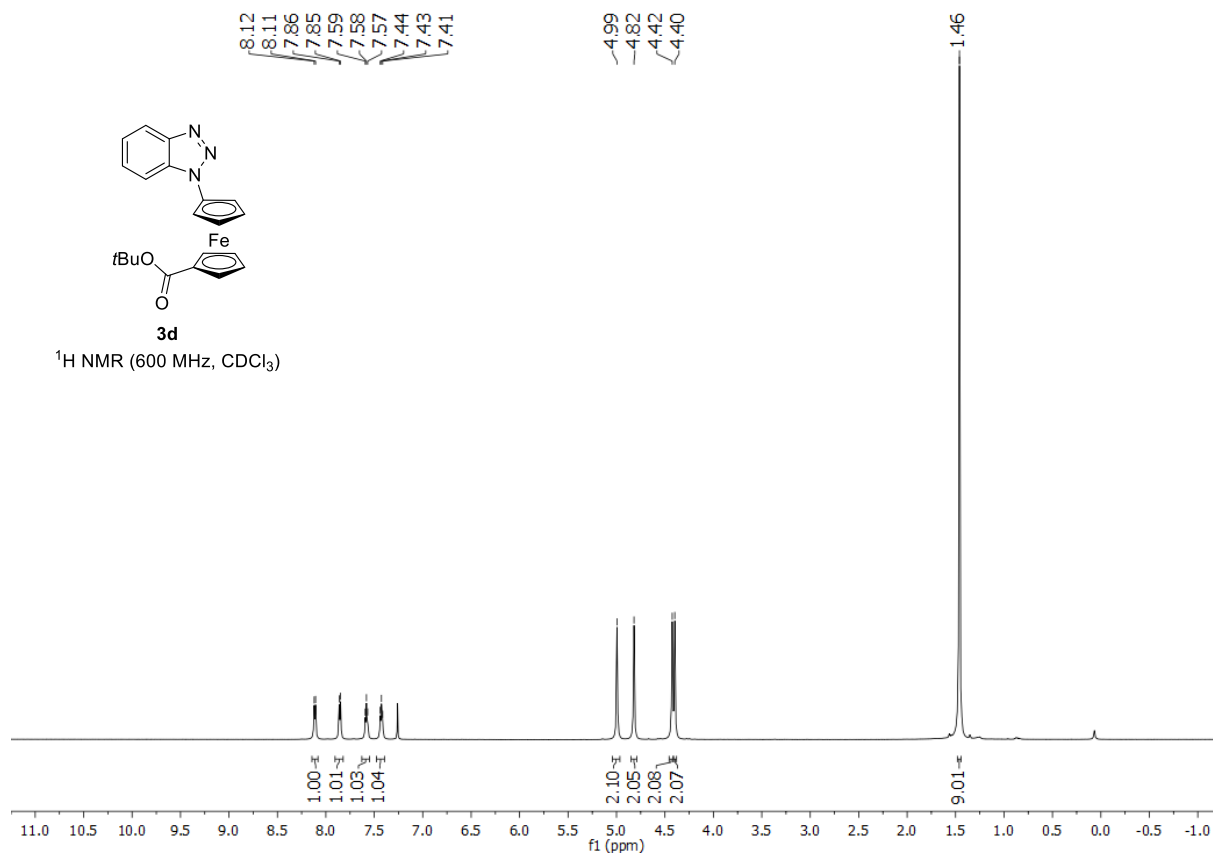
^{19}F NMR (565 MHz, CDCl_3)

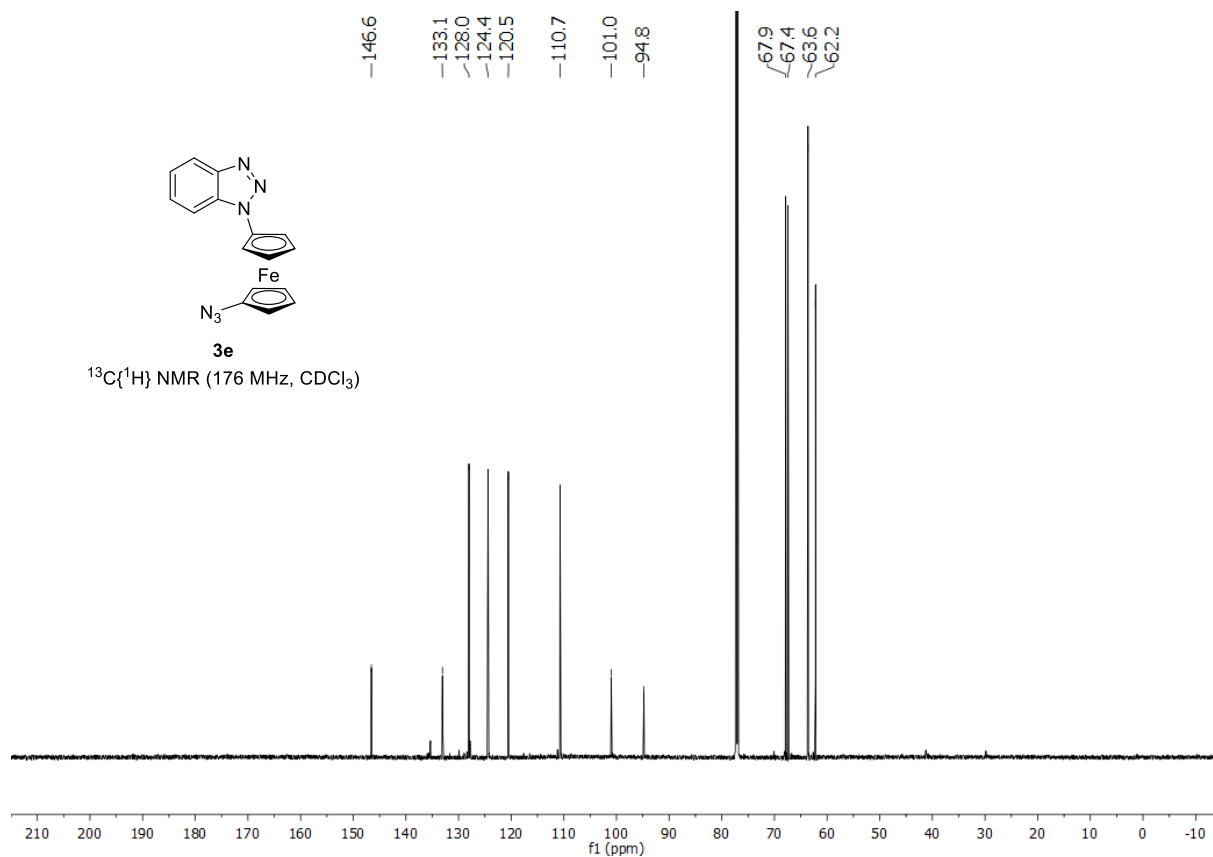
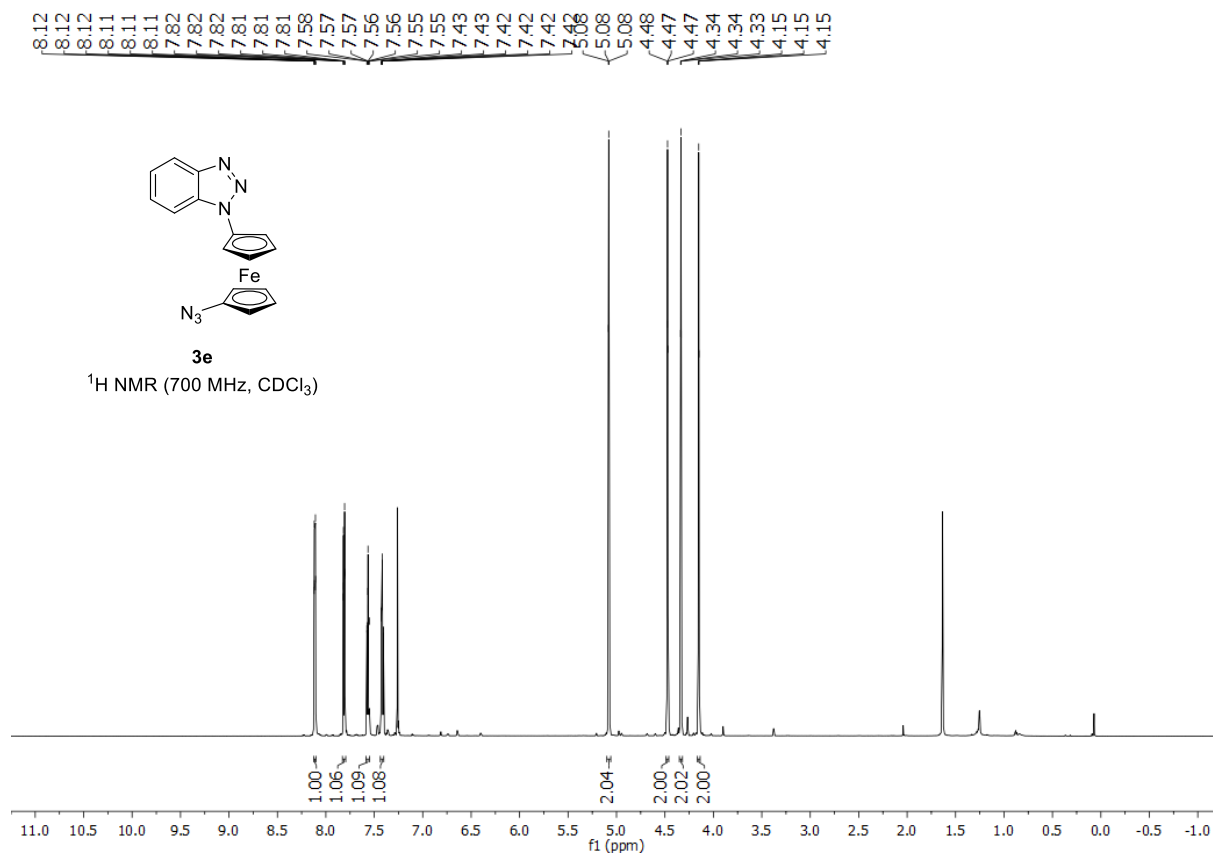


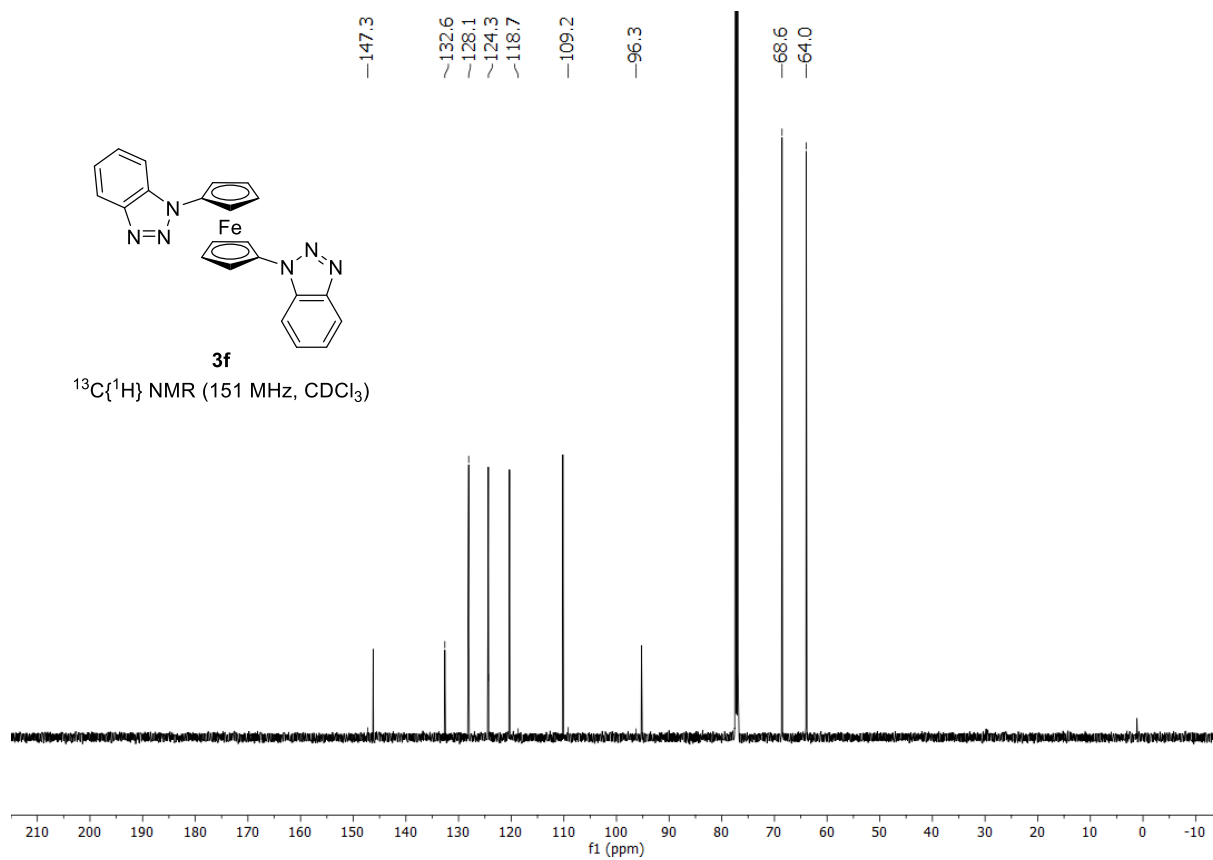
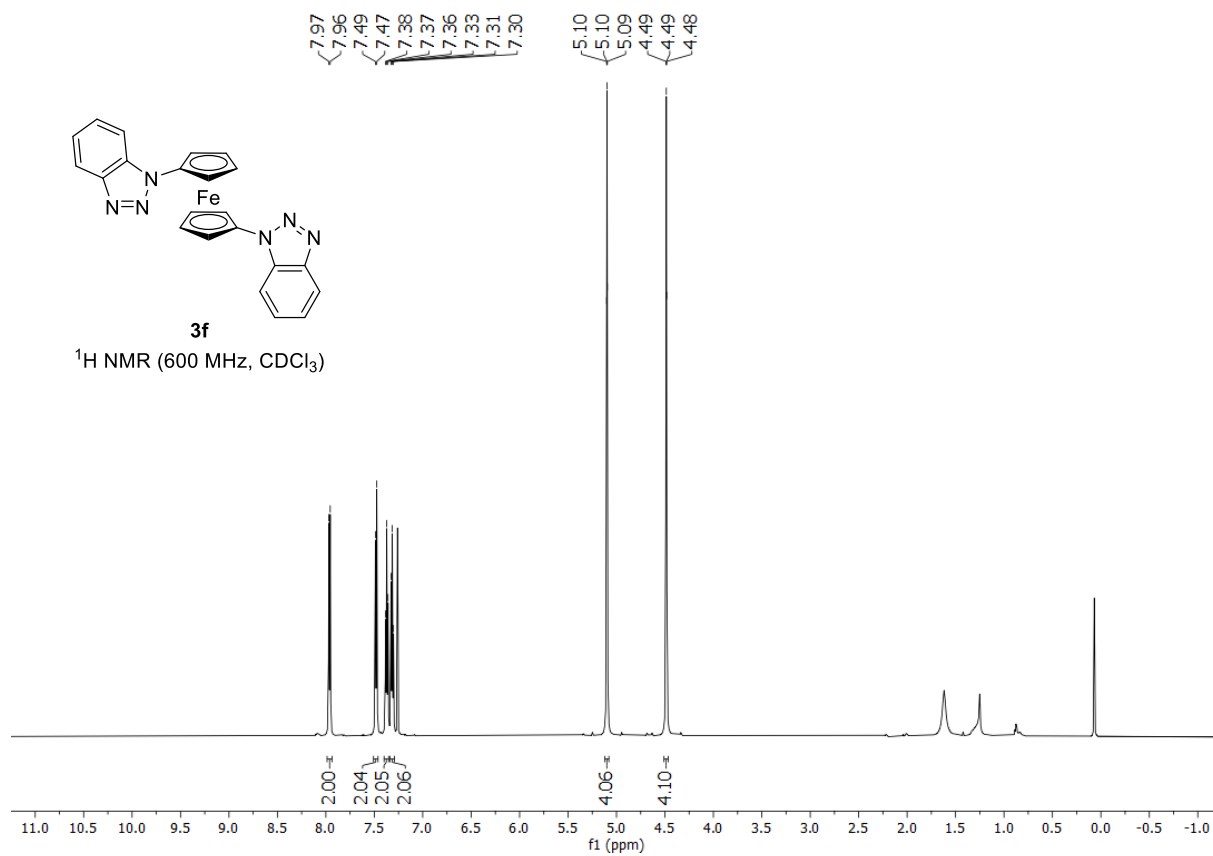


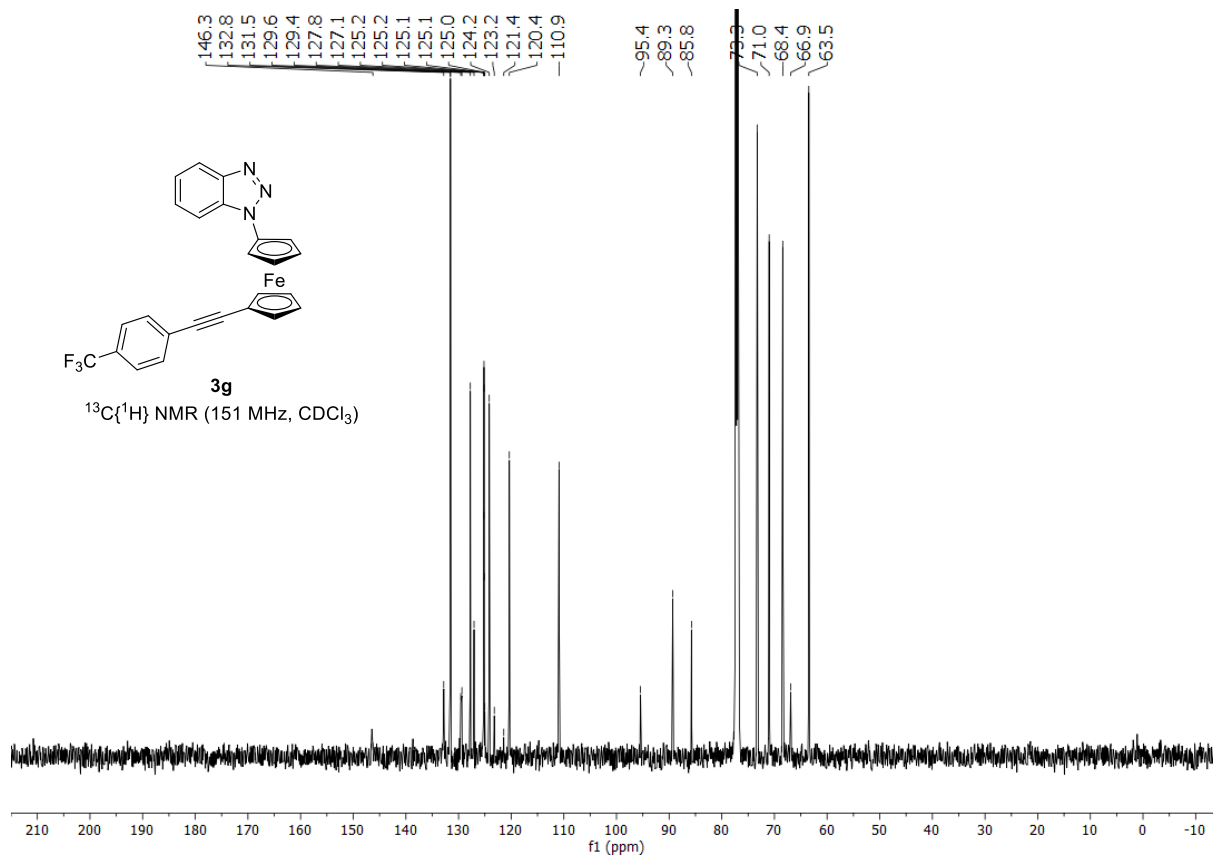
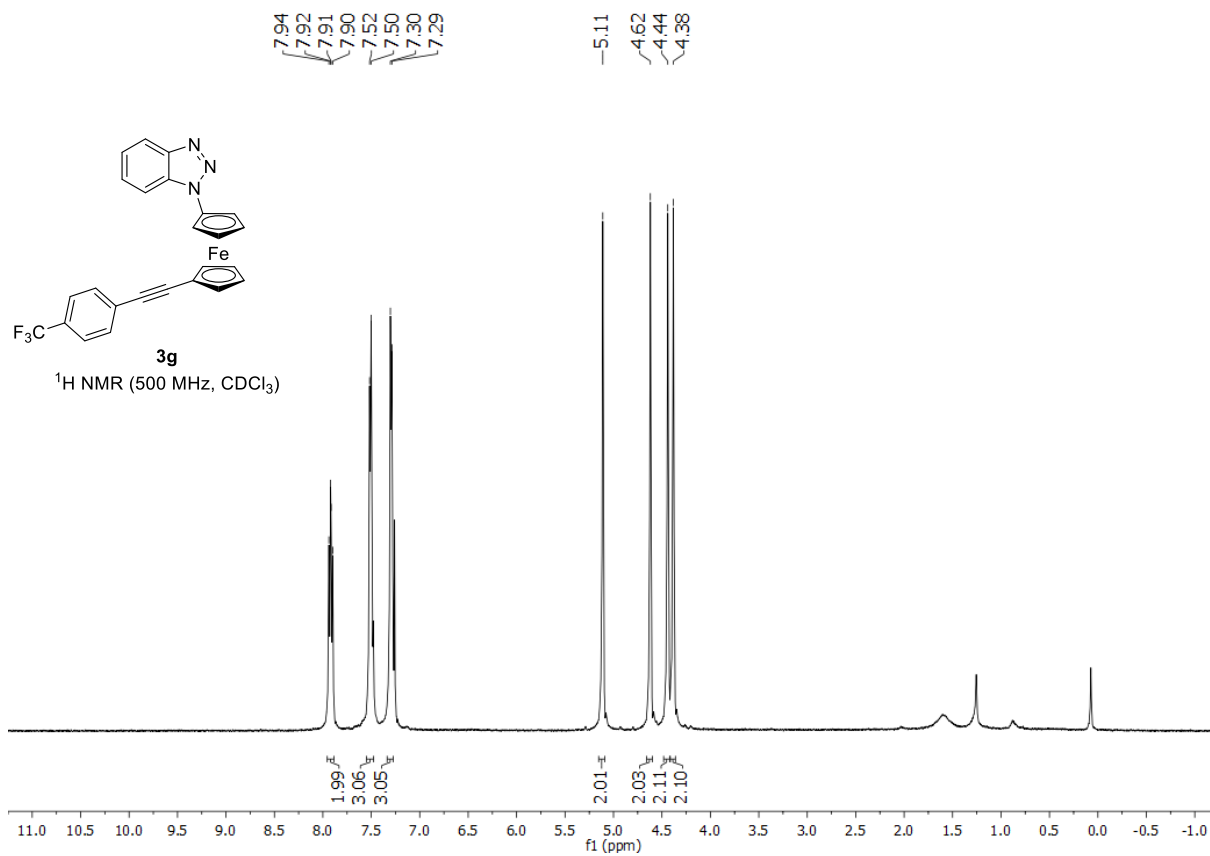


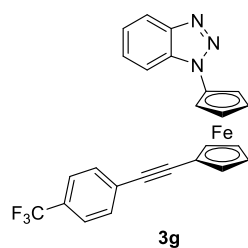




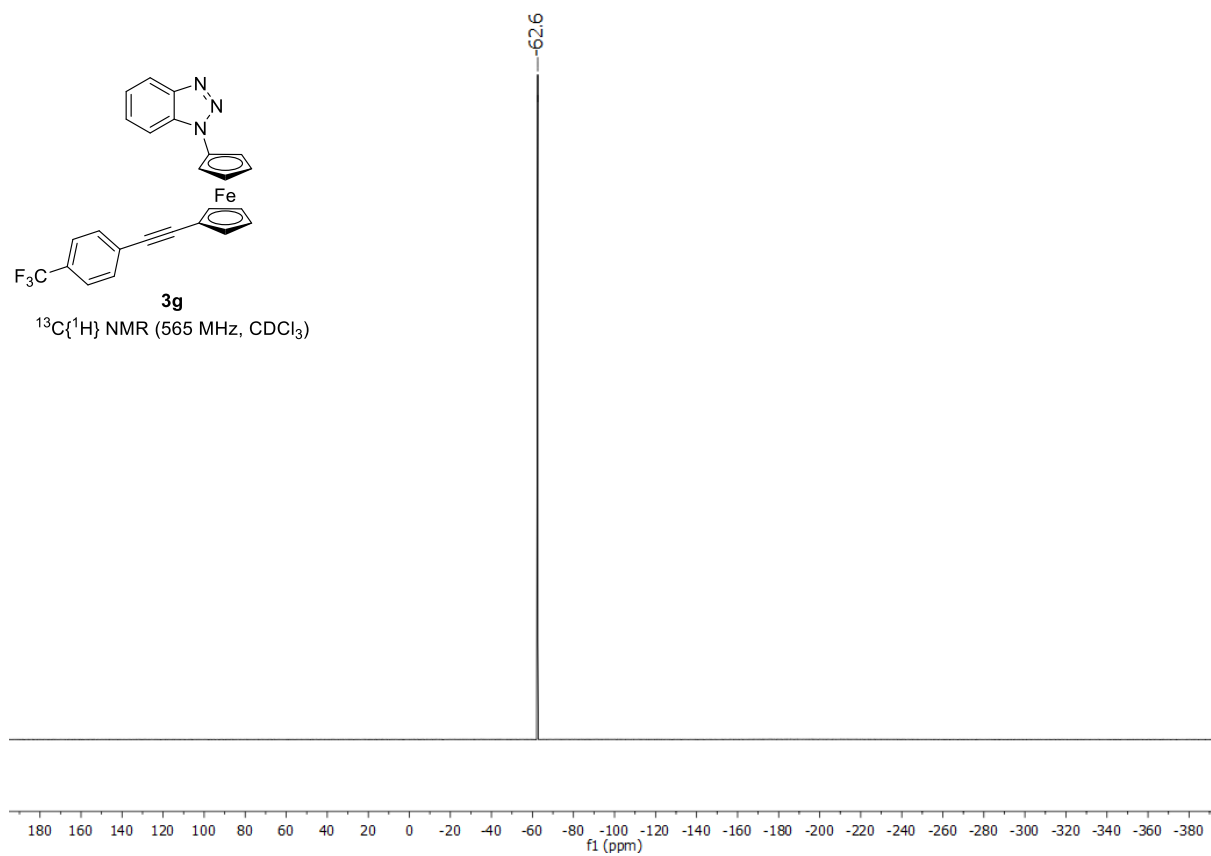


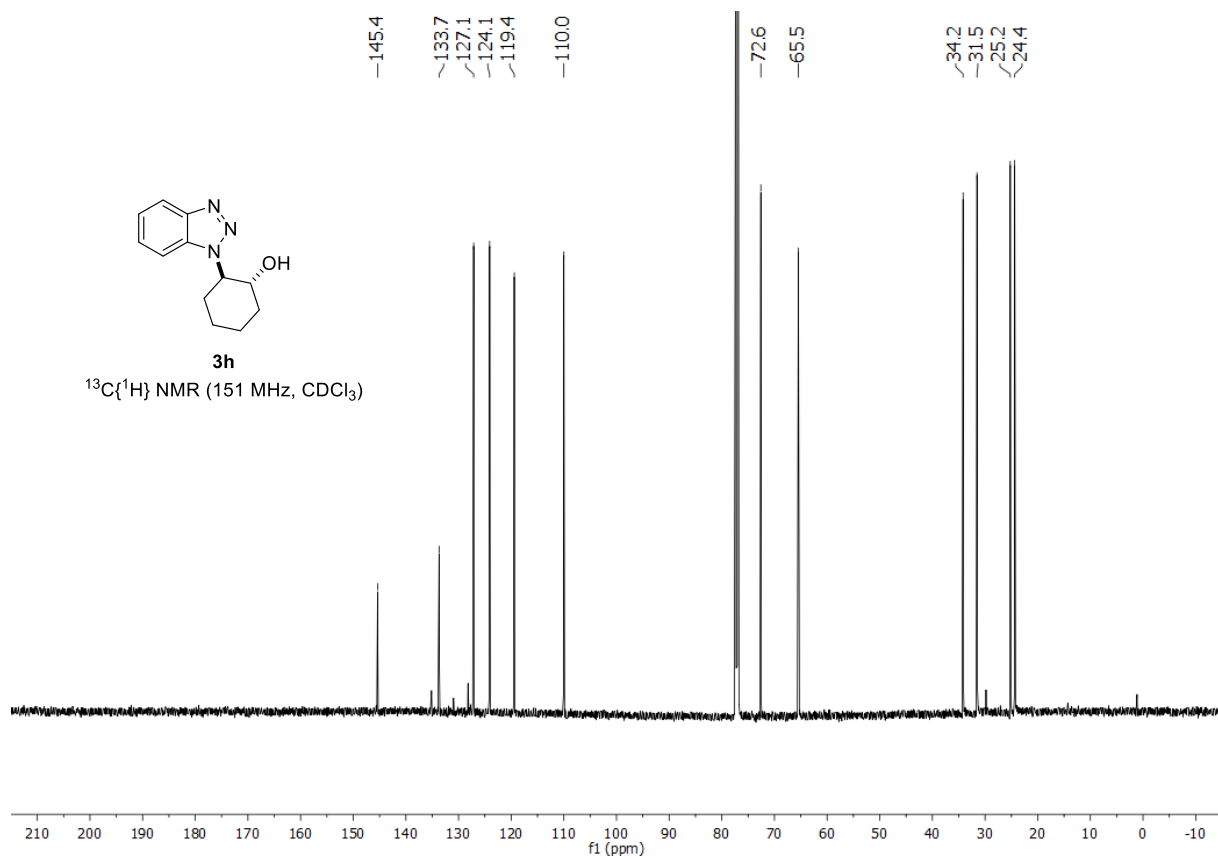
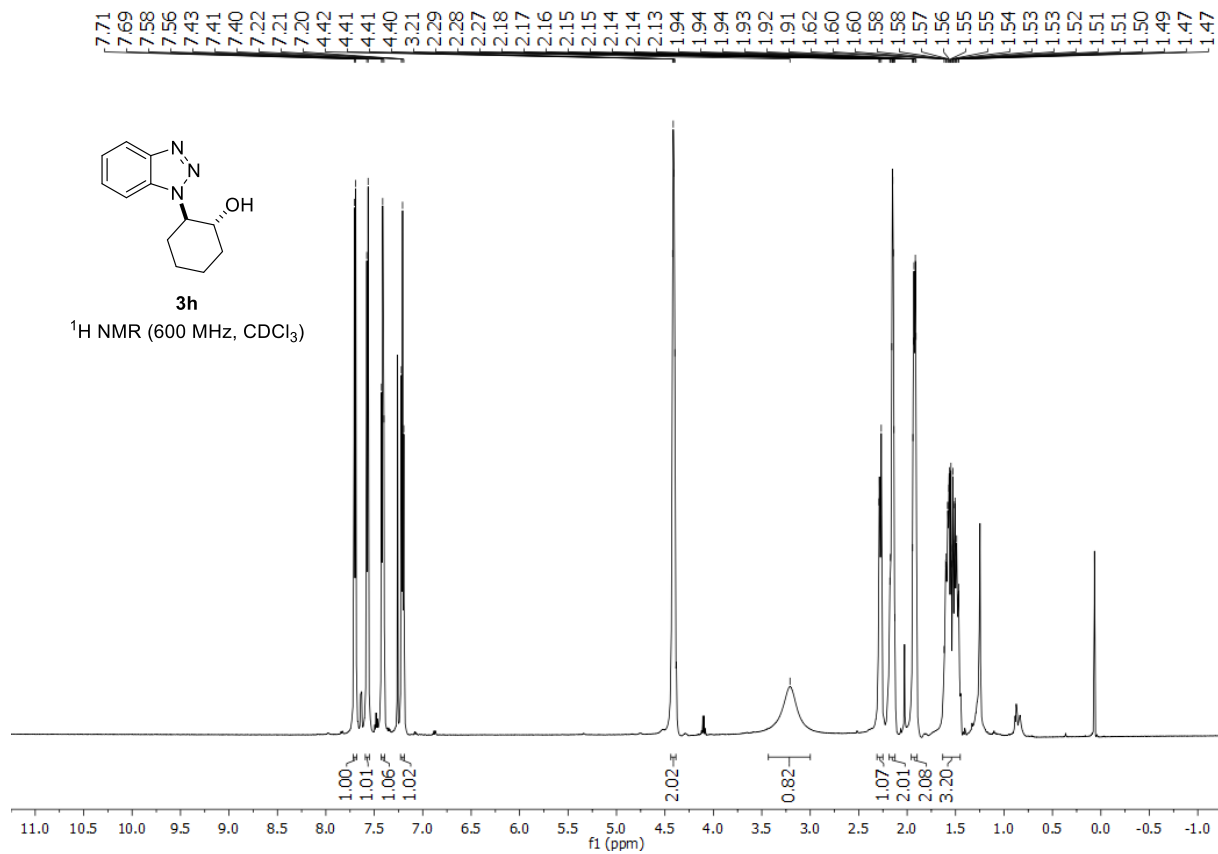


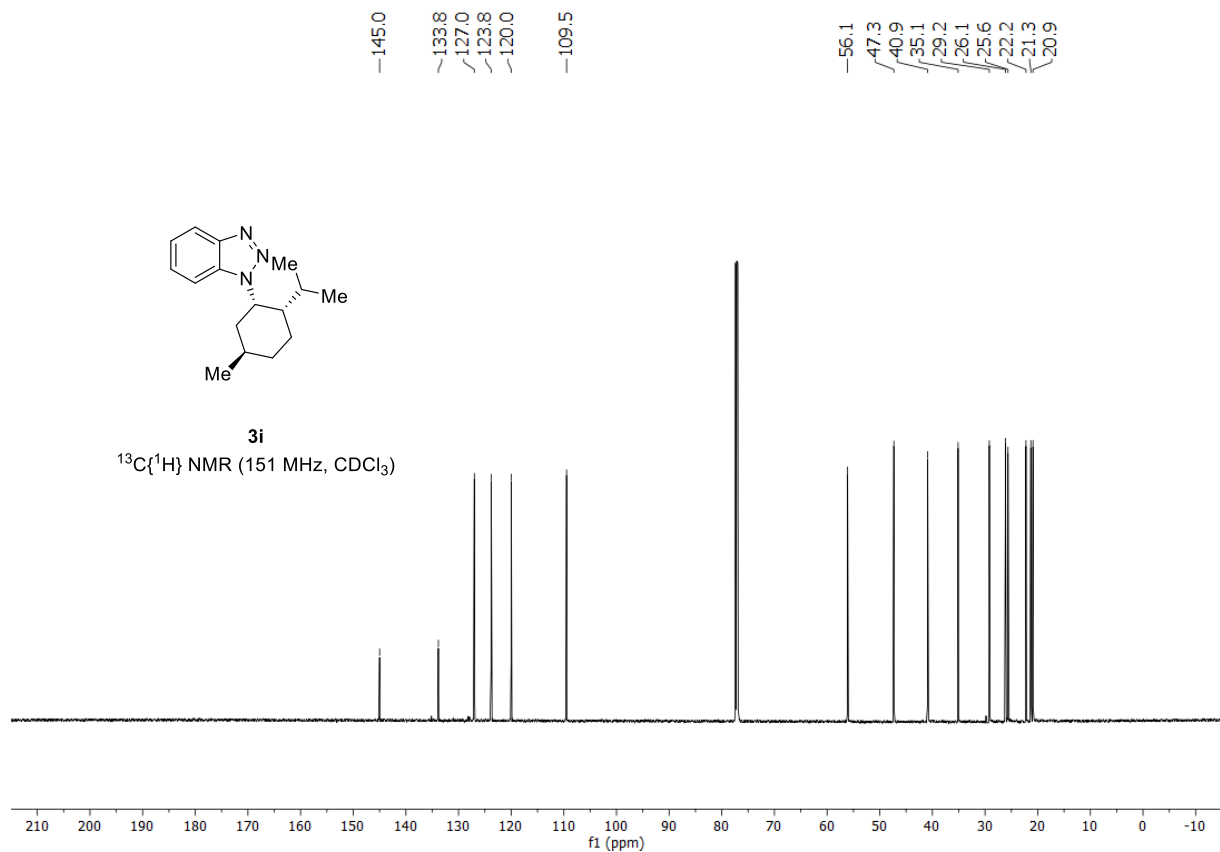
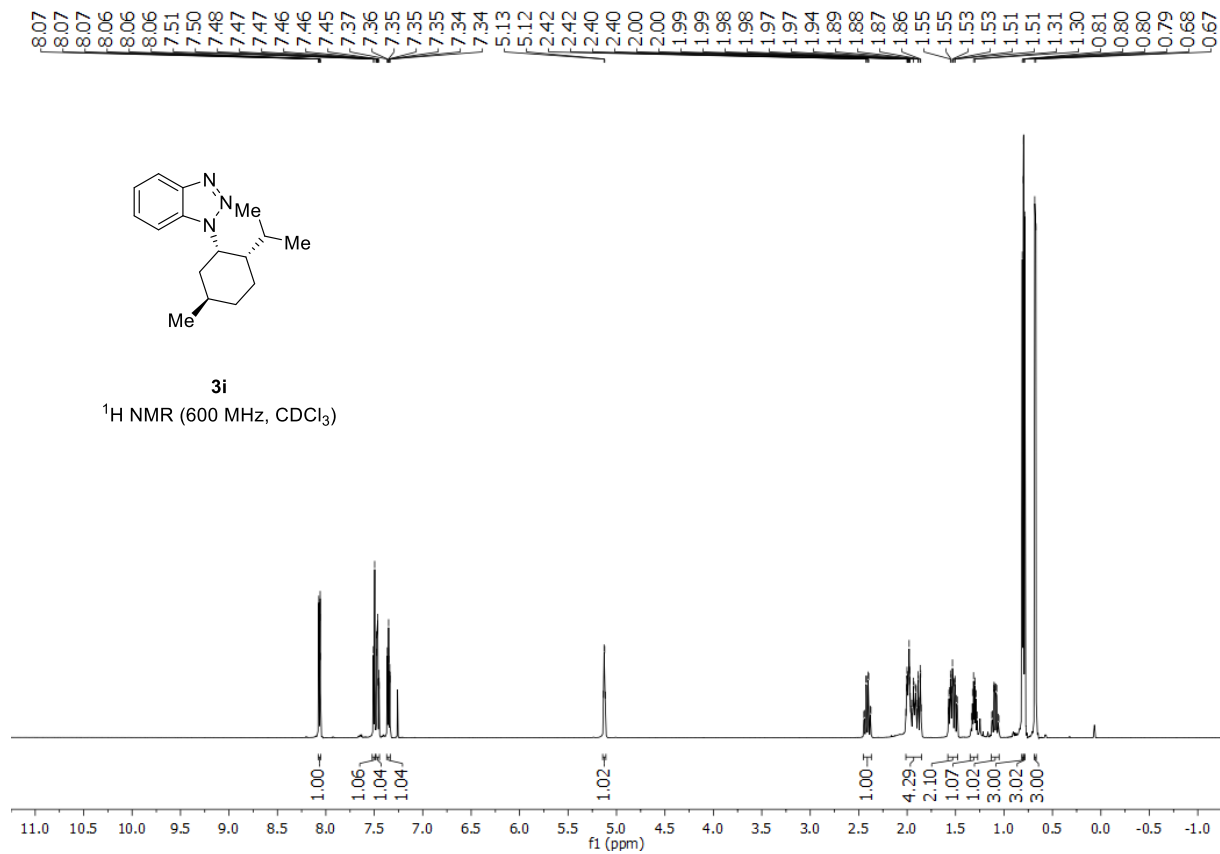


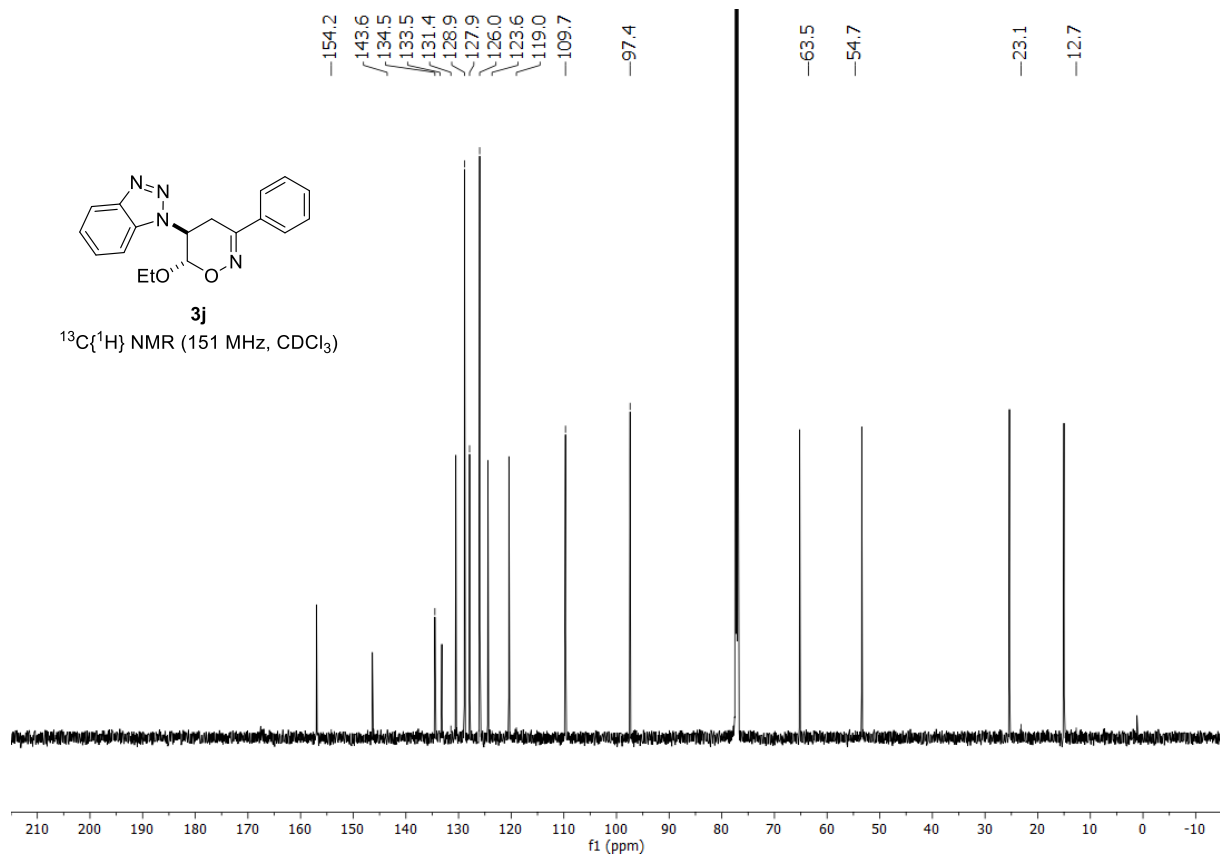
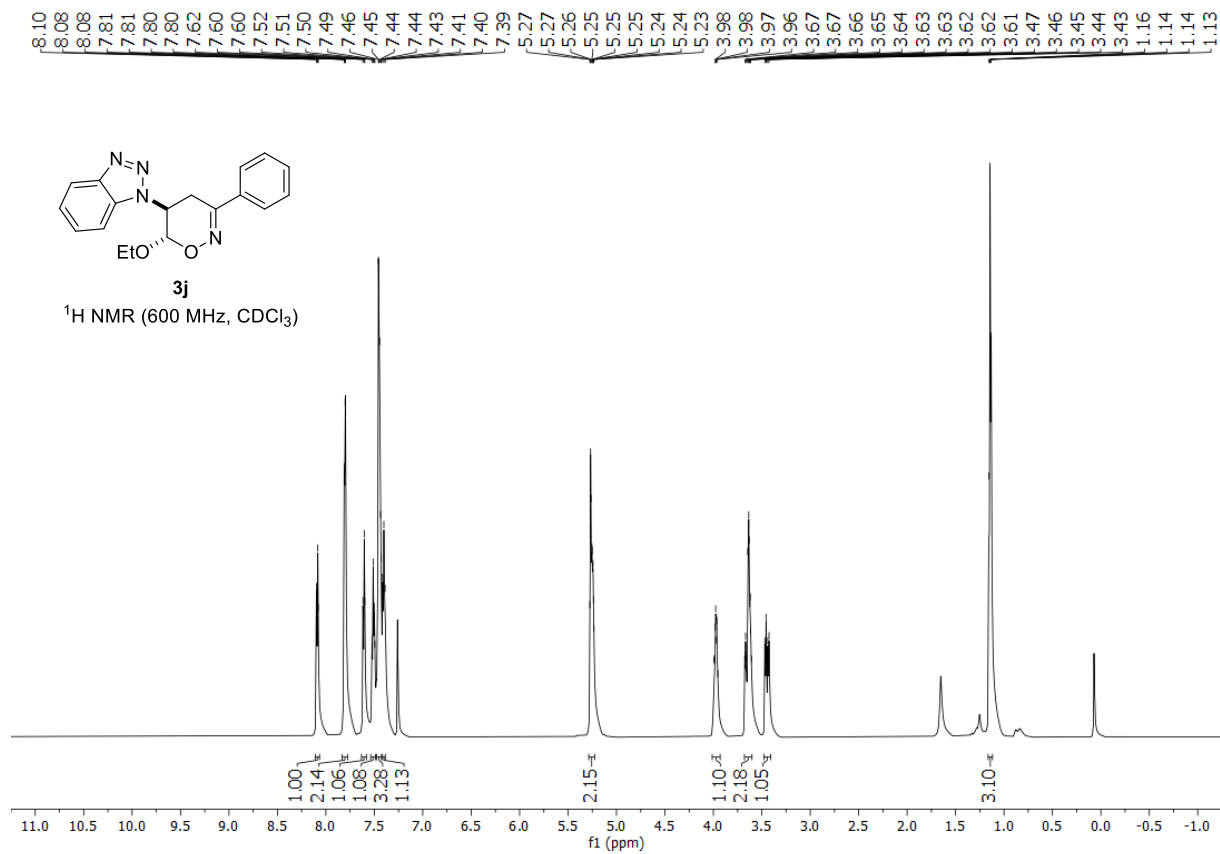


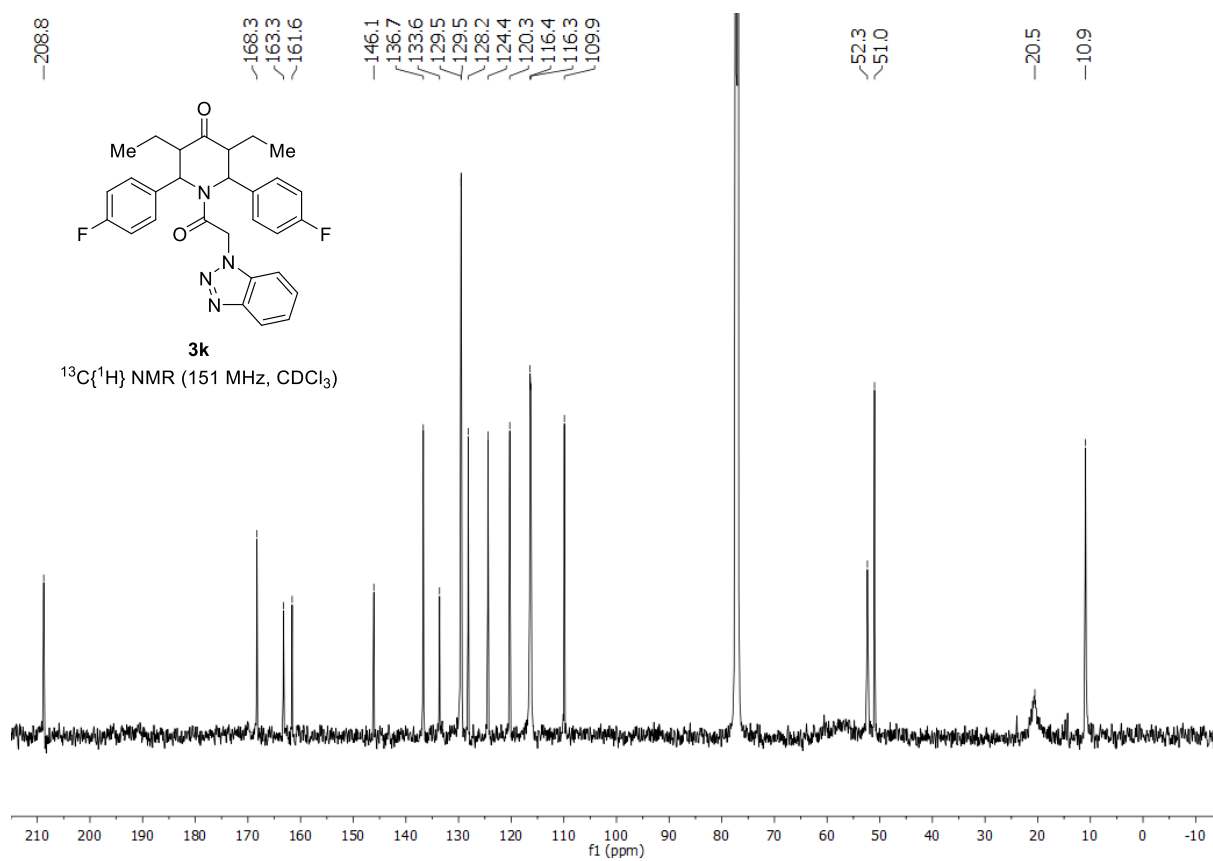
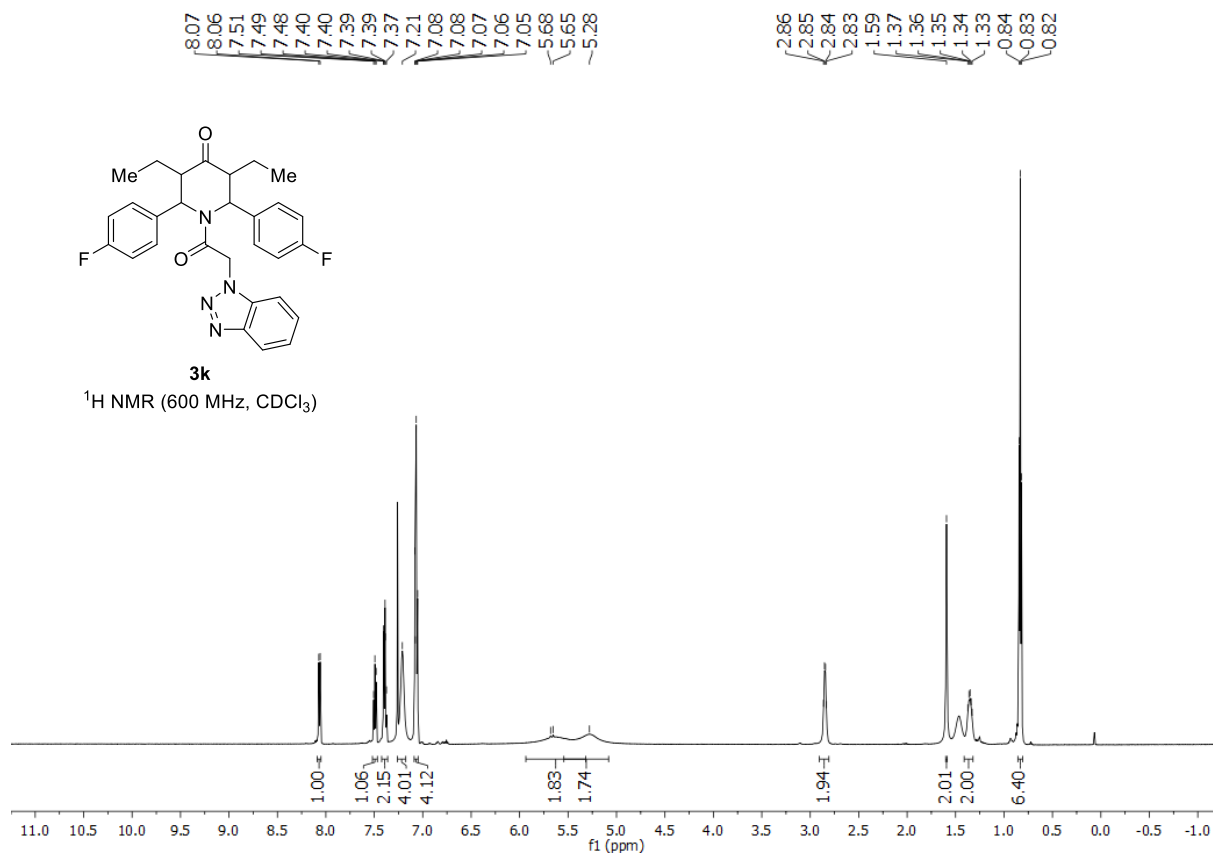
3g
 $^{13}\text{C}\{^1\text{H}\}$ NMR (565 MHz, CDCl_3)

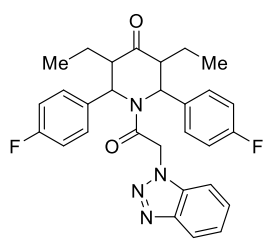






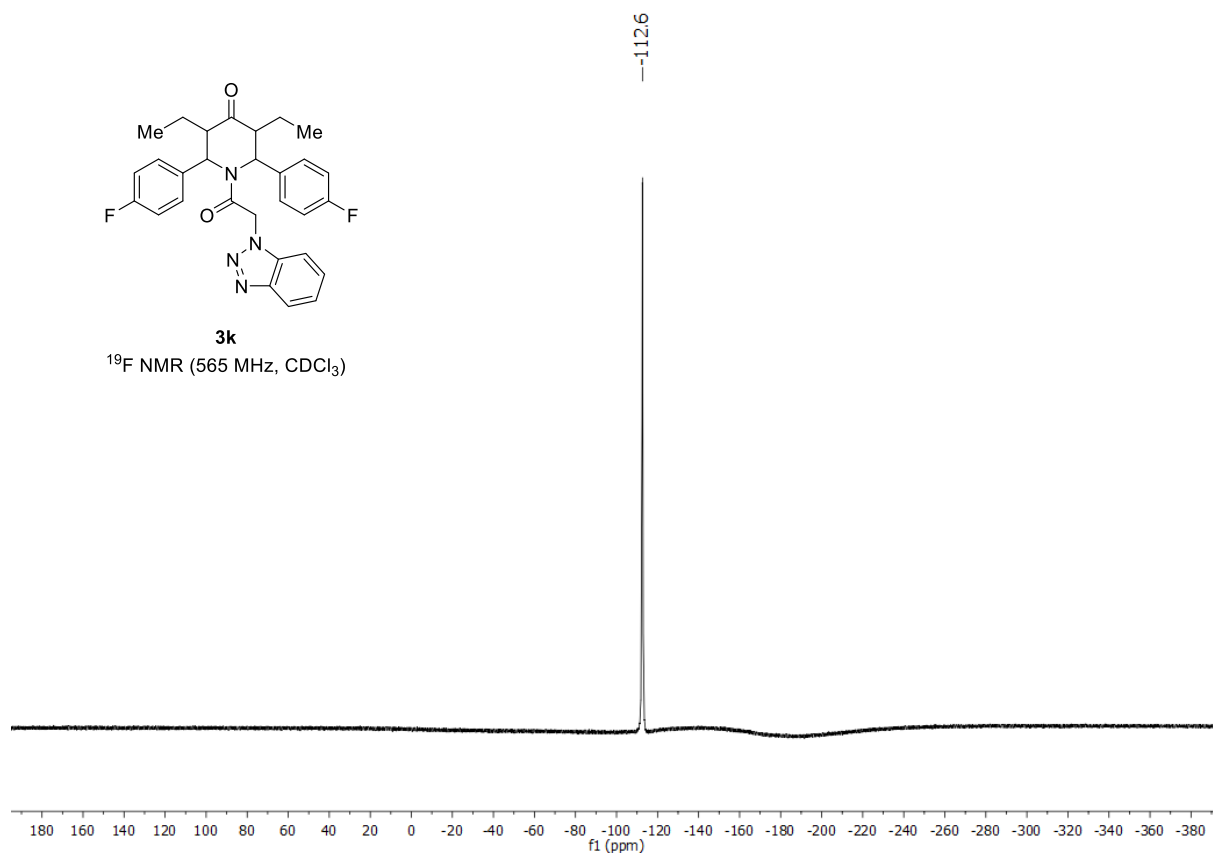


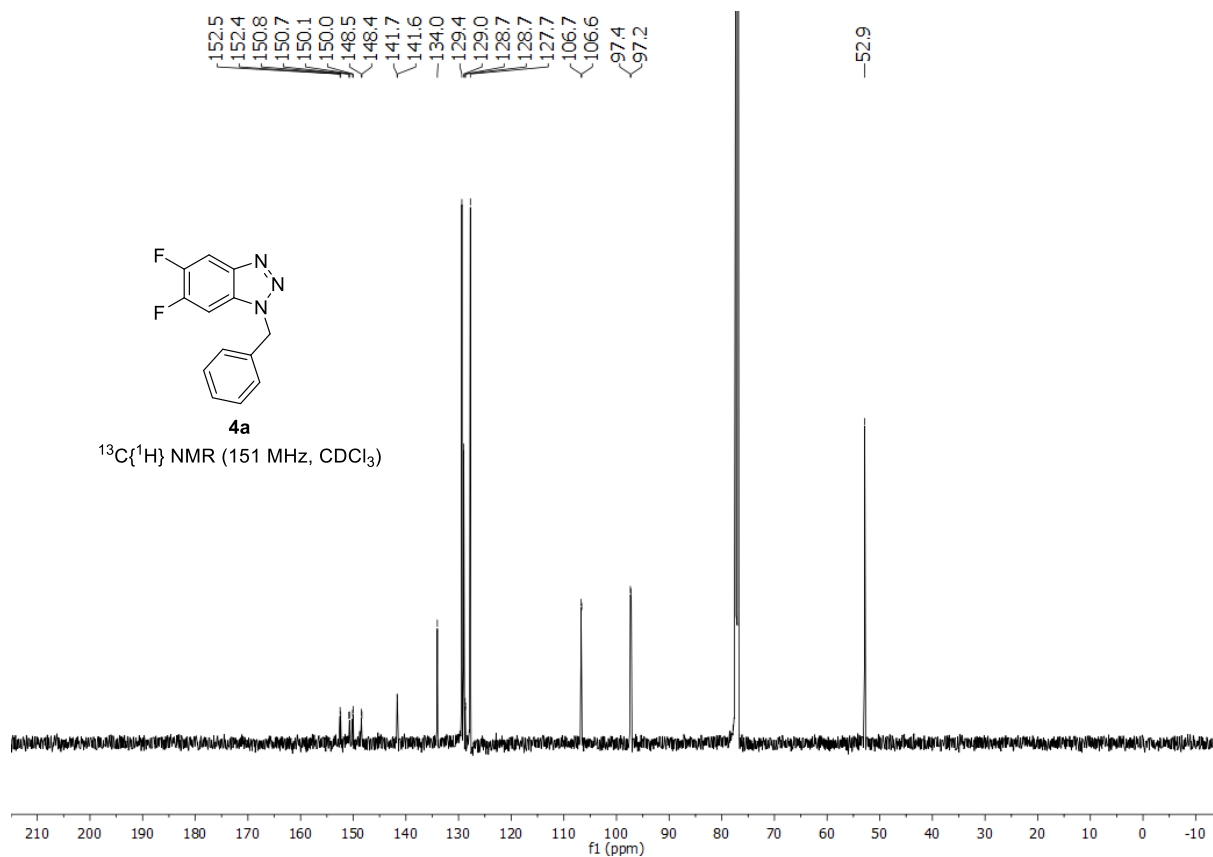
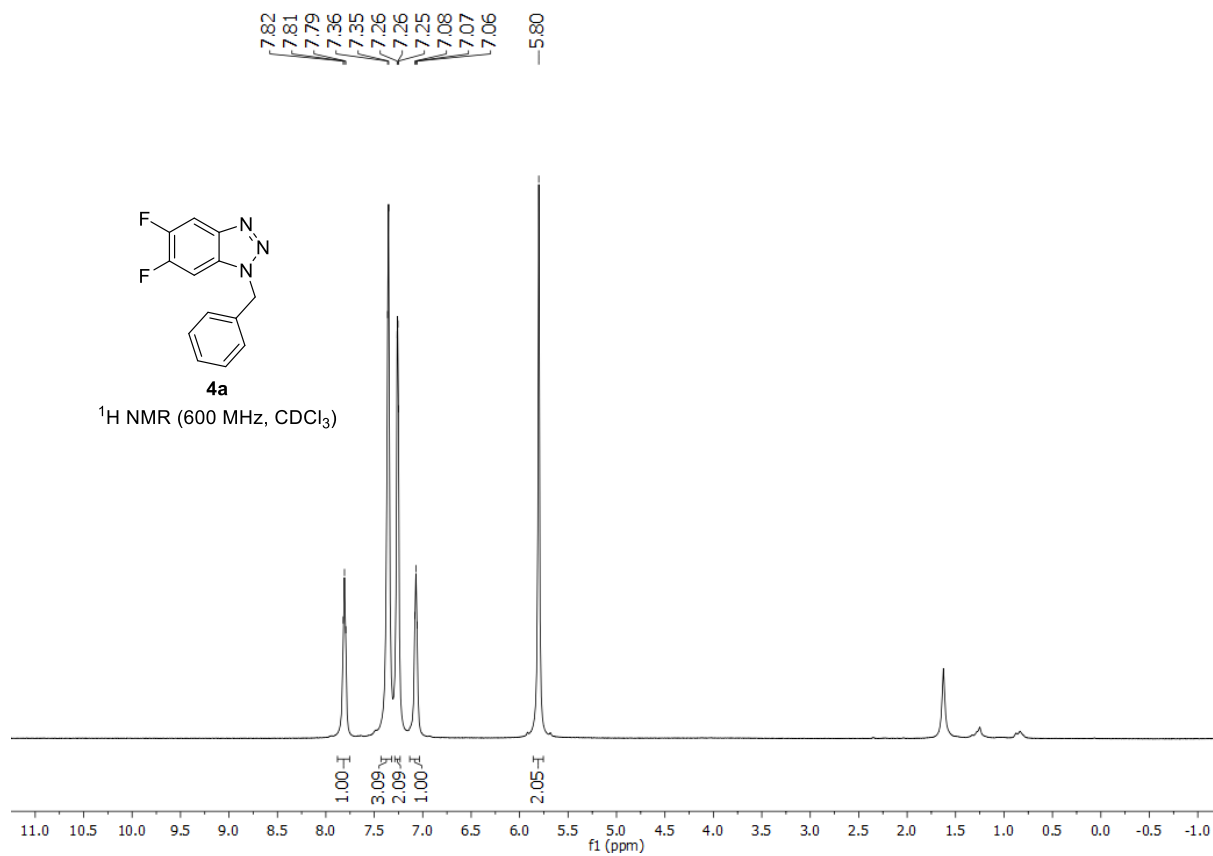


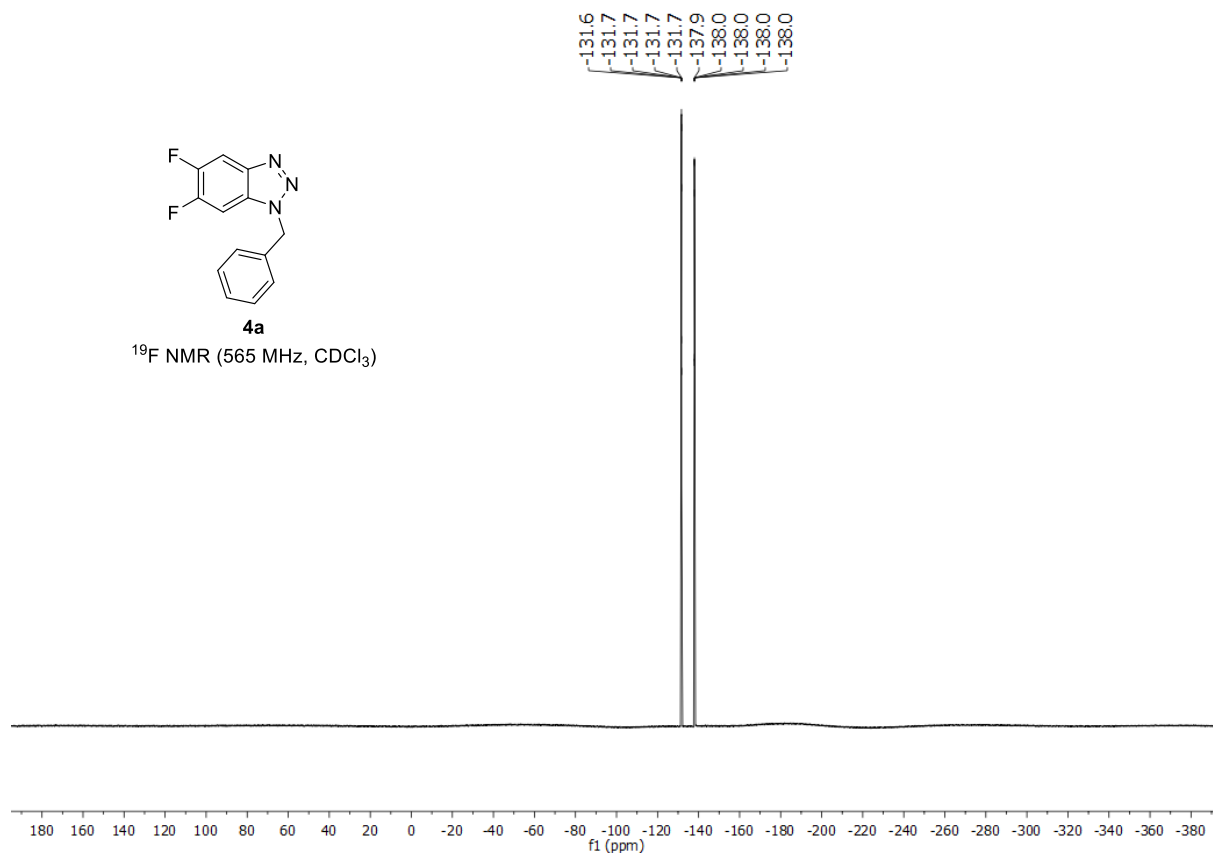


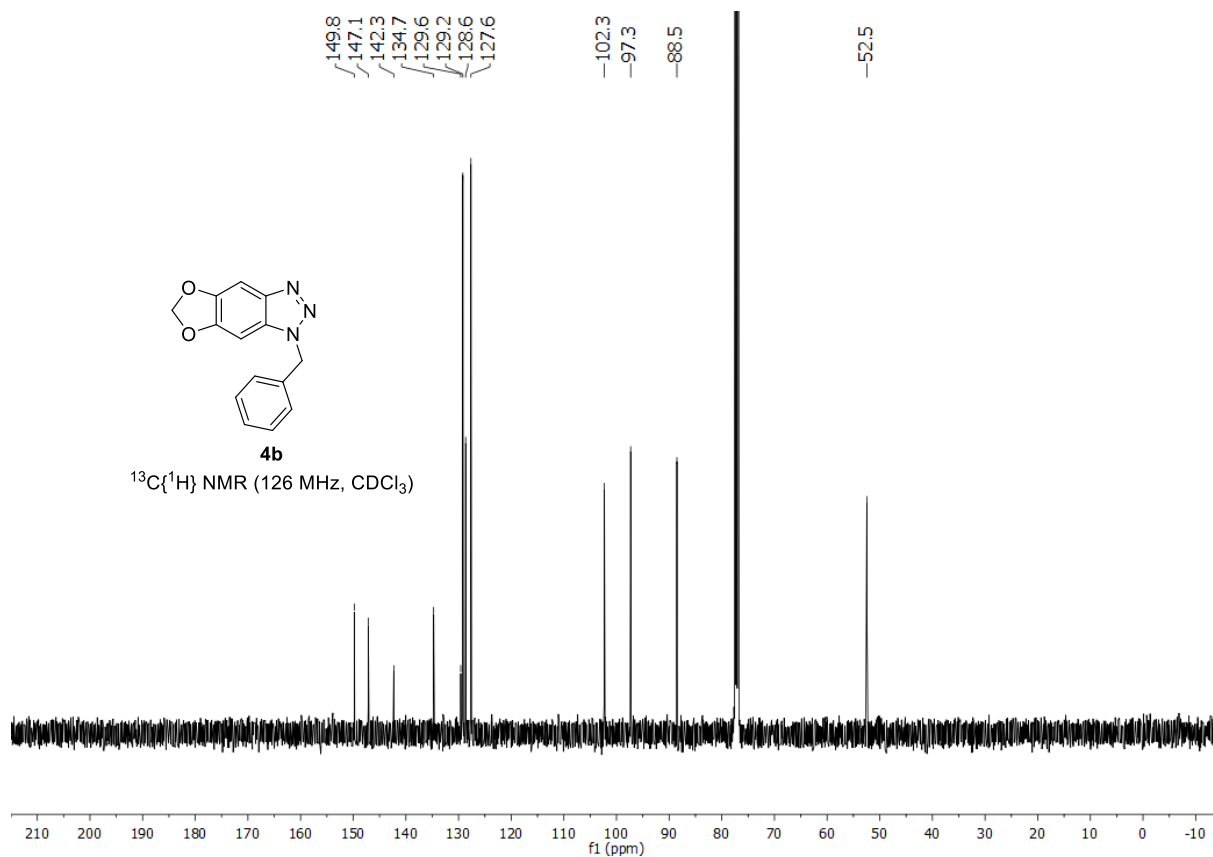
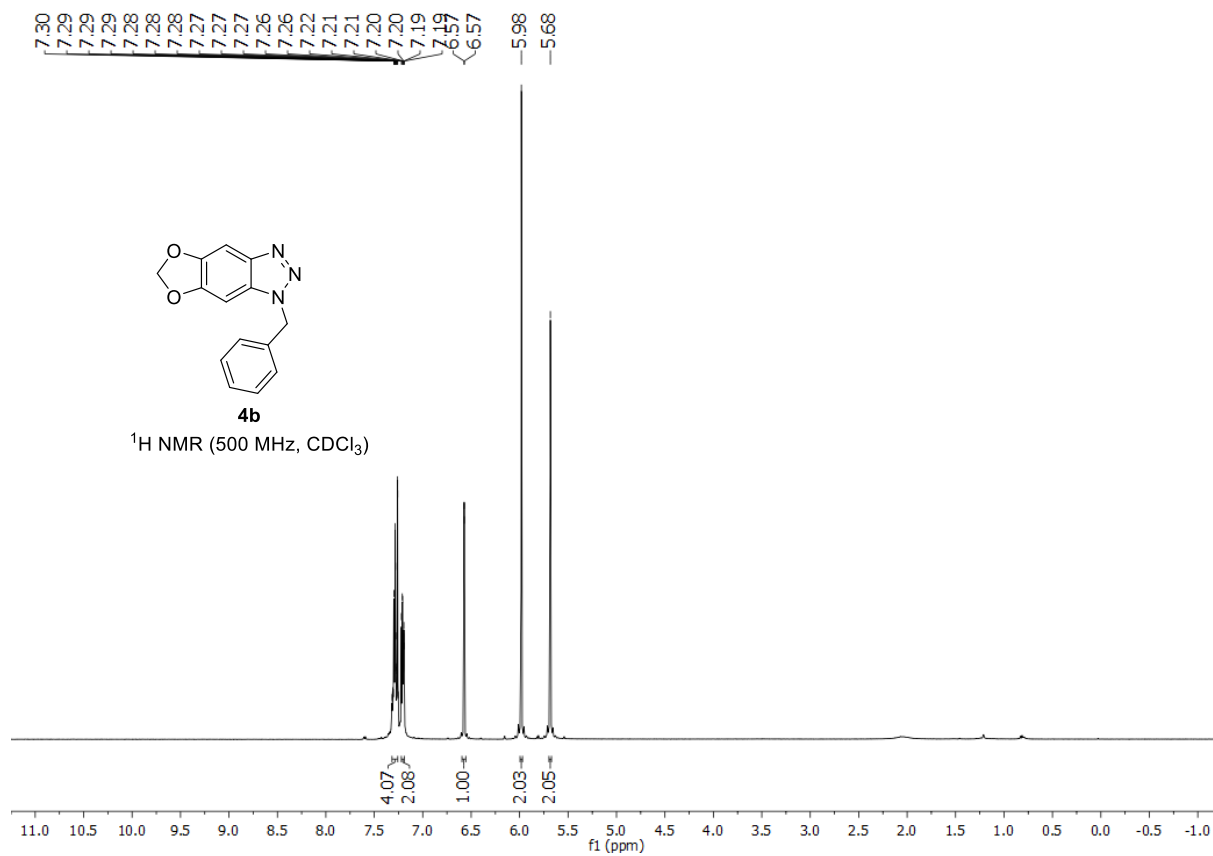
3k

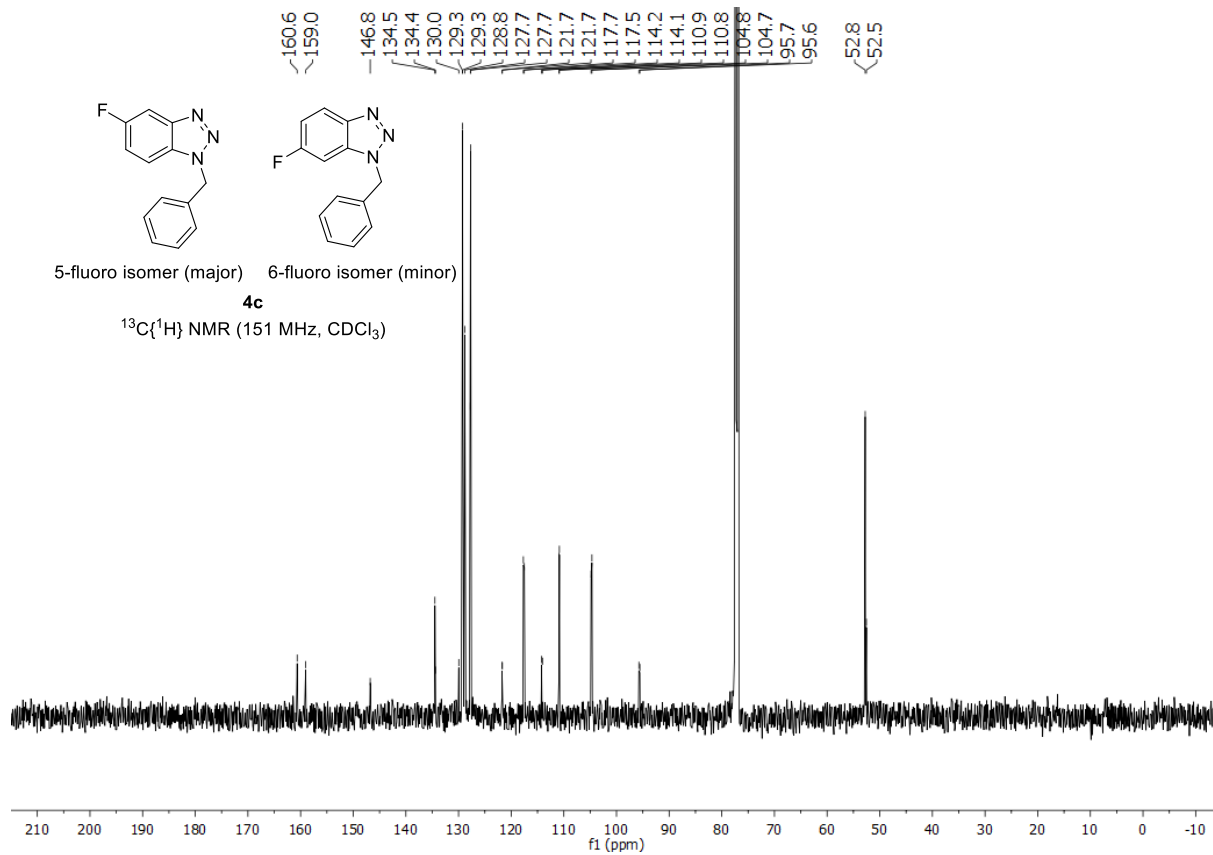
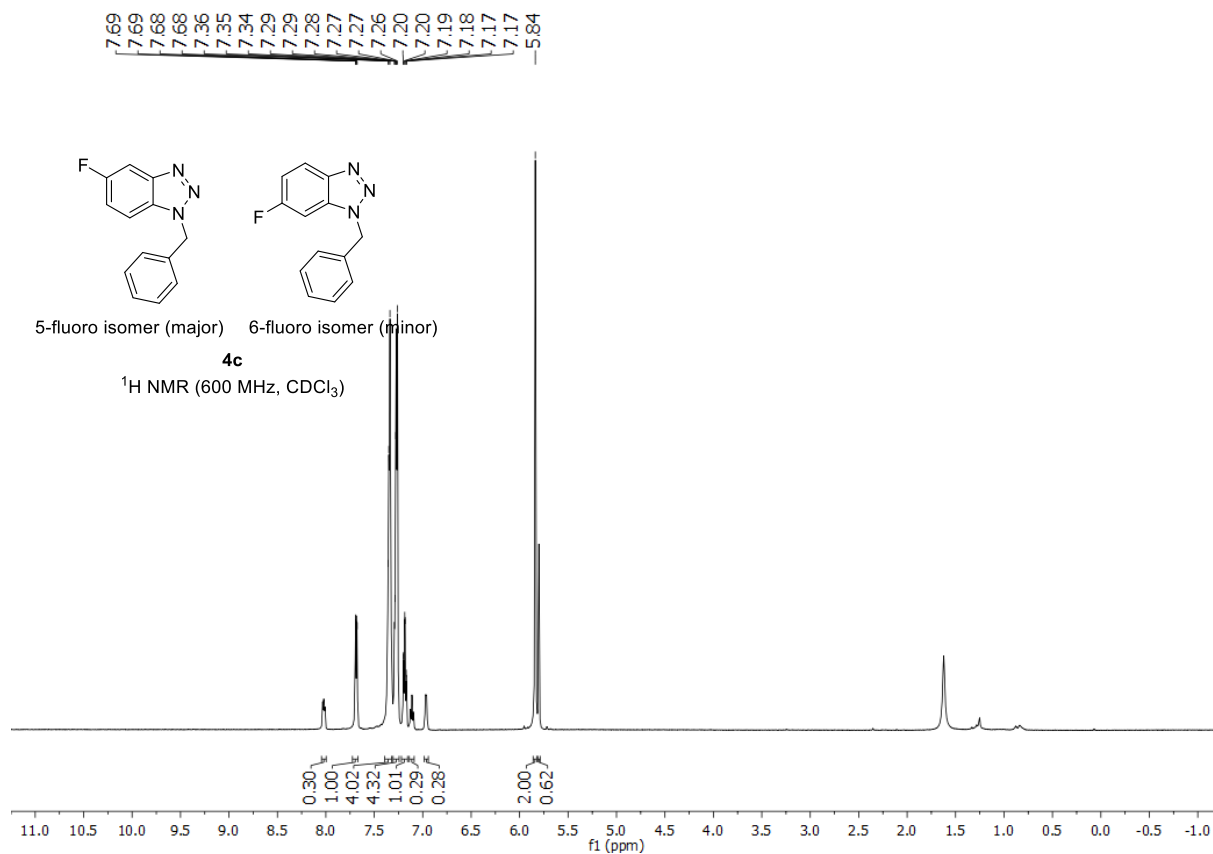
¹⁹F NMR (565 MHz, CDCl₃)

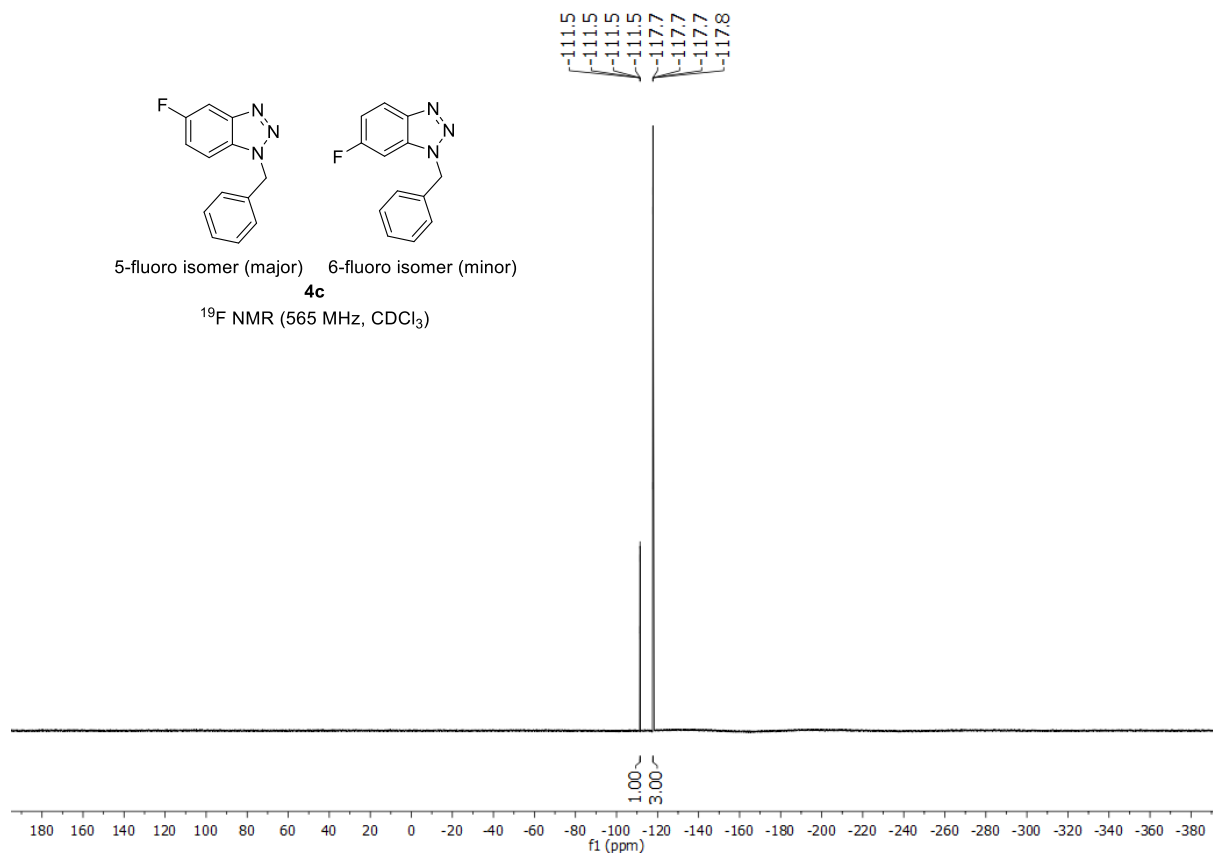


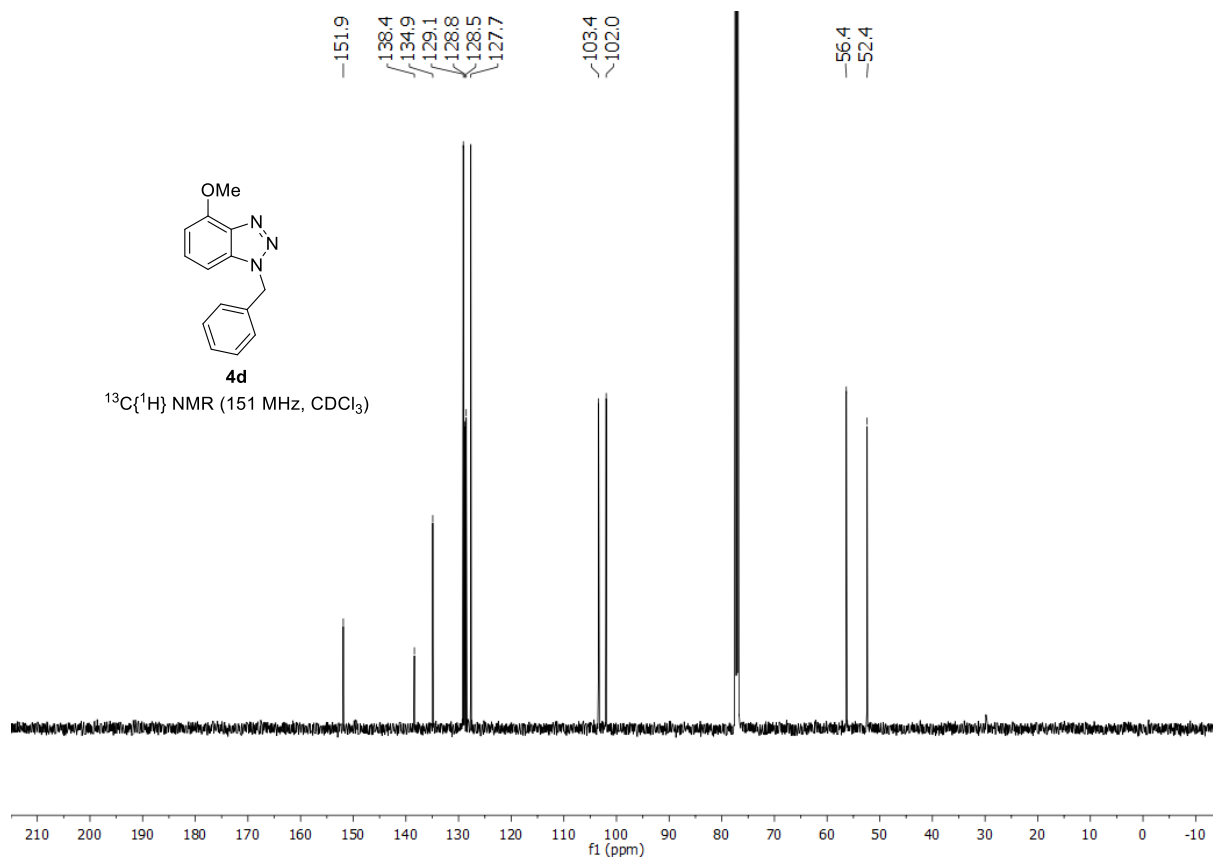
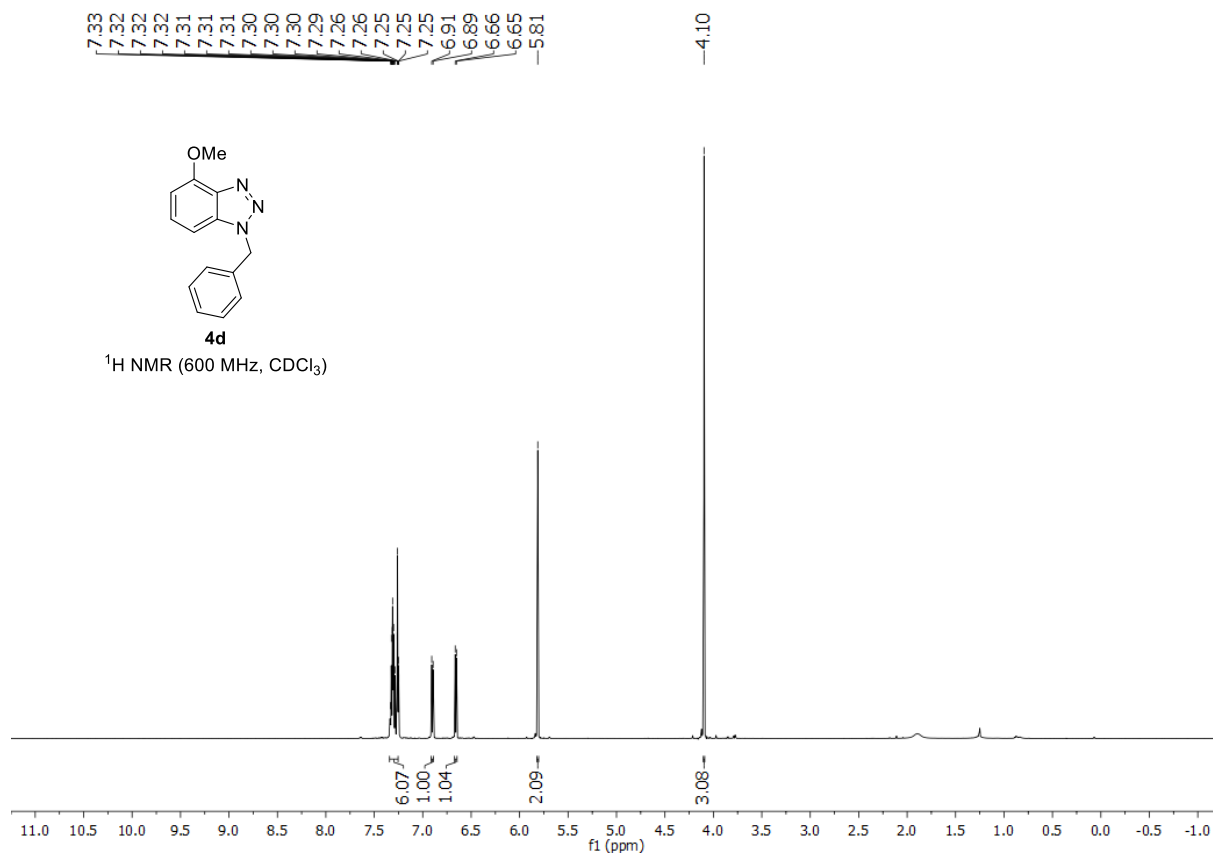




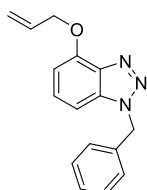






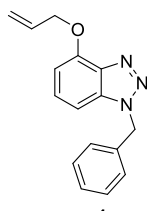
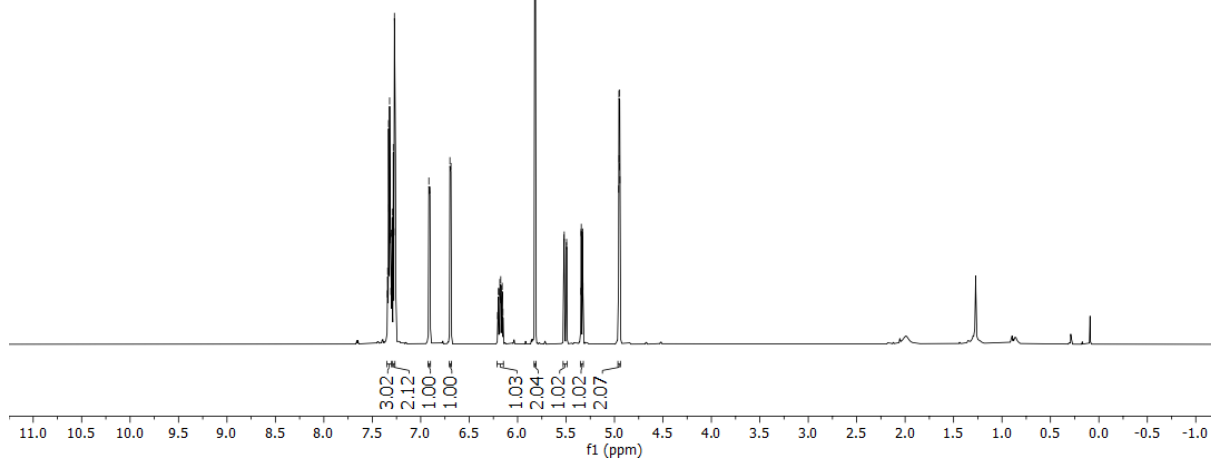


7.34
7.34
7.34
7.33
7.33
7.32
7.32
7.32
7.31
7.31
7.31
7.30
7.29
7.28
7.28
7.27
7.27
6.92
6.90
6.70
6.69
6.21
6.20
6.19
6.18
6.18
6.18
6.17
6.17
6.16
6.15
5.82
5.52
5.52
5.50
5.49
5.35
5.34
5.34
5.34
5.33
5.33
5.33
4.96
4.95
4.95
4.95
4.94



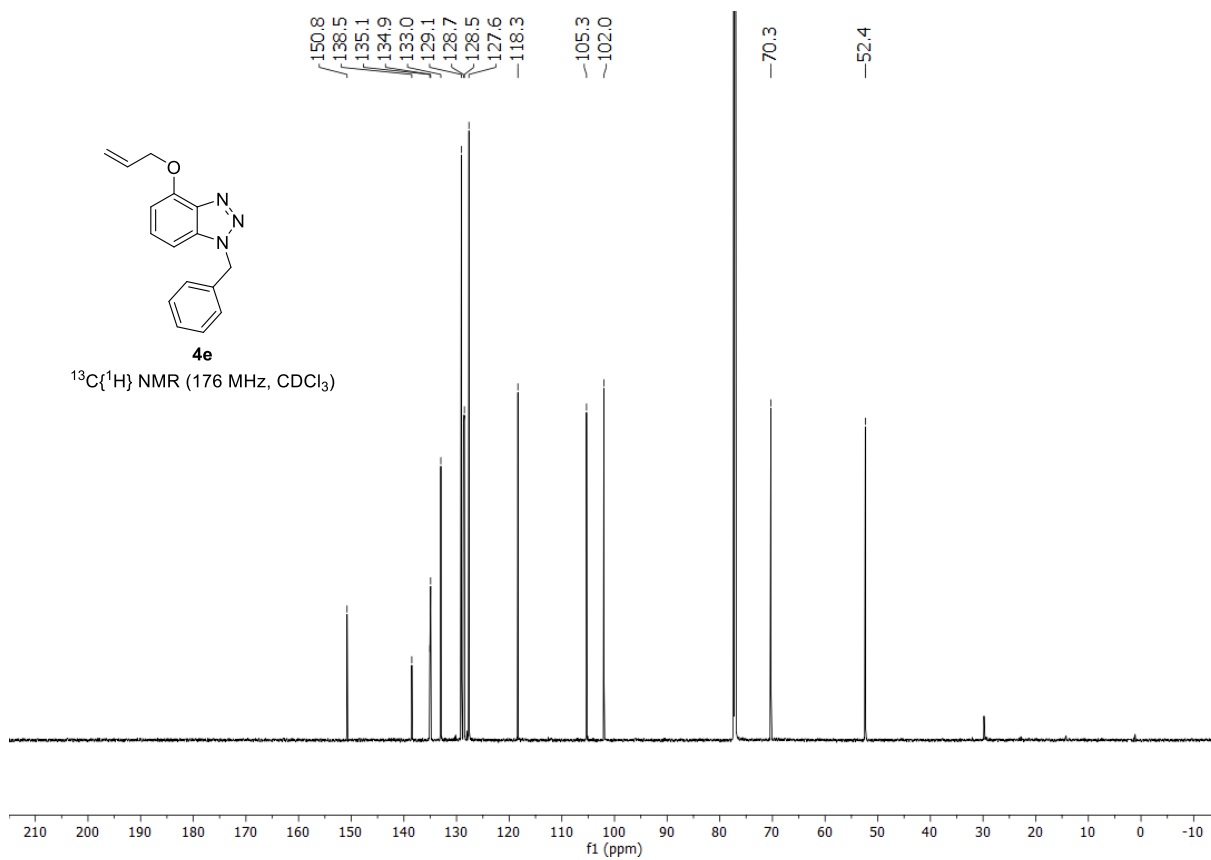
4e

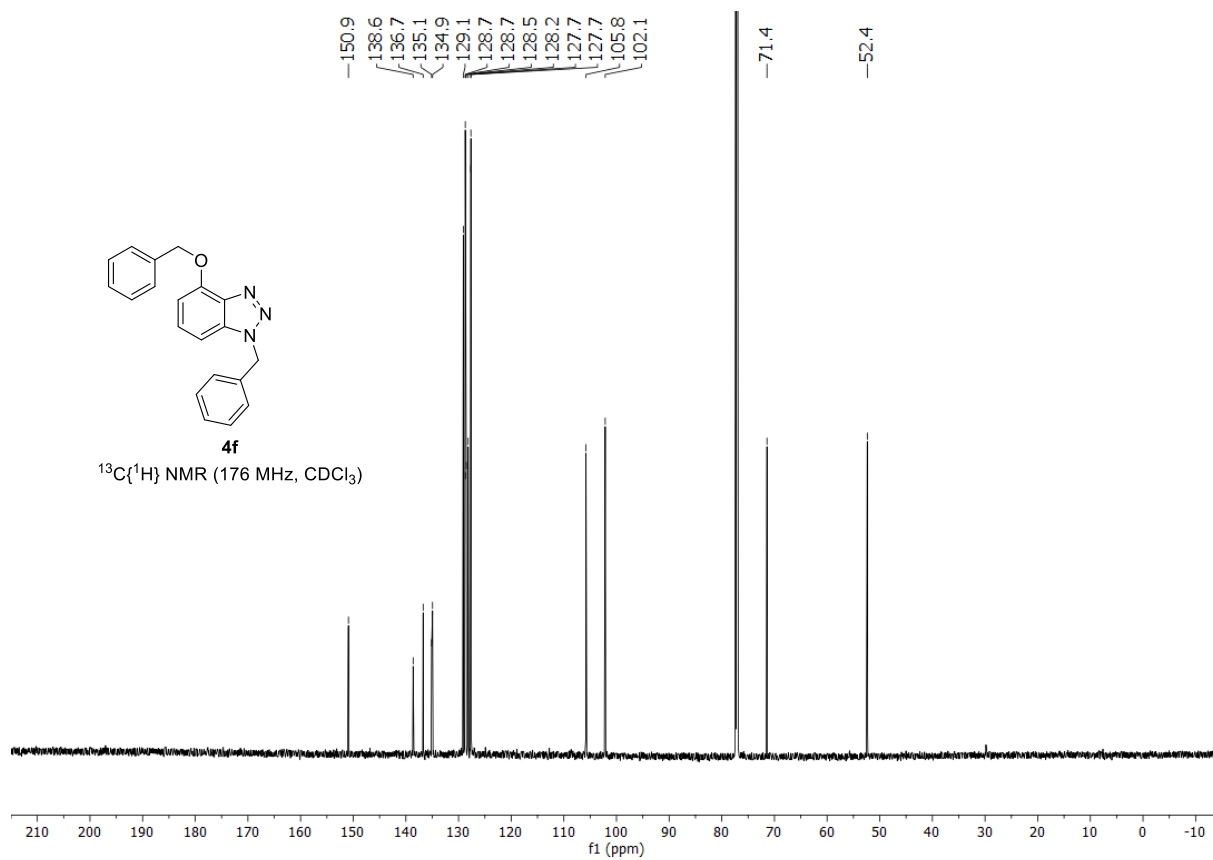
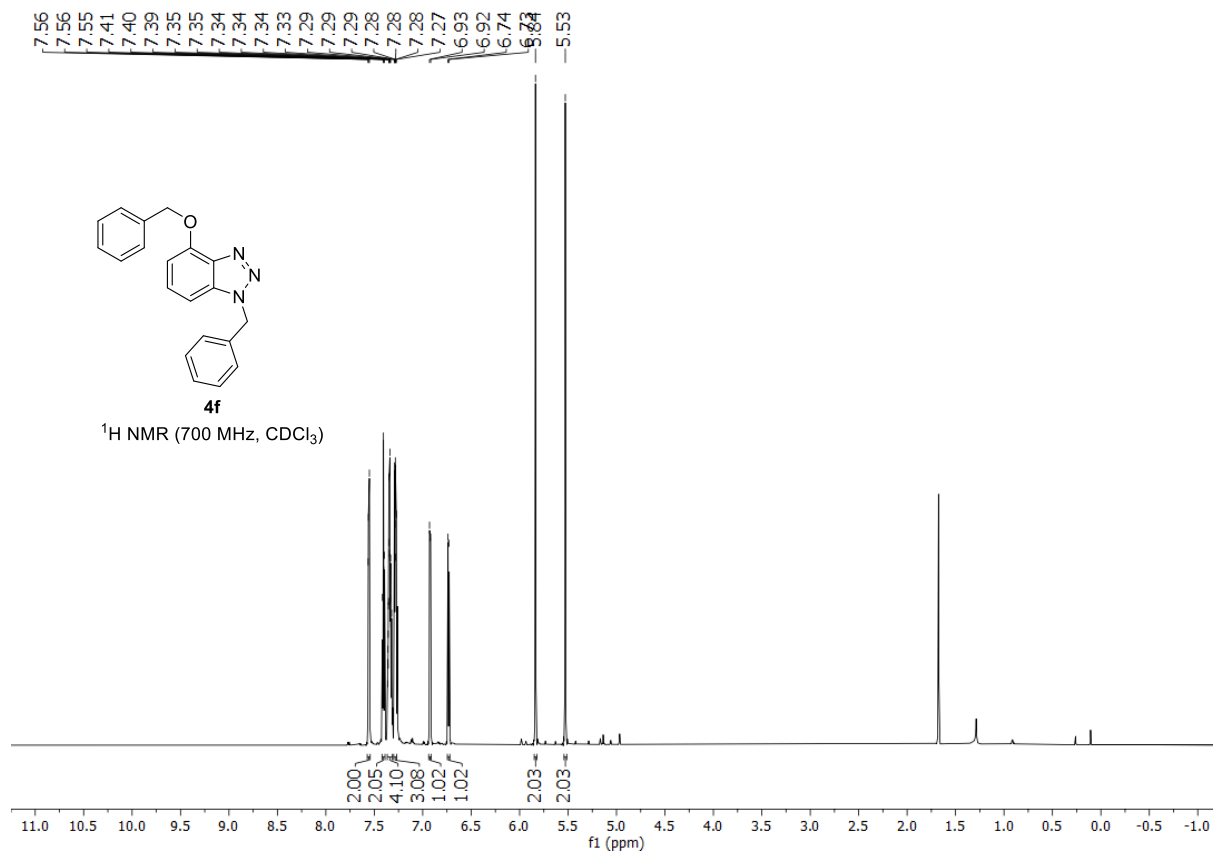
$^1\text{H NMR}$ (700 MHz, CDCl_3)



4e

$^{13}\text{C}\{^1\text{H}\}$ NMR (176 MHz, CDCl_3)





4. References

- [1] X. Li, Y. Sun, X. Huang, L. Zhang, L. Kong, B. Peng, *Org. Lett.* **2017**, *19*, 838–841.
- [2] H. Jiang, Y. Zhang, W. Xiong, J. Cen, L. Wang, R. Cheng, C. Qi, W. Wu, *Org. Lett.* **2019**, *21*, 345–349.
- [3] J. Schwan, M. Kleoff, B. Hartmayer, P. Heretsch, M. Christmann, *Org. Lett.* **2018**, *20*, 7661–7664.
- [4] A. Haito, M. Yamaguchi, N. Chatani, *Asian J. Org. Chem.* **2018**, *7*, 1315–1318.
- [5] M. Kleoff, J. Schwan, L. Boeser, B. Hartmayer, M. Christmann, B. Sarkar, P. Heretsch, *Org. Lett.* **2020**, *22*, 902–907.
- [6] I. D. G. Watson, N. Afagh, A. K. Yudin, *Org. Synth.* **2010**, *87*, 161–169.
- [7] P. Khaligh, P. Salehi, M. Bararjanian, A. Aliahmadi, H. R. Khavasi, S. Nejad-Ebrahimi, *Chem. Pharm. Bull.* **2016**, *64*, 1589–1596.
- [8] M. Kleoff, J. Schwan, M. Christmann, P. Heretsch, *ChemRxiv* **2020**, DOI: 10.26434/chemrxiv.13266260.v1.
- [9] K. Homann, J. Angermann, M. Collas, R. Zimmer, H.-U. Reißig, *J. Prakt. Chem.* **1998**, *340*, 649–655.
- [10] F. Shi, J. P. Waldo, Y. Chen, R. C. Larock, *Org. Lett.* **2008**, *10*, 2409–2412.
- [11] S. Kovács, Á. I. Csincsi, T. Z. Nagy, S. Boros, G. Timári, Z. Novák, *Org. Lett.* **2012**, *14*, 2022–2025.